

## **$\delta$ D in lunar volcanic glasses and melt inclusions: A Carbonaceous chondrite heritage revealed**

A.E. SAAL<sup>1\*</sup>, E.H. HAURI<sup>2</sup>, J.A. VAN ORMAN<sup>3</sup>  
AND M.J. RUTHERFORD<sup>1</sup>

<sup>1</sup>Dept. of Geol. Sc., Brown University, RI, 02912, USA

(\*correspondence: asaal@brown.edu)

<sup>2</sup>DTM, Carnegie Institute of Washington, DC, 20015, USA

<sup>3</sup>Dept. of Geol. Sc., Case Western Reserve University, OH 44106, USA

Water is perhaps the most significant molecule in the solar system, and determining its origin and distribution in planetary interiors has important implications for understanding the evolution of planetary bodies. Here we present the isotopic composition of hydrogen dissolved in lunar volcanic glasses and in their olivine-hosted melt inclusions to establish the source of the lunar magmatic water. These volcanic glasses, returned by the Apollo 15 and 17 missions, represent some of the best-studied and most primitive magmas generated within the Moon. The D/H ratios and H<sub>2</sub>O contents were measured simultaneously in the center of the exposed interiors of individual lunar volcanic glass beads and olivine-hosted melt inclusions, using a Cameca NanoSIMS 50L multicollector ion microprobe. We examined very-low Ti and low-Ti glasses from Apollo 15 15426/27 and high-Ti glasses from Apollo 17 74220. The Apollo 17 high-Ti glasses contain olivine-hosted melt inclusions, small samples of magma trapped within the olivine that grew in the magma before eruption. By virtue of their enclosure within their host crystals, melt inclusions are protected from loss of volatiles by degassing during eruption. After consideration of cosmic ray spallation and degassing processes our results demonstrate that lunar magmatic water has an isotopic composition that is indistinguishable from the bulk water in carbonaceous chondrites and similar to terrestrial water, implying a common origin for the water contained in the interiors of the Earth and Moon. The Moon must have received its water during or shortly after its accretion, before the formation of a robust lunar lithosphere  $\leq 100$  My. Data for highly siderophile elements [1] suggest that a late veneer of meteoritic material delivered to the Moon was too small to be responsible for the lunar volatile budget. Therefore, the simplest scenario consistent with our observations is that the Earth was wet at the time of the Moon-forming event, as predicted by dynamic models [2,3], and that the water was not completely lost during this giant impact.

[1] Day, J. M. D. *et al.* (2007) *Science* **315**, 217-219. [2] Morbidelli, A. *et al.* (2000) *Meteor. Planet. Sci.* **35**, 1309. [3] Walsh, K.J. *et al.* (2012) *Meteor. Planet. Sci.* **47**, 1941.

## **Fluid-mineral reactions during CO<sub>2</sub>-based geothermal energy extraction**

MARTIN O. SAAR, XIANG-ZHAO KONG,  
BENJAMIN M. TUTOLO, ANDREW J. LUHMANN AND  
WILLIAM E. SEYFRIED, JR.<sup>1</sup>

<sup>1</sup>Department of Earth Sciences, University of Minnesota, 310 Pillsbury Dr. SE, Minneapolis, MN 55455, USA.  
saar@umn.edu

Geothermal energy extraction with groundwater as the subsurface heat extraction fluid can result in substantial scaling (mineral precipitation) in pipes, heat exchangers, power conversion equipment, and the subsurface reservoir. A potential solution to this problem is to utilize carbon dioxide (CO<sub>2</sub>) as the subsurface heat extraction fluid. During this approach, CO<sub>2</sub> from an emitter, such as a coal-fired power plant, biofuel plant, or concrete factory, is injected into a geothermal reservoir such as a sedimentary basin or a hydrofractured rock. In the case of the sedimentary basin approach, large amounts of CO<sub>2</sub> are permanently stored underground in the form of a CO<sub>2</sub> plume while a small portion of the geothermally heated CO<sub>2</sub> is circulated back to the surface for power production before reinjection into the reservoir along with the main CO<sub>2</sub> stream. This is referred to as a CO<sub>2</sub>-Plume Geothermal (CPG) system.

When CO<sub>2</sub> is injected into deep saline aquifers, the CO<sub>2</sub> largely displaces the brine although there is a small degree of dissolution at the CO<sub>2</sub>-brine interface. The result is a multicomponent-multiphase plume environment that ranges from virtually pure CO<sub>2</sub> in the center of the plume to CO<sub>2</sub> with dissolved water on the CO<sub>2</sub> side of the CO<sub>2</sub>-water interface, to brine with dissolved CO<sub>2</sub> on the brine side of the interface, to brine with no CO<sub>2</sub> away from the plume.

Here, we present results on the reactions of some of the above described fluid components with various reservoir minerals that are based on flow-through reaction cell experiments under realistic T and P conditions. Pre- and post-experiment X-Ray Computed Tomography analyses provide 3D images of pore-space geometry changes due to the reactions. The 3D images are then used as input in lattice-Boltzmann fluid flow simulations to determine permeability field changes due to the fluid-mineral reactions. The ultimate objective of this work is a parameterization of permeability changes as a function of fluid and mineral chemistry for typical host rocks and T-P conditions which can be included into geothermal reservoir simulators such as TOUGH2.

## Evaluation of different RNA preservation methods to study the active microbial communities in oil sand tailings ponds

SABARI PRAKASAN M.R.<sup>1\*</sup>, NADINE LOICK<sup>2</sup>  
AND CHRIS WEISENER<sup>1</sup>

<sup>1</sup>GLIER, University of Windsor, Windsor, Canada  
(\*mullapus@uwindsor.ca)

<sup>2</sup>Rothamsted Research, Hertfordshire, England

Analysis of RNA is the best approach to understand active microbial populations in an environment. In contrast to DNA, which can persist in soil for several days, RNA is an unstable macromolecule making it more suitable to investigate metabolically active microbial communities. Due to its susceptibility to degradation, the preservation of a sample containing RNA is an important step in molecular studies. In the field of Oil Sand Tailings Research sample-preservation is especially important as due to logistical limitations the extraction of nucleic acids may only be possible days after the samples are taken. The aim of this study is to evaluate the ability of different methods to preserve RNA in Oil Sand Tailings samples both short term (5 days) and long-term (30 days). In our study different preservation solutions including LifeGuard™ Soil Preservation Solution (MoBio Laboratories, Inc.), RNAlater® (Ambion), glycerol and liquid nitrogen are compared to find the best preservative method for soil RNA preservation.

Analysis of different RNA samples shows that all four preservation methods provide significant amounts of RNA for further analysis. After cDNA synthesis T-RFLP analysis is used to compare community structure derived from the differently treated samples. Additionally, during RNA-extraction co-precipitated DNA is also analysed. The community structure data derived from cDNA and DNA provides information on the ability and comparability of the different techniques to preserve microbial communities and demonstrates the importance of RNA (cDNA) in microbial ecology.

## Interaction of Eu(III) with calcium carbonate: Spectroscopic characterization

A. SABĂU<sup>1,2</sup>, N. JORDAN<sup>3</sup>, C. LOMENECH<sup>2</sup>,  
N. MARMIER<sup>2,\*</sup>, V. BRENDLER<sup>3</sup>, A. BARKLEIT<sup>3</sup>, S.  
SURBLÉ<sup>4</sup>, N. TOULHOAT<sup>5,6</sup>, Y. PIPON<sup>5</sup>, N. MONCOFFRE<sup>5</sup>,  
E. GIFFAUT<sup>1</sup>

<sup>1</sup>Agence Nationale pour la gestion des Déchets Radioactifs (ANDRA)

<sup>2</sup>University of Nice - Sophia Antipolis, ECOMERS (\*e-mail: nicolas.marmier@unice.fr)

<sup>3</sup>Helmholtz-Zentrum Dresden-Rossendorf (HZDR)

<sup>4</sup>UMR 3299 CEA/CNRS SIS2M/LEEL

<sup>5</sup>IPNL, CNRS/Université Claude Bernard Lyon

<sup>6</sup>CEA/DEN Saclay, 91191 Gif sur Yvette, France

The present work investigated irreversible sorption processes in the Eu-CO<sub>2</sub>-NaCl-CaCO<sub>3</sub> system, by combining macroscopic with TRLFS and RBS spectroscopic studies.

Powders and single crystals were used due to spectroscopic tools requirements. Sorption of europium was investigated by varying the initial concentration in europium concomitant with the contact time (few hours up to 6 months). TRLFS identified two lifetimes and therefore two species at the calcite/water interface. Lifetimes allow an unambiguous discrimination between sorption processes and incorporation. Values of the lifetimes are comparable to the literature [1] and the total loss of water molecules is a distinctive sign of Eu(III) species incorporation.

RBS confirmed that Eu(III) is associated in two different states with calcite:

- (1) heterogeneous (supported by SEM) surface accumulation, i.e. as a surface precipitate, after 1 month contact time
- (2) incorporation up to depths greater than 160 nm after 1 month.

[1] Fernandes, M. M. *et al.*, *J. Colloid Interface Sci.* **321** (2008) 323-331

## Monazite anamnesis – providing a quantitative timeframe for metamorphic petrogenetic processes

GAVRIL SĂBĂU<sup>1</sup>, ELENA NEGULESCU<sup>1</sup> AND THOMAS THEYE<sup>2</sup>

<sup>1</sup>Geological Institute of Romania, RO-012271 Bucharest, (g\_sabau@yahoo.co.uk)

<sup>2</sup>Institut für Mineralogie und Kristallchemie, DE-70174 Stuttgart, (thomas.theye@imi.uni-stuttgart.de)

Monazite is a privileged phase in metamorphic assemblages, as it has a wide p-T stability field, a complex chemical composition, incorporates high concentrations of radioactive elements and is remarkably refractory to diffusion. Its chemical substitutions represent a very sensitive response to mineral reactions triggered by changing conditions, being recorded and preserved in grain zonations, as well as in regular chemical variations in the monazite populations. Connecting age data with chemical features allows not only dating monazite growth, but also a sometimes surprisingly accurate insight in the concurrent mineral reactions.

We performed several hundred microprobe analyses on monazite in pelitic and gneissic rocks from the South Carpathian basement units, for both chemical characterization and dating. The chemical characterization included structural formulae, ternary plots, normalized plots and elemental ratios therefrom. Relating age point data to compositional trends reveals homogeneous compositional and age domains, as well as regular chemical shifts, having a counterpart in mineral reactions involving monazite, and in variations in the crystallization versus resorption rates of monazite itself.

Monazite acts as a LREE and Th scavenger from decomposing REE-bearing phosphates, carbonates and silicates, and Th (U)-bearing silicates, phosphates and oxides, recording high Th (+Ca, U) and LREE contents in the initial growth stages. Oppositely, monazite resorption is typically indicated by its Nd and Sm enrichment. LREE correlations are variable, reversing differently in different samples with increasing atomic number, whereas the corresponding ratios indicate changes in modal abundance. Y content is buffered by coexisting xenotime and melt, being also markedly fractionated in coexisting garnet, as Y variation strongly and inversely reflects changes in modal garnet abundance. Eu is fractionated in plagioclase (metamorphic or crystallizing from melts) and U in coexisting melts. Heavier MREE are partitioned in xenotime. Monazite chemistry holds thus valuable keys for both identifying and dating thermometamorphic processes, especially those involving melting episodes and garnet growth and decomposition.

## Towards Quantitative Paleohydrology: Reconstructing changes in relative humidity from lipid biomarker $\delta D$ values

DIRK SACHSE<sup>1</sup>, OLIVER RACH<sup>1</sup>, ANSGAR KAHMEN<sup>2</sup>, HEINZ WILKES<sup>3</sup> AND ACHIM BRAUER<sup>3</sup>

<sup>1</sup>University of Potsdam, Institute of Earth and Environmental Science, Karl-Liebknecht-Str. 24-25, 14476 Potsdam-Golm, Germany

<sup>2</sup>ETH Zurich, Institute of Agricultural Sciences, Universitätsstrasse 2, 8092 Zürich, Switzerland

<sup>3</sup>GFZ German Research Centre for Geosciences, Telegrafenberg, 14473 Potsdam, Germany

The stable isotopic composition of meteoric waters, recorded through the hydrogen isotopic composition of lipid biomarkers is an integral of a number of hydrological parameters, such as condensation temperature, precipitation amount, evaporation, moisture pathway. It is often difficult to disentangle these parameters for a true quantitative reconstruction of hydrological variables, such as precipitation amount and relative humidity. Here we review the current state of knowledge of the factors driving leaf wax  $\delta D$  values and evaluate how terrestrial plant lipid biomarker  $\delta D$  values in combination with plant physiological modelling can be used to quantitatively reconstruct changes in relative humidity (rH).

We present a proof-of-concept for this approach by estimating relative humidity changes during the Younger Dryas cold period in Western Europe from the analysis of lipid biomarker  $\delta D$  values from the annually varved sediments of Lake Meerfelder Maar. We use the isotopic difference between aquatic and terrestrial lipid biomarkers as a measure of mean leaf water isotope enrichment. We parameterized a Craig-Gordon leaf water isotope model with plant physiological parameters estimated from available vegetation cover information from palynological records and climate proxy data (such as temperature) and solved this model for rH. Our reconstruction of Younger Dryas rH changes documents profound hydrological changes - likely as a consequence of changes in atmospheric circulation due to the position of North Atlantic Sea Ice - which were the ultimate trigger for the observed environmental changes. While supporting previous suggestions of a dry Younger Dryas in Western Europe our new biomarker and modelling approach delivers for the first time quantitative estimates of hydrological changes (i.e. relative humidity changes), which can be directly compared to the output from climate models.

## The role of organic matter in genesis of sedimentary-hosted stratiform copper deposits in Nahand-Ivand area, NW Iran

\*SADATI N.<sup>1</sup>, YAZDI M.<sup>1</sup>, BEHZADI M.<sup>1</sup>, ADABI M.H.<sup>1</sup>  
AND MOKHTARI A.A.<sup>2</sup>

<sup>1</sup>Department of Geology, Faculty of Earth Science, Shahid Beheshti University, Tehran, Iran (\*correspondence: sadati\_sn@yahoo.com)

<sup>2</sup>Department of Geology, Faculty of Earth Science, Zanjan University, Zanjan, Iran (<sup>2</sup> mokhtari1031@gmail.com)

The study area is located in part of Arasbaran- Sabalan zone in the northwestern part of Iran. Cu mineralization in Nahand - Ivand area is observed in sandstone rock units belonging to the Ghom Red beds Formation of Miocene age[1]. The Ghom Red beds Formation include alternations of red oxidized (iron oxide minerals) sandstones and conglomerates that partly convert to reduced clastic such as sandstone, siltstone, shale, conglomerate, limestone, dolomite and marl, which may contain carbonaceous or organic matter. Also Evaporites such as gypsum and salt are commonly associated. In this study, zones of reduction (grey, white, green) within oxidized red-bed sedimentary rocks are the most favored host rocks. The color of the host rocks ranges from light gray to black, reflecting their high organic matter content.

Mineralization is localized in the organic-rich and pyrite-containing gray rocks that replace the red rocks along the vertical and lateral directions[2]. The main ore minerals in the deposit are copper carbonates such as malachite, azurite and some copper sulfides such as chalcocite[3]. During this study 44 samples were collected from the Ghom Redbeds Formation. Host rock and mineralized samples were analyzed for major and trace element contents by Inductively Coupled Plasma–Mass Spectrometry (ICP- MS). The results showed that In addition to copper, precious metals such as silver are less focused. In this area maximum grade of samples are up to 5.2% Cu with an average of 1.4% Cu. Copper precipitation was possibly promoted by reduction zones from organic matter such as woody fragments and plant fossils[4]. It seems that during the formation of the copper deposits, organic matter played an important role in adsorbing and gathering metallic elements [5].

[1] Sadati et al (2012) MINERALOGIA – SPECIAL PAPERS 40, 124. [2] Gablina *et al.* (2008) Lithology and Mineral Resources 43, 136–153. [3] Cox *et al.* (2007) US Geological 03-107, 1- 50. [4] Stensgaard (2011) Geology and Ore 18, 2-12. [5] Jiajun *et al.* (2002) Ore Geology 20, 55–63.

## REE contents in soils and sediments from the GEMAS and FOREGS data-bases: comparison between different geological contexts in Italy and Sweden

M.SADEGHI<sup>1</sup>, P.PETROSINO<sup>2</sup>, M.ANDERSSON<sup>1</sup>,  
S. ALBANESE<sup>2</sup>, A.LADENBERGER<sup>1</sup>, G. A. MORRIS<sup>1</sup>,  
J.UHLBÄCK<sup>1</sup>, A. LIMA<sup>2</sup> AND B. DE VIVO<sup>2</sup>

<sup>1</sup>Geological Survey of Sweden, BOX 670, S-75128 Uppsala, Sweden (\* correspondance : martiya.sadeghi@sgu.se)

<sup>2</sup>Dipartimento di Scienze della Terra, dell'Ambiente e delle Risorse, Università degli Studi di Napoli Federico II, L.go S. Marcellino 10, 80138 Napoli

Rare Earth Elements (REEs) are rapidly gaining attention as important chemical resources thanks to the increasing number of high-tech applications in which they are required and, as a consequence, scientific interest on REE-bearing minerals and resources is increasing. In this study, REE data from the FOREGS database of solid media chemistry (topsoils, subsoils, stream sediments, floodplains) have been used to constrain elemental distribution maps. Principal Component Analysis (PCA) has been applied to identify patterns within the data set. Detailed investigation of the distribution of REEs in all media for both countries shows the prominent role played by geogenic components. Despite similar REE concentrations in the underlying bedrocks, several significant differences emerge between the two countries driven by climate, morphology of the territory, age of the deposits, presence of mineralisation, type of soils and presence/absence of till.

The same approach has been applied to the GEMAS database to compare the REE distribution in agricultural and grazing land soils, using the same statistical approach as used for solid media from the FOREGS database. In general, high pH alkaline soils show higher REE concentrations. Certain specific anomalies can be correlated to known phosphate and REE mineralizations. The fingerprint of anthropogenic activity, both agricultural fertilizer use and cattle feed, does not influence the geogenic signal. In both Italy and Sweden, REE concentrations in agricultural and grazing land soils are comparable with those obtained for topsoils sampled from unoccupied and undisturbed areas. The main difference between the elemental distribution of REEs is more closely related to the geochemical behaviour of individual elements and their extractability as affected by the source of the elements in the sample media.



## Partitioning behavior of Cs in the matrix of simulated ash residues

A. SAFFARZADEH<sup>1\*</sup> AND T. SHIMAOKA<sup>1</sup>

<sup>1</sup>Kyushu University, Fukuoka 819-0395, Japan

(\*correspondence: amir@doc.kyushu-u.ac.jp)

Tohoku great earthquake and tsunami of March 11, 2011 caused massive explosions at Fukushima I Nuclear Power Plant. Such incidents led to the dissemination of fission products (such as <sup>131</sup>I, <sup>134</sup>Cs, <sup>137</sup>Cs) in a broad geographic area [1, 2]. These radionuclides concentrated in the surrounding natural environments [3] as well as in the debris left from the disaster. Incineration of combustible fraction of disaster debris resulted in the higher level of radioactivity (Cs-related) in the generated ash residues (up to 100,000 Bq/kg in fly ash in some areas), thus banned landfilling.

To model the behavior of radioactive Cs in the ash residues, simulated ash was produced by fusing RDF and Cs salts (non-radioactive) at high temperatures (800-1000 °C). The products mainly consist of glassy matrix (silicate) and a variety of crystalline phases

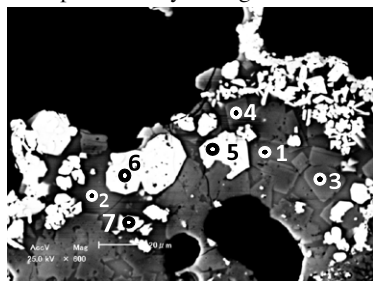


(Fig 1). Microbeam analysis indicates that Cs is essentially distributed within the glassy matrix of the ash with little or no partitioning within the crystalline phases (Table 1). Binding of Cs in the silicate structure of the glass is a good evidence for the entrapment of analogous radioactive Cs. Additional experiments are underway to examine the chemical form of Cs and to improve

**Fig. 1:** SEM image of the ash matrix

| Phases | Glass |       | Crystalline |       |       |       |       |
|--------|-------|-------|-------------|-------|-------|-------|-------|
|        | 1     | 2     | 3           | 4     | 5     | 6     | 7     |
| Cs     | 1.75  | 1.51  | 0.00        | 0.00  | 0.00  | 0.00  | 0.00  |
| Al     | 6.16  | 7.12  | 4.13        | 3.71  | 0.90  | 0.91  | 1.14  |
| Si     | 28.73 | 28.68 | 24.53       | 23.99 | 16.77 | 16.92 | 4.07  |
| Ca     | 5.30  | 4.38  | 20.94       | 19.38 | 23.72 | 23.47 | 2.01  |
| Fe     | 15.65 | 10.70 | 8.22        | 9.03  | 20.96 | 20.42 | 60.93 |
| K      | 2.95  | 2.76  | 0.24        | 0.29  | 0.18  | 0.17  | 0.28  |

the ash quality in order to meet the standards for landfilling.

**Table 1:** Chemical composition of the points in Fig 1 (Wt%).

[1] Kato *et al.* (2012) *J. Env. Radio* **111**, 59-64. [2] Hirose (2012) *J. Env. Radio* **111**, 13-17. [3] Yasunari *et al.* (2011) *PNAS* **108**, 19530-19534.

## The H<sub>2</sub>O-CO<sub>2</sub>-(K, Na)Cl fluids, melting of the tonalite gneiss, and the A-type granitic magmas: Experimental evidence for connection

OLEG SAFONOV

Institute of Experimental Mineralogy, Russian Academy of Science, Chernogolovka, Russia, oleg@iem.ac.ru

The A-type (anorogenic) granites, a specific variety of ferroan granitic rocks forming predominantly during crustal extension, are distinct by their medium-to-high peralkalinity (low Al<sub>2</sub>O<sub>3</sub> and high K<sub>2</sub>O+Na<sub>2</sub>O contents), low CaO, elevated contents of F and Cl. Partial melting of the Archean TTGs in the continental basement is discussed among models to explain origin of these granites. However, neither fluid-absent nor hydrous melting of TTGs at pressures up to 15 kbar can fully satisfy the required parameters of the melts. The influx of K and Na seems to be needed for the formation of the A-type granites. Data on the melting of TTGs in presence of the H<sub>2</sub>O-CO<sub>2</sub> fluids containing alkali salts are absent, so far. In order to trace variations of mineral assemblages and melt composition in dependence on temperature, concentration of salts and K/Na ratio in the fluids, the experiments on interaction of a biotite-hornblende tonalite gneiss with the H<sub>2</sub>O-CO<sub>2</sub>-(K, Na)Cl fluids at 5.5 kbar and 750 and 800°C were performed. The H<sub>2</sub>O-CO<sub>2</sub>-KCl fluids provoke melting only at 800°C. Addition of NaCl assists to melting at 750°C. The increase of the chloride/(H<sub>2</sub>O+CO<sub>2</sub>) ratio in the fluids results in formation at 800°C of the rhyolitic melts with Al<sub>2</sub>O<sub>3</sub> < 13.5 wt. %, CaO < 2 wt. %, K<sub>2</sub>O+Na<sub>2</sub>O > 7 wt. %, FeO/(FeO+MgO) > 0.8, K<sub>2</sub>O/Na<sub>2</sub>O > 1, moderately enriched in Cl (0.2-0.6 wt. %). The melt composition correlate with the coexisting mineral assemblages, varying in the sequence Opx+Amp+Pl+Ti-Mt+Ilm → Opx+Cpx+Ilm → Cpx+Kfs+Ilm. Stabilization of Cpx and Kfs at the high chloride/(H<sub>2</sub>O+CO<sub>2</sub>) ratio in the fluids corresponds to the decrease of CaO and Al<sub>2</sub>O<sub>3</sub> contents in the melts, while increase of the Cl content in these melts promotes the FeO/(FeO+MgO) ratio. Stability of pyroxenes at moderate and high chloride/(H<sub>2</sub>O+CO<sub>2</sub>) ratios in the fluids reflects low *a*<sub>H<sub>2</sub>O</sub> in the melts, i.e. their apparent “dryness”. These characteristics are similar to the A-type granites. At 750°C, the H<sub>2</sub>O-CO<sub>2</sub>-(K, Na)Cl fluids produce trachytic melts, which model syenites, monzonites and other alkalic basic counterparts of the A-type granitic complexes. The experiments support the model for formation of these complexes by crustal melting during high-grade metamorphism in presence of the aqueous-carbonic-salt fluids fluxing in the extensional environments.

## Arsenic contamination in pond sediment of central India

B. L. SAHU<sup>1</sup>, K. S. PATEL<sup>1</sup>, I. WYSOCKA<sup>2</sup>  
AND I. JARON<sup>2</sup>

<sup>1</sup>School of Studies in Chemistry, Pt. Ravishankar Shukla University, Raipur-492010, CG, India, bharatred007@gmail.com

<sup>2</sup>Polish Geological Institute, Rakowiecka, Street-00-975, Warsaw, Poland, iwys@pgi.gov.pl

The pond is widely used for the fish culture and other house hold activities in India. The environment of the Kaudikasa, central India is one of the most arsenic contaminated sites in the World [1]. In this work, the contamination of arsenic and other 33 elements in eight pond sediments (N 20°51' and E 80°45') is described. The sediment samples were collected in summer 2012, and the crushed sample ( $\leq 0.1$  mm) was digested in the micro-oven with acids. The acid extracts were analyzed by using techniques: ICP-AES and ICP-MS. Among 34 elements analyzed, eight elements i.e. Na, K, Mg, Ca, Al, S, P and Fe occurred at macro levels, ranging from 0.01 – 0.06, 0.21 – 0.45, 0.17 – 1.08, 0.18 – 0.76, 1.41 – 3.14, 0.01 – 0.06, 0.02 – 0.03 and 2.8 – 6.3% with mean value of  $0.01\pm 0.01$ ,  $0.33\pm 0.07$ ,  $0.43\pm 0.30$ ,  $0.38\pm 0.14$ ,  $2.12\pm 0.48$ ,  $0.03\pm 0.01$ ,  $0.03\pm 0.01$  and  $4.2\pm 0.9\%$ , respectively. Twelve metals i.e. As, Ba, Sr, Ti, V, Cr, Mn, Co, Ni, Cu, Zn and Pb was present at milligram levels, ranging from 48 – 256, 129 – 264, 12 – 30, 62 – 735, 38 – 144, 29 – 732, 388 – 1109, 12 – 42, 23 – 108, 35 – 73, 40 – 100 and 17 – 40 mg kg<sup>-1</sup> with mean value of  $111\pm 52$ ,  $192\pm 32$ ,  $20\pm 5$ ,  $226\pm 151$ ,  $72\pm 25$ ,  $77\pm 49$ ,  $646\pm 177$ ,  $23\pm 8$ ,  $48\pm 21$ ,  $53\pm 9$ ,  $66\pm 17$  and  $24\pm 6$  mg kg<sup>-1</sup>, respectively. Twelve metals i.e. Li, Rb, Cs, Be, Ga, Tl, Sn, Sb, Bi, Mo, Ag, Cd, Th and U present at lower milligram levels with mean value of 11, 31, 1.3, 1.7, 10, 0.2, 1.5, 0.5, 0.2, 0.8, 0.6, 0.13, 11.7 and 1.24 mg kg<sup>-1</sup>, respectively. Arsenic content was correlated well with the P, Pb and Zn content. The arsenic concentration was found to be several folds higher than the recommended value of 5 mg kg<sup>-1</sup>. The arsenic content in the pond sediment of this region was found to be much more higher than other region of the World [2].

[1] Patel *et al* (2005) *Environ. Geochem. Health* **27**,131-145

[2] Durant *et al*. (2004) *Water Res.* **38**, 2989–3000.

## Microphysical properties of BC in anthropogenic and biomass burning plumes

L. K. SAHU<sup>1</sup>, Y. KONDO<sup>2</sup>, N. MOTEKI<sup>2</sup>, N. TAKEGAWA<sup>3</sup>,  
Y. ZHAO<sup>4</sup>

<sup>1</sup>Physical Research Laboratory, Ahmedabad, India,  
(\*correspondence: lokesh@prl.res.in)

<sup>2</sup>Department of Earth and Planetary Science, Graduate School of Science, The University of Tokyo, Tokyo, Japan,  
kondo@eps.s.u-tokyo.ac.jp, moteki@eps.s.u-tokyo.ac.jp

<sup>3</sup>Research Center for Advanced Science and Technology, University of Tokyo, Tokyo, Japan,  
takegawa@atmos.rcast.u-tokyo.ac.jp

<sup>4</sup>Air Quality Research Center, University of California, Davis, USA, yjzhao@ucdavis.edu

The impact of aerosols on regional air quality necessitates improved understanding of their emission and microphysical properties. The size distributions of black carbon (BC) and light scattering particles (LSP) were measured with a single particle soot photometer on board the NASA DC-8 aircraft during the ARCTAS mission 2008. Air sampling was made in the air plumes of both urban and forest fire emissions over California during the CARB (California Air Resources Board) phase of the mission. Air plumes were identified using tracers for fossil fuel (FF) combustion and biomass burning (BB). Enhancements of BC and LSP in BB plumes were significantly higher compared to those in FF plumes. The average mass concentration of BC in BB plumes was more than twice that in FF plumes. Distinct *emission ratios of BC/CO<sub>2</sub>*, *BC/CH<sub>3</sub>CN*, *CH<sub>3</sub>CN/CO*, and *CO/CO<sub>2</sub>* were estimated for the plumes from the two sources. The size distributions of BC and LSP also showed different behaviours. The BC count median diameter of 115 nm in FF plumes was smaller compared to 141 nm in the BB plumes. BC aerosols were thickly coated in BB plumes as the average shell/core ratios were 1.47 and 1.24 in BB and FF plumes, respectively.

## U-Th systematics and chronology of CH<sub>4</sub>-derived CaCO<sub>3</sub> crusts of the Barents Sea

DIANA SAHY<sup>1\*</sup>, AIVO LEPLAND<sup>2,3</sup>, STEPHEN R. NOBLE<sup>1</sup>, DANIEL J. CONDON<sup>1</sup>, HARALD BRUNSTAD<sup>4</sup>.

<sup>1</sup>NERC Isotope Geoscience Laboratory, Keyworth, UK

(\*correspondence: dihy@bgs.ac.uk)

<sup>2</sup>Geological Survey of Norway, Trondheim, Norway

<sup>3</sup>Tallinn University of Technology, Tallinn, Estonia

<sup>4</sup>Lundin Petroleum, Oslo, Norway

CaCO<sub>3</sub> crusts forming due to methane oxidation at seafloor seepage sites serve as archives of past fluid flow and methane discharges into ocean and atmosphere. U incorporation into CaCO<sub>3</sub> during precipitation offers the opportunity to date the crust formation and growth via U-Th systematics (e.g., Aharon et al., 1997; Teichert *et al.*, 2003).

We present U-Th and <sup>87</sup>Sr/<sup>86</sup>Sr data obtained on such CaCO<sub>3</sub> crusts recovered from the Barents Sea floor using a remotely operated vehicle. CaCO<sub>3</sub> phases occur in different modes within the crusts – disseminated within the siliclastic matrix, porosity- and late cavity- filling. These CaCO<sub>3</sub> domains, sampled by microdrilling, display [<sup>230</sup>Th/<sup>232</sup>Th]<sub>AR</sub> from 0.9 up to ~200 and <sup>232</sup>Th concentrations from ~10 to 7000 ppb. Intra-crust U-Th dates range from ~13.1 ± 0.4 to 8.9 ± 0.4 ka. Older dates come from CaCO<sub>3</sub> disseminated within the sediment matrix while younger dates are from late cavity filling CaCO<sub>3</sub>. Layered cavity fills yield resolvable growth histories on the order of 1.0 kyr. Combined such dating results can be used to constrain the histories of CH<sub>4</sub> seepage in the Barents Sea.

<sup>87</sup>Sr/<sup>86</sup>Sr has been analysed on aliquots drilled adjacent to U-Th sample sites. For the majority of crust samples both <sup>87</sup>Sr/<sup>86</sup>Sr and δ<sup>234</sup>U are close to expected values for modern/Holocene seawater. In addition, a sample of a matrix-dominated tubestone representing a subsurface carbonatized fluid conduit, has more radiogenic <sup>87</sup>Sr/<sup>86</sup>Sr values and δ<sup>234</sup>U closer to secular equilibrium. Such contrasts in <sup>87</sup>Sr/<sup>86</sup>Sr and initial δ<sup>234</sup>U reflect distinctly different fluid chemistries forming surface and subsurface CaCO<sub>3</sub> precipitates. These data, together with crust data from other seeps, demonstrate the utility of U-Th for constraining CH<sub>4</sub> seepage duration and absolute timing.

[1] Aharaon, P., *et al.*, 1997, GSA Bulletin, v. 109, p. 568-579. [2] Teichert, B. M. A., *et al.*, 2003, Geochimica et Cosmochimica Acta, v. 67, p. 3845-3857.

## Distribution of Metalloenzymes in Pacific Ocean Environments as Detected by Proteomic Analysis

MAK A. SAITO<sup>1</sup>, MATTHEW R. MCILVIN<sup>1</sup>, DAWN M. MORAN<sup>1</sup>, ALYSON SANTORO<sup>2</sup>, TYLER J. GOEPFERT<sup>1</sup>, NICHOLAS HAWCO<sup>1</sup>, CARL H. LAMBORG<sup>1</sup>

<sup>1</sup>Marine Chemistry and Geochemistry Department, Woods Hole Oceanographic Institution, Woods Hole MA 02543 USA

<sup>2</sup>University of Maryland, Center for Environmental Science, Horn Point Laboratory, 2020 Horns Point Rd Cambridge, MD 21613 USA

\*Correspondence to msaito@whoi.edu

The use of mass spectrometry based proteomics has the capability for direct measurement of proteins produced by microbial life. These proteins can include biomarkers for nutrient stress or microbial taxonomy, as well as enzymes that are responsible carrying out biogeochemical reactions. Most biogeochemically-relevant enzymes require one or more metal atoms for catalytic activity. We report on the analyses of samples collected from a range of depths in the Equatorial Pacific and Eastern Tropical South Pacific. Analyses involved total protein extractions, enzymatic digestion, multi-dimensional chromatographic separation, mass spectrometry analyses, peptide mapping by high performance computing, and quantitative estimates. Proteins of interest will be discussed with a particular focus on metalloenzymes that contain nickel, cobalt, copper, and iron.

## Origin of atmospheric dust and the associated anthropogenic lead around Omura Bay, West Japan

YU SAITOH<sup>1\*</sup>, YU UMEZAWA<sup>2</sup>, KAZUAKI KAWAMOTO<sup>2</sup>,  
MASAHARU TANIMIZU<sup>3</sup> AND TSUYOSHI ISHIKAWA<sup>3</sup>

<sup>1</sup>CAMCR, Kochi University, B200 Monobe, 783-8502, Japan

(\*correspondence: jm-yu-saitoh@kochi-u.ac.jp)

<sup>2</sup>Graduate School of Fisheries Science and Environmental Studies, Nagasaki University

<sup>3</sup>Kochi Institute for Core Sample Research, JAMSTEC

In order to evaluate the responsibility of the cross-border pollution to the atmospheric environment in West Japan, we measured the trace element concentration and Sr-Pb isotope ratios of aerosol particles collected at the eastern hill of Omura Bay with temporal high resolution from May 2011 to June 2012. The acid-soluble component of the aerosol samples contain more than 10 times the amount of Cd and Pb than the residual dust components contain. This suggests that these elements are mainly of anthropogenic origin. The <sup>87</sup>Sr/<sup>86</sup>Sr of silicate component is high in winter and spring (0.712-0.714), and is lowest in summer (0.706). These high and low ratios are typical of Asian dust and the local sediment, respectively. The seasonal change is considered to reflect the difference of dominant wind direction between winter and summer. Although the correlation between <sup>87</sup>Sr/<sup>86</sup>Sr and soluble Cd and Pb ( $r > 0.7$ ) suggests that the anthropogenic components are transported with the Asian dust, the isotope ratios of soluble Pb (<sup>206</sup>Pb/<sup>207</sup>Pb: 1.16, <sup>208</sup>Pb/<sup>207</sup>Pb: 2.44) suggest that their origin is Japan in spring, when much amount of Asian dust arrives, while those in fall and winter (<sup>206</sup>Pb/<sup>207</sup>Pb: 1.13-1.15, <sup>208</sup>Pb/<sup>207</sup>Pb: 2.42-2.43) suggest far-east Russian and/ or Central Asian origin. Perhaps because dust particles act as adsorbent, lead concentration is highest in the season of Asian dust. Cross-border pollution is highlighted in winter when the coal combustion for heating is at the peak under the wintry atmospheric pressure pattern around East Asia.

## Melting history of the Pozanti-Karsanti ophiolite, Turkey: Implications from whole-rock and mineral compositions

SAMET SAKA<sup>1\*</sup>, IBRAHIM UYSAL<sup>1</sup>, R. MELIH AKMAZ<sup>2</sup>  
AND MELANIE KALIWODA<sup>3</sup>

<sup>1</sup>Karadeniz Technical University, Trabzon, Turkey

(\*correspondence: sakasamet61@gmail.com)

<sup>2</sup>Bülent Ecevit University, Zonguldak, Turkey

<sup>3</sup>Mineralogical State Collection Munich, Germany

Pozanti-Karsanti ophiolite, from the eastern Tauride, Turkey, is represented by mantle unit and overlying crustal sections composed of ultramafic to mafic cumulates and isotropic gabbros. Harzburgitic to dunitic mantle peridotites are characterized by low Al<sub>2</sub>O<sub>3</sub> (0.11–1.01 wt%) and CaO (0.10–1.07 wt%) contents. The low whole rock Al and Ca values are consistent with their high Cr# of spinel values, ranging between 44 and 78. These spinels are generally have low TiO<sub>2</sub> (<0.06% wt%) contents, although spinel in some samples show enrichment up to 0.25 wt%. Chondrite-normalized whole rock and clinopyroxene REE contents show depletion towards HREE to MREE. However, all peridotite samples show marked enrichment of LREE compared to MREE. Both whole rock and clinopyroxene HREE patterns of some peridotite samples follow the melting residue lines, and are modeled ~25–27 fractional melting in spinel stability field. However, depletion of MREE compared to HREE is stronger in some samples and the HREE to MREE patterns do not follow the melting lines produced by various degree of fractional melting in spinel stability field. These samples can be modeled by 5 to 10% fractional melting started at garnet stability field and followed in spinel stability field with additional 22 to 15% melting. The melting degrees obtained from whole rock and clinopyroxene REE data as well as spinel composition are consistent with each other, and confirm that the mantle unit of the Pozanti-Karsanti ophiolite is represented by up to 27% melting at different pressure conditions. The LREE enrichment observed in whole rock and clinopyroxene as well as higher TiO<sub>2</sub> contents of high-Cr# spinels in some samples do not suggest that the mantle unit of the Pozanti-Karsanti ophiolite is the simple melting residue. However, these feature of the peridotites is suggested to be due to the interaction of LREE and TiO<sub>2</sub> rich melts/fluids with formerly depleted peridotites. This interaction, taking place at suprasubduction zone environment, may increase the LREE contents of the peridotites and also cause the equilibration of Ti-depleted spinel to Ti-richer composition.

## Correction of initial-disequilibrium on U-Th-Pb system for dating of young zircons

SHUHEI SAKATA<sup>1\*</sup>, SHINSUKE HIRAKAWA<sup>1</sup>,  
HIDEKI IWANO<sup>2</sup>, TOHRU DANHARA<sup>2</sup>  
AND TAKAHUMI HIRATA<sup>1</sup>

<sup>1</sup>Laboratory for Planetary Sciences, Kyoto University, Kyoto, Japan (junchan@kueps.kyoto-u.ac.jp)

<sup>2</sup>Kyoto Fission Track Co. Ltd., Kyoto 603-8832, Japan

Major analytical problems associated with U-Pb age determination of the young zircons (e.g. < 1 Ma) is the initial-disequilibrium in the U-Th-Pb decay systems through the crystallization of zircon in source magma. To correct the effect of initial disequilibrium, the ratio of the distribution coefficient between source magma and zircon crystal (D) for Th and U ( $f_{Th/U} = D^{Th}/D^U$ ) must be defined [1]. To achieve this, we have determined both the <sup>238</sup>U-<sup>206</sup>Pb and <sup>232</sup>Th-<sup>208</sup>Pb ages obtained for three tephra zircon samples collected from Kirigamine rhyolite (Ar-Ar age is 0.945±0.005 Ma [2]), Bishop tuff (Ar-Ar age is 0.7589±0.0036 Ma [3]) and Toga pumice (Ar-Ar age is 0.42±0.01 Ma [4]) by means of laser ablation-ICPMS technique. The resulting <sup>232</sup>Th-<sup>208</sup>Pb ages were 0.940±0.010 Ma for Kirigamine, 0.759±0.016 Ma for Bishop, and 0.4296±0.0066 Ma for Toga, demonstrating that the resulting ages were consistent with the previously reported values. The  $f_{Th/U}$  values could be calculated based on the measured <sup>232</sup>Th-<sup>208</sup>Pb ages and <sup>206</sup>Pb/<sup>238</sup>U ratios, and the resulting  $f_{Th/U}$  values agreed well within the analytical uncertainties. The disequilibrium-corrected <sup>238</sup>U-<sup>206</sup>Pb age can be calculated under the assumption that the  $f_{Th/U}$  value did not vary significantly among the zircons. To evaluate this, we have measured the <sup>238</sup>U-<sup>206</sup>Pb and <sup>232</sup>Th-<sup>208</sup>Pb ages for zircons from Sanbekisuki tephra [5]. The  $f_{Th/U}$  values used for the correction was based on the average of three  $f_{Th/U}$  values obtained here ( $f_{Th/U} = 0.51 ± 0.11$ ). The corrected <sup>238</sup>U-<sup>206</sup>Pb age was 92.1 ± 8.4 ka, which agreed with the <sup>232</sup>Th-<sup>208</sup>Pb age (90.4 ± 9.5 ka) within the analytical uncertainties. The good agreement in the corrected <sup>238</sup>U-<sup>206</sup>Pb age and <sup>232</sup>Th-<sup>208</sup>Pb age demonstrates clearly that the present  $f_{Th/U}$  value for the Sanbekisuki zircon was consistent with the averaged  $f_{Th/U}$  value calculated above. In conclusion, we can construct more accurate and effective U-Th-Pb dating method based on the  $f_{Th/U}$  value defined in this study, especially for the young zircons (0.1 – 1 Ma).

[1] Schärer (1984) *EPSL*, **67**, 191-204 [2] Wadatsumi *et al.* (1994) *Fission Track News Letters*, **7**, 7-8 [3] Sarna-Wojcicki (2000) *J. Geophys. Res.*, **105** 21, 431-21, 443 [4] Uto *et al.* (2010) *Volcano*, **55**, 201-206 [5] Machida and Arai (2003) *Atlas of Tephra in and around Japan*

## Application of geochemical and statistical approach to assess metal contamination in marine sediments

FANI SAKELLARIADOU<sup>1</sup>

<sup>1</sup>University of Piraeus, Dept of Maritime Studies, fsakelar@unipi.gr

The two principal sources for heavy metals at the sea are lithogenic and anthropogenic ones. Sediments are considered as physical traps for many environmental pollutants [1]. At the present study, sediment samples from Lavrio port (located 60km SW of Athens, in Greece) were analyzed for the determination of metal content. The area is well known for the presence of mixed sulphide mineralisation (galena, sphalerite and pyrite) hosted within marbles and limestones. Samples were digested with a mixture of conc. acids at high temperature [2]. Metal contents were measured by AAS. Data set was treated with multivariate and geostatistical approach. The dendograms provided by hierarchical cluster analysis gave the (Zn, Pb, Mn) and (Cu, Cr, Ni) groups reflecting the mineralization clusters (the latter group representing also, to some extent, the ultramafic association) as well as the (Fe, Al) group standing for clays and other alluvial matter. Application of Principal Component Analysis showed that sampling sites have positive scores for Mn, Zn and Pb. Inter-element correlation coefficients corresponded to values greater than 0,92 for the pair (Zn, Fe), greater than 0,84 for the pairs (Mn, Zn), (Zn, Pb), (Mn, Fe), (Pb, Fe) and (Cr, Al), and greater than 0,68 for the pairs (Al, Fe), (Fe, Cu) and (Cu, Zn). The Simple Kriging geostatistical approach was applied allowing data interpolation [3]. Spatial patterns of Pb, Zn and Cu showed the highest enrichment around the new berth (cited at the eastern part of the harbour), with elevated content around the main harbour area.

[1] Burton (2002) *Limnology*, **3**, 65–75. [2] UNEP (1985) *Reference Methods for Marine Pollution Studies*, No 31-39. [3] Cressie (1990) *Mathematical Geology*, **22**, 239-252.

## Wettability alteration of calcite surface induced by ion exchange

H. SAKUMA<sup>1,2</sup>, M.P. ANDERSSON<sup>1</sup> AND S.L.S. STIPP<sup>1</sup>

<sup>1</sup>Nano-Science Center, Department of Chemistry, University of Copenhagen, Copenhagen, Denmark (\*correspondence: sakuma.h.aa@m.titech.ac.jp, ma@nano.ku.dk, stipp@nano.ku.dk)

<sup>2</sup>Tokyo Institute of Technology, Tokyo 152-8551, Japan

The interaction of water and organic molecules with mineral surfaces controls a range of processes in nature and industry. The thermodynamic property, surface tension, helps describe these interactions. We investigated the change in water affinity for a calcite ( $\text{CaCO}_3$ ) {10.4} surface where  $\text{Ca}^{2+}$  and  $\text{CO}_3^{2-}$  ions were sequentially replaced with  $\text{Mg}^{2+}$  and  $\text{SO}_4^{2-}$ , in the bulk solid and at the surface, which is a system of broad interest, for biomineralisation, oil production, and many others. We used electronic structure calculations based on density functional theory (DFT).

$\text{Mg}^{2+}$  substitution for  $\text{Ca}^{2+}$  is favored but only when  $\text{SO}_4^{2-}$  ions are present and  $\text{MgSO}_4$  incorporates preferentially as ion pairs at the fluid-calcite interface. Mg incorporation weakens organic molecule adhesion, while strengthening water adsorption (Fig. 1). Thus,  $\text{Mg}^{2+}$  substitution renders the calcite surface more water wet, or hydrophilic, making it less favourable for organic compound attachment. We estimated the change in calcite surface tension after ion exchange and determined the resulting change in macroscopic wettability. When only 10% of surface Ca is replaced by Mg, contact angle changes dramatically, i.e. 40 - 70°, converting a hydrophobic surface to a mixed wet surface. Producing magnesium calcite is a simple trick organisms can use for controlling calcite growth and the process helps explain why oil recovery from carbonate reservoirs is enhanced when both  $\text{Mg}^{2+}$  and  $\text{SO}_4^{2-}$  are present in the pore water.

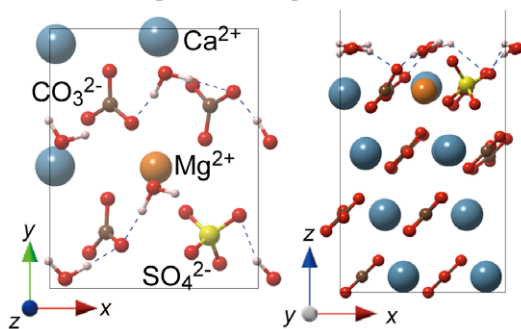


**Figure 1:** The lowest energy configuration for four water molecules on a calcite {10.4} surface with substitution by a Mg  $\text{SO}_4$  ion pair. (Left) Top view. (Right) Side view.

## Characterization and Surface Reactivity of Natural and Synthetic Magnetites

C. SALAZAR-CAMACHO<sup>1</sup>, M. VILLALOBOS<sup>1,\*</sup>  
AND M.D.L.L. RIVAS-SÁNCHEZ

<sup>1</sup>Environmental Bio-Geochemistry Group, Geochemistry Department, Geology Institute (\*correspondence: mariov@geologia.unam.mx)

<sup>2</sup>Laboratorio de Paleomagnetismo, Geophysics Institute UNAM, Coyoacan, CU, Mexico 04510, D.F.

Magnetite is an Fe(II/III) oxide mineral that occurs naturally and potentially as small particles with significant surface reactivity, and although much work is reported on synthetic material [1,2], little work exists for natural samples. The goal of the present work was to carefully characterize four natural magnetite samples from an iron ore deposit [3] and two synthetic commercial reference samples, and to compare their surface characteristics and reactivity with the aim of evaluating their geochemical behavior towards adsorption of environmentally relevant ions, as well as their potential for use as environmental remediation sorbents. In addition, their As(V) adsorption behavior was determined at pH 6, and was analyzed as related to the surface characteristics and particle aggregation behavior determined.

The analyses revealed high magnetite purity in the natural samples, and specific surface areas (SSA) ranging from 1 to 8  $\text{m}^2/\text{g}$ . Small alumino-silicate impurities were found in natural magnetites, apparently occurring at the particle surfaces and significantly lowering the magnetite isoelectric point. All samples are composed of aggregates of 39-52 nm magnetite particle units, but highly aggregated with very large size dispersions. The synthetic sample with the smallest particle size (30 nm in average - 39  $\text{m}^2/\text{g}$ ) showed its entire surface area available for adsorption, despite its highly aggregated state observed, suggesting an open and highly dynamic aggregate framework. The other larger samples showed more complex aggregation behavior, which produced: (1) a widely variable As(V) adsorption behavior with no clear predictable pattern among samples; and (2) a large decrease of the As(V) adsorption maxima with increasing solids concentration (Cs) imposed in the experimental set-up for any one particular sample. Therefore, we recommend high caution in using the BET-SSA and Cs parameters when performing experimental adsorption work with micro-sized magnetite.

[1] Das *et al.* (2010) *J. Radioanal. Nucl. Chem* **285**, 447-454.

[2] Iltou *et al.* (2010) *Environ. Sci. Technol.* **44**, 170-176.

[3] Rivas *et al.* (2009) *Earth Planets Space* **61**, 151-160.

## U-Pb age of a syn-collisional lower continental crust anatetic event, Socorro-Guaxupé Nappe, SE Brazil

C.A. SALAZAR-MORA<sup>1\*</sup> AND M.C. CAMPOS NETO<sup>1</sup>

<sup>1</sup>Geosciences Inst., São Paulo Univ., 05508-080, Brazil.

(\*correspondance: claudio.mora@usp.br; camposnt@usp.br)

The Southern Brasília Orogen, SE Brazil, occurs along the southern border of the São Francisco Craton and is structured as a pile of Ediacaran syn-metamorphic thickened-skinned nappes that diachronically migrate towards the cratonic margin. The Socorro-Guaxupé Nappe (SGN) is the older and upper allochthon that represents an Andean-type magmatic arc [1]. U-Pb ages in zircon from charnockites, mangerites and Grt-granulites [1] indicate an arc activity around 670 Ma in a subduction-related orogenesis followed by ultra-high-T metamorphism and plutonism lasting until 625 Ma. This age is thought [2] to represent the metamorphic peak of the SGN. In the present study we report on new *in situ* U-Pb and Lu-Hf analysis (both LA-ICP-MS) in zircons from syn-tectonic charnockitic leucosomes that comprise the metatextitic unit of the SGN.

Charnockitic leucosomes were generated under Hbl dehydration melting conditions following the reaction  $Hbl + Qtz \rightleftharpoons Opx + Cpx + Pl \pm Melt$ , which implies minimum temperatures of 850°C. The leucosomes presented two zircon tipologies. The first comprises bipyramidal-prismatic grains with oscillatory zoning and high luminescence, sometimes preserving low-luminescence cores with 670 Ma. These high luminescence and oscillatory zoning grains show 19 concordant ages at  $621 \pm 16$  Ma. The second tipology of zircons are isometric and *soccer-ball*-type. These grains show sector zoning and a concordia age of  $608 \pm 4$  Ma. Th/U ratios from the *soccer-ball* grains vary from 1.378 to 2.107, whereas prismatic grains vary from 0.118 to 1.774. Some authors also reported high Th/U values from demonstrably syn-metamorphic, high-T melts [3].  $\varepsilon_{Hf}$  signatures between -13 and -21 in both tipologies of zircon grains provide evidence of crustal reworking. Despite the 16 Ma error in the age of the prismatic grains, Th/U values clearly separate the two tipologies of zircon. The older prismatic grains may be related to the onset of the metamorphic peak (~625 Ma), whereas the isometric ones provide evidence of long-lived high-T conditions until ~608 Ma.

[1] Campos Neto *et al.*, (2011) *JSAES* **32**, 393-406. [2] Janasi (2002) *Prec. Res.* **119**, 301-327. [3] Hakoda & Harley (2004) *JMPS* **33**, 180-190.

## Physico-chemical evolution of Fe-Si-rich interfacial layers during olivine carbonation reactions

G. D. SALDI<sup>1\*</sup>, H. GUO<sup>1</sup>, D. DAVAL<sup>2</sup>, J. DAVIS<sup>1</sup>  
AND K. G. KNAUSS<sup>1</sup>

<sup>1</sup>Earth Sciences Division, Lawrence Berkeley National Laboratory, 1 Cyclotron Road, Berkeley, CA 94720, USA  
gdsaldi@lbl.gov (\*presenting author); hguo@lbl.gov;  
jadavis@lbl.gov; kgknauss@lbl.gov.

<sup>2</sup>LHyGeS, Université de Strasbourg/EOST-CNRS UMR 7517,  
1 rue Blessig, 67084 Strasbourg, France  
ddaval@unistra.fr.

Several recent investigations of mineral carbonation reactions have shown that the formation of Si-rich protective layers at the interface between olivine and aqueous solution can significantly slow down olivine dissolution, thus limiting the rate of conversion to Mg-carbonates.

The experiments conducted on natural Fe-bearing olivine in flexible Au-bags at 90 and 150 °C and with CO<sub>2</sub>-saturated fluids show that the presence of Fe in the mineral+fluid system favors the formation of Fe-Si-rich protective layers. The passivating properties of these coatings originate from the strong interaction between Fe(III) and silica and their action is linked to the permanence of oxidizing conditions in the aqueous fluid.

Transmission electron microscope (TEM) analysis of FIB thin sections of the mineral interfacial region allowed us to study the chemical composition and the physical properties of Fe-Si-rich layers as a function of the progress of the carbonation reaction. In particular, a series of batch experiments of different duration was performed on a natural olivine powder (150-300 μm) at 150 °C and  $pCO_2=100$  bar to describe the evolution of the olivine/water interface over an overall period of one month. During the initial stage of the reaction, the olivine surface is affected by the incipient precipitation of Fe oxide particles, in association with small amounts of amorphous silica, which cover in a non-uniform fashion the mineral surface and prompts the formation of a Fe<sup>3+</sup>-Si layer. The oxidation of the Fe(II) released by dissolution gradually consumes the oxygen initially dissolved in the aqueous volume, leading to reducing conditions. The change of redox conditions brings about the breakdown of the Fe-Si-rich layer and re-activates the dissolution of the coated olivine surface. Increased concentrations of Fe<sup>2+</sup> and Mg<sup>2+</sup> and SiO<sub>(aq)</sub> accelerate the rates of the carbonation process by the formation of Mg-Fe carbonate solid solutions which cover the olivine grains on top of a relatively porous (~2 μm thick) residual coating, composed of abundant amorphous silica.

## SO<sub>2</sub> camera measurements on Stromboli

GIUSEPPE SALERNO<sup>1</sup>, GEORGINA SAWYER<sup>2</sup> AND MICHAEL BURTON<sup>3</sup>

<sup>1</sup>INGV Osservatorio Etneo, Italy, salerno@ct.ingv.it

<sup>2</sup>MetOffice, UK, georgina.sawyer@metoffice.gov.uk

<sup>3</sup>INGV Pisa, Italy, burton@pi.ingv.it

The development of the SO<sub>2</sub> camera, an instrument that allows images of SO<sub>2</sub> amounts to be collected, has opened up new possibilities and insights into degassing behaviour at volcanoes. Here we present recent measurements collected on Stromboli volcano, which reveal patterns in the SO<sub>2</sub> flux emitted from the volcano. Our measurements are compared with the automatic network of scanning spectrometers on the Island which monitor SO<sub>2</sub> emissions. Furthermore we demonstrate a fully integrated retrieval system which takes full account of the light dilution effect, allowing much improved quantification of the measured fluxes.

## Quantitative analysis with the Cameca SXFIVE FE at high lateral resolution: Applications to geochronology and mineralogy

P. SALIOT<sup>1</sup> C. HOMBOURGER<sup>2</sup> AND M. OUTREQUIN<sup>3</sup>

<sup>1</sup>philippe.saliot@ametek.com

<sup>2</sup>chrystel.hombourger@ametek.com

<sup>3</sup>michel.outrequin@ametek.com

The development of the Schottky emitter and its implementation as electron source in Electron Microprobe has significantly improved the characterization of materials in earth sciences and in metallurgy.

The strength of an Electron Probe Microanalysis (EPMA) is the ability to accurately measure and quantify element in traces at few 10's ppm level. The Field Emission (FE) Source allows trace element analysis with high beam currents thanks to the high brightness of the source

Analysis at low beam voltage is used in order to take full advantage of the small spot sizes achievable with a Field Emission Source. Thus, the analytical resolution is not limited anymore by the beam diameter but only by the diameter of the X-ray emission volume.

This will be illustrated, in a first example, by measuring different areas in a Monazite grain. U, Pb and Th are quantitatively analyzed with high precision in order to characterize age domains.

In a second example, quantification of small refractory phases (hibonite, grossite, perovskite, ...) formed by gas condensation in the solar nebula will be presented.



## Magmatic Epidote in Calcaline tonalite, Dehnow (NW Mashhad, NE Iran)

R. SAMADI<sup>1</sup>, S. J. SHEIKH ZAKARIAEE<sup>1</sup>  
AND N. SHIRDASHTZADEH<sup>3</sup>

<sup>1</sup>Department of Geology, Science and Research Branch,  
Islamic Azad University, Tehran, Iran

<sup>3</sup>Department of Geology, Faculty of Science, University of  
Isfahan, Isfahan, Iran

### Introduction

The granitoids of Dehnow in NE Iran are part of a calc-alkaline stock (tonalite to granodiorite and diorite) that intruded the remnants of the Paleo-Tethys Ocean in the Triassic [1]. Epidote is commonly known as primary igneous mineral in intermediate plutonic rock [2]. In Dehnow granitoid it occurred as inclusions in the phenocrystic garnet grains or as subhedral grains associated with biotite.

### Mineral Chemistry

The major element composition of epidote indicates a Xep (Fe/(Fe+Cr+Al-2)) between 0.43 to 0.65. The average pistacite (Ps) component of the epidote is 0.15 and 0.18 for the inclusions in the garnets and Dehnow granitoid, respectively.

### Discussion and Conclusion

Textural criteria may be used to distinguish magmatic and subsolidus (deuteric) epidotes. [3] and [4] argued that euhedral, weakly pleochroic epidote enclosed within biotite is magmatic. The low TiO<sub>2</sub> contents (<0.17%) of most epidote inclusions and epidote in the groundmass suggest that they are primary according to [5], who ascribe TiO<sub>2</sub><0.2% to primary epidote. Based on [6], the Ps values indicate a low *f*O<sub>2</sub> condition but suggesting that the epidote inclusions crystallized under relatively lower *f*O<sub>2</sub> conditions.

[1] Samadi *et al.* (2013) Island Arc (Submitted). [2] Dessimoz & Müntener (2009) Goldschmidt A286. [3] Tulloch (1979) *Con Min Pet* **69**, 105-117. [4] Zen & Hammarstrom (1984) *Geol* **12**, 515-518. [5] Evans and Vance (1987) *Con Min Pet* **96**, 178-185. [6] Sial *et al.* (1999) *Pak J Sci Ind Res* **42**, 342-244.

## Geochemical and isotopic studies of the Hooghly River Estuary, India: Natural vs. anthropogenic sources of organic carbon

SAUMIK SAMANTA<sup>1</sup>, TARUN K. DALAI<sup>1\*</sup>  
AND JITEDNRA K. PATTANAIK<sup>1</sup>

<sup>1</sup>Department of Earth Sciences, Indian Institute of Science  
Education and Research-Kolkata, Mohanpur 741252,  
INDIA (\*correspondence: dalai@iiserkol.ac.in)

Dissolved, suspended and bed loads have been sampled seasonally from the Hooghly River Estuary, the major distributary of the river Ganga. The samples have been analyzed for pH, temperature, TDS, salinity, major ions, δ<sup>18</sup>O of water and δ<sup>13</sup>C of dissolved inorganic carbon (DIC). The results show clear seasonal variations, with lower concentrations of major ions during the monsoon period when the water discharge is the highest. Based on salinity-δ<sup>18</sup>O variation trends, which are similar to those observed earlier [1], freshwater can be characterized by δ<sup>18</sup>O values of ca. -6‰ and ca. -7‰ during the summer and monsoon periods, respectively. This suggests that overall contributions of rainwater to the Hooghly River dominates over those from snow melt in the upper reaches. Calculations made for mixing of seawater and river water suggest that at Gangasagar where the the river drains into the Bay of Bengal, freshwater constitutes ca. 15% and 30% of the water budget during summer and monsoon periods, respectively.

Salinity shows well correlated linear variations with DIC and δ<sup>13</sup>C<sub>DIC</sub> which indicate that mixing exerts the major control on DIC abundances. Based on these trends, it is inferred that δ<sup>13</sup>C<sub>DIC</sub> of freshwater is ca. 1.5‰ lower during monsoon period than in summer. However, δ<sup>13</sup>C<sub>DIC</sub> values are in general lower than those expected due to conservative mixing. Although calcite precipitation may be one of the underlying causes, this seems unlikely in the Hooghly estuary. A more likely explanation is supply of additional organic carbon to the estuary, oxidation of which could add to DIC pool. The source of such organic carbon is most likely pollution and needs to be assessed. δ<sup>13</sup>C<sub>DIC</sub> data of this study suggest that processes such as outgassing of CO<sub>2</sub> from the waters and biological productivity are insignificant in regulating the DIC variation in the estuary.

[1] Somayajulu *et al.* (2002) *Mar. Chem.* **79**, 171-183.

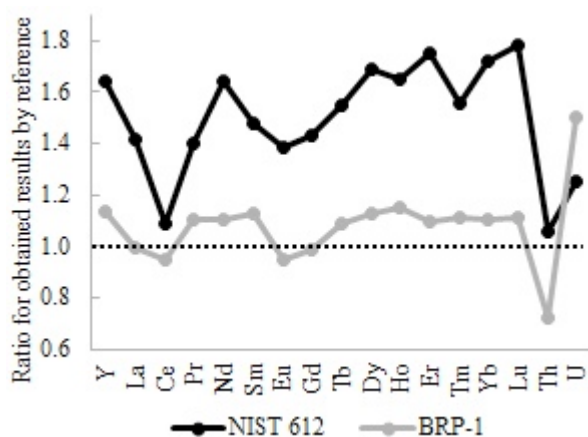
## Determination of trace elements in iron formations by LA-ICP-MS

G.M.S. SAMPAIO<sup>1</sup>, A.T. DE ABREU<sup>1</sup>, H.A. NALINI JR<sup>1\*</sup>  
AND C.C. LANA<sup>1</sup>

<sup>1</sup>Federal University of Ouro Preto, Ouro Preto, MG 35400-000, Brazil (\*correspondence: nalini@degeo.ufop.br)

### Introduction

Here we present a method to measure trace elements (Y, La, Ce, Pr, Nd, Sm, Eu, Gd, Tb, Dy, Ho, Er, Tm, Yb, Lu, Th and U) in banded iron formation. The samples (XRF fused beads) were ablated (spot and raster) in a Nd:YAG 213 nm New Wave Laser coupled to an Agilent 7700x ICP-MS. Internal standards <sup>29</sup>Si and <sup>57</sup>Fe from the certified reference BRP-1 (in fusion beads) and the glass NIST SRM 612 were used to calibrate the unknowns. We discuss our results based on repeated analyses of the reference material IF-G (GIT-IWG, France).



### Results and discussion

The internal standards <sup>29</sup>Si and <sup>57</sup>Fe showed no statistical difference and proved to be suitable for the intended use. Although the slight increase in the instrumental error, the raster pattern showed better mean results than the spot. The calibration with the glass SRM 612 showed a significant bias, as demonstrated in the Figure 1. The best results were obtained by calibration with BRP-1 reducing the matrix effect. Figure 1: Ratio between obtained results using NIST 612 and BRP-1 and values from IF-G certificate.

### Acknowledgments

The authors thank the FAPEMIG and VALE that support this study through the project RDP-00063-10.

## Microflora of native biofilm on activated carbon under filtration of fulvic acids

O. SAMSONI-TODOROVA\*, N. KLYMENKO  
AND T. CHEKHOVSKAIA

Institute of Colloid Chemistry and Chemistry of Water, 42 Vernadsky Avenue, Kyiv, 03680, Ukraine  
(\*correspondence: samsoni@online.ua)

Carbon filters long-term exploitation for drinking water treatment causes the inevitable formation of native biofilms on the surface of porous activated carbon (AC). The aim of this paper was to assess the quantitative and qualitative composition of biofilms microflora that formed spontaneously on AC KAU by filtering of fulvic acids (FC) model solutions in the different conditions. Initial composition of these solutions met Dnieper river water. Filtering time was more than 6 months.

Obtained results are shown in the table 1.

| Samples  | Microorganisms types and quantity, cells/gAC |
|--|--|
| AC with native biofilm that was formed by passing of FA solutions (pH 2) and hydrogen peroxide | Yeast; 2.0·10 <sup>2</sup>                   |
| AC with native biofilm that was formed by passing of FA solutions (pH 2)                       | Fungi, yeast; 6.0·10 <sup>2</sup>            |
| AC with native biofilm that was formed by passing of FA solutions (pH 6) and hydrogen peroxide | Fungi, yeast; 3.5·10 <sup>4</sup>            |
| AC with native biofilm that was formed by passing of ozonated FA solutions (pH 6)              | Fungi, bacteria; 12.1·10 <sup>4</sup>        |

**Table 1:** The qualitative and quantitative composition of native biofilm microorganisms on AC after long-term filtering of FA solutions

Native biofilms were composed from yeast and fungi in the first two cases. This is due to the fact that filtered through charcoal FA solution had low pH, which is more acceptable for the activity of these microorganisms groups. In this case the quantity of microorganisms is lower than by neutral solutions filtering in two orders.

Quantity of live biofilm biomass was about 30% of the total biomass in the biofilm layers near the media and in the outer layers it was about 100%.

## Evolution of deep crustal roots of the Arkhangelsk Diamondiferous Province: Evidences from crustal xenoliths and xenocrysts from Devonian kimberlite pipes

A.V. SAMSONOV<sup>1\*</sup>, J.G. GRIBAN<sup>1</sup>, YU.O. LARIONOVA<sup>1</sup>,  
A.A. NOSOVA<sup>1</sup>, V.V. TRETYACHENKO<sup>2</sup>,  
E.N. LEPEKHINA<sup>3</sup> AND A.N. LARIONOV<sup>3</sup>

<sup>1</sup> IGEM RAS, Moscow, Russia (\*correspondence: samsonovigem@mail.ru);

<sup>2</sup> NIGP AC "ALROSA", Arkhangelsk, Russia;

<sup>3</sup> VSEGEI, St.-Petersburg, Russia

Juvenile continental crust of the Arkhangelsk diamondiferous province (ADP) crystalline basement consists of ca 2.0 Ga calc-alkaline granodiorites, gabbros, metasediments with minor 1.9-1.7 Ga granites. This crust was formed during evolution of the large Lapland-Kola-Dvina orogenic belt [1]. Investigations of crustal xenoliths and zircon xenocrysts from the Devonian kimberlites allow us to recognize several stages in evolution of deep crustal roots of the ADP.

The 2.0 Ga lower-crustal (8-16 kbar) xenoliths of calc-alkaline mafic and intermediate rocks with  $T_{DM}(Nd)$  model ages of 2.0-2.2 Ga possibly represent underplated melts of the subduction stage.

The 1.9-1.7 Ga zircon xenocrysts prevail in a whole zircon population of all kimberlite pipes. The zircons probably grew at collisional and post-collisional stages, because of wide range of geochemical features with distinct high-P garnet-equilibrium population.

The 1.5 Ga zircon xenocrysts occur in all kimberlite pipes and might be captured from deep rapakivi granite plutons that are not recognized on the ADP surface.

The 1.2-1.0 Ga zircon xenocrysts were found in all kimberlite pipes and these zircons might be captured from a lower crust reworked during the Grenville Orogeny event which is not revealed on the ADP surface.

The 0.38 Ga Gar-pyroxenite xenoliths ( $T_{DM}(Nd)$  model ages of 0.7-0.8 Ga) are common for the V.Griba pipe and might be regarded as a cumulus of Devonian mantle magmas buried (?) beneath the crust.

[1] Samsonov *et al.* (2009) Doklady Earth Sciences, 226–230.

## The influence of fault-fracture network activity on fluid geochemistry and mineral precipitation at the Tolhuaca geothermal system, southern Chile

P. SÁNCHEZ<sup>1,2\*</sup>, P. PÉREZ<sup>2,3</sup>, M. REICH<sup>1,2</sup>,  
G. ARANCIBIA<sup>2,3</sup>, J. CEMBRANO<sup>2,3</sup>, E. CAMPOS<sup>2,4</sup>  
AND S. LOHMAR<sup>5</sup>

<sup>1</sup> Universidad de Chile, Santiago, Chile (\*correspondence: vsanchez@ing.uchile.cl; mreich@ing.uchile.cl)

<sup>2</sup> Centro de Excelencia en Geotermia de los Andes

<sup>3</sup> Pontificia Universidad Católica de Chile, Santiago, Chile (pvperez1@uc.cl; garancibia@ing.puc.cl; jcembrano@ing.puc.cl)

<sup>4</sup> Universidad Católica de Antofagasta, Chile (edcampos@ucn.cl)

<sup>5</sup> Mighty River Power Chile (silke.lohmar@geotermia.cl)

The nature of the interplay between active tectonics and fluid flow is a key feature to better understand the chemical evolution of fluids in geothermal and hydrothermal systems.

The objective of our current research is to assess the nature of the interplay between brittle deformation and chemical evolution of fluids and mineral paragenesis in the geothermal field of Tolhuaca in the Southern Andes volcanic zone. Tol-1 is a vertical 1.080 m deep borehole which could yield relevant information regarding the evolution of the Tolhuaca geothermal system. The methodology includes the structural and geochemical analysis of oriented faults, fault-veins and veins in the core. Fluid inclusions analysis by microthermometry, LA-ICP-MS and Raman spectroscopy will allow a better understanding of the feedback between the fluid flow episodes and the mineralization. More than 120 structural measurements were performed and 47 samples were taken for thin & fluid inclusions sections.

Our preliminary results show that there is a strong correlation between abundance of structures and rock type. Lava intervals exhibit more intense fracturing and veining than tuff and volcanoclastic intervals. In the upper 300 m of the core, structures are primarily steeply dipping with a dominant normal sense of displacement (some dextral component). Below a cataclastic zone at 300 m, structures are more variable in dip and sense of motion, with some reverse faults. Fluid inclusions petrography reveals the periodically feedback between fault-fractures networks activation and mineral mineralization sealing the conduits for fluid flow.

## Changes in bacterial diversity and community structure within a geochemically variable uranium-mine water treatment plant

I. SÁNCHEZ-CASTRO<sup>1\*</sup>, M. LÓPEZ-FERNÁNDEZ<sup>1</sup>,  
A. AMADOR-GARCÍA<sup>1</sup>, V. PHROMMAVANH<sup>2</sup>, J. NOS<sup>2</sup>,  
M. DESCOSTES<sup>2</sup> AND M.L. MERROUN<sup>1</sup>

<sup>1</sup>Department of Microbiology, University of Granada, Spain

(\*correspondence: sanchezcastro@ugr.es)

<sup>2</sup>R&D Department, AREVA Mines, France

Monitoring and treatment of mining waters, containing heavy metals and radionuclides, are essential throughout the uranium mining. In order to meet the increasingly demanding regulatory requirements, optimized treatment and remediation strategies must be developed through the use of comprehensive biogeochemical models. Since biotic factors have been described to play a key role in these processes, an exhaustive analysis of the microbial diversity emerges as an important prerequisite.

Therefore, this work aims to assess the bacterial diversity occurring along the drainage treatment settling ponds of a former uranium mine and to link it to the associated geochemical features. A set of four sediment samples were taken along the treatment facility (before treatment, in the two treatment ponds and after treatment).

Highly diverse bacterial communities were observed in all samples by analyzing a total of 400 clones through a PCR-RFLP approach targeting the 16S rRNA gene. The clone libraries were dominated mainly by sequences closely related to the phyla *Acidobacteria*, *Actinobacteria*, *Bacteroidetes*, *Firmicutes*, *Planctomycetes* and specially *Proteobacteria*. Within this predominant phylum, relative abundance of *Alpha*-, *Beta*-, *Delta*- and *Gammaproteobacteria* varied among the different samples indicating specific distribution of the different bacterial populations according to geochemical variations. Links between the bacterial diversity and the geochemistry of the sediments will be discussed. Moreover, detection of sequences affiliated with metal-reducing bacteria (e.g., *Rhodoferrax*, *Ferribacterium*, *Geobacter*, *Geothrix*, *Anaeromyxobacter*) in all four samples, suggests that there is an evident potential for the bioremediation of the studied site.

## Raman spectroscopy evidence for the ikaite-calcite/Vaterite transformation

N. SÁNCHEZ-PASTOR<sup>1\*</sup>, M. OEHLERICH<sup>2</sup>,  
J.M. ASTILLEROS<sup>13</sup>, M. KALIWODA<sup>4</sup>, C.C. MAYR<sup>256</sup>,  
W. W. SCHMAHL<sup>245</sup> AND L. FERNÁNDEZ-DÍAZ<sup>13</sup>

<sup>1</sup>Dpto. Cristalografía y Mineralogía. Universidad Complutense de Madrid, Spain. (\*correspondence: nsanchez@ucm.es)

<sup>2</sup>Dept. Geo und Umweltwissenschaften. Ludwig-Maximilians-Universität, Germany

<sup>3</sup>Institute of Geosciences. CSIC - UCM, Spain

<sup>4</sup>Mineralogische Staatssammlung München, Germany

<sup>5</sup>Geo-Bio-Center. Ludwig-Maximilians-Universität, Germany

<sup>6</sup>Institut für Geography. Friedrich-Alexander-Universität, Germany

Ikaite ( $\text{CaCO}_3 \cdot 6\text{H}_2\text{O}$ ) is a metastable phase that crystallizes from alkaline waters with high phosphate concentrations at temperatures close to 0°C. Above 4°C ikaite crystals transform rapidly to produce calcite pseudomorphs which are considered a valuable paleoclimatic indicator. In this work synthetic ikaite crystals were grown at near-freezing temperatures using an experimental setup that involved the diffusion of  $\text{CaCl}_2$  through a silica gel prepared using natural water from the Argentinian lake "Laguna Potrok Aike". After recovering the crystals from the gel, their transformation was monitored by in situ collecting Raman spectra. The spectra taken in the first stages of the transformation showed the characteristic carbonate vibration modes of ikaite at 1067  $\text{cm}^{-1}$  (symmetric CO stretch) and 700  $\text{cm}^{-1}$  (in plane band). The second most intense band is due to lattice vibrations and found at 200  $\text{cm}^{-1}$ , with secondary peaks at 136, 216 and 265  $\text{cm}^{-1}$ . Moreover, the ikaite spectra show good resolved OH modes at 3180, 3240 and 3424  $\text{cm}^{-1}$  whose intensity changes could be followed. During the transformation new bands at 1081 and 1085  $\text{cm}^{-1}$ , characteristic for vaterite and calcite, appeared in the spectra. After a few hours, the Raman spectrum obtained was identical to that of calcite. However, the external shape of ikaite crystals remained unchanged during the replacement. A mechanism involving the coupling of ikaite dissolution and calcite/vaterite crystallization and the generation of a large amount of porosity is proposed for this transformation.

Acknowledgements: This research was partially funded by DFG-grants in the framework of the ICDP drilling project PASADO and project CGL2010-20134-C02-01 (DGCYT).

## Clay-rich sediments injected into clastic dykes during earthquakes in the Galera fault zone (Guadix-Baza basin, Central Betic Cordillera)

CATALINA SANCHEZ-ROA<sup>1</sup>, JUAN JIMENEZ-MILLAN<sup>1\*</sup>, FERNANDO NIETO<sup>2</sup>, FRANCISCO J. GARCIA-TORTOSA<sup>1</sup>, ISABEL ABAD<sup>1</sup> AND ROSARIO JIMENEZ-ESPINOSA<sup>1</sup>

<sup>1</sup>Department of Geology and CEACTierra, Associated Unit IACT (CSIC-UGR), Faculty of Experimental Science, University of Jaén, Campus Las Lagunillas s/n, 23071 Jaén, Spain (catasroa@ujaen.es; \*correspondence: jmillan@ujaen.es; gtortosa@ujaen.es; miabad@ujaen.es, respino@ujaen.es)

<sup>2</sup>Department of Mineralogy and Petrology and IACT (CSIC-UGR), Faculty of Science, University of Granada, Avda. Fuentenueva s/n 18002, Granada, Spain (nieto@ugr.es)

The Galera Fault zone is a sinistral fault, which is 23 km long and strikes N48°E [1, 2]. The fault zone is 1.5 km wide with several parallel splays dipping NW between 40° and 60°, although vertical dips have also been noted locally.

During field observations within the area, clastic dikes were identified crosscutting the stratification of the sequence as well as filling spaces in between stratification planes. The clastic dikes are composed of medium sand size grains in a matrix of clay minerals. The mineral species identified through x-ray diffraction include quartz, albite, mica, chlorite and smectite. The SEM study reveals prismatic oriented fragments of diatoms. The muscovite and clinocllore crystals show a larger grain size than smectite which exhibits a flaky morphology and its presence is associated with the diatom fragments.

Injection clastic dikes have been previously described as a form of seismites, and their emplacement corresponds to episodic pulses of increasing hydraulic pressure generated by seismic loading [3]. Given that other co-seismic structures such as globular seismites have been identified in the area [4] and considering the clastic origin of the material we could infer that the sediments were saturated with water as a result of fluid circulation associated with the fault zone and later injected into fractures during seismic events.

[1] García Tortosa *et al.* (2011) *Geomorphology* **125**, 517-529. [2] Sanz de Galdeano *et al.* (2012) *Journal of Iberian Geology* **38**, 209-223. [3] Levi *et al.* (2006) *Geochem. Geophys. Geosyst.* **7**, Q12009. [4] Alfaro *et al.* (2010) *Terra Nova* **22**, 172-179.

## Geochemical and microbial signals related to carbonate formation in the subsurface of Rio Tinto

<sup>1</sup>SÁNCHEZ-ROMÁN, <sup>1</sup>FERNÁNDEZ-REMOLAR D, <sup>1</sup>PUENTE-SÁNCHEZ F, <sup>1</sup>RODRIGUEZ N, <sup>1</sup>PARRO V AND <sup>12</sup>AMILS R,

<sup>1</sup>Centro de Astrobiología (INTA-CSIC), 28850 Madrid, Spain. E-mail: msanzroman@cab.inta-csic.es

<sup>2</sup>Centro de Biología Molecular Severo Ochoa (CSIC-UAM), 28049 Madrid, Spain

Rio Tinto is considered a good geochemical terrestrial analogue of Mars due to its high content of iron and extreme acidic pH [1]. The occurrence of carbonates in this extreme environment is very local and they are found to occur under certain conditions of pH and iron concentration [2]. To understand its formation we have recovered and generated samples from cores, taken from wells BH10 and BH11 of depths of 340 and 620 meters, respectively, under anaerobic and sterile conditions. These wells were drilled during the field campaign of the Iberian Pyrite Belt Subsurface Life (IPBSL) project. IPBSL is a drilling project, currently under development, specifically designed to characterize the subsurface ecosystems operating in the Iberian Pyrite Belt (IPB), in the area of Peña de Hierro, and responsible of the extreme acidic conditions existing in the Rio Tinto basin [3]. The present study emphasizes the mineralogical, geological-biochemical and microbial implication for carbonate formation in Rio Tinto. Herein, we show that the formation of carbonate minerals in Rio Tinto is closely related to microbial activity and that can occur under both oxic and anoxic conditions. The formation of carbonates in such extreme environment could explain the occurrence of carbonates on Mars. Finally, this environmental and experimental study provides potential mineralogical biosignatures that may be useful to test life on Mars and other extraterrestrial habitats.

[1] *Planet Space Sci* **55**, 370-381,2007; [2] *Earth Planet Sci Lett* **351**, 13-26, 2012; [3] *Appl Environ Microbiol* **69**, 4853-4865, 2003.

## Thermodynamics of carbon-bearing fluids and oxidized carbon speciation equilibria in subduction zone fluids

CARMEN SANCHEZ-VALLE<sup>1</sup>, DAVIDE MANTEGAZZI<sup>1</sup> AND THOMAS DRIESNER<sup>1</sup>

<sup>1</sup>IGP, ETH Zürich, Switzerland

(correspondence: carmen.sanchez@erdw.ethz.ch)

Subduction zones play an important role in the deep carbon cycle as allow the reintroduction of C into the mantle and the recycling through arc magmatism. The occurrence of diamond-bearing fluid inclusions in HP rocks of oceanic origin suggests that C can be efficiently transferred from the slab to the mantle wedge through dissolution reactions driven by slab-derived aqueous fluids (Frezzotti *et al.*, 2011). A better understanding of the role of aqueous fluids on C recycling thus relies on the development of robust thermodynamic models of the properties of C-bearing aqueous species at relevant conditions.

In this contribution, we present first experimental data on the thermodynamic properties of oxidized carbon species at high P-T that have been used to constrain a model of the speciation of oxidized carbon in aqueous fluids at subduction zone conditions. The thermodynamic properties of oxidized C-bearing aqueous fluids were determined up to 650 °C and 4 GPa from acoustic velocity measurements performed on Na<sub>2</sub>CO<sub>3</sub> and NaHCO<sub>3</sub> aqueous solutions with various concentrations (0.1 to 1 m). Experiments were conducted on externally heated diamond anvil cells by Brillouin scattering spectroscopy. Densities of the fluids directly obtained from the measured acoustic velocities were used to calibrate an equation of state (EoS) able to predict the thermodynamic properties of carbonated fluids at high P-T conditions. Further, the derived partial molar volume and compressibility of aqueous CO<sub>3</sub><sup>2-</sup> and HCO<sub>3</sub><sup>-</sup> ions were used to constrain the effect of P on the equilibrium constant controlling the speciation of oxidized carbon in high temperature fluids:  $\text{HCO}_3^- = \text{H}^+ + \text{CO}_3^{2-}$  (Eq.1). The calculated volume of reaction  $\Delta\bar{V}_r$  for Eq.1 is negative at the investigated P conditions, indicating that aqueous carbonate ions CO<sub>3</sub><sup>2-</sup> are the dominant C-species in high P oxidized fluid. This observation is consistent with direct investigations of the speciation of fluids in equilibrium with carbonate minerals by Raman spectroscopy. The predicted stability of aqueous CO<sub>3</sub><sup>2-</sup> in high P fluids and the enhanced solubility of carbonate minerals under P, indicate that CO<sub>3</sub><sup>2-</sup> ions may be major components in slab-derived fluids and may thus control the mobility of other rock-forming elements in subduction zones.

## Branched tetraethers derived temperature reconstruction from northwestern Black Sea: Proposition of correction and associated sensitivity test

L. SANCHI<sup>1\*</sup>, G. MENOT<sup>1</sup> AND E. BARD<sup>1</sup>

<sup>1</sup>Aix-Marseille Université, CNRS, IRD, Collège de France, CEREGE UM 34, 13545 Aix-en-Provence, France

(\*correspondence: sanchi@cerege.fr, menot@cerege.fr, bard@cerege.fr)

Proxies based on branched GDGT (glycerol dialkyl glycerol tetraether) core lipids are promising tools to reconstruct past continental temperatures. However their use is not always straightforward, notably because of the uncertainties on the source of these biomarkers.

Here we study the relative distribution of branched GDGTs (brGDGTs) in lacustrine sediments from a core retrieved in the northwestern Black Sea (from 40 to 9 cal ka BP). We first discuss the origins of the branched GDGTs. Comparisons to geochemical proxies from the same core support a dominant terrestrial origin of the brGDGTs during the last glacial, and a strong decrease of the soil derived brGDGTs relative proportion toward the Holocene. As this lowering of the soil vs. lacustrine derived brGDGTs is prone to bias the temperature signal reconstructed with a soil calibration, we propose a correction of this signal with a binary mixing model. We further test the sensitivity of this model with a Monte Carlo method. The resulting signals are consistent with (discrete) independent temperature reconstructions from the study area. Moreover the temperature relative evolution provides insights into the millennial scale climate variability in central and eastern Europe. Notably, the imprints of Heinrich event cold spells and late glacial climatic oscillations are in line with other regional paleorecords from the northern hemisphere.

## Calcite step growth velocities; a function of saturation index and the $\text{Ca}^{2+}$ to $\text{CO}_3^{2-}$ activity ratio

K.K. SAND<sup>1\*</sup>, D.J. TOBLER<sup>1</sup>, K.K. LARSEN<sup>2</sup>,  
E. MAKOVICKY<sup>3</sup> AND S.L.S. STIPP<sup>1</sup>

<sup>1</sup>NanoScience-Center, University of Copenhagen,  
Universitetsparken 5, DK-2100 Copenhagen.  
\*kks@nano.ku.dk

<sup>2</sup>Centre for Star and Planet Formation, University of  
Copenhagen, Denmark.

<sup>3</sup>Department of Geography and Geology, University of  
Copenhagen, Denmark

Calcite ( $\text{CaCO}_3$ ) growth rate has an impact on many natural and industrial processes, ranging from biomineralisation to carbon storage and pipe scaling. Larsen *et al.* [1] noted that  $\text{Ca}^{2+}$  to  $\text{CO}_3^{2-}$  activity ratios in natural waters are rarely unity and demonstrated that growth velocities of the calcite acute and the obtuse steps varied with the  $\text{Ca}^{2+}$  to  $\text{CO}_3^{2-}$  ratio at constant states of supersaturation. We have extended the work of Larsen *et al.* to quantify the growth rates for acute and obtuse steps as a function of saturation index (SI) and  $\text{Ca}^{2+}$  to  $\text{CO}_3^{2-}$  activity ratios. Microscopic analysis of growth spirals show that absolute growth velocities change with SI. We have also observed that, independent of SI, acute step velocities are higher than obtuse velocities at low  $\text{Ca}^{2+}$  to  $\text{CO}_3^{2-}$  ratios, whereas obtuse step velocities are higher at higher  $\text{Ca}^{2+}$  to  $\text{CO}_3^{2-}$  ratios (Fig. 1). This shift is certainly related to the different geometries of the acute and obtuse steps.

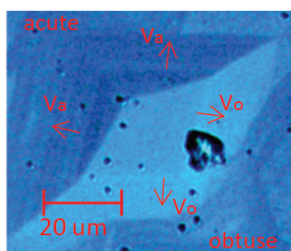


**Figure 1.** Growth spiral at a  $\text{Ca}^{2+}/\text{CO}_3^{2-} = 50$ . The obtuse step velocities are faster ( $V_o$ ) and apex shifts toward the acute corner.

These results have implications for current models of calcite growth and reaffirm that calcite growth cannot simply be described using classical crystal growth theory intended for the high order symmetry of cubic atomic lattices. The rhombohedral symmetry of the calcite atomic structure must be considered.

[1] Larsen *et al.* (2010). *Geochimica et Cosmochimica Acta* **74**, 2099-2109

## Quantification of organic matter redox states by mediated electrochemical analysis

M. SANDER<sup>1</sup>, L. KLÜPFEL<sup>1</sup>, A. PIEPENBROCK<sup>2</sup>,  
A. KAPPLER<sup>2</sup> AND M. AESCHBACHER<sup>1</sup>

<sup>1</sup>Institut für Biogeochemie und Schadstoffdynamik, Swiss  
Federal Institute of Technology Zurich (ETHZ),  
Switzerland (michael.sander@env.ethz.ch)

<sup>2</sup>Geomicrobiology Group, Applied Geosciences, Eberhard  
Karls University Tübingen, Germany

Electron transfer reactions involving organic matter (OM) play a key role in carbon and element cycling in wetlands. Under anoxic conditions, OM may act as terminal electron acceptor in anaerobic microbial respiration. Reduction of OM may competitively suppress electron transfer to  $\text{CO}_2$  and hence methanogenesis. Under oxic conditions, OM is susceptible to enzymatic oxidation, which ultimately leads to OM mineralization and hence  $\text{CO}_2$  emissions. Despite the widely recognized importance of OM redox reactions to the biogeochemistry of wetlands, these reactions were difficult to study in past work as direct quantification methods were missing. We recently introduced mediated electrochemical analysis as a novel approach in which water-soluble organic mediator compounds are used to facilitate electron transfer and redox potential equilibration between OM and electrodes. The approach includes two types of measurements: (i) Mediated electrochemical reduction and oxidation directly quantify (changes in) the numbers of electrons that small OM samples accept and donate in electrochemical cells with well defined redox conditions. (ii) Mediated potentiometric redox potential measurements can be used to determine (changes in) the reduction potentials  $E_h$  of OM samples and on the thermodynamics of redox reactions involving OM. The unique capabilities of mediated electrochemical analysis for the analysis of OM redox dynamics in wetlands will be highlighted by results of two mechanistic laboratory studies. In the first study, mediated electrochemical analysis was used to quantify changes in the redox states of different OM over successive microbial reduction and  $\text{O}_2$ -oxidation cycles. The results demonstrate that electron transfer to and from OM was fully reversible, that system thermodynamics controlled the extents of microbial OM reduction, and that OM accepted electrons over wide  $E_h$  ranges. In the second case study, OM oxidation during incubation with phenoloxidases (i.e., laccases) was quantified, and fast, extensive and irreversible enzymatic oxidation of phenolic moieties in OM was demonstrated. Implications for OM redox dynamics in wetlands under anoxic and oxic conditions will be discussed.



## Aerosol modifications observed at Mt. Cimone (Italy) during the Eyjafjallajökull eruption in 2010

S. SANDRINI<sup>1\*</sup>, L. GIULIANELLI<sup>1</sup>, S. DECESARI<sup>1</sup>, P. CRISTOFANELLI<sup>1</sup>, A. MARINONI<sup>1</sup>, M. CHIARI<sup>2</sup>, G. CALZOLAI<sup>2</sup>, S. CANEPARI<sup>3</sup> AND C. PERRINO<sup>4</sup>

<sup>1</sup>Institute of Atmospheric Sciences and Climate, National Research Council, Bologna, 40129, Italy  
(\*correspondence: s.sandrini@isac.cnr.it)

<sup>2</sup>Italian National Institute for Nuclear Physics, Florence section, Sesto Fiorentino, 50019, Italy

<sup>3</sup>University of Rome "La Sapienza", Chemistry Department, Rome, 00185, Italy

<sup>4</sup>C.N.R. Institute of Atmospheric Pollution, Monterotondo St., Rome, 00015, Italy

Measurements of physical and chemical properties at the Mt. Cimone GAW-WMO Global Station (2165 m a.s.l.) allowed the detection of two volcanic transports occurred during the Eyjafjallajökull Icelandic volcano eruption in Spring 2010. Both episodes were characterized by an abrupt increase of fine and especially coarse mode particles number, with a consistent ash mode at an optical diameter of about 2.5  $\mu\text{m}$  and an accumulation mode peaking at 0.2 - 0.3  $\mu\text{m}$ . To figure out whether and to what extent the local aerosol mass was influenced by the transported volcanic ash the chemical composition of filter samples was derived from different analytical techniques (Ionic Chromatography, PIXE-PIGE and ICP-OES) showing a fine fraction dominated by sulphates and a coarse fraction of mainly crustal origin with a composition in good agreement with that of volcanic ash collected at the eruption site. The concentrations of selected elements (Ti, Al, Fe, Mn) allowed to estimate a volcanic plume contribution of about 10  $\mu\text{g m}^{-3}$ , corresponding to about 40% of the total PM10 mass on 18 May, the most intense of the two events. A comparison with contributions observed in other parts of Europe is presented.

## Characteristics and genesis of ion-adsorption type REE ores

K. SANEMATSU<sup>1,2\*</sup> AND Y. WATANABE<sup>1</sup>

<sup>1</sup>Geological Survey of Japan, AIST, Tsukuba 305-8567, Japan  
(\*correspondence: k-sanematsu@aist.go.jp)

<sup>2</sup>CODES, University of Tasmania, Private Bag 126, Hobart, Tasmania 7001, Australia

Ion-adsorption type REE deposits are the predominant source of HREE and Y in the world, and they have been economically mined only in South China. In order to elucidate the genesis of the deposits, we review petrochemistry of parent granites of ion-adsorption ores, and geochemical and mineralogical characteristics of the ores.

The REE deposits in China consist of weathered granites called ion-adsorption ores which have over 50 % of ion-exchangeable REY relative to whole-rock REY [1, 2]. The parent granites of the deposits are generally characterized by metaluminous to weakly peraluminous ( $ASI < \sim 1.1$ ) compositions and low  $\text{P}_2\text{O}_5$  contents ( $< 0.08\%$ ). The granites contain allanite, titanite and REE fluorocarbonates (e.g., synchysite), which are degraded by chemical weathering, and they are poor in insoluble REE phosphates (monazite and xenotime). The HREE-rich granites are particularly fractionated and underwent deuteric alteration associated with mineralization of REE fluorocarbonates. The LREE/HREE ratios of ion-adsorption ores are constrained by nature and occurrences of these REE-bearing minerals in the granites.

The REE-bearing minerals in granites are degraded by low-pH soil water near the surface, and REE are transported downward in a weathering profile. REE are transported by complexing with humic substances and (bi)carbonate ions or as free ions in soil and ground water at low to near-neutral pH. REE are immobilized by adsorption or incorporation into secondary minerals due to pH increase resulting from the contact of the soil water with rock-forming minerals or higher-pH ground water. Ce is mostly immobilized as  $\text{CeO}_2$  by oxidizing from  $\text{Ce}^{3+}$  to  $\text{Ce}^{4+}$  near the surface. The other  $\text{REE}^{3+}$  are most likely to be adsorbed on the surfaces of kaolinite, halloysite and illite because of their points of zero charge and abundances in the ores. As a result, the weathering profile of the deposits is divided into a REE-leached zone of the upper part of the profile with positive Ce anomaly and a REE-accumulation zone (ion-adsorption ores) in the lower part with negative Ce anomaly. The occurrence of ion-adsorption ore is estimated by the negative Ce anomaly which is positively correlated with ion-exchangeable REE [2].

[1] Bao & Zhao (2008) *Ore Geol. Rev.* **33**, 519-535.

[2] Sanematsu et al. (2013) *Miner. Deposita* **48**, 437-451.



## Mantle-crust interactions in the oceanic lithosphere: Constraints from minor and trace elements in olivine

A. SANFILIPPO<sup>1\*</sup>, R. TRIBUZIO<sup>1,2</sup> AND M. TIEPOLO<sup>2</sup>

<sup>1</sup>Dipartimento di Scienze della Terra e dell'Ambiente, Università di Pavia, 27100 Pavia, Italy (\*correspondence: alessio.sanfilippo@unipv.it)

<sup>2</sup>CNR - Istituto di Geoscienze e Georisorse, U.O. di Pavia, 27100 Pavia, Italy

Minor and trace element compositions of olivines are used as probes into the melt-rock reaction processes occurring at the mantle-crust transitions in the oceanic lithosphere. We considered mantle and lower crustal sections from the Alpine Jurassic ophiolites. In particular, we analyzed olivines from plagioclase-impregnated harzburgites and replacive dunites (Fo 91-90 mol%), and olivines from olivine-rich troctolites, troctolites and olivine-gabbros (Fo 88-82 mol%). The olivines from the harzburgites most likely experienced re-equilibration with the impregnating melts, as indicated by Mn, Ti, Y and HREE variations and the low Na concentrations. The olivines from the dunites have: (i) Mn, Ni, Co and Ca compositions similar to the primitive (Fo 91-89) olivine phenocrysts in MORB [1], and (ii) relatively high Y and HREE contents indicating equilibrium with primitive MORB. We thus reinforce the hypothesis [2] that replacive dunites act as conduits for the extraction of MORB. The involvement of MORB-type melts in the formation of the dunites is substantiated by the spinel compositions ( $Cr\# \sim 35$ ,  $TiO_2 \sim 0.3$  wt%). Notably, the concentrations of Mn, Ni and Co in the dunites olivines produce positive correlations, in agreement with a formation through melt-harzburgite reactions. The preservation of this geochemical inheritance indicates that the liquids migrating along the dunites may change their compositions in response to the dunite-forming reactions. The olivine-rich troctolites are considered to be hybrid rocks formed by interaction between an olivine-rich matrix and MORB-type melts. The olivine chemistry in these rocks is controlled by the composition of the infiltrating melts and provides little information about the nature of the olivine matrix. Fractional crystallization rules the compositions of the olivines from the troctolites. Furthermore, the olivines from the troctolites have higher Y and HREE, and lower Co than the olivines in olivine-gabbros. These variations show that the troctolite/olivine gabbro transition is partly constrained by melt-rock reaction processes.

[1] Sobolev A, Hofmann A, *et al.* (2007), *Science* **316**, 412

[2] Kelemen P, Shimizu N, & Salters V (1995) *Nature*, **375**, 747-753

## Solid - Liquid Equilibria of $K_2SO_4$ -KBr- $H_2O$ System at 373 K

SHIHUA SANG<sup>1,2\*</sup>, TING LI<sup>1</sup> AND YONGXIA HU<sup>1</sup>

<sup>1</sup>College of Materials and Chemistry & Chemical Engineering, Chengdu University of Technology, Chengdu 610059, China. (sangsh@cdut.edu.cn)

<sup>2</sup>State Key Laboratory of Oil and Gas Reservoir Geology and Exploitation (Chengdu University of Technology), Chengdu 610059, P. R. China

Massive high-salinity underground brines are frequently met in the exploitation of oil and gas resources. In particular, the underground gasfield brines in Western Sichuan Basin (China), are very rare liquid mineral resources in the world. The B, K, and Br contents of the brines are far beyond the lower grades of the comprehensive industrial utilization. The ternary system  $K_2SO_4$ -KBr- $H_2O$  is a subsystem of the underground gasfield brines. The solid-liquid equilibria for the ternary system at 373 K were measured experimentally using the method of isothermal solution saturation. In the phase diagram of the ternary system  $K_2SO_4$ -KBr- $H_2O$  at 373 K (Figure 1), there are one invariant point E and two univariant curves DE and CE. Equilibrium solids were KBr and  $K_2SO_4$  in the studied ternary system. The crystallization area of  $K_2SO_4$

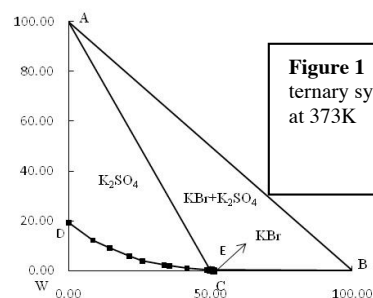


**Figure 1** Phase diagram of the ternary system  $K_2SO_4$ -KBr- $H_2O$  at 373K

(AED field) in the phase diagram is obviously bigger than that of KBr (BEC field).

### Acknowledgements

This work was supported by Open Funds (PLC201204) of State Key Laboratory of Oil and Gas Reservoir Geology and Exploitation (Chengdu University of Technology), the National Natural Science Foundation of China (40973047), the Specialized Research Fund (20125122110015) for the Doctoral Program of Higher Education of China.

## Structural change in molten basalt at deep mantle P-T conditions

C. SANLOUP<sup>1</sup>, J.W.E. DREWITT<sup>1</sup>, P. DALLADAY-SIMPSON<sup>1</sup>, D.M. MORTON<sup>1</sup>, N. RAI<sup>2</sup>, W. VAN WESTRENNEN<sup>2</sup>, Z. KONOPKOVA<sup>3</sup> AND W. MORGENROTH<sup>3;4</sup>

<sup>1</sup>SUPA, Centre for Science at Extreme Conditions and School of Physics and Astronomy, University of Edinburgh, Edinburgh, EH9 3JZ, UK

<sup>2</sup>Faculty of Earth and Life Sciences, VU University Amsterdam, The Netherlands

<sup>3</sup>DESY Photon Science, Notkestr. 85, 22607 Hamburg, Germany

<sup>4</sup>Frankfurt University, Germany

In the recent years, structural and density information on silica glass have been obtained up to record pressures of up to 100 GPa<sup>1</sup>, a first major step towards obtaining data on the molten state.

In this abstract, the structure of molten basalt is reported up to 60 GPa by means of *in situ* x-ray diffraction, and structural changes are evidenced. Silicon coordination increases from 4 at ambient conditions to 6 at 35 GPa, similarly to what has been reported in silica glass<sup>1-3</sup>. Compressibility of the melt after completion of Si coordination change is lower than at lower pressure (**P**) conditions, implying that a single equation of state can not accurately describe density evolution of silicate melts over the whole mantle **P**-range. The transition pressure coincides with a marked change in the **P**-evolution of nickel partitioning between molten iron and molten silicates, indicating that melt compressibility controls siderophile element partitioning.

1. Sato and Funamori, PRL 101, 255502 (2008). 2. Meade *et al.* PRL 69, 1387 (1992). 3. Benmore *et al.*, PRB 81, 054105 (2010).

## Ion microprobe U-Pb dating and Sr isotope measurement of a proto-conodont

YUJI SANO<sup>1\*</sup>, KOSAKU TOYOSHIMA<sup>1</sup>, KOTARO SHIRAI<sup>1</sup>, NAOTO TAKAHATA<sup>1</sup>, AKIZUMI ISHIDA<sup>1</sup> TOMOHIKO SATO<sup>2</sup> AND TSUYOSHI KOMIYA<sup>2</sup>

<sup>1</sup>Atmosphere and Ocean Research Institute, The University of Tokyo, Kashiwanoha, Kashiwa, Chiba 277-8564, Japan (ysano@aori.u-tokyo.ac.jp)

<sup>2</sup>Department of Earth Science and Astronomy, The University of Tokyo, Komaba, Meguroku, Tokyo 153-8902, Japan

We report here *in situ* ion microprobe U-Pb dating of a protoconodont micro-fossil using a NanoSIMS [1,2]. Twenty-three spots on the single fragment of the protoconodont (size: approximately 850  $\mu\text{m}$  x 250  $\mu\text{m}$ ) derived from a sedimentary layer in the Meishucunian formation, Yunnan Province, South China provide a <sup>238</sup>U/<sup>206</sup>Pb isochron age of 547  $\pm$  43 Ma (2 $\sigma$ , MSWD=1.9), which is consistent with the depositional age of the formation, 536.5  $\pm$  2.5 Ma reported by a zircon U-Pb dating [3]. On the other hand, five spots on the small region in the sample yield the isochron age of 416  $\pm$  73 Ma (2 $\sigma$ , MSWD=0.31), apparently younger than the formation age. The younger age may be attributable to the latter metamorphic event, probably Caledonian orogenic activity recorded in the younger zircon with the age of 420 - 440 Ma [4].

We also measured the <sup>87</sup>Sr/<sup>86</sup>Sr ratios of the protoconodont by a NanoSIMS [5]. Nineteen spots on the older age region give the <sup>87</sup>Sr/<sup>86</sup>Sr ratio of 0.71032  $\pm$  0.00023 (2 $\sigma$ ) on the weighted mean average, while seven spots on the younger area provide that of 0.70862  $\pm$  0.00045 (2 $\sigma$ ), significantly smaller than the older part. This is the first finding of U-Pb age and Sr isotope heterogeneity within a single fragment of micro-fossil, even though there is not a large chemical difference measured by a semi-quantitative SEM-EDS analysis.

[1] Sano *et al.* (2006) *Geochem. J.* **40**, 597-608. [2] Takahata *et al.* (2008) *Gond. Res.* **14**, 587-596. [3] Sawaki *et al.* (2008) *Gond. Res.* **14**, 148-158. [4] Guo *et al.* (2009) *Geochem. J.* **43**, 101-122. [5] Sano *et al.* (2008) *App. Geochem.* **23**, 2406-2413.

## On the reliability of paired carbon isotope as a pCO<sub>2</sub> proxy in the Ediacarian Araras platform, Brazil

PIERRE SANSJOFRE<sup>1,2,3\*</sup>, MAGALI ADER<sup>1</sup>,  
RICARDO I.F. TRINDADE<sup>2</sup>, AFONSO C.R. NOGUEIRA<sup>4</sup>

<sup>1</sup>Institut de Physique du Globe de Paris, France (ader@ipgp.fr)

<sup>2</sup>Universidade de São Paulo, Brazil (rtrindad@iag.usp.br)

<sup>3</sup>McGill University, Montréal, Canada (\*correspondence : pierre.sansjofre@mcgill.ca)

<sup>4</sup>Universidade Federal do Pará, Belém, Brazil (anogueira@ufpa.br)

The snowball Earth model accounts for many of the typical geological and geochemical features of the Marinoan glaciation deposits (~635Ma) and of their overlying cap carbonate [1]. Melting this snowball Earth would have required a massive increase of the atmospheric carbon dioxide content (pCO<sub>2</sub>). Recently however, we proposed instead a low atmospheric pCO<sub>2</sub> in the glaciation aftermath [2]. Our interpretation is based on paired carbon isotope data obtained on cap carbonates from Mirassol d'Oeste section (Ediacarian Araras platform, Brazil), together with previous results from cap carbonates of the Doushantuo Fm. and Zhamoketi Fm [3,4]. All three data sets showed low  $\Delta^{13}\text{C}_{\text{carb-org}}$  ( $=\delta^{13}\text{C}_{\text{carb}} - \delta^{13}\text{C}_{\text{org}}$ ). We made the case that these anomalously low values result from a decrease in the photosynthetic fractionation factor ( $\epsilon_p$ ), which can be related to pCO<sub>2</sub> lower than 3000 ppmv at the time of cap carbonate deposition.

We performed here a regional study based on 4 other sections sampled along the Araras carbonate platform. This new data set is broadly consistent with a low atmospheric pCO<sub>2</sub> scenario and allow to explore and identify both the local and global carbon isotopic variations of the Araras carbonate platform. In details, some features indicate that the occurrences of the low  $\Delta^{13}\text{C}_{\text{carb-org}}$  are restricted to shallow depositional environments. In this present contribution, we discuss two alternate hypotheses that can be invoked to explain the low  $\Delta^{13}\text{C}_{\text{carb-org}}$ : (i) a shallow water early diagenetic process inducing a  $\delta^{13}\text{C}_{\text{org}}$  increase and a  $\delta^{13}\text{C}_{\text{carb}}$  decrease or (ii) primary producers presenting lower  $\epsilon_p$  due to other parameter than pCO<sub>2</sub>. In both case, the diagenetic event and the primary producers would remain to be constrained.

[1] Hoffman and Schrag (2002) *Terra Nova* **14**, 129-155. [2] Sansjofre *et al.* (2011) *Nature* **478**, 93-96. [3] Jiang *et al.* (2010) *Earth Planet. Sci. Lett.* **299**, 159-168. [4] Shen *et al.* (2008) *Earth Planet. Sci. Lett.* **265**, 209-228.

## Magnetic susceptibility and $\delta^{18}\text{O}$ characterization of granites related with W, Sn, Mo and Bi (Au) hydrothermal vein deposits

HELENA SANT'OVAIA<sup>1</sup>, HELENA C.B. MARTINS<sup>1</sup> AND  
FERNANDO NORONHA<sup>1</sup>

<sup>1</sup>DGAOT, Centro de Geologia, F.C. Univ. Porto, Portugal, hsantov@fc.up.pt (\* presenting author)

The Northern Portugal mainland comprises an important W-Sn metallogenic province characterized by W-(Mo-Bi), W, W-Sn, and Sn hydrothermal vein deposits related with sinorogenic Variscan granites. These granites are usually classified into two main groups: peraluminous and metaluminous. As the granite rocks reflect redox states of their corresponding melts, the presence of magnetite and/or ilmenite as accessory minerals represent oxidized- and reduced-type respectively. The mineralogical features and magnetic susceptibility (K) of the granites were examined in order to deduce the redox conditions of magma systems, using the magnetic susceptibility data from around 644 sampling stations on different massifs of Variscan Portuguese granites. Whole-rock oxygen-isotope ( $\delta^{18}\text{O}$ ) values were compiled from bibliography [1,2,3,4]. Despite of different petrographic and geochemical characteristics, K values in the majority of the studied granites vary from 20 to 300  $\times 10^{-6}$  SI units corresponding to peraluminous and meta-peraluminous, reduced, ilmenite-type granites. The oxidized or magnetite-type granites are scarce and represented by metaluminous late orogenic with K values ranging from 15 to 20  $\times 10^{-3}$  SI units and low  $\delta^{18}\text{O}$  values ranging from 8.9 to 10.3‰. Major W-Sn ore deposits are related to reduced ilmenite-bearing granites with  $\delta^{18}\text{O}$  enriched (9.3 to 13.5‰); W- (Mo-Bi- Au) deposits are related with oxidized granite series (i.e. magnetite or titanomagnetite-bearing granites). Magnetic susceptibility measurements, represent a powerful tool on mineral exploration of deposits related with intrusive magmatism.

[1] Antunes *et al.* (2008) *Lithos* **103**, 445-465. [2] Martins *et al.* (2009) *Lithos* **111**, 142-155. [3] Neiva *et al.* (2009) *Lithos* **111**, 186-202. [4] Sant'Ovaia *et al.* (2011) *Min. Mag.* **76**, 6, 2325.

This work has been financially supported by PTDC/CTE-GIX/099447/2008 (FCT-Portugal, COMPETE/FEDER).

## Microbial communities in terrestrial CO<sub>2</sub> springs: Insights into the long-term biogeochemical effects of geologic carbon storage

EUGENIO-FELIPE U. SANTILLAN<sup>1\*</sup>, JONATHAN MAJOR<sup>1</sup>  
AND PHILIP C. BENNETT<sup>1</sup>

<sup>1</sup>University of Texas Austin, Austin, TX, USA  
(efu.santillan@utexas.edu \* presenting author)

During carbon sequestration, CO<sub>2</sub> is stored in subsurface reservoirs such as sandstone and basalt formations perturbing native microbial communities. Useful and accessible natural analogues to study long term effects of CO<sub>2</sub> on these communities are high CO<sub>2</sub> springs. Laboratory cultures have shown CO<sub>2</sub> to be toxic for microorganisms starting at 1 atm. Here we present data indicating microbes that can survive up to 10 times that pressure.

In this study, 16S rRNA gene sequences were used to characterize microbial communities from 3 sequestration analogues at depths where PCO<sub>2</sub> is at approximately 2 atm: from a basalt formation in Klickitat (KT), WA containing approximately 700 ppm of total dissolved solids (TDS); from a sedimentary formation along the Little Grand Wash Fault (LGW), UT containing 15,000 ppm TDS; and from a saline water in Bravo Dome (BD), NM containing 50,000 ppm TDS. Results show that the springs were dominated by a few major organisms but still contained more diversity than was expected at toxic CO<sub>2</sub> pressures. LGW sequences had no archaea and were dominated (>85%) by the genus *Acinetobacter*. KT sequences were more diverse than that of LGW and contain methanogens and methanotrophs suggesting CH<sub>4</sub> cycling. Candidate phyla were also detected in KT such as those from the OP, WS, and SPAM divisions. Sequencing for BD is currently underway.

Laboratory cultures also show bacteria at LGW performing lactate fermentation at 10 atm PCO<sub>2</sub>, demonstrating viability at sequestration conditions. This study confirms the presence and viability of microbial communities in CO<sub>2</sub> rich environments that can continue to affect the geochemistry as well as the long-term storage of CO<sub>2</sub>.

## Bioremediation and soil formation processes in bauxite residue tailings

T. C. SANTINI<sup>1,2\*</sup> AND L. A. WARREN<sup>1,3</sup>

<sup>1</sup>McMaster University, GSB218, Hamilton, ON, L8S4K1, Canada (\*correspondence: santini@mcmaster.ca; warrenl@mcmaster.ca)

<sup>2</sup>University of Western Australia, M087, Crawley, WA, 6009, Australia

<sup>3</sup>CSIRO Land and Water, Lucas Heights, NSW, 2234, Australia

Bauxite residue is an alkaline, saline-sodic tailings material generated during the Bayer process, in which alumina is extracted from bauxite. Between 3 and 4 billion tonnes of bauxite residue are estimated to be currently stored in facilities worldwide. *In situ* remediation of bauxite residue by application of inorganic and organic amendments, coupled with natural weathering and soil formation processes, is a cost-effective way to decrease alkalinity and salinity such that the tailings can then support a vegetation cover. Very little information on microbial activity and its potential influence on the geochemistry and mineralogy of bauxite residues currently exists, impeding development of effective remediation strategies. Here, a bauxite residue storage facility was investigated after 15 years of weathering to evaluate the effect of amendments on geochemistry and mineralogy of the bauxite residue, and development of microbial communities.

Illage, and the addition of compost and gypsum, significantly decreased pH and salinity of the tailings. Highly diverse microbial communities were detected in these tailings, indicating that endemic organisms adapted to these materials occur *in situ*. Further, microbial community species composition varied with applied treatments and depth below surface indicating microbial selection of different conditions based on aeration, pH, salinity, and carbon availability. Experiments indicated that endemic communities were able to degrade oxalate, and reduce Fe<sup>3+</sup> and SO<sub>4</sub><sup>2-</sup>, precipitating minerals such as vivianite and siderite; all of which are important steps in the development of soils capable of supporting plant growth. However, the species responsible for carrying out these functions differed between treatments and depths, indicating that knowledge of the specific microbes associated with different conditions is required. Overall, the study demonstrated that microbial communities can influence geochemical cycles and soil formation within bauxite residue deposits, and that the composition and function of microbial communities can be influenced by the application of chemical and physical treatments to bauxite residue.

## Acid rock drainage associated with tropical glacier retreat: Nevado Pastoruri, Perú.

E. SANTOFIMIA<sup>1\*</sup>, E. LÓPEZ PAMO<sup>1</sup>, J. PALOMINO<sup>2</sup>  
AND A. AGUILERA<sup>3</sup>

<sup>1</sup>Instituto Geológico y Minero de España, Madrid, Spain (\*  
correspondence: e.santofimia@igme.es)

<sup>2</sup>Facultad de Ciencias del Ambiente, Huaraz, Perú.

<sup>3</sup>Centro de Astrobiología, Torrejón de Ardoz, Madrid, Spain.

An important glacier retreat has been registered in the Nevado Pastoruri (Huascarán National Park) from 1962 to 2001, reducing its surface a 60% [1]. This process is frequent in glaciers located at Cordillera Blanca. Occasionally, glacier retreat exposed pyrite-rich rock outcrops of the Chicama formation, causing its alteration and the generation of acid rock drainages (ARDs) [2].

In the case of Nevado Pastoruri, the glacier retreat has left exposed to atmospheric conditions the sandstones and lutites with coal enriched in pyrite of the Chimú formation [3].

The proglacial zone presents a lot of lakes, scant vegetation, and intense fluvio-glacial erosion. On morphologies typically glacier are abundant the ARDs, revealing like springs of underground water, runoff or forming lakes. ARDs are clearly identifiable for the colour and the morphology (terraced iron formations), which is associated with the oxidation of Fe(II).

The water sampling was carried out in the proglacial zone. After cluster analysis using 23 samples, two groups were established. The first group (n=8) gathered the most acidic samples, pH 3, showing also the highest concentrations of elements such as SO<sub>4</sub>, Fe, Al, Ca, Mg, Mn and Zn. These samples were directly related to the pyrite alteration (227 mg/L SO<sub>4</sub>, 41 mg/L Fe) and aluminosilicate dissolution (10 mg/L Al), showing especially high values. This group is made up by the ARDs. The average concentration of these samples was an order of magnitude higher than the values showed by second group, which showed a scant mineralize (freshwater).

The ARDs geographical distribution is not disperse. These samples are grouped in a band of 600 m length with N-S direction and 250 m wide, between the elevations of 4925 and 5025 m. The mixing of two water types generates the source of River Pachacoto, showing Fe(III) buffer water (pH 3.1, Fe 0.7 mg/L) and several mg/L of dissolved Al (4.5) that confers mineral acidity to water.

[1] Duran *et al.* (2009) *Investigaciones Sociales* **13**, 59-77. [2] Fortner *et al.* (2011) *Applied Geochemistry* **26**, 1792-1801. [3] INGEMMET (1996) *Geología de los cuadrángulos de Huaraz, Recuay, La Unión y Yanahuanca*, pp. 292.

## Sr and Nd isotope data for arc-related (meta) volcanics (SW Iberia)

J.F. SANTOS<sup>1</sup>, J. MATA<sup>2</sup>, S. RIBEIRO<sup>1</sup>, J. FERNANDES<sup>1</sup>,  
AND J. SILVA<sup>2</sup>

<sup>1</sup>Geobiotec/Dep. Geociências, Un. Aveiro, Portugal,  
jfsantos@ua.pt

<sup>2</sup>Fac. Ciências Univ. Lisboa/ CeGUL, Portugal

In the southern sector of the Ossa-Morena Zone (Iberian Variscan Chain), along its boundaries with the Beja-Acebuches Ophiolite and the South-Portuguese Zone, Upper Palaeozoic igneous mafic and intermediate rocks, both intrusive and extrusive, are widely represented. The so-called Odivelas Unit (Andrade, 1983), include (meta-) basalts and (meta-) andesites, which, according with previous studies, display low-K tholeiitic to calc-alkaline signatures and, therefore, are interpreted as remnants of an active margin volcanic arc. Santos *et al.* (1990) subdivided those volcanics into two groups: in Alfândão-Peroguarda, the tholeiitic nature is dominant; in Odivelas-Penique, the calc-alkaline signature becomes more pronounced. Intercalation of limestone layers provided some age constraints, showing that the subduction-related volcanic activity in the studied area began in the Lower Devonian and continued, at least, through the Middle Devonian (Conde & Andrade, 1974; Machado *et al.*, 2010).

In this work, samples previously studied by Santos *et al.* (1990) and Silva *et al.* (2011) were analysed for Sm-Nd and Rb-Sr isotopes. Considering that the volcanics were systematically affected by hydrothermal metamorphism, it is expected that the Sr signatures show significant disturbance. In contrast, Nd isotope ratios probably reflect the primary features. Alfândão-Peroguarda samples show a very limited range of positive initial  $\epsilon_{Nd}$ , from +5.1 to +4.3 (assuming 400 Ma), showing no evidence for significant crustal assimilation and, therefore, allowing the attribution of negative Nb and Ta anomalies to arc-related processes. On the other hand, <sup>87</sup>Sr/<sup>86</sup>Sr varies from 0.7044 to 0.7060 (for 400Ma). These samples rocks define a horizontal trend on the initial  $\epsilon_{Nd}$  vs. initial <sup>87</sup>Sr/<sup>86</sup>Sr plot, typical of co-genetic rocks that underwent interaction with seawater. On the other hand, Odivelas-Penique volcanics show wide spectra for both initial <sup>87</sup>Sr/<sup>86</sup>Sr (from 0.7038 to 0.7066) and  $\epsilon_{Nd}$  (from +4.6 to -4.1). Significantly, the highest  $\epsilon_{Nd}$  values for this group are within the narrow range defined by Alfândão-Peroguarda tholeiitic basalts, suggesting a common mantle source (or very similar sources) for the most mafic magmas of both sectors.

The whole set of Nd isotope ratios supports the distinction previously proposed between the two groups of volcanics. In addition, the variation from positive to negative initial  $\epsilon_{Nd}$  values in the Odivelas-Penique suite shows that its geochemical features were likely influenced by assimilation of continental crustal material.

Funding: FCT through projects Petrochron (PTDC/CTE-GIX/112561/2009) and Geobiotec (PEst-C/CTE/UI4035/2011).

## Behaviour of rare earth elements (REE) at Funil Reservoir, Southeastern Brazil

J.M.C.O. SANTOS-NEVES<sup>1</sup>, M.M. FERREIRA<sup>1</sup>, M.S.M. VIDAL<sup>1</sup>, A.A. ROCHA<sup>2</sup> AND S.R. PATCHINEELAM\*<sup>1</sup>

<sup>1</sup>Department of Geochemistry and <sup>2</sup>Department of Analytical Chemistry. Institute of Chemistry, Universidade Federal Fluminense, Niterói, Rio de Janeiro State, Brazil.

\*sam\_pat\_br@yahoo.com

Rare earth elements (REE) have specific biogeochemical characteristics, which allow their use as reliable tracers of natural processes at various spatial and temporal scales in aquatic systems [1-3]. This study aims to evaluate the role of Funil Reservoir on REE behaviour. Considering the objectives, water samples were collected in three sample stations, during dry and rainy seasons: (P-01) upstream the Funil reservoir at Queluz, São Paulo State; (P-02) at the reservoir; and (P-03) downstream the Funil Reservoir, at Itatiaia. REE concentrations were determined by ICP-MS.

REE concentrations are presented in Table 1. Calculated ratios from REE normalized by PAAS indicate that values of Gd/Yb > La/Yb, which suggests that there is an enrichment of heavy REE in all sample points in both seasons.

|                     | Rainy season |         |         | Dry season |       |       |
|---------------------|--------------|---------|---------|------------|-------|-------|
|                     | P-01         | P-02    | P-03    | P-01       | P-02  | P-03  |
| $\Sigma$ REE (ng/L) | 72,91        | 54,14   | 102,36  | 77,97      | 87,71 | 83,64 |
| La/Yb               | 0,19333      | 0,17172 | 0,05481 | 0,216      | 0,212 | 0,196 |
| Gd/Yb               | 0,03696      | 0,3308  | 0,17023 | 0,395      | 0,378 | 0,395 |

**Table 1:** REE concentrations and ratios at study area.

Our results indicate that REE abundance is controlled by weathering in drainage basin. During dry season REE concentrations increased. And during rainy season, REE concentrations before and after the reservoir were greater than concentrations at Funil reservoir (P-02). The distinct behaviour observed between dry and rainy seasons is the Funil Reservoir act as geochemical barrier modifying fluvial transport of REE. Another factor that probably affect REE behavior is algal bloom, with dominance of cyanobacteria which occurs during rainy season, which influence the behaviour of REE through the incorporation and release of these metals.

[1] GOLDSTEIN & JACOBSEN (1987) *Chemical Geology*, **48**, 245-272. [2] ELDERFIELD *et al.* (1990) *Geochimica Cosmochimica Acta*, **54**, 971-991. [3] XU & HAN (2009) *Applied Geochemistry*, **24**, 1803-1816.

## Hydromagnesite precipitation in microbial mats from a highly alkaline lake, Central Spain

M. ESTHER SANZ-MONTERO<sup>1\*</sup>, ÓSCAR CABESTRERO<sup>1</sup> AND J. PABLO RODRÍGUEZ-ARANDA<sup>1</sup>

<sup>1</sup>Petrology and geochemistry Department. Facultad de Ciencias Geológicas (UCM), Madrid, Spain. mesanz@geo.ucm.es (\*presenting author)

Microbialites comprised of up to 45% hydromagnesite and 10% of dolomite have been recognized in Las Eras playa-lake, Central Spain. Las Eras is an evaporitic highly alkaline lake, with pH values ranging from 9.4 to 11, that covers an area of 0.1 km<sup>2</sup> [1]. Mg-enriched groundwater flows into this lake, which is supersaturated in hydromagnesite and dolomite. The hydrous Mg-carbonate precipitation occurs in the uppermost layer of benthic microbial mats. This layer is dominated by *Microcoleus* that consists of trichomes in bundles and diatoms embedded in their EPS. Low-vacuum scanning electron microscopy revealed that hydromagnesite nucleation is initiated on the cells of aerobic heterotrophic bacteria that are responsible for the degradation of the microbial biomass. A progressive mineralization of the heterotroph cells by the deposition of plate-like crystals of hydromagnesite on their surface was observed. This resulting in the entombment of the bacteria and the formation of radiating aggregates of hydromagnesite crystals. The degradation and concomitant Mg-carbonate precipitation, finally, led to the lithification of the microbial mat.

This evolution shows that aerobic heterotrophic bacteria play a crucial role in the formation of microbialites in Lake Las Eras by promoting the Mg-carbonates precipitation. This lake is one of the few modern environments where hydromagnesite is a dominant precipitating mineral in microbialites. Thus, it provides a modern analog to use in the interpretation of saline and/or alkaline environments. In turn, the exceptional preservation of bacteria microfossils clustered into magnesite crystals has been already documented in Miocene saline deposits [2].

*The authors greatly appreciate support from MINECO Program (Project CGL2011-26781).*

[1] Sanz-Montero *et al.* (2013) *Geogaceta*, **53**, 97-100. [2] Sanz-Montero, M.E and Rodríguez-Aranda, J.P. (2012) *Sedimentary geology*, **263-264**, 6-15.

## Unravel the role of lake ice cover on the methane budget: A multi-proxy analysis

C.J. SAPART<sup>1</sup>, T. BOEREBOOM<sup>2</sup>, T. RÖCKMANN<sup>1</sup>,  
H. NIEMANN<sup>3</sup>, C. VAN DER VEEN<sup>1</sup>, J-L. TISON<sup>2</sup>

<sup>1</sup>Institute for Marine and Atmospheric research Utrecht,  
Utrecht University, The Netherlands

<sup>2</sup>Laboratoire de Glaciologie, Université Libre de Bruxelles,  
Belgium

<sup>3</sup>Department of Environmental Sciences, University of Basel,  
Switzerland

Large uncertainties exist on the evolution of the atmospheric methane (CH<sub>4</sub>) budget in the future. Concern about possible feedbacks of natural sources in a changing climate is growing, especially concerning the role of thawing of permafrost areas in the Arctic regions. Subarctic lakes are considered as “hotspots” for CH<sub>4</sub> emissions, but the role of the ice cover during the winter period is not well understood to date. Different types of gas bubbles with high CH<sub>4</sub> mixing ratios have been identified in lake ice cover. A recent study revealed that the gas composition of those bubbles depends on, inter alia, the bubble type, the lake depth and the hydrological status of the lakes.

Analysing mixing and stable isotope ratios of CH<sub>4</sub> and CO<sub>2</sub> on those bubbles is an efficient tool to identify the mechanisms involved in the release, the oxidation and transport of CH<sub>4</sub> in permafrost lakes and to better constrain the potential influence of lake characteristics. Those analyses together with lipid biomarkers distribution analysis on lake ice samples reveal that different bubble types contain different isotopic signatures and that oxidation of dissolved CH<sub>4</sub> is the most important process determining the isotopic composition of CH<sub>4</sub> in bubbles. This shows that the increased exchange time between gases coming from the sediments and the water column, due to the capping effect of the lake ice cover, reduces the amount of CH<sub>4</sub> released and favours its oxidation into carbon dioxide.

## Leaching of Zn, Cu and Pb from oxidised sulphidic mine waste as a function of temperature, L/S ratio and leaching reagents

NAEEM SAQIB<sup>1</sup>, MATTIAS BÄCKSTRÖM<sup>2</sup>

<sup>1,2</sup>Man-Technology Environment Research Center, Örebro  
University, SE-701 82, Örebro, Sweden,

<sup>1</sup>(naeem.saqib@oru.se) <sup>2</sup>(mattias.backstrom@oru.se)

Formation of low pH drainage from sulphidic mine waste enhances trace element mobility and posing a serious threat to the surrounding environment [1]. A sustainable and cost effective remediation method is therefore desired. Utilization of the sulphidic waste as a secondary source for metals might be a viable alternative. In this laboratory scale study chemical extraction has been employed to assess the potential of metal release and possible metal recovery from oxidised sulphidic mine waste. Waste from an old copper and lead mine in Kopparberg, mid Sweden, was used for the experiments. Mine waste was extracted with four leaching agents: (i) distilled water, (ii) sulphuric acid, (iii) sodium hydroxide and (iv) sodium bicarbonate (0.01 M), at three liquid solid ratios (5, 10, 20) and at four temperatures (25, 45, 65, 85 °C), for a time of 6 hours during intermittent shaking. Generated solutions were analysed with respect to pH, electrical conductivity, acidity and metal concentrations.

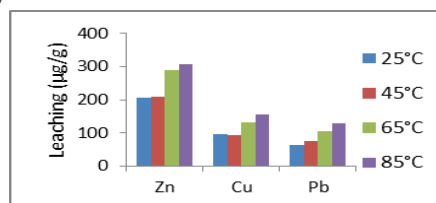


**Figure 1.** Effect of temperature on metal leaching from sulphidic mine waste using sulphuric acid.

Results indicate that increasing temperature enhances extraction of elements due to increase in reaction rates. Increasing L/S ratio increased extraction only to a certain extent after which it decreased or had no prominent effect. Sulphuric acid proved to be the best extraction media extracting as much as 14 % Zn, 10 % Cu and 3 % Pb of the total content. Leaching of Zn and Pb decreased from acid to neutral pH so it is a very crucial factor governing the extraction. Lead extraction with sulphuric acid is probably limited by anglesite (PbSO<sub>4</sub>(s)).

[1] Alena Luptakova, *et al.* (2010) Metals Recovery from Acid Mine Drainage, *Nova Biotechnologica* 23, p 1-10.

## Fuzzy Hierarchical Cross-Clustering of Romanian Mineral Waters

C. SĂRBU

<sup>1</sup>Faculty of Chemistry and Chemical Engineering, Babeş-Bolyai University, Arany Janos Str., No 11, RO-400028, Cluj-Napoca, Romania *E-mail address:* csarbu@chem.ubbcluj.ro

Cluster analysis is a large field, both within fuzzy sets and beyond it. The application of Fuzzy sets in a classification function causes the class membership to become a relative one and consequently an object or sample can belong to several classes at the same time but with different degrees. In this investigation, Fuzzy hierarchical cross-clustering algorithm has been applied for simultaneous clustering of different Romanian mineral water samples and their chemical characteristics (ions concentration), and the results obtained have been allowing an objective interpretation of their similarity and differences, respectively. This very informative fuzzy approach allows the qualitative and quantitative identification of the characteristics responsible for the observed similarities and dissimilarities between mineral water samples. In addition, the fuzzy hierarchical characteristics clustering and fuzzy horizontal characteristics clustering procedures revealed a high similarity between some ions concentration and other features.

## Surfactants from the gas phase may promote aerosol cloud droplet nucleation

NEHA SAREEN<sup>1</sup>, ALLISON SCHWIER<sup>1</sup>, TERRY LATHEM<sup>2</sup>, ATHANASIOS NENES<sup>2,3</sup> AND V. FAYE MCNEILL<sup>1</sup>

<sup>1</sup>Department of Chemical Engineering, Columbia University, New York, NY, USA 10027 vfm2103@columbia.edu

<sup>2</sup>School of Earth and Atmospheric Sciences, Georgia Institute of Technology, Atlanta, GA, USA 30332

<sup>3</sup>School of Chemical and Biomolecular Engineering, Georgia Institute of Technology, Atlanta, GA, USA 30332

The uptake of water-soluble volatile organic compounds (WSVOCs) by wet atmospheric aerosols can lead to the formation of secondary organic aerosol material (SOA). We have performed a series of laboratory studies in order to quantify the impact of WSVOC uptake and aqueous-phase SOA formation on aerosol cloud condensation nuclei (CCN) activity. Deliquesced, acidified submicron ammonium sulfate aerosols at >60% RH were exposed to ppb levels of gas-phase methylglyoxal, acetaldehyde in a continuous-flow aerosol reaction chamber (residence time = 3-5 h). Aerosol size and CCN activity was monitored at the reactor outlet via scanning mobility particle sizer (SMPS) and continuous-flow streamwise thermal gradient chamber CCN counter (CFSTGC), respectively.

Methylglyoxal and acetaldehyde are known to form SOA and suppress surface tension in bulk aqueous aerosol mimics, but both of these species have relatively low Henry's Law constants. We found evidence that adsorption of these species from the gas phase to the gas-aerosol interface significantly impacts aerosol CCN activity, by directly altering the aerosol surface tension. Up to 15% reduction in critical dry diameter for activation was observed without any detectable particle growth due to bulk uptake of organics (Sareen *et al.*, Proc. Natl. Acad. Sci. USA, 2013).

Finally, we have developed a general analytical approach for predicting aerosol surface tension based on gas-phase surfactant loadings, taking into account the effects of both bulk uptake and surface adsorption. These predictions allow calculation of the particle hygroscopicity and predictions of cloud droplet formation. We will present results for atmospheric scenarios and highlight needs for additional experimental work.



## Immobilization of boron in groundwaters by combination of MgO with woodchips

KEIKO SASAKI<sup>1</sup>, XINHONG QIU<sup>1</sup>, HITOSHI TAKAMORI<sup>3</sup>, SAYO MORIYAMA<sup>4</sup>, KEIKO IDETA<sup>5</sup> AND JIN MIYAWAKI<sup>6</sup>

<sup>1</sup>Department of Earth Resources Engineering, Kyushu University, Japan: (keikos@mine.kyushu-u.ac.jp, q-q11@mine.kyushu-u.ac.jp)

<sup>3</sup>Asahi Kasei E-Materials Co. Ltd., Japan: takamori.hf@om.asahi-kasei.co.jp

<sup>4</sup>Fukuoka Institute of Health and Environmental Sciences, Japan: sayo.moriyama@yahoo.com

<sup>5</sup>Institute for Materials Chemistry and Engineering, Kyushu University, Japan: (keiko@cm.kyushu-u.ac.jp, miyawaki@cm.kyushu-u.ac.jp)

Boric acid is one of the most difficult species to immobilize in aqueous environments, because it predominantly exists as a molecular form. Boron specific resin is widely used and well known to immobilize with N-methyl-glucamate groups. However, it requires alkaline pHs and is unsuitable to apply to contaminant sites in a large scale like groundwaters. In the present work, permeable reactive barrier column tests were conducted to remove boron (B) in groundwaters in a laboratory scale for 11 months by using combination of MgO agglomerates with woodchips instead of boron specific resin. MgO agglomerates are one of engineering-assisted geomaterials for handling and main reactive materials here, while woodchips are natural and supplemental ones. <sup>11</sup>B-NMR and XRD results revealed that boron was mainly immobilized as <sup>13</sup>B by co-precipitation with Mg(OH)<sub>2</sub> through destructive sorption of MgO and as <sup>14</sup>B with woodchips through complexation which is in complementary mechanism and facilitated after alkalization by hydration of MgO. SEM images of solid residues MgO agglomerates after immobilization of B were quite different from without woodchips, suggesting that a variety of organic acids in leachate from woodchips affects to Mg<sup>2+</sup> species as a precursor for Mg(OH)<sub>2</sub> precipitate. This affected also to increase the permeability because of avoiding the formation of bulky and needlelike-shaped precipitates of Mg(OH)<sub>2</sub>. As a result, boron specific resin can be alternatively replaced with combination of engineering geomimetics with natural materials, which improved the efficiency to immobilize boron in groundwaters.

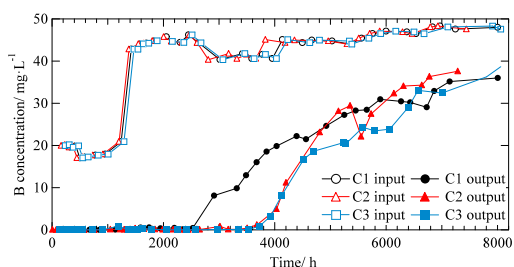


Fig. 1 Changes in B concentrations in input and output solutions with time. C1, MgO; C2, MgO + woodchips; C3, MgO + B specific resin

## Investigation of ancient fluid migration in Ordovician carbonates in the Michigan Basin using secondary minerals

J.K. SASO<sup>1</sup>, R. CALDAS<sup>2</sup>, L. W. DIAMOND<sup>2</sup>, A. PARMENTER<sup>3</sup> AND T. A. AL<sup>1\*</sup>

<sup>1</sup>Earth Sciences, University of New Brunswick, Canada (\*correspondence: TAL@unb.ca)

<sup>2</sup>Institute of Geological Sciences, University of Bern, Switzerland (diamond@geo.unibe.ch)

<sup>3</sup>Nuclear Waste Management Organization, Canada (aparmenter@nwmco.ca)

Investigations of the Upper Ordovician Trenton and Black River group argillaceous limestones in southwest Ontario, Canada, indicate that secondary calcite, dolomite, celestite and anhydrite occur in fracture-filling veins, with dolomite also replacing primary calcite in the limestone. The objectives of this study were to define the paragenetic sequence, identify the source(s) of the fluids, and if possible, place time constraints on the formation of these minerals.

Petrographic studies were conducted by optical and scanning-electron microscopy (SEM). Analyses of  $\delta^{18}\text{O}$  and  $^{87}\text{Sr}/^{86}\text{Sr}$  were conducted by isotope-ratio and thermal ionization mass spectrometry, respectively. Measurements of  $\delta^{18}\text{O}$  were also conducted by ion microprobe. Microthermometric data were collected from doubly-polished 150  $\mu\text{m}$  thick sections.

The paragenetic sequence, from oldest to youngest, is replacement dolomite, vein dolomite, calcite in veins, and late-stage sulphate minerals. Mass-balance calculations indicate that replacement dolomite in the Trenton Group formed under closed conditions, while replacement dolomite in the Black River Group required an external source of Mg. Depth profiles of  $\delta^{18}\text{O}$  and  $^{87}\text{Sr}/^{86}\text{Sr}$  in vein carbonates suggest they formed as  $^{18}\text{O}$ -depleted and  $^{87}\text{Sr}/^{86}\text{Sr}$ -enriched fluid ascended from the underlying shield. The  $^{87}\text{Sr}/^{86}\text{Sr}$  composition of late-stage sulphate minerals suggests they formed from sedimentary basin brine. Fluid-inclusion investigations of the calcite in veins indicate four fluid migration events with homogenization temperatures in the range of 40 to 90  $^{\circ}\text{C}$ . These temperatures are consistent with predictions of temperature associated with peak burial during the Late Carboniferous.

## Osmium isotope evidence for a large impact event in the Late Triassic

H. SATO<sup>1\*</sup>, T. ONOUE<sup>2</sup>, T. NOZAKI<sup>3</sup> AND K. SUZUKI<sup>3</sup>

<sup>1</sup>Kyushu University, Fukuoka 812-8581, Japan

(\*correspondence: 3SC12024G@s.kyushu-u.ac.jp)

<sup>2</sup>Kumamoto University, Kumamoto 860-0862, Japan

(onoue@sci.kumamoto-u.ac.jp)

<sup>3</sup>Japan Agency for Marine-Earth Science Technology

(JAMSTEC), Yokosuka 237-0061, Japan

(nozaki@jamstec.go.jp, katz@jamstec.go.jp)

Seawater <sup>187</sup>Os/<sup>188</sup>Os ratios reflect contributions to the global ocean from riverine (<sup>187</sup>Os/<sup>188</sup>Os ≈ 1.4), and hydrothermal and extraterrestrial inputs (<sup>187</sup>Os/<sup>188</sup>Os ≈ 0.12 - 0.13). Given the distinctive <sup>187</sup>Os/<sup>188</sup>Os ratios of these inputs and the relatively short residence time of Os in the ocean, seawater <sup>187</sup>Os/<sup>188</sup>Os ratios are highly sensitive to change in these fluxes. Thus, Os isotope has been used to demonstrate the 65 Ma impact event at Chixhulub in Mexico [1, 2], based on an abrupt decline in seawater <sup>187</sup>Os/<sup>188</sup>Os ratios during the Cretaceous/Paleogene (K-Pg) boundary.

We report the marine <sup>187</sup>Os/<sup>188</sup>Os ratios of the middle Norian bedded chert and claystone succession in Japan to provide new evidence of an extraterrestrial input. These bedded cherts are considered to be deep-sea sediments that accumulated in a pelagic, open ocean setting within the Upper Triassic paleo-Pacific Ocean (Panthalassa).

The initial <sup>187</sup>Os/<sup>188</sup>Os ratios exhibit an abrupt and marked negative excursion from 0.477 to unradiogenic values of 0.127 in a claystone layer. The Os concentration of this claystone layer is ca. 3 ppb which is three orders of magnitude higher than those of chert layers. Moreover, a plenty amounts of spherule and Ni-rich spinel granules and extraordinary PGE-enrichment was reported from the claystone [3]. The amplitude of this negative Os isotope excursion is comparable to those of the late Eocene (0.5 to 0.28) [4] and the K-Pg boundary (0.4 to 0.157) [1]. These geochemical lines of evidence strongly suggest that a large, kilometer-sized impactor is requisite to explain high Os concentration and unradiogenic <sup>187</sup>Os/<sup>188</sup>Os ratios of the Upper Triassic claystone layer.

[1] Ravizza & Peucker-Ehrenbrink (2003) *Science* **302**, 1392-1395. [2] Luck & Turekian (1983) *Science* **222**, 613-615. [3] Onoue *et al.* (2012) *Proc. Natl. Acad. Sci. USA* **109**, 19134-19139. [4] Paquay *et al.* (2008) *Science* **320**, 214-218.

## Let's use metastable geomaterials in environmental protection: An intelligent geotechnology learnt from natural processes

T. SATO<sup>1\*</sup> AND K. FUKUSHI<sup>2</sup>

<sup>1</sup>Faculty of Engineering, Hokkaido Univ., Kita 13 Nishi 8, Kita-Ku, Sapporo 060-8628 Japan

<sup>2</sup>Institute of Nature and Environmental Technology,

Kanazawa Univ., Kakuma, Kanazawa 920-1192 Japan

\*Correspondence: tomsato@eng.hokudai.ac.jp

In order to ensure sustainable development, engineering technologies used in environmental protection (e.g. purification, remediation) must utilize safe, cost-effective and environmentally efficient materials. As such, the use of ubiquitous geomaterials, rather than synthetic materials, is envisioned. The use of geomaterials for environmental applications, referred to as "geotechnology", is based on principles learnt from natural processes. Therefore, naturally occurring physical, chemical and biological processes can serve as useful analogs in designing cost-effective and intelligent geotechnologies to address environmental problems.

Geomaterials such as clays, carbonates and iron minerals, which are generally stable under Earth surface conditions, have been used widely for environmental applications. This is due to their cost-effectiveness and stability over a range of conditions. However, metastable materials widely observed in nature have been found to be more environmentally efficient due to their higher reactive surface areas and reactivity to hazardous contaminants compared to more stable materials. For example, iron oxides such as hematite, goethite, ferrihydrite and schwertmannite are seen as important naturally occurring sorbents of arsenate and phosphate. However, poorly crystalline and metastable ferrihydrite and schwertmannite exhibit higher capacities for arsenate and phosphate adsorption compared to crystalline goethite and hematite. Similarly, metastable aragonite and monohydrocalcite show better anion adsorption capabilities compared to calcite. Recently, it has been found that the stability of these materials can be modified by the adsorption of certain ions. Therefore, the long-term stability and efficient performance of metastable materials can be controlled in order to maximize their effectiveness. In this presentation, intelligent geotechnologies learnt from natural processes using metastable geomaterials will be introduced, with natural iron oxides and calcium carbonates as examples.

## Analcime alteration of montmorillonite: Growth rates

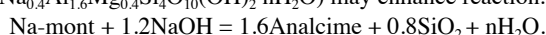
HISAO SATOH<sup>1,2</sup>, KATSUO TSUKAMOTO<sup>2</sup>, HITOSHI OWADA<sup>3</sup> AND TOMOKO ISHII<sup>3</sup>

<sup>1</sup>Mitsubishi Materials Co., Naka 311-0102, Japan

<sup>2</sup>Tohoku University, Sendai 980-8578, Japan

<sup>3</sup>RWMC, Tsukishima, 104-0052, Japan

Analcime is very common zeolite as a low-temperature secondary mineral of alkaline alteration. Growth of analcime was previously studied on precursor Na-clinoptilolite<sup>[1]</sup> and leucite<sup>[2]</sup>. Such an alkaline alteration is predicted in the bentonite barrier of radioactive waste repository by cement-leachates in groundwater<sup>[3]</sup>. Chemical similarity between analcime (NaAlSi<sub>2</sub>O<sub>6</sub>·H<sub>2</sub>O) and montmorillonite (Na<sub>0.4</sub>Al<sub>1.6</sub>Mg<sub>0.4</sub>Si<sub>4</sub>O<sub>10</sub>(OH)<sub>2</sub>·nH<sub>2</sub>O) may enhance reaction:



We investigated growth kinetics of analcime to evaluate the behavior of bentonite barrier under hyperalkaline condition.

Direct measurements of analcime growth rate on substrate, analcime at 90-120 °C were conducted using in-situ phase-shift interferometer (PSI)<sup>[4]</sup>. Supersaturation with respect to analcime was controlled by dissolution of coexisting montmorillonite in the cell with flow of 0.3 M NaOH solution.

The dissolution and growth rates of analcime near equilibrium were observed to be  $-3.6 \times 10^{-3}$  and  $2.7 \times 10^{-3}$  nm/s, at  $\Delta G$  of -11.29 and 8.80 kJ/mol respectively (Fig. 1). Our results agree with previous data<sup>[1]</sup>, which roughly draws a growth rate curve. We conclude that the key of analcime growth is porewater chemistry in montmorillonite. The dissolution of montmorillonite can be affected by porosity (density)<sup>[5]</sup>. Our results can extend the observed alteration towards a mechanistic model involving porosity change.

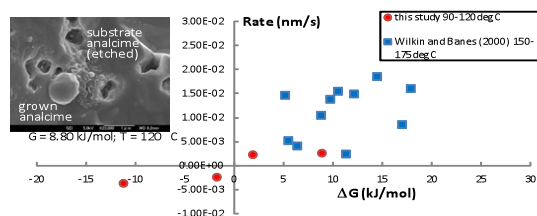


Figure 1: Growth rate curve of analcime and a surface after run showing etch pits and grown grains (FESEM).

[1] Wilkin & Barnes (2000) *Am. Min.* **85**, 1329-1341. [2] Putnis *et al.* (2007) *Am. Min.* **92**, 19-26. [3] Nakayama *et al.* (2004) *Appl. Clay. Sci.* **27**, 53-65. [4] Satoh *et al.* (2007) *Am. Min.* **92**, 503-509. [5] Satoh *et al.* (2013) *Clay Min.* (in press). This research is a part of "Development of the technique for the evaluation of long-term performance of EBS (FY2007-2012)" funded by the ANRE, the METI of Japan.

## Heterogeneity of the uppermost mantle in back-arc settings: Insights from trace-element compositions and water contents in Japanese peridotite xenoliths

TAKAKO SATSUKAWA<sup>1</sup>, MARGUERITE GODARD<sup>2</sup>, SYLVIE DEMOUCHEY<sup>2</sup> AND KATSUYOSHI MICHIBAYASHI<sup>3</sup>

<sup>1</sup>ARC Center of Excellence for Core to Crust Fluid Systems (CCFS) and GEMOC National Key Center, Earth and Planetary Sciences, Macquari University, Sydney, NSW 2109, Australia

<sup>2</sup>Géosciences Montpellier, Université Montpellier 2 and CNRS, Cc 060, Place E. Bataillon, 34095 Montpellier cedex 5, France

<sup>3</sup>Institute of Geosciences, Shizuoka University, Ohya 836, Shizuoka 422-8529, Japan

The uppermost mantle in the back-arc region of a subduction zone is the site of complex interactions between partial melting and fluid migration. To constrain these interactions and reveal the heterogeneity of the uppermost mantle in back-arc setting, we measured geochemical compositions and water contents of spinel peridotite xenoliths obtained from two back-arc volcanoes; Ichinomegata (NE Japan) and Oki-Dogo (SW Japan). The mineral chemistry of Ichinomegata peridotites shows a typical residual peridotite trend, depleted in light rare earth elements (LREE). Some samples of Oki-Dogo peridotites have lower Mg# in olivine (down to 0.88) and are enriched in LREE, indicating that these are affected by melt-rock interactions. Olivine has low water contents in samples from both Ichinomegata and Oki-Dogo. However, the water contents in pyroxenes in Ichinomegata peridotites are significantly higher than in Oki-Dogo. These differences might be due to the different mobility of water during fluid metasomatism versus melt-rock interaction. The water contents of the pyroxenes suggest interactions with water-rich fluids. Hydration incorporation in Ichinomegata peridotite is proposed to be associated with a water-rich metasomatism, which lead to depleted REE patterns in clinopyroxene, and the REE patterns of orthopyroxene are more depleted than for Oki-Dogo samples. However, the chemical composition of Oki-Dogo peridotites shows that they have experienced melt-rock interactions that have lead to the characteristic flat REE pattern of the clinopyroxene. Furthermore, these variations in chemical characteristics between Ichinomegata and Oki-Dogo might be induced by the changes in the subduction system in the Japan Island arc, such as the age and angle of the subducting slab.

## Salt Lakes of Western Australia – Emissions of natural volatile organic compounds

T. SATTLER<sup>1</sup>, T. KRAUSE<sup>1</sup>, H. F. SCHÖLER<sup>1</sup>, K. KAMILLI<sup>2</sup>,  
A. HELD<sup>2</sup>, C. ZETZSCH<sup>2</sup>, J. OFNER<sup>3</sup>, W. JUNKERMANN<sup>4</sup>  
AND E. ATLAS<sup>5</sup>

<sup>1</sup>Inst. of Earth Science, University of Heidelberg, Germany;

<sup>2</sup>Bayreuth Centre of Ecology and Environmental Research,  
University of Bayreuth, Germany;

<sup>3</sup>Vienna University of Technology, Austria;

<sup>4</sup>Inst. for Meteorology and Climate Research, Karlsruhe Inst.  
of Technology, Garmisch-Partenkirchen, Germany

<sup>5</sup>Rosenstiel School of Marine and Atmos. Sci., Miami, USA

Western Australia is a semi-/arid region that is heavily influenced by global climate change and agricultural land use. The area is known for its many saline lakes with a wide range of hydrogeochemical parameters. This area has been repeatedly investigated since 2006 and consists of ephemeral saline and saline groundwater sourced lakes with a pH reaching from 2.5 to 7.1. The semi-/arid region was originally covered by natural eucalyptus forests, but land-use has changed considerably after large scale deforestation from 1950 to 1970. Today the region is mostly used for growing wheat and live stock. The deforestation led to a rising groundwater table, bringing dissolved salts and minerals to the surface.

In the last decades, a concurrent alteration of rain periods has been observed. A reason could be the regional formation of ultra-fine particles that were measured with car-based and airborne instruments around the salt lakes in several campaigns between 2006 and 2011. These ultra-fine particles emitted from the lakes and acting as cloud condensation nuclei can modify cloud microphysics and thus suppress rain events [1]. New data from a campaign in 2012 accentuates the importance of these hyper saline environments for the local climate.

Ground-based particle measurements around the salt lakes in 2012 were accompanied by novel chamber experiments directly on the lakes. The 1.5 m<sup>3</sup> cubic chamber was constructed from transparent PTFE foil permitting photochemistry within while preventing dilution of the air due to lateral wind transport. This experimental setup allows linking the measured data directly to the chemistry of and above the salt lakes. Another advantage of the PTFE chamber is the enrichment of volatile organic compounds (VOC) that are emitted from salt lakes as possible precursors for the ultra-fine particles.

Chamber air was sampled using stainless steel canisters. Sediment, crust and water samples were taken for investigation of potential VOC emissions in the laboratory using GC-MS technique.

Different VOC and halogenated volatile compounds (VOX), exceeding atmospheric background concentrations, were identified from the sampled chamber air. Their enrichment or depletion over the time in the chamber allows for postulated reaction pathways leading to the formation of ultra-fine particles.

## Geochemical and acoustic investigations of hydrocarbon seepage on the continental shelf off northern Norway

S. SAUER<sup>1\*</sup>, J. KNIES<sup>1</sup>, C. SCHUBERT<sup>2</sup>, A. LEPLAND<sup>1</sup>  
AND S. CHAND<sup>1</sup>

<sup>1</sup>Geological Survey of Norway, Trondheim, Norway

(\*correspondence: simone.sauer@ngu.no)

<sup>2</sup>Swiss Federal Institute of Aquatic Science and Technology (EAWAG), Kastanienbaum, Switzerland

Active natural hydrocarbon seepage in the Hola area along the continental shelf off northern Norway has recently been found by Chand *et al.* 2008 [1]. We conducted acoustic and geochemical investigations to gain a better understanding of the extent and history of this gas seepage. Seismics and water column acoustic data were used to reveal potential hydrocarbon pathways to the seafloor and to locate active gas seepage. Methane concentrations are determined in the water column and in sediment pore waters and geomicrobiological analyses of the sediments from the seepage sites are used to assess microbial processes involved in the methane cycle.

We use sulfate and methane sediment pore water profiles to estimate the anaerobic oxidation of methane and stable isotopic analyses of methane are applied to identify biogenic or thermogenic methane sources. Concentration profiles of dissolved iron, ammonium and phosphate provide information on biogeochemical activity in the sediments.

The results of the geochemical investigations of seawater and sediment pore waters will ultimately be combined with the investigation of methane-derived carbonate crusts whose presence has recently been documented in the Hola area with an AUV based on photo and synthetic aperture sonar images. U-Th dating of these carbonate crusts will provide insights into past methane release and possible links with climate variations.

[1] Chand, S., Rise, L., Bellec, V., Dolan, M., Bøe, R., Thorsnes, T., Buhl-Mortensen, P., 2008. Active Venting System Offshore Northern Norway. *Eos, Transactions American Geophysical Union* 89, 261-262.

## Mobility of Au in the mantle

\*J. EDWARD SAUNDERS<sup>1</sup>, N. J. PEARSON<sup>1</sup>, SUZANNE Y. O'REILLY<sup>1</sup>, W. L. GRIFFIN<sup>1</sup>

<sup>1</sup>ARC Centre of Excellence for Core to Crust Fluid Systems (CCFS) and GEMOC, Macquarie University, NSW, 2109, Australia, (\*Correspondence: james.saunders@mq.edu.au)

Sulfides are the main host for Au in the silicate earth [1,2], but there are few reliable analyses of Au in mantle sulfides. As both a chalcophile and a highly siderophile element, Au is an important tracer of differentiation/ metasomatism in the mantle. Sulfides melt incongruently in the mantle, and are mobile in a range of melts and fluids; thus this component is readily modified during mantle processes. *In-situ* analyses are important for unravelling these processes, because multiple generations of sulfides are commonly present in mantle xenoliths [2, 3, 4].

We have analysed Au in sulfides hosted in peridotite xenoliths from eastern Australia, southeastern China and Spitsbergen (Arctic Norway). These data have been used to assess the average abundance of Au in mantle sulfides, and investigate how mantle processes affect their Au content. The variety of metasomatic characteristics, in terms of style and strength of metasomatism, in the three sample sets makes it ideal for understanding how Au behaves in the mantle.

The Au content in sulfides in mantle peridotites across all datasets is  $1.3 \pm 4.1$  ppm. This is similar to the limited data in the literature (global average Au =  $1.5 \pm 4$  ppm). Both this study, and the data in the literature indicate that sulfides in the continental lithospheric mantle contain less Au than would be calculated using whole-rock PUM values ( $\sim 2.5$  ppm). The pyroxenites studied have even lower Au contents (average Au =  $0.08 \pm 0.10$  ppm). This difference has important implications for the ability of mantle melts to transport Au, and as metasomatic agents.

While globally, mantle sulfides hosted in peridotites have a similar average and range of Au concentrations, there are important differences at local scales. This study shows the relationship between mantle metasomatism, as defined by silicate chemistry, and Au concentration in mantle sulfides. A significant amount of metasomatic sulfides can be introduced associated with the modification of the silicates, and these typically have a reduced Au content, similar to the low concentration observed in the pyroxenite melts analysed.

[1] Mitchell & Keays (1981) *GCA* **45**, 2425-2442. [2] Alard *et al.*, (2000) *Nature* **407**, 891-894 [3] Alard *et al.*, (2002) *EPSL* **203**, 651 – 663. [4] Griffin *et al.*, (2012) *Lithos*, **149**, 115- 135.

## Radiolysis and life in deep subseafloor sediment of the South Pacific Gyre

J. SAUVAGE<sup>1</sup>, A.J. SPIVACK<sup>1</sup>, A. G. DUNLEA<sup>2</sup>, R.W. MURRAY<sup>2</sup>, R. POCKALNY<sup>1</sup>, S. D'HONDT<sup>1</sup>  
AND IODP EXPEDITION 329 SHIPBOARD SCIENTIFIC PARTY

<sup>1</sup>Graduate School of Oceanography, University of Rhode Island, Narragansett, RI 02882, USA  
(\*correspondence :justine\_sauvage@my.uri.edu)

<sup>2</sup>Department of Earth and Environment, Boston University, Boston, MA 02215, USA.

The nature of the energy yielding mechanisms in the low-energy organic-poor sedimentary environment underlying the South Pacific Gyre (SPG) is not fully constrained. We used the approach of Wang *et al.* (2008) to quantify rates of organic-fuelled metabolic activities at most IODP Expedition 329 Sites (U1365 through U1370). At Site U1366 and U1370 net rates of oxygen-reducing organic oxidation averaged  $1.77\text{E-}2$  and  $1.64\text{E-}3$  fmol O<sub>2</sub> cell<sup>-1</sup> yr<sup>-1</sup>, respectively, representing a tremendously low cellular metabolism. At Site U1370, we observe net oxygen reduction throughout the entire sediment column. At Site U1366, statistically significant net oxygen reduction is not detected at depths greater than 11 meters below seafloor. Despite these low rates of organic oxidation, most cell counts are above the minimum detection limit throughout the entire sequence at both sites.

Hydrogen from natural radioactive splitting of water has been hypothesized to be a significant electron donor in organic-poor sediment of the SPG. Because water radiolysis produces H<sub>2</sub> and  $\frac{1}{2}$  O<sub>2</sub> simultaneously, oxidation of this H<sub>2</sub> does not contribute to net O<sub>2</sub> reduction in the sediment. Our calculation of radiolytic H<sub>2</sub> production, based on radioactive element content and sediment physical properties, indicate that on average  $5.63\text{E-}1$  and  $9.79\text{E-}2$  fmol H<sub>2</sub> yr<sup>-1</sup> cell<sup>-1</sup> is available throughout the sequence at Sites U1366 and U1370, respectively. Despite these relatively high production rates, dissolved H<sub>2</sub> abundances are below detection at both sites. These results suggest that H<sub>2</sub> from in situ water radiolysis fuels the predominant energy-yielding pathway for microbes in SPG sediment.

## O, Si, Fe isotopes and Ge/Si constraints on the preservation of signatures inherited from the formation of Isua BIFs

LUDIVINE SAUVAGE<sup>1\*</sup>, MARC CHAUSSIDON<sup>1</sup>,  
BÉATRICE LUIS<sup>1</sup> AND CLAIRE ROLLION-BARD<sup>1</sup>

<sup>1</sup>CRPG UMR 7358 CNRS-Univ. Lorraine, BP 20, 54501  
Vandoeuvre-lès-Nancy, France (\*lsauvage@crpg.cnrs-  
nancy.fr)

A 5.7 cm long sample, made of 9 alternating magnetite-rich and quartz-rich layers, of the oldest known example of archaean BIF (3.7-3.8 old Isua sample IF-G) was studied by ion microprobe for its O, Si and Fe isotopic compositions, and by laser ICP-MS for its trace element concentrations (Ge/Si ratios). Isotopic profiles across the layers were obtained with a resolution of 50-100 $\mu$ m (spot size 25 $\mu$ m) to look for systematic isotopic variations (total of 580  $\delta^{18}\text{O}$  data in quartz and magnetite, 441  $\delta^{30}\text{Si}$  in quartz and 641  $\delta^{56}\text{Fe}$  in magnetite). Ge contents in quartz were measured in parallel with a spot size of  $\sim$ 120 $\mu$ m.

$\delta^{56}\text{Fe}$  values range from -0.1 to +2.4‰ and are quite homogeneous ( $\pm$ 0.8‰,  $2\sigma$ ) within a given magnetite layer, with no significant differences between two successive layers, in agreement with previously published values [1, 2, 3]. Up to 3‰ variations in  $\delta^{18}\text{O}$  values are present in the magnetite and quartz layers (except one showing larger variations) with an average  $\sim$ 8‰ difference in  $\delta^{18}\text{O}$  between quartz (either in the quartz layers or in the magnetite layers) and magnetite, in agreement with isotopic equilibration under amphibolite facies metamorphism. In contrast to  $\delta^{18}\text{O}$  and  $\delta^{56}\text{Fe}$  values,  $\delta^{30}\text{Si}$  values show systematic "stratigraphic" isotopic variations (from -3.5 to 0‰) with significant differences between quartz in the quartz-rich and the magnetite-rich layers. Ge/Si ratios vary from 0.6 to  $1.2 \times 10^{-5}$  mole/mole (i.e., 7-14 ppm Ge). There are significantly lower than published data on bulk quartz layers from a Isua sample (Ge/Si  $> 2 \times 10^{-5}$  mole/mole [4]) due to the occurrence of Ge-rich amphiboles. Ge/Si variations seem to follow those of  $\delta^{30}\text{Si}$ . Because quartz is resistant to Si isotopic exchanges,  $\delta^{30}\text{Si}$  are likely to reflect variations in the conditions of formation and diagenesis of the Isua BIFs. Ge/Si ratios could trace temperature fluctuations and parent fluids of different origin.

[1] Dauphas, N. et al. (2007) *Geochim. et Cosmochim. Acta* **71**, 4745-4770. [2] Whitehouse M.J. and Fedo C.M. (2007) *Geology* **35**, 719-722. [3] Czaja, A.D. et al. (2013) *Earth Planet. Sci. Lett.* **363**, 192-203. [4] Frei R. & Polat A. (2007) *Earth Planet. Sci. Lett.* **253**, 266-281.

## How kimberlites form: Clues from olivine geochemistry

L. SAUZEAT<sup>1</sup>, C. CORDIER<sup>1</sup> AND N.T. ARNDT<sup>1\*</sup>

<sup>1</sup>ISTerre, Université de Grenoble, France (\*correspondence:  
Nicholas.Arndt@ujf-grenoble.fr)

The formation of olivine in kimberlites is not well understood. In most kimberlites, olivine occurs as large rounded single or polycrystalline nodules (1-10mm) and as small single crystals in the matrix. It is widely accepted that majority of them are xenocrysts produced by reaction and elimination of minerals from mantle peridotite either within kimberlite melts in transit toward the surface or within the mantle before. The compositions of the cores of olivines in polycrystalline nodules range widely, from about Fo92 to Fo83, whereas the rims have more restricted compositions, usually about Fo88.

In this study, we focus on very well preserved kimberlites from Kangamiut in Greenland. We conducted petrological studies and microprobe analyses along several profiles in one unusual polycrystalline nodule. This nodule is an assemblage of small closely packed fragments, most with the uniform composition Fo92, but some fragments have rims with lower Fo contents. Our results show that the fragment rims are complex and comprise an internal zone with variable forsterite contents (Fo88 to Fo92) but roughly constant minor element contents (e.g. 0.07 wt.% CaO and 0.35 wt.% NiO), and an external zone with near-constant Fo (Fo88) but variable minor element concentrations (0.09-0.41 wt.% CaO and 0.19-0.29% wt. NiO). This external zone is similar to the thin rim surrounding all the polycrystalline nodule. We attribute these compositions to two major processes. The first, which is responsible for the internal zone, occurred before the incorporation of the nodule in the kimberlitic magma and is related to "defertilisation" of peridotite in the lithosphere; i.e. reaction with CO<sub>2</sub>-rich fluids that removed pyroxene and garnet to produce a dunitic lithology. The second, which is responsible for the external zone, resulted from crystallization of olivine from the kimberlitic magma.

## Agés and deformation of felsic dikes within granulites and gneisses of the Gruf Complex, Central Alps.

J. SAVAGE<sup>1</sup>, A. MÖLLER<sup>1</sup>, J. OALMANN<sup>1</sup>  
AND R. BOUSQUET<sup>2</sup>

<sup>1</sup>Department of Geology, University of Kansas, USA,  
jsav1013@ku.edu, amoller@ku.edu, joalmann@ku.edu  
<sup>2</sup>Institute of Geosciences, Christian-Albrechts-Universität zu  
Kiel, Germany, bousquet@min.uni-kiel.de

Magmatic leucosomes and dikes in metamorphic terranes provide an opportunity to correlate accessory phase crystallization ages with the timing of deformation and metamorphic events as well as larger scale magmatic intrusions.

The Gruf Complex consists of migmatitic gneisses plus scarce charnockites and UHT sapphirine granulites. We identified several mineralogically distinct types of leucosomes and dikes: 1) foliation-defining, biotite-bearing leucosomes that are commonly folded; 2) medium-grained hornblende- and/or biotite-bearing granite pods crosscutting these leucosomes; 3) biotite-bearing pegmatite dikes, boudinaged or crosscutting the main foliation; 4) pegmatitic muscovite-, garnet-, beryll-bearing dikes, crosscutting all other rock types. Field observations indicate changing melt composition during and after regional metamorphism and associated deformation. Zircons from these dikes were dated by LA-ICP-MS to constrain deformation and metamorphism.

All analyzed samples contain oscillatory-zoned zircons with ages of 250–300 Ma. A leucosome within a brecciated metaperidotite enclave contains equant, sector-zoned  $32.2 \pm 0.2$  Ma zircons. Most dike sample zircons have rims of 28–30 Ma. An undeformed muscovite-bearing pegmatite dike crystallized at  $25.6 \pm 0.3$  Ma. Another muscovite-bearing pegmatite dike lacks zircon domains <28 Ma, probably due to insufficient Zr in the melt.

Apparent zircon saturation temperatures ( $T_{Zrs}$ ) for dike and leucosome samples are 680–890°C and uncorrelated with age. We attribute the wide  $T_{Zrs}$ -range to inherited zircon that did not dissolve in the melt. The pegmatite without <28 Ma zircon has a  $T_{Zrs}$  of 730°C suggesting its parental magma formed by partial melting of material similar to the deformed dikes, but did not exceed 730°C.

Conclusions: partial melting in the migmatites is coeval with the 30–32 Ma Bergell intrusion and main deformation. Dike emplacement and deformation continued until c. 24 Ma, coinciding with intrusion of the Novate granite and cooling of the granulites below the  $T_c$  of rutile at c. 500°C. The presence of 32 Ma zircons in all dikes indicates remelting of older leucosomes and dikes as the mechanism to produce the more fractionated pegmatites.

## The copper isotope composition of bulk Earth: A new paradox?

PAUL S. SAVAGE<sup>1\*</sup>, HENG CHEN<sup>1</sup>, GREGORY SHOFNER<sup>2</sup>,  
JAMES BADRO<sup>2</sup> AND FRÉDÉRIC MOYNIER<sup>1</sup>

<sup>1</sup>Washington University in St. Louis, MO 63130, USA  
(\*correspondence: savage@levee.wustl.edu,  
chenheng@levee.wustl.edu, moynier@levee.wustl.edu)  
<sup>2</sup>IPGP, Paris, France (gshofner@gmail.com, badro@ipdp.fr)

It is estimated that two thirds of terrestrial Cu is held in the core [1]; hence, to constrain the bulk Earth Cu isotope composition,  $\delta^{65}\text{Cu}$  estimates for both mantle (BSE) and core are required. By analysing a representative suite ( $n \sim 50$ ) of basaltic samples and their differentiates, we have investigated the behaviour of Cu isotopes during mantle melting and magmatic differentiation, and established a robust  $\delta^{65}\text{Cu}$  value for BSE. Our results show that, during fractional crystallisation, Cu isotopes can be fractionated to both lighter and heavier compositions, depending on crystallising phase. However, during partial melting, there is no resolvable fractionation. This implies that primitive basaltic melts are a good proxy for the Cu isotope composition of the mantle. Such analyses give an average  $\delta^{65}\text{Cu}_{\text{BSE}}$  value of  $0.07 \pm 0.12$  ‰ (2sd; relative to the standard NIST 976).

To estimate the Cu isotope composition of the Earth's core, we performed a series of piston-cylinder experiments to determine the  $\text{Cu}_{\text{metal/silicate}}$  isotope fractionation factor. These show that metal is preferentially enriched in the heavier Cu isotope, which agrees with empirical data from silicate-bearing iron meteorites [2]. Using these data to estimate a  $\delta^{65}\text{Cu}_{\text{CORE}}$  value, we calculate the Cu isotope composition of bulk Earth to be  $\delta^{65}\text{Cu}_{\text{BE}} \approx 0.16$  ‰. The “paradox” is as such: bulk Earth has a heavier Cu isotope composition than most (if not all) of the thus-far analysed chondritic meteorite groups [3, 4].

Assuming chondrites = bulk Earth, to explain this “missing  $^{63}\text{Cu}$ ”, we tentatively propose two possibilities:

- 1) Isotopically light Cu entered the Earth's core as a sulphide phase, or is stored in a thus-far unsampled part of the mantle, again in sulphides.
- 2) The light Cu isotope was preferentially lost as a result of volatile processes during Earth's accretion.

Alternatively, the current  $\delta^{65}\text{Cu}$  chondrite dataset does not represent bulk Earth, and further analyses are required.

[1] McDonough, *ToG*, 2003; [2] Williams and Archer, *GCA* **75**, 2011; [3] Luck *et al.*, *GCA* **67**, 2003 [4] Barrat *et al.*, *GCA* **83**, 2012.



## Nitrate and its N and O isotopes in a tropical marine boundary layer

J. SAVARINO<sup>1</sup>\* S. MORIN<sup>2</sup>, J. ERBLAND<sup>1</sup>, M. D. PATEY<sup>3</sup>,  
W. VICARS<sup>1</sup>, B. ALEXANDER<sup>4</sup> AND E. P. ACHTERBERG<sup>3</sup>

<sup>1</sup>LGGE/CNRS/UJF, BP 96, 38402 St Martin d'Hères, France  
(\*correspondance joel.savarino@ujf-grenoble.fr)

<sup>2</sup>CEN/Météo-France/CNRS, 38402 St Martin d'Hères, France  
(samuel.morin@meteo.fr)

<sup>3</sup>School of Ocean and Earth Science, University of  
Southampton, Southampton SO14 3ZH, UK  
(eric@noc.soton.ac.uk)

<sup>4</sup>Dept. of Atmospheric Sciences, University of Washington,  
Seattle, WA 98195-1640, USA (beckya@uw.edu)

Isotopic investigations are instrumental in deciphering sources and processes affecting atmospheric nitrate. Combining the analysis of the <sup>17</sup>O-excess ( $\Delta^{17}\text{O} = \delta^{17}\text{O} - 0.52 \delta^{18}\text{O}$ ) with the nitrogen stable isotope ratio (<sup>15</sup>N/<sup>14</sup>N) on the same sample is a powerful tool to reveal unexpected processes happening in the air [1].

Despite recent successes in using the isotope composition of nitrate for deciphering atmospheric chemical processes in polar and mid latitude regions [2, 3], the strong oxidative atmosphere of the sub tropical and tropical regions has been largely forgotten [4]. In order to partially fill this gap, we present a full seasonal cycle of the nitrate isotope systematic at the Cap Verde (Lat 16° 85'N, Long. 24° 87' W, Alt. 20m), characteristic of a tropical marine boundary layer (MBL).

While the concentration of nitrate at this MBL do not show any season variations, the oxygen isotopic characteristics display a pronounced seasonal cycle that is compatible with nitrate formation chemistry, which includes the BrNO<sub>3</sub> sink at a level of ca. 20 ± 10% of nitrate formation pathways. The results also suggest that the N<sub>2</sub>O<sub>5</sub> pathway is a negligible NO<sub>x</sub> sink in this environment. Observations further indicate a possible link between the NO<sub>2</sub>/NO<sub>x</sub> ratio and the nitrogen isotopic content of nitrate in this low NO<sub>x</sub> environment, possibly reflecting the seasonal change in the photochemical equilibrium among NO<sub>x</sub> species.

[1] Thiemens, M. H. (2006) *Annual Review of Earth and Planetary Sciences*, **34**, 217-262. [2] Morin, S. *et al. Science*, **322**, 730-732, doi: 10.1126/science.1161910. Michalski, G. *et al. (2003) Geophys Res Lett*, **30**, 1870, doi: 10.1029/2003gl017015. [4] Alexander, *et al. (2009), Atmos Chem Phys*, **9**, 5043-5056, doi: 10.5194/acp-9-5043-2009.

## Experimental modeling of silicates phosphatization in the hypergenesis zone

A.V. SAVENKO

Moscow M.V. Lomonosov State University, 119991, Moscow, Russia (correspondence: Alla\_Savenko@rambler.ru)

Now there was a concept that immobilization of dissolved phosphates on silicate minerals in the hypergenesis zone occurs on the mechanism of superficial adsorption. At the same time it is possible to assume that alongside with it process of silicates phosphatization similar to widespread process of silicates carbonatization proceeds. This hypothesis was verified during the longtime experiments.

The phosphatization of two basic clay minerals (kaolin and montmorillonite) was studied after two-year long interaction with 0.25–5.0 mM orthophosphate solutions under acidity conditions ranged pH 1.8–8.8. The results have shown (figure) that variation of dissolved phosphorus and silicon concentrations at pH 3.7–8.8 is close to equivalent:  $\Delta[\text{Si}] \approx -\Delta[\text{P}]$  whereas  $\Delta[\text{Si}]$  value at pH 1.8 is in 1.5–2 times exceeds decrease in phosphates concentration. Quantity of phosphorus immobilized by clay minerals is in direct proportion of its equilibrium concentration in the solution:  $-\Delta[\text{P}] = k[\text{P}]_{eq}$ . The proportionality factor  $k$  is identical to all studied samples and decreases from 0.58 till 0.44 at the pH increase with 1.8 up to 8.8. Quantity of silicon passing in the dissolved forms reaches 6–20% of total amount of silica in the solid phase. It specifies phosphatization of clay minerals which products are dissolved silica and poorly soluble basic aluminium phosphates.

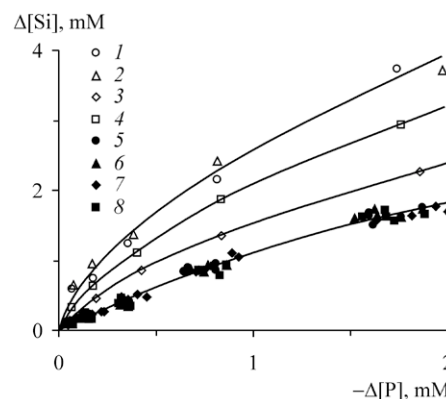


**Figure:** Relationship between variation of dissolved phosphorus and silicon concentrations at the clay minerals phosphatization. pH 1.8/3.7–8.8: 1/5 – kaolin, Glukhoveck; 2/6 – ditto, Podolsk; 3/7 – montmorillonite, Askanija, sample 1; 4/8 – ditto, sample 2.



## Multi-proxy investigation of Holocene climate in West Siberia using peat deposits

YU. V. SAVINYKH,<sup>1</sup> N. PEDENTCHOUK,<sup>2</sup> YU.I. PREIS<sup>3</sup> AND E.V.GULAYA<sup>1</sup>

<sup>1</sup>Institute of Petroleum Chemistry SB RAS, Tomsk, Russia, [yu-sav2007@yandex.ru](mailto:yu-sav2007@yandex.ru)

<sup>2</sup>School of Env. Sciences, University of East Anglia, Norwich, UK

<sup>3</sup>Institute of Monitoring of Climatic and Ecological Systems SB RAS, Tomsk, Russia

West Siberia is a vast region that covers a large part of northern Asia and, in spite of its size, is relatively homogenous in terms of topography and climate. It is an ideal target for studying palaeoclimate, because even a relatively limited number of sites would provide representative data for investigating climate changes that affect large areas of this region. This project uses a multi-proxy approach to study Holocene climate change in West Siberia.

A peat core was obtained from an ombrotrophic bog located in the vicinity of Tomsk. Bog vegetation is dominated by peat moss, but also comprises a substantial number of vascular plant species. The base of the 6.5-m-long core was dated at 10,500 cal yr BP. Organic matter was subjected to palynological, biomarker, and stable isotopic analyses.

Our preliminary testate amoebae (analyst I.V.Kurina) and *n*-C<sub>23</sub> alkane (sourced mainly by *Sphagnum* spp.)  $\delta$ D in the upper 260 cm of the core show the following patterns. The percentage of hydrophilic testate amoebae starts to increase from the background level at 140-135 cm, reaches its peak at 125-115 cm, drops to a minimum at 85-65 cm, and then undergoes an increase towards the top of the core. The  $\delta$ D values of *n*-C<sub>23</sub> decrease from -170‰ at c. 200 cm to -225‰ at 105-100 cm, change sharply to -210‰ at 95-85 cm and then reach -190‰ at the top. Because more negative  $\delta$ D values of *Sphagnum* spp. could indicate colder or wetter (or a combination of both) climate, we suggest that these two data sets point to a period of wetter climate during the time interval recorded by the peat sequence between 140 and 100 cm. The integration of our data with palynology from previously published reconstructions of West Siberian climate from 500 and 1700 cal yr BP, corresponding to c. 150-50 cm of our core, suggests a period of cold and wet climate. Our ongoing work on biomarker and stable isotopic compositions of various sources of organic matter in this core will allow us to provide more detail with regards to palaeoclimatic changes during this and earlier time intervals in the Holocene.

## Boron isotopes in boninites from the Izu-Bonin-Mariana arc system: Insights into subduction initiation

IVAN P. SAVOV<sup>1</sup> AND SAMUELE AGOSTINI<sup>2</sup>

<sup>1</sup>Univ. Leeds, School of Earth & Environment, Leeds LS2-9JT, UK; [i.savov@leeds.ac.uk](mailto:i.savov@leeds.ac.uk); <sup>2</sup>Istituto di Geoscienze

e Georisorse- CNR, Pisa, Italy [s.agostini@igg.cnr.it](mailto:s.agostini@igg.cnr.it)

The origin of boninites has long been debated and several mechanisms for their formation have been proposed [1]. These rocks have both high MgO contents and somewhat LREE+LILE enrichments, thus their genesis should involve large percentage melting of highly melt-depleted but also highly fluid metasomatized mantle sources. One mechanism to explain boninite generation in the Izu-Bonin-Marianas (IBM) arc-basin system invokes sinking of cold Pacific oceanic slabs, trench retreat and intense backarc spreading [1]- all resulting in anomalous mantle melting conditions and voluminous boninite eruptions close in time and space to the oldest mafic volcanic arc rocks in IBM at ~ 51 Ma [2]. Since the mantle is extremely depleted in B and has very negative  $\delta^{11}\text{B}$  ratios and the slab fluids have very positive  $\delta^{11}\text{B}$  signatures, B and B isotope ratios are able to trace the slab-fluid additions and the resulting boninite generation. We have selected a suite of representative boninites from the the Izu-Bonin (Bonin Ridge) and the Marianas (Guam Island) segments of the IBM. The boninites all have remarkably similar  $^{87}\text{Sr}/^{86}\text{Sr}$  (0.7042-0.7049) and  $^{143}\text{Nd}/^{144}\text{Nd}$  (0.51283-0.51297) isotope signatures. Interestingly the boninites  $\delta^{11}\text{B}$  ranges from +0.9 to +5.1 permil (data always better than  $\pm 1$  per mil), supporting models for early slab fluid liberation via dehydration of old foundering Pacific slabs. Such fluid additions are necessary for lowering the melting temperature of the depleted mantle wedge and for boninite generation. Based on the isotope (B, Nd, Sr) and trace element similarities we envision the boninite sources to be chemically similar to blueschist-containing serpentinite muds and serpentinitized peridotites erupted today via mud volcanoes in the IBM forearc and successfully drilled during ODP Legs 195 and 125 [3]. Links between high Mg arc volcanic rocks and serpentinite-derived fluids are becoming increasingly common [4] and we will discuss possible links between metamorphic petrology of the slab inventory, island arc magma generation and the usefulness of B isotopes as tracer.

[1] Leng & Gurnis (2011), *Geochem. Geophys. Geosyst.*,12,Q12018; [3] Ishizuka *et al.* (2011), *EPSL* 306; [3] Savov *et al.* (2007), *JGR-Solid Earth* 112, B09205 [4] Tonarini *et al.* (2007), *Geochem. Geophys. Geosyst.*,8, Q09014.

## Stable C and O isotope ranges of African land snail shells

Y. SAWADA<sup>1\*</sup>, D. L. DETTMAN<sup>2</sup> AND M. PICKFORD<sup>3</sup>

<sup>1</sup>Shimane Univ. 402-1 Fukushima, Kurashiki 710-0048, Japan  
(\*correspondence: yoshipikotan4306@sky.megaegg.ne.jp)

<sup>2</sup>Environ. Isotope Lab. Dept. Geosciences, Univ. Arizona,  
Tucson, AZ85721 (dettman@email.arizona.edu)

<sup>3</sup>Muséum National d'Histoire Naturelle, France  
(pickford@mnhn.fr)

Cenozoic fossil land snails can be found in many continental sections (Pickford, *J. African Earth Sci.*1995). We show how stable C and O isotope ranges of modern land snail shell from various ecosystems in Africa are related to snail genus, climate, and diet. Sequential powdered samples are drilled following growth lines through multiple years of shell growth to document stable isotope response to seasonal environmental variation. Results are summarized as follows:  $\delta^{13}\text{C}$ : Variation within one specimen is small. Shell  $\delta^{13}\text{C}$  primarily responds to differences in diet, i.e. C3 plants, C4 plants, and the ingestion of carbonate from detritus, bedrock or soil.

$\delta^{18}\text{O}$ : (1) Snails of the same genus from same ecosystem have similar values. (2) Oxygen isotope ranges from tropical forest, upland forest, coastal steppe, semi-desert and desert are small, with forest values generally lower than desert or semi-desert. (3) Regions with pronounced dry and wet seasonality (savannah, Mediterranean) can have large seasonal variation in  $\delta^{18}\text{O}$ . Within one climate type, snails of different genus often have similar ranges, although sometimes ranges are different. Habitat/climate has a stronger control on shell chemistry than taxonomy.

The  $\delta^{13}\text{C}$  and  $\delta^{18}\text{O}$  ranges of land snail shells reflect ecosystems, diet, and perhaps micro-habitat preference. Land snail fossils are potential targets for paleoenvironmental reconstruction based on a combination of faunal analysis and stable isotope geochemistry. [abbreviation] C:  $\delta^{13}\text{C}$  VPDB, O:  $\delta^{18}\text{O}$ , VPDB.

[Tropical forest: Gabon, Uganda, Tanz.] *Leptocala* C: -11.28 ~ -13.28; O: -0.97 ~ -3.29; *Trochonanina* C: -14.20 ~ -15.56; O: +0.39 ~ -1.74; *Thapsia* C: -11.80 ~ -13.35; O: -1.37 ~ -3.55; *Limicolaria* C: -12.68 ~ -15.36; O: +1.01 ~ -3.85; *Achatina* C: -8.45 ~ -13.02; O: +0.13 ~ -2.83 [Upland forest: Kenya, Ug.] *Limicolaria* C: -9.37 ~ -11.41; O: +1.41 ~ -2.13; C: -7.90 ~ -10.02; O: +3.45 ~ -0.07; C: -8.35 ~ -12.33; O: +2.03 ~ -2.23; *Trochonanina* C: -0.24 ~ -5.22; O: +1.63 ~ -1.25 [Savannah woodland: Namibia, Kenya, Mozambique] *Xeroceratus* C: -6.37 ~ -7.99; O: -2.31 ~ -7.76; *Achatina* C: -5.96 ~ -10.90; O: +5.38 ~ -5.42; C: -4.84 ~ -13.83; O: +5.59 ~ -4.65; C: -8.37 ~ -13.82; O: +1.33 ~ -8.16; *Limicolaria* C: -1.82 ~ -7.92; O: +2.91 ~ -4.64 [Mediterranean: Morocco] *Helicopsis* C: -3.19 ~ -4.62; O: +0.74 ~ -0.99; *Rumina* C: -9.27 ~ -9.80; O: +5.76 ~ -1.08; *Kabylia* C: -5.31 ~ -7.01; O: +3.48 ~ -0.07 [Coastal steppe: Oman] *Rochebrunia* C: -4.49 ~ -7.67; O: +2.95 ~ +0.92; *Euryptyxis* C: -9.28 ~ -10.88; O: +0.80 ~ +0.37; *Obeliscella* C: -7.88 ~ -9.52; O: +1.42 ~ -1.02 [Semi-desert: Nam. Ug.] *Dorcasia* C: -5.91 ~ -8.58; O: +3.89 ~ -0.12; *Bloyetia* C: -5.96 ~ -7.32; O: +2.79 ~ -1.21 [Desert: Nam.] *Dorcasia* C: -0.18 ~ -1.03; O: +3.37 ~ +1.26; *Trigonephrus* C: -0.20 ~ -2.75; O: +5.70 ~ +3.27.

## Seasonal methane fluxes and sulfate reduction rates in a eutrophied Baltic estuarine system

JOANNA E. SAWICKA\*, CAMILLA OLSSON AND VOLKER BRÜCHERT

Department of Geological Sciences, Stockholm University  
Svante Arrhenius Väg 8, 10691 Stockholm, Sweden  
(\*joanna.sawicka@geo.su.se)

Estuaries and shelves are thought to be the source of 75% of the oceanic  $\text{CH}_4$  emissions to the atmosphere, but to date relatively few data are available that report spatial and seasonal variations in production and emission of  $\text{CH}_4$  from sediments in eutrophied coastal settings. Himmerfjärden (Baltic Sea, Sweden) is an estuary with a surface area of 174  $\text{km}^2$ . The estuary has a well-described eutrophication gradient from the inner part of the estuary to the opening, which is due to a sewage treatment plant (STP) in the inner estuary that has been discharging treated sewage since 1973. The sediments in the bay consist of organic-rich postglacial mud, sand, and glacial clay.  $\text{CH}_4$  fluxes at sediment/water interface, pore water concentrations of  $\text{SO}_4^{2-}$ ,  $\text{CH}_4$ , and  $\text{H}_2\text{S}$ , and  $^{35}\text{S}$ -sulfate reduction rates were measured in the spring, summer, autumn, and winter in the estuary at two stations, one close to the STP and one at a reference site outside the estuary. Additionally, sea-air fluxes and  $\text{CH}_4$  water column concentrations were measured at the two stations.

Benthic methane fluxes were determined from ex-situ incubations and showed seasonal and spatial variations. The lowest  $\text{CH}_4$  flux ( $0.1 \text{ mmol m}^{-2}\text{d}^{-1}$ ) was observed in winter at the reference site and the highest  $\text{CH}_4$  flux ( $8.74 \text{ mmol m}^{-2}\text{d}^{-1}$ ) was recorded in the summer in Himmerfjärden sediment. For the other seasons,  $\text{CH}_4$  fluxes at both stations were between  $1 \text{ mmol m}^{-2}\text{d}^{-1}$  and  $2 \text{ mmol m}^{-2}\text{d}^{-1}$ . Sulfate reduction rates showed spatial variability and were consistently 10-fold higher in Himmerfjärden ( $\sim 0.3 \mu\text{mol cm}^{-3}\text{d}^{-1}$ ) than at the reference site. There was a distinct zone of organoclastic sulfate reduction in both sediments at 3-7 cm depth. In the contaminated sediments near the STP, the sulphate-methane transition zone (SMT) was observed persistently during the year at depths 12-16 cm, indicating the presence of anaerobic methane oxidation, but was not detected above 40 cm depth at the reference site. Water column  $\text{CH}_4$  concentration profiles showed that the sediments are the major source of  $\text{CH}_4$  in the water column, as there was a pronounced increase in concentrations towards the bottom. Near-bottom water  $\text{CH}_4$  concentrations were between 109 and 131  $\text{nmol/l}$ . Concentrations at the surface were generally two-fold lower indicating efficient methane oxidation in the water column. Nevertheless, surface waters at both stations were oversaturated with respect to  $\text{CH}_4$  throughout the year indicating that Himmerfjärden is an annual net source of  $\text{CH}_4$  to the atmosphere.

## Thermodynamics of the C-H-O fluid at extreme conditions

S.K. SAXENA<sup>1\*</sup>, R. HRUBIAK<sup>1</sup>, V. DROZD<sup>1</sup>,  
A.B. BELONOSHKO<sup>2</sup>, P. SHI<sup>3</sup> AND G. ERIKSSON<sup>4</sup>

<sup>1</sup>Department of mechanical and materials engineering, Florida International University, Miami, FL 33199, USA (\*correspondence: saxenas@fiu.edu)

<sup>2</sup>Department of Metallurgy, Royal Technical University, Stockholm, Sweden

<sup>3</sup>Thermo-Calc AB, Stockholm, Sweden

<sup>4</sup>GTT-Technologies, Aachen, Germany

The superfluid model [1] for calculation of high pressure-temperature fluid fugacities builds on the combination of experimental data on pure and mixed fluids at temperatures lower than 1000 K over several kilobars and molecular dynamics generated data at extreme conditions (> 5 kbar and up to 100 GPa and 4000 K). The model is found to be generally consistent with post-publication (since 1992) experimental data. The calculated data on water at low pressure differs significantly from the Brodholt-Wood fluid inclusion data [2] but closely reproduces the densities measured by Abramson and Brown [3]. The superfluid model and the model of Zhang and Duan [4] are closely similar.

We have used the model to calculate high pressure and temperature phase equilibrium in binary (MgO-CO<sub>2</sub>, Al-H<sub>2</sub>), ternary (Fe-H<sub>2</sub>O-C, wustite-H<sub>2</sub>O-C) and multicomponent (carbonaceous chondrite) systems. The results show that while a carbonate may be stable over the entire range of the mantle pressures and temperatures, it is not stable if the mantle is chondritic in composition. Iron carbide (Fe<sub>3</sub>C), on the other hand, is stable to extreme pressure and temperatures in the ternary as well as in chondritic composition and may be a good candidate to be assimilated in the core. The conclusions are that a) the carbonate may not be the storage for CO<sub>2</sub> in the deep earth and b) carbon is more likely stored in Earth's core as carbide and as diamond in the mantle.

The authors wish to acknowledge the support and collaboration of the Deep Carbon Observatory.

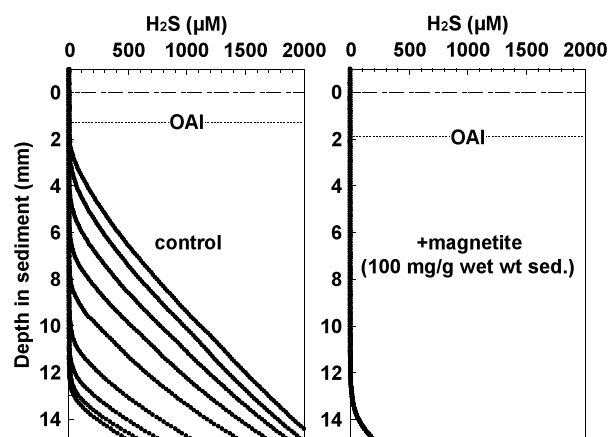
[1] Belonoshko, A.B., Shi, P., Saxena, S.K. (1992) *Computer and Geosciences* **18**, 1267–1269. [2] Brodholt, J.P., Wood, B.J. (1994) *Geochim. Cosmochim. Acta* **58**, 2143–2148. [3] Abramson, E.H., Brown, J.M. (2004) *Geochim. Cosmochim. Acta* **68**, 1827–1835. [4] Zhang, C., Duan, Z. (2009) *Geochimica et Cosmochimica Acta* **73**, 2089–2102.

## Effect of magnetite addition on H<sub>2</sub>S dynamics in coastal marine sediment

M. SAYAMA

National Institute of Advanced Industrial Science and Technology (AIST), Tsukuba 305-8569, Japan  
(m.sayama@aist.go.jp)

It has been well known that magnetite is poorly reactive towards dissolved sulfide (H<sub>2</sub>S) on a time scale of hours to days (Canfield *et al.*, 1992; Raiswell and Canfield, 1996; poultou *et al.*, 2004). However, microprofiles of H<sub>2</sub>S in experimental sediment cores made with coastal marine surficial sediment showed a dramatic change by the addition of magnetite (Fig. 1). The depth of H<sub>2</sub>S front at which H<sub>2</sub>S concentration starts to increase stayed at the original even after four days incubation in the core with magnetite addition (Fig. 1, right), whereas the H<sub>2</sub>S front moved up quickly and reached to the oxic-anoxic interface (OAI) within 24 hours in the control core (without magnetite addition) (Fig. 1, left). Possible mechanism to explain these results might be electrochemical oxidation of H<sub>2</sub>S at deep with long distance electron (e<sup>-</sup>)-transfer through solid state cycling of structural Fe<sup>2+</sup> and Fe<sup>3+</sup> in magnetite (Latta *et al.*, 2011).



## The partitioning of trace elements between clinopyroxene and trachybasaltic melt during rapid cooling

P. SCARLATO<sup>1</sup>, S. MOLLO<sup>1</sup>, J. D. BLUNDY<sup>2</sup>, G. IEZZI<sup>3</sup>  
AND A. LANGONE<sup>4</sup>

<sup>1</sup>Istituto Nazionale di Geofisica e Vulcanologia, Via di Vigna Murata 605 00143 Rome, Italy (\*correspondance: mollo@ingv.it)

<sup>2</sup>School of Earth Sciences, University of Bristol, Wills Memorial Building, Bristol BS8 1RJ, UK

<sup>3</sup>Dipartimento INGEO, Università G. d'Annunzio, Via Dei Vestini 30, 66013 Chieti, Italy

<sup>4</sup>C.N.R.- Istituto di Geoscienze e Georisorse, UOS Pavia, via Ferrata 1 27100 Pavia, Italy

### Variation of trace element partition coefficients

We present the variation of trace element partition coefficients measured at the interface between rapidly cooled clinopyroxene crystals and co-existing melts. Results indicate that, Ds for REE, HFSE and TE increase with increasing cooling rate, in response to clinopyroxene compositional variations. The entry of REE into the M2 site is facilitated by a coupled substitution where either Na substitutes for Ca on M2 site or Al<sup>iv</sup> substitutes for Si in the tetrahedral site. Due to the lower concentration of Ca in rapidly cooled clinopyroxenes, LILE on M2 decrease at the expense of monovalent cations. Conversely, higher concentrations of HFSE and TE on the M1 site are facilitated as the average charge on this site increases with the replacement of divalent-charged cations by Al<sup>vi</sup>. At both equilibrium and cooling rate conditions, Ds for isovalent cations define parabola-like curves when plotted against ionic radius, consistent with the lattice strain model.

### Implications

Although crystallization kinetics alter clinopyroxene composition, deviations from equilibrium partitioning are insufficient to change the tendency of a trace element to be compatible or incompatible. Consequently, there are regular relationships between ionic radius, valence of the trace element and D. Under both equilibrium and cooling rate conditions, the partitioning of trace elements is driven by charge-balance mechanisms; cation substitution reactions can be treated in terms of the energetics of the various charge-imbalanced configurations.

## A Pilot Br Isotopic Study of Arid Playa Lakes and Ordinary Chondrites

BRUCE F SCHAEFER<sup>1</sup>

<sup>1</sup>CCFS, Department of Earth and Planetary Sciences, Macquarie University, NSW 2109, Australia  
(Bruce.Schaefer@mq.edu.au)

**Introduction:** Bromine possesses a chemistry broadly comparable to that of Cl and F, however its heavier mass and lower abundance results in slightly different behaviours in geochemical cycling. For example it is disproportionately enriched in sea water with respect to Cl. Br can be considered to be a “hydrophile” element, and hence its behaviour is in governed by that of water. It possesses two isotopes <sup>79</sup>Br (50.686%) and <sup>81</sup>Br (49.314%).

This study has developed new chemical extraction, and most significantly, new mass spectrometric protocols for Br isotopes on silicates, evaporites and waters using N-TIMS methodologies. Existing CF-IRMS methodologies offer internal precision of ~0.3‰ (1SD, [1]), whereas N-TIMS measurements of laboratory HBr and seawater standards produce external reproducibility of <0.07‰ (1SD) over an 18 month period with internal precision typically <0.06‰ (1SD) on single analyses.

This study presents the first high precision, N-TIMS isotopic data on playa lake evaporites and ordinary chondrites, recording a >5‰ variation in solar system <sup>81</sup>Br/<sup>79</sup>Br.

[1] Shouaker-Stash *et al.*, *Anal. Chem.*, **77**; p4027-4033, 2005.

## New data on anisotropy and composition dependence of Na/K-interdiffusion in alkali feldspar

A.-K. SCHAEFFER<sup>1</sup>, E. PETRISHCHEVA<sup>1</sup>, G. HABLER<sup>1</sup>, R. ABART<sup>1</sup> AND D. RHEDE<sup>2</sup>

<sup>1</sup>University of Vienna, Department of Lithospheric Research, Vienna, Austria (anne-kathrin.schaeffer@univie.ac.at)

<sup>2</sup>GFZ German Research Centre for Geosciences, Telegrafenberg, 14473 Potsdam, Germany

Cation exchange experiments have been conducted using crystallographically oriented plates of gem quality sanidine as starting material.

The observed geometry of the diffusion fronts can be explained by a composition dependence of the interdiffusion coefficient. We extracted the composition dependence of the interdiffusion coefficient from our measured data by use of the Boltzmann transformation in the composition interval between  $X_{Or}$  0.5 and 1 for the directions (001) and (010).

At 850°C the interdiffusion coefficient  $D$  is nearly constant at  $0.3 \times 10^{-15} \text{m}^2 \text{s}^{-1}$  over the composition range  $X_{Or}$  0.50 to 0.95 and then rises steeply to values of  $2.5 \times 10^{-15} \text{m}^2 \text{s}^{-1}$  for profiles normal to (001). Normal to (010)  $D$  is nearly constant at  $0.03 \times 10^{-15} \text{m}^2 \text{s}^{-1}$  over the composition range  $X_{Or}$  0.5 to 0.97 before, too, rising steeply at higher  $X_{Or}$ . Thus interdiffusion normal to (001) is faster by a factor of about ten than interdiffusion normal to (010).

Christoffersen *et al.* [1] measured interdiffusion coefficients in the composition range between  $X_{Or}$  0.1 to 0.8 in diffusion couple experiments. They observed a similar anisotropy but they find a composition dependence of  $D$  for intermediate compositions which disagrees with our findings. Also, their absolute values for the interdiffusion coefficient at a given composition are smaller by about a factor of ten.

Comparison with theoretical calculations of the interdiffusion coefficient from self-diffusion data found in literature [2, 3] using the Manning relation for interdiffusion in ionic crystals shows a rough fit for interdiffusion normal to (001) while the slower interdiffusion normal to (010) deviates significantly from what would be expected.

The activation energy also shows an anisotropy; normal to (001) it is about 340 kJ/mole while it is 250 kJ/mole normal to (010).

[1] Christoffersen *et al.* (1983) *American Mineralogist*, **68**, 1126-1133. [2] Foland (1974) *Geochemical Transport and Kinetics*, 77-98. [3] Kasper (1975) *Ph.D. thesis, Brown University*.

## The geochronological signal of a dying magma system

U. SCHALTEGGER<sup>1</sup>, C. BRODERICK<sup>1</sup> AND J.F. WOTZLAW<sup>1</sup>

<sup>1</sup>Section of Earth and Environmental Sciences, University of Geneva (urs.schaltegger@unige.ch, joern.wotzlaw@unige.ch, cindy.broderick@unige.ch)

U-Pb dating of zircon is the most commonly used geochronometer for temporal quantification of pluton and batholith forming processes. High-precision zircon  $^{206}\text{Pb}/^{238}\text{U}$  dating repeatedly produces a dispersion of ~50-200 ka between the oldest and youngest zircon of the same sample, and of up to 1 Ma within a plutonic unit, pointing to a prolonged magmatic evolution with non-monotonously varying parameters like melt temperature, crystallinity and melt composition. Combining high-precision U-Pb dates with trace element and Hf isotope analysis on the same dated volume of zircon, we are able to trace different processes acting during the assembly of a pluton and quantify their timing: 1) changing melt composition due to fractional crystallization of zircon and of other accessory minerals (e.g., titanite) over time; 2) quantify the evolution of overall crystallinity of a magmatic body over time; 3) changes in magma temperature by identifying periods of enhanced and suppressed zircon crystallization, and correlate them with periods of mafic magma recharge and thermal rejuvenation of the system; 4) changing sources of incoming melts over time by linking initial Hf isotopes to crystallization age.

Probability density functions of  $^{206}\text{Pb}/^{238}\text{U}$  zircon dates of a pluton usually point to several peaks of enhanced zircon crystallization during a prolonged period of increasing crystallinity of the magma, leading to stalling of the crystal mush and subsequent complete solidification at upper crustal levels. The non-steady decrease of the volume of potentially eruptible crystal-poor liquid leads eventually to the "plutonic death" of a magmatic system.

## Labile structures in organic matter under the influence of multivalent cations – an issue for dynamic interfaces?

GABRIELE ELLEN SCHAUMANN<sup>1</sup>

<sup>1</sup>University Koblenz-Landau, Insitute for Environmental Sciences, Fortstr. 7, Landau, Germany, schaumann@uni-landau.de

Soil organic matter (SOM) controls large part of the processes occurring at biogeochemical interfaces in soil and may contribute to sequestration of organic chemicals. In this contribution, the idea that sequestration of organic chemicals is driven by physicochemical SOM matrix aging, and its consequences for transport processes will be discussed. In contrast to chemical aging processes, physical matrix aging involves changes in the supramolecular arrangement of SOM molecules and molecule segments. Organic chemicals can be entrapped in nanovoids, which can transform to a semi-persistent cage. Persistence of entrapment directly depends on the rigidity and stability of the cage. Water molecule bridges (WaMB) and cation bridges (CaB) between segments of soil organic matter (SOM) have been found to stabilize the supramolecular SOM matrix and are therefore suspected to control immobilization of organic chemicals in soil. Contaminants sequestered by WaMB or CaB can be immobilized or released suddenly upon changes in environmental conditions like moisture, temperature or melting. Understanding their dynamics is highly important to model the reaction of soil as well as release and transport of organic chemicals on changes in climatic conditions. While the idea of CaB in solid soil organic matter is more and more accepted, there is increasing evidence that such cross-links are not relevant in all types of soil organic matter, depending on the spatial distribution of charged functional groups in the OM. Only if distances between functional groups are sufficient, CaB can form. Larger distances can be bridged by CaB-WaMB associations. Also interfacial properties are dynamic. Soil wettability can with increasing involvement of functional groups in CaB-WaMB associations. In the extreme case, high concentrations of multivalent cations can hydrophobize surfaces of SOM. Associations of CaB and WaMB evolve slowly and form a supramolecular network in SOM. Those dynamic associations can fix molecular arrangements inducing water repellency and increase kinetic barriers for the release and uptake of water and sorption and transport of organic chemicals in soil.

## The role of soil Cu in chelate mediated Fe acquisition by plants

W.D.C. SCHENKEVELD<sup>1\*</sup> AND S.M. KRAEMER<sup>1</sup>

<sup>1</sup>University of Vienna. Dept. of Environmental Geosciences, Althanstrasse 14, 1090 Wien, Austria  
walter.schenkeveld@univie.ac.at (\* presenting author)

Iron is an essential micronutrient to plants. In soils with a neutral to alkaline pH, the solubility of Fe bearing minerals is very low and can become limiting for plant growth. To avoid Fe deficiency in plants grown on such soils, the solubility of Fe needs to be increased. This can be established by means of chelating agents, which strongly bind Fe and form a soluble Fe complex. These chelating agents can either have a natural or an antropogenic origin.

Grasses (including wheat, barley and rice) are very efficient in preventing Fe deficiency, because their Fe acquisition strategy includes the exudation of chelating agents called phytosiderophores (PS). These PS can dissolve soil Fe and the resulting FePS complex can be taken up by a high affinity membrane transporter. In agricultural practice, plant species that are less efficient in acquiring Fe are commonly supplied with micronutrient fertilizers based on synthetic chelating agents. For Fe fertilization on calcareous soils, FeEDDHA (iron ethylene diamine bis-N,N'-hydroxyphenyl acetic acid) is among the most effective.

Soils contain several metals that can compete with Fe for binding to chelating agents, thereby compromising the efficiency of the chelate mediated Fe uptake mechanism. Cu is among the stronger competitors and occurs in soil in quantities that could substantially compromise Fe uptake.

It will be shown and discussed that the extent to which Cu effectively competes with Fe for complexation under soil conditions is controlled by both thermodynamic and kinetic factors. These factors include the specific affinity of the chelating agent for Fe and Cu, the Fe and Cu activity in the soil, the extent to which metal complexes adsorb to reactive soil components, the mobilization rate of Fe and Cu, and the displacement rate of Fe from the Fe-chelate by Cu. Both with PS and synthetic Fe chelates, Cu may considerably limit the time-span the chelating agent remains effective as Fe transporter.

## New insights into simultaneous determination of mass-dependent isotopic fractionation and radiogenic isotope variations of strontium by multi-collector ICPMS

HOWIE D. SCHER<sup>1</sup>, ELIZABETH M. GRIFFITH<sup>2</sup>  
AND WAYNE P. BUCKLEY JR.<sup>1</sup>

<sup>1</sup>Department of Earth and Ocean Sciences, University of South Carolina, hscher@geol.sc.edu

<sup>2</sup>Department of Earth and Environmental Sciences, University of Texas at Arlington, lgriff@uta.edu

Variability of Sr isotope ratios are due to radioactive decay and mass dependent fractionation through various physiochemical reactions. Radiogenic Sr ratios are used for geochronology and provenance while stable isotope ratios of Sr reveal mechanisms of sample formation and resolve mass balance in geochemical systems.

Accurate and precise measurements of stable Sr isotope ratios (e.g., <sup>88</sup>Sr/<sup>86</sup>Sr) are possible if the ratio can be corrected for mass-discrimination effects during analysis. Ohno and Hirata (2007) developed a method where Sr solutions were doped with Zr, and measured <sup>88</sup>Sr/<sup>86</sup>Sr ratios were normalized to <sup>91</sup>Zr/<sup>90</sup>Zr=0.2181, while simultaneously measuring <sup>87</sup>Sr/<sup>86</sup>Sr. Using standard sample bracketing combined with a Zr correction, we tested three variables that influence the mass-discrimination effect on the multi-collector ICPMS. All stable isotope ratios are reported relative to SRM987.

First, solutions of 500 ppb SRM987 with Ba/Sr from 0.002 to 200 were analyzed by bracketing against a SRM987 solution with no Ba. Deviations from  $\delta^{88}\text{Sr}=0\text{‰}$  occur above Ba/Sr ratios of 10. Deviations from our long term <sup>87</sup>Sr/<sup>86</sup>Sr value also occur above this level of Ba.

Second, seawater was processed through standard microcolumn extraction with SrSpec resin (Eichrom). Eluted Sr was adjusted to 250 ppb and Zr was added so that Sr/Zr was ~1. We repeated the Ba doping experiment using the Zr correction. When Ba/Sr<10 the measured  $\delta^{88}\text{Sr}$  is  $0.37\pm 0.05\text{‰}$  (2 $\sigma$ , n=28) which is within analytical precision of published values for seawater (0.35 to 0.39). Deviations occur above Ba/Sr = 10.

Lastly we tested the Zr/Sr ratio on the measurements of  $\delta^{88}\text{Sr}$  in seawater. We determined that the ideal Zr/Sr ratio is slightly lower than unity, and that high Zr/Sr ratios result in inaccurate  $\delta^{88}\text{Sr}$  determinations.

[1] Ohno T., and Hirata T. (2007) *Analytical Sciences*, **23**, 1275-1280

## Dahomeyan Neoproterozoic imprint on Eburnean Palaeoproterozoic rocks in southeast Ghana – Rubust Ar, flimsy Pb

ANDERS SCHERSTÉN<sup>1</sup>, LAURENCE PAGE<sup>1</sup>, PER KALVIG<sup>2</sup>,  
ANDREAS PETERSSON<sup>1</sup> AND SOLOMON ANUM<sup>3</sup>,

<sup>1</sup>Department of Geology, Lund University, Sölvegatan 12, SE-223 62 Lund, Sweden. anders.schersten@geol.lu.se; laurence.page@geol.lu.se; andreas.petersson@geol.lu.se;

<sup>2</sup>Geological Survey of Denmark and Greenland, Øster Voldgade 10 DK-1350, København, Denmark. pka@geus.dk

<sup>3</sup>Geological Survey Department, Ghana, P.O. Box M 80 Accra, Ghana. anumsolo@yahoo.com

The Dahomeyan belt formed during Pan-African suture between juvenile island arcs rocks that were amalgamated to the >2.0 Ga West African craton (WAC). Arc accretion and subsequent continent collision is manifested through eclogites and mafic to felsic granulites. Pre-collisional passive margin sediments were thrust westward over the WAC. A combined zircon U-Pb and hornblende/mica <sup>40</sup>Ar/<sup>39</sup>Ar profile across the Eburnean-Dahomeyan orogens was made to constrain Dahomeyan imprint on the Eburnean rocks in the WAC. Hornblende ages are 2.06 Ga, while micas yield 2.0 Ga. Zircon U-Pb ages yield igneous crystallisation ages >2.1 Ga, however some samples display significant Pb-loss with lower intercept ages that are consistent with a 0.6 Ga Dahomeyan imprint. This probably reflect fluid induced variable resetting of the zircon U-Pb system, while mica and hornblende remained below their blocking temperatures and where inert to the fluids that affected the zircon. A granulite and a zoned plagioclase porphyritic metavolcanic rock from within the Dahomeyan belt, yield 0.614 and 0.577 Ga zircon ages respectively. The 0.577 Ga population represent igneous crystallisation as represented by prismatic zoned crystals. The 0.614 Ga population is represented by rounded featureless zircon, and date granulite facies metamorphism. Hornblende from the granulite yield 0.59 Ga <sup>40</sup>Ar/<sup>39</sup>Ar plateaux, dating post granulite facies cooling through ~525 °C, correspond to a cooling rate of at least 10 °C/Myr.

These result highlights the imprint of the Dahomeyan orogen on the >2 Ga Eburnean rocks of the WAC in southeast Ghana. No resetting of Ar-ages is noted in mica or hornblende in the Eburnean rocks, while zircon is variably reset.

## Physical evolution of olivine-hosted melt inclusions during high- $T$ homogenization treatments

F. SCHIAVI\*, A. PROVOST, P. SCHIANO AND N. CLUZEL

Laboratoire Magmas et Volcans, Univ. Blaise Pascal, CNRS, IRD, 5 rue Kessler, 63038 Clermont-Ferrand, France

(\*correspondence: f.schiavi@opgc.univ-bpclermont.fr)

Silicate melt inclusions (MIs) form in thermodynamic equilibrium with their host mineral. After entrapment, during the ascent of the host magma and its cooling upon eruption, MIs may undergo physical and chemical changes, part of which are irreversible. Thus, to properly interpret petrological information recorded by MIs, a full understanding of their physico-chemical behaviour when submitted to variations of external temperature ( $T$ ) and pressure is required. Homogenization temperature ( $T_h$ ) of the inclusion content (gas + glass  $\pm$  crystals) is thought to correspond to minimum entrapment temperature ( $T_e$ ). However,  $T_h$  in olivine is observed to increase systematically with time during high- $T$  treatments, thus revealing the occurrence of irreversible physico-chemical changes in the MI-host system.

To figure out what processes are responsible for  $T_h$  increase, we performed heating experiments on  $H_2O$ -rich (Vulcano Is., Italy) and  $H_2O$ -poor (Famous-Zone MORB, East Atlantic) olivine-hosted MIs. Equilibrium between melt and olivine compositions suggests  $T_e \approx 1210^\circ C$  for Vulcano MIs and  $\approx 1220^\circ C$  for Famous-Zone MIs. Each experiment consisted of several heating-cooling cycles performed in a rapid-quench optically-controlled Vernadsky heating stage.

In our experiments large variations of  $T_h$  with time were measured, along with high first  $T_h$  (1230-1300°C for Vulcano MIs;  $T_h \geq 1315^\circ C$ , more often  $\approx 1430^\circ C$  for Famous-Zone MIs), which are inconsistent with calculated  $T_e$ .  $T_h$  increase from one cycle to the next is associated with an increase of low- $T$  bubble size and a slower reduction of bubble volume at high  $T$ . Images taken during the experiments on Famous-Zone MIs allowed us to measure expansions of MI cavities up to  $\sim 30$  vol% of the starting volume. Volume expansion occurred quite rapidly (after 10-80 min at  $T > 1100^\circ C$ ) and increased with time. Its amount, and the associated first  $T_h$  as well, seem to be related with MI size, distance of MI walls from olivine faces, and ratio between bubble and MI volumes.  $T_h$  increase essentially results from the plastic deformation of host olivine (elastic deformation and dissolution/precipitation interfere but are reversible). Though diffusive water loss may interfere too during the first hours at high  $T$ , it cannot explain the observed cavity expansion nor the large and sustained increase in  $T_h$ .

## Pace of soil formation based on soil structure indices

JASMIN SCHIEFER<sup>1</sup>, GEORG J. LAIR<sup>1,2</sup>  
AND WINFRIED E.H. BLUM<sup>1</sup>

<sup>1</sup>Institute of Soil Research, University of Natural Resources and Life Sciences, Vienna, Austria

<sup>2</sup>Institute of Ecology, University of Innsbruck, Austria.

E-mail: jasmin.schiefer@boku.ac.at, georg.lair@boku.ac.at

Clay sized aggregates play a key role in soil formation as they accumulate and preserve organic matter (OM) by physical protection against microbial decomposition [1]. However, the development of microaggregates during soil formation is not well understood. For our study we collected soils of a chronosequence of approximately 10 to 10000 years in an alluvial plain of the River Danube [2]. A- and AC-horizons of Fluvisols and Chernozems under cropland, grassland and forest were sampled. Microaggregates ( $< 2\mu m$ ), gained by ultrasonic dispersion and centrifugation, as well as bulk soil were physically and chemically analysed.

Microaggregates under semi-natural forest showed a steep increase of OM content and a depletion of amorphous Fe-(hydr)oxides in the first years of soil development. In the soils older than about 350 years, OM content in the clay sized aggregates remain more or less constant over time, indicating a possible saturation of the clay sized particles with OM. In contrast, the initially low OM content in the microaggregates under cropland was continuously increasing with soil age. A characterisation of OM in the microaggregates (e.g. by STA) revealed that with time less degradable compounds are accumulating, especially in the AC-horizon. In the AC-horizon of a 2000 - 3000 year old soil the amount of labile and stable OM in the clay sized aggregates was about the same.

Soil structure build-up was strongly influenced by bioturbation (e.g. earthworms) and plant material inputs (roots, litter). A calculation of the annual soil formation rate, based on the depths of the A-horizons, indicates a very high soil formation rate up to  $\sim 4$  mm/year at the beginning, decreasing to  $\sim 0.1$  mm/year after 2000 years.

[1] Chenu and Plante (2006), *Europ. J. of Soil Science* **57** (4), 596-607. [2] Lair *et al.* (2009), *Quat. Geochr.* **4** (3), 260-266.



## Using increment cores of eastern cottonwood trees (*Populus deltoides*) to assess the timing of Cd pollution

JOHAN SCHIJF<sup>1\*</sup> AND MARY C. GARVIN<sup>2</sup>

<sup>1</sup>Chesapeake Biological Laboratory, P.O. Box 38, Solomons, MD 20688, USA (\*correspondence: schijf@umces.edu)

<sup>2</sup>Oberlin College, Department of Biology, 119 Woodland St., Oberlin, OH 44074, USA (Mary.Garvin@oberlin.edu)

We measured the concentrations of 8 trace metals in the trunk wood of ~40 eastern cottonwoods (*P. deltoides*), a fast-growing dioecious angiosperm common throughout much of eastern North America. Large trees were selected more or less at random from an area in northern Ohio (USA) that has a known history of soil pollution with a variety of metals and organic compounds, as well as from an equally sized control area. Two increment cores (L < 40 cm, Ø 5 mm) were taken from each tree at chest level. To avoid contamination, annual growth rings were marked on one core and the markings were used to guide cutting of the sample core with tungsten carbide surgical tools into eight 5-year sections covering the period 1970–2009. The older and younger rings were not analyzed. All sections were completely microwave-digested (10 min at 200°C) in a mixture of 16 M nitric acid and 30% hydrogen peroxide, along with one blank and one pine wood SRM (NJV 94-5). The cooled digests were then weighed, diluted 100-fold, and analyzed by Octopole Reaction System ICP-MS (Agilent) for As, Cd, Co, Cr, Cu, Ni, Pb, and V.

While some metals (As, V) are always below the method detection limit (DL) and others appear to vary arbitrarily, Cd is the only one showing behavior that may be interpretable in terms of both space and time. Blanks were always below the DL (~15 ng Cd per g dry wood), there was no evidence of sample contamination, and analytical recovery of the SRM was excellent (>98%). The ~40 trees fall into three distinct groups: 1. Trees with low mean Cd concentrations (270 ng/g) and little temporal variability ( $n = 20$ ); 2. Trees with a clear maximum or temporal trend in the Cd concentration of up to 1300 ng/g ( $n = 14$ ); 3. Three trees with extremely high Cd concentrations (>2500 ng/g). Replicate cores taken from a single tree as well as from separate trees at a single location yielded satisfactory reproducibility (10–20%). Although the timing of maximum Cd concentrations varies, high amounts are not found in the most recent 10 years of any tree. All trees in group 3 and all but one tree in group 2 are located in the polluted area, whereas all but one tree in the control area are from group 1. A simple statistical test indicates that this distribution has an almost negligible probability of occurring by chance ( $\chi^2 = 8.819$ ,  $p = 0.003$ ).

## Mg isotope evidence for ancient magmatic differentiation on the angrite parent body

M. SCHILLER<sup>1\*</sup>, T. MIKOUCHI<sup>2</sup>, J. N. CONNELLY<sup>1</sup>  
AND M. BIZZARRO<sup>1</sup>

<sup>1</sup>Centre for Star and Planet Formation, Natural History Museum of Denmark, University of Copenhagen, Copenhagen, Denmark (\*email: schiller@snm.ku.dk)

<sup>2</sup>Department of Earth & Planet. Science, University of Tokyo, Tokyo, Japan

Angrite meteorites are the most alkali-depleted rocks in our solar system and they can be divided into plutonic and volcanic angrites [1]. Of the group of volcanic angrites, NWA 1670 is particularly interesting because it contains significant amounts of olivine xenocrysts of up to 5 mm in size that are chemically distinct from the groundmass [2,3]. The existence of xenocryst olivine not in chemical equilibrium with the groundmass offers the potential for a resolvable temporal difference between both phases. Therefore, considering the old age for this angrite [4], the xenocrysts may reflect an earlier magmatic event.

Here we apply the <sup>26</sup>Al to <sup>26</sup>Mg ( $t_{1/2} = 0.7$  Myr) chronometer to examine the temporal relationship of olivine xenocrysts and basaltic groundmass in NWA 1670. Mg isotope data for individual olivine grains and groundmass separates were obtained using the Neptune MC-ICPMS. All olivine xenocrysts have negative  $\mu^{26}\text{Mg}^*$  with a mean of  $-10.7 \pm 3.1$  ppm. Measured  $\mu^{26}\text{Mg}^*$  of the groundmass ranges from  $-5.3$  to  $+4.3$  ppm and are positively correlated with <sup>27</sup>Al/<sup>24</sup>Mg ratios. Both sets of data form an apparent isochron suggesting a similar <sup>26</sup>Al/<sup>27</sup>Al abundance at time of their formation to that of other old angrites. However, the negative intercept of the isochron cannot be reconciled with the low <sup>26</sup>Al/<sup>27</sup>Al abundance and suggests that the correlation is best explained as a two component mixing trend. Model ages for single xenocryst olivine range from 0.36 to 1.18 Myr after CAIs. A model age for the most anomalous groundmass sample yields an age of 3.9 Myr after CAIs, consistent with the Mg isochron ages for other volcanic angrites. These data demonstrate that olivine entrained in NWA 1670 are products of ancient magmatic differentiation on the angrite parent body shortly after solar system formation, which significantly predates the formation of volcanic angrites.

[1] K. Keil (2012), *Chem. Erde-Geochem.*, 72, 191–218. [2] T. Mikouchi *et al.* (2003), *Meteorit. Planet. Sci. Suppl.*, 38, 5218. [3] A. Jambon *et al.* (2008) *Meteorit. Planet. Sci.*, 43, 1783–1795 [4] Sugiura *et al.* (2005), *Earth Planets Space*, 57, e13-e16.

## Origin of natural gas-fed “eternal flames” in the Northern Appalachian Basin, USA

ARNDT SCHIMMELMANN<sup>1</sup>, GIUSEPPE ETIOPE<sup>2</sup>  
AND AGNIESZKA DROBNIAK<sup>3</sup>

Department of Geological Sciences, Indiana University, 1001  
E 10th Street, Bloomington, IN 47405-1405, USA,  
aschimme@indiana.edu

<sup>2</sup>Istituto Nazionale di Geofisica e Vulcanologia, Sezione Roma  
2, via V. Murata 605, 00143 Roma, Italy, and Faculty of  
Environmental Science and Engineering, Babes-Bolyai  
University Cluj-Napoca, Romania,  
giuseppe.etiope@ingv.it

<sup>3</sup>Indiana Geological Survey, Indiana University, 611 N Walnut  
Grove, Bloomington, IN 47405, USA,  
agdrobni@indiana.edu

Hydrocarbon gas seeps are surface expressions of petroleum seepage systems, whereby gas is ascending through faults and conduits from pressurized reservoirs that are typically associated with sandstones or limestones. The region around the states of New York and Pennsylvania marks the birthplace of commercial gas production from shales dating back into the 19<sup>th</sup> century. We sampled two burning seeps in New York and Pennsylvania that had not yet received geochemical scrutiny, including compound-specific stable isotope ratios of hydrogen and carbon. A spectacular “eternal flame” in Chestnut Ridge County Park (Erie County, western New York State) marks a natural gas macroseep of dominantly thermogenic origin emanating directly from deep shale source rocks, which makes this a rare case in contrast to most Petroleum Seepage Systems where gas derives from conventional reservoirs. The main flaming seep releases about 1 kg of methane per day and seems to feature the highest ethane and propane (C<sub>2</sub>+C<sub>3</sub>) concentration ever reported for a natural gas seep (~35 vol. %). The same gas is also released to the atmosphere through nearby invisible and diffuse seepages from the ground. The synopsis of our chemical and stable isotope data with available gas-geochemical data of reservoir gases in the region and the stratigraphy of underlying shales suggests that the thermogenic gas originates from Upper Devonian shales without intermediation of a conventional reservoir. A similar investigation on a second “eternal flame” near Clarrington in Pennsylvania suggests that gas is migrating from a conventional sandstone pool and that the seep is probably not natural but results from an undocumented and abandoned gas or oil well.

## High-precision <sup>10</sup>Be-dating and Little Ice Age glacier advances at Steingletscher (Swiss Alps)

IRENE SCHIMMELPFENNIG<sup>1,2</sup>, JOERG M. SCHAEFER<sup>1</sup>,  
NAKI AKÇAR<sup>3</sup>, SUSAN IVY-OCHS<sup>4</sup>, ROBERT FINKEL<sup>5</sup>,  
SUSAN ZIMMERMAN<sup>6</sup> AND CHRISTIAN SCHLUECHTER<sup>3</sup>

<sup>1</sup>Lamont-Doherty Earth Observatory/Columbia University,  
Palisades, NY-10964, USA

<sup>2</sup>CEREGE, 13545 Aix en Provence, France

<sup>3</sup>Institute of Geological Sciences, University of Bern,  
Switzerland

<sup>4</sup>Laboratory of Ion Beam Physics, ETH, Zürich, Switzerland

<sup>5</sup>Earth and Planetary Science Department, University of  
California-Berkeley, Berkeley, California, USA

<sup>6</sup>Lawrence Livermore Natl Lab, Ctr Accelerator Mass  
Spectrometry, Livermore, CA-94550 USA

The increase in sensitivity of the cosmogenic <sup>10</sup>Be technique now provides novel insights into glacier and climate change by giving dates throughout the Holocene and up to present day from moraines around the globe.

We show the first <sup>10</sup>Be chronology for Steingletscher in the Central Swiss Alps (47°N, ~2000 m altitude), consisting of 30 boulder ages. The chronology includes early Holocene glacier positions, which most likely reflect glacier responses to abrupt cold spells identified in other Northern Hemisphere paleoclimate records. On the younger inner moraines, fourteen <sup>10</sup>Be boulder ages from individual ridges are in stratigraphic order ranging from 170 to 530 years. We relate these boulder ages to glacier advances during the Little Ice Age (LIA, 14<sup>th</sup> to 19<sup>th</sup> century in the Swiss Alps). Two samples from moraine ridges inside the LIA limit of Steingletscher yield ages of 170 ± 10 years and 130 ± 10 years. These latter samples potentially allow for quantification of the amount of <sup>10</sup>Be inherited during prior periods of exposure, on the order of a thousand atoms per gram.

Our <sup>10</sup>Be data from boulders deposited during the last millennium are based on quartz samples as small as 5 g, facilitating routine processing for <sup>10</sup>Be dating even on such young samples. Comparing the Steingletscher data with other emerging <sup>10</sup>Be chronologies of recent glacier advances, we will discuss the current analytical limits of <sup>10</sup>Be dating together with the relevance of cosmogenic nuclide inheritance and other sources of natural uncertainty for the overall sensitivity of <sup>10</sup>Be surface exposure dating.

## CO<sub>2</sub> fluxes in the submarine hydrothermal system of Panarea

M. SCHIPEK\*, R. SIELAND, D. STEINBRÜCKNER, M. PONEPAL, K. BAUER AND B. MERKEL<sup>1</sup>

<sup>1</sup>TU Bergakademie Freiberg, Scientific Diving Center, 09596 Freiberg, Germany

(\* correspondence: mandy.schipek@gmail.com)

The measurement of CO<sub>2</sub> fluxes in terrestrial and submarine hydrothermal systems is affected by large uncertainties. Different methodologies were applied by scientific divers to estimate areal gas fluxes and determine massive gas discharges in water depths between 8 and 30 m in the hydrothermal system of Panarea, Italy.

Because several hundreds of hydrothermal vents exist in the submerged caldera of Panarea it is impossible to measure each gas discharge directly. Therefore gas discharges were classified in 5 groups with respect to their amount of gas release. Class A to D (0 to < 40 l/min) discharges were measured by displacement of water in a graduated container according to [1].

By visual counting and classifying discharge points within areas of increased hydrothermal activity, a rough estimation of diffuse gas release was realized. Massive gas discharges (class E, 40 – 100 l/min) were determined by means of a device based on impeller and temperature readings [2]. Corrections concerning gas temperature and hydrostatic pressure were performed.

A substantial percentage of the investigated gas discharge points (75 – 95%, n ≈ 700) was classified as weak (class A – D). About 10 fumaroles were identified as very intense gas releases (class E). Small gas discharges had been estimated to release up to 30 ± 14.5 t/d CO<sub>2</sub>, while massive outlets account for 5 ± 0.6 t/d CO<sub>2</sub> in the submarine area of the caldera. The total CO<sub>2</sub> flux was calculated by considering the dissolution of CO<sub>2</sub> during the ascent to the sea floor [3]. Assuming 20 – 40% of gas dissolution, the total CO<sub>2</sub> flux in the submarine hydrothermal system of Panarea was estimated to be 47 ± 15.1 t/d CO<sub>2</sub>. This is about 26% of the CO<sub>2</sub> emission of the nearby terrestrial volcano Vulcano [4] and <0.47% compared to all Mediterranean hydrothermal emissions [5].

[1] Italiano & Nuccio (1991) *J. Volcanol. Geotherm. Res.* **46**, 125-41. [2] Ponepal *et al.* (2010) *Miscellanea* **7**, 66-70. [3] Caracausi *et al.* (2005) *Geochim Cosmochim Acta* **69**, 3045-59. [4] Baubron *et al.* (1990) *Nature* **344**, 51-53. [5] Dando *et al.* (1991) *Prog Oceanogr* **44**, 333-67.

## Structure, evolution and function of the root bacterial microbiota of *Arabidopsis* species

K. SCHLAEPPI<sup>1,2\*</sup>, N. DOMBROWSKI<sup>1</sup>, E. VER LOREN VAN THEMAAT<sup>1</sup> AND P. SCHULZE-LEFERT<sup>1</sup>

<sup>1</sup>Department of Plant Microbe Interactions, Max Planck Institute for Plant Breeding Research, Cologne, Germany

<sup>2</sup>Swiss Federal Research Institute Agroscope, Reckenholzstrasse 191, 8046 Zurich, Switzerland  
(\*correspondence: klaus.schlaepi@agroscope.admin.ch)

Plants touch with their roots soil - one of the richest microbial ecosystems on earth. At this contact zone, the secretion of poorly characterized root exudates fuels the differentiation of a distinct rhizosphere bacterial microbiota compared to the surrounding soil. Rhizobacteria provide microbial services affecting plant growth and health and contribute to ecosystem functioning. We examined the composition and evolution of the bacterial root microbiota within a phylogenetic framework of host species, including *Arabidopsis thaliana* and its sister species *Arabidopsis halleri* and *Arabidopsis lyrata* and evolutionarily ancient *Cardamine hirsuta* with pyrosequencing of 16S rRNA gene amplicon libraries. The composition of rhizobacterial communities varies most as a function of environmental condition and consists of a taxonomically narrow and evolutionarily conserved core microbiota consisting of Actinomycetales, Burkholderiales, and Flavobacteriales. We identified few root microbiota members that provide unique signatures for each host species, possibly reflecting host-specific requirements in a given environment. Most of these host species-dependent microbiota signatures were found for the phylogenetically oldest *C. hirsuta*, indicating that root microbiota diversification is linked to the evolutionary divergence time of the host species. *A. halleri* is the only plant among the tested species that grows on heavy metal (e.g. Cadmium) contaminated soils, tolerating high levels of Cd and accumulating high levels of Cd in leaves. We have initiated the examination of rhizobacterial communities of *A. halleri* grown in soils with elevated heavy metals coupled with community profiling of enrichment cultures and metal uptake measures in leaves. In this context, first insights into microbiota services will be provided.

## Continuous soil gas monitoring related to CCS – Lessons learned from a 5-year case study

SCHLOEMER, S.<sup>1</sup>, MÖLLER, I.<sup>1</sup> AND FURCHE, M.<sup>1</sup>

<sup>1</sup>Federal Institute for Geosciences and Natural Resources, Hannover, Germany, s.schloemer@bgr.de

The development of adequate monitoring strategies for CO<sub>2</sub> storage sites is one of the most vigorously discussed subjects related to carbon capture and storage (CCS), both in the public and in the scientific community. Public acceptance of CO<sub>2</sub> sequestration will only be achieved if secure and comprehensible monitoring methods for the natural environment are applied in a transparent way. Deep geological monitoring is mostly related to large scale migration of injected carbon dioxide in the storage formations. In contrast, detection and quantification of different gas species in the vadose zone of soil column and/or in the atmospheric boundary layer is a key method in many fields of near-surface environmental research and geohazards as well as CCS. As CO<sub>2</sub> soil gas concentrations vary over broad ranges, reliable statements on CO<sub>2</sub> seepage can only be made by using continuous long-term gas concentration measurements. We describe lessons learned from the first continuous monitoring program applied on a proposed CO<sub>2</sub> storage site in the Altmark area (Germany).

We will focus on our technical experiences, data interpretation and recommendations for further monitoring programs related to CCS. The most important topic is the reliability of a single station's data quality. Each selected site needs a thorough pre-investigation, e.g. regarding the depth of the biologically active zone and potential free water level. Based on our long lasting experience from field studies and including recent monitoring programs, we strongly recommend that baseline monitoring schemes for CO<sub>2</sub> storage sites should start at least 3 years before the gas injection into the reservoir. We will show that vadose zone monitoring can be considerably more sensitive to small seepage rates than surface flux measurements under favourable conditions but will also address pitfalls and limitations of the method.

## Sorption of uranium and neptunium onto diorite from Äspö HRL

K. SCHMEIDE\*, S. GÜRTLER, K. MÜLLER, R. STEUDTNER, C. JOSEPH, F. BOK AND V. BRENDLER

Helmholtz-Zentrum Dresden-Rossendorf, Institute of Resource Ecology, P.O. Box 510119, 01314 Dresden, Germany (\* k.schmeide@hzdr.de)

Granitic subsurface environments are considered as potential host rock formations for the deep underground disposal of radioactive waste. The retention behavior of the crystalline rock diorite from the Äspö Hard Rock Laboratory (HRL, Sweden) towards the redox-sensitive actinides U and Np was studied by means of batch sorption experiments. The influence of various parameters, such as grain size (0.063 – 0.2 mm, 0.5 – 1 mm, 1 – 2 mm), temperature (25 and 10°C), atmosphere and sorption time (5 to 108 days) was studied using a synthetic Äspö groundwater (pH 7.8,  $I = 0.178$  M) as background electrolyte. For U(VI), sorption isotherms were recorded ( $5 \times 10^{-9}$  M to  $7 \times 10^{-5}$  M). Distribution coefficients,  $K_d$  values, were determined. The  $K_d$  values decrease with increasing grain size of the diorite and with decreasing temperature. The  $K_d$  values determined under oxic conditions are lower than those determined under anoxic conditions.

In the U sorption system, the speciation of U(VI) in solution and thus, its sorption onto diorite is strongly influenced by the groundwater composition. It was found by time-resolved laser-induced fluorescence spectroscopy that  $\text{Ca}_2\text{UO}_2(\text{CO}_3)_3(\text{aq})$  is the dominating species in solution. Hence, calcium and carbonate ions leached out of diorite significantly affect U(VI) sorption. Kinetic experiments showed that sorption equilibrium ( $K_d = 1.44 \pm 0.30$ , 1 – 2 mm fraction) is reached relatively fast (after 10 to 20 days). As predominant surface species on diorite,  $\text{UO}_2(\text{CO}_3)_3^{4-}$  was identified by in situ time-resolved attenuated total reflection Fourier-transform infrared (ATR FT-IR) spectroscopy. About 50% of the sorbed U can be desorbed with Äspö ground water. This part occurs predominantly as U(VI) (94%) as shown by TTA solvent extraction.

In the Np sorption system, the effect of the groundwater composition on speciation and sorption behavior is weak. By ATR FT-IR spectroscopy,  $\text{NpO}_2^+$  was detected in solution. During sorption experiments under anoxic conditions (up to 108 days), Np(V) is reduced to Np(IV) by the Fe(II) of the diorite which leads to a very strong Np sorption (95% sorption for  $[\text{Np}]_0 = 1 \times 10^{-6}$  M, S/L = 200 g/L). Consequently, only 5–6% of the sorbed Np can be desorbed with Äspö ground water. This small amount was identified as Np(V) by TTA solvent extraction.

## Reactivity of nanoscale zero-valent iron particles used for *in situ* groundwater remediation

D. SCHMID, S. LAUMANN, V. MICIĆ AND T. HOFMANN\*

Department of Environmental Geosciences, University of Vienna, Vienna, Austria (\*correspondence: thilo.hofmann@univie.ac.at)

Nanoscale zero-valent iron (nZVI) is a powerful reducing agent and has therefore been proposed as a tool for *in situ* groundwater remediation [1]. It has a high potential for transformation of a broad range of contaminants, including chlorinated solvents, redox active toxic metals/metalloids and radionuclides, chemical warfare agents, and pharmaceuticals [2,3,4]. The effectiveness of this remediation technique depends on the reactivity of nZVI particles, which is influenced e.g., by particle properties, hydrochemical conditions, and nature of the contaminants.

The aim of this study is to investigate the reactivity of two commercially available nZVI using iopromide in batch and column reactors under pH values typically found in groundwater (pH 7 and 8). Iopromide is a halogenated X-ray contrast media and serves as a model contaminant.

The investigated nZVI included polyelectrolyte-coated nZVI and non-coated nZVI, both in aqueous suspension (NANOIRON s.r.o., Czech Republic). All experiments were carried out under anoxic conditions with the same molar ratio of Fe<sup>0</sup> and iopromide.

First results show that the degradation of iopromide with both nZVI studied follows a pseudo-first order kinetics. Non-coated nZVI appeared to be more reactive. Both types of nZVI were able to fully degrade iopromide in nearly ten minutes under the applied laboratory conditions. The surface area normalized reaction rate constant ( $K_{SA}$ ) depends on the pH value and the type of nZVI. The non-coated nZVI reacted 2–3 times faster than the polyelectrolyte-coated nZVI. At the pH of 7 the  $K_{SA}$  increases from 330 L m<sup>-2</sup> h<sup>-1</sup> for coated nZVI to 940 L m<sup>-2</sup> h<sup>-1</sup> for non-coated nZVI. At a pH value of 8 the  $K_{SA}$  values are 3–4 times lower, varying from 110 L m<sup>-2</sup> h<sup>-1</sup> for coated nZVI to 240 L m<sup>-2</sup> h<sup>-1</sup> for non-coated nZVI.

Further experiments will be conducted in column reactors under similar hydrochemical conditions and iopromide concentrations in order to simulate the nZVI-mediated iopromide reduction in groundwater and to compare the reaction rate constants with these obtained in batch reactors.

[1] Karn *et al.* (2009): *Envir. Health Perspect.* 117, 1823–1831. [2] Zboril *et al.* (2012): *Hazard. Mater.* (211–212), 126–130. [3] Zhang, W. (2003): *J. Nanopart. Res.* 5, 323–332. [4] Stieber *et al.* (2011): *ES&T* 45 (11), 4944–4950.

## Alpine metamorphism of the Pan-African gneiss basement in the Menderes/Çine massif, SW Turkey, revealed by garnet Lu-Hf geochronology

ALEXANDER SCHMIDT<sup>1a</sup> AND ROLAND OBERHÄNSLI<sup>1b</sup>

<sup>1</sup>Institute of Earth- & Environmental Sciences, University of Potsdam, Germany

<sup>a</sup>alexander.schmidt@geo.uni-potsdam.de

<sup>b</sup>roob@geo.uni-potsdam.de

The Menderes Massif is one of the large Alpine metamorphic complexes of Turkey. Its southern part, precisely the Çine submassif, is described as a high-grade gneissic core of Precambrian basement covered by a lower-grade series of Paleozoic schists and Cenozoic-Mesozoic marbles. The geochronology of the gneiss basement in this complex so far highly depends on U-Pb ages of zircons, which yield protolith ages between 560 to 540 Ma. Its metamorphic period has been constrained at Alpine ages between 63 and 25 Ma using Ar/Ar and Rb-Sr geochronology. However garnet, one of the most abundant minerals in schists of this region, has yet to be the focus of geochronological work. Here we present the first Lu-Hf ages of garnet crystals from garnet-biotite schists of the southern margin of the Çine submassif. Lu-Hf analysis have been performed on 4–6 cm sized euhedral garnet crystals by the use of a micro-sampling technique, which permits the analysis of the isotopic composition of cores and rims of garnets, and a set number of intermediate radii. Different zones of these garnet crystals were recognized based on trace element distributions in core to rim profiles. The Lu-Hf results so far reveal at least two events, i.e. the beginning of garnet growth represented by a garnet core age of ca. 60 Ma, and an age of ca. 40 to 38 Ma at an intermediate radius of the garnet crystal ( $r \sim 50\%$ ), which also corresponds to a pronounced change in the distribution of heavy to medium rare earth elements. The Fe, Mg, Mn and Ca as well as the heavy rare earth element distributions in the garnet crystals indicate the preservation of a classical growth zoning pattern, i.e. bell-shaped Mn, constant decrease in Fe/(Fe+Mg), and HREE enrichment in garnet cores. Therefore it is clear that the Lu-Hf analysis yield growth ages rather than retrograde overprinting, hence the evidence for the Alpine metamorphism of the Çine submassif.

## Quartz solubility and $\text{CO}_3^{2-}$ – $\text{HCO}_3^-$ equilibrium in $\text{H}_2\text{O}+\text{Na}_2\text{CO}_3$ and $\text{H}_2\text{O}+\text{NaHCO}_3$ fluids at high $P$ and $T$

C. SCHMIDT<sup>1</sup>

<sup>1</sup>Deutsches GeoForschungsZentrum (GFZ), 14473 Potsdam, Germany (Christian.Schmidt@gfz.potsdam.de)

Alkali hydrogencarbonate and carbonate in aqueous fluids may play an important role in the mobilization of the REE and other elements at crustal conditions [1] and in subduction zones [2]. Here, the  $\text{CO}_3^{2-}$ – $\text{HCO}_3^-$  equilibrium and the quartz solubility in aqueous 4.65 molal  $\text{NaHCO}_3$  and 1.6 molal  $\text{Na}_2\text{CO}_3$  solutions were studied to 600 °C and 1.53 GPa using a hydrothermal diamond-anvil cell. The recorded spectra were normalized to the temperature dependence of the Stokes-Raman scattering intensity, the frequency and scattering factor, density, and reflection at the diamond-fluid interface [3,4]. The  $\text{HCO}_3^-(\text{aq})$  and  $\text{CO}_3^{2-}(\text{aq})$  concentrations were obtained from the integrated intensities of the Raman bands at  $\sim 1000$  and  $\sim 1060$   $\text{cm}^{-1}$  assuming that the ratio of the relative molar scattering factors  $J_{1000}/J_{1060}=0.1667/0.2434$  [3] is independent of pressure ( $P$ ) and temperature ( $T$ ). In the  $\text{Na}_2\text{CO}_3$  solution, the fraction of the species  $\text{CO}_3^{2-}(\text{aq})$  did not show a significant dependence on pressure, but decreased with temperature from  $\sim 0.77$  at 100 °C to  $\sim 0.69$  at 200 °C to  $\sim 0.41$  at 600 °C. Before equilibration at 600 °C, the  $\text{CO}_3^{2-}(\text{aq})$  fraction at vapor pressure was  $\sim 0.99$  at 100 °C and  $\sim 0.91$  at 200 °C. No  $\text{CO}_2$  or  $\text{CH}_4$  were detected. In the  $\text{NaHCO}_3$  solution, the  $\text{CO}_3^{2-}(\text{aq})$  fraction increased with temperature and decreased with pressure along all studied isotherms from 200 to 600 °C, e.g. at 600 °C from 0.16 at 0.63 GPa to 0.1 at 1.5 GPa. Thus,  $\text{HCO}_3^-$  ions can be stable in lower crustal and upper mantle fluids. The only detectable Raman band from dissolved silica was at  $\sim 770$   $\text{cm}^{-1}$ , which indicates a predominantly monomeric silica speciation. The calibrated integrated intensity of this band was used to determine the  $\text{SiO}_2(\text{aq})$  molality. The quartz solubility in 1.6 molal  $\text{Na}_2\text{CO}_3$  increased with  $P$  and  $T$ , but was always much higher than the solubility of quartz in water at the same  $P$ - $T$  condition. The quartz solubility in 4.65 molal  $\text{NaHCO}_3$  increased with  $T$ , decreased with  $P$  along the 500 and 600 °C isotherms to values below the solubility in water, and was approximately constant at 300 and 400 °C. For lower pressure isobars, there was a distinct drop in the solubility between 500 and 400 °C.

[1] Thomas *et al.* (2011) *Contrib. Mineral. Petrol.* **161**, 315–329. [2] Martinez *et al.* (2004) *Chem. Geol.* **207**, 47–58. [3] Rudolph *et al.* (2008) *Dalton Trans.*, 900–908. [4] Schmidt (2009) *Geochim. Cosmochim. Acta* **73**, 425–437.

## Molecular-level comparison of water-soluble sedimentary organic matter extracted by two methods

FRAUKE SCHMIDT<sup>1\*</sup>, BORIS P. KOCH<sup>2</sup>, MATTHIAS WITT<sup>3</sup> AND KAI-UWE HINRICHS<sup>1</sup>

<sup>1</sup>MARUM – Center for Marine Environmental Sciences, University of Bremen, Leobener Straße, D-28359 Bremen, Germany (\*correspondence: frauke.schmidt@uni-bremen.de)

<sup>2</sup>Alfred-Wegener-Institut Helmholtz-Zentrum für Polar- und Meeresforschung, Am Handelshafen 12, D-27570 Bremerhaven, Germany

<sup>3</sup>Bruker Daltonik GmbH, Fahrenheitstraße 4, 28359 Bremen, Germany

Organic matter in marine sediments is a complex mixture of numerous individual molecules, which are central reactants in various biogeochemical processes and serve as a substrate for benthic organisms. The fate of organic matter and its bioavailability is largely controlled by composition, size and reactivity of the individual organic molecules. In this study, we aim at a molecular characterization of the easily mobilized and thus accessible fraction of organic matter in marine sediments. We compared the molecular composition of (i) the mobile dissolved organic matter (DOM) pool in interstitial waters, extracted with rhizons, with (ii) the organic matter that was extracted from the associated sediment with water in a Soxhlet apparatus. After solid phase extraction, both DOM fractions were subjected to molecular-level analysis by ultra-high resolution Fourier Transform Ion Cyclotron Resonance Mass Spectrometry (FT-ICR-MS). We selected four different sediment horizons of a core from the Black Sea that represented different ages, depositional and geochemical conditions. FT-ICR mass spectra of the Soxhlet extracted DOM yielded 2- to 3-times higher numbers of molecules compared to the interstitial water DOM, with the former being distributed over a larger mass range and exhibiting higher abundances of heteroatom-bearing molecules. We related the molecular-level differences between both DOM pools to age and sediment geochemistry. The Soxhlet-extractable DOM pool was up to 30-times more concentrated than the DOM pool in the interstitial waters. Soxhlet extraction of sediments in combination with FT-ICR-MS analyses opens a window to studying a so far uncharacterized sedimentary organic matter pool that is potentially the major precursor of “traditional” DOM.

## Discrimination scheme for Fe-Mn deposits based on REY, HFSE and Th

KATJA SCHMIDT<sup>1\*</sup>, MICHAEL BAU<sup>1</sup>  
AND ANDREA KOSCHINSKY<sup>1</sup>

<sup>1</sup>School of Engineering and Science, Jacobs University  
Bremen, 28759 Bremen, Germany, \*correspondence:  
k.schmidt@jacobs-university.de

Marine Fe-Mn deposits can be distinguished based upon the type of aqueous fluid from which they precipitate and their specific setting: While hydrogenetic crusts slowly precipitate from ambient seawater and attain their constituents from this source, diagenetic nodules form within the sediment, with pore water as major source of elements. In the vicinity of hydrothermal vents, hydrothermal crusts precipitate from both hydrothermal fluid and seawater as possible source fluid. Variable concentrations of economically important elements characterize these groups. The individual groups can be separated using discrimination diagrams such as Ce/Ce\*<sub>SN</sub> vs. Nd, Ce/Ce\*<sub>SN</sub> vs. Y/Ho<sub>SN</sub>, Nb vs. Ta, and Ce/Ce\*<sub>SN</sub> vs. Th, Zr, Hf, Nb, Ta, which combine the effects of redox, growth rate and mineralogy on the trace metal content of Fe-Mn deposits. The redox-sensitive Ce, and HFSE and Th are continuously scavenged during crust growth, while the other REY are controlled by an exchange equilibrium. In contrast to REY, HFSE and Th are mainly scavenged from the Fe oxide phase relative to the Mn oxide phase, and together with the low mobility of these elements during diagenesis, this can be used to separate the individual groups. Hydrogenetic crusts display positive Ce anomalies, negative Y anomalies and high concentrations of REY, HFSE and Th, reflecting slow precipitation from seawater. Diagenetic nodules differ from hydrogenetic crusts and nodules as they display negative Ce anomalies at lower Nd concentrations, related to the low mobility of Ce<sup>4+</sup> in sub-oxic porewaters. Seawater-dominated hydrothermal crusts differ from hydrogenetic crusts and diagenetic nodules as this is the only group which display positive Y anomalies, together with negative Ce anomalies and low Nd concentrations. This signature reflect the rapid scavenging of REY from ambient seawater on hydrothermal oxide particles, without strong fractionation. In contrast to these hydrothermal crusts, hydrothermal Mn crusts which gained significant proportions of their REY content from the mantle via hydrothermal fluids (up to 30%, based on Nd isotopes), often cover the same regions as diagenetic nodules in Ce/Ce\*<sub>SN</sub> vs. Y/Ho<sub>SN</sub> and Ce/Ce\*<sub>SN</sub> vs. Nd diagrams. Both groups can be further be separated in Ce/Ce\*<sub>SN</sub> vs. Th and Nb vs. Ta diagrams.

## Geochemical diversity and K-rich compositions found by the MSL APXS in Gale Crater, Mars

M.E. SCHMIDT<sup>1</sup>, P.L. KING<sup>2</sup>, R. GELLERT<sup>3</sup>, B. ELLIOTT<sup>4</sup>,  
L. THOMPSON<sup>4</sup>, J.A. BERGER<sup>5</sup>, J. BRIDGES<sup>6</sup>, J.L.  
CAMPBELL<sup>3</sup>, B. EHLMANN<sup>7</sup>, J. GROTZINGER<sup>7</sup>, J.  
HUROWITZ<sup>7</sup>, L. LESHIN<sup>8</sup>, K.W. LEWIS<sup>9</sup>, S.M.  
MCLENNAN<sup>10</sup>, D.W. MING<sup>11</sup>, G.M. PERRETT<sup>3</sup>, I.  
PRADLER<sup>3</sup>, E.M. STOLPER<sup>7</sup>, S.W. SQUYRES<sup>12</sup>, A.H.  
TRIEMAN<sup>13</sup> AND THE MSL SCIENCE TEAM

<sup>1</sup>Brock Univ, St. Catharines ON L2S2A1 Canada,  
\*correspondance: mschmidt2@brocku.ca;

<sup>2</sup>Aust. Nat. Univ., Canberra ACT 0200 Australia;

<sup>3</sup>Univ. Guelph, ON N1G2M7 Canada;

<sup>4</sup>Univ. New Brunswick, Fredericton, NB E3B5A3 Canada;

<sup>5</sup>Univ. Western Ontario, London, ON N6A3K7 Canada;

<sup>6</sup>Univ. Leicester, LE1 7RH, UK;

<sup>7</sup>Calif. Inst. Tech., Pasadena, CA 91125, USA;

<sup>8</sup>Rensselaer Polytech. Inst., Troy, NY 121808 USA;

<sup>9</sup>Princeton Univ., NJ 08540, USA;

<sup>10</sup>Geosciences, SUNY Stony Brook, NY 11794 USA;

<sup>11</sup>NASA JSC, Houston, TX 77058 USA;

<sup>12</sup>Cornell Univ., Ithaca, NY 14850 USA;

<sup>13</sup>Lunar Planet. Inst., Houston, TX 77058 USA

Along the Curiosity rover's traverse toward Glenelg (through sol 102) the Alpha Particle X-ray Spectrometer (APXS) analysed four rocks and one soil. Microscopic images and compositions of unbrushed rock surfaces are consistent with 5-20% dust contamination. Nevertheless, the underlying characteristics of these rocks may still be discerned. As a group, they span nearly the entire range in FeO\* and MnO of the Martian dataset. In addition, they are particularly enriched in volatile metals (K, Zn, Ge), and these elements do not correlate with Cl or S. One rock, Jake\_Matijevic is notably alkaline and evolved; its composition is that of a nepheline-normative mugearite. The other three rocks plot in the basanite field of a TAS diagram, with high K<sub>2</sub>O (up to 3.0%) and low SiO<sub>2</sub>. These three rocks are otherwise SNC-like (high Fe and low Al). Three out of the four rocks (including Jake\_Matijevic) plot along a line in variation diagrams, suggesting mixing of Fe-rich and Al-rich components, likely by sedimentary processes.

With only four rocks analyzed so far and ambiguity as to their geologic context (e.g. outcrop vs. float; igneous vs. sedimentary) additional measurements are needed to fully understand the region. It is nevertheless clear that Curiosity landed in a lithologically diverse, K-rich region of Mars.

## The influence of Perchlorate ( $\text{ClO}_4^-$ ) on the sorption behavior of Th(IV) on the Muscovite (001) basal plane

M. SCHMIDT<sup>1</sup>, S. S. LEE<sup>2</sup>, R. E. WILSON<sup>2</sup>, K. E. KNOPE<sup>2</sup>, P. FENTER<sup>2</sup> AND L. SODERHOLM<sup>2</sup>

<sup>1</sup>Karlsruhe Institute of Technology (KIT), Institute for Nuclear Waste Disposal, Karlsruhe, Germany

<sup>2</sup>Argonne National Laboratory, Chemical Sciences and Engineering Division, Argonne, IL, U.S.A.

In many sorption as well as other geochemical studies the perchlorate anion ( $\text{ClO}_4^-$ ) is used as a constituent of the background electrolyte for its non-coordinating behavior. It is assumed that by restricting the competitive coordination reaction in solution it is possible to study the unperturbed sorption reaction. The adsorption of tetravalent thorium to the muscovite (001) basal plane gives a cautionary example, where the change from a weakly coordinating anion ( $\text{Cl}^-$ ) to a non-coordinating anion ( $\text{ClO}_4^-$ ) has a drastic and unexpected effect on the sorption behavior of the cation.

Results from surface x-ray diffraction techniques in combination with alpha-spectrometry measurements will be presented. On the basis of these results we will demonstrate that Th(IV) exhibits a straightforward sorption behavior driven by electrostatic attraction and, to a lesser degree solution complexation and hydrolysis, when the reaction is studied in NaCl background electrolyte media (Schmidt *et al.*, 2012). Thorium adsorbs up to a slightly higher than charge compensating coverage of 0.4 Th/ $A_{\text{UC}}$  predominantly as an extended outer sphere complex with two intact hydration spheres.

By the same method and under the same solution conditions – but with  $\text{NaClO}_4$  instead of NaCl – the adsorption behavior changes drastically: no interaction of Th with the interface can be detected under these conditions. The changes in solution chemistry are comparably minor, and it appears unlikely that changes in the complexation behavior can explain this observation. Potential interfacial reaction mechanisms underlying this unanticipated behavior will be discussed.

[1] Schmidt, M., Lee, S.S., Wilson, R.E., Soderholm, L. and Fenter, P. (2012) Sorption of tetravalent thorium on muscovite. *Geochimica et Cosmochimica Acta*, **88**, 66-76.

## Distribution and enrichment processes of lithium and other solutes in the Salar de Uyuni brine

NADJA SCHMIDT\*, ROBERT SIELAND AND BRODER MERKEL

TU Bergakademie Freiberg, Department of Hydrogeology, D-09599 Freiberg, Germany (\*correspondence: Nadja.Schmidt@geo.tu-freiberg.de)

The world's largest salt pan, the Salar de Uyuni, is located in the Bolivian Altiplano, at 3650 masl between the eastern and western cordilleras of the Andes. Although it hosts one of the world's most promising lithium deposits, accumulation and horizontal distribution of lithium and other solutes in the brine are not satisfactorily understood.

During various drilling and sampling campaigns (2009-2012) numerous brine samples were taken from boreholes down to 12 m all over the salt lake. Further brine samples were gained from one meter deep drilling holes along three transects from the center to the border in the northeastern part of the Salar. All samples were investigated by IC and ICP-MS as well as for stable isotopes.

Li concentrations in the brine vary between 200 and 1500 mg/L, whereby a vertical gradient could not be observed in the upper 12 m. Li is peaking near the northeastern and southeastern shore, with concentration gradients of 100 mg/L/km (own data) and 40 mg/L/km [1], respectively. Li peaks match with the delta areas of former and recent inflowing rivers. Hence, more than one major tributary as a source of lithium exist, which is in contradiction to results of former investigations supposing the Rio Grande to be the only feeder of lithium to the salt lake basin [2].

The surface in areas where increased Li concentrations occur is characterized by muddy sediments interspersed with crystals of halite and other evaporites. Because clay is decreasing in direction from the shore a temporary fixation and release of Li on clay is assumed as controlling factor leading to an effective enrichment in the brine.

[1] F. Risacher & B. Fritz (2000) *Chemical Geology* 167: 373-392. [2] S.L. Rettig, B.F. Jones, F. Risacher (1980) *Chemical Geology* 30: 57-79



## Calcium isotope fractionations from roots to shoots

SCHMITT A.-D.<sup>1,2\*</sup>, STILLE P.<sup>1</sup>, LABOLLE F.<sup>3</sup>, COBERT F.<sup>1,4</sup>, BOURGEADE P.<sup>2</sup>, CHABAUX F.<sup>1</sup> AND GANGLOFF S.<sup>1</sup>

<sup>1</sup>Université de Strasbourg et CNRS-UMR 7517,

LHyGeS/EOST ; 1 rue Blessig, F-67000 Strasbourg

<sup>2</sup>Université de Franche-Comté et CNRS-UMR 6249, Chrono-

environnement ; 16, route de Gray, F-25000 Besançon

<sup>3</sup>Université de Strasbourg, Institut de Zoologie et de Biologie végétale, 12, rue de l'université, F-67000 Strasbourg

<sup>4</sup>Université de Liège, Faculté d'agronomie de Gembloux; 27 avenue du maréchal Juin, B-5030 Gembloux

\* adschmitt@unistra.fr

Recent studies have shown that Ca isotope ratios have the potential to be important tracers of biological activities in forested ecosystems or more generally in plant physiology and in biogeochemistry.

Field studies performed in forested watersheds point to the importance of Ca isotope fractionations in soil solutions due to biological activity in the surficial soil horizons. Hydroponic experiments, performed on rapid growing bean plants, that allow to have a complete growth cycle, helped to identify the mechanisms responsible for these Ca isotope fractionations (Cobert *et al.*, 2011; Schmitt *et al.*, 2013). Indeed, the adsorption of Ca by lateral roots, that are enriched in <sup>40</sup>Ca compared to the nutritive medium, follows a closed-system equilibrium fractionation with a fractionation factor of 0.9988, suggesting that Ca forms exchangeable bonds with the RCOO<sup>-</sup> groups in the cell wall structure of the lateral roots. Two other fractionation levels have been identified within the plant during the Ca transfer from roots to shoots. When the xylem sap goes to the shoots, <sup>40</sup>Ca is preferentially bound to the polygalacturonic acids (pectins) of the middle lamella of the xylem cell wall. Finally, a third fractionation occurs in the reproductive organs also caused by cation-exchange processes with pectins. The fractionation mechanisms are the same whatever the Ca content and pH of the nutritive solution. Only the bean plants average signature as well as the amplitude of the Ca isotopic fractionation within plant organs are highly dependent on the composition of the nutritive solution. A comparative field study is installed to examine the Ca isotopic fractionation in trees of a forested watershed.

[1] Cobert *et al.* 2011, *GCA* **75**, 5467-5482; [2] Schmitt *et al.*, 2013. *GCA* **110**, 70-83.

## Atmospheric CF<sub>4</sub> trapped in polar ice – A new proxy for granite weathering

J. SCHMITT<sup>1\*</sup>, B. SETH<sup>1</sup>, P. KÖHLER<sup>2</sup>, J. WILLENBRING<sup>3</sup> AND H. FISCHER<sup>1</sup>

<sup>1</sup>Climate and Environmental Physics & Oeschger Centre for Climate Change Research, University of Bern, CH,

(\*correspondence: schmitt@climate.unibe.ch)

<sup>2</sup>Alfred Wegener Institute Helmholtz Centre for Polar and Marine Research, Bremerhaven, Germany

<sup>3</sup>University of Pennsylvania, Department of Earth & Environmental Sciences, Philadelphia, USA

The reconstruction of continental weathering rates using trace elements and their isotopes measured on marine sediments and crusts is a vigorously growing field. Here, we use a novel approach using the ppt-level trace gas CF<sub>4</sub>, tetrafluoromethane, which can be analysed in air trapped in ice cores. CF<sub>4</sub> is a trace impurity in granites and other plutonic rocks, and during weathering this gas escapes into the atmosphere. In preindustrial times, this release from granitic rocks was the only natural source of CF<sub>4</sub>. Because CF<sub>4</sub> is inert to destruction processes in the tropo- and stratospheres, its only sink is destruction by UV radiation and radicals in the mesosphere. This chemical inertness is responsible for an exceptionally long atmospheric lifetime which is expected to range between 50 kyr and 400 kyr. Although the globally integrated CF<sub>4</sub> emission flux from weathering is only a few tons per year, the exceptionally long lifetime allows to establish a long-term atmospheric concentration of about 33 ppt. We developed a vacuum melt-extraction system for ice core samples coupled to a mass spectrometry detector to precisely measure these trace amounts of CF<sub>4</sub> found in past atmosphere and applied this method to ice over the entire Dome C ice core. During the last 800 kyr, atmospheric CF<sub>4</sub> varied in a narrow band between 31 ppt and 35 ppt, i.e. only 10-15 % variability, providing a first estimate of the long-term weathering rate fluctuations. Our record shows that CF<sub>4</sub> increases during interglacials and falls during the coldest, glacial phases. However, our CF<sub>4</sub> record shows also a pronounced shift toward higher CF<sub>4</sub> levels after 430 kyr (the Mid-Brunhes Event). With the beginning of Marine Isotope stage 11, we find a steep rise in CF<sub>4</sub> that probably relates to intense weathering during the first full interglacial after a series of lukewarm interglacials.

## CF<sub>4</sub> and CO<sub>2</sub> - coupling weathering and carbon cycle

J. SCHMITT<sup>1\*</sup>, B. SETH<sup>1</sup>, P. KÖHLER<sup>2</sup>, J. WILLENBRING<sup>3</sup>  
AND H. FISCHER<sup>1</sup>

<sup>1</sup>Climate and Environmental Physics & Oeschger Centre for Climate Change Research, University of Bern, CH, (\*correspondence schmitt@climate.unibe.ch)

<sup>2</sup>Alfred Wegener Institute Helmholtz Centre for Polar and Marine Research, Bremerhaven, Germany

<sup>3</sup>University of Pennsylvania, Department of Earth & Environmental Sciences, Philadelphia, USA

The analysis of CO<sub>2</sub> and its stable carbon isotopes from ice cores revealed large changes of atmospheric CO<sub>2</sub> related to changes in ocean circulation, marine biological processes and contributions from the terrestrial carbon storage. These processes dominate the glacial/interglacial CO<sub>2</sub> variations. Yet, CO<sub>2</sub> is also modulated by the marine alkalinity balance. The net alkalinity influx to the ocean is driven by silicate weathering drawing down atmospheric CO<sub>2</sub>. Conversely, alkalinity is lost when CaCO<sub>3</sub> is buried in marine sediments. On orbital time scales, these fluxes are assumed to be almost balanced as atmospheric CO<sub>2</sub> and its climatic effects feedback on the weathering rates providing a negative feedback loop.

Trace elements from marine sediments are widely applied to derive weathering rates or changes in the weathering style for a certain region. Here, we use a novel approach to provide a global weathering estimate using the ppt-level trace gas CF<sub>4</sub> archived in polar ice cores. CF<sub>4</sub> is found as a trace gas in granites, and during weathering it escapes to the atmosphere. Because CF<sub>4</sub> is inert in the lower atmosphere, its only sink is destruction by UV radiation in the mesosphere. This chemical inertness is responsible for an exceptionally long atmospheric lifetime which is expected to range between 50 kyr and 400 kyr. We developed a vacuum melt-extraction system for ice core samples to precisely measure these trace amounts of CF<sub>4</sub> and applied it to ice over the entire Dome C ice core. During the last 800 kyr, atmospheric CF<sub>4</sub> varied in a narrow band between 31 ppt and 35 ppt, i.e. only 10-15 % variability, providing a first estimate of the long-term weathering rate fluctuations. Our record shows that CF<sub>4</sub> increases during interglacials and falls during the coldest, glacial phases. However, our CF<sub>4</sub> record also shows a pronounced shift toward higher CF<sub>4</sub> levels after 430 kyr. With the beginning of MIS 11, we find a rise in CF<sub>4</sub> that probably relates to intense weathering during the first full interglacial after a series of lukewarm interglacials. This dataset lends support to a strong positive coupling of continental weathering and climate.

## Multitracer paleoclimate and recharge study of groundwater in the North China Plain

T. SCHNEIDER<sup>1\*</sup>, G. CAO<sup>2</sup>, C. ZHENG<sup>2,3</sup>  
AND W. AESCHBACH-HERTIG<sup>1</sup>

<sup>1</sup>Institute of Environmental Physics, Heidelberg University, Im Neuenheimer Feld 229, 69117 Heidelberg, Germany (\*correspondence: Tim.Schneider@iup.uni-heidelberg.de)

<sup>2</sup>Center for Water Research, College of Engineering, Peking University, Beijing 100871, China

<sup>3</sup>Department of Geological Sciences, University of Alabama, Tuscaloosa, Alabama, USA

A multitracer study of groundwater in the North China Plain (NCP) was conducted in the framework of a Chinese-German cooperation project whose main objective is to obtain groundwater ages and recharge rates in order to refine a groundwater flow model of the NCP and to help find ways for sustainable groundwater management [1]. Additionally, the obtained data adds to an existing data set from a previous paleoclimate and groundwater recharge study in the NCP [2][3].

Samples were taken on two sampling campaigns in 2011 and 2012 from 36 wells along a transect in the northern NCP starting at the mountains in the west, passing south of Beijing and leading to the Bohai Sea at Tianjin. In addition, seven wells were sampled on a short transect near Handan, further south in the NCP.

Dating tracers being used are <sup>3</sup>H-<sup>3</sup>He, SF<sub>6</sub> and CFCs 11, 12 and 113 for young ages and <sup>14</sup>C as well as <sup>4</sup>He for a longer time scale. The climate information is obtained through dissolved noble gases and stable isotopes. The combined use of SF<sub>6</sub> and CFCs allows us to identify and correct for possible SF<sub>6</sub> from natural sources and CFC contamination in the highly industrialized area near Beijing.

Dating results show that the groundwater age mainly increases with depth rather than distance along the transect, with an abrupt rise at a depth of around 100m. Enhanced concentrations of both SF<sub>6</sub> and CFCs are unrelated, indicating different sources. The noble gas temperatures suggest a temperature difference between the Holocene and the last glacial period of about 5°C. Overall, the new data confirm and complement previous results from the NCP [2][3].

[1] Cao *et al.* (2013), *Water Resour. Res.* **49**, 159-175. [2] Kreuzer *et al.* (2009), *Chem. Geol.* **259**, 168-180. [3] von Rohden *et al.* (2010), *Water Resour. Res.* **46**, W05511

## **$^{241}\text{Am}$ supporting $^{210}\text{Pb}$ and $^{137}\text{Cs}$ dating**

BERNHARD SCHNETGER<sup>1</sup> KATHARINA HÄUSLER<sup>2</sup>  
AND OLAF DELLWIG<sup>2</sup>

<sup>1</sup>ICBM, Carl-von-Ossietzky University, 26111 Oldenburg, Germany; b.schnetger@icbm.de

<sup>2</sup>Leibniz Institute for Baltic Sea Research (IOW), Rostock, Germany; katharina.hauesler@io-warnemuende.de; olaf.dellwig@io-warnemuende.de

$^{210}\text{Pb}$  dating is usually supported by radioactive  $^{137}\text{Cs}$  to verify age models. Atmospheric nuclear bomb testing in the 50<sup>th</sup> and 60<sup>th</sup> as well as the Chernobyl accident in 1986 has introduced not only measurable amounts of radioactive Cs but also Pu nuclides into the environment. Due to the relatively short half-life of  $^{241}\text{Pu}$  (14.35 a) measurable activities of the daughter  $^{241}\text{Am}$  are now present and can directly be analysed by modern gamma-ray detectors (Appleby *et al.* 1991). The advantages of using  $^{241}\text{Am}$  over  $^{137}\text{Cs}$  are a) its high particle reactivity causing rapid sedimentary burial and b) its immobile behaviour after deposition minimizing redistribution. While the 1963 peak in  $^{137}\text{Cs}$  is prone for a large dispersion in the sedimentary environment,  $^{241}\text{Am}$  forms sharp peaks in undisturbed sediments. Even the frequency of atmospheric nuclear bomb testing can be identified by high-resolution sampling of geological archives resulting in more trustful age determinations. In sediments where both  $^{210}\text{Pb}$  and  $^{137}\text{Cs}$  fail to give reliable ages,  $^{241}\text{Am}$  can be used for a rough age estimation of sediment intervals. In such cases the following  $^{241}\text{Am}$  time markers can be used: increased activities due to the frequency of atmospheric bomb testing in 1951, first maximum in 1958, second maximum in 1962 and a narrow peak in 1986 (Chernobyl) and possibly in the future 2011 (Fukushima). Between these markers, sediment velocities or sedimentation rates (if dry bulk density is known) can be calculated spanning at least a half century back in time. The sharp peaks originating from accidents can easily be missed by low-resolution sampling. Due to the much longer half-life of  $^{241}\text{Am}$  (432a) compared to  $^{137}\text{Cs}$  (30.17a) this tracer can be used when  $^{137}\text{Cs}$  cannot be detected in the environment any more. For instance,  $^{137}\text{Cs}$  in 1962 sediment layers will be decayed after app. eight half-lives in 2075. In addition, sediment data from the euxinic Landsort and Gotland Deeps (Baltic Sea) indicate a significant influence on  $^{137}\text{Cs}$  and  $^{210}\text{Pb}$  burial over time due to the Mn-pump within the redoxline.

[1] Appleby P.G., Richardson N., & Nolan P.J. (1991):  $^{241}\text{Am}$  dating of lake sediments. *Hydrobiologia* 214, 35-42.

## **Cr isotopic variations in Neoproterozoic near-surface chemical sediments**

R. SCHOENBERG<sup>1\*</sup>, I.C. KLEINHANN<sup>1</sup>, M. WILLE<sup>1</sup>,  
M. VAN ZUILEN<sup>2</sup>, R.B. PEDERSEN<sup>3</sup>, V. MELEZHNIK<sup>3,4</sup>  
AND N. BEUKES<sup>5</sup>

<sup>1</sup>Dept. of Geoscience, University of Tuebingen, Germany  
(\*correspondence: schoenberg@ifg.uni-tuebingen.de)

<sup>2</sup>Institute de Physique de Globe de Paris, France

<sup>3</sup>Centre for Geobiology, University of Bergen, Norway

<sup>4</sup>Geological Survey of Norway (NGU), Trondheim, Norway

<sup>5</sup>Dept. of Geology, University of Johannesburg, South Africa

Recent studies explored the potential of stable Cr isotopic variations in oceanic sedimentary archives as tracer for atmospheric oxygen levels through Earth's history [1,2]. Thereby, the stable Cr isotopic variations in up to 2.75 Ga old BIFs were interpreted to indicate oxidative chromium weathering on the continents initiated by an accumulation of small levels of free atmospheric oxygen some 350 Ma before the ca. 2.4 to 2.32 Ga great oxidation event (GOE) [1]. This interpretation, however, was challenged by others [3], who propose that the Cr isotopic variations in these predominantly Algoma type BIFs are due to non-redox isotopic effects caused by rapid precipitation from their deep-water hydrothermal source.

In order to shed light on the applicability of stable Cr isotopes as paleo-redox tracer we investigated carbonates from well-defined supra-, intra- and subtidal depositional environments from the ca. 2.55-2.48 Ga old Malmani Subgroup of the Transvaal Basin in South Africa and 2.06 Ga old lacustrine carbonates, marine stromatolites and near-shore jaspilites from the Pechenga Greenstone Belt, as well as 2.0 Ga organic-rich, siliceous deposits from the Onega Basin, both situated in the NW Fennoscandian Shield. The relatively large variations (ca. +1.4‰ to -1.2‰ in  $\delta^{53/52}\text{Cr}$ ) found in post-GOE sedimentary archives from the Fennoscandian Shield support chromium redox-cycling associated with oxidative chromium weathering on the continental surface. Compared to the large Cr isotope variations of these post-GOE deposits, the range in  $\delta^{53/52}\text{Cr}$  values of late Archean sedimentary archives appears to be much smaller. Possible scenarios to explain the observed Cr isotopic variations in these sedimentary archives and their implications to the presence of free atmospheric oxygen will be discussed.

[1] Frei *et al.* (2009) *Nature* **461**, 250-253. [2] Frei *et al.* (2011) *EPSL* **312**, 114-125. [3] Konhauser *et al.* (2011) *Nature* **478**, 369-373.

## From date to process: Integrating geochemistry and geochronology on very short and very long timescales

BLAIR SCHOENE

219 Guyot Hall, Department of Geosciences, Princeton University, Princeton, NJ, USA.  
(bschoene@princeton.edu)

How continental crust is created, preserved and recycled, and whether or not these processes have changed through Earth history are important for a) understanding the geochemical and petrological stratification of the crust and b) quantifying long term geochemical and isotopic cycling in the Earth's crust and mantle. Developing models for crustal evolution requires robust geochronology on both the short and long timescales, targeting relatively rapid geologic phenomena (e.g. magma production and differentiation) as well as long term secular change. This contribution highlights recent efforts to better apply high-precision U-Pb geochronology to continental magmatic systems and to develop techniques comparing magmatic systems through Earth history.

Models describing the transfer of mass and heat through the crust during orogenesis demand age constraints with increasing precision and accuracy. While modern ID-TIMS U-Pb geochronology can resolve the timescales of zircon crystallization in single pulses of magma, much work is needed to relate dates to processes such as magma production, transport, differentiation, and emplacement. Our recent work focuses on integrating zircon crystallization ages and geochemistry to both understand the growth history of single zircons on <50 ka timescales and to build a framework for longer timescale geochemical evolution of two Alpine magmatic systems.

To compare differences in magmatic differentiation during crustal magmatism from the Archean to present, we develop statistical methodologies for analyzing large geochemical databases (Earthchem, etc.). Substantial differences in both crustal inputs (basalts) and indicators of differentiation to high-Si compositions suggest either secular changes in magmatic/metamorphic processes during crustal genesis and modification, or preservation bias. These results motivate further detailed investigation of Archean terranes, although robust comparison between any number of orogenic belts, Archean or modern, require geochronology with precision that is relevant to tectonomagmatic processes. Sub-million year precision is now achievable in Archean rocks by ID-TIMS U-Pb geochronology, but necessitates careful integration of field, geochemical, and geochronological data with numerical modelling studies.

## Evolution of temperature and precipitation during Marine Isotope Stage 5 recorded in speleothems from the Hüttenbläuserschachthöhle, western Germany

D. SCHOLZ<sup>1,2\*</sup>, D. HOFFMANN<sup>2,3</sup>, C. SPÖTL<sup>4</sup>, Y. KOCOT<sup>1</sup>  
AND P. HOPCROFT<sup>5</sup>

<sup>1</sup>Institute for Geosciences, University of Mainz, Johann-Joachim-Becher-Weg 21, 55128 Mainz, Germany  
(\*correspondence: scholz@uni-mainz.de)

<sup>2</sup>Bristol Isotope Group (BIG), School of Geographical Sciences, University of Bristol, University Road, BS8 1SS Bristol, United Kingdom

<sup>3</sup>CENIEH, Paseo Sierra de Atapuerca s/n, 09002-Burgos, Spain

<sup>4</sup>Institut für Geologie und Paläontologie, Leopold-Franzens-Universität, Innrain 52, 6020 Innsbruck, Austria

<sup>5</sup>Bristol Research Initiative for the Dynamic Global Environment (BRIDGE), School of Geographical Sciences, University of Bristol, University Road, BS8 1SS Bristol, United Kingdom

We present high-resolution  $\delta^{18}\text{O}$ ,  $\delta^{13}\text{C}$  and trace element profiles for two stalagmites from Hüttenbläuserschachthöhle, western Germany, which grew during Marine Isotope Stage (MIS) 5.

HBSH-1 provides a climate record with decadal to centennial resolution between 130 and 80 ka, which shows four growth interruptions coinciding with the Greenland Stadials. This shows that stalagmite growth is a very sensitive proxy for cool and dry conditions in the northern hemisphere.

We interpret stalagmite  $\delta^{18}\text{O}$  as a proxy for past temperature changes, whereas stalagmite  $\delta^{13}\text{C}$  rather reflects changes in the hydrologic balance. The  $\delta^{13}\text{C}$  record shows three pronounced negative peaks during MIS 5, and the timing of those is in agreement with MIS 5e, 5c and 5a. This suggests warm and relatively humid climate in western Germany for these phases.

During the Last Interglacial, the evolution of  $\delta^{18}\text{O}$  and  $\delta^{13}\text{C}$  is opposite. Whereas the  $\delta^{18}\text{O}$  signal suggests the warmest conditions around 125 ka followed by a gradual decrease, the  $\delta^{13}\text{C}$  signal indicates wetter conditions towards the end of the Last Interglacial. This 'decoupling' of temperature and humidity during MIS 5e is also visible in a series of snapshot simulations performed with the general circulation model FAMOUS.

## Chemical and isotopic composition of soil solutions from cambisols in Styria (Austria) - Seasonality, evaporation and interstitial distribution

W. SCHÖN<sup>1\*</sup>, A. LEIS<sup>2</sup> AND M. DIETZEL<sup>1</sup>

<sup>1</sup>Institute of Applied Geosciences, Graz University of Technology, Rechbauerstraße 12, 8010 Graz, Austria, (\*correspondence: w.schoen@student.tugraz.at)

<sup>2</sup>Institute of Water, Energy and Sustainability, Joanneum Research, Elisabethstraße 18, 8010 Graz, Austria

In most natural surroundings soil solutions are primarily gained from the uptake of meteoric water. Subsequently infiltration, capillary exchange, bioresponse, evaporation etc. result in complex and individual gas-water-solid systems. Knowledge on the isotopic and chemical evolution of soil solutions and its interstitial distribution is highly relevant for environmental and forensic studies, but respective systematic and combined field and experimental studies are rare.

Therefore we investigated the composition of solids and interstitial solutions of individual horizons for three cambisols in Styria (Austria). The solutions were separated from the soils by compaction method at hydraulic pressures of 27.4 and 54.9 MPa, corresponding to respective matric potentials (mp).

The soils consist mainly of quartz, chlorite, muscovite, plagioclase with associated silicates like kaolinite and vermiculite, but without a significant vertical variability. The pH of the separated soil solutions typically increases with depths and elevated mp. Concentrations of dissolved ions such as Ca<sup>2+</sup> and Mg<sup>2+</sup> increase at high mp, which correspond to higher  $\delta D$  and  $\delta^{18}O$  values. Lab experiments for evaporation and wetting indicate a systematic correlation of the combined isotope data and solution chemistry. The field-related and experimental results are discussed in respect to the impact of seasonality, evaporation, and mp-related interstitial distribution of the (isotope) geochemical composition of the separated soil solutions.

## X-ray tomography links macroscopic silicate fabric and AMS fabric

A. SCHÖPA<sup>\*1</sup>, D. FLOESS<sup>2</sup>, M. DE SAINT BLANQUAT<sup>3</sup>, P. LAURNEAU<sup>4</sup>, C. ANNEN<sup>1</sup> AND L. BAUMGARTNER<sup>2</sup>

<sup>1</sup>School of Earth Sciences, University of Bristol, Wills Memorial Building, BS8 1RJ Bristol, UK

(\*correspondence: anne.schopa@bristol.ac.uk)

<sup>2</sup>Université de Lausanne, Batiment Geopolis, 1015 Lausanne, Switzerland

<sup>3</sup>Géosciences Environnement Toulouse / Observatoire Midi-Pyrénées, 31400 Toulouse, France

<sup>4</sup>Laboratoire de Planétologie et Géodynamique de Nantes, CNRS/Université de Nantes, 44322 Nantes, France

Anisotropy of magnetic susceptibility (AMS) has been widely applied to gain insight into magnetic fabrics in granitic intrusions, basalt lava flows and dikes. In order to draw this generic link, it is assumed that the AMS fabric reflects the silicate fabric and hence gives information about magma flow, emplacement related strain and/or tectonic strain. However, a detailed analysis of this link between macroscopic magmatic fabric and AMS fabric is still lacking.

We present the first comparison between different fabric datasets to show how the macroscopic silicate fabric is linked to the magnetite-controlled AMS fabric on the grain-size scale. Datasets include 1) macroscopic silicate fabric measured directly in the field; 2) macroscopic silicate fabric derived from image analysis of rock slab pictures and sample pictures [1]; 3) shape preferred orientation (SPO) of mafic silicates from X-ray tomography images; 4) SPO of magnetite grains from X-ray tomography images [2]; 5) calculated distribution of magnetite grains from X-ray tomography images; 6) AMS fabric. The data were collected in the granitic intrusion of the Lago della Vacca Complex, Adamello Batholith, Italy.

Macroscopic mineral fabrics measured in the field and obtained with image analysis agree with each other and with the SPO of mafic silicates calculated from the tomography scans. Furthermore, the tomography results show that the SPO of mafic silicates and of the magnetite grains are consistent with the AMS data whereas the distribution of the magnetites is less compatible with the AMS fabric.

The consistent results obtained from a variety of methods demonstrate that the orientation of the AMS ellipsoid coincides with the macroscopic silicate fabric. This enforces the application of AMS as a robust tool to characterise magmatic fabrics in granitic intrusions.

[1] Launeau *et al.* (2010) *Tectonophysics* **492**, 230-239. [2] Ketchum (2005) *J Struct Geol* **27**, 1217-1228.

## Controls on the isotope composition of trace metals in calcite - New tools for paleo-reconstructions

J. SCHOTT<sup>1\*</sup>, V. MAVROMATIS<sup>1</sup> AND E. H. OELKERS<sup>1</sup>

<sup>1</sup>Université de Toulouse & CNRS, GET, Toulouse, France,  
(\*presenting author jacques.schott@get.obs-mip.fr,  
mavromat@get.obs-mip.fr, oelkers@get.obs-mip.fr)

Divalent metals including Ba, Mg, Sr, Cd, Co, Cu, Mn, and Zn exhibit contrasting ion size, diffusivity, hydration energy (or rate of exchange of water molecules in their hydration sphere), and affinity to hydrolyze or form inorganic and organic ligands. A large number of past studies have shown that these contrasting properties affect calcite-fluid partition constants, and how these partition coefficients vary with calcite growth rate.

In an effort to extend these observations to isotopic fractionation we have performed a number of related experimentally studies showing how crystal growth rates, and fluid pH and speciation impact the isotopic composition of the divalent metals incorporated into the calcite lattice. For example, the extent of Mg isotope fractionation between calcite and the fluid phase increases considerably with **decreasing** calcite growth rate<sup>1</sup>. In contrast, Ba, Sr, and Zn isotope fractionation increases with **increasing** calcite growth rate. Equally, Ca and Mg isotope fractionation increase with calcite and magnesite growth rate, respectively<sup>2</sup>. The distinct behavior of Mg stems from the reduced lability of water molecules in its coordination sphere compared to Ca, Ba, Sr, or Zn, and provides new insight on carbonate growth mechanisms. Moreover, Mg kinetic isotope fractionation can be quantified using three isotope diagrams<sup>3</sup> which allow the precise determination of equilibrium fractionation factors and provides a new tool to quantify the growth rates of calcite precipitated in the deep past. Such tools also provide insight into the saturation state of the fluids present when the calcite precipitated. Similarly, the measurement of Zn and Cu concentration and isotope compositions during calcite growth at fixed rates, pH, saturation state, and concentration of selected inorganic and organic ligands, allow quantification of the equilibrium isotope composition of Zn and Cu incorporated in the lattice and its dependence on the aqueous fluid composition. Such observations provide new insight into the metal incorporation mechanisms during calcite growth. Our experimental calibrations, validated by the quantification of Mg, Zn and Cu chemical and isotope fractionation in calcite-precipitating springs, are providing new and powerful tools to reconstruct paleo-environmental conditions from the isotope compositions recorded in carbonate sediments.

[1] Mavromatis *et al.* (2013) *Geochim. Cosmochim. Acta* (in press). [2] Pearce *et al.* (2012) *Geochim. Cosmochim. Acta* **92**, 170-183. [3] Young *et al.* (2002) *Geochim. Cosmochim. Acta* **66**, 683-698.

## Serpentinization, Microbial Activities, and Carbon Flow in the Deep Biosphere

MATTHEW O. SCHRENK<sup>1</sup>

<sup>1</sup>East Carolina University, Greenville, NC, USA

Serpentinizing ultramafic rocks are conduits for the exchange of carbon and energy between the deep Earth and the surface environment and are ubiquitous, occurring on each of the continents and over vast portions of the seafloor. Serpentinization commonly generates high pH (>11), highly reducing conditions rich in hydrogen and methane that can sustain deep subsurface microbial communities which play important roles in controlling the composition and mobility of carbon-bearing compounds. Due to a complex interplay of nutrient sources and sinks and because they are perched near the limits of life, the significance of microbial processes in serpentinites has proven difficult to constrain. Recently, concerted studies of serpentinites in both continental and marine settings have begun to identify the functional potential of serpentinite-associated microbial communities, their energy sources, and their impacts upon carbon speciation. Metagenomic and functional genomic analyses document evidence of both consumption and production of hydrogen and methane in certain environments and in some cases for microbially-mediated sulfur and iron red-ox transformations. These studies also provide evidence for CO and CO<sub>2</sub> assimilation and the potential for the fermentation of organic matter derived from deep Earth materials. These data provide important targets for quantification of subsurface biogeochemical processes and their impact upon the characteristics of circulating fluids and their host rocks. By linking microbiological data with geochemical data, these studies also provide the opportunity to develop new paradigms for understanding microbial adaptations and evolution in the deep subsurface environment.

## Intact polar lipids and diagenetic processes in sub-seafloor sediments in the Black Sea

JAN M. SCHRÖDER<sup>1\*</sup>, IVANO W. AIELLO<sup>2</sup>, TOBIAS GOLDHAMMER<sup>1</sup>, VERENA B. HEUER<sup>1</sup>, MARCUS ELVERT<sup>1</sup>, MATTHIAS ZABEL<sup>1</sup> AND KAI-UWE HINRICHS<sup>1</sup>

<sup>1</sup> MARUM – Center for Marine Environmental Sciences and Dept. of Geosciences, University of Bremen, Germany (\*correspondance: jschroeder@marum.de)

<sup>2</sup> Moss Landing Marine Laboratories, Moss Landing, CA, USA

The Black Sea is the world's largest anoxic basin where the water column beneath 100 m depth as well as the underlying sediments are devoid of oxygen. FS Meteor cruise M84/1 (DARCSEAS) [1] investigated site GeoB 15105 in the SW Black Sea and obtained an 8 m-sedimentary record of complex Late Pleistocene environmental change due to the transition from a limnic to a brackish marine system. The resulting diagenetic regime in these sediments is unusual and exhibits signals of overlapping sulfate reduction, methanogenesis, and Fe reduction, coupled with variable concentrations of total organic carbon. This is consistent with evidence for abundant sulfate-reducing bacteria in the methanogenic zone [2]. Using a strongly improved set of methods for extraction, preparation and detection of microbial intact polar lipids (IPL), we examined signals of the sedimentary microbial communities in relation to the complex diagenetic regime and sedimentary history as determined by pore-water analysis of electron donors and acceptors and sedimentological examination, respectively.

We found that IPLs were present throughout the whole sediment core with a maximum in a sapropel layer at around four meters. IPL concentrations were highly variable and archaeal glycolipids (e.g., mono- and diglycosidic glyceroldibiphytanyltetraethers) as well as bacterial phospholipids (e.g., diether based phosphatidylethanolamines) were observed down to a depth of eight meters. Furthermore, varying ratios of archaeal to bacterial lipids between 0.1 and 0.6 revealed regional differences of microbial abundance and could also be related to methane oxidation processes. Our study provides new insights into the relationship of microbial communities, diagenetic processes and the sedimentary history in the Black Sea sediments.

[1] Zabel (2011) RV METEOR, *Cruise Report M84/1 2011*, DFG. [2] Leloup *et al.* (2007) *Env. Microbiol.* **9**, 131-142.

## Sediment traps in Lake Baikal reveal strong changes in productivity over the last decade

C.J. SCHUBERT<sup>1\*</sup>, J. NIGGEMANN<sup>2</sup> AND M. STURM<sup>1</sup>

<sup>1</sup>Surf, Eawag, 6047 Kastanienbaum, Switzerland (\*correspondence: carsten.schubert@eawag.ch, mike.sturm@eawag.ch)

<sup>2</sup>Max Planck Research Group for Marine Geochemistry University of Oldenburg, 26129 Oldenburg, Germany, (jniggema@mpi-bremen.de)

### More than 10 years of monitoring

Lake Baikal is one of the largest lakes in the world and with a maximum water depth of ~1640 m also the deepest. This makes it unique and comparable to an ocean also since due to efficient vertical mixing oxygen concentrations are high throughout the water column.

We have moored sediment traps which were recovered and renewed every year since 1999. Up to 18 traps were deployed over the whole water column. Organic carbon and nitrogen concentrations and isotopes as well as chlorin concentrations and chlorin indices were measured to estimate productivity and the composition of the organic material. C/N ratios between 10 and 13 hint to a strong autochthonous together with some allochthonous contribution to the organic material.  $\delta^{13}\text{C}_{\text{org}}$  values around -31 ‰ (rather light for freshwater systems) were described before by Qiu *et al* [1] and related to diatom blooms. Chlorin measurements showed very strong, i.e., up to 5-fold variations in productivity. Chlorin indices [2] varied from 0.5 to 1.5 indicating differences in organic material freshness over the years.

[1] Qiu *et al.* (1993) *Geology* **21**, 25-28. [2] Schubert *et al.* (2005) *Geochem. Geophys. Geosyst.* **6**, Q03005, doi:10.1029/2004GC000837

## Rn in water detection by LSC – sample volume optimization

MICHAEL SCHUBERT<sup>1</sup> AND JUERGEN KOPITZ<sup>2</sup>

<sup>1</sup>Helmholtz Centre for Environmental Research Leipzig, Germany; (michael.schubert@ufz.de)

<sup>2</sup>Universitätsklinikums Heidelberg, Germany; (Juergen.Kopitz@med.uni-heidelberg.de)

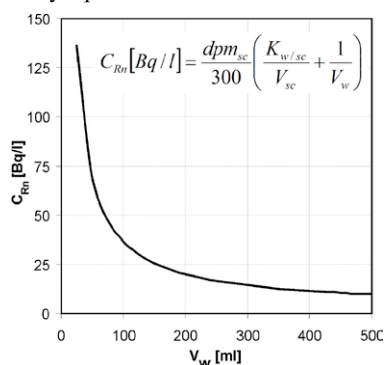
Radon (<sup>222</sup>Rn) is, amongst the noble gases, of particular interest as tracer in groundwater / surface water interaction studies. In related applications radon-in-water concentrations can be detected either directly in the field by using a mobile radon-in-gas monitor or after a water sampling campaign by liquid scintillation counting (LSC) in the laboratory.

If LSC is applied the radon has to be transferred from the water sample of a certain volume  $V_w$  [l] into the scintillation cocktail of the volume  $V_{sc}$  [l]. Whereas  $V_{sc}$  is preset by the size of the LSC vials (usually 20 ml)  $V_w$  is not specified. Aim of the presented study is an optimization of  $V_w$ .

The equation given in the figure allows calculating the <sup>222</sup>Rn concentration that was originally present in the water sample  $C_{Rn}$  [Bq/l] based on  $V_{sc}$  and  $V_w$ , on the water/cocktail partition coefficient for radon  $K_{w/sc}$  and on the dpm value detected in the cocktail  $dpm_{sc}$ . The equation is based on the assumption that  $dpm_{sc}$  represents the total dpm of <sup>222</sup>Rn and its four short-lived progeny (after 3 h equilibration time), i.e. of five radionuclides in decay equilibrium.

Plotting the equation for an exemplary  $dpm_{sc}$  value (e.g. 1000), for a  $K_{w/sc}$  value of 0.019 (valid for 21°C) and for varying values for  $V_w$  and  $V_{sc}$  results in a 3D image. Setting  $V_{sc}$  to 20 ml (the cocktail volume that is

usually applied) results in the 2D plot for  $C_{Rn}/V_w$  shown in the diagram. It becomes obvious that the gradient of the function flattens significantly if  $V_w$  increases over about 350 ml. That implies that an increase of the water sample volume over about 350 ml does *not* result in significantly higher counting rates (and neither in better counting statistics). On the other hand, a water volume that is significantly smaller than about 250 ml results in a significantly smaller radon concentration in the cocktail and hence in poorer counting statistics. Thus, water sample volumes of about 250 - 350 ml should be chosen if 20 ml vials are applied for radon-in-water detection by LSC.



## Transformational faulting in high pressure polymorphs – two case studies in quartz and olivine

ALEXANDRE SCHUBNEL<sup>1</sup>, FABRICE BRUNET<sup>2</sup>, NADÈGE HILAIRET<sup>3</sup>, JULIEN GASC<sup>4</sup>, YANBIN WANG<sup>4</sup> AND HARRY W. GREEN II<sup>5</sup>

<sup>1</sup>Laboratoire de Géologie, ENS<sup>2</sup> Paris, France

<sup>2</sup>ISTERRE, Université Joseph Fourier, Grenoble, France

<sup>3</sup>UMET, Université de Lille, Lille, France

<sup>4</sup>GSECARS, University of Chicago, Argonne, IL., USA

<sup>5</sup>Dept of Earth Sciences, UC at Riverside, CA, USA

Intermediate and deep focus earthquakes (100 -700 km) occur in a pressure and temperature regime where rocks are expected to deform plastically. The idea that they may be triggered by phase transformations in cold subducting lithosphere is appealing. However, the relationship between phase transformation and faulting remains unclear.

Coesite has been recognized as a reliable marker of ultrahigh-pressure (UHP) metamorphic environments in continental collision zones. Recent careful relocation of subduction-zone earthquakes have also shown that at depths of 100–250 km, seismicity occurs in the uppermost part of the slab, where the former oceanic crust has already been converted to eclogite. In the mantle transition zone, olivine undergoes two phase transformations while deep focus earthquakes locate inside the coldest part of slab, where metastable olivine bodies have sometimes been identified.

Here, we provide experimental evidence that, under differential stress at high pressure and temperature conditions ( $\Delta\sigma=2GPa$ ,  $P=2-5GPa$  and  $T=1150\pm 50K$ ), shear fractures nucleate and propagate at the onset of the olivine  $\rightarrow$  spinel transition in the  $Mg_2GeO_4$  analogue system. Similar observations were performed for quartz  $\rightarrow$  coesite ( $\Delta\sigma=4GPa$ ,  $P=3-4GPa$  and  $T=1300\pm 50K$ ) in samples of Arkansas novaculite. In both cases, fracture propagation is sufficiently rapid to radiate energy in the form of intense acoustic emissions. These follow the Gutenberg-Richter law over 4 orders of moment magnitudes and like intermediate and deep-focus earthquakes, require no volumetric strain.

Microstructural analysis shows the development of macroscopic faults, filled with a gouge composed exclusively of the HP polymorph (spinel or coesite). Within the gouge, the material is so fine (1-50 nm) that diffusion accommodated grain boundary sliding may have provided a mechanism viable at “co-seismic” strain rates ( $>10^4 s^{-1}$ ). Our results seem to indicate as a rule that HP polymorphic transformations are mechanically unstable under stress, simply because they are exothermic and induce large negative  $\Delta V$ . This clearly opens the prospects of revisiting a large number of phase transitions to assess their role in the triggering of deep seismicity.



## How mass balance affects isotope ratios in the weathering zone

J.A. SCHUESSLER, J. BOUCHEZ  
AND F. VON BLANCKENBURG

GFZ German Research Centre for Geosciences, Helmholtz  
Centre Potsdam, Potsdam, Germany  
(bouchez@gfz-potsdam.de)

The novel stable isotope signatures in the compartments of the weathering zone are controlled not only by isotope fractionation factors that are characteristic of the chemical processes at play in the weathering zone, but are also controlled by the elemental fluxes between the different compartments, *i.e.* by mass balance effects. To deconvolve these two effects, we designed a steady state, batch reactor, mass balance model representing the weathering zone from the soil scale to the large river scale. We assume the main fractionating processes being formation of secondary precipitates, such as clays, and uptake by plants [1]. The model shows that:

$$\delta_{diss}^X - \delta_{rock}^X = -\Delta^X \cdot \frac{E_{org+sec}^X}{S_{rock+prim}^X} \quad (1)$$

where  $\delta_{diss}^X$  and  $\delta_{rock}^X$  are the isotope composition of the metal element  $X$  in the dissolved load and in the source rock, respectively,  $\Delta^X$  the flux-weighted combined isotope fractionation factor,  $E_{org+sec}^X$  the export flux of  $X$  in isotopically fractionated solids (organics and secondary precipitates),  $S_{rock+prim}^X$  the release flux of  $X$  to water through primary mineral dissolution.

The main predictions are: (a) For very “soluble” elements (*i.e.* those with a low affinity for secondary precipitates and easily redissolved from plant litter), no fractionated  $\delta_{diss}^X$  solid is exported, and is likely to be close to the source rock,  $\delta_{rock}^X$ . Therefore, such elements are not viable tracers of weathering processes. (b) Equation (1) predicts that the largest difference in isotope ratios that can be observed between source rock and dissolved species and is equal to the combined isotope fractionation factor of the processes at play in the weathering zone.

The validity of these predictions are verified using an extensive database of measured water and rock isotope compositions and a compilation of experimentally determined isotope fractionation factors for Li, B, Mg, Si and Ca. It is observed that most  $\delta_{diss}^X - \delta_{rock}^X$  data fall indeed between 0 (source rocks) and the best estimate of  $-\Delta^X$ . Moreover, most of the  $\delta_{diss}^{Ca} - \delta_{rock}^{Ca}$  values are small compared to estimates of  $-\Delta^{Ca}$ , due to its high solubility.

[1] Bouchez *et al.*, *Amer. J. Sci.* **313**, 2013

## Early stage Ostwald ripening of submicrometer calcite

L.N. SCHULTZ\*, K. DIDERIKSEN, D. MÜTER,  
S.S. HAKIM AND S.L.S. STIPP

Nano-Science Center, Department of Chemistry, University of  
Copenhagen, Denmark (\*correspondence:  
lschultz@nano.ku.dk)

Ostwald ripening, also known as grain coarsening, occurs when crystals are at equilibrium with surrounding fluids. Over time, recrystallization favors larger and more thermodynamically stable particles. For calcite ( $\text{CaCO}_3$ ), this affects diagenesis, relevant for aquifers and oil reservoirs and plays a role in industrial products where a thin adsorbed water layer covers crystal surfaces. While saturated conditions are common in nature and industry, rates and consequences of recrystallization at equilibrium are much less known and understood than growth and dissolution far from equilibrium.

We exposed submicrometer scale calcite, with a surface area of  $11.8 \text{ m}^2/\text{g}$ , to saturated solutions at  $23 \text{ }^\circ\text{C}$ ,  $100 \text{ }^\circ\text{C}$  and  $200 \text{ }^\circ\text{C}$  and we observed grain coarsening for up to 261 days. Scanning electron microscopy (SEM) showed visible calcite crystal coarsening at  $100 \text{ }^\circ\text{C}$  and  $200 \text{ }^\circ\text{C}$  (Figure 1) within one day. BET surface area decreased by an order of magnitude and the average diameter grew to  $2 \text{ }\mu\text{m}$  or larger. We measured change in particle size distribution and determined that the lognormal shape is indicative of early stage Ostwald ripening, consistent with classical theory.

Coarsening at  $23 \text{ }^\circ\text{C}$  was not observable by BET or SEM, but changes in X-ray diffraction peak widths suggest an evolving surface, characterized by crystallite coarsening and fewer defects. These changes affect surface properties during the early stages of Ostwald ripening and have implications in our understanding of Ostwald ripening theories, behaviour in calcitic reservoirs and commercial calcite powder stability.

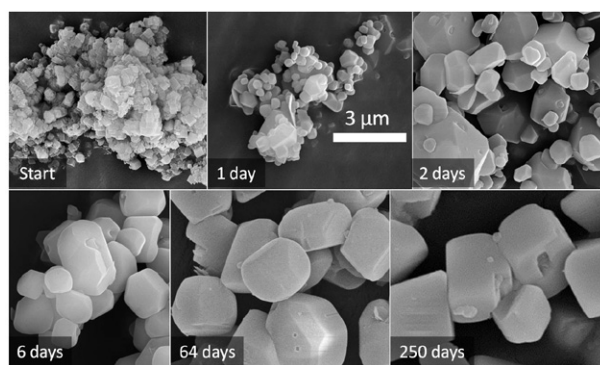


**Figure 1.** Calcite coarsening at  $200 \text{ }^\circ\text{C}$  in saturated solution. The scale bar applies for all images.

## Dehydration of metasomatic rocks along subduction and cold diapiric P-T trajectories

JOHN C. SCHUMACHER<sup>1</sup> AND HORST R. MARSCHALL<sup>2</sup>

<sup>1</sup>School of Earth Sciences, University of Bristol, Wills Memorial Building, Queen's Road, Bristol BS8 1RJ, UK  
(\*correspondence: j.c.schumacher@bristol.ac.uk)

<sup>2</sup>Department of Geology & Geophysics, Woods Hole Oceanographic Institution, Woods Hole, MA 02543, USA  
(hmarschall@whoi.edu)

Material from the subducting slabs is chemically linked to the source region of magmas produced at convergent plate margins. Hydrous fluids and chemical components from (1) subducted altered-oceanic crust and (2) the thin sedimentary veneer are added to (3) depleted mantle-wedge peridotite are invoked as the source of these melts. Exhumed subduction zone mélanges show new rock compositions develop through metasomatism and advection during early subduction where metabasic rocks and other rock types are juxtaposed with serpentinites. In large enough amounts in the source, these new (metasomatic) rock compositions may alter or expand the P-T region over which large amounts of fluid or key trace elements are either retained in or released from the source rocks relative to conditions predicted by the widely applied three-component source models.

This study examines the petrologic changes along a subduction P-T trajectory followed by a cold diapiric rise into the mantle wedge; the high-P, metasomatic rock compositions used for the calculations are from the island of Syros, Greece. These following metasomatic assemblages developed under blueschist-facies conditions and were preserved between garnet-epidote-glaucophane schist and serpentinite:

- (1) glaucophane+epidote+phengite+chlorite;
- (2) glaucophane+epidote+chlorite+omphacite;
- (3) epidote+chlorite+omphacite; (4) chlorite; (5) chlorite+talc.

The calculated phase relations for the metasomatic rocks compositions show that water-rich mineral like chlorite from these rocks could be stable to higher pressures, temperatures, and be more abundant than in hydrated basalt. Chlorite-rich metasomatic compositions produce more garnet than is expected from metabasalts. For example at about 805°C & 21 kbar, metasomatic rock (3) becomes 37 vol% garnet, 19 vol% pyroxene, 37 vol% amphibole; at about 910°C & 20 kbar, metasomatic rock (4) becomes 45 vol% garnet, 15 vol% spinel, 35 vol% olivine.

## A decadal lipid biomarker paleohydrological record during the onset of the Younger Dryas from Northeastern Germany

KATHRIN SCHÜTRUMPF<sup>1</sup>, ACHIM BRAUER<sup>2</sup>, INA NEUGEBAUER<sup>2</sup>, OLIVER RACH<sup>1</sup> AND DIRK SACHSE<sup>1</sup>

<sup>1</sup>University of Potsdam, Institute of Earth & Environmental Science, Karl-Liebknecht-Str. 24-25 14476 Potsdam-Golm Germany

(correspondence: k.schuetrumpf@googlemail.de)

<sup>2</sup>GeoForschungsZentrum Potsdam Section 5.2, Climate Dynamics and Landscape Evolution, Telegrafenberg C109 14473 Potsdam

Regional expressions of global climatic changes, especially their effect on the hydrological cycle, are difficult to predict. However, their impacts, in the form of droughts or extreme precipitation events can be severe for societies and ecosystems. Therefore, a better understanding of the complex hydrological feedback mechanisms during past abrupt climate changes may ultimately lead to better predictions of regional climate changes.

High-resolution proxy data from well dated lacustrine sedimentary archives are particularly well suited for the reconstruction of regional climate changes in the past. Here we are investigating the hydrological impacts of the abrupt climate change during the onset of the Younger Dryas (YD) cold period between 13.000 and 12.400 years BP from the paleolake Rehwiess in Berlin in Northeastern Germany.

We extracted lipid biomarkers from a 122,10 cm sedimentary sequence covering a period of 600 years during the onset of the YD. We identified abundant mid- and long-chained n-alkanes, usually attributed to aquatic macrophytes and higher terrestrial plants, respectively. In addition, we found hopanes of bacterial origin as well as branched alkanes. Dinosterol, a characteristic biomarker for dinoflagellates, was also detected.

Using these samples we construct a record of hydrological changes in decadal resolution. Therefore, we are analyzing the hydrogen isotope composition of lipid biomarkers (D/H). We will evaluate this palaeohydrological record in conjunction with micro-facies, geochemical and palynological data in order to understand the hydrological evolution of regional climate during the onset of the YD in Northeastern Germany.

## The Geobiology of Weathering: The 13<sup>th</sup> Hypothesis

D.W. SCHWARTZMAN<sup>1\*</sup> AND S. BRANTLEY<sup>2</sup>

<sup>1</sup>Department of Biology, Howard Univ., Washington DC 20059, USA (\*correspondence: dschwartzman@gmail.com)

<sup>2</sup>Department of Geosciences, Pennsylvania State Univ., University Park, State College, PA 16802, USA (sxb7@psu.edu)

The magnitude of the biotic enhancement of weathering (BEW) has profound implications for the long-term carbon cycle [1, 2]. The BEW ratio is defined as how much faster the silicate weathering carbon sink is under biotic conditions than under abiotic conditions at the same atmospheric  $p\text{CO}_2$  level and surface temperature. Thus, a 13<sup>th</sup> hypothesis could be added to the 12 outlined by Brantley *et al.* [3] regarding the geobiology of weathering: The BEW factor and its evolution over geological time can be inferred from “meta-analysis” of empirical and theoretical weathering studies. We present estimates of the global magnitude of the BEW drawing from lab, field, watershed and models of the long-term carbon cycle, with values ranging from one to two orders of magnitude.

[1] Schwartzman and Volk (1989) *Nature* **340**, 457-460. [2] Schwartzman (1999 2002) *Life, Temperature, and the Earth: The Self-Organizing Biosphere*. Columbia Univ. Press. [3] Brantley *et al.* (2011) *Geobiology* **9**(2), 140-165.

## Serpentinization history of the Santa Elena complex peridotites, Costa Rica

ESTHER M. SCHWARZENBACH<sup>1\*</sup> AND ESTEBAN GAZEL<sup>2</sup>

Department of Geosciences, Virginia Tech, Blacksburg, VA, United States

(\*correspondence: esther11@vt.edu; <sup>2</sup>egazel@vt.edu)

Serpentinization is a widespread process where ultramafic rocks react with water or fluids along oceanic ridges or within subduction zones. On the Santa Elena peninsula (Costa Rica) variably serpentinized peridotites outcrop together with layered and pegmatitic gabbros and are intruded by mafic dikes. However, the original tectonic setting of the Santa Elena complex and the origin of the peridotites has not yet conclusively been determined and interpretations range from a supra-subduction zone to an oceanic ridge setting. In this study we identify the alteration history and the sources of the hydrothermal fluids that affected these peridotites by studying the petrology and sulfur geochemistry. Our goal is to contribute to the understanding of the tectonic evolution of Central America.

The Santa Elena ultramafic complex includes lherzolites, cpx-bearing harzburgites and minor dunites. Extent of serpentinization varies between 30 and 100%. Locally clinopyroxene is replaced by amphibole (tremolite, Mg-hornblende, edenite, and pargasite). The peridotites preserve opaque mineral assemblages including pentlandite, awaruite, pyrrhotite, heazlewoodite, magnetite, and locally violarite and smythite. Additionally, most samples contain native Cu and a chemically wide range of Cu-sulfide assemblages including chalcocite, cubanite, bornite, chalcopyrite, samaniite [Cu(Fe,Ni)<sub>8</sub>S<sub>8</sub>], and sugakite [Cu<sub>2</sub>(Fe,Ni)<sub>7</sub>S<sub>8</sub>]. Elemental mapping revealed that native copper abundantly forms dendritic rims around pentlandite, while pentlandite is variably replaced by Cu-sulfides.

The mineralogical observations and the opaque mineral assemblages of the peridotites generally reflect i) highly reducing conditions during serpentinization and very low water rock ratios ( $\ll 1$ ), ii) that both formation of amphibole and Cu-alteration occurred subsequent to serpentinization, and iii) that serpentinization occurred at  $\leq 250^\circ\text{C}$ , but that locally fluid temperatures exceeded  $300\text{--}350^\circ\text{C}$ . Thus, our new data indicates that the peridotites of the Santa Elena complex experienced several stages of hydrothermal alteration and that serpentinization was likely overprinted by a later high temperature hydrothermal event.

## Geochemical characterization of thermal springs in the Tete Province, Northern Mozambique

A. SCIARRA\*, M. PROCESI, F. QUATTROCCHI  
AND D. CINTI

Istituto Nazionale di Geofisica e Vulcanologia, Rome, Italy

(\*correspondence: [alessandra.sciarra@ingv.it](mailto:alessandra.sciarra@ingv.it))

A first geochemical survey was carried out in the Northern Mozambique in March-April 2013, with the aim to investigate chemistry and origin of some thermal springs in the Tete Province. The investigated area is located in the East African Rift, adjacent to the marginal sedimentary Mozambique Basin. This area is crossed by the *Rio Zambezi*, one of the main river in Africa and explored during the 19<sup>th</sup> century by David Livingstone.

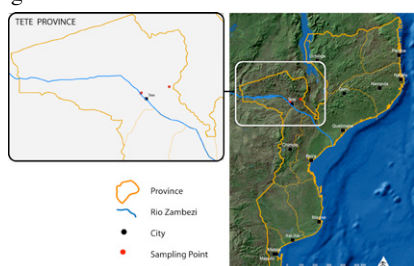


Figure 1: Location of the study area.

Many thermal springs are present in this province due to the proximity with the rift, but considerably little geochemical and geothermal studies have been done, due to the difficulties related both to the site accessibility and social interaction with local tribes. Three thermal springs were sampled close to the *Missao de Boroma*, Tete, crossing the Rio Zambezi by a traditional pirogue. Collected samples are being analysed to determine major, minor and trace elements,  $\delta^{18}\text{O}$  and  $\delta\text{D}$ , dissolved gas, carbon isotopic ratios of TDIC (Total Dissolved Inorganic Carbon) (expressed as  $\delta^{13}\text{C}\text{‰}$  vs. VPDB), the  $^3\text{He}/^4\text{He}$  and the dissolved Radon. The measured temperature ranges between 66°C to 42°C and the pH from 7.9 to 8. The conductivity is around 2400  $\mu\text{S}/\text{cm}$  and the Eh is between -208 to -404 mV. The chemical and isotopic analysis are in progress, anyway this first sampling suggests the need to plan and perform a national geochemical survey of the thermal springs in Mozambique. Data should be organized in organic geodatabase and geographic information systems. This information could have a big relevance not only for the geochemical, hydrogeological and geological knowledge of the Country but also for a potential geothermal exploration and exploitation.

## Age of the Bird River Sill (Manitoba, Canada) and the Secular Variation of Layered Intrusion-hosted Stratiform Chromite Mineralization

JAMES S. SCOATES<sup>1</sup>, R.F. JON SCOATES<sup>2</sup>  
AND COREY J. WALL<sup>1</sup>

<sup>1</sup>Pacific Centre for Isotopic and Geochemical Research,  
EOAS, University of British Columbia, Vancouver, BC,  
Canada, ([jscoates@eos.ubc.ca](mailto:jscoates@eos.ubc.ca), [cwall@eos.ubc.ca](mailto:cwall@eos.ubc.ca))

<sup>2</sup>2502 Holyrood Drive, Nanaimo, BC, Canada,  
([jscoates@telus.net](mailto:jscoates@telus.net))

The Archean Bird River Sill, a 20 km long and up to 800 m thick mafic-ultramafic layered intrusion in the Bird River greenstone belt of southeastern Manitoba, Canada, contains significant resources of chromium and nickel-copper, and locally anomalous concentrations of platinum group elements (PGE). Stratiform chromitite, displaying both remarkable lateral continuity and local irregularities due to synmagmatic disruption, occurs in up to six main intervals over a thickness of ~60 m in the Chromitiferous Zone of the lower ultramafic part of the intrusion. Ni-Cu sulfide mineralization is hosted in ultramafic rocks at the base of, or just below, the sill (e.g., past-producing Maskwa-Dumbarton mines). We report U-Pb zircon ages (chemical abrasion, single grains, ID-TIMS) for cumulates from below and above the Chromitiferous Zone, including (1) a locally pegmatitic, sulfide-bearing, feldspathic peridotite from the PGE Zone beneath the lowermost chromitite horizon (Lower Group) of  $2743.72 \pm 0.31$  Ma ( $n=6$ ), and (2) a leucogabbro in the Lower Gabbro Zone, approximately 35 m above the uppermost chromitite horizon (Upper Paired Group) of  $2743.19 \pm 0.31$  Ma ( $n=9$ ; revised from [1]). These ages are interpreted as the age of crystallization of the sill and they define the timing of the associated Cr-Ni-Cu±PGE mineralization. Other Neoproterozoic mafic-ultramafic intrusions containing economic concentrations of chromite and/or Ni-Cu-(PGE) occur in the northwestern part of the Superior Province in the Canadian Shield (e.g., McFaulds Lake, Big Trout Lake, Puddy Lake, Shebandowan) and share broadly similar geologic relationships. The age of significant intrusion-hosted stratiform chromite mineralization worldwide ranges from Eoarchean (e.g., Akilia, Greenland) to Paleoproterozoic (e.g., Bushveld, South Africa), which is comparable to the range for komatiite-related Ni deposits. This temporal restriction is consistent with both deposit types requiring the involvement of high-MgO, Cr-rich parent magmas produced during large degrees of mantle melting early in Earth history.

[1] Scoates & Scoates (2013) *Econ. Geol.* **108**, 13 p.

## Ageing of the Thetyan crust documented by xenoliths from Hyblaean diatremes (Sicily): Implication for crustal assimilation during magma emplacement

VITTORIO SCRIBANO\* AND MARCO VICCARO

<sup>1</sup>Dipartimento di Scienze Biol., Geol., Amb., Univ. Catania, Corso Italia 55, 95127 Catania, Italy (Correspondence: scribano@unict.it, m.viccaro@unict.it)

Previous study on xenoliths from Miocene diatremes from Hyblaean area (Sicily) suggested that the local Mesozoic sedimentary and volcanic sequence rests upon a fossil oceanic core-complex belonging to the Ionian Thetyan lithospheric domain. Hyblaean xenoliths have also suggested that the postulated core-complex hosted long living hydrothermal systems which have produced diverse geochemical and mineralogical modification to the host ultramafic and gabbroic rocks (e.g. hydration, alkalinization, sulfidization, carbonation) through time, as well the deposition of hydrothermal brines at different crustal levels. The Upper Miocene volcanic rocks cropping out in the Central-Eastern section of the area were erupted after a 50 Ma non-magmatic period (the Eocene hiatus). The interaction between ascending magmas and the fossil hydrothermal system produced dehydration of the serpentinite wall rock with formation of fluidized eruptive systems (i.e. diatremes). The basalt magma assimilated some hydrous peralkaline anatectitic melts thereby attaining a silica-undersaturated, sodic (nephelinitic) character. Magmas that fed the Pleistocene volcanism in the northern margin of the Plateau intersected a section of the fossil hydrothermal system, which was particularly rich in hydrothermal evaporites as testified by the high contents in S, Cl, F, H<sub>2</sub>O, Ca, Na, Sr, Ba, relatively high Zr/Hf and occurrence of sodalite series phenocrysts. More in general, we put forward the idea that selective assimilation of hydrothermally altered wall rocks may explain the geochemical paradox of the Hyblaean basaltic lavas, which display Nd-Sr isotope ratios distinctive of MORB-type magmas and distribution of some trace elements more typical of alkaline-series magmas.

## Evidence of intergranular melt pools and melt films in lower crustal granite: Products of fluxing by water derived from deformation of nominally anhydrous minerals

S.J. SEAMAN<sup>1\*</sup>, M.L. WILLIAMS, M.J. JERCINOVIC, G.C. KOTEAS<sup>2</sup> AND L. BROWN

<sup>1</sup>Department of Geosciences, University of Massachusetts, Amherst, MA 01003, USA (\*correspondence: sjs@geo.umass.edu)

<sup>2</sup>Department of Geology, Norwich University, Northfield, VT 05663, USA

Water in nominally anhydrous minerals in lower crustal granitoids may move from structural sites and fluid inclusions in nominally anhydrous minerals to grain boundaries during deformation. Along grain boundaries, this water can lower the solidus, facilitating the production of small amounts of partial melt. Outcrops of the 2.6 Ga Stevenson granite, a lower crustal granite in the Athabasca granulite terrane, Saskatchewan, range from K-feldspar megacrystic granite to ribbon mylonite. With increasing deformation, water concentration in quartz and feldspar crystals decreases, and very fine-grained (2-10 micron) brown colored grain boundary films and intergranular pools are progressively developed. The fine-grained multi-phase material on grain boundaries and at grain triple junctions has been interpreted as former melt films and melt pools, respectively. The interpreted melt films have a distinctive pocked texture and a multiphase assemblage with quartz, 2 feldspars and fine (1-2 microns) Fe oxides. Melt films on the grain boundaries of plagioclase, potassium feldspar and quartz are approximately 20 microns wide. Melt pools are up to 100<sup>+</sup> microns in diameter. In some zones of the rock, melt pools are nearly interconnected, possibly beginning to mobilize, approaching a situation in which a melt conduit would be established. Water in nominally anhydrous minerals has the potential to lower the solidus significantly enough to initiate partial melting in lower crustal granitoids at high ambient temperatures. 3000 ppm water in quartz and feldspars that make up large volumes of lower crustal granitoids would lower the dry solidus of granite by 96°C at 1 GPa, facilitating the production of small volumes of partial melt that wet the grain boundaries along which it is produced.

## Tracing denitrification using isotopic composition of nitrogen in soils and plants

MATHIEU SEBILLO<sup>1\*</sup>, AURELIE MOTHET<sup>1</sup>, LIZ HAMILTON<sup>2</sup>, EDWARD MALONE<sup>2</sup>, VERONIQUE VAURY<sup>1</sup>, OLIVIER GROS<sup>3</sup> AND GILLES PINAY<sup>4</sup>

<sup>1</sup>UPMC Univ Paris 06, UMR Bioemco, 4 place Jussieu, 75252 Paris Cedex 05, France

amathieu.sebilo@upmc.fr (\*presenting author)

<sup>2</sup>University of Birmingham, School of Geography, Earth and Environmental Sciences, Birmingham, B15 2TT, UK

<sup>3</sup>Département de Biologie, UMR 7138 SAE, Université des Antilles et de la Guyane, 97159 Point à Pitre Cedex, Guadeloupe, France

<sup>4</sup>Observatoire des Sciences de l'Univers de Rennes, UMR Ecobio, Campus Beaulieu, bât. 14. 263 av du Général Leclerc 35042 Rennes Cedex, France.

One of the major challenges of current research on the functioning of the continental ecosphere is to develop integrative approaches allowing scale changes. Isotopic biogeochemistry is an interested integrating tool. The basic idea is that the isotopic composition of a chemical species ( $\delta^{15}\text{N}$  for nitrogen) at a definite location reflects (i) its various sources and (ii) processes which affect its concentration. Denitrification generates an isotopic enrichment of  $^{15}\text{N}$  and  $^{18}\text{O}$  of the residual nitrate in soils or in waters (surface or groundwater).

However, denitrification is intermittent and occurs in hot spots. In order to get insights into this process involved at regional scale, it is important to trace the succession of denitrification in soils and test the hypothesis whether plants could integrate the signal of denitrification occurring in soils. First results show that for a same type of soil,  $\delta^{15}\text{N}$  is much higher for agricultural soils than for meadows, forest or mangrove soils. This is mostly likely due to higher gaseous losses processes occurring in agricultural soils such as denitrification.

Moreover,  $\delta^{15}\text{N}$  of plants increase with increasing of  $\delta^{15}\text{N}$  of soils. This confirms that the  $\delta^{15}\text{N}$  of soil organic nitrogen could be an indicator of the intensity of denitrification

## Physical and geochemical processes during groundwater replenishment with highly treated wastewater

S. SEIBERT<sup>2</sup>, H. PROMMER<sup>1,2,3,\*</sup>, A. SIADE<sup>1,3</sup> AND O. ATTEIA<sup>4</sup>

<sup>1</sup>University of Western Australia, Crawley, Australia

Henning.Prommer@csiro.au (\* presenting author)

<sup>2</sup>CSIRO Land and Water, Wembley, Australia

<sup>3</sup>NCGRT, Australia

<sup>4</sup>EGID, Pessac Cedex, France

Decreasing availability of ground and surface water resources in conjunction with increasing water demands has motivated the exploration of unconventional new water sources in Australia and other places. Among possible solutions recycling of municipal wastewater through advanced tertiary treatment techniques presents a promising option to augment existing drinking water supplies. During this treatment process reverse osmosis (RO) plays a critical role in the removal of undesired solutes and results in low ionic strength product water. The purified, desalinated water can be stored underground for protection against evaporation loss and introduce, where required, an additional aquifer treatment step for the removal of trace pollutants (e.g., pharmaceuticals, disinfectant-byproducts). As the recycled low ionic strength water is typically in chemical disequilibrium with the native aquifer conditions, the injection into aquifers often triggers a complex range of coupled physical and geochemical processes that can strongly affect the quality of the groundwater in the recharged aquifer. In this study we present field observations and a model-based interpretation of the data collected during a large-scale groundwater replenishment trial using highly treated waste water in Perth, Western Australia. The trial injection was conducted between November 2010 and December 2012 to clarify the technical feasibility and societal acceptance of a large-scale implementation of this approach. The first phase of the modelling study was dedicated to obtaining an accurate understanding and description of the injectant and temperature propagation within the highly heterogeneous sedimentary aquifer.

The calibrated conservative transport model was then subsequently used to identify and quantify the geochemical reactions that were induced by the injection. In agreement with earlier laboratory results from respirometer tests (e.g., [1,2]) the simulation results show that pyrite oxidation acts as the major driver for reaction-induced concentration changes within the aquifer. Pyrite oxidation showed to cause a rapid removal of oxygen and also the removal of the nitrate contained in the injectant. The acidity produced by the pyrite oxidation showed to be partially buffered by the alkalinity contained in the injected water but also by a range of mineral reactions, including Fe-carbonate and feldspar dissolution. Understanding the nature and longevity of the mineral buffering mechanisms is crucial for the design of future large-scale implementations of groundwater replenishment.

[1] Descourvieres *et al.* (2010a) *Appl. Geochem* **25**, 261–275.

[2] Descourvieres *et al.* (2010b) *Env. Sci. Technol.*, **44**, 6698–6705.

## Competition for sulfide in marine sediments: Electrogenic Filamentous Bacteria versus *Beggiatoa*

DORINA SEITAJ<sup>1\*</sup>, SAIRAH Y. MALKIN<sup>2</sup>, REGINA SCHAUER<sup>3</sup> AND FILIP J.R. MEYSMAN<sup>1,2</sup>

<sup>1</sup>Netherlands Institute of Sea Research (NIOZ), Ecosystem Studies Department, Korringaweg 7, 4401 NT, Yerseke, Netherlands (\*correspondence: Dorina.Seitaj@nioz.nl)

<sup>2</sup>Free University of Brussels (VUB), Department of Analytical and Environmental Chemistry, Pleinlaan 2, 1050 Brussels, Belgium

<sup>3</sup>Aarhus University, Department of Bioscience, Center of Geomicrobiology, Ny Munkegade 116, 8000 Aarhus, Denmark

Recently, a novel mechanism of sulfide oxidation has been described from marine sediments, whereby long filamentous bacteria (ElectroFilaments) couple the reduction of oxygen at the surface to the oxidation of sulfide at centimeters depth via electrical currents. This creates a wide suboxic zone similar to that created by the large sulphur bacteria of the genus *Beggiatoa*. These latter bacteria are motile and capable of intracellular nitrate storage, and in this way, *Beggiatoa* can transport nitrate to deeper sediment layers to oxidize H<sub>2</sub>S. In the seasonally hypoxic Lake Grevelingen, The Netherlands, both types of sulfur oxidizing bacteria have recently been observed. This rises the question how these different modes of microbial sulfide oxidation compete?

We conducted a yearlong study of monthly sampling campaigns in Lake Grevelingen. Microsensor profiling of O<sub>2</sub>, pH and H<sub>2</sub>S revealed the geochemical fingerprint of the dominant microbial process over time (both mechanisms generate a very distinct pH profile). In addition, FISH tagging for *Desulphobulbus* and microscopic counting of *Beggiatoa* allowed to quantify the abundance of the two competing bacteria. Our results show that both modes of microbial sulfide oxidation follow a predictable seasonal succession, where *Beggiatoa* are dominant in autumn right after summer hypoxia, while Electrofilaments become dominant in spring. Field data and additional mesocosm experiments suggest that bottom water oxygenation, nitrate availability and physical disturbance are the main environmental factors controlling the outcome of this microbial competition. These two competing microbial pathways of sulfur oxidation strongly affect the biogeochemical cycling, but in a very different way, and so, the predominance of either mechanism can have a strong impact on the elemental cycling in coastal sediments.

## Tracing the origin of sulphur in Darzila karst cave, NE Iraq

A. SEITHER<sup>1,3\*</sup>, K. HEILAND<sup>2,3</sup> AND S. KUMMER<sup>3</sup>

<sup>1</sup>Norges Geologiske Undersøkelse, 7040 Trondheim, Norway (\*correspondence: anna.seither@ngu.no)

<sup>2</sup>Ingenieurbüro für Grundwasser GmbH, 04229 Leipzig, Germany (k.heiland@ibgw-leipzig.de)

<sup>3</sup>TU Bergakademie Freiberg, 09596 Freiberg, Germany

Darzila cave, located in the Sangaw district in Northern Iraq, develops by the dissolution of limestone by sulphuric acid through oxidation of H<sub>2</sub>S. The hydrogen sulphide may either originate from oil-rich reservoirs, such as the nearby Kirkuk oil field, or from gypsum of the Lower Fars Formation.

Samples from these possible endmembers were subject to isotopic analyses ( $\delta^{34}\text{S}$ ,  $\delta^{18}\text{O}$ ). The water of three prominent floor feeders inside the cave was analyzed for its content of major ions, trace elements, total organic carbon, as well as for the stable isotopic composition of water ( $\delta\text{D}$ ,  $\delta^{18}\text{O}$ ), dissolved sulphate ( $\delta^{34}\text{S}$ ,  $\delta^{18}\text{O}$ ) and sulphide ( $\delta^{34}\text{S}$ ).

Investigations of water samples pointed towards a potential influence of hydrocarbon-bearing layers at two sites. Indices were significantly elevated SO<sub>4</sub><sup>2-</sup>/Ca<sup>2+</sup> ratios, an increased content of total dissolved solids (10-31 g/L) and dissolved organic carbon (14-20 mg/L), and relative enrichments of trace elements such as Cr, Be, Ga, Ni, Co, Mn, and V. The isotopic investigations confirmed the influence of H<sub>2</sub>S affluxes from hydrocarbons ( $\delta^{34}\text{S} \approx -9\text{‰}$  VCDT) at these sites. Further evidence was given by depleted  $\delta^{34}\text{S}$  and  $\delta^{18}\text{O}$  values in sulphate, small differences between the sulphur isotopic signature of sulphate and sulphide, as well as elevated  $\delta\text{D}$  values in ambient water.

The third floor feeder had an entirely different isotopic signature, showing distinct signs of bacterial sulphate reduction and therefore pointing towards primary gypsum from the Lower Fars Formation ( $\delta^{34}\text{S} \approx +22\text{‰}$  VCDT) as sulphur source. Main indications were a  $\delta^{34}\text{S}$  value of sulphate above that of gypsum and strongly depleted sulphide. However, it appears that sulphate reduction was superimposed by several secondary transformation processes.

## Partial melting of rhyolites in the Chaltén Contact Aureole (Patagonia, Argentina)

S. SEITZ<sup>1\*</sup>, B. PUTLITZ<sup>1</sup>, L.P. BAUMGARTNER<sup>1</sup>,  
S. LERESCHE<sup>1</sup> AND P. NESCHER<sup>1</sup>

<sup>1</sup>Institute of Earth Sciences, University of Lausanne, 1015  
Lausanne, Switzerland (\* correspondence:  
susanne.seitz@unil.ch)

The Chaltén Plutonic Complex (CHPC) consists of mafic and granitic calc-alkaline intrusive rocks emplaced in several successive batches. High-precision U/Pb zircon dating yield ages between  $16.9 \pm 0.05$  Ma and  $16.37 \pm 0.02$  Ma [1]. The host-rocks are formed by a Paleozoic clastic sequence, Jurassic rhyolites and volcanoclastics, and a Cretaceous pelitic sequences. The intrusion of the CHPC post-dates major regional deformation.

Partial melting in the Chaltén contact aureole is limited to small zones at gabbro and tonalite contacts with rhyolites. Partial melting does not occur at the granite-rhyolite contact. The rhyolitic migmatites are characterized by an anastomosing network of veins of quartz, feldspar and almandine-rich garnet. This network is most prominent at 10m to 15m from the contact. Some cm-scale shear zones concentrated partial melt. On a microstructural scale partial melt is segregated along quartz-feldspar grain boundaries. They show typically cusped grain boundaries with melt penetrating along the edges. Petrologic investigations show that melting is to the result of biotite breakdown to cordierite or garnet.

Thermodynamic calculation for these peraluminous rhyolites indicate that first melt occurs at 650-700°C and pressures around 3kbar. Simple thermal calculations yield maximum temperatures of about 550°C at the mafic-rhyolite contact, which is 100-150°C lower than the required temperature for partial melting. Melting in the rhyolitic migmatites was intense enough to partially reset U/Pb ages as indicated by the younging of zircon ages (obtained by laser ablation). We are currently studying the mechanism of partial resetting of the zircon ages, as well as the kinetics of oxygen isotope exchange between quartz phenocrysts and the rhyolite matrix. Preliminary modeling suggests, that oxygen isotopes can be re-equilibrated dominantly by diffusion, while zircon most likely recrystallized.

[1] Ramírez de Arellano *et al.* (2012), *Tectonics* **31**, 1-18

## Silicate-natrocarbonate immiscibility in ijolites at Oldoinyo Lengai, Tanzania: Melt inclusion study

V.S. SEKISOVA<sup>1,2</sup>, V.V. SHARYGIN<sup>2\*</sup> AND A.N. ZAITSEV<sup>3</sup>

<sup>1</sup>Novosibirsk State University, Novosibirsk 630090, Russia  
<sup>2</sup>V.S. Sobolev Institute of Geology and Mineralogy SD RAS,  
Novosibirsk 630090, Russia (\*correspondence:  
sharygin@igm.nsc.ru)

<sup>3</sup>St. Petersburg State University, St. Petersburg 199034, Russia

Xenoliths of plutonic rocks (ijolite, jacupirangite, etc.) in the Oldoinyo Lengai pyroclastics are considered to be cumulates forming in an intermediate chamber from a parental olivine nephelinite magma [1].

Melt inclusions with silicate-carbonate immiscibility were found in nepheline and Ti-magnetite of olivine-mica ijolite. Other minerals (pyroxene, etc.) contains inclusions without immiscibility; fluorapatite bears natrocarbonate inclusions. Phase composition of inclusions in nepheline (5-100  $\mu$ m) is silicate glass + vapor-carbonate globule  $\pm$  daughter/trapped crystals  $\pm$  sulfide bleb. Vapor-carbonate globule (up to 20  $\mu$ m) consists of gas bubble ( $\approx$ 60%) and nyerereite-rich carbonate aggregate ( $\approx$ 40%). Some inclusions may also contain numerous submicron carbonate globules in glass. Heating experiments with inclusions indicated the following events: (1) carbonate component melted instantaneously at 540-560°C; (2) melting of silicate glass occurred at 580-640°C; (3) all globules gradually coalesced into one large vapor-carbonate globule at 640-800°C; (4) homogenization in this globule occurred at 900-920°C; (5) complete homogenization (miscibility of carbonate and silicate liquids) was not achieved with temperature increase up to 1100°C.

Our study of inclusions advocates very complex history of the Lengai ijolite and evolution of initial silicate melt in an intermediate chamber. Crystallization of ijolites occurred in conditions of silicate-natrocarnatite immiscibility in very broad temperature (540-1100°C). During formation nepheline and other minerals trapped as inclusions at least two immiscible liquids. After entrapment additional carbonate fraction was separated from silicate liquid within inclusion with decreasing temperature. The immiscibility phenomenon was recently recorded in the Oldoinyo nephelinites [2-4].

This work is supported by RFBR (grant 11-05-00875).

[1] Dawson *et al.* (1995) *J Petrol* **36**, 797-826. [2] Mitchell (2009) *Contrib Mineral Petrol* **158**, 589-598. [3] Mitchell & Dawson (2012) *Lithos* **152**, 40-46. [4] Sharygin *et al.* (2012) *Lithos* **152**, 23-39.



## Ensemble Simulation of the Atmospheric Radionuclides Discharged by the Fukushima Nuclear Accident

T. T. SEKIYAMA\*, M. KAJINO AND M. KUNII

Meteorological Research Institute, Tsukuba 305-0052, Japan

(\*correspondence: tsekiyam@mri-jma.go.jp)

Enormous amounts of radionuclides were discharged into the atmosphere by a nuclear accident at the Fukushima Daiichi nuclear power plant (FDNPP) after the earthquake and tsunami on 11 March 2011. The radionuclides were dispersed from the power plant and deposited mainly over eastern Japan and the North Pacific Ocean. A lot of numerical simulations of the radionuclide dispersion and deposition had been attempted repeatedly since the nuclear accident. However, none of them were able to perfectly simulate the distribution of dose rates observed after the accident over eastern Japan. This was partly due to the error of the wind vectors and precipitations used in the numerical simulations. Unfortunately, their deterministic simulations could not deal with the probability distribution of the simulation errors.

Therefore, an ensemble simulation of the atmospheric radionuclides was performed using the ensemble Kalman filter (EnKF) data assimilation system coupled with the Japan Meteorological Agency (JMA) non-hydrostatic mesoscale model (NHM). The JMA-NHM has been used operationally for weather forecasts by JMA. Through this ensemble data assimilation, twenty members of the meteorological analysis over eastern Japan from 11 to 31 March 2011 were successfully obtained. Using this meteorological analysis, the radionuclide behavior in the atmosphere such as advection, convection, diffusion, dry deposition, and wet deposition was simulated. This ensemble simulation provided the multiple results of the radionuclide dispersion and distribution. Because the large (small) ensemble-spread of the multiple results indicates the low (high) accuracy of the numerical simulation, the probability distribution of the simulation errors is obtainable from the ensemble simulation. These statistics can provide information useful for the probabilistic prediction of atmospheric radionuclides.

Numerical simulations are able to collaborate with field observations in depicting the full picture of the radionuclide contamination in Fukushima.

## Imaging the reactivity and transport of $^{99}\text{Tc}$ through Fe-cement/rock barriers

A. F. SELIMAN<sup>1</sup>, J. BRIDGE<sup>2</sup>, S.A. BANWART<sup>1</sup>  
AND M.E. ROMERO-GONZÁLEZ<sup>1\*</sup>

<sup>1</sup>Cell-Mineral Research Centre, Kroto Research Institute, The University of Sheffield, Sheffield S3 7HQ, UK  
(\*m.e.romero-gonzalez@sheffield.ac.uk)

<sup>2</sup>School of Engineering, University of Liverpool, Liverpool L69 3GH, UK. (j.brigde@liverpool.ac.uk)

Geological disposal of radioactive waste requires a detailed understanding of the critical processes affecting geochemical transformations at laboratory and field scale. The interfaces between storage containers, repository and geological substrata can be viewed as a series of continuous barriers with varying porosity and chemical composition that governs flow and physical-chemical transformation of radionuclides during their long term transport. Using this approach, we have investigated the mobility of  $^{99}\text{TcO}_4^-$  transport through Fe-cement/sandstone engineered barriers using flow through experiment and gamma imaging of  $^{99\text{m}}\text{Tc}$  isotope. A flow cell packed with nirex vault reference backfill material (NRVB) containing zero valent iron (ZVI) or magnetite and Sherwood sandstone in a barrier fashion was used. The transport of  $^{99\text{m}}\text{Tc}$  in synthetic groundwater at pH 10 was imaged using a medical gamma camera at a flow rate of  $5.7\text{ml h}^{-1}$ . The Fe-bearing material was prepared to obtain a uniform distribution of 20% ZVI or 10% magnetite representative of steel materials that may create reactive hotspots in the disposal site. The results showed that the unmodified NRBV/sandstone systems have not capacity to retain  $^{99\text{m}}\text{Tc}$ . In contrast,  $^{99\text{m}}\text{Tc}$  was not transported through the NRBV containing ZVI and it was retained entirely by the modified barrier. The NRBV/sandstone system modified with magnetite showed retardation of  $^{99\text{m}}\text{Tc}$  that was overcome over long periods of time, allowing the radionuclide to be eventually transported out of the flow cell. The results showed that  $^{99}\text{Tc}$  transport is conservative through cement and sandstone. The implication is that this radionuclide will be transported to the outside natural environment surrounding the geological disposal. However, amendment with Fe-bearing materials, especially ZVI increases confinement of the radionuclide within the geological disposal reducing the risk of long term environmental contamination.

## Direct observation of gas hydrate formation in a sedimentary matrix on the microscale

K. SELL<sup>1\*</sup>, M. CHAOUACHI<sup>2</sup>, F. ENZMANN<sup>1</sup>, W.F. KUHS<sup>2</sup>,  
M. KERSTEN<sup>1</sup>, B. PINZER<sup>3</sup> AND E.H. SAENGER<sup>4</sup>

<sup>1</sup>Gutenberg-University, Mainz 55099, Germany

(\*correspondence: sell@uni-mainz.de)

<sup>2</sup>GZG, University Göttingen 37077, Germany

<sup>3</sup>PSI, Tomcat Beamline, 5232 Villigen, Switzerland

<sup>4</sup>ETH, Zurich 8006, Switzerland

Gas hydrates (GH) are ice-like solid compounds comprised of gas molecules and water [1]. As it is very difficult to recover natural GH samples due to their fast decomposition under ambient conditions, a lot of open questions are left concerning the microstructure and distribution of hydrates in sediments. This study represents the first direct observation of gas hydrate growth in a sedimentary matrix using time-resolved synchrotron-based tomography leading to first insights on the nucleation and growth of gas hydrates at a high spatial resolution of 740 nm. The time-sequences of the GH formation in the medium reveal that the reaction clearly started at the gas-water interface forming a several  $\mu\text{m}$  thick hydrate film (Fig.1). In contradiction to some earlier conjectures a nucleation on the grain surface was not observed. At a later stage the water is replaced by GH of more or less isometric shape with pore space in between. Some of our observations show that water remains as a thin film between grains and hydrate but this needs to be corroborated. Seismic anomalies observed in field studies might be explained by the presence of thin water films in hydrate-bearing sediments. In a next step the full 3D data set will be used as a direct input to model the effective elastic properties.

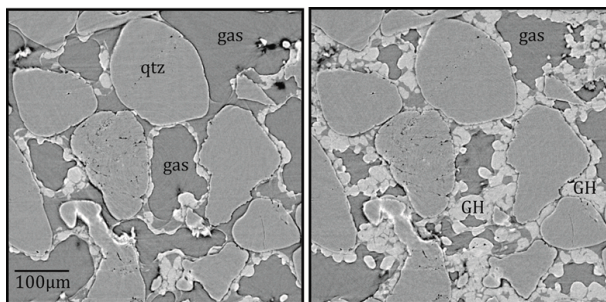


**Figure 1:** 2D slices depicting the stepwise hydrate growth within the sedimentary matrix.

[1] Sloan & Koh (2008) In: Clathrate hydrates of natural gases. CRC Press, Boca Raton, 752.

## Application of mineral thermometers and barometers to shoshonitic-ultrapotassic rocks: The Simav Graben (Western Anatolia, Turkey)

B.SEMIZ

Dep of Geological Engineering, Pamukkale University, 20070, Denizli, Turkey (bsemiz@pau.edu.tr)

The study area is located at the intersection of E–W-trending Plio-Quaternary Simav Graben and NE–SW-trending Neogene Selendi and Uşak-Güre basins in the western Anatolia. Due to their morphological, stratigraphical positions and petrographical features in the field, the investigated shoshonitic-ultrapotassic rocks are called Inceğiz, Gediz, Dereköy, Naşa, Kestel basalts, Saphanedağı and Ilıcaksu Lamproites. All the SHO-UK rocks display similar petrographic characteristics.

Fourteen samples, representing the SHO-UK units in the eastern parts of the Simav Graben have been used for mineral chemical studies and for estimation of the temperature and pressure conditions of magmatic crystallization. These samples are porphyritic, hyaloplitic, pilotaxitic in texture and with the following mineral assemblages; clinopyroxene ( $\text{En}_{40-52}$ ,  $\text{Wo}_{39-48}$ ), olivine ( $\text{Fo}_{63-92}$ ), rarely phlogopite (Mg# 65-91), plagioclase ( $\text{An}_{62-88}$ ), and sanidine ( $\text{Or}_{52-84}$ ). Ti-magnetite, ilmenite and chrome-spinel (5-18% MgO, 39-54%  $\text{Cr}_2\text{O}_3$ ) are common accessory minerals.

Application of clinopyroxene [1] and olivine-spinel [2] geobarometric studies for the SHO-UK, equilibrium pressure between  $\sim 7.6$ -10.3 and  $\sim 16.2$ -16.8 kbar has been estimated, corresponding to 25-51 km depth, respectively. Oxygen fugacity ranges from -11.9 and -13.8. Olivine [3], Olivine-spinel [4], clinopyroxene [5] and magnetite-ilmenite pairs [6] geothermometers have been applied for estimating the crystallization temperatures of minerals. Calculated crystallization temperatures are 1193-1262°C for olivines, 1086-1191°C for clinopyroxene and 793-851°C for magnetite-ilmenite pairs. The estimates of magmatic parameters indicate that the magmas forming the SHO-UK rocks crystallized at different levels, from mantle depths toward deep-level magma chambers.

[1] Nimis, (1995) *Contrib Mineral Petrol.* **121**, 115-125. [2] O'Neil, (1981) *Contrib Mineral Petrol.* **77**, 185-194. [3] Putrika, (2008) *Reviews in Mineral. & Geochem.* **69**, 61-120. [4] O'Neil and Wall, (1987) *J Petrol.* **28**, 1169-1191. [5] Putrika *et al.*, (2003) *Am Mineral.* **88**, 1542-1554. [6] Stomer, (1983) *Am. Mineral.* **68**, 586-594.

## Trace element composition of clinopyroxenes from the Kızıldağ ophiolite (S-Turkey): Implication for multi-stage fractionational melting in a SSZ setting

AHMET D. SEN<sup>1</sup>, İBRAHİM UYSAL<sup>2</sup>, MARGUERITE GODARD<sup>3</sup>, SAMET SAKA<sup>2</sup>, RECEP.M. AKMAZ<sup>2</sup>, MELANİE KALIWODA<sup>4</sup> AND UTKU BAGCI<sup>5</sup>

<sup>1</sup>Gümüşhane University, Gümüşhane, Turkey

<sup>2</sup>Karadeniz Technical University, Trabzon, Turkey

<sup>3</sup>Géosciences Montpellier, Montpellier, France

<sup>4</sup>Mineralogical State Collection Munich, LMU, Germany

<sup>5</sup>Mersin University, Mersin, Turkey

Trace-element composition of clinopyroxenes from the mantle peridotites of Kızıldağ ophiolite (Hatay, S-Turkey) were determined by laser ablation ICP-MS to better understand the geochemical processes and the formation of the ophiolite. The peridotite sequence is composed of tectonized harzburgite and ultramafic cumulate rocks representing refractory mantle source and Moho Transition Zone (MTZ), respectively. Harzburgites contain spinel with Cr# 47-70 and Mg# 37-66, indicating that they are residue of high degrees of partial melting. Ultramafic cumulates are mainly dunite and wehrlites. Tectonized harzburgites show two different types of compositions. First type of harzburgites are refractory and have primary pyroxene crystals with ductile deformation signs. Second type of harzburgites are more fertile and have interstitial clinopyroxenes showing similar characteristics with rocks from MTZ. Chondrite-normalized rare earth element (REE) patterns of clinopyroxenes from Kızıldağ ophiolite are clearly depleted in light REE (LREE) ( $[Lu/La]_N > 100$ ), and have slightly similar patterns with clinopyroxenes of abyssal peridotites from normal mid-ocean ridges (MOR). Interstitial clinopyroxenes in MTZ dunites have flatter patterns ( $[Lu/La]_N \sim 10$ ) comparable with those from other dunites of all the Tethyan ophiolites (e.g. Oman, Troodos). Clinopyroxenes in tectonized harzburgites having extremely downward REE patterns, characterized by a strong depletion of heavy REE (HREE) to middle REE (MREE), suggest that they are residue of first stage fractional melting in the garnet stability field in a MOR setting. Interstitial clinopyroxene from impregnated harzburgites have more enriched REE patterns than those of depleted harzburgites, indicating spinel field melting in a SSZ setting where melts can percolate within upwelling mantle.

## The possible source mantle and magma genesis of basalts from Pitcairn island: Implication from highly siderophile elements and Os isotope ratios

RYOKO SENDA<sup>1\*</sup>, TAKESHI HANYU<sup>1</sup>, AKIRA ISHIKAWA<sup>1,2</sup>, HIROSHI KAWABATA<sup>1,3</sup>, TOSHIRO TAKAHASHI<sup>1</sup> AND KATSUHIKO SUZUKI<sup>1</sup>

<sup>1</sup>FREE, JAMSTEC, Yokosuka 237-0061, Japan

(\*Correspondence: rsenda@jamstec.go.jp)

<sup>2</sup>Earth Science and Astronomy, The University of Tokyo, Tokyo 153-8902, Japan

<sup>3</sup>Research and Education Faculty, Kochi University, Kochi 780-8520, Japan

It is well known that recycled materials are involved in producing the chemical and isotopic heterogeneities observed in oceanic island basalts (OIB). The type of recycled material present in the Enriched Mantle 1 (EM-1) reservoir has been widely debated. Oceanic crust with pelagic sediment (e.g., Chauvel *et al.*, 1992), delaminated subcontinental lithospheric mantle (SCLM) (e.g., Hauri and Hart, 1993), subducted oceanic plateaus (Gasperini *et al.*, 2000) and just single melting process involving pristine mantle (Collerson *et al.*, 2010) have all been invoked as contributing to EM-1 source. The chemical composition of EM-1 is characterized by radiogenic Sr, unradiogenic Nd, unradiogenic Pb and radiogenic Os isotope compositions compared to the depleted mantle.

We measured Os isotope ratios and highly siderophile elements (HSE) abundances in basalts from Pitcairn Island, south Pacific, which represent strong EM-1 flavor to identify the possible source components of these magmas. The Os isotope ratios (0.138-0.161) have similar to or slightly higher range than, those measured in previous studies on EM-1-type basalts (~0.150). The HSE patterns normalized by chondrites are characterized by fractionation between IPGE (Os, Ir, Ru) and Pd. Among IPGE, Ir abundances of some basalts are depleted compared to Os and Ru. Pt abundances of most basalts also show depleted pattern from Ru and Pd. These characteristics are similar to some picrites from Hawaii (Ireland *et al.*, 2009). However the abundances of HSE in Pitcairn basalts are clearly lower than those of Hawaiian picrites with similar range of MgO. The Os isotope ratios of Pitcairn basalts are higher than those of picrites. We will discuss the components of the source mantle of EM-1 and the magma genesis of Pitcairn Island basalts combining our data with previous studies.

## Composition and structure of fresh and aged Fe oxidation products

A.-C. SENN\*, R. KAEGI, S.J. HUG,  
J.G. HERING AND A. VOEGELIN

Eawag, Swiss Federal Institute of Aquatic Science and  
Technology, Überlandstrasse 133, CH-8600 Dübendorf,  
(\*correspondence: anna-caterina.senn@eawag.ch)

The oxidation of dissolved Fe(II) by O<sub>2</sub> leads to the formation of amorphous to poorly crystalline Fe(III)-precipitates. These precipitates control the fate of major and trace elements at redox-interfaces and play an important role in many natural and technical systems. Dissolved phosphate (P), silicate and Ca are major factors controlling composition and structure of fresh Fe(III)-precipitates [1, 2]. In this study, we therefore investigated (i) the effects of silicate and Ca over a wide range of P/Fe ratios on the composition and structure of fresh Fe(III)-precipitates formed by oxidation of 0.5 mM Fe(II) in bicarbonate-buffered solution at pH 7.0 and (ii) changes in precipitate composition and structure during aging for 30 days at 40 °C.

During Fe(II) oxidation, mostly lepidocrocite (Lp) is formed at initial P/Fe ratios below ~0.1. Phosphate was nearly completely co-precipitated with Fe(III) up to an initial molar P/Fe ratio of ~0.55 in the absence of Ca and ~0.75 in the presence of dissolved Ca. Above these P/Fe ratios, only amorphous Fe(III)-phosphate formed and phosphate removal was incomplete. Enhanced co-precipitation of phosphate and Ca with Fe(III) was attributed to electrostatic effects and to the formation of mixed Ca-Fe(III)-phosphates. Silicate did not interfere with the initial phosphate uptake but inhibited lepidocrocite formation at low P/Fe ratios, instead promoting the formation of hydrous ferric oxide (HFO; ferrihydrite-like polymers with limited corner-sharing linkage of Fe(III)-octahedra). Continuing Fe(III) polymerization during aging led to the remobilization of phosphate, especially in the absence of Ca and silicate. Phosphate remobilization was limited in the presence of Ca, which stabilizes mixed Ca-Fe(III)-phosphate, and especially silicate, which inhibits Fe(III) polymerization into crystalline Fe(III)-precipitates.

The results from this study form the basis for an improved mechanistic and quantitative understanding of Fe(III)-precipitate formation and trace element co-sequestration at aquatic redox-interfaces and in technical systems, for example drinking water treatment for As removal.

[1] Voegelin *et al.* (2010) *Geochim. Cosmochim. Acta* **74**, 164-186. [2] Kaegi *et al.* (2010) *Geochim. Cosmochim. Acta* **74**, 5798-5816.

## The occurrence of very high-grade pyrometamorphic xenocrysts/xenoliths in the plutonic rocks of the Alvand plutonic complex, Hamedan, Iran

ALI A. SEPAHI

Department of Geology, Bu-Ali Sina University, Hamedan,  
Iran, E-mail: aasepahi@gmail.com, sepahi@basu.ac.ir

The Alvand plutonic complex and a sequence of poly-metamorphic rocks are situated near to Hamedan, Sanandaj-Sirjan zone, Iran. Restites, xenoliths and xenocrysts are abundant in granitoids of the complex but they are rare in gabbroic rocks. Restitic xenocrysts of garnet, sillimanite/andalusite and cordierite which subsequently reacted with granitic magmas are common in granitoids. In gabbroic rocks, especially in a wherlitic olivine gabbro, scarce xenocrysts of andalusite occur which have been converted to sillimanite and a pelitic xenolith in this rocks has been pyrometamorphosed to a very high grade mineral assemblage (e.g. a spinel, sillimanite, mullite and sanidine-bearing assemblage). Thermometric studies have indicated that this very high grade pyrometamorphic assemblage has been formed at peak temperature of more than 1000 °C (up to 1300-1400 °C) when mafic-ultramafic host magma interacted with Al-rich xenoliths.

## Tectonomagmatic origin of the Late Jurassic volcanism in the Patagonia Province, Argentina

L. SERRANO<sup>1,2\*</sup>, V. KAMENETSKY<sup>2</sup>, A. MARZOLI<sup>1</sup>, M. MARQUEZ<sup>3</sup>, G. BELLINI<sup>1</sup>, H. BERTRAND<sup>4</sup>  
AND C. BALLHAUS<sup>5</sup>.

<sup>1</sup>Uni Padua, Italy (linamaria.serranoduran@studenti.unipd.it)

<sup>2</sup>CODES, University of Tasmania, 7001, Hobart Australia

<sup>3</sup>Uni Nac. de Patagonia, Comodoro Rivadavia, Argentina

<sup>4</sup>Lab. Géologie, Ecole Normale Supérieure de Lyon, France

<sup>5</sup>Steinman Inst., University of Bonn, 53115, Germany

A thick sequence of the Late Jurassic magmatic rocks in Patagonia (Argentina) extends over  $1 \times 10^6$  km<sup>2</sup> from the Atlantic to the Andes [1]. Although bimodal in composition, the Patagonia Province (PP) is one of the largest silicic (felsic) LIPs on Earth. It consists of rhyolites and ignimbrites of the Marifil (~187-177Ma) [2,4] and Chon Aike (~168-151Ma) [2,3] Formations (Fm), with a minor andesitic component represented by the Bajo Pobre (BP) (~164-153Ma) [2,3] and Locontrapial Fm. Thus the total duration of magmatism is ~36 Ma. Our new U-Pb ages on zircons for the Marifil Fm confirm that the first felsic pulse coincided with the Karoo-Ferrar magmatic event (~184-178Ma) [4]. However, the main peak activity in the PP is ~10 Ma younger. Basaltic volcanism of the Cañadon Asfalto (CA) Fm fills an extensional basin contemporaneous with the volcanism of the PP. This magmatism was associated with a complex geodynamic evolution during the Gondwana break-up. The setting comprised continental rifts and a subduction zone in the western continental margin, possibly accompanied by back-arc rifting. Andesites from the BP Fm and basalts from CA Fm are Opx rich rocks with occasional anhedral olivine crystals with Cr-spinel inclusions (Mg# 0.48-0.25; Cr# 0.47-0.37). The most primitive Cr-spinel grains from the BP and CA have contrasting compositions in terms of Al<sub>2</sub>O<sub>3</sub> (25-28 and 10-12 wt%) and TiO<sub>2</sub> (1.3-1.4 and 0.4-1.3 wt%, respectively). Accordingly, parental melt compositions can be correlated with MORB for BP and island-arc magmas for CA [5]. Compositions of the Late Jurassic volcanic rocks combined with quartz- and pyroxene-hosted melt inclusion and Cr-spinel study will be discussed and applied to understanding the tectono-magmatic environment of this LIP.

[1] Pankhurst & Rapela (1995) *EPSL* 134, 23-26. [2] Feraud *et al* (1999) *EPSL* 172, 83-96. [3] Pankhurst *et al* (2000) *J. Pet.* 41, 602-625. [4] Jourdan *et al* (2005) *Geology* 33, 745-748. [5] Kamenetsky *et al* (2001) *J. Pet.* 42, 655-671.

## Natural and synthetic plagioclases for the interpretation of planetary surfaces

SERVENTI G.<sup>1</sup>, CARLI C.<sup>2</sup>, ORLANDO A.<sup>3</sup>, BORRINI D.<sup>4</sup>, PRATESI G.<sup>4</sup>, SGAVETTI M.<sup>1</sup> AND CAPACCIONI F.<sup>2</sup>

<sup>1</sup>Department of Physics and Earth Sciences, University of Parma (giovanna.serventi@unipr.it)

<sup>2</sup>Inaf-IAPS Tor Vergata, Roma (cristian.carli@iaps.inaf.it)

<sup>3</sup>Institute of Geosciences and Earth Resources, C.N.R., Firenze (orlando@igg.cnr.it)

<sup>4</sup>Department of Earth Sciences, University of Firenze

Plagioclase, pl, is an important constituent of planetary surfaces, e.g. Moon and Mercury. Spectrometers detected crystalline pl on the lunar surface [1], with composition of ~An90 and variable FeO content. New data from XRS and GRS on the Hermean surface show contents of Na [2] that are compatible with low-An (<90) pl.

### Natural and synthetic plagioclase spectroscopy

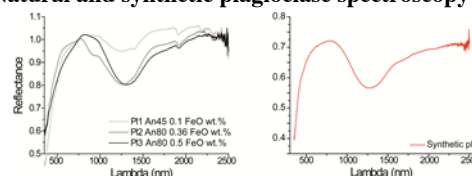


Fig. 1 Natural (left) and synthetic (right) spectra of pl.

Visible and near-infrared reflectance (VNIR) spectroscopy is the most used technique to map the surface of Solar System bodies. Pl, often considered a spectrally neutral phase, shows a clear absorption at ~1.25  $\mu$ m, even for very low FeO contents (Fig. 1, left); furthermore, an increase of this component, causes an increase of the absorption band depth, while its position moves to the IR region. We synthesized pl with different An and FeO content, in order to investigate how these parameters control the absorption band in the VNIR. A Pl, An90 with 0.5 wt% FeO, was synthesized from oxides and carbonate at  $\log f_{O_2} = -9$ ; the mixture was first heated at 1600 °C for 15 minutes, quenched and then re-heated at 1400 °C for 24 hours. XRD and EPMA confirmed both the presence of a crystalline phase and its compositional homogeneity. The spectrum is reported in Fig. 1, right.

The synthesis of different pl will allow to create a VNIR spectra database which will be invaluable to better constrain the composition of the crust of Solar System bodies.

[1] Ohtake M. *et al.* (2009) *Nature*, 461, 236-241. [2] Evans *et al.* (2013) *LPSC XLIV*, Abstract #2033.

## Bioaerosols in ECHAM5-HAM

ANA SESARTIC<sup>1</sup>, ULRIKE LOHMANN<sup>1</sup>,  
AND TRUDE STORELVMO<sup>2</sup>

<sup>1</sup>ETH Zurich, Institute for Atmospheric and Climate Science,  
Zurich, Switzerland (ana.sesartic@env.ethz.ch,  
ulrike.lohmann@env.ethz.ch)

<sup>2</sup>Department of Geology and Geophysics, Yale University,  
210 Whitney Ave., USA-06520-8109 New Haven (CT)

Interest in primary biological aerosol particles (bioaerosols) like bacteria and fungal spores is mainly related to their health effects, impacts on agriculture, ice nucleation and cloud droplet activation, as well as atmospheric chemistry [1].

In our study we investigated the impact of bacteria and fungal spores acting as ice nuclei on clouds and precipitation on a global scale. Bacteria [2] and fungal spores [3] as a new aerosol species were introduced into the global climate model ECHAM5-HAM using observational data compiled by [4] for fungal spores and [5] for bacteria.

The addition of bioaerosols into ECHAM lead to only minor changes in cloud formation and precipitation on a global level, however, changes in the liquid water path and ice water path as well as stratiform precipitation in the model were observed in the boreal regions where tundra and forests act as sources bacteria and fungal spores.

This goes hand in hand with a decreased ICNC and increased effective radius of ice crystals. An increase in stratiform precipitation and snowfall can be observed in the model results for those regions as well.

Although bacteria and fungal spores contribute to heterogeneous freezing, their impact in the model was reduced by their low numbers compared to other heterogeneous ice nuclei like mineral dust.

To the best of our knowledge, the influence of bioaerosols on the global climate appears to be small. However, there are still several uncertainties constraining bioaerosol modelling, for example their exact emissions (especially over remote regions and the oceans), the impact of coating and ageing on the bacterial IN-ability, etc. Standardised long-term observations with world-wide coverage of ecosystems, as well as further laboratory data, are therefore necessary for a more precise model evaluation.

[1] Morris *et al.* (2011) *Biogeosciences* **8**, 17-25. [2] Sesartic *et al.* (2012) *Atmos. Chem. Phys.* **12**, 8645-8661. [3] Sesartic *et al.* (2013) *Environ. Res. Lett.* **8**, 014029. [4] Sesartic & Dallafior (2011) *Biogeosciences* **8**, 1181-1192. [5] Burrows *et al.* (2009) *Atmos. Chem. Phys.* **9**, 9281-9297.

## N<sub>2</sub>O and δ<sup>15</sup>N-N<sub>2</sub>O data in ice cores: atmospheric versus in situ signal

BARBARA SETH, JOCHEN SCHMITT,  
MICHAEL BOCK AND HUBERTUS FISCHER

Climate and Environmental Physics & Oeschger Centre for  
Climate Change Research, University of Bern,  
Switzerland, (\*correspondence: seth@climate.unibe.ch)

N<sub>2</sub>O is an important greenhouse gas which has several sources in both terrestrial and marine ecosystems. N<sub>2</sub>O mixing ratios and stable isotopes measured from air entrapped in ice cores allow to identify different processes driving changes in these sources. We present a new δ<sup>15</sup>N-N<sub>2</sub>O record covering the past 15'000 years and discuss possible explanations for the long-term decrease during the Early Holocene.

However, comparative analyses of different ice cores show offsets in the mixing ratios suggesting that elevated mixing ratios are due to in situ production, especially in glacial ice with higher impurity content.

However, the pathways leading to in situ production of N<sub>2</sub>O in ice cores are not yet identified. Sowers [1] observes N<sub>2</sub>O isotope anomalies in Vostok ice core samples and supposes that microorganisms might use ammonium (NH<sub>4</sub><sup>+</sup>) in ice to produce N<sub>2</sub>O. EPICA Dome C (EDC) ice samples suspect to in situ production show fairly heavy δ<sup>15</sup>N-N<sub>2</sub>O values as well, however, the isotope signature of N<sub>2</sub>O produced from ammonium is expected to be rather light. Thus, it is unlikely that in situ produced N<sub>2</sub>O in the EDC ice core can be related to NH<sub>4</sub><sup>+</sup> oxidation.

Alternatively, we propose that in situ N<sub>2</sub>O in the EDC ice is produced from nitrate (NO<sub>3</sub><sup>-</sup>). Low accumulation sites like EDC show extremely enriched δ<sup>15</sup>N-NO<sub>3</sub><sup>-</sup> values due to intense post-depositional loss processes [2], while sites with higher accumulation have lighter δ<sup>15</sup>N-NO<sub>3</sub> values [3] and we found a lighter δ<sup>15</sup>N-N<sub>2</sub>O in situ signature for those samples. More knowledge about in situ N<sub>2</sub>O could help to verify hidden in situ production or identify ice cores and time intervals suitable to derive the atmospheric history for both mixing ratios and isotopic signature of N<sub>2</sub>O.

[1] Sowers (2001), *JGR* **106**, 31903-31914. [2] Blunier *et al.* (2005), *GRL* **32**, L13501. [3] Hastings *et al.* (2005), *GBC* **19**, GB4024.

## Competition between microbial and abiotic Fe(II) oxidation: A kinetic modeling approach

M. SETO<sup>1\*</sup> AND P. VAN CAPPELLEN<sup>2</sup>

<sup>1</sup>Dept. of Information and Computer Science, Nara Women's University, Nara 630-8222, Japan, seto@ics.nara-wu.ac.jp (\*presenting author)

<sup>2</sup>Ecohydrology Research Group, University of Waterloo, Waterloo, Canada

Neutrophilic Fe(II) oxidising bacteria (FeOB) are ubiquitous in soils and sediments. It has been proposed that under low oxygen conditions they are able to successfully outcompete abiotic Fe(II) oxidation. Not only do FeOB catalyse Fe(II) oxidation, they may also hinder the autocatalytic growth of Fe(III) oxides, possibly through the binding of Fe(II) and Fe(III) to cell surfaces or extracellular polymeric substances. We present a simple kinetic model of neutrophilic Fe(II) oxidation, which explicitly accounts for the inhibitory effect of FeOB on the autocatalytic Fe(II) oxidation pathway. The model comprises kinetic equations for the different forms of Fe in systems with and without FeOB. The microbial Fe(II) oxidation rate is assumed to be a function of the FeOB cell concentration, the O<sub>2</sub> concentration, and the cell-bound Fe(II) concentration. The latter is related to the aqueous Fe(II) by an isotherm. In the proposed model, cell-bound Fe(II) and Fe(III) are intermediates in the transformation of aqueous Fe(II) to Fe(III) oxides. The validity of the model is statistically examined, using data of Fe(II) oxidation batch experiments in the presence of the bacterium *Leptothrix cholodnii* Appels [1]. The observed microbial Fe(II) oxidation kinetics are well described by the model. Compared to the abiotic experiments, the presence of the bacteria increases the initial Fe(II) oxidation rate by nearly a factor of 3, but decreases the subsequent autocatalytic Fe(II) oxidation rate by about 50%. The results suggest that neutrophilic FeOB may broaden their geochemical niche by slowing down the autocatalytic growth of Fe(III) oxides in low O<sub>2</sub> environments.

[1] Vollrath *et al.* (2012) *Geomicrobiol J.*, **29**, 550-560

## Sr-Nd isotope geochemistry of the troctolitic-gabbroic Bell Rock Range, Giles Complex, central Australia

R. E. B. SEUBERT<sup>1</sup>, R. R. KEAYS<sup>1</sup>, S. M. JOWITT<sup>1</sup>  
AND A. G. TOMKINS<sup>1</sup>

<sup>1</sup>School of Geosciences, Monash University, Clayton, VIC 3800, Australia, roland.seubert@monash.edu

The Mesoproterozoic Giles Complex of the Musgrave Province, central Australia, forms part of the c. 1075 Ma Warakurna Large Igneous Province. Here, we provide new Sr-Nd isotope data for a troctolite-gabbro member (Bell Rock Range) of the Giles Complex and compare them with other members of the Giles Complex; these data provide new insights into the formation and evolution of this under-researched magmatic province.

The most primitive melt within the Bell Rock Range is represented by a sample from the top of the intrusion that has an initial  $\epsilon\text{Nd}$  value of +4.8, higher than the main troctolitic body of the range ( $\epsilon\text{Nd}$  of -0.3 to +1.3), and  $\epsilon\text{Nd}$  values of the gabbroic-ultramafic Wingellina Hills, Ewarara, Kalka and Gosse Pile intrusions range from -5.1 to +0.5 [1]. In comparison, the basal part of the Bell Rock Range has  $\epsilon\text{Nd}$  values of -4 to 1.1, identical to later dykes that cross-cut the range, and indicative of formation from magmas that underwent crustal contamination or were derived from an enriched mantle source. Although the troctolites at Bell Rock Range yield a range of  $\epsilon\text{Nd}$  and MgO values, they have relatively uniform initial  $^{87}\text{Sr}/^{86}\text{Sr}$  values compared to all other lithologies in our database.

These data shed new light onto the petrogenesis of the Giles Complex, and indicate that it is unlikely that any of the the magmas that formed this complex were derived from a depleted region of the mantle. The magmas that formed this complex must have either been sourced from an enriched region of the mantle or have undergone variable crustal contamination, resulting in the range of isotopic compositions observed within this suite of co-magmatic rocks.

The relatively uniform  $^{87}\text{Sr}/^{86}\text{Sr}$  compositions of the Bell Rock Range troctolites suggests that they represent an uncontaminated end-member style of Giles Complex magmatism, whereas gabbroic-ultramafic cumulates in the same area represent true mixing between mantle-derived melts and crustal rocks indicative of significant crustal contamination. These findings will contribute to an understanding of the tectonic setting of the Giles Complex.

[1] Wade (2006) PhD thesis, University of Adelaide, Australia.

## Iodide Ion Hydration in Aqueous Solution to 360°C: Insight from XAS and Ab Initio MD

T.M. SEWARD<sup>1</sup>, HENDERSON C.M.B.<sup>2</sup>, SULEIMENOV O.M.<sup>1</sup> AND CHARNOCK J.M.<sup>2</sup>

<sup>1</sup>Victoria University of Wellington, Wellington 6140, New Zealand; terry.seward@vuw.ac.nz

<sup>2</sup>University of Manchester, Manchester M13 9PL, UK

The interaction of solute species with solvent molecules is a fundamental aspect of aqueous solutions and changes with increasing temperature and pressure in response to changes in the hydrogen bonding of water solvent. The varying nature of ion hydration in hydrothermal systems plays an important role in many geochemical processes including water stable isotope fractionation, mineral solubility and precipitation, metal complexing and transport reactions.

Anion-solvent interaction is still poorly known at elevated temperatures and pressures and no data exist for iodide solvation above ambient temperatures (Seward and Driesner, 2004). We have therefore studied the first shell hydration of iodide using X-ray absorption spectroscopy from 35 to 350°C at equilibrium vapour pressures. The Exafs of 1.00m RbI as well as 0.10m CsI and SrI<sub>2</sub> was measured using a high temperature X-ray optical cell containing silica glass and/or cvd diamond windows. With increasing temperature from 35 to 350°C, iodide-oxygen(water) distance increased from 3.56 to 3.61Å as the first shell waters are "dragged" away from the iodide ion by expanding bulk water solvent to which they are hydrogen bonded. Over the same temperature range, the number of first solvation shell waters apparently decreases from 7 to 4.

We have also performed ab initio molecular dynamics simulations using the Car-Parinello scheme (Car and Parinello, 1985). The present density functional theory calculations utilised norm-conserving pseudopotentials of Troullier and Martins (1991) to describe the core of all atoms except for hydrogen for which a von Barth-Car analytical pseudopotential was used. The simulation cell was cubic with periodic boundary conditions containing 32 waters and one iodide ion. At 27°C, the iodide-oxygen(water) distance was 3.53Å and increased to 3.59Å at 350°C, in good agreement with our results from XAS.

Car R. and Parinello (1985) Phys. Rev. Lett. 55, 2471.  
Seward T.M. and Driesner T. (2004) In: Aqueous Systems at Elevated Temperatures and Pressures (Elsevier), chap. 5.  
Troullier and Martins (1991) Phys. Rev. B, 43.

## Fluid-mediated re-equilibration and self-irradiation in complex U-Th-rich assemblages of pegmatites: A case from Norway and implications for U-Th-Pb dating of ore deposits.

A.M. SEYDOUX-GUILLAUME\*<sup>1</sup>, B. BINGEN<sup>2</sup>, C. DURAN<sup>3</sup>, V. BOSSE<sup>4</sup>, J.L. PAQUETTE<sup>4</sup>, D. GUILLAUME<sup>1</sup>, PH. DE PARSEVAL<sup>1</sup> AND J. INGRIN<sup>5</sup>

<sup>1</sup> GET, UMR5563 CNRS-UPS-IRD, Université de Toulouse, 14 av E. Belin, 31400 Toulouse, France

<sup>2</sup> Geological Survey of Norway, 7491 Trondheim, Norway

<sup>3</sup> Département des sciences appliquées, 555 Boulevard de l'Université, Chicoutimi, Québec, Canada, G7H 2B1

<sup>4</sup> LMV, Université Blaise Pascal, 5 rue Kessler, 63000 Clermont-Ferrand, France

<sup>5</sup> UMET, UMR 8207 CNRS, Université Lille1, 59655 Villeneuve d'Ascq, France

In most rocks, uranium and thorium are concentrated in favorable crystallographic sites in few minerals such as zircon, monazite, titanite, and rarely uraninite, thorianite, thorite / huttonite, euxenite. These minerals are submitted to intense self-irradiation that can lead to amorphization and also modify their environment by irradiating the host minerals. Here, we focus on accessory minerals in rare-metal-rich pegmatites from southern Norway (Kragerev, Iveland-Evje); some of these minerals are rich in U (e.g. up to 15wt % for euxenite). A complex paragenesis of zircon + monazite + xenotime + euxenite was studied by multiple methods including optical and electron microscopy and U-Pb geochronology (SIMS and LA-ICP-MS). Observations show that complex relationships exist between the different minerals (especially zircon-euxenite) and the various processes (alteration by fluids and radiation effects) which have repercussions on the U-Th-Pb geochronology response. Irradiation (self and out), destroy the crystal lattice (amorphization) promoting the alteration of more or less destroyed parts. Amorphization induces volume increase, leading to the formation of cracks which eventually connected into a network through the rock. This fracturing allows fluid circulation, and promotes alteration of source minerals and dispersion of elements (e.g. Pb and U). Our results demonstrate however that monazite and xenotime crystals, even altered, have a greater potential for U-Th-Pb dating [1].

[1] Seydoux-Guillaume *et al.* (2012) *Chem. Geol.* **330-331**, 140-158.



## High-spatial resolution imaging of the distribution and inter-element correlation of metals in modern and ancient stromatolites

M.C. SFORNA<sup>1\*</sup>, P. PHILIPPOT<sup>1</sup>, M. VAN ZUILEN<sup>1</sup>,  
A. SOMOGYI<sup>2</sup>, K. MEDJOUBI<sup>2</sup>, P.T. VISSCHER<sup>3</sup>  
AND C. DUPRAZ<sup>3</sup>

<sup>1</sup> Institut de Physique du Globe de Paris, Sorbonne Paris Cité,  
Paris, France (\*correspondence : sforna@ipgp.fr)

<sup>2</sup> Synchrotron Soleil, Saint-Aubin, Gif-sur-Yvette, France

<sup>3</sup> Department of Marine Sciences, University of Connecticut,  
Groton, Connecticut, USA

Metals, which are widely used by all microorganisms, could act as indicators in the rock record of past microbial activity if we are able to distinguish between biological uptake and late stage contamination associated with diagenesis. Here we present the results of the study of the distribution, inter-element correlation and speciation of trace metals in modern and ancient stromatolites from Big Pond, a hypersaline lake in the Bahamas and the 2.7 Ga-old Tumbiana formation in Western Australia. Results were obtained using synchrotron-based techniques.

In a cm-scale drill core of an extant stromatolite from the Bahamas, the Fe, Ti, Zn, Cu and As contents in the organic fraction of the stromatolite structure increase with depth. We attributed this to metal uptake during early diagenesis. Both in the Bahamas and in the Tumbiana stromatolites, high-spatial resolution imaging at different scales (from the cm- to the nm-scale) reveals different types of metal distribution and inter-element correlations. Although most of the metal enrichments are of diagenetic origin, the occurrence of specific species in isolated organic structures that are preserved in the core of the stromatolite domes most likely reflects remains of past biological activity.

## Insights of the Mt. Etna volcanic activity through multiparametric data recorded by the NEMO-SN1 seafloor observatory

T. SGROI\*, M. DE CARO, N. LO BUE AND P. FAVALI  
Istituto Nazionale di Geofisica e Vulcanologia, Rome, Italy

In the last years the use of seafloor observatories improves the possibility to perform long-term monitoring in abyssal area as far not easily accessible, interested by geophysical processes like volcanism, seismicity or fluid emissions. Presently many programmes to establish permanent underwater networks are launched at global scale (e.g., EMSO in Europe, OOI in USA, NEPTUNE in Canada and DONET in Japan). Recently, a multidisciplinary approach has proven to be a very important tool in the monitoring of volcanic areas. In fact, the different instruments hosted in the seafloor observatory permit to perform multidisciplinary analyses, better focusing on the dynamics of volcanic system.

In the Italian territory, the NEMO-SN1 seafloor cabled observatory is running in the Western Ionian Sea at a depth of 2100 m, about 25 km off-shore Eastern Sicily, as node of EMSO infrastructure (<http://www.emso-eu.org>). Eastern Sicily is of great scientific interest, due to the proximity to seismogenic structures which originated the most destructive earthquakes of the area and to Mt. Etna. The underwater observatory fills the gap in the off-shore sector of the Mt. Etna, focusing on its deeper feeding system. SN1 was able to record also the low-frequency seismic signals linked to Etna volcanic activity, as the volcanic tremor associated to the 2002-2003 eruptive activity. In this work, the joint analyses of seismological, gravimetric and oceanographic data are used to highlight the dynamics of Mt. Etna. The inferences of background noise from volcanic activity and ocean processes are investigated through the cross-analyses of different kind of geophysical data to improve the confidence of volcanic hazard assessment.

## Mantle xenoliths from Bir Ali (Yemen)

SGUALDO P.\*, BECCALUVA L., BIANCHINI G.  
AND SIENA F.

Dip. Fisica e Scienze della Terra, Università di Ferrara  
(\*sglpla@unife.it)

Mantle xenoliths from the Bir Ali diatrema (southern Yemen) consist of spinel peridotites and clinopyroxenites. In this contribution we present bulk rock (XRF, ICP-MS) and mineral (EMPA, LA-ICP-MS) major and trace element analyses carried out on a collection of 62 samples in order to characterize the lithospheric mantle of the area and constrain its relative petrological evolution. Peridotites are mainly equilibrated at 950-1000 °C and include fertile lherzolites and more refractory harzburgites and dunites, suggesting that partial melting processes variably affected the pristine mantle composition. Subsequent metasomatic reactions are evidenced by: a) glassy films and/or patches; b) interstitial plagioclase; c) rare pargasite amphibole (observed only in one sample). Further evidence of metasomatic interactions is given by anomalously low Fo content (<0.87) of olivine and low Mg# of pyroxene (<0.88). These metasomatic events are confirmed by the bulk rock trace element budget that reveal enrichments in the most incompatible elements, especially in the most refractory dunites ( $La_N/Yb_N$  up to 4.1). Coherently, enrichments in the most incompatible elements are also observed in diopsidic clinopyroxene ( $La_N/Yb_N$  up to 3.9) and glasses ( $La_N/Yb_N$  up to 9.9). Trace element discrimination ratios [1] suggest that the causative metasomatic agents were mainly represented by alkali-silicate melts. Noteworthy, samples characterized by plagioclase impregnation show unfractionated (flat) bulk-rock and clinopyroxene REE patterns suggesting refertilization by subalkaline metasomatic melts. Therefore, the considered lithospheric section appears to be characterized by remarkable heterogeneity, in contrast with what observed in mantle xenoliths collected from the Ethiopian plateau area that display clear evidence of pervasive refertilization by CFB melts [2]. This suggests that the lithospheric mantle of southern Yemen wasn't affected by the thermochemical effects of the Afar plume.

[1] Coltorti *et al.* 2000. *Earth Planet. Sc. Lett.* **183**, 303-320.

[2] Beccaluva *et al.*, 2011. *GSA Special Paper* **478**, 77-104.

## Pore-scale simulation of calcite dissolution and precipitation using lattice-Boltzmann method

B. SHAFEI<sup>1\*</sup>, C. HUBER<sup>2</sup> AND A. PARMIGIANI<sup>3</sup>

<sup>1</sup>School of Earth and Atmospheric Sciences, Georgia Institute of Technology, Atlanta, GA 30332, USA.

babak.shafei@eas.gatech.edu

<sup>2</sup>christian.huber@eas.gatech.edu

<sup>3</sup>andrea.parmigiani81@gmail.com

Calcium carbonate dissolution and precipitation plays an important role in the context of CO<sub>2</sub> storage in geologic formation, or as a pH buffer during diagenesis of marine sediments. Using the parallel open-source library palabos (www.palabos.org), we have developed a new multi-species pore-scale model based on the lattice Boltzmann method to investigate the effect of physical and chemical heterogeneities on geochemical behavior of carbonate system in a complex porous media. The model has been successfully applied to study the permeability change of a porous medium associated with a given porosity change during dissolution and precipitation and arsenic sorption on Fe-bearing minerals.

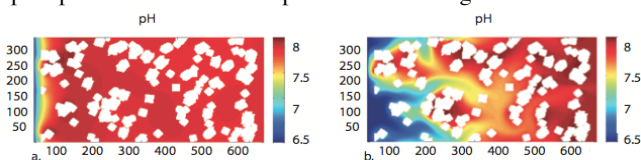


**Fig 1.** Pore-scale pH distribution at steady-state for a) low Peclet number (Pe=1) and b) high Peclet number (Pe=5).

In this study, we consider standard geochemical pathways for the carbonate system including 7 species (i.e. H<sup>+</sup>, OH<sup>-</sup>, H<sub>2</sub>CO<sub>3</sub>, HCO<sub>3</sub><sup>-</sup>, CO<sub>3</sub><sup>2-</sup>, Ca<sup>2+</sup> and CaHCO<sub>3</sub><sup>+</sup>) and 5 mixed kinetic-equilibrium reactions. The focus of our study is to investigate how spatial distribution of the pH is affected by: 1) the kinetic rates of heterogeneous calcite dissolution and precipitation (i.e. pH-dependent vs. pH-independent rate constants), 2) transport regime (i.e. Peclet numbers) and 3) chemical composition of initial and boundary conditions resulting in spatially variable saturation index with respect to calcite. Results showed that the development of pore-scale concentration gradients is a combined effect of heterogeneous reactions and pore-scale flow within the porous medium. In high Pe simulations (Fig 1.a), both depth of penetration and spatial heterogeneity increase compared to low Peclet scenario (Fig 1.b). Calculated minimum, maximum and average pH values in the computational domain are function of Pe, chemical composition of inflow and initial solution in the domain, and type of rate constants.

## Geochemistry and petrogenesis of volcanic rocks in the Lahrud region, of the Ardebil province, Iran

HABIB SHAHBAZI SHIRAN

Department of Archaeology, University of Mohaghegh  
Ardabili, Ardebil, Iran (Shahbazihabib@yahoo.com)

Compositional analyses of materials from prehistoric contexts have become an important component of most scientifically oriented archaeological projects. Characterizing the elemental signature of materials (obsidian, metals, stones) helps determine provenance and technological production techniques, and therefore is useful for reconstructing trade and interaction between people prehistorically.

Simple petrographic descriptions can provide useful information on raw material provenance, but for some lithic materials more sophisticated techniques are required. Geochemistry can provide this sophisticated tool, trace and interpret the bedrock or the source of the ancient lithic materials. Geochemists have determined the geologic, magmatic and/or tectonic affinities of igneous rocks for decades. This project reports on mineral assemblages and whole-rock geochemistry that mafic rocks used to make lithic artifacts and especially building stones in the Ardebil province, northwestern Iran, have two bedrock sources.

## New insights into the isotope exchange reaction between O<sub>3</sub> and CO<sub>2</sub> via O(<sup>1</sup>D) from laboratory experiments

ROBINA SHAHEEN<sup>1</sup>, THOMAS RÖCKMANN<sup>2</sup>, BELA TUZSON<sup>3</sup> AND CHRISTOF JANSSEN<sup>4</sup>

<sup>1</sup>University of California at San Diego, Department of Chemistry and Biochemistry, 9500 Gilman Dr, La Jolla, CA 92093 USA, roshaheen@ucsd.edu

<sup>2</sup>Institute for Marine and Atmospheric Research Utrecht, Utrecht University, Princetonplein 5, 3584 CC Utrecht, The Netherlands, t.roeckmann@uu.nl

<sup>3</sup>Empa, Swiss Federal Laboratories for Materials Science and Technology, Laboratory for Air Pollution and Environmental Technology, Überlandstr.129, 8600 Dübendorf, Switzerland, Bela.Tuzson@empa.ch

<sup>4</sup>Laboratoire de Physique Moléculaire pour l'Atmosphère et l'Astrophysique, 4 Place Jussieu, 75005 Paris, France, christof.janssen@upmc.fr

Stratospheric CO<sub>2</sub> shows a marked oxygen triple isotope anomaly that is derived from O<sub>3</sub> via O(<sup>1</sup>D). So far the precise isotopic composition of the isotope exchange partner of CO<sub>2</sub> has not been identified and it is not clear whether normal mass dependent or anomalous isotope effects contribute during the exchange process. From laboratory experiments using simultaneous mass spectrometric analysis of CO<sub>2</sub> and laser spectroscopy based symmetry selective analysis of O<sub>3</sub> isotopomers, we present experimental evidence that the O(<sup>1</sup>D) mediated isotope transfer is coupled to the asymmetric O<sub>3</sub> isotopomers and follows a standard mass dependence. Recently investigated alternative pathways for oxygen isotope exchange between CO<sub>2</sub> and hyperthermal O atoms or O<sub>2</sub> molecules are unlikely to compete significantly with isotope exchange via O(<sup>1</sup>D). Existing measurements also indicate unresolved discrepancies for the isotope anomaly of O<sub>3</sub> produced in the laboratory under different photochemical conditions, which may originate from highly energetic oxygen species generated in the photolysis of O<sub>2</sub> and/or O<sub>3</sub>. Such variations would be directly transferred to CO<sub>2</sub>, and further combined measurements of the isotopic composition of CO<sub>2</sub> and symmetry resolved O<sub>3</sub> are needed to fully unravel all aspects of the isotope exchange.

## Dynamics of H<sub>2</sub>O<sub>2</sub> in the external *milieu* of corals – from single organism to the reef

YEALA SHAKED<sup>1,2\*</sup> AND RACHEL ARMOZA-ZVULONI<sup>1,2</sup>

<sup>1</sup>Inst of Earth Sciences, Hebrew Univ., Jerusalem, Israel  
(\*correspondence: yshaked@vms.huji.ac.il)

<sup>2</sup>Interuniversity Inst. for Marine Sciences, Eilat, Israel  
(rachelar@post.tau.ac.il)

Symbiont-bearing corals are subjected to internal fluxes of reactive oxygen species (ROS) from their symbiotic algae as well as external fluxes from photochemically generated ROS in overlying waters. Here, combining sensitive methods, kinetic approaches and statistical tools, we characterized the dynamics of the membrane permeable ROS - hydrogen peroxide (H<sub>2</sub>O<sub>2</sub>) - in the external *milieu* of corals in a laboratory setting and in a natural coral reef. On the organism level, we observed flow-induced release of H<sub>2</sub>O<sub>2</sub> and antioxidants from intact corals over 2-4 hour periods. In the absence of flow we found that antioxidants associated with the coral quickly degraded externally applied H<sub>2</sub>O<sub>2</sub>. Scaling up to the ecosystem level, we observed coral-induced changes in H<sub>2</sub>O<sub>2</sub> concentrations and elevated antioxidant activities in the proximity of a coral knoll and in the reef lagoon. This newly described ability of corals to change the chemistry of their surrounding water by releasing both H<sub>2</sub>O<sub>2</sub> and antioxidants may have important implications for coral physiology and interactions with the environment. External antioxidant activity may enable corals to offset exogenous H<sub>2</sub>O<sub>2</sub> whereas the flow induced H<sub>2</sub>O<sub>2</sub> release may aid corals in discarding internal H<sub>2</sub>O<sub>2</sub>.

## Traffic-associated heavy metal pollution and source discrimination in Jiangxi Province, China

SHAO LI<sup>1,2</sup>, XIAO HUAYUN<sup>3\*</sup> AND WU DAISHE<sup>1</sup>

<sup>1</sup>Environmental and Chemical Engineering College, Nanchang University, Nanchang, 330031, China

<sup>2</sup>The Key Lab of Poyang Lake Environment and Resource Utilization of Ministry of Education, Nanchang, 330031, China

<sup>3</sup>State Key Laboratory of Environment Geochemistry, Institute of Geochemistry, Chinese Academy of Sciences, Guiyang, 550002, China

Road traffic is recognized as an important source of heavy metals. In order to identify the levels and sources of heavy metal contamination on three highways in Jiangxi Province, concentrations of Zn, Cu, Pb, Sb, Cd in different chemical forms in airborne particles, road dusts and soils were analyzed. All of the Zn, Cu, Pb, Sb, Cd concentrations in road dusts and soils exceeded background values. And the heavy metal concentrations in road dusts were higher than those in soils. Heavy metal concentrations in airborne particles, road dusts and soils presented similar rules: Zn > Cu, Pb > Sb, Cd. Zinc, Cu, Pb, Sb, Cd concentrations in airborne particles, road dusts and soils were all significantly correlated with vehicle number, indicating that road traffic was one of the main source of these metals. For all these metals, we also found that the ratios were higher near the toll stations than on normal driving road, indicative of an increased heavy metal emission rates under the conditions of low driving velocity and discontinuous movement of vehicles. The sources of the heavy metals were also identified by comparing chemical forms of the heavy metals in airborne particles, road dusts and soils. Lead in airborne particles was dominated by the acid soluble/exchangeable fractions (67%) while that in road dusts and soils was dominated by the residual fractions (45.3% and 43.8%, respectively), which suggested that Pb in airborne particles was derived from traffic, and that in road dusts and soils resulted mainly from the use of leaded gasoline in the past. In raining days, Zn concentrations in PM10 increased possibly because tire abrasion turned to be weak due to the lubrication of rainwater and so more small particles were emitted from the tyre wear. The difference in chemical forms of the heavy metals in airborne particles, road dusts and soils was associated with concentrations of organic matters. Bioavailability of heavy metals in airborne particles was much higher than that in road dusts and soils..

Corresponding author. E-mail: xiaohuayun@vip.skleg.cn.

## Redox control on the water column distribution of Ra in a stratified lake - Lake Kinneret, Israel

G. SHARABI<sup>1,2\*</sup>, Y. KOLODNY<sup>1</sup>, L. HALICZ<sup>1</sup>, A. NISHRI<sup>3</sup>  
AND B. LAZAR<sup>1</sup>,

<sup>1</sup> Institute of Earth Sciences, The Hebrew University of Jerusalem, ISRAEL 91904

(\*Correspondence: galit@gsi.gov.il)

<sup>2</sup> Geological Survey of Israel, Jerusalem, ISRAEL 95501

<sup>3</sup> Israel Oceanographic and Limnological Research Ltd., P.O. Box 447, Migdal, ISRAEL 14950

The vertical distribution of transition metals in holomictic lakes is controlled by the seasonal mixing/stratification regime that change the redox state in the water column. We studied the control of the Mn redox system on water column distribution of Ra, an element with invariant oxidation state. The study was conducted in Lake Kinneret (The Sea of Galilee), Israel, a warm monomictic lake in northern Jordan valley. Lake Kinneret fluctuates between periods of stratification (spring/summer) and mixing (fall/winter), with full depth mixing (~37 m) in February. The mixed layer (epilimnion) is always well oxygenated while below it (hypolimnion), anoxic conditions prevail.

Vertical profiles of Mn, <sup>226</sup>Ra ( $T_{1/2}=1,600$  y) and <sup>224</sup>Ra ( $T_{1/2}=3.7$  d) were measured during October 2012. Practically all the Mn in the well-oxygenated mixed layer (0-15 m) was particulate ( $10 \mu\text{g}\cdot\text{L}^{-1}$ ). A large peak of dissolved Mn ( $500 \mu\text{g}\cdot\text{L}^{-1}$ ), appeared at the oxycline ~17.5 m. The reducing hypolimnion, below 20 m, contained ~60  $\mu\text{g}\cdot\text{L}^{-1}$  of dissolved Mn and was virtually deficient of solid Mn-oxides. The water column profile of <sup>226</sup>Ra and <sup>224</sup>Ra were remarkably similar.

Mn speciation along the Kinneret water column is redox sensitive: it appears mainly as solid Mn-oxide in the oxygenated epilimnion, and as dissolved Mn(II) in the anoxic hypolimnion. Hence, the particles of Mn-oxide that sink through the water column, dissolve in the epilimnion-hypolimnion interface and form an extremely large and narrow peak of dissolved Mn(II). The Ra water column profile resembled that of Mn, despite being a redox-insensitive element. This is attributed to adsorption of dissolved Ra on solid Mn-oxides in the epilimnion and its desorption in the hypolimnion. We use the <sup>224</sup>Ra/<sup>226</sup>Ra ratios and the large difference in their half-lives to obtain a field estimate of the reduction rate of Mn-oxide.

## Magmatic systems of the Paleoproterozoic large igneous provinces: Evidence from the eastern Fennoscandian Shield

E.V. SHARKOV\*, M.M. BOGINA AND A.V. CHISTYAKOV  
IGEM RAS, Staromonetny per. 35, Moscow, Russia 119017  
(sharkov@igem.ru)

It is known that large igneous provinces are usually formed by lava plateaus, dyke swarms and subvolcanic sills, which are united into volcano-plutonic associations. At the same time, rocks within lava plateau were subjected to crystallization differentiation and crustal assimilation, which caused wide variations in their composition. This leaves us with questions where and how this occurred?

For this aim we presented the results of our study of two Paleoproterozoic large igneous provinces in the eastern Fennoscandian Shield: (1) early Paleoproterozoic (2.5-2.35 Ga) province of siliceous high-Mg series, and (2) middle Paleoproterozoic (2.35-1.9 Ga) province composed by high- and low-Ti alkaline and tholeiite basalts. The peculiar feature of these provinces is the presence of layered mafic-ultramafic complexes: dunitite-harzburgite-bronzitite-norite-gabbro-norite-anorthosite (Monchegorsky, Fedorovo-Pansky, Burakovsky, etc.) and wehrlite-clinopyroxenite-gabbro-alkaline gabbro (Elet'ozero and Greymykh-Vyrmes), respectively. The formation of these complexes was controlled by replenishment of fresh magmas in solidified intrusive chambers and impregnation of melts into already solidified rocks (multistage formation). Geochemical data indicate that all rocks of these centers are related in different degree, being often close in major and trace-element composition to volcanics in lava plateaus.

So, we suggest that these layered intrusive complexes represent deep-seated long-lived transitional magmatic chambers where melts, derived from magma-generation zones were accumulated and experienced crystallization differentiation, while evolved melts were mixed with fresh magma portions. Cumulates retained in the crust. Correspondingly, the primary magmas partially lost their components and derived evolved magmas continue their ascent to the surface. The evolved magmas arrived at the surface and formed lava piles of different composition. Thus, it is difficult for primary melts to reach surface; as a rule, they are subjected to transformations in such transitional chambers.

## Melting phase relations in Udachnaya-East kimberlite and search for parental melt composition

I.S. SHARYGIN<sup>1\*</sup>, K.D. LITASOV<sup>1</sup>, A. SHATSKIY<sup>1</sup>,  
A.V. GOLOVIN<sup>1</sup>, E. OHTANI<sup>2</sup> AND N.P. POKHILENKO<sup>1</sup>

<sup>1</sup>Sobolev Institute Geology and Mineralogy, Novosibirsk  
630090, Russia (\*igor.sharygin@gmail.com)

<sup>2</sup>Tohoku University, Sendai 980-8578, Japan.

Udachnaya-East kimberlite (UEK) is an unique example of unaltered Group I kimberlites, exhibiting lack of serpentinisation and containing abundant alkaline carbonate and chloride minerals in the groundmass [1]. We studied phase relation in UEK in using multianvil experiments at 3-6.5 GPa and 900-1500 °C [2]. Super-solidus assemblage consists of olivine (Ol), Ca-rich garnet (Gt), Al-spinel (Sp), perovskite (Pv), CaCO<sub>3</sub>, and apatite at 3-6.5 GPa with addition of clinopyroxene at 3-4 GPa and Na-Ca carbonate at 6.5 GPa and 900 °C. The subliquidus phase assemblage (Ol + Gt + Sp + Pv) differs from common mantle lithologies, which may be due to unaccounted CO<sub>2</sub> lost during kimberlite degassing at shallow depth. UEK did not achieve complete melting even at 1500°C and 6.5 GPa. This indicates that kimberlite magma below 90 km depth was a mixture of the melt and xenogenic materials (mainly Ol). In the studied *P-T* range, melt has Ca-carbonatite composition (Ca/(Ca+Mg) = 0.6-0.8) with high alkali and Cl contents (2.8-6.7 wt.% K<sub>2</sub>O, 7.3-11.6 wt.% Na<sub>2</sub>O, 1.2-3.7 wt.% Cl). The K, Na and Cl contents and Ca/(Ca+Mg) ratio decrease with temperature. The SiO<sub>2</sub> content in the partial melt increases with temperature and decreases with pressure (Fig. 1). Consequently, the ascending melt dissolved increasingly more SiO<sub>2</sub> (Fig. 1) and evolved from essentially carbonatite (<5 wt.% SiO<sub>2</sub>) toward carbonate-silicate composition (up to 25 wt.% SiO<sub>2</sub>).

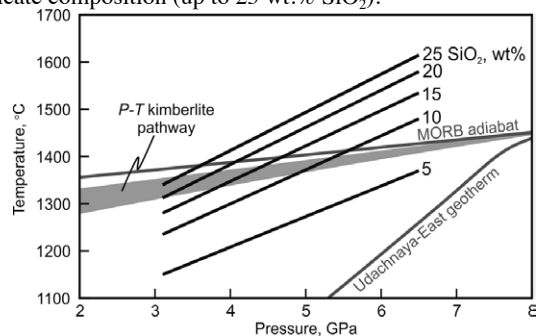


**Figure 1:** *P-T* plot for UEK melt with SiO<sub>2</sub> isopleths.

[1] Kamenetsky *et al.* (2012) *Lithos* **152**, 173-186. [2] Sharygin *et al.* (2013) *Dokl. Earth Sci.* **448**, 200-205.

## Mineralogy of the Chelyabinsk meteorite, Russia

V.V. SHARYGIN<sup>1\*</sup>, T.YU. TIMINA<sup>1</sup>, N.S. KARMANOV<sup>1</sup>,  
A.A. TOMILENKO<sup>1</sup> AND N.M. PODGORNYKH<sup>1</sup>

<sup>1</sup>V.S. Sobolev Institute of Geology and Mineralogy SD RAS,  
Novosibirsk 630090, Russia (\*correspondence:  
sharygin@igm.nsc.ru)

The entry in the Earth's atmosphere, further blasting and impact of the Chelyabinsk meteor body have been fixed 15 February 2013. We studied small fragments collected in the area of abundant meteorite shower (nearby towns Emanzhelinsk and Korkino, South Urals).

The Chelyabinsk meteorite was classified as an ordinary LL5 chondrite (S4, W0) [GEOKHI RAS]. It is very similar in mineral composition to other LL5 chondrites such as Salzwedel, Hautes Fagnes and Al Zarnkh [1-3]. All meteorite fragments consist of coarse- to fine-grained matrix, rare submillimetre chondrules and thin fusion crust. Some fragments show brecciated texture.

Olivine (Fo<sub>68-72</sub>Fa<sub>28-31</sub>Ln<sub><0.5</sub>), orthopyroxene (En<sub>70-74</sub>Fs<sub>25-28</sub>Wo<sub>1-2</sub>), Fe-Ni-metal, troilite, chromite and Na-plagioclase (Ab<sub>77-86</sub>An<sub>10-20</sub>Or<sub>3-10</sub>) are major primary minerals in the inner part. Ilmenite, Cr-diopside (Wo<sub>46-48</sub>En<sub>43-45</sub>Fs<sub>16-18</sub>, Cr<sub>2</sub>O<sub>3</sub> – 0.6-0.8 wt%), chlorapatite, merrillite and feldspathic glass are minor. Coarse- to medium-grained matrix mainly contains primary minerals (olivine, pyroxenes, etc.); some areas show fine recrystallization due to melting and further quenching with formation of skeletal crystals of olivine (Fa<sub>29-46</sub>Ln<sub>1-3</sub>), orthopyroxene, subcalcium pyroxene (Wo<sub>22-42</sub>En<sub>45-65</sub>Fs<sub>13-22</sub>) in feldspathic glass (plagioclase). Metal-sulfide assemblage (up to 10 vol%) is represented by kamasite-taenite intergrowths (or their individuals) and troilite; pentlandite and native copper occur rarely. Chondrules are different in mineralogy. Some of them show well-oriented "barred" texture and consist of olivine and Na-plagioclase (feldspathic glass) with minor chromite and chlorapatite. Other chondrules are similar in mineral composition to the matrix and their oriented texture is less pronounced.

Fusion crust (up to 1 mm) contains relics of primary minerals, mafic-ultramafic brown glass, abundant gas bubbles, newly-formed minerals (zoned skeletal crystals of Cr-Ni-rich magnetite, forsterite-fayalite, wüstite, etc.) and Ni-rich metal-sulfide globules (heazlewoodite, awaruite-taenite, godlevskite, rarely Os-Ir-Pt-Ni alloy).

[1] Matthes (1995) *Chem Erde-Geochem* **55**, 257-261. [2] Gismelseed *et al.* (2005) *Meteorit Planet Sci* **40**, 255-259. [3] Vandeginste *et al.* (2012) *Geol Belg* **15**, 96-104.

## Evidence for formation of alluvial diamonds from North-East of Siberian platform in subduction environment

V.S. SHATSKY<sup>1,2\*</sup>, D.A. ZEDGENIZOV<sup>2</sup>, A.L. RAGOZIN<sup>2</sup>  
AND V.V. KALININA<sup>2</sup>

<sup>1</sup>Vinogradov Institute of Geochemistry SB RAS, 1a Favorsky str., Irkutsk, 664033, Russia, (\*correspondence: shatsky@igc.irk.ru)

<sup>2</sup>Sobolev Institute of Geology and Mineralogy SB RAS, 3 Koptyuga ave., Novosibirsk, 630090, Russia

Diamonds from placers show large variability in nitrogen content ranging from below detection to 3500 at.ppm. Nitrogen contents in diamonds with eclogitic inclusions are generally high (average of 950 at.ppm) as compared with diamonds of ultramafic suite (average of 513 at.ppm).  $\delta^{13}\text{C}$  values of the diamonds range from -27 to -3‰ (n=28) for eclogitic diamonds and from -7.1 to -0.5‰ (n=16) for peridotitic diamonds. The 265 diamonds were polished to expose their mineral inclusions. Inclusions of eclogite suite are predominant (74%). The diamonds of the eclogitic suite contain garnet, omphacitic clinopyroxene, coesite, K-feldspar, rutile, corundum. The peridotitic diamonds contain olivine, Cr-pyrope garnet, orthopyroxene and chromite. Majoritic garnets of both peridotitic and eclogitic parageneses were identified in 4 diamonds. The olivines have Fo contents between 89.7 and 93.8 mol.% (average – 92.4). Eclogitic garnet and Cpx inclusions are within the range of eclogitic inclusions of worldwide. For an assumed pressure of 5 GPa eclogitic garnet and clinopyroxene gave temperatures in the range 1028-1290°C. The majority of eclogitic diamonds show positive Eu-anomalies. High-Ca group garnets are LREE depleted, show strong positive Eu (up to 4.25) and Sr anomalies and have HREE contents that are less than the low- and intermediate-Ca group samples. Eclogitic Cpx inclusions are characterized by convex REE<sub>N</sub> patterns with maxima at Nd or Sm. The presence of majorite inclusions indicate that the portion of the diamonds is of sublithospheric origin. Multiple inclusions from diamond and their carbon isotopes composition are consistent with a mixing model in which they result from the interaction of slab-derived melt/fluid with surrounding mantle. The nature of the variations in the carbon isotope composition and the nitrogen contents indicate that the diamonds growth medium have at least two sources (mantle and recycled earth crust via subduction zone). Mantle carbon was involved in the diamond formation process during the final stages of growth.

## Telluride-gold-sulfide mineralization in silicification zones of gabbro-dolerite bodies of hengursk complex (Russia, Pay-Khoy)

R.I. SHAYBEKOV

Institute of Geology Komi SC UB RAS, Syktyvkar, Russia, 54 Pervomayskaya st. (\*correspondence: shaybekov@geo.komisc.ru)

According to the previous studies gold-telluride mineralization has been found only in the gabbro-dolerite bodies of Pay-Khoy hengursk complex at the districts "Pervyi" and "Savabeysky" in copper and nickel ores [1]. The studies of sulfide (chalcopyrite highly) mineralization in quartz veins of district "Krutoy" revealed silver-gold-telluride phases with later hydrothermal origin.

Telluride-gold-sulphide mineralization is characterized by a fairly stable composition - chalcopyrite, covellite, wurtzite, gold, silver, coloradoite (found for the first time in Pay-Khoy) and native phase. The composition of coloradoite has minor changes from the classic mineral which could be explained by the specificity of mineral formation or inaccurate analysis due to the small size of the grains. The impurities of silver and lead in insignificant quantities were found, which allowed distinguishing of two kinds - silver-lead and silver. The formation of this type of mineralization occurred in a low-, medium-temperature hydrothermal process in the veins of gold-bearing sulphide mineralization.

The work was made with the support of the program of the presidium RAS №27 (12-П-5-1027) and SC-1310.2012

[1] Shaybekov R.I. Mineral assemblages and genesis of platinum sulphide mineralization in gabbro-dolerite Pay-Khoy (Russia, the Nenets Autonomous District) // Notes RMS, 2011. № 6, pp. 70–86.

## Use of passive sampling to measure organic chemicals and metabolites in water and soil: Application to human health risk assessment in developing countries

D. SHEA\*, T. HONG, X. XIA, X. KONG, K. O'NEAL, AND P. LAZARO

North Carolina State University, Raleigh, NC 27695-7617  
USA (\*correspondence: d\_shea@ncsu.edu)

Measuring chronic exposure to broad chemical mixtures at trace levels is currently not practical because traditional *grab* samples do not capture temporal variations in exposure and thus provide little information on chronic exposure unless many samples are collected and analyzed. This problem is even greater in developing countries where resources for sampling and chemical analysis can be extremely limited. We will report on the use of passive sampling devices (PSDs) to provide a cost-effective means of estimating chronic exposure and toxic response in water and soil. PSDs sequester and preconcentrate organic chemicals from water and from soil and sediment via desorption to water. Using laboratory-derived and field-verified uptake rates (calibration), PSDs were deployed in the field for a known amount of time (e.g., 1 month), the accumulated chemical residue was measured, and then the average exposure calculated based on the calibration. Extracts of the PSDs also were used in high throughput cell-based assays to measure various toxic endpoints such as genotoxicity and endocrine disruption. We will illustrate the potential utility of PSDs using data from the Red River, Vietnam. In surface waters, we found very good agreement between measured chemicals in the PSDs and synoptically deployed aquatic test organisms, providing strong evidence that PSDs accumulate only the bioavailable fraction of a chemical. In soil, we also found good agreement between PSDs and accumulation in earthworms. In both water and soil, there was generally good agreement between PSD chemical residues and toxic response variables. We will discuss the current utility and limitations for using PSDs for both human and ecological health risk assessments and provide an example of the spatial and temporal variation in human health risk to chemical exposure in the Red River, Vietnam.

## Effect of hydrothermal alteration on magnetic susceptibility of Challu Pluton, SE Damghan- Iran

M. SHEIBI<sup>1\*</sup>, P. MAJIDI<sup>2</sup> AND M. REZAEI KHKHAYY<sup>3</sup>

<sup>1,3</sup> Faculty Member, Department of Geology, Shahrood University of Technology, Iran (\*correspondence: sheibi@shahroodut.ac.ir, Mehdi.Rezaei@khayam.ut.ac.ir)

<sup>2</sup> MSc. student of Petrology, Department of Geology, Shahrood University of Technology, Iran (parvinmajidi91@gmail.com)

Challu pluton located in the northern part of Central Iran structural zone, SE Damghan. Based on mineralogy and geochemistry, the pluton is I-type granite and compositionally ranges from monzodiorite and monzonite. The pluton intruded in Eocene volcano-plutonic series of Toroud-Chah Shirin. During the crystallization and cooling, a magmatic-dominated hydrothermal system caused extensive hydrothermal alteration and Fe mineralization.

Challu granitoidic body has been studied using by anisotropy of magnetic susceptibility (AMS). The method carried out by (MFK1-FA) Kappbridge susceptometer (AGICO, Brno) operating at low field ( $4 \times 10^{-4}$ T; 920 Hz) at Geomagnetic Lab of Shahrood University of Technology. According to the measurements (32 stations, 96 cores and 384 fragments), the average magnetic susceptibility ( $K_m$ , in  $\mu$ SI) of monzonites and monzodiorites are 9323 and 28776, respectively. Therefore, the rocks belong to the ferromagnetic granitoids (bulk susceptibility  $\geq 500 \mu$ SI). Magnetite is the main carrier of the magnetic behavior and pyroxene, biotite and sphene are other carriers. Due to presence of extensive propylitic mineral assemblages (epidote, calcite and chlorite) in the south eastern margin and importance of their effect on AMS, the magnetic susceptibility of some grains of epidotes was determined. The obtained data shows that presence of this mineral has no effect on bulk susceptibility but the grain size of magnetic, its loss and damage during hydrothermal alteration reduced the amount of magnetic susceptibility.



## Microbial communities correlate with Lemon Creek Glacier meltwater discharge

CODY S. SHEIK<sup>1</sup>, EMILY I. STEVENSON<sup>1</sup>, PAUL DEN UYL<sup>1</sup>, SARAH M. ACIEGO<sup>1</sup>, AND GREGORY J. DICK<sup>1,2\*</sup>

<sup>1</sup>Dept. Earth and Environmental Sciences, <sup>2</sup>Dept. of Ecology and Evolutionary Biology, University of Michigan, Ann Arbor, MI, 48109, USA. (\*Correspondence gddick@umich.edu)

Mineral weathering has long been recognized as an important ecological process that is mediated in part by microorganisms. Recently, microorganisms have been implicated in the weathering of rock in the interstitial waters between bedrock and overlying glaciers (1,2), a process which may directly impact carbon cycling in the the northern Atlantic Ocean (3). Here we surveyed microbial communities associated with sub-glacial meltwaters and mixed sediments over the course of four months as they were discharged from the Lemon Creek Glacier located near Juneau Alaska, USA. Utilizing a high throughput small subunit ribosomal RNA gene sequencing approach, the diversity and structure of microbial communities was quantified and correlated to changes in the water geochemistry.

Microbial communities were consistently dominated by *Proteobacteria* classes *Beta*, *Alpha*, *Gamma* and *Delta* (in descending order of abundance), which accounted for 40-70% of the total community). Many sequences from uncultured groups often associated with anoxic environments were also recovered, including candidate divisions BD1-5, OD1 and TM7 (1-5%) and novel methanogenic Archaea (<0.1%). Phylogenetic richness was high in most samples (15-85 unique lineages) and resembled typical sediment community diversity. Community structure was distinct in each sample and was significantly correlated with time of discharge and sampling location (*e.g.* lower glacial fed lake, glacial outflow channel, and sub-glacial interstitial waters).

Our results suggest that interstitial microbial weathering supports diverse microbial communities that resemble those from anoxic environments, are highly dynamic with respect to time of discharge, yet retain a consistent phylum level taxonomic structure. Furthermore this work highlights ice-water-sediment interfaces as important microbial habitats that are potential analogs for other low temperature geochemically active environments such as the deep subsurface.

[1] Sharp, M., *et al.* (1999) *Geology* 27:107-110. [2] Skidmore, M., *et al.* (2005) *Appl Environ Microbiol* 71:6986-6997. [3] Bhatia, M.P., *et al.* (2013) *Nat Geosci* 6:274-278.

## Causes and consequences of low atmospheric pCO<sub>2</sub> in the Late Mesoproterozoic

NATHAN D. SHELDON<sup>1</sup>

<sup>1</sup> Department of Earth and Environmental Sciences, University of Michigan, Ann Arbor, MI, USA, (nsheldon@umich.edu)

Based upon various proxy, theoretical, and model constraints, Paleoproterozoic atmospheric pCO<sub>2</sub> [1] was much higher than Phanerozoic levels [*e.g.*, 2]. However, relatively little is known about the transition between the two climate states. Here, geochemical mass-balance from ~1.1 Ga old Midcontinent Rift System (USA) paleosols is used to reconstruct atmospheric pCO<sub>2</sub> during the Mesoproterozoic. The calculations robustly indicate low atmospheric pCO<sub>2</sub> (<10 times Preindustrial levels). Results are consistent between seven paleosols at one site, between paleosols at different Midcontinental Rift sites, and between the new results and previously published pencontemporaneous paleosol [3] and microfossil reconstructions [4-5]. In spite of the lower than expected pCO<sub>2</sub> values, climate models driven by the reconstructed pCO<sub>2</sub> levels predict equable conditions [6]. The newly recognized Mesoproterozoic pCO<sub>2</sub> minimum is best explained as the culmination of a long-term C burial event by the biosphere that is also indicated by marine carbonate δ<sup>13</sup>C changes during the Mesoproterozoic, and which is consistent with changes in the biosphere including increased stromatolite abundance and diversity, evolution of sulfur-utilizing bacteria, and the spread of microbial mats into continental environments. One potential testable consequence of this hypothesis is that it should be accompanied by a gradual rise in atmospheric pO<sub>2</sub> throughout the “boring billion.”

[1] Sheldon (2006) *Precambrian Research* 147, 148-155. [2] Royer *et al.* (2007) *Nature* 446, 530-532. [3] Mitchell and Sheldon (2010) *Precambrian Research* 183, 738-748. [4] Kaufman and Xiao (2003) *Nature* 425, 279-282. [5] Kah and Riding (2007) *Geology* 35, 799-802. [6] Domagal-Goldman and Sheldon (2012) *AGU P13B-1936*.

## What caused Mongolian Mesozoic magmatism: Was it crustal or mantle driven?

T. SHELDRIK<sup>1\*</sup>, T.L. BARRY<sup>1</sup> AND A.D. SAUNDERS<sup>1</sup>

<sup>1</sup>University of Leicester, Leicester, LE1 7RH, UK.

(\*correspondence: thomassheldrick@gmail.com, tlb2@le.ac.uk, ads@le.ac.uk)

Prior to the Himalayan orogeny, the last major phase of continent collision and amalgamation in mainland Asia was the mid-late Mesozoic closure of the Mongol-Okhotsk ocean. Rapidly following on from the collisional event came extensive and widespread basaltic magmatism that infilled extensional basins across parts of eastern and southern Mongolia, and northern China. The production of voluminous basalts soon after an orogenic event has led some to propose that a mantle plume may have interacted with the crust during this period<sup>[1]</sup>. Opposing this theory are suggestions of slab delamination<sup>[2]</sup>, post-orogenic collapse<sup>[3]</sup> or lithospheric overthickening and delamination<sup>[4]</sup>. This study aims to assess the plausibility of these models by constraining the mechanisms of magma genesis for these mildly alkali basalts. Then, using these constraints, we plan to test local and regional tectonic syntheses.

To this end, a large suite of basaltic samples have been collected from the most western limit of the Mesozoic volcanism, from the Gobi, Mongolia. Samples have been analysed for major, trace and REE elements (XRF & ICP-MS) with results showing that the basalts are LREE enriched (high La/Ti) and slightly HREE depleted with variable Mg#’s, Pb & Nb anomalies and Th/Nb ratios. The chemistry and a limited amount of isotope data shows that fractionation and crustal contamination processes were important for melt generation. Further sampling and a more extensive isotope study will help to elucidate some of the processes that produced these enigmatic basalts and thereby test models for melt generation.

[1] Yarmolyuk & Kovalenko 2001. *Tectonics, magmatism and metallogeny of Mongolia*, London. [2] Tomurtugoo *et al.*, 2005. *Jour Geol Soc* 162, 125-134. [3] Fan *et al.*, 2005. *Geo Res.* 121, 115-135. [4] Wang *et al.*, 2006. *Earth & Planet papers* 251, 179-198.

## Mg isotope evidence for early dolomite formation in a Marinoan cap carbonate

BING SHEN<sup>1</sup>, JOSHUA WIMPENNY<sup>2</sup>, QING-ZHU YIN<sup>2</sup>, CINTY LEE<sup>3</sup>, SHUHAI XIAO<sup>4</sup> AND CHUANMING ZHOU<sup>5</sup>

<sup>1</sup>School of Earth and Space Science, Beijing University, Beijing, 100871, bingshen@pke.edu.cn

<sup>2</sup>Department of Geology, University of California, Davis, CA, 95616, jbwimpenny@ucdavis.edu, qyin@ucdavis.edu

<sup>3</sup>Department of Earth Science, Rice University, Houston, TX, 77002, ctlee@rice.edu

<sup>4</sup>Department of Geoscience, Virginia Tech, Blacksburg, VA, 24060, xiao@vt.edu

<sup>5</sup>Nanjing Institute of Geology and Palaeontology, CAS, Nanjing, 210008, cmzhou@nigpas.ac.cn

The global deposition of cap carbonates after the Marinoan glaciation (635Ma) is key evidence supporting the Snowball Earth hypothesis [1]. The cap carbonate is almost exclusively composed of dolostone with rare occurrences of limestone [2]. Thus, this interval is the only time in the Earth’s history when deposition of dolostone occurred globally, suggesting a unique marine geochemistry after the Marinoan glaciation. Here, we report the Mg isotopic composition ( $\delta^{26}\text{Mg}$ ) of the Zhamoketi cap carbonates from two sections in the Quruqtagh area, NW China [3], which contain both limestone and dolostone. Our data show an enrichment of heavy Mg in the cap limestone samples, indicating scavenging of light Mg from seawater consistent with global dolostone precipitation. Compared with their Phanerozoic counterparts, the Zhamoketi cap limestones and dolostones have very similar  $\delta^{26}\text{Mg}$  values [4, 5], which may indicate early formation of Marinoan cap dolostone driving seawater to heavier  $\delta^{26}\text{Mg}$  values. This study suggests that the sharp transition from extreme icehouse to extreme greenhouse conditions during the meltdown of Marinoan Snowball Earth might have created a suitable environment for global dolostone formation.

[1] P.F. Hoffman, *et al.*, *Science*, 281 (1998) 1342. [2] P.F. Hoffman, *et al.*, *Palaeo, Palaeo, Palaeo*, 277 (2009) 158. [3] S. Xiao, *et al.*, *Precambrian Research*, 130 (2004) 1. [4] A. Galy, *et al.*, *EPSL*, 201 (2002) 105. [5] E.D. Young, *et al.*, *Rev.Mineral.Geoch.*, 55 (2004) 197.

## Carbon stable isotope composition in modern snail shell aragonite and its climatic significance

X. F. SHENG, L. L. ZHU AND L. W. LIU

Key Laboratory of Earth Surface Geochemistry, Ministry of Education, School of Earth Sciences and Engineering, Nanjing University, Nanjing 210093, China (shenxuer@nju.edu.cn)

Stable isotope signatures recorded in land snail shells have been widely used to characterize the information of paleo-climate and paleo-environment.  $\delta^{13}\text{C}$  values of the land snail shells can be used to discuss and estimate the compositions of local vegetations, namely the ratio of plants  $\text{C}_3$  to plants  $\text{C}_4$  in the ecosystem, which can examine the drought degree of ancient ecological system.

Here we explored the relationships between the  $\delta^{13}\text{C}$  of modern snail shells and associated climatic factors in east part of China in an attempt to develop transfer functions that can be applied to retrieve the climatic information stored in snail shells. Totally 400  $\delta^{13}\text{C}$  values of modern land snail shell aragonite from the field collected were measured from 18 localities in a widely spatial scale, with the result shows the  $\delta^{13}\text{C}$  of modern snail shells are obviously related to precipitation, elevation and weakly related to temperature and latitude. The analysis exhibits that the negative correlations between the  $\delta^{13}\text{C}$  of shells with the living season precipitation and temperature as the former is robust ( $R^2=0.47$ ) and the latter is weak ( $R^2=0.27$ ). However, correlations between the  $\delta^{13}\text{C}$  of shells with elevation and latitude is positive with the former was robust ( $R^2=0.48$ ) and the latter was weak ( $R^2=0.34$ ).

Furthermore, under the condition that the humidity stayed relatively stable, the indoor snail feeding experiment was carried out and the study comes to the conclusion that the food is the dominant factor influencing the  $\delta^{13}\text{C}$  of snail shells, and the fractionation value between the diet and snail shells is calculated as 14.72‰. The study simultaneously confirmed that the temperature does not affect the  $\delta^{13}\text{C}$  of snail shell under laboratory conditions. In summary, we discussed that the impact effect from the environmental factors on the  $\delta^{13}\text{C}$  of snail shells is not a direct action, but through regulating and altering the local vegetation types and compositions in an ecosystem.

The research was financially supported by the NSF of China through Grant 41073065.

## A review of radionuclides impact in South Sinai, Egypt: Case study of Sharm El Sheikh area

MAHMOUD I. SHERIF<sup>1</sup>, MOHAMED F. GHONEIM<sup>1</sup>, MOHAMED TH. S. HEIKAL<sup>1</sup>, BOTHINA T. EL DOSUKY<sup>1</sup>, MOHAMED M. EL GALY<sup>2</sup>

<sup>1</sup>Geology Department, Faculty of Science, Tanta University, Tanta 31527, Egypt

<sup>2</sup>Nuclear Material Authority, Cairo, Egypt

The area of Sharm El Sheikh consists mainly of granitic rocks of alkaline type. Alkaline granite is the most favourable host rock for uranium and thorium mineralization. The activity concentration of natural radionuclides ( $^{238}\text{U}$ ,  $^{232}\text{Th}$ ,  $^{226}\text{Ra}$  &  $^{40}\text{K}$ ) of 100 samples around the studied area, including granites, dikes and stream sediments were investigated using  $\gamma$ -ray spectrometry. The radium equivalent activity ( $R_{\text{eq}}$ ), gamma activity concentration index (I), external hazard index (Hex) internal hazard index (Hin) and annual effective dose rate (AEDR) have been calculated and compared with the internationally approved values.

The permissible values for each index revealed that all exposures of granite and mafic dikes have values below safety limits of radiation. The stream sediments within the major wadis are also safe. However, the felsic dikes that more or less occur far from the inhabited areas of Sharm El Sheikh town exceed the permissible radiation limits indicating their hazardous effect.

Thereby, it was recommended to restrict land use in a buffer zone adjacent to the felsic dikes of very limited distributions. Moreover, a planned major town extension of Sharm El Sheikh area has to be stopped around and within these dikes sites, but alternative future residential areas could be delineated to the northwest of the town.

## Electronic structures of transition metal oxides and sulfides: Applications to the physics and chemistry of the Earth

DAVID M. SHERMAN<sup>1</sup>

<sup>1</sup>School of Earth Sciences, University of Bristol, Bristol BS8 1RJ UNITED KINGDOM (dave.sherman@bris.ac.uk)

A variety of geochemical and geophysical processes result from electronic transitions in minerals and aqueous complexes. In aquatic environments, photochemical excitations on mineral surfaces release dissolved micronutrients and may have played a role in prebiotic synthesis. In the deep Earth, pressure-induced electronic transitions such as spin-pairing, metallization and changes in the band gap/Fermi energies of phases affect the density, transport properties and element partitioning in the core and mantle.

Density functional theory, using approximate exchange-correlation functionals, has enabled us to accurately predict structures and vibrational energies of minerals and aqueous complexes. We can now predict the thermodynamics, phase transitions and seismic properties of minerals in the deep earth and even the thermodynamics of metal complexation in hydrothermal solutions. However, exchange-correlation functionals such as the generalized gradient approximation (GGA) are still based on the local density approximation. Consequently, these functionals still contain an error associated with incorrectly including the electron self-interaction. The self-interaction error yields incorrect electronic structures and band gaps and precludes accurate predictions of electronic transition energies. For the case of a material like FeO, standard GGA functionals incorrectly yield a metallic ground state that becomes Pauli-paramagnetic (rather than a diamagnetic low-spin state) with pressure. Charge-transfer band gaps in Fe<sub>2</sub>O<sub>3</sub> are too low. Physicists have addressed this problem using the “Hubbard U” correction to the local density approximation. However the U parameter is an empirical correction. Chemists, however, have recognized that the Hartree-Fock formalism exactly includes the self-interaction correction. A variety of “hybrid” exchange functionals have been developed (e.g., B3LYP) that empirically mix Hartree-Fock exchange with the GGA exchange-correlation functional. Here, I will present several examples to illustrate the application of these functionals to transition metal oxides and sulfides and show how the hybrid functionals predict electronic transitions of importance in geochemistry and geophysics.

## Reduced gas flux from Precambrian cratons – Implications for subsurface microbiology

B. SHERWOOD LOLLAR<sup>1\*</sup>, G. HOLLAND<sup>2</sup>, L. LI<sup>1</sup>,  
G. LACRAMPE-COULOUME<sup>1</sup>, G.F. SLATER<sup>3</sup>,  
T.C. ONSTOTT<sup>4</sup> AND C.J. BALLENTINE<sup>5</sup>

<sup>1</sup>Dept. of Earth Sciences, University of Toronto, ON, Canada M5S 3B1 (\*bslollar@chem.utoronto.ca)

<sup>2</sup>LEC, University, Lancaster LA1 4YQ UK

<sup>3</sup>SGG, McMaster University, Hamilton ON Canada L8S 4K1

<sup>4</sup>Dept. of Geosciences, Princeton University, Princeton, N.J., USA

<sup>5</sup>SEAES, Manchester University, Manchester M13 9PL UK

Quantification of global H<sub>2</sub> flux has to date been based primarily on thermodynamic and geochemical modelling, or on H<sub>2</sub> measurements at a number of marine systems such as the Rainbow and Logatchev hydrothermal vents, the off-axis Lost City field, and more recently, at diffuse vents. H<sub>2</sub> sources from continental systems are significantly less well constrained. Recent exploration of saline fracture waters more than a km below the Earth’s surface in Precambrian continental crust however has identified environments equally as H<sub>2</sub>-rich as the hydrothermal vents and spreading centers, and sustaining microbial communities of H<sub>2</sub>-utilizing methanogens and sulfate reducers [1]. Here we report on results from > 30 sites and > 250 samples and boreholes in continental Precambrian sites worldwide. Fracture waters accessed via mines and underground research laboratories contain mM concentrations of reduced gases (H<sub>2</sub>, CH<sub>4</sub>, ethane, propane, butane) as well as high concentrations of noble gases.

First identified in Ne isotope results from the Witwatersrand basin in South Africa [2], novel radiogenic isotope signatures have now been shown to be a consistent feature of these deep waters [3]. Integration of the noble gas signatures with compositional and isotopic information for the reduced gases provide constraints on the residence time of the fracture waters, the degree of interconnectivity of different groundwater systems, and an estimate of the amount of time these waters have been isolated from the surface. This presentation will address the distribution of ancient fluids at selected key reference sites; and the controls of this deep hydrosphere on the biodiversity and distribution of the subsurface microbial biosphere and carbon cycle.

[1] Lin *et al.* (2006) *Science* **314**, 479-482. [2] Lippmann-Pipke *et al.* (2011) *Chem. Geol.* **283**, 287-296. [3] Holland *et al.*, (2013) *Nature*, *in press*.

## Geodynamic constraints on the recycling of ancient SCLM and genesis of Tibetan diamondiferous ophiolites

R.D. SHI<sup>1,2\*</sup>, W.L. GRIFFIN<sup>2</sup>, S. Y. O'REILLY<sup>2</sup>, X.R. ZHANG<sup>1,3</sup>, Q.S. HUANG<sup>1</sup>, X.H. GONG<sup>1</sup> AND L. DING<sup>1</sup>

<sup>1</sup> Institute of Tibetan Plateau Research, CAS, Beijing 100101 China (\*correspondence: shirendeng@itpcas.ac.cn)

<sup>2</sup> GEMOC/CCFS, Earth and Planetary Sciences, Macquarie University, NSW 2109 Australia

<sup>3</sup> Department of Earth Sciences, The University of Hong Kong, Pokfulam Road, Hong Kong, China

Natural diamonds have been found *in situ* in the chromitites and peridotites of Tibetan ophiolites [1,2]. Whole-rock <sup>187</sup>Os/<sup>188</sup>Os values of these diamond-bearing peridotites and chromitites vary from 0.1038 to 0.1266, yielding  $T_{RD}$  ages back to 3.4 Ga. This suggests that part of the Tibetan Tethys Ocean (TTO) was underlain by a fragment of ancient subcontinental lithospheric mantle (SCLM), left stranded in the oceanic lithosphere during the opening of TTO [3]. However, there has been little geological evidence to support the geodynamics required to recycle ancient SCLM in the Tibetan ophiolites. Here we present the metamorphic ages (peak age: 191 Ma; retrogression age: 181 Ma) of Amdo HP granulites formed by the subduction of TTO crust, the age (184 Ma) of the Naqu ophiolite representing the initial subduction (SI) of TTO at the south margin of the Amdo micro-terrene, and the age (160 Ma) of the Amdo ophiolite, representing the back-arc basin developed by mantle convection in the supra-subduction zone. These ages indicate that TTO in the Amdo area is older than 191 Ma, consistent with a major PGM Os-isotope  $T_{RD}$  age peak (243 Ma) [4]. Fig.1 shows the geodynamic situation of the Tibetan Tethys ophiolites, in which the Amdo micro-terrene was isolated in the TTO during the rifting of Gondwana along listric faults, then subducted to >150 km depth, before exhumation.

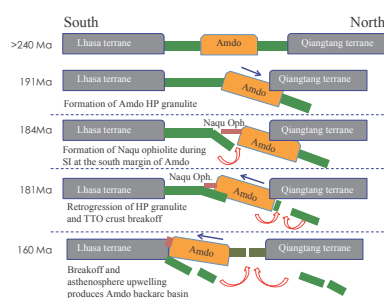


Fig. 1 Recycling of ancient SCLM in the Tibetan ophiolites

[1] Yang *et al.* (2013) *Science* (subm.); [2] Griffin *et al.* (2013) this conference; [3] Shi *et al.* (2012) *Geological Review*, 58(4): 643-652; [4] Shi *et al.* (2007) *EPSL*, 261: 33-48.

This research was funded by the National Natural Science Foundation of China (Grant no. 41172059)

## Reconstruction of Oil-filling History by Fluid Inclusion Analysis: A Case Study of Tahe Oil Field, Tarim Basin, NW China

WEIJUN SHI, ZHIRONG ZHANG, JOHN K. VOLKMAN, JIANZHONG QIN AND TENGGER, BINBIN XI

Sinopec Key Laboratory of Petroleum Accumulation Mechanisms, Wuxi Institute of Petroleum Geology, SINOPEC Research Institute of Petroleum Exploration and Production, 100 Jinxi Road, Binhu District, Wuxi, Jiangsu, China. shiwj.syky@sinopec.com

The Tahe oil field in the Tarim Basin of NW China, has Ordovician carbonates as the main reservoir strata. Core samples from the reservoirs in the eastern Tahe oil field were collected for analysis of fluid inclusions (FIs). FIs occurred mainly in calcite and quartz cements and within calcite veins in the carbonate rock matrix. From the homogenization temperatures, molecular compositions obtained by laser ablation and on-line GC-MS analysis, and simulations for fluid pressures and trapping temperature, we determined that 2 types of oil-bearing inclusions representing the 2 main petroleum charging events in the region were present. The early stage of the petroleum-filling occurred about 245 ~ 255 Ma, during the late Permian to early Triassic (late Hercynian). The late charging occurred in the Pliocene (Himalayan Orogeny).

The dominant FIs have blue fluorescence and relatively high maturity (VR of 0.75%  $R_o$  from MPI and 1.22%  $R_o$  from MPR aromatic maturity parameters). Homogenization temperatures of the associated aqueous inclusions vary from 74 to 92 °C. Results from laser ablation GC-MS analysis showed higher proportions of saturated hydrocarbons and gaseous hydrocarbons. The simulated paleo trapping temperature ranged from 150.6 to 156.9 °C, and fluid pressures ranged from 565.9 to 599.8 bar.

The second type of oil-bearing inclusions displays yellow fluorescence and relatively low maturity (VR of 0.59%  $R_o$  from MPI and 1.17%  $R_o$  from MPR), and homogenization temperatures from 58 to 113 °C. The yellow fluorescing inclusions contain much more water-soluble aromatic hydrocarbons than in the blue ones. The simulated paleo trapping temperature range from 79.2 to 83.5 °C, and fluid pressures range from 221.8 to 245.3 bar.

## Iron dissolution kinetics in mineral dust under more realistic aerosol conditions: Re-considering pH scale

ZONGBO SHI

School of Geography, Earth and Environmental Sciences,  
University of Birmingham, B15 2TT, UK Email:  
z.shi@bham.ac.uk

Iron (Fe) is a micronutrient that mediates the primary productivity in the global ocean. A significant source of such Fe in the surface ocean is from dust. It is therefore important to quantify the flux of bioavailable Fe from dust, which is strongly dependent on Fe solubility. Fe in dust is mostly insoluble, but such Fe may become soluble after reacting with acidic species during transport. In the last 20 years, many laboratory studies have been conducted to measure the dissolution kinetics of Fe in dust at pH from 1 to 5. It is now known that clouds may actually decrease Fe solubility because of its higher pH, e.g., >4. In contrast, aerosol water can be more acidic but more complicated in composition. However, most of the previous lab studies were conducted under much simplified conditions compared to those in aerosol water. These results, when applied, could lead to large bias in global models. In this work, I measured Fe dissolution kinetics in dust under conditions closer to aerosol water.

The results showed that at the same  $[H^+]$  concentration at (1 g dust L<sup>-1</sup> solution), (i) (NH<sub>4</sub>)<sub>2</sub>SO<sub>4</sub> at 1 mol L<sup>-1</sup> slows down Fe dissolution; and (ii) NH<sub>4</sub>Cl at 1 mol L<sup>-1</sup> accelerates the Fe dissolution in dust. Based on these results, I propose to use an effective pH scale for simulating Fe dissolution kinetics in aged dust in models. This pH scale considers the activity of H<sup>+</sup> ion and [HSO<sub>4</sub><sup>+</sup>], both of which can be predicted by the AIM thermodynamic model (<http://www.aim.env.uea.ac.uk/aim/aim.php>).

In addition, oxalate (0.03 M Na<sub>2</sub>C<sub>2</sub>O<sub>4</sub>) significantly accelerates the dissolution of Fe in dust (1 g dust L<sup>-1</sup> solution, 0.1 N H<sub>2</sub>SO<sub>4</sub> or 0.01 N H<sub>2</sub>SO<sub>4</sub>, and 1 M (NH<sub>4</sub>)<sub>2</sub>SO<sub>4</sub>).

## Changes in <sup>238</sup>U/<sup>235</sup>U associated with reductive immobilization of uranium in groundwater

ALYSSA E. SHIEL<sup>1\*</sup>, CRAIG C. LUNDSTROM<sup>1</sup>, THOMAS M. JOHNSON<sup>1</sup>, PARKER LAUBACH<sup>1</sup>, PHILIP E. LONG<sup>2</sup> AND KENNETH H. WILLIAMS<sup>2</sup>

<sup>1</sup>Dept. of Geology, University of Illinois at Urbana-Champaign, Urbana, IL USA; ashiel@illinois.edu (\*presenting author)

<sup>2</sup>Lawrence Berkeley National Laboratory, Berkeley, CA USA

The prevalence of groundwater contamination associated with uranium (U) mining and milling activities has driven the need for the development of effective and economically feasible remediation strategies. U is mobile in its oxidized state, U(VI), but immobile and much less toxic in its reduced state, U(IV). Thus, U(VI) reduction to U(IV) is proposed as a remediation strategy for U contaminated groundwaters. The former U mill site in Rifle, Colorado (USA) hosts experiments that investigate the rates and mechanisms of targeted U immobilization techniques. Our research focuses on the development of <sup>238</sup>U/<sup>235</sup>U (discussed as δ<sup>238</sup>U) as a tool for evaluating immobilization in the subsurface.

U concentrations and <sup>238</sup>U/<sup>235</sup>U values have been monitored over the course of three field experiments at the Rifle, CO field site in 2010–11, 2011–12 and 2012–13. These experiments examined changes in U concentrations and <sup>238</sup>U/<sup>235</sup>U values associated with biostimulation, desorption and re-oxidation. Large variations accompany acetate-induced biostimulation under both iron reducing and sulfate reducing conditions. In both cases, <sup>238</sup>U is preferentially reduced to U(IV), leaving the remaining groundwater U(VI) relatively isotopically light (Δ<sup>238</sup>U = -1.3 and -1.9‰, respectively). Changes in <sup>238</sup>U/<sup>235</sup>U accompany changes in the U concentration (dropping from ~150–200 ppb U prior to the acetate injection to ~10 ppb U). During the post-injection phase, as concentrations rebounded, absence of <sup>238</sup>U/<sup>235</sup>U greater than pre-injection values implies the primary source of U is advection of U(VI), rather than re-oxidation of U(IV). Bicarbonate-induced desorption, which led to a doubling in the U concentration, has been demonstrated to result in no significant U isotopic fractionation [1].

Our research demonstrates the potential for <sup>238</sup>U/<sup>235</sup>U to detect U reductive immobilization in the subsurface and to distinguish between removal by this process and relatively temporary processes such as sorption. U isotopes join the growing number of heavy stable isotopes with demonstrated potential for use in environmental monitoring.

[1] Shiel *et al.* (2013) *Environ. Sci. Technol.* **47**, 2535–2541.

## Estimate of residence time of groundwater in Mt. Fuji area, central Japan

N. SHIKAZONO, T. UMEMURA AND T. ARAKAWA

3-14-1, Hiyoshi, Kohoku-ku, Yokohama 223-8522 Japan  
(sikazono@applc.keio.ac.jp)

Many groundwater samples were collected from Mt. Fuji area, central Japan which is totally composed of basaltic materials. The samples were analyzed for Na<sup>+</sup>, K<sup>+</sup>, Ca<sup>2+</sup>, Mg<sup>2+</sup>, Si, Al<sup>3+</sup>, Fe<sup>2+</sup>, Fe<sup>3+</sup>, TC (total dissolved carbon), Cl<sup>-</sup>, NO<sub>3</sub><sup>-</sup>, SO<sub>4</sub><sup>2-</sup>. Analytical data plotted against altitude indicate that alkali and alkali earth element and Si concentrations increase with decreasing altitude, indicating that the dissolution of silicates in basaltic materials control the trends. Ca and Mg concentrations positively correlate with each other. This is consistent with CaO/MgO molal ratio of basalt which is 1.47. Therefore, it is inferred that Ca and Mg in groundwater were derived mainly from the congruent dissolution of basalt. Ca/Si concentration ratio determined by the dissolution reactions of basalt accompanied by the precipitation of allophane is 0.29 that is lower than 0.48 estimated from the analytical data on groundwater. This lower value could be due to the precipitation of silica mineral (SiO<sub>2</sub>). The agreement between theoretical and analytical results indicate that Ca, Mg and Si concentrations of groundwater are governed by dissolution and precipitation reactions. In order to interpret groundwater chemistry and estimate residence time of groundwater the simplified coupled dissolution kinetics-fluid flow model was used. Assuming reasonable values of parameters (reactive surface area, mass of groundwater, temperature etc) and using rate constant experimentally determined, residence time of groundwater in southeastern and northern part of Mt. Fuji area was estimated to be several years to 30 years. This estimated residence time is consistent with isotope data (beryllium isotope, tritium concentration and CFCs). The calculation indicates that the reasonable residence time (10-30 years) was obtained, if dissolution rate constant of Si for basaltic glass determined by fluid flow experiments but unreasonable one by closed system experiments. It is just conceivable that whether etch pits formed or not and/or heterogeneous dissolution occurred or not has significant impact on dissolution rate of basalt.

## Dissolved gallium and gallium/aluminum ratios in the US GEOTRACES North Atlantic zonal section

A.M. SHILLER<sup>1\*</sup>, M. HATTA<sup>2</sup> AND C.I. MEASURES<sup>2</sup>

<sup>1</sup>Dept. of Marine Science, Univ. Southern Mississippi, Stennis, MS 39529, USA (\*correspondence: alan.shiller@usm.edu)

<sup>2</sup>Dept. of Oceanography, Univ. Hawaii, Honolulu, HI 96822  
(mhatta@hawaii.edu, chrism@soest.hawaii.edu)

Gallium has a solution chemistry and geochemical behavior similar to aluminum; however, gallium appears to be less reactive than aluminum. Thus, fractionation of gallium from aluminum has the potential to shed light on aluminum input and removal processes with gallium behaving like a "super-heavy isotope" of aluminum. The 2010/2011 US GEOTRACES North Atlantic zonal section provided an opportunity to create a first detailed ocean section of dissolved gallium. Thirty-two profiles plus ancillary surface water samples were obtained and analyzed for dissolved gallium and aluminum.

In general, this new Ga section is consistent with previous observations: deep and bottom waters ranged between 30 and 35 pmol/kg; a distinct Ga minimum is observed in the Antarctic Intermediate Water; a slight maximum is found in Mediterranean Outflow Water; and, surface waters show a distinct north-westward increase. The surface water trend could be reflective of a residence time effect (i.e., accumulation of dust-derived Ga during North Atlantic gyral circulation) or of greater dust dissolution input. The biggest surprise is the observation of a ~20% increase in Ga in deep waters in the vicinity of the Mid-Atlantic Ridge.

The dissolved Ga/Al ratios are also instructive. Low (i.e., more rock-like) ratios in the Med water and hydrothermally-influenced waters are suggestive of recent inputs of these elements. In contrast, high Ga/Al ratios along the African margin are suggestive of preferential Al scavenging removal. Interestingly, high Ga/Al ratios in Labrador Sea Water along the western margin are actually lower than ratios in the Labrador Sea itself, suggesting accumulation of Al during transit. In surface waters of the eastern part of the section, where there is a significant gradient in chlorophyll fluorescence, the Ga/Al ratio increases with increasing fluorescence. This is consistent with preferential scavenging removal of Al from surface waters.

## Spin Transition of Iron in Amorphous Mg-Silicates at Mantle-Related Pressures

S.-H. DAN SHIM<sup>1</sup>, C. GU<sup>2</sup>, K. CATALI<sup>3</sup>,  
B. GROCHOLSKI<sup>4</sup>, L. GAO<sup>5</sup>, E. ALP<sup>5</sup>, P. CHOW<sup>6</sup>,  
Y. XIAO<sup>6</sup>, H. CYNN<sup>3</sup> AND W. J. EVANS<sup>3</sup>

<sup>1</sup>Arizona State University, SHDShim@asu.edu, USA

<sup>2</sup>Massachusetts Institute of Technology, USA

<sup>3</sup>Livermore National Laboratory, USA

<sup>4</sup>Argonne National Laboratory, USA

<sup>5</sup>Smithsonian Institution, USA

<sup>6</sup>Carnegie Institute of Washington, USA

A sharp increase in iron partitioning into melt with respect to mineral phases was reported at 70 GPa in an Al-free system [Nomura *et al.* 2011]. Based on the report, it was proposed that melt may be neutrally or negatively buoyant in the deep mantle. Nomura *et al.* [2011] attributed the iron partitioning change to a sharp high-spin to low-spin change in iron, which was found in their measurements on a Fe-diluted (5%) Mg-silicate glass at a similar pressure. However, Andrault *et al.* [2012] found no sharp change in iron partitioning between silicate melt and minerals in an Al-bearing system up to 120 GPa.

We measured the electronic configuration of iron in two different iron-rich (20%) Mg-silicate glasses at high pressure and 300 K in the diamond-anvil cell combined with X-ray Emission Spectroscopy (XES) and Nuclear Forward Scattering (NFS): Al-free glass up to 135 GPa and Al-bearing glass up to 93 GPa. We found no sharp changes in the spin state of iron up to our maximum pressure. Instead, the population of low-spin iron increases gradually from 1 bar in both glasses, but significant population of iron still remains high spin (40-50%) even at 90-135 GPa. Our observation is consistent with the expectation of gradual response of disordered systems to compression due to the existence of diverse coordination environments for iron in the glasses and continuous structural adjustment of the disordered system with pressure. If our results on Mg-silicate glasses can provide some insights for iron in mantle melts, the spin transition in iron should be gradual and further smeared out at the high temperatures of mantle melts [Sturhahn *et al.*, 2005], and therefore unlikely to induce a sharp change in iron partitioning in the deep mantle.

[1] C. Gu, K. Catalli, B. Grocholski, L. Gao, E. Alp, P. Chow, Y. Xiao, H. Cynn, W. J. Evans, and S.-H. Shim. Electronic structure of iron in magnesium silicate glasses at high pressure. *Geophys. Res. Lett.*, 39:L24304, 2012.

## Volatile element content of the mid-ocean ridge mantle

K. SHIMIZU<sup>1\*</sup>, A.E. SAAL<sup>1</sup>, E.H. HAURI<sup>2</sup>,  
V.S. KAMENETSKY<sup>3</sup> AND R. HÉKINIAN<sup>4</sup>

<sup>1</sup>Dept. of Geological Sciences, Brown University, Providence, RI, 02912, USA

(\*correspondence: Kei\_Shimizu@brown.edu)

<sup>2</sup>DTM Carnegie Institute of Washington, DC, 20015, USA

<sup>3</sup>CODES, University of Tasmania, Hobart, Australia

<sup>4</sup>Keryunan, 29290 Saint Renan, France

Volatile element (H<sub>2</sub>O, CO<sub>2</sub>, F, Cl, S) budget of mid-ocean ridge mantle (DMM) is crucial for understanding mantle melting, rheology, and convection. The isotopic composition of MORB demonstrates that the mantle beneath ridges is heterogeneous. MORB from Garrett transform fault and Macquarie Island defines the depleted and enriched end-members respectively. We have analyzed H<sub>2</sub>O, CO<sub>2</sub>, F, Cl, S contents of Garrett TF and Macquarie Is. MORB to determine the volatile budget of these end-member components.

28 glasses from Garrett TF [1] and 52 glasses from the Macquarie Is. [2] were analyzed for major, trace, and volatile elements by triplicate analyses. Previous works reported the isotopic composition of a subset of our samples from the Garrett TF [3] (minimum <sup>87</sup>Sr/<sup>86</sup>Sr = 0.7022) and the Macquarie Is. [2] (maximum <sup>87</sup>Sr/<sup>86</sup>Sr = 0.7033), which correlates with the degree of trace element enrichment (e.g. Th/La) indicating a long-lived depletion and enrichment of their mantle sources.

We first considered shallow level processes, such as volatile degassing, sulfide saturation and interaction of melt with hydrothermally altered material. Degassing has affected the CO<sub>2</sub> concentration of the glasses except for a few CO<sub>2</sub> undersaturated samples, but it did not affect H<sub>2</sub>O, F, Cl, and S. Samples that were sulfide saturated [4] and contaminated by seawater or hydrothermally altered material (high Cl/K) were filtered out.

The CO<sub>2</sub>/Nb of the depleted MORB determined using the CO<sub>2</sub> undersaturated Garrett TF glasses MORB is 250, consistent with Saal *et al.* [5]. We use Cl-Nb-CO<sub>2</sub> correlations to determine a CO<sub>2</sub>/Nb of ~ 600 for degassed Macquarie Is. MORB, consistent with the work by Cartigny *et al.* [6]. The H<sub>2</sub>O/Ce of the depleted and enriched sources are 120 and 170 respectively. The F/Nd, Cl/K, and S/Dy ratios of our samples expand beyond the range of previous reported values.

[1] Hékinian, R. *et al.* (1992) *EPSL* **108**, 259-275. [2] Kamenetsky, V. S. *et al.* (2000) *J. Petrology* **41**, 411-430. [3] Wendt, J. I. *et al.* (1999) *EPSL* **173**, 271-284. [4] Liu, Y. *et al.* (2007) *GCA* **71**, 1783-1799. [5] Saal, A. E. *et al.* (2002) *Nature* **419**, 451-455. [6] Cartigny, P. *et al.* (2008) *EPSL* **265**, 672-685.



## Electrochemical Impedance Spectroscopic Study of the Hematite/Water Interface

KENICHI SHIMIZU<sup>1\*</sup> AND JEAN-FRANÇOIS BOILY<sup>1</sup>

<sup>1</sup>Department of Chemistry, Umeå University, Sweden,  
\*kenichi.shimizu@chem.umu.se

Hematite is one of the most abundant and stable iron minerals in Earth's upper crust, and thus inevitably plays an important role in various bio-geochemical processes, including mass transport, pollutant migration, and microbial metabolism. This mineral is also a promising material in the search for renewable forms of energy, such as in Li-ion batteries and water splitting. The intrinsic activity of hematite surfaces notably concerns interactions with water and electrolyte ions. Recent cryogenic X-ray photoelectron spectroscopy (XPS) work in our group have addressed such issues by monitoring electrolyte ion loadings and binding mechanisms at nano-sized hematite particle surfaces.[1,2,3]

In an effort to further our understanding of reactions taking place at the hematite/water interface, we used electrochemical impedance spectroscopy (EIS) to extract interfacial properties such as adsorption resistance and electric double layer capacitance using a specially constructed set-up to study surfaces of single body semi-conductive hematite specimens.[4] EIS measurements of crystallographically oriented electrode surfaces contacted with electrolyte solutions (0.1 M NaCl, NaCl/Na<sub>2</sub>CO<sub>3</sub>, and NH<sub>4</sub>Cl) were carried out both in the absence and presence of light in the 4-12 pH range. The resulting spectra were thereafter analyzed using an equivalent electrical circuit model accounting for solution, interface and bulk hematite electrochemical processes. These efforts showed, for instance, that double layer capacitances of the basal (001) plane are insensitive to solution pH and electrolyte type whereas those of the (012) are considerably affected by them. This can be attributed to differences in amphoteric attributes of these two planes. Results revealed that the ammonium ion has a greater influence on charge development than the bicarbonate ion. This finding is consistent with a cryogenic XPS study from our group [3] pointing to hydrogen-bonded interactions between ammonium and hematite surface hydroxo groups.

Photo-irradiation decreased open circuit potentials relative to dark conditions on both (001) and (012) surfaces due to photo-reduction reactions. Impedance spectra show that the (012) is affected more indicating the greater photo-reactivity of this plane. Results also show that the charge transfer resistance within bulk hematite crystal was lower through the (012) plane than on the (001) plane, as can be expected from the anisotropic nature of this mineral.

[1] Shimizu, Shchukarev, Kozin & Boily (2012), *Surf. Sci.* 66, 1005.[2] Shimizu, Shchukarev, Kozin & Boily (2013), *Langmuir* 29, 2623.[3] Shimizu, Shchukarev & Boily (2011), *J. Phys. Chem. C* 115, 6796.[4] Shimizu, Lasia & Boily (2012), *Langmuir*. 28, 7914.

## Volatile behavior in an immature subduction zone inferred from boninitic melt inclusions in Cr-spinel

KENJI SHIMIZU<sup>1,2</sup> AND NOBUMICHI SHIMIZU<sup>2</sup>

<sup>1</sup>Japan Agency for Marine-Earth Science and Technology, Yokosuka, 237-0061, Japan, shimmy@jamstec.go.jp  
<sup>2</sup>Woods Hole Oceanographic Institution, Woods Hole, MA, 02543, United States

Recent studies suggest that boninites formed at the immature stage of subduction zone, whereas related arc tholeiites erupted 0-7 Myrs after boninites at Izu-Bonin-Mariana Arc (e.g. Ishizuka *et al.*, 2011, EPSL), indicating significant changes in conditions of subduction within this period. We have analysed volatile contents and sulfur isotopic compositions of melt inclusions (MIs) in Cr-spinel from beach sands of fore-arc volcanic islands of boninite (Muko, Chichi) and tholeiite (Mukoo and Guam), using secondary ion mass spectrometry (ims-1280). Major element compositions of MIs fully cover compositional ranges of whole-rocks. Some boninitic MIs have MgO higher than 20 wt%, showing that they are very primitive magmas. H<sub>2</sub>O and CO<sub>2</sub> contents of MIs are contrasting between boninites and tholeiites, with boninitic MIs are high (up to 4 wt%) in H<sub>2</sub>O and low (< 50 ppm) in CO<sub>2</sub>, whereas tholeiitic MIs are lower (H<sub>2</sub>O ~1-2 wt%) and higher (CO<sub>2</sub> up to ~1300ppm) than boninitic MIs. Except for H<sub>2</sub>O, volatiles of boninitic MIs (Cl <500ppm; S ~150ppm) are considerably lower than those in tholeiite MIs (Cl and S up to 3000ppm).  $\delta^{34}\text{S}_{\text{VCDT}}$  of boninitic MIs are low (-10 to 0 ‰), whereas those of tholeiite MIs ( $\delta^{34}\text{S}_{\text{VCDT}} = +2$  to +7 ‰) are comparable to reported arc tholeiite data. The results suggest that different sources for S were involved in the formation of boninitic and tholeiitic magmas.

## Buried ikaite precipitates in Antarctic sediments: Are they fossil indicators of microbial sulfate reduction or AOM?

MEGUMI SHIMIZU<sup>1\*</sup>, MARCOS Y. YOSHINAGA<sup>2</sup>,  
KAI-UWE HINRICHS<sup>2</sup> AND CINDY VAN DOVER<sup>1</sup>

<sup>1</sup>Duke University Marine Laboratory, Nicholas School of Environment, Duke University, Beaufort, NC, USA  
(\*correspondence: megumi.shimizu@duke.edu)

<sup>2</sup>MARUM Center for Marine Environmental Sciences, University of Bremen, 28334 Bremen, Germany

Ikaite is a calcium carbonate hexahydrate ( $\text{CaCO}_3 \cdot 6\text{H}_2\text{O}$ ) formed at low temperature and high concentration of dissolved inorganic carbon (DIC) in organic-rich sediments [1]. Two microbial processes, bacterial sulfate reduction of organic matter and anaerobic methane oxidation (AOM) by archaeal/bacterial consortia can trigger ikaite precipitation by increasing DIC concentration. To determine which of these processes may contribute to ikaite formation, we studied a 500-cm sediment core from the northern Antarctic Peninsula that contained 4 large ikaite crystals ( $\sim 50 \text{ cm}^3$  each) at depths > 300 cm. Apolar (fossil) lipids were extracted from six sediment horizons: at the surface, within the modern sulfate-methane transition zone (85 cm), and the four horizons where ikaite was found (304, 454, 480 and 505 cm). Stable carbon isotopic compositions of bacterial fatty acids (FA), and archaeal biphytanes (BP), archaeol (AR), and hydroxy-archaeol (OH-AR) were analyzed.  $\delta^{13}\text{C}$  values of FA and BP ranged from -30‰ to -20‰ (ave =  $-23 \pm 2.3$  ‰) from the six sample horizons. AR and OH-AR was extracted from the same horizons, but isotope values were only measurable at the 454 and 500-cm horizons due to low concentrations. In these two horizons, AR was depleted in  $^{13}\text{C}$  (ave = -49‰) as well as OH-AR (ave = -87‰). The  $^{13}\text{C}$ -enriched values of  $\text{C}_{15-18}$  FA (bacterial markers for AOM) and of BP (archaeal marker for AOM) suggest they are not derived from AOM because lipids derived from AOM are significantly depleted (-110‰ to -60‰) [2,3]. Although the  $^{13}\text{C}$ -depleted AR and OH-AR can from AOM related Archea, they could be also from methanogenic Archaea [4].  $\delta^{13}\text{C}$  in ikaite, DIC and methane will provide a scope on ancient carbon flow and help to reveal ancient microbial activities contributed kaite formaiton.

[1] Suess (1982) *Science* **216**, 1128-1131. [2] Elvert (2003) *Geomicrobiology Journal* **20**, 403-419. [3] Hinrichs (1999) *Nature* **398**, 802-805. [4] Londry (2008) *Organic Geochemistry* **39**, 608-621.

## Boron and sulfur isotopic variations during subduction of hydrated lithosphere: The Erro Tobbio case

N. SHIMIZU<sup>1</sup>, M. SCAMBELLURI<sup>2</sup>, D. SANTIAGO RAMOS<sup>3</sup>  
AND S. TONARINI<sup>4</sup>

<sup>1</sup>Woods Hole Oceanographic Inst., Woods Hole, MA, USA

<sup>2</sup>University of Genova, Genova, Italy

<sup>3</sup>Amherst College, Amherst, MA, USA

<sup>4</sup>Istituto Geosci. Geores-CNR, Pisa, Italy

Exhumed high-pressure serpentinites provide unique opportunities for advancing our understanding of geochemical changes in hydrated lithosphere during subduction and deep recycling of elements. The Erro Tobbio serpentinitized peridotites represent Jurassic oceanic lithosphere which underwent low-T hydration ( $T < 300^\circ\text{C}$ ) followed by high-T serpentinitization and recrystallization at  $\sim 550^\circ\text{C}$ , 2 – 2.5 GPa during Alpine subduction. Covariations observed for whole-rock  $\delta\text{D}$ ,  $\delta^{18}\text{O}$ , Sr, and  $\text{H}_2\text{O}$  indicate that hydration continued at high temperatures, placing the Erro Tobbio massif in the mantle wedge. During hydration whole-rock boron concentrations varied from 10 to 32 ppm with  $\delta^{11}\text{B}$  from +3.8 to +23‰ for low-T serpentinites, and from 12 to 36 ppm with  $\delta^{11}\text{B}$  from +17 to +24‰ for high-T rocks. In-situ analysis of sulfur isotopic composition of individual sulfide grains (pentlandite with minor heazlewoodite) has revealed that  $\delta^{34}\text{S}$  varies from -2.5 to +4‰ for low-T rocks, consistent with whole-rock data (Alt *et al.*, 2012), while high-T rocks display a much larger range in  $\delta^{34}\text{S}$  from -2 to +18‰ with significant increases in modal sulphide. B isotopes, S isotopes, and other geochemical variations observed for the Erro Tobbio peridotites suggest that hydration and mass transfer from slab to wedge occurred at relatively shallow level, resulting in the formation of hydrated mantle wedge with high  $\delta^{11}\text{B}$ , high  $\delta^{34}\text{S}$ , enrichment in B, Sr, and other fluid-mobile elements, suitable for the sources for arc magmas and heterogeneous sources for MORB and OIB.

## FOZO-HIMU connection: Link to chemical heterogeneity of MORB and variable degree of dehydration

G. SHIMODA\*<sup>1</sup> AND T. KOGISO<sup>2</sup>

<sup>1</sup> Geological Survey of Japan, National Institute of Advanced Industrial Science and Technology, Tsukuba 305-8567, Japan (\*correspondence: h-shimoda@aist.go.jp)

<sup>2</sup> Graduate School of Human and Environmental Studies, Kyoto University, Kyoto, 606-8501, Japan (kogiso@gaia.h.kyoto-u.ac.jp)

It has been considered that source materials of HIMU and FOZO could be recycled oceanic crust. From this perspective, the arising question is what process is responsible for the geochemical difference between HIMU and FOZO. Additionally, coupled production of low Rb/Sr and high U/Pb and Th/Pb ratios of HIMU and FOZO has been controversial. To solve the issue, many studies have been conducted to evaluate the origin of the HIMU source using hydrothermal alteration and/or dehydration reaction. These studies can successfully explain the origin of HIMU and FOZO source. However, they may neglect effect of global chemical trend of MORB composition that should result in variation in isotopic composition of recycled MORB. In addition, variation in condition of subduction process (e.g., amount of dehydrated fluid) should greatly affect the isotopic composition of recycled oceanic crust.

In the present study, geochemical modeling has been conducted to evaluate the origin of HIMU and FOZO reservoirs on the basis of global chemical trend of MORB and variation in subduction processes. For the modeling, MORB compositions from East Pacific rise and Mid-Atlantic ridge are compiled from published data (PetDB: <http://www.earthchem.org/petdb>). The results suggest that crystal fractionation at a mid-ocean ridge can increase U and Th concentrations relative to Pb content, producing high U/Pb and Th/Pb ratios in evolved MORBs. In addition, high degree of dehydration beneath a subduction zone can increase U/Pb and Th/Pb ratios of subducting oceanic crust compared to less dehydrated oceanic crust, suggesting that strongly dehydrated oceanic crust can be a suitable source for HIMU and less dehydrated MORBs can produce material with FOZO isotopic signature. In this context, magma evolution at mid-ocean ridges and variable degree of dehydration beneath subduction zones play an essential role in producing the isotopic variations between HIMU and FOZO.

## Occurrence of >3.9 Ga “Nanok” gneiss from Saglek Block, northern Labrador, Canada

M. SHIMOJO<sup>1\*</sup>, S. YAMAMOTO<sup>1</sup>, S. AOKI<sup>1</sup>, S. SAKATA<sup>2</sup>, K. MAKI<sup>2</sup>, K. KOSHIDA<sup>1</sup>, A. ISHIKAWA<sup>1</sup>, T. HIRATA<sup>2</sup>, K.D. COLLERSON<sup>3</sup> AND T. KOMIYA<sup>1</sup>

<sup>1</sup>Department of Earth Science and Astronomy, The University of Tokyo, Komaba, Meguro, Tokyo, 153-8902, Japan

(\*correspondence: shimojo@ea.c.u-tokyo.ac.jp)

<sup>2</sup>Laboratory for Planetary Sciences, Kyoto University, Japan

<sup>3</sup>The University of Queensland, Brisbane Qld 4072, Australia

The Saglek Block is underlain by the Early to Late Archean suites including ca. 3.73 Ga Uivak I Gneiss, ca. 3.62 Ga Uivak II Gneiss, ca. 3.24 Ga Lister Gneiss and ca. 2.5 Ga granite [e.g. 1]. Those rocks underwent high-grade metamorphism, locally reaching granulite facies at 2.8-2.7 Ga [1]. Additionally, presence of over 3.8 Ga, up to 3.91 Ga, zircon cores in the Uivak I Gneiss suggested pre-Uivak I Gneiss rocks [1, 2], named as Nanok Gneiss [2]. However, the origin of the old zircon cores is still unclear: inherited from pre-Uivak I materials or precipitated from an older suite of the Uivak I felsic magma. Thus, we examined the internal structures of zircons using cathodoluminescence (CL) images and conducted laser-ablation ICP-MS U-Pb dating.

The result of the 11 orthogneiss samples from the south of St. John's Harbor is the following. The CL images or microscopic observations clearly display that most of the zircon grains comprise three domains: Zone I to III, respectively. Zone I is located in their central regions, and display clear oscillatory zoning. It is characterized by low U contents and high Th/U ratios. The Zone II lacks obvious oscillatory zoning, and is very dark. It is characterized by high U contents and low Th/U ratio, compared with Zone I. Zone III is a very thin layer in the outermost part of grains or does not exist. The U-Pb ages of Zone I and II shows a peak at 3.96-3.85 Ga and around 2.7 Ga, respectively. Those ages are well-correlated with observations of CL images, U contents and Th/U ratios. The age of the Zone II is in agreement with metamorphic age of previous study. Hence, the age of Zone I can be interpreted lower limit of the magmatic age of the protoliths of the orthogneisses, older than the conventional age of the Uivak Gneiss [1]. We concluded that the granitoid, the precursor of the Nanok Gneiss, were emplaced at 3.96 Ga in the Saglek block, Labrador.

[1] Schiøtte *et al.* (1989) *Can. J. Earth Sci.* **26**, 1533-1556. [2] Collerson (1983) *Lunar planet. Inst. Tech. Rep.* **83-03**, 28-33.

## Determination of Boron using Isotope dilution MC-ICP-MS

HYUNG SEON SHIN\* , MIN SEOK CHOI, JONG-SIK RYU  
AND KWAN SOO HONG

Korea Basic Science Institute, Chungbuk, Korea  
(\*correspondence: h2shin@kbsi.re.kr)

A new technology applying to the isotope dilution method was used to estimate the amount of B (boron) in geological samples and was determined to be a viable method to minimize naturally occurring B background signals. The B ratios in geological sample (SDC-1 and SGR-1) were measured using a double-focusing multiple collector inductively coupled plasma mass spectrometer (Neptune). High naturally occurring B background signals and  $^{40}\text{Ar}^{+4}$  interference were improved using a low RF power technique. A  $\text{H}_3\text{PO}_4$  in mixed acid ( $\text{HNO}_3 + \text{HF}$ ) was used to reduce the loss of B form ( $\text{BF}_3$ ) in the sample dissolution process.

Boron isotopes were measured using a multi-collector, inductively coupled plasma mass spectrometer (Neptune, Thermo-Finnigan, Bremen, Germany). The present study determined an alternative method to minimize B isotope background signals. The B background signal was improved using a low RF power technique. The 800 W setting represents an excellent compromise between lower interference and the reduced matrix effect experienced at 1200 W. The results at 800 W (SGR:  $55.246 \pm 0.003$  and SDC:  $13.273 \pm 0.003$  mg g<sup>-1</sup>) were equivalent to the reference values (SGR:  $54 \pm 3$  and SDC: 13 mg g<sup>-1</sup>). However, the values obtained using 1200 W (SGR:  $48.600 \pm 0.001$  and SDC:  $11.127 \pm 0.004$  mg g<sup>-1</sup>) were slightly lower than the 800 W values. Furthermore, the addition of  $\text{H}_3\text{PO}_4$  prevented the loss of boron within the sample dissolution process. The SDC-1 and SGR-1 results obtained by the isotope dilution method were within the range of the reference values. Overall, the high performance of our proposed analytical technique (decreased B background signal under low RF power,  $\text{H}_3\text{PO}_4$ , isotope dilution method and MC-ICP-MS) makes it suitable for use in the determination of B in geological samples

1. J. K. Aggarwal, D. Sheppard, K. Mezger and E. Pernicka, *Chem. Geol.*, 2003, **199**, 331-342. 2. L. Zhao, Q. Chen, C. Li and G. Shi, *Sol. Energy Mater. Sol. Cells*, 2007, **91**, 1811-1815. 3. T. Fujisakia, A. Yamadab and M. Konagai, *Sol. Energy Mater. Sol. Cells*, 2002, **74**, 331-337. 4. M. Betti, *Int. J. Mass Spectrom.*, 2005, **242**, 169-182.

## Boron and other trace element constraints on the slab-derived component in Miocene volcanic rocks from the Setouchi Volcanic Belt in SW Japan

HIRONAO SHINJOE<sup>1</sup>, YUJI ORIHASHI<sup>2</sup>  
AND TOMOAKI SUMII<sup>3</sup>

<sup>1</sup>Tokyo Keizai University, Tokyo, JAPAN (\*correspondence: shinjoe@tku.ac.jp)

<sup>2</sup>Earthquake Reserch Instutiute, Univ. of Tokyo, Tokyo, JAPAN

<sup>3</sup>Geological Surv. Japan, AIST, Tsukuba, JAPAN

We present a dataset for boron and other trace element contents for basalts and high-Mg andesites (HMA) obtained from the middle Miocene Setouchi Volcanic Belt (SVB) in SW Japan. SVB was formed along the SW Japan Arc, immediately after the opening of the Japan Sea and clockwise rotation of SW Japan with the subduction of young hence hot Shikoku Basin of the Philippine Sea plate. Previous studies on HMA and basalt of SVB, laid stress on the contribution of subducting sediment, particularly partial melt of terrigenous sediments to the magma source mainly based on their Sr, Nd, Pb isotopic compositions.

Analyzed samples show a large negative Nb and Ta anomalies, and enrichment of alkaline earth elements and Pb, which are features of typical island arc volcanic rocks. Boron content of basalts and HMA is highly variable (7 – 71 ppm).

Trace element compositions of altered oceanic crust-derived fluid, sediment-derived fluid, and sediment melt are modeled, and resultant fluid mobile/immobile element ratios (B/Nb, Ba/Nb, Pb/Nb, and K/Nb) are used to examine slab-derived component to mantle source. Most of element ratios are explained by <5% contamination of sediment melt to depleted mantle except for some HMAs with rather high B/Na ratios. Mantle source for these HMAs may be enriched with some trace elements including boron before the addition of slab-derived melt.

## Mechanism and crystallochemical signature of nano-particle formation by microorganisms

H. SHIOTSU<sup>1</sup>, M. JIANG<sup>1</sup>, Y. NAKAMATSU<sup>1</sup>, T. OHNUKI<sup>2</sup>  
AND S. UTSUNOMIYA<sup>1</sup>

<sup>1</sup>Department of Chemistry, Kyushu University, Fukuoka 812-8581, Japan (utsunomiya.satoshi.998@m.kyushu-u.ac.jp)

<sup>2</sup>ASRC, Japan Atomic Energy Agency, Tokai, Ibaraki, Japan

Interaction between rare earth elements (REEs) and microorganisms have attracted increasing attention due to the ubiquitous occurrence of microorganisms in the subsurface environment and to implication to the safety assessment of nuclear waste disposal, as REEs are used as a surrogate of trivalent actinides. Post-adsorption nano-mineralization by microorganisms is a key process that can constrain the migration of REEs; however, the mechanisms and factors controlling the process are still unclear. This study demonstrates the REEs (La-Lu) accumulation experiments to understand the effect of pH, coexistent REEs and the functional group of cells surfaces on the crystal chemistry of biogenic nanoparticle formation.

During the exposure of yeast to REE solution at 25 °C, all REEs were removed from the solution by 24 h at pH 4 and 5, while 50 % of the initial amount remained in the solution at pH 3 after 24 h. Deprotonation of the functional groups on the cell surface merely occurs at pH 3 as evidenced by the other experiments at 4 °C. In contrast, 10 % of REEs were adsorbed to the cell surfaces at pH 4 and 5. Particles at the size of ~100 nm precipitated on the cell surfaces at pH 3, while ~30 nm-sized nano-particles were observed at pH 4 and 5 at 25 °C. These nano-particles were characterized as phosphate containing a series of REEs. The nano-particles at pH 3 had monazite structure, while the particles forming at pH 4 and 5 were amorphous, indicating that crystallization took place only at pH 3. REE phosphate inorganically synthesized at room temperature revealed crystalline structure (monazite, xenotime or rhabdophane) depending on the element. Additional inorganic model experiments using the CMC, Ln resin and Cellulose Phosphate, which have the functional groups similar to cell surfaces, demonstrated that the nano-particles precipitated without structure. Based on these data it is suggested that adsorption to the functional groups on the cell surfaces constrain the shape and structure of nanoparticles.

As for the REE pattern, the difference between the distribution coefficient,  $K_d$  (ml/g), of LREE and of HREE increased with time increasing. At 24 h, the  $K_d$  ratio of Nd to Tm ( $K_{d, Nd}/K_{d, Tm}$ ) is 1.72, 4.61, and 6.86 at pH 3, 4, and 5, respectively. The  $K_d$  ratios greater than 1 indicate the preferential uptake of LREE by the microorganisms, which are attributed to the lower solubility products of REE phosphate. As a consequence, the present study underscores the important role of cell surfaces and biological activity on the kinetics, mechanisms and crystal chemistry of nanoparticle formation as well as the physico-chemical properties of nanoparticles.

## Sub-daily elemental fluctuation in mussel shell

KOTARO SHIRAI<sup>1\*</sup>, TSUZUMI MIYAJI<sup>2</sup>, BERND R. SCHÖNE<sup>3</sup> AND KAZUSHIGE TANABE<sup>4</sup>

<sup>1</sup>Atmosphere and Ocean Research Institute, The University of Tokyo, Kashiwa 277-8564 Japan (\* correspondence: kshirai@aori.u-tokyo.ac.jp)

<sup>2</sup>Department of Natural History of Science, Hokkaido University, Sapporo 060-0810 Japan

<sup>3</sup>Institute of Geoscience, University of Mainz 55128 Mainz Germany

<sup>4</sup>The University Museum, The University of Tokyo, Tokyo 133-0033 Japan

Shells of bivalve mollusks such as mytiloids serve as excellent paleoenvironmental archives. They exhibit a broad biogeographic distribution, occur in large numbers in the fossil record and contain a temporally aligned and highly resolved record of past environmental parameters. For example, Mg/Ca ratios of mussel shells have been explored as a temperature proxy. According to several studies, however, the suitability of the Mg/Ca thermometer is limited by vital effects. In order to extract reliable environmental information from the shell through geochemical analyses it is essential to understand the mechanism of elemental incorporation into the shell during calcification and growth.

In the present study, we have analyzed Mg/Ca Sr/Ca and S/Ca ratios of two shells of the Mediterranean mussel *Mytilus galloprovincialis* collected alive from Tokyo Bay, Japan. Environmental parameters were monitored at the sampling site. The elemental distribution was determined in polished cross-sections by means of electron probe micro analysis. Growth patterns were used to place the geochemical data in a temporal context.

Growth lines (which formed during low tide) showed higher Mg/Ca ratios compared to adjacent growth increments. S/Ca ratios were also high at the growth line. However, the Mg/Ca and S/Ca do not show linear correlation. Both Mg/Ca and S/Ca ratios showed significant periodic fluctuations at the sub-seasonal scale. These fluctuations likely indicate that the shell Mg/Ca ratios primarily reflect biological changes caused by tidal cycle and do not record temperature.

## Composition of serpentine after olivine and orthopyroxene: Serpentinized peridotites of Nain ophiolite (Isfahan Province, Iran)

N. SHIRDASHTZADEH<sup>1</sup>, G. TORABI<sup>1</sup> AND R. SAMADI<sup>2</sup>

<sup>1</sup>Department of Geology, Faculty of Science, University of Isfahan, Isfahan, Iran

<sup>2</sup>Department of Geology, Science and Research Branch, Islamic Azad University, Tehran, Iran

### Introduction

The Nain ophiolite is one of the most complete ophiolitic suits at the East of Central-East Iranian Microcontinent - ophiolitic belt and it comprises a high proportion of serpentinized mantle peridotites [1]. As a possible alteration product of Nain mantle peridotites, serpentine constructed the veinlets and the mesh texture, characterized with a pale green-white chalky feature. The fibrous serpentine filled the cracks and veinlets are crossing the mesh texture and this indicates their former formation.

### Raman Spectrometry and Microprobe Data

Raman Spectrometry of the serpentine suggests that the mesh texture is made of lizardite and the rock veinlets are filled by chrysotile. Based on major element data, lizardite is  $Mg_{3.00}Fe_{0.31}Ni_{0.01}Si_{1.84}$ , with  $Al_2O_3 = 0.00$  wt%,  $Mg\# = 0.91$ ,  $Cr\# = 0.00$  in composition and chrysotile is  $Mg_{2.14}Fe_{0.10}Al_{0.23}Cr_{0.02}Si_{2.18}$ , with  $Al_2O_3 = 2.84-5.97$  wt%,  $Mg\# = 0.96$ ,  $Cr\# = 0.10$ .

### Discussion of Results

Lizardite is characterized with higher Mg, Fe and Ni in while chrysotile is higher in  $Al_2O_3$  and Cr#. [2] suggested that serpentine after orthopyroxene (bastite) are generally low in MgO (~ 34–37 wt%), but have silica similar to serpentine after olivine (38–42 wt%). MgO of the studied chrysotile (~ 30–32 wt%), formed after orthopyroxene are generally higher than MgO of lizardite (~ 29 wt%), formed after olivine (i.e. lizardite), but the silica has a similar range (~ 43–54 wt%) in chrysotile and lizardite. The low Mg and high Cr and Al of chrysotile is a consequence of the composition of the original orthopyroxene (e.g., [3]; [4], [2]). Therefore, Al-rich serpentine of chrysotile is found in orthopyroxene bastite with lower MgO and FeO contents, and higher  $Al_2O_3$  and  $Cr_2O_3$  concentrations, while the lizardite is the serpentinization product of olivine.

[1] Shirdashtzadeh *et al.* (2013) *Lithos* (Submitted). [2] Shervais *et al.* (2005) *Inter Geol Rev* **47**, 1-23. [3] Dungan (1979) *Can Min* **17**, 771-784. [4] Wicks & Plant (1979) *Can Min* **17**, 785-830.

## Water content of inclusions in superdeep diamonds

S.B. SHIREY<sup>1</sup>, E.H. HAURI<sup>1</sup>, A.R. THOMSON<sup>2</sup>, G.P. BULANOVA<sup>2</sup>, C.B. SMITH<sup>2</sup>, S.C. KOHN<sup>2</sup> AND M.J. WALTER<sup>2</sup>

<sup>1</sup>DTM, Carnegie Institution of Washington, Washington DC 20015, USA (shirey@dtm.ciw.edu, hauri@dtm.ciw.edu)

<sup>2</sup>Dept Earth Sciences, University of Bristol, Queen's Road, Bristol BS8 1RJ, UK (andrew.thomson@bristol.ac.uk)

The water content of the mantle strongly influences mantle convection and partial melting. Previously, direct measurements of mantle water content have been limited to peridotites or inferred from basalts. Superdeep or sublithospheric diamonds from the transition zone and lower mantle carry ultra-high pressure silicate and oxide micro-inclusions that provide an unparalleled opportunity to directly sample the composition, mineralogy and water content of deep mantle minerals.

We measured mineral inclusions in Type II (<20 ppm N) diamonds from the 93 Myr old Collier 4 kimberlite pipe in the Juina field of Brazil for their water content with the DTM NanoSIMS 50L. Studies of these diamonds showed complex growth structures, diverse inclusion assemblages, and heterogeneous C isotopic compositions (-5‰ to -25‰) interpreted as being due to subducted components entrained in the Trinidade plume [1]. Simultaneous scanning ion imaging of <sup>12</sup>C, <sup>16</sup>O<sup>1</sup>H, <sup>18</sup>O, <sup>19</sup>F, <sup>30</sup>Si and <sup>56</sup>Fe was employed and data reduced using the *L'image* (© LR Nittler, DTM) image-processing software. H<sub>2</sub>O contents vary from nominally-anhydrous phases such as majorite (30 ppm, J9), walstromite after CaSi-perovskite (74 ppm, J14), and Mg-Al spinel (245 ppm, J2) to more water-rich phases such as Mg-pyroxene (former MgSi-perovskite, 2600 ppm, J2), Fo<sub>91</sub> olivine (2300 ppm, J20) and K-feldspar (7800 ppm, J2). Mg-silicate phases along an internal fracture (J9) have 2.3 to 3.8 wt% H<sub>2</sub>O and may be epigenetic or compromised.

Inferences on the mineralogy and H<sub>2</sub>O contents of the inclusions at the time of trapping depend on identification of retrograde phases, final retrograde pressure, and H<sub>2</sub>O storage capacity of the retrograde mineral assemblages. Correspondence of lowest measured water with the most anhydrous phases suggests some retention of original water content, however. Forsteritic olivine with 2300 ppm H<sub>2</sub>O, and aluminous Mg-pyroxene with 2600 ppm H<sub>2</sub>O, are consistent with H<sub>2</sub>O saturation at pressures ≥ 7 GPa [2] and represent lower limits on the original H<sub>2</sub>O content of these inclusions if their trapping depths were greater than 200 km.

[1] Bulanova *et al.* (2010) *Cont. Min. Petrol.* 160 489-510. [2] Hauri *et al.* (2006) *Earth Planet. Sci. Lett.* 248, 715-734.

## Simultaneous mantle metasomatism, diamond growth and crustal events in the Archean and Proterozoic of South Africa

Q. SHU<sup>1,2\*</sup>, G.P. BREY<sup>1</sup>, A. GERDES<sup>1</sup> AND H. E. HOEFER<sup>1</sup>

<sup>1</sup>Institut für Geowissenschaften, Goethe-Universität, Altenhöferallee 1, D-60438 Frankfurt, Germany; <sup>2</sup>China University of Geosciences (Beijing), Xueyuan Road 29, Haidian, Beijing, China. 100083; \*shu@em.uni-frankfurt.de

Subcalcic garnets from harzburgites are proxies of the chemical and isotope composition of their bulk rock. The present study and previous work [1,2] on the Sm-Nd and Lu-Hf isotope systematics show that they can be excellent recorders of multiple mantle events. Subcalcic garnets with sinusoidal REE patterns are the results of high degrees of partial melting of their protolith at shallow pressures followed by subduction and re-enrichment by (silico-)carbonatitic melts. Metasomatism in a previously depleted mantle ( $\epsilon_{\text{Hf}} = +16$ ) occurred underneath the crust the East Kaapvaal craton at around 3.2 Ga. Simultaneously, the crust was affected by widespread activity around that time and Sm-Nd model dates of similar age from pooled peridotitic garnet inclusions in diamonds were interpreted as oldest diamond growth ages. Oceanic lithosphere was created between the West- and East-Kaapvaal around 2.95 Ga [2] and subducted underneath the West-block before the collision around 2.88 Ga. This also caused enrichment process in an overlying, highly depleted mantle wedge 2.9 Ga ago [2] and apparently triggered a major growth period of diamonds as demonstrated by similar Re-Os ages from sulfide inclusions in diamonds from Kimberley and Botswana. Further enrichment in the West-Kaapvaal mantle at 2.62 Ga [1] coincides with the 2.6-2.8 Ga Ventersdoorp magmatism and with a 2.6 Ga Re-Os isochron from E-type sulfide inclusions from Koffiefontein. The attachment of the Kheis-Magondi belt to the Kaapvaal craton caused further metasomatism around 1.90 Ga [2] in the mantle along the Western margin of the Kaapvaal craton. The latest stages of mantle metasomatism lie between 0.9-1.3 Ga, coincident with the Namaqua-Natal belt orogeny. Periods of diamond growth younger than 2.6 Ga cannot be related directly to any mantle or crustal event. Major geotectonic events and plume activity episodically remobilized low melting portions in the mantle keel which lead to episodic (auto) metasomatism of the depleted mantle, episodic diamond growth and destruction of the lithospheric keel.

[1] Lazarov *et al.*, 2009, Earth Planet. Sci. Lett. **27**, 1–10.

[2] Shu *et al.*, 2013, Geochim. Cosmochim. Acta, in press

## The differentiation mechanism of W and Sn of Qitianling granite in Hunan province, south China

SHUANG YAN<sup>1,2</sup> AND XIANG XIAOJUN<sup>1,2</sup>

<sup>1</sup>Chongqing Key Laboratory of Exogenic Mineralization and Mine Environment, Chongqing Institute of Geology and Mineral Resources, Chongqing 400042, China;

<sup>2</sup>Chongqing Research Center of State Key Laboratory of Coal Resources and Safe Mining, Chongqing 400042, China  
E-Mail: shy810124@yahoo.com

Both large-scale tungsten and tin mineralization took place mostly in Nanling Mountains, South China. The two elements are usually related and accompanied with granitic rocks. Hua *et al* (2010) proposed that the eastern sector of the Nanling Mountains is characterized by strong and dense W mineralization, while Sn mineralization becomes stronger westwards. This study attempts to discuss reasons that cause the two elements differentiation, in the light of the study on the fluid inclusions of Furong Sn deposit and Xintianling W deposit, of which both have genetic relations to the Qitianling granitic rocks in Nanling Mountains, South China.

According to the study on the fluid inclusions of the two deposits, aqueous two-phase inclusions and daughter mineral-bearing inclusions are found in Furong Sn deposit, located in the south of Qitianling granites. The ore forming fluids have the composition of CaCl<sub>2</sub>-NaCl-H<sub>2</sub>O system with high salinity (36.99-42.45 wt% NaCl eq.) and temperature (462-494°C). While in the Xintianling W deposit, the CO<sub>2</sub>-riched inclusion has been observed as the major inclusion. The ore forming fluids are characterised with low salinity (below 6%) and high temperature (367-392°C). The first melt temperatures of CO<sub>2</sub> range between -66.6~61.1°C.

These findings suggest that CO<sub>2</sub>-enriched hydrothermal fluid differentiated from the Qitianling granites is conducive to the separation of W from the granitic magma system. In the later evolutionary tertiary of the magma, the hydrothermal fluid is characterized with high level of Cl<sup>-</sup>, which favor Sn enrichment in the ore-forming fluids. Accordingly, the difference of the ore-forming fluids of the two deposit maybe is the major factors responsible for the differentiation of W and Sn.

This research project was financially supported by the National Natural Science Foundation of China (41003024) and the Open Foundation of the State Key Laboratory of Ore Deposit Geochemistry (201103)

## Studies of nuclear waste form glasses with synchrotron radiation

D.K. SHUH<sup>1\*</sup>, W.W. LUKENS<sup>1</sup>, J.P. ICENHOWER<sup>1</sup>,  
J.G. DARAB<sup>2</sup>, T. TYLISZCZAK<sup>1</sup>, H. BLUHM<sup>1</sup>,  
D. A. MCKEOWN, A. C. BUECHELE, I.S. MULLER  
AND I.L. PEGG

<sup>1</sup>Lawrence Berkeley National Laboratory (LBNL), Berkeley, CA 94720, USA (\*correspondence: DKShuh@lbl.gov; WWLukens@lbl.gov, JPicenhower@lbl.gov, Tolek@lbl.gov, HBlum@lbl.gov)

<sup>2</sup>J.G. Darab, MEL Chemicals Inc., NJ 08822 USA (JDarab@MEIchem.com)

<sup>3</sup>Catholic University of America, Washington, D.C. 20064, USA (davidm@vsl.cua.edu, andrewb@vsl.cua.edu, isabellem@vsl.cua.edu, ianp@vsl.cua.edu)

The speciation of several radionuclide and surrogate metal ions in specific formulations of nuclear waste form glasses has been investigated by synchrotron radiation methods. The primary technique to determine the oxidation state and structural information, and chemical behavior in many of these studies has been hard x-ray absorption fine structure (XAFS) [1]. There has been considerable effort utilizing XAFS to understand the conditions under which surrogates, in large part Re for Tc but also including specific metal ions such as Ce and Hf for Pu, are suitable chemical and structural analogs for the actual radionuclides of interest. Similar approaches have been utilized to validate the reliability of surrogates in glass waste form characteristics under processing and alteration conditions [2].

Recently, studies of glass waste form materials have been initiated using new soft synchrotron radiation tools that include the scanning transmission x-ray microscope (STXM) and ambient pressure x-ray photoelectron spectroscopy (APPES) endstations at the Molecular Environmental Sciences Beamline of the Advanced Light Source at LBNL [3]. Spectromicroscopy studies have been conducted using soft x-ray absorption spectroscopy of light atom constituents and metal ions in glasses with STXM, investigating the early stages of the interaction of water with glass surfaces with PES under more realistic conditions of approximately 10 Torr. New opportunities to address critical issues in nuclear waste form glass science with emerging synchrotron radiation methods will be presented and discussed.

[1] Booth *et al.* (1999) *J. Mater. Res.* **14**, 2628-2639.

[2] McKeown, *et al.* (2012) *J. Nucl. Mater.* **429**, 159-165.

[3] Bluhm *et al.* (2006) *J. Electron Spectros. Rel. Phenom.* **150**, 86-104.

## A novel <sup>190</sup>Pt-<sup>4</sup>He method of isotope geochronology for the direct dating of native minerals of platinum

YURIY A. SHUKOLYUKOV<sup>1,2,\*</sup>, OLGA V. YAKUBOVICH<sup>1,2,\*\*</sup>, ALEXANDER G. MOCHALOV<sup>1</sup>  
AND ALEXANDER B. KOTOV<sup>1</sup>

<sup>1</sup>IPGG RAS, Makarova 2, 199034, Saint-Petersburg, Russia (\*\* correspondence: olya.v.yakubovich@gmail.com)

<sup>2</sup>Saint-Petersburg State University, Universitetskay 7/9, 199034, Saint-Petersburg, Russia

\*deceased

Retention of radiogenic <sup>4</sup>He in crystals of most minerals is very low. Helium can escape easily from minerals in a course of their geological history. However, in a group of minerals, namely native metals, the retention of radiogenic helium is anomalously high [1]. Very low solubility of helium in metals leads to formation of atomic clusters of helium atoms, which manifest themselves as nanometer-scale bubbles. Migration of such "bubbles" in the crystal structure requires relatively high temperature close to the metal melting temperature.

The tendency of helium to form stable bubbles in native metals allows to propose a novel method in isotope geochronology for the direct dating of native minerals of platinum that is based on the  $\alpha$ -decay of <sup>190</sup>Pt isotope [2].

We present nuclear-physical, isotope-geochemical and methodological aspects of the novel <sup>190</sup>Pt-<sup>4</sup>He method. We validate the method on a set of new experimental <sup>190</sup>Pt-<sup>4</sup>He dating measurements of four platinum deposits: (i) the Galmoenan massif, a gabbro-dunite-pyroxenite massif in the Koryak Highlands, Russia; the alkaline-ultramafic massifs of (ii) Kondyor, (iii) Inagli and (iv) Chad in the Aldanian shield, Russia. Our experimental measurements confirm the successful applicability of <sup>190</sup>Pt-<sup>4</sup>He for the direct dating of the native minerals of platinum.

[1] Shukolyukov (2012) *Petrology*, **20.1.**, 1-20 [2] Shukolyukov (2012) *Petrology*, **20.6.**, 491-505



## Microbial production and transformation of dissolved organic matter in the hydrothermal system

N.A. SHULGA<sup>1</sup>, V.I. PERESYPKIN<sup>1</sup> AND I.I. RUSANOV<sup>2</sup>

<sup>1</sup>P.P. Shirshov Institute of Oceanology of the RAS,  
Nahimovski prospect 36, Moscow, Russia, 117997,  
(nash.ocean@gmail.com)

<sup>2</sup>Winogradsky Institute of Microbiology RAS, Prospekt 60-  
letiya Oktyabrya 7, 117312, Moscow, Russia  
(rusanov\_igor@mail.ru)

This study was inspired by the lack of information on the microbial production of dissolved organic matter in course of chemosynthesis and methane oxidation at hydrothermal fields: most of studies didn't take into account the production of dissolved organic matter (DOM), considering only formed and consumed microbial biomass in the processes of microbial transformation of endogenous gases coming from hydrothermal solutions.

It is well known that the formation of organic compounds in the zones of hydrothermal activity proceeds under the influence of a number of physicochemical and biogeochemical (extremophile consortiums of bacteria and archaea) factors. We present i) radioisotope measurements of the activity of microbial communities in the hydrothermal fields of the Mid-Atlantic Ridge (MAR) and the East Pacific Rise (EPR), ii) investigation of the rates of microbial CO<sub>2</sub> assimilation, sulfate reduction, methane oxidation, lithotrophic and acetoclastic methanogenesis, and assimilation and oxidation of organic carbon, iii) analysis of samples of sulfide, sulfate, and carbonate hydrothermal deposits of various morphological types. Special attention was paid to the measurement of microbial DOM. We show for deep-sea hydrothermal systems, that in the process of microbial methane oxidation and dark assimilation of carbon dioxide at various temperature gradients of microbial production of DOM in most cases significantly higher than biomass production. Intensities of sulfate reduction and methanogenesis have been measured for the first time at different temperatures and dilution of the hydrothermal solution, not only in anaerobic sediments and solutions, but also in water samples of the contact zone and the plume.

The different content of organic compounds in microbiological samples and ore deposits from hydrothermal systems related to basalt volcanism and serpentinization of ultrabasic rocks testifies the different genesis of DOM.

This work was supported by grant RFBR № 10-05-01116-a, 12-05-31259\_МОН-а.

## Production and diffusion of cosmogenic noble gases: Using open-system behavior to study surface processes

DAVID L. SHUSTER<sup>1,2</sup>, MARISSA M. TREMBLAY<sup>1,2</sup>  
AND GREG BALCO<sup>2</sup>

<sup>1</sup>Dept. of Earth and Planetary Science, University of  
California, Berkeley, CA 94720 USA

<sup>2</sup>Berkeley Geochronology Center, Berkeley, CA 94709 USA

We present a new geochemical approach to obtaining information about the temperature and surface exposure history of rocks and sediments. The approach is based on the simultaneous production and diffusion of cosmogenic noble gases in minerals at and near Earth's surface, and aims to take advantage of "open-system" behavior that has previously been viewed only as an undesirable obstacle to surface exposure dating. Given knowledge of diffusion kinetics, the relative abundances of cosmogenic <sup>3</sup>He, <sup>21</sup>Ne and other cosmogenic nuclides in natural samples constrain their temperature histories during surface exposure. When interpreted with a simple theoretical framework, and using laboratory-determined kinetics of He and Ne diffusion [1-3], our preliminary results indicate several pairs of common minerals and easily measurable cosmogenic noble gases that display partial retention at Earth surface temperatures. We focus initially on the minerals quartz and feldspars; these provide sets of nuclide-mineral systems that can be selected and optimized to constrain mean surface temperatures (and changes therein) across a range of climate settings and lithologies over the last few Ma. As an example, we present preliminary results from quartz-bearing Antarctic sandstones that constrain a mean, effective temperature of approximately -15 °C over 5-10 ka of surface exposure. We present the basic theory and fundamental assumptions of this approach, and discuss potential complexity and limitations to the interpretation of these data.

1. Gourbet, L., et al., Neon diffusion kinetics in olivine, pyroxene and feldspar: Retentivity of cosmogenic and nucleogenic neon. *Geochimica et Cosmochimica Acta*, 2012. 86: p. 21-36; 2. Shuster, D.L. and K.A. Farley, Diffusion kinetics of proton-induced <sup>21</sup>Ne, <sup>3</sup>He, and <sup>4</sup>He in quartz. *Geochimica et cosmochimica acta*, 2005. 69(9): p. 2349-2359; 3. Tremblay, M.M., D.L. Shuster, and G. Balco, Quantifying the open-system behavior of cosmogenic noble gases in quartz. *Goldschmidt 2013* (this meeting).

## The Study of Cadmium Accumulation by Floating Macrophytes using Natural Modeling Approach

O.V. SHUVAEVA<sup>1,2\*</sup>, L.A. BELCHENKO<sup>2</sup>  
AND T.E. ROMANOVA<sup>1,2</sup>

<sup>1</sup>Institute of Inorganic Chemistry SB RAS, 3, Ac. Lavrent'ev Pr., 630090, Novosibirsk, Russia, olga@niic.nsc.ru

<sup>2</sup>Novosibirsk State University, 2, Pirogova, 63090, Novosibirsk, Russia, lab305@lab.nsu.ru

<sup>3</sup>Novosibirsk State University, 2, Pirogova, 63090, Novosibirsk, Russia, romanova\_toma@mail.ru

It is known that phytoremediation technology became an effective method of environment clearing after it has been found the plant's ability to accumulate the contaminants at high concentration level. The floating macrophytes (*FM*) *Eichhornia crassipes* (*EC*) and *Pistia stratiotes* (*PS*) are applied most often to waste waters purification.

The goal of this investigation was to study the efficiency of the metal's bioaccumulation by *EC* and *PS* when exposed to cadmium with an emphasis on the mechanism of transport and transformation of pollutant within the plant and its fate during accumulation act.

To estimate hit consequences of pollutant on ecosystem an experiment was carried out in the conditions close to the natural using an approach of natural modeling consisting in a statement of natural experiments with the use of mesocosms, established directly in a reservoir into which one enters the set portion of pollutant and then supervises the dynamics of its concentration.

As a result it was found that the degree of cadmium extraction by *FM* from contaminated natural water while maintaining the viability of the plants depends on the way of pollutant introducing and the maximum is observed in the case of its gradual entry. Herewith at the first stage of cadmium uptake the sorption of the metal on the surface of the roots takes place where cadmium mainly localized in rhizodermis, and then the pollutant penetrates into the tissues of the stem according to its translocation factor

In contrast to the traditional black-box approach, detailed investigations of pollutant transport and distribution in plant tissues have given sound understanding of the phytoremediation phenomenon. Such advancements could provide a basis for future improving the efficacy of the biological remediation processes.

## Modelling fluid-mineral equilibria in two-phase fluid systems

YU. V. SHVAROV<sup>1</sup>, E. N. BASTRAKOV<sup>2\*</sup>, T.P. MERNAGH<sup>2</sup>  
AND N. N. AKINFIEV<sup>3</sup>

<sup>1</sup>Moscow State University, Moscow 12345, Russia

<sup>2</sup>Geoscience Australia, Canberra, ACT 2601, Australia

(\*correspondence: Evgeniy.Bastrakov@ga.gov.au)

<sup>3</sup>IGEM RAS, 119017, Moscow 119017, Russia

There is a demand for modeling fluid-rock interaction in geological systems that contain two fluid phases (e.g., liquid + gas) or experience a transition from supercritical to subcritical state of fluids. The relevant problems include CO<sub>2</sub> sequestration into geological formations; exploitation of gas-rich geothermal systems; quantification of metal transport by low-density fluids in porphyry, epithermal, and lode-gold mineral systems. Modelling of geochemical processes in these systems requires software that allows simultaneous prediction of the accurate phase composition of the fluid part of the system and "conventional" water-rock or gas-rock equilibria. Recent experimental and theoretical studies start to provide thermodynamic models to expand these calculations into the realm of metal bearing fluids [1].

To address these challenges, we employ the HCh software package [2] that uses the Gibbs Free Energy minimization approach for equilibrium calculations. To calculate fluid-fluid equilibria, we have incorporated a customised version of the PRSV equation-of-state [3], where thermodynamic properties of *pure water* at a given temperature and pressure are calculated according to the comprehensive Haar-Gallagher-Kell model [4]. The incorporated algorithms were calibrated and tested against available experimental and theoretical data for the binary H<sub>2</sub>O-CO<sub>2</sub> and H<sub>2</sub>O-CH<sub>4</sub> systems, and the ternary H<sub>2</sub>O-CO<sub>2</sub>-CH<sub>4</sub> system.

A practical application of the software to economic geology problems is illustrated by calculation of H<sub>2</sub>S concentrations in a supercritical fluid and subcritical gas and liquid phases in equilibrium with mineral assemblages containing iron sulfides and oxides. An equilibrium between pyrite-pyrrhotite mineral pair and the H<sub>2</sub>O-CO<sub>2</sub>-CH<sub>4</sub>-H<sub>2</sub>O-H<sub>2</sub>S-H<sub>2</sub> fluid offers a plausible explanation of the H<sub>2</sub>S concentrations measured in the vapor-rich inclusions from the Missouri lode gold deposit.

- [1] Migdisov & Williams-Jones (2013) *GCA* **104**, 123-135. [2] Shvarov (2008) *Geochem. Int* **46**, 834-839. [3] Stryjek & Vera (1986) *Can. J. Chem. Eng* **64**, 323-333. [4] Kestin *et al.* (1984) *J. Phys. Chem. Ref. Data* **13**, 175-183.

## Hg as a proxy for volcanic activity during extreme environmental turnover: the K-T boundary

A. N. SIAL<sup>1\*</sup>, L. D. LACERDA<sup>2</sup>, V. P. FERREIRA<sup>1</sup>, R. FREI<sup>3</sup>, R. A. MARQUILLAS<sup>4</sup>, J. A. BARBOSA<sup>1</sup>, C. GAUCHER<sup>5</sup>, C. C. WINDMÖLLER<sup>6</sup> AND N. S. PEREIRA<sup>1</sup>

<sup>1</sup>NEG-LABISE and Dept. Geology, UFPE, Recife, Brazil  
(\*correspondence: sial@ufpe.br)

<sup>2</sup>LABOMAR, UFC, Fortaleza, Brazil

<sup>3</sup>Inst. Geogr./Geol., Univ. of Copenhagen, Denmark, 1350

<sup>4</sup>Univ. Salta, Salta, Argentina

<sup>5</sup>Fac. Ciencias, Univ. de La Republica, Montevideo, Uruguay

<sup>6</sup>Dept. Chem., UFMG, Belo Horizonte, Brazil

Hg tends to concentrate in sediments deposited right after major glacial events as a result from leaching of volcanogenic Hg from land surface and accumulation along argillaceous sediments. Low geological background concentrations of Hg makes it suitable for identifying accumulation pulses during sedimentation that can be tentatively related to weathering processes and thus to climatic changes. Intense volcanism was, perhaps, responsible for climatic changes, decrease in biodiversity and mass extinction in the K-T boundary (KTB).

We have used Hg as a proxy for volcanic activity and atmospheric Hg and CO<sub>2</sub> buildup across the KTB in the Yacoraite Fm., Argentina, where Hg up to 250 ng.g<sup>-1</sup> has been found. In drill cores across the KTB in the Paraiba Basin, NE Brazil, Hg also increased from late Maastrichtian to early Danian. Hg spikes predating the KTB are, perhaps, the record of volcanic activity very close to this transition. At Stevns Klint, Denmark, Hg contents reached ~ 250 ng.g<sup>-1</sup> within a clay layer that comprises the KTB, and exhibits marked <sup>87</sup>Sr/<sup>86</sup>Sr positive excursion and <sup>206</sup>Pb/<sup>204</sup>Pb and <sup>187</sup>Os/<sup>188</sup>Os (t = 65Ma) negative ones. Highest Hg values in the Yacoraite Fm. and at Stevns Klint (~250 ng.g<sup>-1</sup>) are similar to volcanogenic Hg contents in Neoproterozoic cap carbonates (~ 280 ng.g<sup>-1</sup>), deposited in the aftermath of Snowball glaciation, a comparative extreme environmental turnover, in absence of meteorite impact. Co-variation between Hg and Al<sub>2</sub>O<sub>3</sub> is observed in all studied sections suggesting that Hg is adsorbed onto clays. Thermo-desorption experiments in samples from the Yacoraite Fm. showed Hg<sup>+2</sup> as the major species present, in agreement with a volcanic origin. Combined Hg and C-isotope stratigraphies may become a powerful tool for the eventual assessment of the role of volcanic activity during extreme climatic and biotic events, such as those during the Cretaceous-Tertiary or Permian-Triassic boundaries.

## The age of eclogitisation underneath the Kaapvaal craton – A composite xenolith from Roberts Victor

M. SIEBER\*, G.P. BREY, H.-M. SEITZ, A. GERDES AND H.E. HOEFER

Institut für Geowissenschaften, Goethe-Universität,  
Altenhöferallee 1, D-60438 Frankfurt, Germany;  
\*melanie-sieber@stud.uni-frankfurt.de

We have studied a composite, 16x11x5 cm sized, biminerale eclogite xenolith (texturally Type II) from the Roberts Victor diamond mine (South Africa) with a 1 cm thick layer along its longer side of green, Cr-rich cpx with exsolution lamellae (presumably opx which is now completely replaced by calcite) plus a Cr-rich garnet (up to 6 wt% Cr<sub>2</sub>O<sub>3</sub>) which gradually change into the dark coloured cpx's (without exsolution lamellae and heavily altered in places) and Cr-free garnets in the major part of the eclogite. Electron microprobe traverses across the xenolith show that the individual mineral grains (~4 mm in size) are homogeneous but that there is a gradient of mineral compositions from the Cr-rich layer into the Cr-free part which appears like a diffusional gradient. For example, Al<sub>2</sub>O<sub>3</sub> in garnet increases from 18 to a constant level of 23 wt% over a distance of 3 cm and Cr concomitantly decreases from 6 to practically zero wt%. The Mg-value increases over the same distance from 50 to 57. Clinopyroxenes change in composition complementary to the garnets. This concomitant change also holds for the trace elements which were determined by laser ablation ICP MS. The grt-cpx partitioning of the trace elements is the same throughout the xenolith except for a dependency on the Cr-content of garnet.

The temperature of 915 °C of last equilibration were calculated with the Krogh 1988 grt-cpx thermometer at 4.2 GPa.

We interpret the compositional profile as the reflection of the passage of a basaltic melt through peridotite. A contact zone with Cr-rich cpx and a compositional gradient was formed and the whole package was subsequently metamorphosed to eclogite. The aim is to determine the age of eclogitisation with the Sm-Nd and Lu-Hf isotope systems from garnet separates obtained from rock slices parallel to the Cr-rich layer.

## Molybdenum isotope fractionation in the Great Artesian Basin, Australia

C.SIEBERT<sup>1\*</sup>, P. POGGE VON STRANDMANN<sup>2</sup>  
AND K. BURTON<sup>3</sup>

<sup>1</sup>GEOMAR, Helmholtz Center for Ocean Research, Kiel, Germany

<sup>2</sup>Univ. of Oxford, Dept. of Earth Sciences, Oxford, UK

<sup>3</sup>Univ. of Durham, Dept. of Earth Sciences, Durham, UK

\* (correspondence: csiebert@geomar.de)

Over the last decade, Molybdenum (Mo) isotopes have become a valuable proxy for redox conditions in marine sediments. More recently, the behavior of Mo and its isotopes during weathering and erosion have been investigated to constrain inputs to the oceans. This study aims to investigate another aspect of terrestrial Mo cycling, namely its behavior in groundwater aquifers. Recent studies suggest that groundwater input could have a significant impact on oceanic elemental and isotopic budgets. Concentrations and isotope compositions of elements in groundwater are usually controlled by the recharging water (e.g. precipitation) and processes within the aquifer such as chemical weathering. We investigated these processes for Mo in the Australian Great Artesian Basin (GAB), the world's largest confined aquifer underlying ~22% of the Australian continent. The GAB consists of alternating layers of waterbearing sandstone aquifers and non-waterbearing siltstones and mudstones. The thickness of this sequence varies from less than 100 metres at the Basin edges to 3000 metres in the centre. Groundwater in the GAB flows generally west and south with a flow rate between 1 and 5 m/a. Recharge occurs by rainfall into outcropping sandstone along the eastern margins of the Basin. Samples are from the eastern portion of the GAB and range in age from 36 (close to the recharge area) to 700 kyr over a distance of 600 km along the flow of the groundwater.

Molybdenum concentrations and isotopes vary widely throughout the sampled area ([Mo]: 0.4 to 13 ppb and  $\delta^{98}\text{Mo}$ : -0.2 to 1.4 ‰). The isotopes show correlations with [U] and [SO<sub>4</sub>], but are not or only weakly correlated with [Mo], [Mn], [Fe] or  $\delta^7\text{Li}$ . The observed patterns point to fractionation of Mo isotopes by a sequestering mineral phase. A systematic change of Mo isotope values with distance from the recharge area indicates that the size as well as the processes within the aquifer could impact the isotope composition of groundwater input to the oceans. The results emphasize the role of groundwater processes for the fractionation of Mo isotopes. However, the quantitative impact of this fractionation on the oceanic budget remains to be determined.

## Experimental study of accretion and early differentiation of the Earth

JULIEN SIEBERT<sup>1\*</sup>, JAMES BADRO<sup>2</sup>, DANIELE ANTONANGELI<sup>1</sup> AND FREDERICK J. RYERSON<sup>3</sup>

<sup>1</sup>Institut de Minéralogie et de Physique des Milieux

Condensés, Université Pierre et Marie Curie, Paris, France

(\*correspondence: julien.siebert@impmc.upmc.fr)

<sup>2</sup>Institut de Physique du Globe de Paris, Paris, France

<sup>3</sup>Lawrence Livermore National Laboratory, California, USA

The pattern of siderophile (iron-loving) element abundance in the silicate portion of the Earth is a consequence of metal separation during core formation. Thermodynamic expressions used to constrain the metal-silicate partitioning behavior of siderophile elements are mainly established from large volume press experiments that do not cover the full range of potential P-T conditions for core-mantle equilibrium. Using the laser-heated diamond anvil cell technique, we have extended metal-silicate partitioning measurements to 75 GPa and 4400 K, exceeding the liquidus temperatures for both metal and silicate and, therefore, achieving thermodynamic conditions directly equivalent to the full range of P-T conditions relevant to metal-silicate equilibration at the base of a deep magma ocean. Partitioning results obtained for siderophile elements (Ni, Co, V, Cr, Mn, Nb) and light elements (Si, O) are used to constrain a mechanism for terrestrial accretion and core formation reconciling the observed mantle concentrations of V, Cr and geophysical constraints on light elements in the core. The experiments were performed in the P-T ranges of 35-74 GPa and 3100-4400 K. The metal-silicate partition coefficients for nickel and cobalt decrease with increasing pressure and reach the values required to yield present mantle concentrations at ~50 GPa [1]. Enhanced solubility of oxygen in the metal perturbs the metal-silicate partitioning of V and Cr, precluding extrapolation of previous results (Siebert *et al.* 2013). We will present new continuous core formation models for different redox paths showing that terrestrial accretion under highly reduced conditions as proposed by most core formation models [3, 4] could be reconsidered.

[1] Siebert *et al.* (2012) *EPSL* **321-322**, 189-197. [2] Siebert *et al.* (2013) *Science* **339**, 1194-1197. [3] Wood *et al.* (2006) *Nature* **441**, 825-833. [4] Rubie *et al.* (2011) *EPSL* **301**, 31-42.

## Heat producing element enrichment in granitic rocks & zircon Hf isotopic constraints on crustal evolution in NE Queensland, Australia

C.SIEGEL<sup>1,3\*</sup>, S.E. BRYAN<sup>1,3</sup>, C.M. ALLEN<sup>1</sup>, D.J. PURDY<sup>2</sup>  
AND D.A. GUST<sup>1</sup>

<sup>1</sup>EEBS, Queensland University of Technology, Australia  
(\*correspondence:c.siegel@qut.edu.au)

<sup>2</sup>Geological Survey of Queensland, Australia

<sup>3</sup>QGECE, The University of Queensland, Australia

The primary processes causing enrichment of incompatible Heat Producing Elements (HPE; U, Th & K) in granitic rocks are still poorly understood and are topical in light of increasing interest in engineered geothermal systems. Differentiation of the continental crust, through successive events of granitic magmatism, is expected to lead to a HPE-enriched upper crust and a depleted lower crust. In such a closed system crust model, younger granitic rocks should be more isotopically evolved. Instead, our study of granitic rocks, emplaced within a relatively restricted area (~200x100km), reveals a paradox: isotopic systems become more primitive over time, but HPE concentrations are more elevated. The study area has had ~360 Myr history of granitic magmatism with mainly I- to minor A-type granitic rocks of Carboniferous, Permian, Triassic, Cretaceous & Tertiary age.

Long-term compositional trends are recognised: modal mineralogy and bulk-rock composition record enrichment of K-feldspar and the increase of HPE concentration from the Permo-Carboniferous to the Cretaceous. In contrast, new MC-ICP-MS zircon Hf isotope data indicate secular changes to bulk crustal source compositions. Triassic ( $\epsilon_{\text{Hf}}$ : +4.9 to +8.5) and Cretaceous ( $\epsilon_{\text{Hf}}$ : +8.3 to +10.8) zircons are generally more isotopically primitive compared to Permo-Carboniferous ( $\epsilon_{\text{Hf}}$ : -7.3 to +1.2 & +3.6 to +9.8) and Tertiary ( $\epsilon_{\text{Hf}}$ : +0.5 to +5.1) zircons. The restriction of more isotopically primitive zircons in Triassic and Cretaceous rocks does not favor the model of a simple differentiated crust but rather an open crust system and progressive basification of the lower crust. Paradoxically, the isotopically primitive Mesozoic intrusions are also the most compositionally evolved, and have the highest HPE enrichments. To explain this, we interpret that fluid fluxing associated with a subduction-related contractional event in the Late Permian-Triassic was important for fertilising the lower crust and enriching it in HPE. This overcame the effects of basification by underplating during earlier back-arc extensional events. Cretaceous-Tertiary intraplate igneous events then provided important catalysts for more typical crustal differentiation.

## Hydraulic and geochemical survey of the lithium-resources in the Salar de Uyuni (Bolivia)

ROBERT SIELAND\*, NADJA SCHMIDT  
AND BRODER MERKEL

TU Bergakademie Freiberg, Department of Hydrogeology, D-09599 Freiberg, Germany

(\*correspondence: Robert.Sieland@geo.tu-freiberg.de,  
Nadja.Schmidt@geo.tu-freiberg.de,  
Broder.Merkel@geo.tu-freiberg.de)

The Salar de Uyuni, located in the southern Altiplano of the Bolivian Andes, is the largest salt flat in the world (10,000 km<sup>2</sup>, 3,653 m a.s.l.). Its alternating sequence of salt, mainly composed of halite, and lacustrine sediments contain a brine which is highly enriched in lithium (up to 4.7 g/L) among other elements [1]. Moreover, it is considered to be the largest lithium-brine deposit in the world.

Between 2009 and 2012 exploration drillings which completely penetrate the upper salt layer (with a maximum thickness of 11 m) as well as brine sampling were conducted at various sites on the salt flat. Porosity measurement of salt cores was realized gravimetrically on dried (70°C, until  $\Delta_{\text{weight loss}} < 1\%$ ) core samples. Additionally, X-ray tomography on selected core samples was used to verify porosity results. Geochemical analyses on brine samples were conducted using ICP-MS.

Porosity data showed large horizontal differences of the salt crust. While the uppermost two meters of the salt are characterized by total porosities between 25 and 40%, deeper parts of the salt crust showed significantly lower porosities between 5 and 18%. Chemical analyses revealed an inhomogeneous distribution pattern for different elements. Among others, highest lithium concentrations were found close to the main tributary in the south as well as in a small fringe in the north of the salt flat.

Using stratigraphic information from drill cores, porosity data as well as the distribution pattern of lithium concentrations in the brine, a conceptual model was developed in order to estimate the total volume of brine occurring in the salt flat as well as the lithium-resource. The total amount of lithium in the Salar de Uyuni is estimated to around 6.6 million tons. This is in contradiction to previous publications [1, 2] which assume the lithium-resources to be about 35% higher.

[1] F. Risacher, B. Fritz (1991) *Chemical Geology* **90**: 211-231 [2] USGS (2012) *Mineral Commodity Summaries 2012*, p. 94-95

## Ca, Mo and U isotopes suggest Neoproterozoic-like ocean conditions during the Late Permian Mass Extinction

SILVA-TAMAYO, J.C.<sup>1</sup>, PAYNE, J.L.<sup>1</sup>, WIGNALL P.B.<sup>2</sup>,  
 NEWTON R.J.<sup>2</sup>, NEUBERT, N.<sup>4</sup>, BRUESKE, A.<sup>4</sup>,  
 EISENHAEUER A.<sup>3</sup>, WEYER, S.<sup>4</sup>, FIETZKE, J.<sup>3</sup>  
 AND MAHER, K.<sup>1</sup>.

<sup>1</sup>Stanford University. cuore@stanford.edu,  
 jlpayne@stanford.edu, kmaher@stanford.edu

<sup>2</sup>University of Leeds. P.B.wignall@leed.ac.uk,  
 R.B.newton@leeds.ac.edu

<sup>3</sup>Helmholtz Center for Ocean Research Kiel  
 aeisenhauer@geomar.de, fietzke@geomar.de

<sup>4</sup>Leibniz Universitat Hannover. s.weyer@mineralogie.uni-hannover.de, n.neubert@mineralogie.uni-hannover.de

The most catastrophic extinction event in the history of animal life occurred at the end of the Permian Period, ca. 252 Mya. Ocean acidification and global oceanic euxinia have each been proposed as causes of this biotic crisis, but the magnitude and timing of change in global ocean chemistry remains poorly constrained.

Here we use Ca, Mo and U isotopes applied to globally distributed, well dated late Permian- early Triassic sedimentary sections to better constrain the magnitude and timing of change in ocean chemistry through this interval. All the investigated carbonate successions (Turkey, Italy and China) exhibit decreasing  $\delta^{44/40}\text{Ca}$  compositions, paralleling a major decrease in  $\delta^{13}\text{C}$  values. These findings support an episode of ocean acidification coincident with the major biotic crisis. The Mo and U isotope records exhibit significant rapid negative anomalies at the onset of the main extinction interval, suggesting rapid expansion of anoxic and euxinic marine bottom waters during the extinction interval. The rapidity of the isotope excursions in Mo and U suggests substantially reduced residence times of these elements in seawater relative to the modern, consistent with expectations for a time of widespread anoxia. The large C-isotope variability during the early Triassic, which is similar to that of the early-middle Cambrian, suggests imply largely biogenetically controlled perturbations of the oceanic carbon cycle. These findings strengthen the evidence for a global ocean acidification event coupled with rapid expansion of anoxic zones as drivers of end-Permian extinction in the oceans.

## Shiveluch volcano: Mineralogical records of geodynamic complexity

SIMAKIN A.<sup>1,2\*</sup>, SALOVA T.<sup>2</sup>, GORDEYCHIK B.<sup>2</sup>  
 AND CHYURIKOVA T.<sup>3</sup>

<sup>1</sup>Institute Physics Earth, Moscow Russia, simakin@ifz.ru

<sup>2</sup>Institute Experim. Mineral., Chernogolovka, Russia

<sup>3</sup>Inst. Volcanol. Seism., Petropavlovsk-Kamchatskii, Russia

Shiveluch is the most north active andesite volcano on Kamchatka. Several types of magmas mix and interact in Shiveluch magmatic system. There are only two centres of the basaltic eruptions on Shiveluch. Olivine-plagioclase basalts form dyke complex of the NW orientation on the northern edge of caldera. Second centre was found recently on the western slope of volcano. Complex structure of the magma localization in the thick crust of Northern Kamchatka is revealed by the seismic tomography (Lees *et al.*, 2007). Contrasted low Vp zones are traced at the depths 5-7, 13-17, 25-30 km with horizontal dimensions up to 100 km larger than typical intervolcano distances. Results of the magmatic amphibole barometry (new barometer-Simakin *et al.*, 2012a) also clustered around three observed geophysically levels. Detailed mineralogical study of two types of Shiveluch basalts demonstrates heterogeneity of the whole rock and even individual crystals. Oxygen fugacity estimates with clinopyroxene geo-oxobarometer (Simakin *et al.*, 2012b) yield bi-modal distributions with  $f\text{O}_2$  around NNO+1(0.5) and NNO+1.6(2.5). Second maximum is close to the high  $f\text{O}_2$  estimates (c.a. NNO+2) typical for the high pressure (up to 10-11 kbar) amphiboles.

Compositions of Holocene volcanites around Shiveluch on  $\text{SiO}_2$ -Ba diagram are separated into several evolutionary series with different initial Ba content. The upper  $\text{SiO}_2$ -Ba set (Sedanka volcanic centre with several Shiveluch compositions) on the Th/Yb – Nb/Yb diagram adjoins decompressional mantle partial melts array. These magmas presumably originate at the mantle upgoing flow near the subducting plate edge. Low Ba basalts (Baidarnaya centre) belong to the Bezymianny-Klyuchevskoy volcanoes compositions set forming on the Nb/Yb – Th/Yb diagram vertical array between normal IAB and N-MORB compositions. Effective melting of the underplated thick continental crust near the Moho depth produces oxidized siliceous amphibole-bearing magmas of adacite affinities. These three components mix and undergo crystallization differentiation before being erupted on Shiveluch.

[1] Lees *et al.*, Geoph. Monograph Series 172, 2007. [2] Simakin A. *et al.*, Earth Science Res., 1(2), 2012a. [3] Simakin A. *et al.*, Petrology, 20(7), 2012b.

## Ni sorption at the Particle Edges of Synthetic and Biogenic Birnessite

ANNA A. SIMANOVA<sup>1\*</sup>, SHARON E. BONE<sup>2</sup>, JOHN R. BARGAR<sup>3</sup>, GARRISON SPOSITO<sup>2</sup> AND JASQUELIN PEÑA<sup>1</sup>

<sup>1</sup>University of Lausanne, Switzerland, (\*correspondence: anna.simanova@unil.ch, jasquelin.pena@unil.ch)

<sup>2</sup>Lawrence Berkeley National Laboratory, Berkeley, USA sbone@lbl.gov, gsposito@berkeley.edu

<sup>3</sup>Stanford Synchrotron Radiation Lightsource, Menlo Park, USA, bargar@slac.stanford.edu

Biogenically produced manganese oxides play an important role in trace metal scavenging in the environment. The metal sorption capacity of the Mn oxides arises mainly from the presence of negatively charged Mn(IV) vacancy sites in the MnO<sub>2</sub> sheets. For example, recent extended X-ray absorption fine structure (EXAFS) studies showed that Ni binds to vacancy sites in biogenic Mn oxides via two preferential coordination geometries: as a triple-corner-sharing complex (Ni-TCS) at circumneutral pH and a mixture of Ni-TCS and Ni incorporated into the MnO<sub>2</sub> sheet at higher pH [1,2]. However, under-coordinated oxygen atoms at particle edges offer additional sites for metal coordination. Metal sorption by particle edges has been reported for chemically synthesized birnessites, but is poorly understood for biogenic minerals where the admixing of organic and mineral functional groups in these microbe-mineral assemblages may modify the reactivity at the particle edges.

In this work, we used  $\delta$ -MnO<sub>2</sub> as a synthetic analog of biogenic birnessite to study the reactivity of the birnessite edge since it has fewer vacancies and contains no biomass. We studied adsorption of Ni at the surface of  $\delta$ -MnO<sub>2</sub> as a function of pH and surface loadings using a combination of wet chemistry methods and Ni K-edge EXAFS spectroscopy and compared these data to Ni adsorption at the surface of the biogenic birnessite produced by *Pseudomonas putida* strain GB-1 [1]. At pH 8 the surface speciation and reactivity of  $\delta$ -MnO<sub>2</sub> was similar to biogenic birnessite, while at lower pH values we detected an additional surface species that likely formed at the particle edges of  $\delta$ -MnO<sub>2</sub>. The absence of this species in biogenic birnessite suggests that the bacterial cells and extracellular substances decrease the reactivity of the the particle edges of biogenic MnO<sub>2</sub>.

[1] Pena, J., Kwon, K. D., Refson, K., Bargar, J. R., Sposito, G. (2010) *Geochim. Cosmochim. Acta* 74, 3076-3089. [2] Pena J., Bargar J.R., Sposito G. (2011) *Environ. Sci. Technol.* 45, 7338-7344.

## Lithium in HED meteorites – Implications for planetary crusts

M.ŠIMČÍKOVÁ<sup>1</sup>, T. MAGNA<sup>1</sup> AND F. MOYNIER<sup>2</sup>

<sup>1</sup>Czech Geological Survey, Klárov 3, CZ-11821 Prague, Czech Republic; tomas.magna@geology.cz

<sup>2</sup>Dept. Earth Planetary Sciences, Washington University, St. Louis, MO 63130, USA

The Li contents and isotope compositions are presented for a suite of howardites, eucrites and diogenites (HEDs) thought to originate from asteroid Vesta. The Li contents show notable differences between Li-poor diogenites and Li-rich eucrites whereas howardites have moderate Li contents. Contrary to elemental differences, Li isotope compositions are irresolvable among the individual groups of HEDs, attesting to insignificant Li isotope fractionation during formation of thick basaltic crust by melting of Vesta's mantle.

Several observations are derived. (i) All HEDs span an extremely narrow  $\delta^7\text{Li}$  range (2.2–4.9‰), except for LAP 03569 and Cachari. This asteroidal homogeneity is surprising provided that Vesta experienced core segregation, magma ocean and solidification, and thermal metamorphism some of which could fractionate Li isotopes. The derived bulk mean  $\delta^7\text{Li}$  of Vesta is  $3.7 \pm 1.1\text{‰}$  ( $2\sigma$ ) which is within the range of the mean  $\delta^7\text{Li}$  values derived for the Earth ( $\sim 3.3\text{‰}$ ), Mars ( $\sim 4.0\text{‰}$ ) and the Moon ( $\sim 4.1\text{‰}$ ). (ii) Ordinary chondrites, considered to represent the bulk composition of Vesta, are on average isotopically  $\sim 1\text{‰}$  lighter than HEDs while  $\delta^7\text{Li}$  values of carbonaceous chondrites fall within the range of HEDs. (iii) Oxygen isotopes in Pasamonte hint to its origin from another parent body than the other HEDs. However, proximity of its  $\delta^7\text{Li}$  provides strong evidence for rapid magmatic evolution and basaltic crust differentiation on other bodies akin to Vesta. This implies the existence of planetary embryos in the infancy of the Solar System that were large enough to sustain large-scale magmatism and yet preserving Li isotope compositions intact during their ephemeral magmatic histories. (iv) Unlike Fe isotopes,  $\delta^7\text{Li}$  of Stannern-trend eucrites do not differ from the main group eucrites implying no particular Li isotope difference of residual enriched melts that were involved in their genesis. (v) No elemental Li depletion is recorded in HEDs relative to chondrites which is contrary to other volatile elements such as Zn or Cd that experienced massive loss. This suggests effective retaining of Li in Vesta despite its later impact history which is compatible with moderately volatile behavior of Li at high temperatures and/or during planetary melting. Thus, the lack of evolved crustal rocks and prevalence of 'juvenile' basaltic lavas at asteroidal levels may be discerned with Li.

## The importance of iron mobility in magmatic-hydrothermal systems

ADAM SIMON<sup>1\*</sup>, LAURA BILENKER<sup>1</sup> AND AARON BELL<sup>2</sup>

<sup>1</sup>Earth & Environmental Sciences, University of Michigan  
[\*simonac@umich.edu]

<sup>2</sup>Institute of Meteoritics, University of New Mexico

Iron is a ubiquitous component of arc-related magmas and porphyry-, high-sulfidation, iron-oxide-copper-gold (IOCG), and iron-oxide-apatite (IOA) ore deposits. Iron is present as an essential structural constituent in ferromagnesian silicate minerals, magnetite, sulfide crystals, and sulfide liquids, as well as aqueous fluids that exsolve from silicate melt. The observation that the oxidation state for different arc magma systems varies over approximately five orders of magnitude, from approximately one log unit below the FMQ (fayalite-magnetite-quartz) buffer to the HM (hematite-magnetite) buffer, indicates that iron exists in both ferrous and ferric forms in most arc magmas. The valence of iron is proportionally dominated by Fe<sup>2+</sup> in most common ferromagnesian silicate minerals, is 2/3 Fe<sup>3+</sup> and 1/3 Fe<sup>2+</sup> in magnetite, is Fe<sup>2+</sup> in sulfides, and is Fe<sup>2+</sup> in Cl-bearing aqueous fluid. Interestingly, there does not appear to be a sliding scale for the oxidation state of iron in aqueous fluids, in contrast to silicate liquids. The observation that aqueous fluids contain only a single valence state of Fe across five orders of magnitude of fO<sub>2</sub> space is fundamentally different than sulfur, which exists as both H<sub>2</sub>S and SO<sub>2</sub> in aqueous fluid and the relative proportion of each is dictated by the fO<sub>2</sub> of the system. These observations have critical implications for magmatic systems.

We continue to investigate experimentally the importance of the mass transfer of iron from melt to aqueous fluid, and the many reactions among aqueous fluid, silicate melt, magnetite, and sulfide phases. Our data confirm field-based hypotheses that the transfer of iron from melt to aqueous fluid increases the ratio of Fe<sup>3+</sup> / Fe<sup>2+</sup> in the degassed melt. This has implications for the composition of ferromagnesian silicates and the stability of sulfide phases during degassing. The mass transfer of iron affects the oxidation state of sulfur in the melt, driving sulfur from sulfide to sulfate, which in turn has implications for the mass transfer of ore metals (Cu, Au) from melt to aqueous fluid. This also may affect the fractionation of iron isotopes, and their ability to serve as geochemical fingerprints for source reservoirs of iron in IOCG and IOA deposits. We will present new data and discuss the incredible role that iron plays in moderating phase equilibria of silicate magmas, and the potential use of iron isotopes to assess the evolving oxidation state and source reservoir characteristics of arc magmas.

## Insight to the local melt structures and their influence on the fractionation of rare earth elements (La, Gd, Yb, Y)

S.SIMON<sup>1\*</sup>, M. WILKE<sup>1</sup>, S. KLEMME<sup>2</sup>, W. A. CALIEBE<sup>3</sup>, R. CHERNIKOV<sup>3</sup> AND K. O. KVASHNINA<sup>4</sup>

<sup>1</sup>GFZ, German Research Centre For Geosciences, Potsdam, Germany (\*correspondence: ssimon@gfz-potsdam.de)

<sup>2</sup>Westfälische Wilhelms-Universität, Münster, Germany

<sup>3</sup>Deutsches Elektronen-Synchrotron, Hamburg, Germany

<sup>4</sup>European Synchrotron Radiation Facility, Grenoble, France

Knowledge of the local structure around rare earth elements (REE) in aluminosilicate melts is of great interest for the geochemistry of magmatic processes, particularly for understanding the partitioning of REE between melt and the coexisting crystals in a more comprehensive way. Several studies already proposed a significant influence of the melt composition on REE fractionation [1 – 4]. In a fundamental study Ponader & Brown [5] showed that the local environment around La, Gd and Yb changes with polymerization of the melt, this was used to explain differences in element partitioning. However, no direct correlation between partitioning data and structural informations was provided.

In this study, melt compositions taken from Prowatke & Klemme [4] and various haplogranitic, -basaltic compositions were doped with La, Gd, Yb or Y and synthesized as glass. EXAFS was used to gather quantitative information on the local environment of Gd, Yb and Y and XANES for qualitative information on the local environment of La in the glasses. Additional high temperature (HT) in situ Y-EXAFS was performed to prove, if the local structure of Y above T<sub>G</sub> corresponds to the local structure in the quenched melts. Analysis of the EXAFS data shows that the average bond length, the width and skewness of the REE-O pair distribution function increase with increasing polymerization of the melt for Gd, Yb and Y [6]. XANES spectra confirm a similar trend for La. The HT Y-EXAFS shows no significant change of the local structure above T<sub>G</sub>. Finally, correlations of structural parameters and partitioning data from Prowatke & Klemme [4] were obtained.

[1] Blundy & Wood (2003) *Earth Planet. Sci. Lett.* **210**, 383-397. [2] Watson (1976) *Contrib. Mineral. Petrol.* **56**, 119-134. [3] Ryerson & Hess (1978) *Geochim. Cosmochim. Acta* **42**, 921-932. [4] Prowatke & Klemme (2005) *Geochim. Cosmochim. Acta* **69**, 695-709. [5] Ponader & Brown (1989) *Geochim. Cosmochim. Acta* **53**, 2893-2903. [6] Simon et. al. (2012) *Chem. Geol.*, **in press**.



## Oxygen isotope fractionation in formation of CO<sub>2</sub>

D. SIMONE<sup>1\*</sup>, L.M.T. JOELSSON<sup>2\*</sup>, C. JANSSEN<sup>1</sup>  
AND M.S. JOHNSON<sup>2</sup>

<sup>1</sup>LPMAA, UMR 7092 UPMC/CNRS, Paris, France  
[daniela.simone@etu.upmc.fr]

<sup>2</sup>Department of Chemistry, University of Copenhagen,  
Denmark [joelsson@chem.ku.dk]

\*DS and LMTJ contributed equally to the work.

The discovery of mass independent isotope fractionation (MIF) of oxygen isotopes [1] opened a new dimension in environmental research. Much subsequent research has focused on isotope effects in ozone formation [2,3]. Despite the apparent similarity to formation of ozone, relatively little attention has been given to the possibility of MIF in the formation of CO<sub>2</sub> through the reaction CO + O(<sup>3</sup>P) + M → CO<sub>2</sub> + M [4]. A better understanding of the isotope fractionation in CO<sub>2</sub> may give insights into mechanisms of MIF.

The photochemical reactor at the Copenhagen Centre of Atmospheric Research [5] was used to study the reaction CO + O(<sup>3</sup>P) + M → CO<sub>2</sub> + M experimentally. O(<sup>3</sup>P) radicals were obtained from photolysis of O<sub>3</sub> in the visible region. The use of ordinary commercial LED lamps ensured that no O(<sup>1</sup>D) and subsequently no OH was formed. An enriched sample of CO (90% <sup>13</sup>C<sup>16</sup>O, 10% <sup>13</sup>C<sup>18</sup>O, trace amounts of <sup>13</sup>C<sup>17</sup>O) was used to distinguish the reaction of interest from possible fluctuations in the background concentrations of <sup>12</sup>CO and <sup>12</sup>CO<sub>2</sub> in the reactor. Infrared spectra were recorded with a Bruker IFS 66v/s Fourier Transform Infrared spectrometer. The spectra were analysed using the non-linear least squares algorithm MALT [6]. Experiments were conducted at pressures ranging from 200 to 980 mbar and the isotope chemical kinetics has been modelled using the chemical kinetics software package KPP [7]. Isotope effects were calculated as:

$\alpha_n = \frac{\ln([C^nO]_{t=0}/[C^nO](t))}{\ln([C^{16}O]_{t=0}/[C^{16}O](t))}$ . We present first results, which show unusual ratios of ( $\alpha_{17}-1$ )/( $\alpha_{18}-1$ ). However, as in earlier experiments [4], unambiguous assignment of this MIF is complicated by the presence of side reactions.

[1] Clayton *et al.* (1973), *Science*, 182, 485-488. [2] Brenninkmeijer *et al.*, *Chem. Rev.*, 103(12). [3] Thiemens (2006), *Annu. Rev. Earth Planet. Sci.* **34** 217-62. [4] Pandey and Bhattacharya (2006), *J. Chem. Phys.* 124 234301. [5] Nilsson *et al.* (2009), *Atmos. Environ.* 43 3029-3033. [6] Griffith (1996), *Appl. Spectrosc.* 50 59-70. [7] V. Damian *et al.*: *Comp. Chem. Eng.*, 26, 1567-79, 2002

## Estimating uncertainties in base cation weathering rates according to mass balance

MAGNUS SIMONSSON<sup>1\*</sup>, JOHAN BERGHOLM<sup>2</sup>,  
BENGT OLSSON<sup>2</sup> AND INGRID ÖBORN<sup>3</sup>

<sup>1</sup>Dep. of Soil and Environment, Swedish University of Agricultural Sciences (SLU), P.O. Box 7014, S-750 07 Uppsala, Sweden (\*correspondence: magnus.simonsson@slu.se)

<sup>2</sup>Dep. of Ecology, SLU, Uppsala

<sup>3</sup>World Agroforestry Centre, Nairobi, Kenya

Because forestry is often allocated to soils with low weathering capacity, intensive harvesting practices may deteriorate plant nutrition. Reliable estimates of weathering rates are therefore crucial in analyses of sustainability of, e.g., whole-tree and stump harvesting. By the mass balance approach present base cation cycling may be estimated from data on leaching, deposition, and accumulation in biomass and soil. Insight in the uncertainties in the weathering estimates is crucial for the interpretation of the data.

| Weathering rate of: | Ca                                      | Mg   | K    | Na   |
|---------------------|---|------|------|------|
|                     | (kg ha <sup>-1</sup> yr <sup>-1</sup> ) |      |      |      |
| Average             | 4.0                                     | 1.4  | 3.3  | -3.3 |
| Conf. int.          | ±3.8                                    | ±1.6 | ±4.4 | ±15  |

**Table 1:** Average weathering rates and approximate confidence intervals (ca 95% level) based on spatial variability and uncertainties in allometric functions etc.

| Term in balance          | Ca  | Mg  | K    | Na  |
|--------------------------|-----|-----|------|-----|
| Deposition               | 8%  | 43% | 2%   | 26% |
| $\Delta K_{\text{exch}}$ | 3%  | 5%  | 1%   | 0%  |
| Leaching                 | 4%  | 28% | 0.4% | 74% |
| Biomass accumul          | 86% | 25% | 97%  | 0%  |

**Table 2:** Contributions to overall uncertainty in weathering rates according to soil balance.

The present study was carried out in a Norway spruce (*Picea abies* Karst. (L.)) stand on a podzolic soil in SW Sweden. The results pinpoint the difficulty in assessing low weathering rates in general (Table 1), and demonstrates that the influence of the different terms of the balance varies considerably among the different base cations (Table 2). Details of the uncertainty contributions in the different terms of the balance is shown on a poster with the same title.

## Assessment and geochemical evolution of springs at Hazaribagh District, Jharkhand, India

HEMANT K SINGH<sup>1</sup>, D. CHANDRASEKHARAM<sup>2</sup>, TRUPTI G.<sup>3</sup> AND B. SINGH<sup>4,5,6</sup>

<sup>1</sup>Department of Earth Sciences, IIT Bombay, Mumbai, India-400076 and (\*correspondence: hemantksingh25@gmail.com)

<sup>2</sup>Department of Earth Sciences, IIT Bombay, Mumbai, India-400076 (dchandra@iitb.ac.in)

<sup>3</sup>Department of Earth Sciences, IIT Bombay, Mumbai, India-400076 (trupti@iitb.ac.in)

<sup>4</sup>Department of Earth Sciences, IIT Bombay, Mumbai, India-400076 (banambar.iitb@gmail.com)

<sup>5</sup>IITB-Monash Research Academy, IIT Bombay, Mumbai, India-400076

<sup>6</sup>Civil Engineering Department, Monash University, Clayton, Melbourne, Australia, 3800

Group of thermal and cold springs in Hazaribagh District, Jharkhand with temperatures from 32 to 90 °C and 25 to 27 °C respectively. Three thermal springs and two cold springs are located at Surajkund area, and one thermal spring in Katkamshandi village 15 km from the main town. These springs are located in the Archean Chotanagpur Gneissic Complex (CGC) in the eastern part of Peninsular India. pH of the thermal water ranges from 8.3 to 9, which indicates the springs are alkaline in nature. The water types of thermal springs and cold spring are Na-Cl-SO<sub>4</sub> type. Piper diagram suggests that the geothermal waters circulating through the granitic host rocks have their chemistry compatible with that of the host rock. Since the HCO<sub>3</sub> to Cl ratio is less than one suggest that thermal water is believed to be fast ascending without any major mixing with near surface groundwater but for mild to moderate dilution with groundwater. However anion variation shows sifting toward the SO<sub>4</sub> field suggesting addition of SO<sub>4</sub> from ancient volcanic rocks of the region (Rajmahal volcanics). Mineral saturation index suggest that thermal water is saturated with silica. Two thermal springs of Surajkund area having similar Na/K ratios indicates that they are fed by the same reservoir. Estimated reservoir temperature based on chemical geothermometers is in the range of 150 to 210 °C.

## Dissolved barium distribution and cycling in the Bay of Bengal

SATINDER PAL SINGH<sup>1\*</sup> AND SUNIL KUMAR SINGH<sup>2</sup>

<sup>1</sup>Physical Research Laboartory, Ahmedabad, India, satinder@prl.res.in (\* presenting author)

<sup>2</sup>Physical Research Laboartory, Ahmedabad, India, sunil@prl.res.in

Eight depth profiles of dissolved barium concentrations have been measured in the Bay of Bengal (BoB) along the 87°E transect (~6°N to ~21°N) to track the dispersion of its large influx from the Ganga–Brahmaputra (G–B) river system and the outflow to the equatorial Indian Ocean. A typical Ba concentration–depth profile shows relatively higher Ba concentrations in surface waters (depth ≤5 m) followed by a minimum in the depth interval ~50–150 m and a further increase with depth. The Ba data in the upper layers (depth <100 m), excluding a very high Ba ~112.8 nmol/kg at salinity 24.5 near mouth of the Hooghly estuary, show a North–South trend with a strong and significant inverse correlation with salinity ( $R^2 = 0.75$ ;  $P < 0.0001$ ). This indicates the southward flow of dissolved Ba from the G–B river system that also includes its contributions by particle release and SGD. The subsurface Ba minimum is ubiquitous and most probably is a result of Ba uptake on settling particulates. On the other hand, the Ba concentrations in deep waters (depth ≥500 m) is controlled dominantly by water mixing as suggested by a very strong and significant inverse correlation with salinity ( $R^2 > 0.95$ ;  $P < 0.0001$ ). Exceptions to this conservative behavior are the “hot-spots” of dissolved Ba in bottom waters, which are resulted by the dissolution of sediments at and/or below the sediment–water interface.

Attempts were made to budget the Ba abundance in the Bay of Bengal using a two box model approach, surface (top ~100 m) and deep waters (below ~100 m). Under the steady state the annual Ba influx from the Ganga–Brahmaputra river system seems to be balanced through its removal via sinking particulates as a result there is no lateral outflow of dissolved Ba from the G–B to the equatorial Indian Ocean through top ~100 m of the BoB. Most of this sinking particulate Ba (~95 %) is regenerated again in the lower box, preferentially in the intermediate waters ~100–500 m.

## Diffusion-driven isotopic fractionations in olivine in laboratory and natural settings

C.K. SIO<sup>1</sup>, M. ROSKOSZ<sup>2</sup>, M. CHAUSSIDON<sup>3</sup>,  
N. DAUPHAS<sup>1</sup>, R. MENDYBAEV<sup>1</sup>, F. RICHTER<sup>1</sup>,  
AND F.-Z. TENG<sup>4</sup>

<sup>1</sup>The University of Chicago, (ksio@uchicago.edu)

<sup>2</sup>Université de Lille 1, France

<sup>3</sup>CNRS-CRPG, Nancy, France

<sup>4</sup>University of Washington

Our previous *in situ* measurements of a zoned olivine from Kilauea Iki lava lake revealed large and negatively-coupled Mg-Fe isotopic fractionations [1]. We estimated the relative diffusivities of the isotopes of Mg and Fe in olivine, scaled as  $D_1/D_2 = (m_2/m_1)^{\beta}$ , with  $\beta_{\text{Fe}} \sim 0.25$  and  $\beta_{\text{Mg}} \sim 0.15$  for an olivine zoned from Fo<sub>80</sub> to Fo<sub>83.6</sub>.

Olivine diffusion experiments were run with the goal to quantify  $\beta$ -values and to compare them with the values estimated from the natural sample. In each experiment, crystallographically oriented Fo<sub>100</sub> (synthetic) and Fo<sub>0</sub> (Rockport fayalite) crystals were placed in an alumina crucible, held together by gravity, and the rest of the crucible was hand-packed with FeO powder. A total of six crucibles were placed together in the hot spot of a gas-flowing furnace at the Université de Lille 1. Each pair of crucibles were quenched at a time by moving them to a cold spot in the furnace after 10 and 20 days; all crucibles were taken out of the furnace after 30 days. Contacts were made across some Fo<sub>100</sub>-Fo<sub>0</sub> and all Fo<sub>100</sub>-FeO interfaces. The Fo<sub>100</sub>-Fo<sub>0</sub> profiles were fitted using the diffusion equation of [2], while that of Fo<sub>100</sub>-FeO required slower diffusion coefficients.

The longest profile (Fo<sub>100</sub>-Fo<sub>0</sub>, 30 days, diffusion along c-axis) was analyzed for its Mg isotopic compositions using SIMS (IMS 1280) at CRPG, Nancy. Matrix standards (Fo# 6, 16, 64, 76, 79, 85, 90, and 95) were previously measured by solution for their  $\delta^{26}\text{Mg}$ , and were used to monitor matrix effects. We find that matrix correction is critical in obtaining accurate  $\beta$ -values and that more matrix standards may be required. Our preliminary data shows > 10% fractionation in  $\delta^{26}\text{Mg}$ , which suggests a  $\beta_{\text{Mg}}$  of about 0.1 or less in olivine.

We are currently analyzing more experimental samples and investigating the cause of the apparent discrepancy of the  $\beta$ -value.

[1] C.K. Sio *et al.*, GCA, (in revision). [2] R. Dohmen and S. Chakraborty, (2007). Phys Chem Min. 34, 597-598.

## Experimental study of the system Mg<sub>4</sub>Si<sub>4</sub>O<sub>12</sub>-Mg<sub>3</sub>Cr<sub>2</sub>Si<sub>3</sub>O<sub>12</sub> at 12-25 GPa and 1600 °C

E. A. SIROTKINA<sup>1\*</sup>, A.V. BOBROV<sup>1</sup>, L. BINDI<sup>2</sup>,  
AND T. IRIFUNE<sup>3</sup>

<sup>1</sup>Moscow State University, Russia (\*correspondence: katty.ea@mail.ru, archi3@yandex.ru)

<sup>2</sup>University of Florence, Italy (luca.bindi@unifi.it)

<sup>3</sup>Ehime University, Japan (irifune@dpc.ehime-u.ac.jp)

Pyrope-rich garnets of the ultrabasic paragenesis widely abundant as inclusions in diamonds are characterized by significant admixture of the knorringite, Mg<sub>3</sub>Cr<sub>2</sub>Si<sub>3</sub>O<sub>12</sub>, end-member. Such garnets often contain majoritic component, (Ca,Fe,Mg)SiO<sub>3</sub>, which is an indicator of the sub-lithospheric mantle conditions. Although both components are important for barometry of mantle mineral associations, high-pressure phase relations in the system MgSiO<sub>3</sub>-Mg<sub>3</sub>Cr<sub>2</sub>Si<sub>3</sub>O<sub>12</sub> have been not studied yet. In this study we report the first results of experiments on the majorite-knorringite join at 12–25 GPa and 1600 °C aimed on investigation of conditions of the formation, structural peculiarities, and evolution of the composition of Cr-bearing majoritic garnets.

We investigated the full range of starting compositions with steps of 10–20 mol% and 2–3 GPa in multi-anvil experiments, which allowed us to plot the preliminary phase diagram for the system MgSiO<sub>3</sub>-Mg<sub>3</sub>Cr<sub>2</sub>Si<sub>3</sub>O<sub>12</sub> and synthesize garnets of a wide compositional range. The phase assemblages for majorite-rich starting materials (<30 mol % knorringite) include garnet, enstatite, and eskolaite (Cr<sub>2</sub>O<sub>3</sub>). With the increase of knorringite content in the starting composition, garnet + eskolaite association is formed. Typically synthetic garnets contain significant portion of majorite (>15 mol %) even for pure Mg<sub>3</sub>Cr<sub>2</sub>Si<sub>3</sub>O<sub>12</sub> starting composition. The stability of garnet on the phase diagram is limited by pressure: MgSiO<sub>3</sub> ilmenite containing up to 7 wt% Cr<sub>2</sub>O<sub>3</sub> appears together with eskolaite at  $P > 20$  GPa. Single-crystal X-ray diffraction studies carried out on the produced garnets demonstrated their cubic symmetry in the studied compositional range and allowed us to study structural peculiarities of garnets. The lattice parameter of garnet (in parentheses) linearly increases with increasing the Mg<sub>3</sub>Cr<sub>2</sub>Si<sub>3</sub>O<sub>12</sub> component: 11.4725(4) Å (Mg<sub>3.88</sub>Cr<sub>0.24</sub>Si<sub>3.88</sub>O<sub>12</sub>), 11.5187(6) Å (Mg<sub>3.58</sub>Cr<sub>0.84</sub>Si<sub>3.58</sub>O<sub>12</sub>), 11.5445(5) Å (Mg<sub>3.38</sub>Cr<sub>1.24</sub>Si<sub>3.38</sub>O<sub>12</sub>), and 11.5718(1) Å (Mg<sub>3.21</sub>Cr<sub>1.58</sub>Si<sub>3.21</sub>O<sub>12</sub>).

## Characterization of indigenous oil field microorganisms for microbially enhanced oil recovery (MEOR)

J. SITTE<sup>1</sup>, E. BIEGEL<sup>2</sup>, A. HEROLD<sup>2</sup>, H. ALKAN<sup>3</sup>  
AND M. KRÜGER<sup>1</sup>

<sup>1</sup>BGR, Geomicrobiologie, D-30655 Hannover

<sup>2</sup>BASF SE, GVF/H, D-67056 Ludwigshafen

<sup>3</sup>Wintershall Holding GmbH, R&D, D-34119 Kassel

Microbial activities and their resulting metabolites became a focus of attention for enhanced oil recovery (MEOR, microbial enhanced oil recovery) in the recent years. In order to develop a strategy for a MEOR application in a German oil field operated by Wintershall experiments were performed to investigate different sampling strategies and the microbial communities found in these samples. The objectives of this study were (1) to characterize the indigenous microbial communities, (2) to investigate the dependency of microbial activity/diversity on the different sampling strategies, and (3) to study the influence of the *in situ* pressure on bacterial growth and metabolite production. Fluids were sampled at the well head (surface) and *in situ* in approx. 785 m depth to collect uncontaminated production water directly from the reservoir horizon and under the *in situ* pressure of 31 bar (subsurface). In the lab the pressure was either released quickly or slowly to assess the sensitivity of microorganisms to rapid pressure changes. Quantitative PCR resulted in higher microbial cell numbers in the subsurface than in the surface sample. Biogenic CO<sub>2</sub> and CH<sub>4</sub> formation rates were determined under atmospheric and high pressure conditions in the original fluids, with highest rates found in the surface fluid. Interestingly, no methane was formed in the native fluid samples. While nitrate reduction was exclusively detected in the surface samples, sulfide formation also occurred in the subsurface fluids. Increased CO<sub>2</sub> formation was measured after addition of a variety of substrates in the surface fluids, while only fructose and glucose showed a stimulating effect on CO<sub>2</sub> production for the subsurface sample. Stable enrichment cultures were obtained in complex medium inoculated with the subsurface fluid, both under atmospheric and *in situ* pressure. Growth experiments with constant or changing pressure, and subsequent DGGE analysis of bacterial 16S rRNA genes, revealed that the pressure treatment did not affect the bacterial community composition. Our results show that bacteria in the enrichment culture can tolerate pressure changes between atmospheric and *in situ* reservoir pressure, which makes them promising candidates for further MEOR tests. Since substantial differences in microbial activities were observed between the surface and subsurface fluids, the selection of the sampling strategy should also be considered for MEOR research and industrial application.

## Uranium accumulation by plants covering piles and dumps in uranium post-mining area in SW Poland

A. SKŁODOWSKA<sup>1\*</sup>, D. LECH<sup>2</sup> AND D. RUSZKOWSKI<sup>1</sup>

<sup>1</sup>Faculty of Biology, University of Warsaw, Miecznikowa 1, 02-096 Warsaw, Poland; (\*correspondence: asklodowska@biol.uw.edu.pl)

<sup>2</sup>Polish Geological Institute, 4, Rakowiecka Street, 00-975 Warsaw, Poland (dariusz.lech@pgi.gov.pl)

The uranium exploration and exploitation in the South-West Poland (Lower Silesia District) had been carried out since 1925 when the first 9 Mg of uranium ore were mined from which 690 mg of radium was extracted and the mining ceased in 1962 (total amount of 704 Mg of U was derived). Nevertheless the old subsurface mines, piles and dumps are still involved in the geochemical cycle of the area. Leaching of uranium and radionuclides may be a serious environmental problem in many countries.

Investigations of the influence of mining activity on the natural environment revealed the local-scale radioactive contamination limited to the dumps and their nearest vicinity at four localities: Kowary-Podgorze, Radoniów, Kopaniec/Kromnow and Grzmiaca. Standard ecological test "MARA" performed on 54 samples of wastes and water taken in 15 localities showed moderate toxicity in 5 waste samples and 1 water sample. Another standard test MicroTox showed minor toxicity in 2 waste samples and did not show ecotoxicity of any water sample.

Accumulation of uranium by plants covering the surface of 5 piles containing the most radioactive wastes (dose 1.94-97 μSv/h) was examined. Grasses were found as hyper-accumulator of uranium in all examined places. Maximum uranium concentration 817.15 mg/kg d.w. was noted in the roots of fescue (*Festuca* sp.) growing in Kopaniec pile and 178.85 mg/kg d.w. in the roots of meadow grass (*Poa* sp.) growing in Grzmiaca. Aerial parts of these plants contained 10-20 lower concentration of uranium. Dicotyledonous plants accumulate uranium in the roots up to 196.22 mg/kg d.w. and in leaf up to 138.56 mg/kg d.w. (hawkweed in Kopaniec). Hyper accumulation of uranium was noted in mosses (mainly in *Hypnum cupressiforme*) occurring in streams in the nearest vicinity of piles (up to 700 mg/kg d.w. in Kowary).

These results clearly show that plants actively participate in uranium geochemical cycling what is important factor in environmental risk assessment and may be valuable indication for planning remediation processes.

## New experimental constraints on slab top conditions

S. SKORA<sup>1\*</sup>, M. MARTINDALE<sup>1,2</sup>, L. CARTER<sup>1,3</sup>,  
J. BLUNDY<sup>1</sup>, T. ELLIOTT<sup>1</sup> AND J. PICKLES<sup>1</sup>

<sup>1</sup>Dept of Earth Sciences, University of Bristol, BS8 1RJ  
(\*correspondence: Susanne.Skora@bristol.ac.uk)

<sup>2</sup>Dept of Earth and Ocean Sciences, University of British  
Columbia, 6339 Stores Road, Vancouver, BC V6T1Z4

<sup>3</sup>Dept of Earth Sciences, Rice University, 6100 Main Street,  
Houston Texas, 77005

Subduction zones give rise to arc volcanism because fluids and/or hydrous melts that are released from the slowly heating subducted slab trigger melting in the overlying mantle wedge. The arc geochemical signature points towards a ternary mixture of a melt from subducted sediment, fluid from basaltic oceanic crust and depleted mantle peridotite. The use of the arc geochemical signature in combination with experimental petrology on phase relations, melting and trace element behaviour is therefore key for constraining the P,T,fO<sub>2</sub> conditions in subducted slabs. The aim of this presentation is to place such constraints, using our latest experimental results on subducted sediment and basalt.

A nice example is given by the geochemical signal of the Mariana Arc. Here, the pelagic sediments dominate the incompatible trace element budget over volcanoclastics in the sedimentary column, whereas the volcanoclastics are predominant in the arc geochemical signature. Our study on the melting phase relations of natural volcanoclastic sediments at 3-6 GPa and 800-900°C [1] has revealed that biotite control melting at these conditions in this lithology. The vapour-saturated solidus for volcanoclastic sediments is higher (825-850°C) than in other, phengite bearing marine sediments (700-750°C) at 3 GPa. This trend is reversed at high-pressure conditions (6 GPa) where the biotite melting reaction occurs at lower temperatures (800-850°C) when compared to the phengite melting reaction (900-1000°C). This places tight constraints on slab top temperatures beneath the Mariana Arc at 180 km depth (6 GPa). It must be above the biotite melting reaction (>800°C) but below the phengite melting reaction (<900°C), preventing pelagic sediments from releasing all their incompatible elements into the liquid phase. Another set of experiments using natural altered oceanic crust provide further constraints. Here, we find that the elevated Ba/Th ratio characteristic of many (sediment-starved) arc basalts is only generated within a narrow temperature field (800-850°C), above phengite breakdown but below epidote-out.

[1] Martindale *et al.* (2013), *Chem Geol* **342** 94-109.

## Micromorphology of diamond resorption at 100 kPa: The role of metal ions

V.L. SKVORTSOVA<sup>1\*</sup>, Y.FEDORTCHOUK<sup>2</sup>  
AND A.A.SHIRYAEV<sup>3</sup>

<sup>1</sup>MSU, Moscow, 119991, Russia (\*correspondance:  
valskvor@yahoo.com)

<sup>2</sup>Dalhousie University, Halifax, B3H 4R2, Canada

<sup>3</sup>IPhCE, RAS, Moscow, 119071, Russia

Natural diamonds show various resorption features produced during ascent in kimberlite magma. Experiments conducted at 100 kPa and 900 °C in KOH melts with constant flow of H<sub>2</sub>O vapor or CO<sub>2</sub> gas in the presence of ions of elements common in natural kimberlites (Mg, Ca, Sr, Al, Si, Fe, Cr, Ni, Co, REE) and in mantle minerals (olivine, ilmenite) demonstrated strong catalytic effect of some metal ions on diamond dissolution rate. We report a detailed investigation of micromorphological features induced on diamond surface in these experiments. We examine individually the effects of the oxidizing media, of the catalytic ion, and of the pre-existing defects in diamonds.

The study uses crystals of natural diamonds after loss of 50-80% of the initial weight. Field-Emission SEM and Atomic Force Microscope were used for surface characterisation. It is shown that for the same catalyser ions etching in aqueous fluids leads to smoother surfaces, whereas CO<sub>2</sub>-fluids leaves extremely rough surfaces. In presence of the strongest catalysers (Fe, Cr, Ni ions) the {110} faces show rounded steps. Other strong catalysers (Sr,Cr + Si, ilmenite) produce deep positive trigons of various shapes and sizes on {111} faces. The weakest catalysers (Ca, Mg, Si ions, olivine, natural kimberlite) reveal fine details of {110} faces and shallow trigons on {111} even at low H<sub>2</sub>O and CO<sub>2</sub> concentrations. In fragmented diamonds severe resorption exhibited internal growth structure and defects. Besides influence of extensive parameters, heterogeneities of internal structure (e.g. growth/resorption features); traces of deformation-related features and other defects play important role in formation of final surface morphology.

## Imaging of spatial trace-element distribution in apatite using various X-ray based and spectral analytical methods

SLABY E.<sup>1</sup>, LISOWIEC K.<sup>1</sup>, MICHALAK P.P.<sup>2</sup>, GÖTZE J.U.<sup>2</sup>, MUNNIK F.<sup>3</sup>, FÖRSTER H.-J.<sup>4</sup> AND RHEDE D.<sup>4</sup>

<sup>1</sup>ING PAN, Warsaw, PL, e.slaby@twarda.pan.pl

<sup>2</sup>TUBAF, Freiberg, DE, s.michalak@hzdr.de,

<sup>3</sup>HZDR, Dresden, DE, f.munnik@hzdr.de

<sup>4</sup>GFZ, Potsdam, DE, forhj@gfz-potsdam.de

Magmatic apatites formed in a composite granitoid pluton usually exhibit distinct zonation patterns caused by changes in trace-element composition, such as REEs and Y. Such compositional variations can be used to describe various petrological and geochemical processes, e.g. mixing of magmas of different composition. Apatites from Karkonosze Massif of Poland were studied using various X-ray-based and spectral analytical methods: FE-EPMA – Field Emission Electron Microprobe (including BSE images), PIXE/PIGE – Particle Induced X-ray/Gamma Emission and CL – Cathodoluminescence. Each method was employed to visualize (mappings) and quantify (spot analyses, line profiles) trace-element distribution patterns in single apatite grains. Slightly different suites of trace elements possessing various detection limits were analyzed with each method, with the largest number of elements measured by EPMA and the lowest detection limits achieved by PIXE. PIGE was proved to be most sensitive for analyzing light elements, such as F and Cl. Cathodoluminescence turned out to be the method best suited for visualizing zonation patterns with subtle, very thin zones not seen either on BSE images or X-ray maps. Because each method has advantages and limitations, their combined application is required to best visualize trace-element variations in apatite, which then can be used for modelling magma- differentiation processes.

## Evolution of rhyolite magmas in the Halle Volcanic Complex – A record from Hf and O isotope and Hf concentrations in zircon

SŁODCZYK ELŻBIETA<sup>1\*</sup>, PIETRANIK ANNA<sup>1</sup>, BREITKREUZ CHRISTOPH<sup>2</sup> AND FANNING MARK<sup>3</sup>

<sup>1</sup>University of Wrocław, Geological Sciences, Poland; elzbieta.slodczyk@ing.uni.wroc.pl (\* presenting author) anna.pietranik@ing.uni.wroc.pl

<sup>2</sup>TU Bergakademie Freiberg, Geology and Paleontology, Germany, cbreit@geo.tu-freiberg.de

<sup>3</sup>The Australian National University, Australia, Mark.Fanning@anu.edu.au

The Halle Volcanic Complex (HVC) is located in the northeastern Saale Basin in NE Germany. The region is underlain by the Mid – German Crystalline Zone. The HVC is dominated by rhyolitic rocks (c. 200 km<sup>3</sup>), which were mainly emplaced as large laccoliths. The U/Pb age of zircons ranges from 289 to 301 Ma, inherited zircons are scarce [1].

We have chosen four localities within the HVC for detailed isotopic and chemical analyses of magmatic zircon: Spitzberg, Wettin, 1044 and 1390 [1].  $\epsilon_{\text{Hf}}$ ,  $\delta^{18}\text{O}$  and elemental concentrations of Zr, Hf have been measured in previously dated zircons from these localities. On the basis of Hf content we divided zircon in two groups: zoned grains with low Hf core (8 - 9000 ppm) and high Hf rim (10 - 12000 ppm) and unzoned grains with constant low Hf concentration through grains (6 - 9000 ppm). High Hf rims occur also as magmatic overgrowths on inherited cores. Most of high Hf zircon fragments are also characterized by higher  $\epsilon_{\text{Hf}}$  compared to low Hf zircon. The diversity in  $\delta^{18}\text{O}$  (6.3 - 8.1 ‰) does not correlate with Hf concentration and  $\epsilon_{\text{Hf}}$ .

Generally, the isotope and chemical characteristic of zircon grains is similar between localities and suggest an input of higher  $\epsilon_{\text{Hf}}$  magma towards the late stage of magma evolution, probably shortly prior to the final emplacement. Lack of correlation between  $\epsilon_{\text{Hf}}$  and  $\delta^{18}\text{O}$  implies that at least three sources contributed material [2] to the ca. 300 Ma magmatism contrary to the simple two source contribution observed for the NE German Basin [3].

[1] Breitzkreuz *et al.* (2009), Z. Dt. Ges. Geowiss. 160:173-190. [2] Romer *et al.* (2001), CMP, 141:201-221. [3] Pietranik *et al.* (2013), J. Petrol – in press

## The role of ultramafic veins in mafic alkaline magmatism: Contrary evidence from continental intra-plate settings

K.A. SMART<sup>1\*</sup>, S. TAPPE<sup>1,2</sup>, A. STRACKE<sup>3</sup>, R. L. ROMER<sup>4</sup>  
AND D. PRELEVIĆ<sup>5</sup>

<sup>1</sup>University of the Witwatersrand, Johannesburg, South Africa  
(\*katie.smart2@wits.ac.za)

<sup>2</sup>De Beers Group Exploration, Johannesburg, South Africa

<sup>3</sup>Westfälische Wilhelms-Universität, Münster, Germany

<sup>4</sup>GFZ Potsdam, Germany

<sup>5</sup>University of Mainz, Mainz, Germany

Continental and oceanic mafic alkaline magmas have comparable major and trace element compositions that point towards similar P-T and volatile conditions during partial melting of their upper mantle source regions. While it is now widely accepted that OIB source regions must contain small amounts of recycled mafic components that contribute disproportionately to the magmatism, the geochemical and isotopic heterogeneity of equivalent magmas beneath continental interiors are more commonly explained by the contribution of partial melts of ultramafic veins at the base of the lithosphere. Vein-style metasomatism has also been suggested to explain the isotopic heterogeneity observed in OIBs formed on thick oceanic lithosphere, such that recycling of oceanic crust may not be the dominant source of mantle heterogeneity [1].

We analysed a suite of Mesozoic primitive mafic alkaline basalts and Permian alkaline lamprophyres from southern Sweden (Baltic Shield) for their major and trace element, and Sr-Nd-Hf-Pb isotope compositions. Although the Mesozoic alkaline basalts exhibit trace element features typically ascribed to melting of hydrous potassic phases within the mantle lithosphere, relatively homogeneous, moderately depleted radiogenic isotope compositions argue against derivation from old vein-metasomatized lithosphere. Isotopic modelling of hydrous metasomatic veins (represented by the Permian lamprophyres) potentially introduced to the lithospheric mantle beneath the Baltic Shield during Permo-Carboniferous plume magmatism suggests that such vein material, if it persisted to the Mesozoic, did not play a role in later mafic alkaline magmatism. In contrast, our data show that low-volume alkaline basaltic magmas beneath a thick continental lid 'oversampled' recycled oceanic crust from an otherwise highly depleted convecting upper mantle, similar to OIBs and E-MORBs.

[1] Pilet *et al.* (2008). *Science* **320**, 916 – 919.

## Wintertime nitrate isotope dynamics in the Atlantic Sector of the Southern Ocean

S.M. SMART<sup>1\*</sup>, D.M. SIGMAN<sup>2</sup>, S.E. FAWCETT<sup>2</sup>,  
S.J. THOMALLA<sup>3</sup>, M.A. WEIGAND<sup>2</sup> AND C.J.C. REASON<sup>1</sup>

<sup>1</sup>Department of Oceanography, University of Cape Town,  
Private Bag, Rondebosch, 7700, South Africa  
(\*correspondence: sandimsmart@gmail.com)

<sup>2</sup>Department of Geosciences, Princeton University, Princeton,  
New Jersey 08544, USA

<sup>3</sup>Ocean Systems and Climate Group, CSIR, P.O. Box 320,  
Stellenbosch, 7599, South Africa

We provide the first data on the wintertime patterns of seawater nitrate isotopes (<sup>15</sup>N/<sup>14</sup>N and <sup>18</sup>O/<sup>16</sup>O) for the region south of Africa. Water column profile and underway surface samples collected in July 2012 span a range of latitudes from the subtropics to 57.8°S, just beyond the Antarctic winter sea-ice edge (56.7°S). The data are used in the context of simple models of nitrate consumption (including the Rayleigh model) to estimate the isotope effect (the degree of isotope discrimination) associated with the assimilation of nitrate by phytoplankton. Within the Antarctic, application of the Rayleigh model to depth profile N isotope data yields lower isotope effect estimates than are derived from the spatial variations within the mixed layer (the latter yielding isotope effect estimates near the commonly observed value of 5‰). The data from the Subantarctic Zone, both profiles and surface variations, also yield markedly low estimates for the assimilation isotope effect when analysed with the Rayleigh model. Similar behaviour observed in the N and O isotopes of nitrate suggest that the isotope effect is underestimated by the Rayleigh model due to mixing of waters across a wide range of nitrate concentrations in this more northern domain of the Southern Ocean. The nitrate N-to-O isotope relationship (i.e. Δ(15-18), defined as δ<sup>15</sup>N-δ<sup>18</sup>O) is remarkably uniform across the entire sampled Southern Ocean surface; however, there is a measurable Δ(15-18) difference between the surface mixed layer and the underlying deep water. The significance of these observations will be presented.

## Unraveling the CaCO<sub>3</sub>/PSS Mesocrystal Formation Mechanism by *in situ* TEM and *in situ* AFM

P.J.M. SMEETS<sup>1,2</sup>, K. R. CHO<sup>1</sup>, D. LI<sup>1</sup>, M.H. NIELSEN<sup>1</sup>,  
N.A.J.M. SOMMERDIJK<sup>2</sup> AND J.J. DE YOREO<sup>1,3\*</sup>

<sup>1</sup>The Molecular Foundry, Lawrence Berkeley National Laboratory, Berkeley, CA 94720, USA

<sup>2</sup>Laboratory of Materials and Interface Chemistry, Eindhoven University of Technology, 5600 MB Eindhoven, Netherlands

<sup>3</sup>Pacific Northwest National Laboratory, Richland, WA 99352, USA (\*James.DeYoreo@pnl.gov)

The interplay between mineral and organic species is central to the control of microbial systems over biomineral formation. Deciphering the underlying mechanisms requires *in vitro* studies in which the physical and chemical parameters can be well controlled.

Using negatively charged polyelectrolyte polystyrene sulfonate (PSS) as a proxy for a bio-organic mediator, we investigate particle-mediated crystallization of CaCO<sub>3</sub>, one of the most abundant materials for biomineralization. To induce growth, we use a calcium source in combination with the ammonium carbonate diffusion method. Utilizing similar conditions, Wang *et al.* showed that this approach yielded a family of well-defined calcite-PSS mesocrystals – i.e. 3D regular but porous scaffolds composed of easily distinguished and almost perfectly aligned nanocrystals [1]. Although mesocrystal formation was suggested to proceed via assembly of an amorphous precursor, direct proof of this mechanism is lacking. Here we use *in situ* TEM and *in situ* AFM to follow the formation process. For *in situ* TEM a custom designed fluid cell was utilized, containing two Si/Si<sub>3</sub>N<sub>4</sub> wafers with electron transparent Si<sub>3</sub>N<sub>4</sub> membranes.

We find that the observed mesocrystal morphology can be obtained merely through CaCO<sub>3</sub> overgrowth in PSS solution on a single crystal seed, and *in situ* AFM demonstrates that the development of this morphology is due to polymer poisoning of atomic steps during classical layer-by-layer calcite growth. However, both *in situ* TEM and AFM reveal a complex pathway during the initial stages of formation. Ca- PSS particles first adsorb onto the substrate. After about 2h of reaction with ammonium carbonate in the TEM fluid cell, these then appear to transform into larger amorphous aggregates. We are now attempting to detail the structural evolution of these initial particles and draw inferences about their formation mechanism and role in crystallization.

[1] Wang *et al.* (2005), *J. Am. Chem. Soc.* **127**, 3246-3247

## The Discovery and Role of Non-Stoichiometric Complexes of Calcium Carbonate in the Solution Precipitation of Vaterite

P.J.M. SMEETS<sup>1</sup>, W.J.E.M. HABRAKEN<sup>1,2</sup>,  
L. BERTINETTI<sup>2</sup>, F. NUDELMAN<sup>1,3</sup>,  
AND N.A.J.M. SOMMERDIJK<sup>1,3\*</sup>

<sup>1</sup>Laboratory of Materials and Interface Chemistry, Eindhoven University of Technology, 5600 MB Eindhoven, Netherlands

<sup>2</sup>Max-Planck-Institute of Colloids and Interfaces, 14424 Potsdam, Germany

<sup>3</sup>SoftMatter CryoTEM Unit, Eindhoven University of Technology, 5600 MB Eindhoven, Netherlands  
(\*correspondence: N.Sommerdijk@tue.nl)

Calcium carbonate (CaC) is the most abundant biogenic mineral, found in marine organisms and their fossilized deposits. Its crystallization mechanism is heavily debated since recent studies proposed a non-classical crystallization pathway via pre-nucleation clusters [1]. In the present study, we used cryo-TEM in combination with a titration set-up and demonstrated the existence of subnanometer-sized complexes (~0.4-0.6 nm) as prevalent pre-nucleation species in CaC mineralization, even in under-saturated regimes, which persisted after nucleation.

We show that these pre-nucleation species contain only one calcium in the equilibrium structure, which makes them complexes rather than clusters, similar as what was recently shown for calcium phosphate [2]. From a detailed analysis of the titration data we calculated that the average CaC-pre-nucleation complex chemistry represents a Ca/C ratio <<1, contains at least 50 mol% of bicarbonate and has an overall negative charge. This observation is in contrast to the previously proposed neutral CaCO<sub>3</sub> clusters that have been reported to exist under similar conditions [1]. We used *ab-initio* calculations to identify the structure of these complexes.

Furthermore, a dense liquid phase [3] of sub-micron sized assemblies of complexes exist already before the nucleation event. We propose a nucleation mechanism in which a calcium carbonate nucleus forms within these assemblies through a transformation of the complexes, after which the bulk phase (vaterite) propagates by ion growth.

[1] Gebauer *et al.* (2008), *Science* **322**, 1819-1822. [2] Habraken *et al.* (2013), *Nature Communications* **4**, 1507. [3] Bewernitz *et al.* (2012), *Faraday Discussions* **159**, 291-312



## Lu-Hf and Sm-Nd garnet geochronology: Closure revisited and new applications in lithosphere studies

MATTHIJS A. SMIT<sup>1,2,3</sup>, ERIK E. SCHERER<sup>2</sup>,  
KLAUS MEZGER<sup>4</sup>, LOTHAR RATSCHBACHER<sup>5</sup>,  
ELLEN KOOIJMAN<sup>2,6</sup> AND BRADLEY R. HACKER<sup>1</sup>

<sup>1</sup>Department of Earth Sciences, UC Santa Barbara, USA

<sup>2</sup>Institut für Mineralogie, WWU, Münster, Germany

<sup>3</sup>Institute for Geography and Geology, University of Copenhagen, Denmark

<sup>4</sup>Institut für Geologie, Universität Bern, Switzerland

<sup>5</sup>institut für Geologie, TU Bergakademie, Freiberg, Germany

<sup>6</sup>Swedish Museum of Natural History, Stockholm, Sweden

The link between <sup>176</sup>Lu-<sup>176</sup>Hf and <sup>147</sup>Sm-<sup>143</sup>Nd dates and *P-T* information from garnet is still subject to uncertainty because closure systematics are not well constrained. To progress in this field, we performed <sup>176</sup>Lu-<sup>176</sup>Hf and <sup>147</sup>Sm-<sup>143</sup>Nd geochronology on garnet crystals of different size ( $\emptyset = 0.90\text{--}6.2$  mm) from a granulite from the Archean Pikwitonei Granulite Domain, Superior Province, Canada. Metamorphism in this region started at  $\sim 2716 \pm 4$  Ma and peak metamorphism (760 °C [1]) occurred at  $2639 \pm 2$  Ma [2].

The <sup>176</sup>Lu-<sup>176</sup>Hf dates for the larger size fractions ( $\emptyset > 2.5$  mm) yielded  $2714 \pm 6$  Ma, identical to the age of first garnet growth. Smaller grains exhibit slight younging to  $\sim 2680$  Ma. In contrast, the <sup>147</sup>Sm-<sup>143</sup>Nd dates are equal to or younger than the age of peak metamorphism. The age trends cannot be explained by inclusion effects or REE zoning, but instead relate to diffusive loss of radiogenic <sup>176</sup>Hf and <sup>143</sup>Nd.

The data enable the quantitative evaluation of the closure systematics of the <sup>176</sup>Lu-<sup>176</sup>Hf and <sup>147</sup>Sm-<sup>143</sup>Nd chronometers in garnet: <sup>176</sup>Lu-<sup>176</sup>Hf dates for garnet of a typical grain size ( $\emptyset > 0.5$  mm) represent (re-)crystallization of the phase. The same applies to <sup>147</sup>Sm-<sup>143</sup>Nd, except for UHT rocks and cases where *dT/dt* is much lower than commonly observed in tectonic settings.

These constraints enable the use of garnet geochronology in unravelling prograde histories of deep-crustal rocks. We used this approach to assess the enigmatic history of the deep crust underlying the Pamir-Tibetan Plateau. We obtained a detailed record of near-isobaric heating between 37.0 and 26.5 Ma and relate this directly to high mantle heat flow induced by roll-back or breakoff of the Indian plate.

[1] Kooijman *et al.* (2012) *J. Metamorph. Geol.* **30**, 397-412.

[2] Heaman *et al.* (2011) *Can. J. Earth Sci.* **48**, 205-245.

## Geomicrobiological activity in the Mesoarchean Witwatersrand-Mozaan Succession: Evidence from iron formations and shales

A.J.B. SMITH<sup>1\*</sup>, N.J. BEUKES<sup>1</sup> AND J. GUTZMER<sup>1,2</sup>

<sup>1</sup>PPM, Department of Geology, University of Johannesburg, Johannesburg, South Africa (\*correspondence: bertuss@uj.ac.za)

<sup>2</sup>Helmholtz Institute Freiberg for Resource Technology, Halsbruecker Str. 34, 09599 Freiberg, Saxony, Germany

The Mesoarchean ( $\sim 2.96\text{--}2.92$  Ga) Witwatersrand-Mozaan Succession of southern Africa is one of the oldest, well preserved supracratonic successions in the world. Numerous iron-rich units occur in this succession in the form of iron formations and iron-rich shales. Detailed studies of multiple deep level drill cores have led to the reconstruction of the lateral facies distribution of these iron-rich units. The iron formations are distal deposits, and change from hematite-magnetite, magnetite, mixed magnetite-carbonate to mixed carbonate-silicate facies towards proximal environments [1]. Proximal to the banded iron formations are iron-rich shales with manganese-rich carbonate concretions, grading into iron-poor shales and eventually sandstones [2]. This facies distribution illustrates that iron deposition only took place below wave base, likely below the photic zone. Distribution of iron was likely controlled by ferrous iron- and reduced manganese-rich hydrothermal plumes with a limited vertical extent due to neutral buoyancy [3]. Chemolithoautotrophic iron-oxidizing bacteria are inferred to have caused the precipitation of iron as ferric oxyhydroxides, with hematite preserved where the plume was not in contact with the sediment. Magnetite and isotopically light iron-rich carbonate, in contrast, formed diagenetically through interaction of the hydrothermal plume and organic carbon sourced from biological activity in the sediment [1]. The manganese-rich carbonate concretions in the more proximal iron-rich shale show evidence for dissimilatory manganese reduction of manganese originally precipitated by manganese-oxidizing bacteria [2]. Microbial oxidation of iron below the photic zone in iron formations and of manganese in shales suggest that free molecular oxygen at micro-oxic conditions were developed at depth in the the Witwatersrand-Mozaan basin since known geomicrobial processes require micro-oxic conditions.

[1] Smith *et al.* (2013) *Ec Geo.* **108**, 111-134. [2] Smith *et al.* (2010) *Geochim Cosmochim* **74** suppl 1, A973. [3] Isley (1995) *J Geol* **103**, 169-185.

## Millennial Scale Holocene Climate Variability: Iberian Precipitation Reconstructed from two Speleothems

A.C. SMITH<sup>1\*</sup>, P.M. WYNN<sup>1</sup>, P. A. BARKER<sup>1</sup>, M.J. LENG<sup>2</sup> AND S. NOBLE<sup>2</sup>.

<sup>1</sup>Environment Centre, Lancaster Univ., LA1 4YQ, UK

(\*correspondence: a.smith8@lancs.ac.uk, p.wynn@lancs.ac.uk, p.barker@lancs.ac.uk)

<sup>2</sup>NERC Isotope Geosciences Laboratory, Nottingham, UK (mjl@bgs.ac.uk, srn@bgs.ac.uk)

Palaeoclimate records from the Northern Iberian Peninsula are ideally suited to provide detailed insight into terrestrial climate change and oceanic variability. However, long duration unaltered palaeoclimate records are rare in this region. Two speleothems from a small cave in Matienzo (Cantabria) have been used in conjunction with cave monitoring to develop a continuous, high resolution isotope and trace element palaeoclimate record, which spans the Holocene and Younger Dryas. This speleothem record is interpreted in terms of changing winter precipitation amount, driven by moisture deliverance from the North Atlantic Ocean [1]. Oxygen isotope maxima occur at 1200, 3100, 4500, 5200, 8000 and 9500 years BP, suggesting significant periods of relative winter aridity throughout the Holocene.

Precipitation minima occur in phase with North Atlantic cold periods marked by IRD and identified by Bond *et al.* 1997 [2]. Concurrent alterations in oceanic and atmospheric circulation are known to cause significant reductions in moisture availability, in this case limiting precipitation in Southern Europe. The high correlation between the timing of North Atlantic cold events and speleothem isotope maxima suggests a rapid atmospheric response to changes in oceanic conditions and strong teleconnections between the northern Atlantic Ocean and mid latitudes. This speleothem offers one of the first high resolution, continuous terrestrial records of North Atlantic Ocean cold SST events. These large-scale oceanic processes appear to have dramatically influenced precipitation in northern Iberia and may have played a decisive role in environmental development in the region.

[1] Drunmond *et al.* (2011) *Climate Res.* **48**,193-201. [2] Bond *et al.* (1997) *Science* **278**, 1257-1266.

## Chemostratigraphy of Pennsylvanian Core Shale Cyclothems, Illinois Basin, Southern Indiana

CHRISTOPHER N. SMITH<sup>1,2\*</sup>, CLINTON BROACH<sup>2</sup>, HAMED CHOK<sup>1</sup>, WILLIAM S. ELLIOTT JR.<sup>3</sup> AND WILLIAM P. GILHOOLY III<sup>2</sup>

<sup>1</sup>Weatherford International Ltd  
christopher.smith4@weatherford.com\*,  
hamed.chok@weatherford.com

<sup>2</sup>Department of Earth Sciences, Indiana University-Purdue University Indianapolis  
cbroach@umail.iu.edu, wgilhool@iupui.edu

<sup>3</sup>Department of Geology and Physics, University of Southern Indiana  
wselliott@usi.edu

Major and trace element data from five Late Middle Pennsylvanian cores (Carbondale Group) were determined to investigate sediment sources and chemical conditions in the water column during organic matter deposition. A series of limestone, gray and black shale (including the Excello Shale), siltstone, sandstone and coals from a coal bed methane exploration well that penetrated the Linton and Petersburg Formations, Vanderburgh County, Southern Indiana were sampled to provide 99 core samples used in this study. These sequences were deposited in a near-shore intracratonic basin flooded by shallow epeiric seas.

Exploratory data analyses including principal component analysis (PCA) and hierarchical clustering analysis (Ward's Linkage HCA) were used to analyze the data for significant groupings of elements by lithology and total organic carbon (TOC) content. Principal component 1 (PC1) accounts for 49% of the total variance in the data and can be used to distinguish between clastic (Si, Al, K, Na, Ti) and carbonate (Ca, Sr) related elements. Principal component 2 (PC2) accounts for 19% of the total variance and is indicative of the presence or absence of redox sensitive trace element proxies for total organic carbon (Mo, U, V, Cr, Ni, Zn and Hg). Clustering analysis of sandstone and siltstones form a largely homogenous grouping for sequences interpreted as marine and non-marine, whereas there is greater heterogeneity in the groupings of both gray and black shales.

The Excello black shale shows the strongest enrichment in redox sensitive trace metal proxies for TOC. Finally, low TOC gray shales exhibit a relative enrichment in rare earth elements relative to the black shales and the North American Shale Composite (NASC), that may also reflect different sediment sources or diagenetic processes.

## Adopting a combined U-Th-Pb strategy to date speleothems >200 ka

CHRISTOPHER J.M. SMITH<sup>1\*</sup>, DAVID A. RICHARDS<sup>1</sup>, DANIEL J. CONDON<sup>2</sup>, MATTHEW S.A. HORSTWOOD<sup>2</sup>, RANDALL R. PARRISH<sup>2</sup>, JON WOODHEAD<sup>3</sup> AND DEREK C. FORD<sup>4</sup>

<sup>1</sup>School of Geographical Sciences, University of Bristol, UK (\*correspondence: chris.smith@bristol.ac.uk)

<sup>2</sup>NERC Isotope Geosciences Laboratory, British Geological Survey, UK

<sup>3</sup>School of Earth Sciences, University of Melbourne, Australia

<sup>4</sup>School of Geography and Earth Sciences, McMaster University, Canada

Speleothems are widely recognised as valuable records of palaeoenvironmental and landscape change with robust and precise chronologies to ~500 ka, principally based on the U-Th decay scheme. However, the practical upper limit for speleothem dating can be extended by the adoption of U-Th-Pb methodologies that account for disequilibrium in the decay chain, see review by Woodhead & Pickering (2012) [1]. While the range of applications is expanding, widespread adoption of these methods is hampered by the need to accurately predict, with high precision, the initial state of U-series disequilibrium (i.e.  $(^{234}\text{U}/^{238}\text{U})_{\text{initial}}$ ), and also analyse material with a sufficient range of U/Pb to provide high precision isochron age determinations.

For a suite of speleothems spanning the late Pliocene to late Pleistocene exhibiting variable U (1-100  $\mu\text{g g}^{-1}$ ) and low non-radiogenic Pb (<50  $\text{ng g}^{-1}$ ), we have adopted a combined U-Th-Pb dating strategy to take full advantage of the sensitivity and spatial resolution of available techniques. For individual growth layers, we have used: (1) rapid in-situ U-Pb LA-MC-ICPMS (193 nm ArF excimer laser) techniques, which enables fast throughput, high spatial resolution and a wide range in U/Pb for individual spots; (2) conventional U-Pb ID TIMS, for high-precision three-dimensional isochrons at lower spatial lower resolution; (3) U-Th MC-ICPMS static Faraday methods, to obtain high-precision estimates of initial  $^{234}\text{U}/^{238}\text{U}$  for material  $\geq 500$  ka.

We discuss the relative merits of each of the above methods and their combined use, focusing in particular on the compromises that have to be made between spatial resolution and age precision for speleothems with different growth rates and ages.

[1] Woodhead & Pickering, (2012) *Chem Geol* **322-323**, 290-299.

## Diamond inclusions reveal fugitive mantle nitrogen

E.M. SMITH<sup>1\*</sup>, M.G. KOPYLOVA<sup>1</sup>, M.L. FREZZOTTI<sup>2</sup> AND V.P. AFANASIEV<sup>3</sup>

<sup>1</sup>Department of Earth, Ocean and Atmospheric Sciences, University of British Columbia, 2207 Main Mall, Vancouver, BC V6T 1Z4, Canada (\*correspondence: esmith@eos.ubc.ca)

<sup>2</sup>Department of Geological Sciences and Geotechnologies, University of Milano-Bicocca, Piazza della Scienza 4, 20126 Milano, Italy

<sup>3</sup>Sobolev Institute of Geology and Mineralogy, Siberian Branch of the Russian Academy of Sciences, pr. Akademika Koptuyuga 3, Novosibirsk, 630090, Russia

Mantle volatiles in mid-ocean ridge basalts and fluid inclusions in mantle xenoliths are dominated by  $\text{CO}_2$ . Nitrogen generally appears as a trace component. However, we report diamonds from three different localities, the Kaapvaal, Congo, and Siberian cratons, that have N-rich fluid inclusions and melt inclusions.

Nitrogen in the inclusions was analyzed with micro-Raman spectroscopy. Fluid inclusions in the Siberian diamond are  $\text{CO}_2\text{-N}_2$  mixtures with  $40\pm 4$  mol%  $\text{N}_2$ . Melt inclusions in the diamonds from the Kaapvaal and Congo cratons contain exsolved bubbles of volatiles that are nearly pure  $\text{N}_2$ , with <9 mol%  $\text{CO}_2$ . At the time of trapping, the silicate melt would have contained ~1 wt% dissolved  $\text{N}_2$ .

These melt and fluid inclusions are well-preserved samples of mobile, undegassed mantle phases. Such N-rich fluids/melts reveal an unrecognized type of concentrated N flux escaping the convecting mantle. This critical observation casts uncertainty on current flux models, which otherwise suggest considerable net influx to the mantle via subduction that does not return to surface (at mid-ocean ridges, volcanic arcs, back-arc basins, and hotspots).

We propose that the  $\text{N}_2$  in our samples was liberated by oxidation from  $\text{NH}_4^+$ -bearing silicates. The coexistence of  $\text{N}_2$  and oxidized carbon species in fluid/melt inclusions supports the idea that oxidizing conditions help to mobilize N and C. This implies redox conditions control mantle nitrogen behaviour, both in terms of storage and geodynamic cycling.

Additionally, the oxidation of  $\text{NH}_4^+$  to  $\text{N}_2$  could be accompanied by isotopic fractionation. This would allow isotopically light  $\text{N}_2$  (low  $^{15}\text{N}/^{14}\text{N}$ ) to be derived from isotopically heavy subducted or stored  $\text{NH}_4^+$  (higher  $^{15}\text{N}/^{14}\text{N}$ ). This isotopic fractionation may explain the gross mismatch between isotopically heavy N influxed by subduction and the isotopically light N effluxed from the mantle, in diamonds and mid-ocean ridge basalts, for example.

## An inert desolvating nebulizer system and rapid washout accessory for tungsten isotope measurements with multicollector ICP-MS

F.G.SMITH<sup>1\*</sup>, J. HOLST<sup>2</sup>, C.PATON<sup>2</sup> AND M. BIZARRO<sup>2</sup>

<sup>1</sup>CETAC Technologies, Omaha, NE 68144 USA  
(\*correspondence: fsmith@cetac.com)

<sup>2</sup>Center for Star and Planet Formation, Natural History Museum of Denmark, University of Copenhagen, Copenhagen DK-1350, Denmark

Multicollector ICP-MS instruments are specialized devices for high-precision isotope ratio measurements. Prepared liquid samples may be concentrated (100 to 1000 mg/L) in elements of interest; these higher concentrations can cause longer analyte washout times and signal spikes. This poster will describe an inert, low flow (50 to 200  $\mu$ L/min) desolvating nebulizer system with a rapid washout accessory. This nebulizer system can also be equipped with a dedicated autosampler that features a dual-flowing rinse capability to minimize sample carryover. Wetted parts are composed of fluoropolymers such as PFA (perfluoroalkoxy) for lowest trace metal blanks and maximum chemical resistance. Optimum operating conditions for the nebulizer system with a contemporary multicollector ICP-MS for tungsten measurements will be detailed. Figures of merit will include signal enhancement, isotope ratio measurements and long-term (12 hour) ratio stability, and rinse out characteristics with and without the rapid washout accessory [1].

[1] Holst *et al.* (in review), "<sup>182</sup>Hf-<sup>182</sup>W age dating of a <sup>26</sup>Al-poor inclusion and implications for the origin of short-lived radionuclides in the early solar system." Proceedings of the National Academy of Sciences.

## Biogenic new particle formation and its potential impacts on climate

J. N. SMITH<sup>1,2\*</sup>, M. LAWLER<sup>2</sup>, P. WINKLER<sup>3</sup>, J. ZHAO<sup>4</sup>, AND P. MCMURRY<sup>4</sup>

<sup>1</sup>National Center for Atmospheric Research, Boulder, CO 80307 USA (\*correspondence: jimsmith@ucar.edu)

<sup>2</sup>University of Eastern Finland, 70211 Kuopio, Finland

<sup>3</sup>University of Vienna, 1090 Vienna, Austria

<sup>4</sup>University of Minnesota, Minneapolis, MN 55455 USA

Observations show that growth rates of freshly nucleated atmospheric nanoparticles are about 5-10 times higher than can be accounted for by sulfuric acid condensation. This additional growth is primarily due to the uptake of organic compounds, often of biogenic origin, by processes that are not yet understood and that might include condensation of low-volatility vapors or reactions that occur on or within particles. If the growth of freshly nucleated atmospheric aerosols is sufficiently fast, these particles can reach sizes required to serve as cloud condensation nuclei (CCN), and may thereby potentially affect the climate.

We have performed laboratory and field measurements focusing on understanding the role of biogenic organic compounds in the formation and growth of atmospheric aerosols. Measurements were made using the Thermal Desorption Chemical Ionization Mass Spectrometer (TDCIMS), an instrument capable of realtime measurements of the molecular composition of ambient aerosols as small as 10 nm in diameter. In recent laboratory experiments of new particle formation from  $\alpha$ -pinene ozonolysis, high molecular weight ( $m/z$  430-560) low volatility gases correlated with initial stages of particle formation [1]. Additional work has focused on identifying particle phase compounds present in nanoparticles of varying size during the earliest stages of growth: in those studies organic acids were observed in the smallest particles formed by nucleation [2].

Our laboratory results are also compared to field observations of nanoparticle composition and gas phase precursors at sites in which biogenic emissions dominate. These include an isoprene-dominated region (Columbia, MO), and several sites with a mixture of terpene emissions (Hyytiälä, Finland, Manitou Forest, Colorado). These observations show that atmospheric nanoparticles are often enriched with organic acids and nitrogen-containing compounds. These particles are often quite hygroscopic, and thus may have a far greater effect on cloud formation than previously thought.

[1] Zhao *et al.* (2013) ACPD **13**, 9319-9354. [2] Winkler *et al.* (2012) GRL **29**, L20815.

## Western Oregon as a low-sediment end member of particulate organic carbon export from temperate forested uplands

J.C. SMITH<sup>1\*</sup>, A. GALY<sup>1,2</sup>, N. HOVIUS<sup>3</sup> AND A. TYE<sup>4</sup>

<sup>1</sup>Department of Earth Sciences, University of Cambridge, Cambridge CB2 3EQ, United Kingdom (\*correspondence: jcs74@cam.ac.uk)

<sup>2</sup>(ajbg2@cam.ac.uk)

<sup>3</sup>German Research Centre for Geosciences GFZ, 14473 Potsdam, Germany (hovius@gfz-potsdam.de)

<sup>4</sup>British Geological Survey, Keyworth, Nottingham NG12 5GG, United Kingdom (atye@bgs.ac.uk)

The transfer of continental biomass to geological storage has the potential to sequester considerable amounts of carbon dioxide. Despite an initial focus on active mountain belts as prime locations for this erosion, temperate forested uplands might also have a significant role to play.

In some temperate catchments with high connectivity between hillslopes and actively incising channels, clastic yield is high, but soil is preferentially mobilised by overland flow beyond a moderate discharge threshold, resulting in the export of globally significant amounts of biomass [1]. However, these processes are not universal in temperate forested uplands. Using organic carbon and nitrogen elemental and isotopic ratios, we present results revealing contrasting particulate organic carbon dynamics in the headwaters of Western Oregon. Suspended sediment concentrations are typically very low, while organic carbon concentrations frequently reach 30%. A lack of active incision has led to the development of flat, thickly vegetated riparian zones which isolate hillslopes. Nevertheless, considerable amounts of soil and plant material are eroded from the channel and immediately adjacent areas during rain. Such settings export non-fossil organic carbon at rates of  $\sim 6 \text{ t km}^{-2} \text{ yr}^{-1}$ , around half the rate from the high-sediment temperate end member. Contrasts between the two systems suggest that ecosystem biology is the principal control on POC export style in temperate forested uplands.

Comparison of our results with studies made downstream of these headwaters at their entry to the Pacific Ocean [2, 3] offers new insights into the fate of biomass mobilised in Oregon's uplands and similar settings.

[1] Smith *et al.* (2013), *Earth Planet Sc Lett* **365**, 198-208. [2] Hatten, Goñi & Wheatcroft (2012), *Biogeochemistry* **107**, 3-66. [3] Goñi *et al.* (2013), *J Geophys Res-Bioge* **118**, 1-23.

## Helium equilibrium between pore water and quartz: A clever, but limited tool

S.D. SMITH<sup>1,2\*</sup>, G.A. HARRINGTON<sup>1</sup>, B.D. SMERDON<sup>1</sup> AND D.K. SOLOMON<sup>2</sup>

<sup>1</sup>CSIRO Water for a Healthy Country Flagship, Urrbrae, SA 5064, Australia

(\*correspondence: stan.smith@csiro.au)

(glenn.harrington@csiro.au, brian.smerdon@csiro.au)

<sup>2</sup>Dept. of Geology and Geophysics, Univ. of Utah, Salt Lake City, UT 84112, USA (kip.solomon@utah.edu)

Pore water helium concentrations calculated from quartz helium concentrations [1] offer a unique tool to determine helium distribution in low permeability formations. Analyses have been carried out on shale and sandstone core samples from the San Juan Basin, USA and the Eromanga and Surat basins, Australia.

Comparing quartz-derived helium concentrations to direct pore water concentrations reveal up to an order of magnitude difference between the two. This uncertainty is unacceptable for modelling vertical helium transport to constrain estimates of fluid flux. However, in the San Juan Basin, <sup>3</sup>He/<sup>4</sup>He ratios agree between methods. In the Eromanga Basin, modelling indicates >90% equilibrium is expected, however, when compared with direct pore water measurements [2], as low as 10% of equilibrium is observed. Regardless of present-day equilibrium, the method could be useful for paleohydrology studies, provided the timing of equilibrium can be constrained.

The method appears more promising in deeper (thus hotter) basins where the equilibrium time between pore water and quartz is reduced significantly. In shallow systems, the equilibrium time may greatly exceed the lifespan of shallow, quasi-steady state hydrological systems. Further testing of the method in additional basins may result in an adequate screening method to find where the method is applicable. The possibility exists that this method will not come to fruition as too much uncertainty remains and equilibrium is found in theory instead of in the samples.

[1] Lehmann, Waber, Tolstikhin, Kamensky, Gannibal, & Kalashnikov (2003) *Geophys Res Lett* **30**, 4. [2] Gardner, Harrington, & Smerdon (2012) *J. Hydrol* **468**, 63-75.

## Using tephra layers to provide absolute and relative chronologies for sedimentary archives: An example from the Lake Suigetsu SG06 record from Japan

V.C. SMITH<sup>1</sup>, R.A. STAFF<sup>1</sup>, D. F. MARK<sup>2</sup>,  
S.P.E. BLOCKLEY<sup>3</sup>, C. BRONK RAMSEY<sup>1</sup>  
AND T. NAKAGAWA<sup>4</sup>

<sup>1</sup>Research Laboratory for Archaeology and the History of Art, University of Oxford, Oxford OX1 3QY, U.K.  
(victoria.smith@rlaha.ox.ac.uk)

<sup>2</sup>Scottish Universities Environmental Research Centre (SUERC), East Kilbride G75 0QF, U.K.

<sup>3</sup>Centre for Quaternary Research, Royal Holloway University of London, Egham TW20 0EX, U.K.

<sup>4</sup>Department of Geography, University of Newcastle, Newcastle Upon Tyne NE1 7RU, U.K.

The Lake Suigetsu SG06 sedimentary archive from Honshu Island, central Japan, provides a high-resolution palaeoenvironmental record for the last 150 kyrs. The 73 m-long record contains numerous layers tephra (30 visible and numerous cryptotephra) sourced from explosive volcanism from Japan and South Korea. These marker layers can be used for both relative and absolute chronology.

The glass chemistry of these tephra is typically unique, therefore most of the layers can be correlated to those in other archives and to specific eruptions [1]. Since many of these layers are widespread (>600 km from source) these isochrons allow for the assessment of leads and lags in palaeoclimate across the region.

The tephra can also be dated using <sup>40</sup>Ar/<sup>39</sup>Ar methods. These <sup>40</sup>Ar/<sup>39</sup>Ar ages are crucial for constraining the pre-50 ka SG06 age model. Correlating these distal SG06 tephra layers to proximal deposits is essential as large crystals are required to obtain precise and <sup>40</sup>Ar/<sup>39</sup>Ar ages and these are only abundant in the coarser proximal deposits [2].

Precise radiocarbon dates have been obtained for all the post-50 ka visible SG06 tephra layers [1] using the modelled radiocarbon data and varve chronology [3]. These radiocarbon dates and <sup>40</sup>Ar/<sup>39</sup>Ar ages of the eruptions can significantly improve the age models of other archives in which the tephra are found.

[1] Smith *et al.* (2013) *Quaternary Science Reviews* **67**, 121-137. [2] Smith *et al.* (2011) *Quaternary Science Reviews* **30**, 2845-2850. [3] Bronk Ramsey *et al.* (2012) *Science* **338**, 370-374.

## Molecular simulation of aqueous electrolyte solutions

WILLIAM R. SMITH<sup>1,2</sup>\*, FILIP MOUČKA<sup>3</sup>  
AND IVO NEZBEDA<sup>4</sup>

<sup>1</sup>University of Ontario Institute of Technology, Faculty of Science;

<sup>2</sup>University of Guelph, Mathematics and Statistics,  
(william.smith@uoit.ca \*presenting author)

<sup>3</sup>J.E. Purkinje University, Physics, (fmoucka@seznam.cz)

<sup>4</sup>J.E. Purkinje University, Chemistry, (inezbeda@icpf.cz)

We employ the Osmotic Ensemble Monte Carlo (OEMC) algorithm [1] to predict the solute and water chemical potentials in aqueous electrolyte solutions. OEMC implements a Semi-Grand Canonical Ensemble simulation of the solution phase, which can be viewed as an application of the Reaction Ensemble Monte Carlo algorithm [2] to the case of an inter-phase chemical reaction, including speciation reactions as appropriate.

Focusing on aqueous NaCl at ambient conditions, we present the following:

1. An improved electrolyte force field based on SPC/E water and a simple charged Lennard-Jones sphere model, determined by fitting the concentration dependence of the density and chemical potential, and the solubility.
2. Calculations of the concentration dependence of the water chemical potential and demonstration of thermodynamic consistency with the electrolyte chemical potential using the Gibbs-Duhem equation.
3. Electrolyte chemical potentials at finite concentrations for polarizable force fields for water and the electrolyte, using the Multi-Particle Move Monte Carlo method [3].
4. Calculations predicting the onset of homogeneous nucleation in supersaturated aqueous electrolyte solutions.

[1] F. Moučka, I. Nezbeda, W.R. Smith, *J. Phys. Chem.* **B116**, 5468 (2012); *idem*, *J. Chem. Phys.*, in press (2013). [2] W.R. Smith, B. Tríska, *J. Chem. Phys.* **100**, 3019 (1994) [3] F. Moučka, M. Rouha, and I. Nezbeda, *J. Chem. Phys.* **126**, 224106 (2007).

## The North Australian Craton: A Palaeoproterozoic accretionary orogen

R.G. SMITS<sup>1,2\*</sup>, W.J. COLLINS<sup>2</sup> AND M. HAND<sup>1</sup>

<sup>1</sup>Centre for Tectonics, Resources and Exploration, University of Adelaide, S.A. 5005, Australia, russell.smits@adelaide.edu.au

<sup>2</sup>School of Environmental and Life Sciences, University of Newcastle, NSW 2308, Australia,

The North Australian Craton (NAC) is 1,830,000 km<sup>2</sup>, making up almost one quarter of Australia. The development of this system has a broad spatial and temporal organization such that sedimentation, magmatism and tectonism generally migrated southward over the interval ~2000 to 1700 Ma, and at least in the northern parts of the craton, appears to have a late Archaean substrate. In most regions, within 10-20 Ma, sedimentation was followed by deformation and granite-dominated magmatism associated with high thermal gradient metamorphism, pointing to a systematic pattern of crustal consolidation as the craton developed.

Detrital zircon spectra, maximum depositional of sediments, distribution of mafic intrusives and Hf isotopes over the NAC indicates a southerly migration of depositional activity from the Pine Creek Orogen in the north to the Arunta Orogen in the south, with two main phases of basin formation between 1880-1850 and 1830-1780 Ma. The sediments of these basins share common zircon detritus populations, particularly Neoproterozoic sources. A general trend toward more primitive Hf values with time is typical for retreating accretionary orogens. The Archean detrital populations recorded in sediments from all regions of the NAC, Hf isotopic data coupled with the systematic spatial and temporal pattern of magmatism and deformation/metamorphism is consistent with an Archean substrate that migrated southwards over a period of ~300 Ma. We can envisage such a migration as being controlled by a long-lived retreating margin, with distinct "pulses" of magmatism related to periods of accelerated extension. This scenario suggests that the NAC developed in an oceanic back arc setting, rather than in an intracratonic setting as has been recently proposed. The model implies that formation of Palaeoproterozoic continental lithosphere can be efficiently achieved in back arc settings, similar to the modern-day western Pacific.

## Terrestrial temperature response during Early Eocene hyperthermals

K.E. SNELL<sup>1\*</sup>, H.C. FRICKE<sup>2</sup>, W.C. CLYDE<sup>3</sup>  
AND J. M. EILER<sup>1</sup>

<sup>1</sup>Div. of Geological and Plan. Sci., Caltech, Pasadena, CA 91125 (\*correspondence: ksnell@caltech.edu)

<sup>2</sup>Geology Dept., Colorado College, Colorado Springs, CO 80903

<sup>3</sup>Dept. of Earth Sciences, Univ. of New Hampshire, Durham, NH 03824

The Early Eocene is marked by a number of rapid global warming events called hyperthermals that are associated with negative carbon isotope excursions (CIE) in both marine and terrestrial records. Each theory to explain the connection of these hyperthermals with the CIEs predicts a different climatic response. Characterizing the timing, duration and magnitude of temperature change will help establish their cause and possibly establish whether or not they are driven by a single process. It is possible that all share a common underlying cause; if so, we might predict that the temperature change during each hyperthermal is proportional to the magnitude of its associated CIE (and perhaps exhibit other similarities, such as the relative amplitudes of marine and terrestrial temperature change). To our knowledge, the only hyperthermal for which we know the terrestrial temperature change is the Paleocene-Eocene Thermal Maximum (PETM).

Here we use carbonate clumped isotope ( $\Delta_{47}$ ) thermometry of paleosol carbonates from the Bighorn Basin (Wyoming, USA) to produce paleotemperature estimates at high temporal resolution for Early Eocene hyperthermals ETM2 and H2. Average baseline temperatures (which likely reflect near-peak summer ground temperatures) before and after the two hyperthermals are ~28°C and increase to ~38°C during the apex of each CIE; temperatures appear to recover close to baseline temperatures between ETM2 and H2. These data (combined with previous constraints on the PETM) suggest that both the absolute temperatures and the magnitudes of temperature change associated with the PETM, ETM2 and H2 are similar (within error); the magnitudes of temperature change (~10°C) also appear similar to/slightly greater than that found in arctic sediments [1]. In addition, our record shows a cooling interval within the peak of ETM2 that is similar in pattern to an event that is present in the arctic record [1]. These results suggest that the temperature change associated with the hyperthermals does not necessarily scale with the magnitude of the local CIEs from paleosol carbonate nodules (~6‰ for the PETM and ~4‰ for ETM2). For ETM2, the CIE appears to precede warming.

[1] Sluijs *et al.* (2009) *Nature Geoscience*, 2, 777-780.

## Dissolution rates and surface chemistry of calcium aluminosilicate glasses in cementitious systems

R. SNELLINGS<sup>1\*</sup> AND K. SCRIVENER<sup>1</sup>

<sup>1</sup>Institute of Materials, EPFL, Lausanne, Switzerland  
(\*correspondence: ruben.snellings@epfl.ch)

Waste calcium aluminosilicate (CAS) glasses are widely used as supplementary cementitious materials in Portland-cement based construction materials for environmental, economical and technical reasons. The amount of cement that can be replaced by waste CAS is largely depending on their reactivity and composition. Understanding the reactivity or rates of dissolution of these wastes in typical Portland cement pore solutions of high ionic strength and alkalinity (pH  $\approx$  13) is of great importance to optimise the performance, durability and sustainability of the blended Portland cements.

Water quenched synthetic CAS glasses of selected compositions ranging from pure silica framework to CaO-rich depolymerized glasses were subjected to batch dissolution reactions avoiding hydration product precipitation. The obtained dissolution rates scaled linearly with the Ca/(Al+Si) molar ratio, and showed a large difference in reactivity between framework and partially depolymerised glasses (Fig. 1).

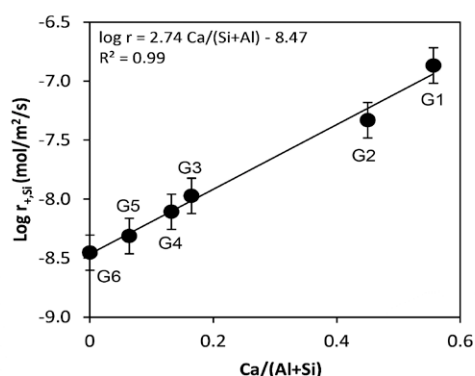


**Figure 1:** Dependence of glass dissolution rate at pH 13 on the molar Ca(Al+Si) ratio of the glass.

Glass dissolution rates also depended on solution composition. Increasing Al activity decreased dissolution rates of framework glasses, while increasing Ca activity decreased dissolution rates of all glasses. The glass surface chemistry as a function of solution pH and composition was investigated by XPS, zeta potential measurements and surface titrations and lead to a model of CAS glass dissolution for high pH cement type environments.

## Isotopic Tomography of Monazite

DAVID R. SNOEYENBOS<sup>1\*</sup>, EMILY M. PETERMAN<sup>2</sup>,  
MICHAEL J. JERCINOVIC<sup>3</sup>, MICHAEL L. WILLIAMS<sup>3</sup> AND  
DAVID A REINHARD<sup>4</sup>

<sup>1</sup>Box 513, Chesterfield, MA 01012 USA

\*correspondence: kyanite@mac.com

<sup>2</sup>Bowdoin College, Brunswick, ME 04011 USA

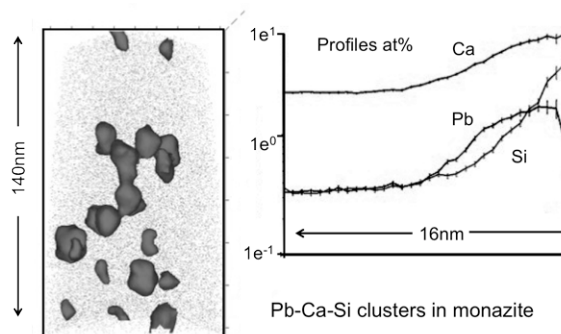
<sup>3</sup>University of Massachusetts, Amherst, MA 01002 USA

<sup>4</sup>Cameca Instruments Inc., Madison, WI 53711 USA

In Atom Probe Tomography (APT) a specimen is evaporated atom by atom, and the mass/charge and original position (X,Y, Z to 0.2nm) of each detected atom is recorded to produce a quantitative 3-D reconstruction at the atomic scale. APT can also provide *in situ* atomic scale isotopic tomography of U, Th and radiogenic Pb, allowing access to otherwise cryptic thermochronologic information.

A polymetamorphic monazite grain from the Churchill Province, Canada was selected for analysis by APT. Prior EPMA analysis indicates monazite crystallization at 2.55Ga, overgrowth at 2.37Ga, and fracture-infill and further overgrowth at 1.84Ga. Datasets of up to 200 million atoms were collected, sampling the various domains and their mutual interfaces.

Distinct clusters of Pb atoms <10nm dia. and spaced at 20–30nm were observed in the older, reheated domain. These clusters contain up to 1.7 at.% Pb, 4 at.% Si and 7 at.% Ca in a radial structure. These clusters closely resemble those found by APT in reheated zircon [1. Valley *et al.*]. The presence of <sup>208</sup>Pb, <sup>207</sup>Pb and <sup>206</sup>Pb in the clusters indicates post-crystallization segregation of radiogenic Pb from both the Th and U decay chains. Because Th and U enter the monazite structure via coupled substitution (e.g. Th+Ca, Th+Si and U+Si), Si and Ca in the clusters may represent the unpaired atoms after radionuclide decay. To measure an isotopic age at this scale, precise <sup>207</sup>Pb/<sup>206</sup>Pb determination requires a minor correction for interfering species such as (ThPO<sub>3</sub>)<sub>3</sub>+



[1] Valley, J. W. *et al.* (2012) Elemental and isotopic tomography at Single-Atom-Scale in 4.0 and 2.4 Ga zircons. Abstract V12A-05 presented at 2012 Fall Meeting, AGU, San Francisco, Calif., 3-7 Dec.



## Potential temperatures of convecting mantle based on Al partitioning between olivine and spinel

A.V.SOBOLEV<sup>1,2</sup>, V.G.BATANOVA<sup>1,2</sup>, D.V.KUZMIN<sup>3</sup>  
AND N.T.ARNDT<sup>1</sup>

<sup>1</sup>ISTerre, University J. Fourier, Grenoble, France,  
alexander.sobolev@ujf-grenoble.fr

<sup>2</sup>Vernadsky Institute of Geochemistry RAS, Moscow, Russia

<sup>3</sup>Sobolev Inst. of Geol and Min, SBRAS Novosibirsk, Russia

Knowledge of potential temperatures of convecting mantle is required for the understanding the global processes on the Earth [1]. The common way to estimate these is the reconstruction of primary melt compositions and liquidus temperatures based on the Fe-Mg partitioning between olivine and melt. This approach requires knowledge of the compositions of primitive melts in equilibrium with olivine alone as well as composition of olivine equilibrium with primary melts. This information is in most cases unavailable or of questionable quality. Here we report a new approach to obtain crystallization temperatures of primary melts based on the olivine-spinel Al-Cr geothermometer [2]. The advantages of this approach are: (1) common presence of spinel in assemblage with high-Mg olivine and (2) low rate of diffusion of Al in the olivine, which promises to preserve high magmatic temperatures.

We analysed over one thousand spinel inclusions and high-Mg host olivines from different MORB, OIB and Archean komatiites on the JXA-8230 EPMA at ISTerre, Grenoble, France. Concentrations of Al, Ti, Na, P, Zn, Cr, Mn, Ca, Co, Ni were determined with a precision of 10 ppm (2 standard errors) using a newly developed protocol [3]. When available, we also analysed matrix glass and glass inclusions in olivine and found that temperature estimations from olivine-spinel (Al-Cr) and olivine-melt (Fe-Mg)[4] equilibrium match within (+/-30 degree C).

The results show contrasting crystallization temperatures of Mg-rich olivine of the same Fo content from different types of mantle-derived magmas, from the lowest (down to 1220 degree C) for MORB to the highest (up to 1500 degree C) for komatiites. These results match predictions from Fe-Mg olivine-melt equilibrium and confirm the relatively low temperature of the convecting mantle source of MORB and higher temperatures in the mantle plumes that produce the OIB of Iceland, Hawaii, Gorgona, and Archean komatiites.

[1] McKenzie & Bickle, 1988, *J. Petr.* 29, p 625-679. [2] Wan et al, 2008, *Am. Min.* 93, p1142-1147. [3] Batanova & Sobolev, 2013, *Min. Mag.* (this issue). [4] Ford et al, 1983, *J. Petr.* 24, p 256-265.

## Crystallization of P-rich minerals from the high phosphorus rare-metal magma of East-Kalguty dyke belt (S.Altay, Russia)

SOKOLOVA E<sup>1,2\*</sup> AND SMIRNOV S.Z.<sup>1,2</sup>

<sup>1</sup> V.S. Sobolev Institute of Geology and Mineralogy SB RAS, Novosibirsk, Russia

(\*correspondence: ekaterina@igm.nsc.ru)

<sup>2</sup> Novosibirsk State University, Novosibirsk, Russia

High phosphorus content is an important feature of some highly evolved peraluminous Ca-poor granitoids, associated with ore deposits. East-Kalguty dyke belt (South Altai, Russia) is one of the few representatives of rare-metal rich felsic high-phosphorus rocks (avg 0.39 wt % P<sub>2</sub>O<sub>5</sub> and ASI=1.23). In this case alkali feldspars (Af) represent significant reservoir of phosphorus, containing 0.14 wt % P<sub>2</sub>O<sub>5</sub> in average. Incorporation of P into feldspars involves the substitution  $2\text{Si}^{4+} = \text{Al}^{3+} + \text{P}^{5+}$ [1].

Average P-content 0.27 wt % of P<sub>2</sub>O<sub>5</sub> in the melt equilibrated with Af phenocrysts from dyke rocks was calculated from dependence  $\text{ASI} = 0.7273 * \text{D}[\text{P}]/\text{Af}/\text{melt} + 0.7818$  derived by D.London on the basis of experimental data [1].

Direct measurement of P<sub>2</sub>O<sub>5</sub> by EMPA in melt inclusions in quartz phenocrysts showed 0.29 wt %, which is in good agreement with the calculated value. This means that Af crystallized from the same melt with quartz phenocrysts.

Comparison of Ca and P content, and Ca/P ratio in the melt inclusions and rocks shows that apatite crystallized before entrapment of the melt inclusions in quartz. Low Ca content results in excess of phosphorus in the evolved melts, which was later incorporated into feldspars and ambligonite LiAl[PO<sub>4</sub>](OH). Main intrusive phase of the Kalguty granite massif, preceding to rare-metal dykes, have P-content close to the clark of felsic rocks [2]. The increase of P in latest dykes, which reaches a maximum in the rare-metal rich dykes is explained by introduction of phosphorus by external fluids into magmatic system with subsequent its accumulation in the course of magma differentiation.

*This study was supported by grants RFBR 12-05-31-290 and 13-05-00471.*

[1] London (1992), *American Mineralogist* 77, 126-145. [2] Vinogradov (1962), *Geochemistry* 7, 555-565

## Reactive transport modeling of cement/concrete – rock interaction: The Tournemire and Maqarin cases

JOSEP M. SOLER<sup>1</sup>

<sup>1</sup>IDAEA-CSIC, 08034 Barcelona, Catalonia, Spain

In the framework of the GTS-LCS project (JAEA-Japan, NAGRA-Switzerland, NDA-UK, POSIVA-Finland, SKB-Sweden), reactive transport modeling of 2 analogues of cement-rock interaction in a repository is being performed: The DM borehole at Tournemire (France) and the Eastern Springs hyperalkaline system at Maqarin (Jordan). In Tournemire solute transport is dominated by diffusion between concrete and rock (mudstone); in Maqarin there is flow along a fracture zone from a cement-like metamorphic rock body with diffusion between fracture and wall rock (clay-containing limestone). The two cases are examples of diffusion (Tournemire) and fracture-flow (Maqarin) dominated systems. In the modeling presented here, calculations have been performed with the CrunchFlow reactive transport code. Results are compared with observations.

Results for the Tournemire case (concrete-mudstone interaction during 15 years) show sealing of porosity at the rock side of the interface (mm scale) due to the precipitation of C-A-S-H, calcite and ettringite, together with clay dissolution. The location of sealing is influenced by cation exchange. Without exchange, sealing is at the concrete side of the interface.

The hyperalkaline system at Maqarin may have been active for tens or several hundreds of thousands of years. The high-pH solution flows along the full length of the fracture (ca. 80 m), with intense mineral alteration in the wall rock (cm scale). Major secondary minerals include ettringite-thaumasite, C-S-H/C-A-S-H and calcite. C-S-H/C-A-S-H precipitation is controlled by the dissolution of primary silicates. Ettringite precipitation is controlled by diffusion of sulfate and aluminum from the wall rock to the fracture, with aluminum provided by the dissolution of albite. Calcite precipitation is controlled by diffusion of carbonate from the wall rock. Extents of porosity sealing along the fracture and in the fracture-wall rock interface depend on assumptions regarding flow velocity and composition of the high-pH solution. The multiple episodes of fracture sealing and reactivation evidenced in the fracture infills were not included in the simulations.

Financial support from POSIVA and the many discussions with the LCS team are gratefully acknowledged.

## Spatial heterogeneity of benthic methane dynamics in the subaquatic canyons of the Rhone River Delta (Lake Geneva)

S. SOLLBERGER<sup>1,2\*</sup>, J.P. CORELLA<sup>3</sup>, S. GIRARD CLOS<sup>3</sup>, M.-E. RANDLETT<sup>1,2</sup>, C.J. SCHUBERT<sup>1</sup>, D. SENN<sup>1,2</sup>, B. WEHRLI<sup>1,2</sup> AND T. DELSONTRO<sup>1,2</sup>

<sup>1</sup>Eawag, Swiss Federal Institute of Aquatic Science and Technology, CH-6047 Kastanienbaum, Switzerland

<sup>2</sup>Institute of Biogeochemistry and Pollutant Dynamics, ETH Zurich, CH-8092 Zurich, Switzerland

<sup>3</sup>Environmental Science Institute (ISE) and Dept. of Geology and Paleontology, University of Geneva, CH-1205 Geneva, Switzerland

\* *correspondence*: sebastien.sollberger@eawag.ch

Heterogeneous benthic methane (CH<sub>4</sub>) dynamics from river deltas, resulting from variable organic matter accumulation, have been recently reported in various aquatic and marine environments. The spatial heterogeneity of CH<sub>4</sub> sediment release from the Rhone delta of Lake Geneva (Switzerland/France) was thus investigated. Methane benthic dynamics were compared (1) between three underwater canyons of different sedimentation regimes, (2) along a longitudinal transect of the canyon most influenced by the Rhone River, and (3) laterally across a canyon. Results indicate higher CH<sub>4</sub> diffusion rates in the canyon, which continuously receives loads from the Rhone River compared to the other canyons, as well as in intermediate sites instead of proximal and distal reaches of the canyon. The lateral canyon survey results were inconclusive due to the shorter length of the cores. The more allochthonous material is found in higher sedimentation rate environments and partially explained the greater CH<sub>4</sub> diffusion rates. The lower river velocity in the intermediate region characterized by a smaller fraction of coarser sediment allowed more organic matter to settle down and be preserved. This induced higher CH<sub>4</sub> diffusion rates than in the proximal region, where the upper layer of sediments were potentially more disturbed by a stronger river inflow. Total CH<sub>4</sub> sediment release was found to range from 0.9 to 1.2 x 10<sup>4</sup> t CH<sub>4</sub> yr<sup>-1</sup> for the entire delta, although it is most likely oxidized before CH<sub>4</sub> reaches the atmosphere due to the oxic water column. Finally, turbidites were shown to act as sealing layers beneath which CH<sub>4</sub> could accumulate in high amounts and potentially act as source layers for ebullition.

## Spatial microbial community structure of a shallow-water hydrothermal system

MIRIAM SOLLICH<sup>1,2\*</sup>, IOULIA SANTI<sup>3</sup>, PETRA POP RISTOVA<sup>1</sup>, THOMAS PICHLER<sup>2</sup>, KAI-UWE HINRICHS<sup>1,2</sup> AND SOLVEIG I. BÜHRING<sup>1</sup>

<sup>1</sup>MARUM & <sup>2</sup>Dept. of Geosciences, University of Bremen, Bremen, Germany (\*correspondence: msollich@uni-bremen.de)

<sup>3</sup>Max Planck Institute for Marine Microbiology, Bremen, Germany

Marine shallow-water hydrothermal systems are extreme environments, characterized by discharge of hot and often acidic fluids with elevated concentrations of reduced compounds. Steep physico-chemical gradients on small spatial scales lead to the formation of various microniches for microbial communities. In contrast to deep-sea hydrothermal systems, the sun light in shallow systems results in a combination of photoautotrophic and chemoautotrophic primary production. Despite the comparably easy accessibility of shallow-water hydrothermal systems, little is known about the spatial microbial community structure and its relationship to physico-chemical conditions.

Here, we present data for the system off Milos island, one of the most hydrothermally active regions in the Mediterranean Sea. A combined approach of gene- and lipid-based techniques (ARISA and intact polar lipids) with porewater geochemistry data was applied along a temperature gradient to investigate the spatial microbial community structure.

Supported by statistical analyses, ARISA data revealed significant changes of the bacterial community structure along the temperature gradient and depth profiles from hydrothermally unaffected areas towards the vent orifices. Intact polar lipid results are consistent with the ARISA data and clearly differentiate samples from close to the vent outlet from those in less affected areas. Changes from phospho- and betaine lipids within the top layer of the unaffected area to glyco- and ornithine lipids in the hydrothermally influenced sediment layers show a change from photoautotrophic algae to a bacteria-dominated community.

Statistical analyses revealed that changes in the microbial community structure were mostly related to spatial heterogeneity in pH and sulfide and less to temperature.

The innovative approach to combine gene- and lipid-based methods proved to be very useful to describe the spatial microbial structure.

## Biogeochemical features of the behavior of arsenic in Sherlovogorsk mining district of the Zabaikalsky Krai (Russia)

M.A. SOLODUKHINA AND G.A. YURGENSON

Federal state budget institution of science, Institute of Nature Recourses, Ecology and Cryology, Siberian Branch of Russian Academy of Sciences, Chita, Russia (mabn@ya.ru, yurgga@mail.ru)

As a result of multiyear research (2002-2012 gg.) conducted in Sherlovogorsk mining district of the Zabaikalsky Krai, the peculiarities of biogeochemical behaviour As in the components of the landscape. Shows the sources of his income, concentration, regularities of the spatial distribution of the soil, especially biological capture and accumulation in plants.

The spatial distribution of arsenic (As) on the territory of the region is due to the regularities of the development of the second phase of formation of Sherlovogorsk of ore-magmatic system, which is associated with the formation of tin-polymetallic Deposit.

All of the components of landscapes Sherlovogorsk ore district has considerably enriched with As. It is established, that in natural soils background of the site content As in 6 times exceeds MPC and in 2 times - soil Clark. On the territory of the fields maximum Clark concentration (CC) in the soil (the ratio of the average content in the soil to the soil Clark) is 1183, and the excess of MPC in 1005 times. In техноземе career-dumping landscape respectively QC=340, and the excess of MPC in 289 times. Sherlovogorsk ore area can be identified as arsenic biogeochemical province.

The main form of location As in soils is the residual. In the permafrost meadow-forest, in gravelly low-power soil, Chernozem without carbonates, in the chestnut carbonate soil more than 50% As fixed in a stationary position in the oxidation products arsenopyrite, first of all skorodit and other arsenates.

Capture As different plants varies considerably. Herbaceous plants and shrubs more intensively involve As in biological Cycling, than shrubland. Of wood and shrub of plants *Crataegus sanguinea* Pallas and *Betula pendula* Roth do not have гипераккумуляцией As, in contrast to the bushes: *Pentaphylloides fruticosus* (L.) O. Schwarz, *Pentaphylloides parvifolia* (Fischer ex Lehm.) Sojak and *Artemisia gmelinii* Weber ex Stechm. In them, just as in the grassy plants of natural-technogenic landscape detected toxic and critical concentration As (more than 5 mg/kg).

For the majority of the studied plants tend maximum capture As roots and leaves, by the end of the vegetation period is marked its accumulation in these bodies. Minimum contents As found in fruits and seeds.

The obvious hubs, As are herbaceous plants: *Potentilla acervata* Sojak, *Aconogonon angustifolium* (Pall.), *Gallium verum* L. and subshrubs - *Artemisia gmelinii* Weber ex Stechm.

## Melting and breakdown of MgCO<sub>3</sub> at high pressures

N.A. SOLOPOVA<sup>1,2,\*</sup>, A.V. SPIVAK<sup>2</sup>, YU.A. LITVIN<sup>2</sup>  
AND L. S. DUBROVINSKY<sup>1</sup>

<sup>1</sup>Bayerisches Geoinstitut, University of Bayreuth, Bayreuth, Germany, (\*corresponds: solopenok@yandex.ru)

<sup>2</sup>Institute of Experimental Mineralogy of the Russian Academy of Sciences, Chernogolovka, Moscow region, Russia

Studies inclusions in ultra-deep diamonds suggest that magnesite can be major stable carbonate in the lower mantle. It can play an important role for the carbon cycle in the Earth's interior. New form of magnesite II was reported at the high-pressure and high-temperature [1]. However, the information about melting of magnesite at high pressure is limited [2].

We study high-pressure high-temperature behavior of magnesite, stability of the melt and its decomposition in static compression experiments between 10 and 60 GPa and temperatures up to 3500 K using diamond anvil cell technique with laser heating. Special methodology was used for determining the melting point. The spherical boron doped diamonds were used as a heat absorber for laser heating.

In accordance with thermodynamic analysis [3] our experimental results showed that magnesite does not decompose to MgO and CO<sub>2</sub> under conditions of the Earth's lower mantle and demonstrate extended field of congruent melting of magnesite. We observed also formation of MgO and diamond or graphite as a result of decomposition of MgCO<sub>3</sub> melt. Formation of diamond and graphite may be explained by a two stage reaction: MgCO<sub>3</sub>=MgO+CO<sub>2</sub>; CO<sub>2</sub>=C+O<sub>2</sub>.

The obtained results allow to determine the phase relations of MgCO<sub>3</sub> at high pressures and high temperatures, and important for constraining the conditions of diamond crystallization from the carbonate-bearing parental media in the Earth's lower mantle.

[1] Isshiki, Irifune, Hirose & Ono (2004), *Nature* 427, 60-62.

[2] Katsura & Ito (1990), *Earth and Planetary Science Letters* 99, 110-117. [3] Dorogokupets (2007), *Geokhimiya* 6, 624-631.

This work was funded by grant RFBR 12-05-33044.

## Complex C-O-H-N-S fluids and sulphide-silicate melt immiscibility in the upper mantle

I. SOLOVOVA<sup>1,\*</sup>, A. BOUIKINE<sup>2</sup>, L. KOGARKO<sup>2</sup>  
AND A.B. VERCHOVSKY<sup>3</sup>

<sup>1</sup>Institute of Geology of Ore Deposits solovova@igem.ru

<sup>2</sup>Vernadsky Institute of Russian Academy of Sciences,

<sup>3</sup>The Open University, Milton Keynes, UK

The minerals (Ol, Opx, Cpx) of metasomatized garnet lherzolite xenoliths from East Antarctica contain diverse microinclusions of melt, fluid, and fluid-silicate-sulphide inclusions with typical liquid immiscibility textures. At room temperature, the fluid inclusions contain one (liquid), two (liquid and gas) or three (H<sub>2</sub>O and CO<sub>2</sub> liquids and gas) phases. All the inclusions are CO<sub>2</sub>-dominated. The obtained data suggest the existence of two sources of fluids. Fluid of fluid-silicate-sulphide inclusions show homogenization temperatures of up to -64.8°C, and densities of up to 1.17 g/cm<sup>3</sup>, which correspond to pressures ≥13 kbar at the moment of fluid entrapment (at 1000°C). Phase transitions at -151°C are close to the critical point of N<sub>2</sub> (-147°C). The Raman spectra of fluid inclusions display lines of CO<sub>2</sub>, H<sub>2</sub>S and N<sub>2</sub>. The high-pressure fluid inclusions have low C/N<sub>2</sub> and N<sub>2</sub>/Ar, heavy nitrogen isotope compositions and elevated <sup>40</sup>Ar/<sup>36</sup>Ar values (up to 530). Second type inclusions have lower densities (≤0.82 g/cm<sup>3</sup>) and, correspondingly, lower entrapment pressures (≤7 kbar). Their Raman spectra exhibit a distinct H<sub>2</sub>O line. Their fluid has higher C/N<sub>2</sub> and C/Ar, lower δ<sup>13</sup>C, and close to atmospheric N<sub>2</sub>/Ar and <sup>40</sup>Ar/<sup>36</sup>Ar values. It is suggested that the observed fluids are products of mixing between a mantle derived fluid and atmospheric air or/and seawater.

## Fe(II) uptake mechanisms on montmorillonite clay minerals: A multidisciplinary approach

D. SOLTERMANN<sup>1,2,\*</sup>, M. MARQUES FERNANDES<sup>1</sup>,  
B. BAEYENS<sup>1</sup>, M.H. BRADBURY<sup>1</sup> AND R. DÄHN<sup>1</sup>

<sup>1</sup>Laboratory for Waste Management, Paul Scherrer Institut, Villigen PSI, Switzerland, (\*daniela.soltermann@psi.ch).

<sup>2</sup>Institute of Biogeochemistry and Pollutant Dynamics, ETH Zürich, Zürich, Switzerland

Virtually all radioactive waste repository designs contain large amounts of iron (steel canisters) and reducing conditions will prevail in the long-term. Due to the corrosion of steel canisters, high ferrous iron (Fe<sup>2+</sup>) concentrations in the interstitial porewaters in the near- and far-fields might be expected, which could have a significant influence on the sorption behaviour of other radionuclides through sorption competition effects. The best suited approach investigating the sorption of Fe<sup>2+</sup> on clay minerals and the influence of high aqueous Fe<sup>2+</sup> concentrations on the radionuclide retention by clay minerals is a multi-disciplinary one, consisting of macroscopic sorption experiments, geochemical modelling and advanced spectroscopic techniques, such as X-ray absorption spectroscopy (XAS). Fe<sup>2+</sup> uptake on an iron-free synthetic montmorillonite in the absence of any competing metal was measured by batch sorption experiments under anoxic conditions (O<sub>2</sub> <0.1 ppm). A two-site protolysis nonelectrostatic surface complexation and cation exchange sorption model<sup>1</sup> was used to quantitatively describe the uptake of Fe<sup>2+</sup> on montmorillonite. Two types of clay surface binding sites, so-called strong ( $\equiv\text{S}^{\text{S}}\text{OH}$ ) and weak ( $\equiv\text{S}^{\text{W}}\text{OH}$ ) edge sites, were required to model the Fe<sup>2+</sup> sorption isotherms. XAS data showed spectroscopic differences between Fe sorbed at low and medium concentrations, which were chosen to be characteristic for uptake on strong and weak sites, respectively. The XAS data analysis indicated that Fe is located in the continuity of the octahedral sheet.<sup>2</sup>

Sorption competition experiments of divalent metals Fe and Zn were carried out to further elucidate the uptake processes at the clay mineral-water interface. The competition experiments were performed for the combinations of Zn(II)/Fe(II) and Fe(II)/Zn(II), where the former represents the trace index metal and the latter the blocking metal at high concentration. The results of the wet chemistry and XAS measurements indicate that Fe(II) is competing with Zn(II) if the Fe(II) is present in excess (blocking metal). However, no competition effects between Fe(II) and Zn(II) were observed if Zn(II) is the blocking metal. These results can be explained by a selective uptake of trace Fe on montmorillonite due to Fe(II)/Fe(III) redox processes taking place at the clay surface.<sup>2</sup> The outcome of this study contributes to an improved molecular understanding of the Fe-clay interaction under anoxic conditions in the absence and presence of other divalent metals.

[1] Bradbury&Baeyens. *J. Contam. Hydrol.*, 1997, **27**(3-4), 223-248. [2] Soltermann *et al. Environ. Sci. Technol.*, 2012, doi: 10.1021/es304270c.

## Application of portable XRF analyzers in Au and PGE exploration: An example from the Bushveld Complex, South Africa

ALIREZA SOMARIN

Thermo Fisher Scientific, Tewksbury, MA 01876  
alireza.somarin@thermofisher.com

Field portable X-ray fluorescence (FPXRF) analyzers are used worldwide in exploration and mining of various types of metallic and non-metallic deposits from base metals to REEs, precious metals and even hydrocarbons. FPXRF application in base metal and REE exploration and mining is relatively easy and straight forward due to their high economic threshold combined with low detection limit of these metals by FPXRF. Application in precious metal projects needs good understanding of the limitations of the technique; however, FPXRF can still be utilized in such cases using pathfinder elements. This paper summarizes one of these cases in Au-PGE exploration in the Bushveld Complex, South Africa.

In this study, the pathfinder elements were defined using lab assays of 63 samples that were collected along a stratigraphic section. Elements with highest correlation with the target metals (Au, Pt and Pd) were classified as pathfinder elements. These elements were Ni and Cu in this case study (Figure 1). Analyzes of the samples (both direct shot and pulp samples) by FPXRF indicate that all anomalous zones of Au, Pt and Pd can be easily identified by locating anomalies of Ni and Cu on prepared (pulp) and even un-prepared samples. Such anomalous samples have target elements lower than detection limit of FPXRF and should be analyzed by laboratory techniques.

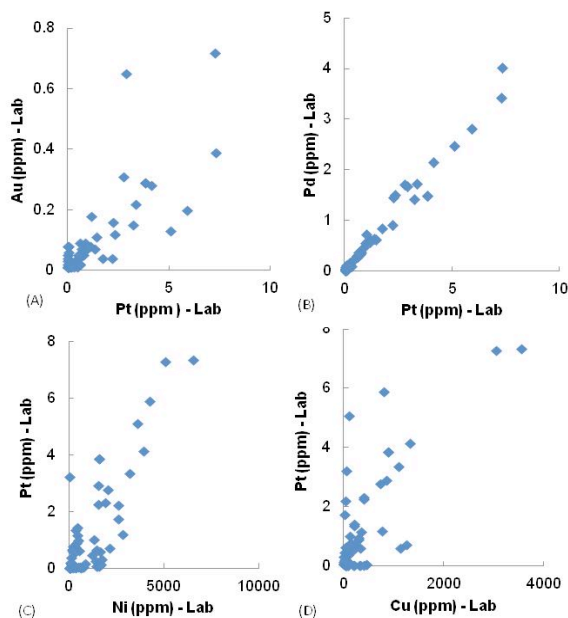


**Figure 1:** A and B) Correlation between target elements. C and D) Correlation between Pt and pathfinder elements (Ni and Cu).

## The Neoproterozoic magmatic evolution in Northern Guangxi, China

SONG HAO<sup>1,2</sup>, XU ZHENGQI<sup>1,2\*</sup>, NI SHIJUN<sup>1,2</sup>  
AND ZHANG CHENGJIANG<sup>1,2</sup>

<sup>1</sup> Department of Geochemistry and Nuclear Resources Engineering, Chengdu University of Technology, Chengdu 610059, China (\*Correspondence: xuzhengqi@cdut.cn)

<sup>2</sup> Key Laboratory of Nuclear Techniques in Geosciences of Sichuan Province, Chengdu 610059, China

As a Neoproterozoic giant intrusion, Motianling Pluton in North Guangxi remains a long-standing controversy in the diagenetic age. Based on a series of U-Pb dating in the Motianling Granites, the study of volcanic rocks in the study area mainly aims at retracing the tectono-magmatic evolutionary history in Jinningian epoch of Northern Guangxi. However, the relationship between the Danzhou Group and the Motianling Granites is still in great dispute [1]. This paper attempt to clarify the relationship between Danzhou Group and the Motianling Granites.

With long elongation time in the diagenesis, the Danzhou Group and the Motianling Granites have the time-overlap part and are formed within nearly 100 million years. And the main granite body is formed in the middle-late period of sedimentation of the Danzhou Group, with the later persistent granitic magmatic activity even after the deposition epoch during the formation period of the patched granite body in the Motianling Granites. The severe subsidence of earth surface is resulted from the orogenic extension, which results in the formation of the fine clastic sedimentary of the Danzhou Group (part of Sibao Group can be included). And the partial melting of the crust is resulted from the lithospheric delamination accompanying with the granitic magmatic activity. Through combining the U-Pb dating results with the element geochemistry, the main granite body and the diabase bodies/veins are formed after the Bendong granodiorite, then display the increasing tendency in acidity (SiO<sub>2</sub>) and decrease tendency in alkali (Na<sub>2</sub>O+K<sub>2</sub>O) in the patched granite bodies.

This work is supported financially by the National Natural Scientific Foundation of China (Grants No. 41173059) and the Foundation of China Nuclear Geology (Grants No. 201148 and 200995).

[1] Li Z X *et al.* (1999) *Earth and Planetary Science Letters* **173**, 171-181.

## The Triassic Igneous rocks in the Northeastern part of the South Korea

KYO-YOUNG SONG<sup>1</sup>

<sup>1</sup>Korea Institute of Geoscience & Mineral Resources, Daejeon, Korea (kysong@kigam.re.kr)

The Triassic igneous rocks, gabbroic to granite in composition, occur scattered throughout the Yangyang and Gangneung areas in the northeastern part of the South Korea. The total alkali versus silica composition of these igneous rocks shows a series of differentiation well and large variation from gabbro to alkali granite. So these igneous rocks can be classified to the Yangyang suite on the concept of granite suite.

The Yangyang suite is consist of gabbro, two mica granite, biotite granite, the Namhangjin diorite, the Yangyang syenite, the Yangyang granite and the Hajodae granite. The Yangyang suite is divided into two groups by whole-rock geochemistry analysis, alkali and subalkali rocks group. These means the Yangyang suite is consist of two subsuite. The geochemistry and isotopic composition of these two subsuites indicate that these are thought to be derived from the different granitic magma source. Alkali rocks group contains gabbro, the Namhangjin diorite, the Yangyang syenite and the Yangyang granite, subalkali rocks group contains two mica granite, biotite granite and the Hajodae granite.

The SHRIMP zircon U-Pb ages of the Yangyang suite range from 234±2.9 to 226.5±1.8 Ma.

This Yangyang suite is very important to understand and explain the indentation model which the South China Blocks had collided into the North China Blocks in the Korean peninsula as a wedge-shaped.

## Water Vapor Interactions with FeOOH Particle Surfaces

XIAOWEI SONG\* AND JEAN-FRANÇOIS BOILY

Department of Chemistry, Umeå University, Sweden \*Email: xiaowei.song@chem.umu.se

Iron oxyhydroxide (FeOOH) minerals play important roles in a variety of atmospheric, terrestrial and technological settings. Interactions with water vapor are particularly important given the predominance of water-bearing gases in the environment. In this work, molecular details of water adsorption reactions at FeOOH surfaces were resolved using vibrational spectroscopy, quartz crystal microbalance and molecular dynamics. Acidified and alkalified mineral surfaces were investigated to determine protonation effects on interfacial water loadings and structures. The effects of residual salts on the surfaces were further studied by resolving competitive hydration processes between surface-bound Cl<sup>-</sup> ions and hydroxyl groups.

This work reveals the initial mechanisms of formation of thin water films on mineral surfaces under atmospheric conditions [1]. We show that thin films of adsorbed water display liquid water-like attributes. The affinity of surface (hydr)oxo groups for water molecules is strongly dependent on their abilities at forming hydrogen bonds. Coordination number and site accessibility/steric constraints are main factors. These groups have moreover stronger affinities for water than chemisorbed water (-OH<sub>2</sub>) and Cl-exchanged group (e.g. -Cl, μ-Cl). Finally, we identified a *surface memory effect* showing that original surface protonation states can be retrieved by evacuating surfaces from surface-bound waters. This confirms that the original surfaces were at thermodynamic equilibrium prior water uptake reactions and that all reactions are reversible. This reversibility may further hold in mineral particles undergoing several water condensation-evaporation cycles in nature. This work thus opens a path for understanding water structure as well as condensation reactions on these important mineral particles.

[1] Song X.W., Boily J.-F. (2013), Chem. Phys. Lett. 560, 1-9.

## A stable isotope perspective on tracing natural and anthropogenic Hg emissions at the global scale.

JEROEN E. SONKE

Observatoire Midi-Pyrénées, 14 avenue E. Belin 31400 Toulouse, sonke@get.obs-mip.fr

A decade of research on the natural variations in mercury (Hg) stable isotope abundances has shown large variations across biogeochemical reservoirs. These variations result from the gradual separation of heavy/light or even/odd Hg isotopes during the numerous physicochemical processes that shuttle Hg across the Earth's surface. As a result, a Hg isotopic measurement gives rise to four useful isotope fingerprints that may characterize its source, or code for the transformations that Hg has undergone in the past.

Tracing the dominant natural and anthropogenic Hg emissions at the global level is a challenge. The further Hg emissions travel from their source, the more likely it is that oxidation/reduction, sorption or (de-)methylation reactions modify the original source Hg isotope signatures. This presentation illustrates an integrated approach to evaluate Hg isotope tracing at the global scale. Similar to modern and historic Hg emission inventories, a parallel Hg isotope library needs to be built per industrial sector and geographical region. Industrial processes include Hg transformations that may change isotope signatures and need to be understood. Monitoring of the isotopic composition of emitted Hg species and associated Hg deposition at different spatiotemporal scales is necessary. Finally, monitoring of critical receptor environments on continents and oceans and on different time scales (modern, geologic) will tell if globally relevant emission sources can be recognized. All of these tasks are compatible with box and process models of the global Hg cycle, so that Hg isotopic information may in the near future be integrated in global models to help understand Hg cycling.

The approach will be illustrated for coal fired power plant (CFPP) emissions: A coal Hg isotope library, containing ~200 coal samples from historically dominant coal burning regions has been made. A study on two large Chinese coal fired power plants suggests that stack emission Hg isotope signatures are slightly modified from feed coal signatures by emission control technologies. Bi-weekly monitoring of gaseous and particulate Hg isotope signatures in Asian urban-industrial environments is compatible with a dominant CFPP source. Finally, a preliminary attempt to integrate an emission isotope library in a global Hg box model will be compared to historical records of Hg deposition and isotopic variation in peat bogs.

## (Non-?) Traditional Hg stable isotope geochemistry in the early 1920's

J. E. SONKE<sup>1</sup>, N. ESTRADE<sup>2</sup>, O.F.X DONARD<sup>3</sup>  
AND J. CARIGNAN<sup>2</sup>

<sup>1</sup> Observatoire Midi-Pyrénées, CNRS-GET-Université de Toulouse, France, sonke@get.obs-mip.fr

<sup>2</sup> CRPG, UMR 7358, CNRS-Université de Lorraine, Nancy, France

<sup>3</sup> IPREM/LCABIE, UMR 5254, CNRS-Université de Pau et des Pays de l'Adour, Pau, France

In 1919 Sir Francis Aston discovered the multiple stable isotopes of mercury (Hg) using his mass spectrograph. Only one year later Johannes N Brønsted and György de Hevesy used high precision density measurements to prove that liquid Hg distillation into a vacuum fractionates Hg isotopes as a function of isotope mass. In more detailed studies during the 1920's Brønsted and colleagues managed to produce Hg vapors and residual liquids that were heavily fractionated by up to -84‰ and +74‰ on the  $\delta^{202}\text{Hg}$  scale. They derived the kinetic isotope fractionation law, and used Rayleigh equations and diagrams to estimate Hg isotope separation factors. They also explored the natural variations in Hg isotope abundances, by converting cinnabar (HgS) into liquid Hg and measuring its density. By sheer coincidence they did not find any density variations for nine global cinnabar deposits, within their measurement uncertainty of 0.4 - 1.2 ‰ on the  $\delta^{202}\text{Hg}$  scale. Today we know that the  $\delta^{202}\text{Hg}$  of cinnabar may vary by up to 5 ‰ across a single cinnabar deposit.

In 2006 Jean Carignan was interested in the potential isotopic fractionation of volatile metals under natural and industrial conditions. He proposed to examine the distillation of liquid Hg in a vacuum, without knowing that nearly one century before him scientists had looked at the issue. Using MC-ICPMS, we made nearly identical observations as Brønsted and co-workers: a kinetic isotope fractionation factor of 1.0067 for the  $^{202}\text{Hg}/^{198}\text{Hg}$  pair (Estrade *et al.*, 2009). We also performed Hg isotope analysis of Hg vapor that is in equilibrium with liquid Hg. Here we observed deviations from theoretical mass dependency for the two odd Hg isotopes,  $^{199}\text{Hg}$  and  $^{201}\text{Hg}$ , in what has become the first experimental evidence for nuclear volume fractionation of Hg isotopes. This contribution will look back on both the early and more recent measurements.

[1] Estrade, N., Carignan, J., Sonke, J.E., Donard, O.F.X., 2009. Mercury isotope fractionation during liquid-vapor evaporation experiments. *Geochimica et Cosmochimica Acta*, 73: 2693-2711.

## Satellite and aircraft views of relationships between particles, cloud water, and rain water

ARMIN SOROOSHIAN<sup>1\*</sup>, ZHEN WANG<sup>2</sup>, GRAHAM FEINGOLD<sup>3</sup>, TRISTAN L'ECUYER<sup>4</sup>  
AND HAFLIDI H. JONSSON<sup>5</sup>

<sup>1</sup> Chemical and Environmental Engineering, University of Arizona, Tucson, AZ, United States

(\*correspondence: armin@email.arizona.edu)

<sup>2</sup> Chemical and Environmental Engineering, University of Arizona, Tucson, AZ, United States  
(zhenw@email.arizona.edu)

<sup>3</sup> Earth Systems Research Laboratory, NOAA, Boulder, CO, United States (graham.feingold@noaa.gov)

<sup>4</sup> Department of Atmospheric and Oceanic Sciences, University of Wisconsin, Madison, WI, United States  
(Tristan@aos.wisc.edu)

<sup>5</sup> Center for Interdisciplinary Remotely Piloted Aircraft Studies, Naval Postgraduate School, Monterey, CA, United States (hjonsson@nps.edu)

A poorly characterized process in warm clouds is the conversion of cloud water to rain water especially with regard to the rate by which this complex process occurs. Using a satellite remote sensing data set, this conversion process is examined in a global sense over oceans to identify regional differences and relationships with relevant environmental parameters [1]. We show that a faster conversion process coincides with conditions of reduced atmospheric stability, higher low-level wind speeds, and low aerosol index values. Aircraft measurements are used in a stratocumulus cloud environment to provide more views on relationships between environmental factors influencing water in clouds [2].

[1] Sorooshian, Wang, Feingold & L'Ecuyer (2013), A satellite perspective on cloud water to rain water conversion rates and relationships with aerosol types and atmospheric stability. *Geophys. Res. Atmos.*, 118, doi: 10.1002/jgrd.50523  
[2] Sorooshian, Wang, Coggon, Jonsson, Ervens (2013), Observations of sharp oxalate reductions in stratocumulus clouds at variable altitudes: organic acid and metal measurements during the 2011 E-PEACE campaign. *Environ. Sci. Technol.*, doi: 10.1021/es4012383.



## Iron isotope geochemistry of the Balmuccia peridotite massif and the composition of the upper mantle

PAOLO A. SOSSI<sup>1\*</sup>, HUGH ST.C. O'NEILL<sup>1</sup>  
AND MARCO BELTRANDO<sup>2</sup>

<sup>1</sup>Research School of Earth Sciences, Australian National University, Canberra, ACT, 0200

<sup>2</sup>Dipartimento di Scienze della Terra, Università di Torino, Via Valperga Caluso 35, 10125 Torino, Italy

Extensive work on global, unmetasomatised oceanic and lithospheric mantle-derived peridotites reveals a scatter of  $\pm 0.1\%$   $\delta^{57}\text{Fe}$  around the 0‰ value (vs. IRMM-014) [e.g. 1, 2]. Contrastingly, most primitive basaltic lavas cluster about  $\delta^{57}\text{Fe} \approx 0.1\%$  [3]. This disparity has typically been ascribed to iron isotope fractionation during partial melting [4]. However, recent studies place the composition of primitive, undepleted mantle at  $\approx +0.1\%$ , obviating the need for such melting-induced fractionation [5]

In order to constrain the relative effects of partial melting and metasomatism on the iron isotope composition of the upper mantle, we present data from the remarkably fresh and well-characterised Balmuccia orogenic peridotite massif of the Ivrea Zone in northern Italy [6]. A spectrum of cogenetic ultramafic samples were analysed, comprising pyroxenites to lherzolites, harzburgites and dunites, faithfully capturing the variation recorded in the massif.

The starting composition of the Balmuccia lherzolite has about 39% MgO, 3.1% Al<sub>2</sub>O<sub>3</sub>, 2.9% CaO and 8.3% FeO, which could be explained by the extraction of  $\approx 5 \pm 0.33\%$  MORB from primitive mantle. This initial composition has a  $\delta^{57}\text{Fe} \approx 0.013\% \pm 0.005\%$  and defines an anchor point from which trends of pyroxene-addition, melt depletion and Fe-metasomatism are identified. Residual harzburgites extend to lighter  $\delta^{57}\text{Fe}$  and higher Mg#s, while Fe-enriched harzburgites and dunites are typified by heavier iron isotope compositions and near-constant Mg# with respect to the lherzolites.

Lherzolites with lower MgO contents also exhibit heavier  $\delta^{57}\text{Fe}$  values, nearing +0.05‰ at the MgO content of the primitive mantle (36.77%). However, given that MORBs, with  $\delta^{57}\text{Fe} \approx 0.15\%$  [3] are derived from depleted mantle, a source of Fe isotope fractionation between partial melting and their eruption onto the ocean floor seems to be required.

[1] Weyer and Ionov, 2007, EPSL; [2] Huang *et al.*, 2011, GCA, 75; [3] Teng *et al.*, 2013, GCA; [4] Dauphas *et al.*, 2009, EPSL; [5] Poitrasson *et al.*, 2013, CMP; [6] Hartmann and Wedepohl, 1993, GCA

## Hf isotope systematics of Archean anorthosites: The Manfred Complex, Yilgarn Craton, Western Australia

A.K. SOUDERS<sup>1\*</sup>, P.J. SYLVESTER<sup>1</sup>, J.L. CROWLEY<sup>2</sup>  
AND J.S. MYERS<sup>3</sup>

<sup>1</sup>Department of Earth Sciences, Memorial University, St. John's, NL A1B 3X5, Canada (\*kate.souders@mun.ca)

<sup>2</sup>Department of Geosciences, Boise State University, 1910 University Drive, Boise, Idaho 83725-1535 USA

<sup>3</sup>Department of Applied Geology, Curtin University, Perth, WA 6845, Australia

Archean anorthosite complexes represent a minor, yet distinct rock type found within many Archean terranes. These mantle-derived melts are commonly found in layers with associated leucogabbro, gabbro, and ultramafic units of similar origin. Most Archean anorthosites are intensely deformed and metamorphosed yet preserved igneous minerals have been identified within several complexes. It has become obvious that Archean anorthosites contain zircon crystals, which can be used to establish robust crystallization ages for anorthosite complexes. These minerals are also ideal targets for in situ Lu-Hf isotopic analysis to further characterize the source of Archean anorthosites and provide insight into the formation and evolution of the continental crust during the Archean.

The ca. 3.7 Ga Manfred Complex is exposed northeast of Mount Narryer within the Narryer Gneiss Terrane, Yilgarn Craton, Western Australia. The layered anorthosite-gabbro-ultramafic intrusion outcrops in pods and lenses, engulfed by granitic gneisses [1, 2, 3]. We have sampled anorthosites, leucogabbros and gabbros from the Manfred Complex and determined their age by LA-ICPMS U-Pb zircon geochronology. Zircons separated from these rocks give ages of 3.63 Ga to 3.73 Ga. LA-MC-ICPMS Lu-Hf isotope analyses were performed by focusing the laser spot directly on top of the U-Pb analysis location for each zircon grain. Initial Hf isotope compositions of zircon grains from the Manfred complex range from ca.  $\epsilon_{\text{Hf}} +2$  to  $-3$ . This range suggests contributions from both depleted mantle and ancient crustal sources to the parent magma of the Manfred Complex.

[1] Kinny *et al.* (1988) Prec. Res. 38, 325-341. [2] Myers (1988) Prec. Res. 38, 309-323. [3] Williams & Myers (1987) WA Geol. Surv. Rpt. 22, 32 pp.

## Secondary Organic Aerosols in the coupled climate aerosol model ECHAM-HAM: Insights into production dependencies and climate impacts

G.SOUSA SANTOS<sup>1\*</sup>, T. STANELLE<sup>1</sup>, I. BEY<sup>1</sup>  
AND U. LOHMANN<sup>1</sup>

<sup>1</sup>Institute for Atmospheric and Climate Science, ETH Zurich, Universitaetstrasse 16, 8092 Zurich (\*correspondence: gabriela.sousa-santos@env.ethz.ch)

Aerosols are an integral part of the climate system, because they play essential roles in the atmosphere's radiation budget and in the hydrological cycle. An important fraction of the aerosols in the troposphere are organic. So far, most models only considered Primary Organic Aerosol (POA) emissions into the atmosphere. However, Secondary Organic Aerosols (SOA) are a non negligible fraction of the total organic.

We aim to investigate SOA processing and impacts on the climate system using two sets of simulations with ECHAM-HAM: two equilibrium simulations for 2000 conditions without SOA and with interactive computation of SOA, and a 50-year hindcast (1960-2010).

The hindcast simulation shows a general increase in SOA burdens in the Northern Hemisphere from 1960 to 2010. SOA production increases from 25 to 30Tg/yr globally and 0.75 to 1.3Tg/yr in Europe. This translates in a increase in SOA surface concentrations of roughly 30% globally and 40% in Europe. In Europe, the reported changes mainly resulted from an increase in biogenic precursor emissions, which are, in turn, most likely connected to changes in anthropogenic land cover and in a lower degree to changes in surface radiation. In other regions of the world other factors like anthropogenic precursor emissions and temperature changes have higher importance. According to the model, SOA has impact on the Earth radiation budget, with a direct radiative effect at the top-of-the-atmosphere (TOA) of  $-0.35\text{W/m}^2$ . We will present details of the effect on other climate variables, especially on cloud properties at the conference.

## Best practices for reducing energy poverty and (as a result) emissions of methane, carbon dioxide, and black carbon/aerosols

BENJAMIN K. SOVACOOOL

Institute for Energy and the Environment, Vermont Law School, bsovacool@vermontlaw.edu

This presentation demonstrates how small-scale renewable energy technologies such as solar panels, cookstoves, biogas digesters, microhydro units, and wind turbines are helping Asia eradicate energy poverty and (as a result) reduce greenhouse gas emissions. Through an in-depth exploration of case studies in Bangladesh, China, India, Laos, Indonesia, Malaysia, Mongolia, Nepal, Papua New Guinea, and Sri Lanka, the presentation highlights the applicability of different approaches to the promotion of renewable energy in developing countries. It also illuminates how household and commercial innovations occur (or fail to occur) within particular energy governance regimes. It lastly, and uniquely, explores successful case studies alongside failures or "worst practice" examples that are often just as revealing as those that met their targets. Based on these successes and failures, the presentation concludes by presenting twelve salient lessons for policymakers and practitioners wishing to expand energy access and raise standards of living in some of the world's poorest communities.

## Benthic fluxes and early diagenesis processes in Adriatic Sea

F. SPAGNOLI<sup>1\*</sup>, G. BARTHOLINI<sup>2</sup> AND P. GIORDANO<sup>3</sup>

<sup>1</sup>CNR-ISMAR, Largo Fiera della Pesca, 60125, Ancona, Italy

<sup>2</sup>Università di Bologna, Dipartimento di Scienze Biologiche, Geologiche e Ambientali, Piazza di Porta S. Donato, 1, Bologna

<sup>3</sup>CNR-ISMAR, Via Gobetti, 101, 40120, Bologna, Italy

During the last decades various researches in the Adriatic and Ionian Sea allowed the individuation of different area characterized by various early diagenesis environments that generate dissolved fluxes at the sediment-water interface with different intensity.

North of the Po River a thin and discontinuous band of terrigenous fine carbonate sediment and with different reactivity of organic matter produces benthic fluxes extremely variable in functions of the fresh organic matter entered by the main rivers

In front of the Po River a limited area, with high sedimentation rate and high continental and autochthonous organic matter inputs, generates high nutrient benthic fluxes.

In the western Adriatic sediments are characterised by progressive southward decrease of sedimentation rate and reactive organic matter that generate decreasing benthic fluxes. The central Adriatic Sea bottom sediment area is characterized by prevalently carbonate sediments and low fluxes of nutrients due to little organic and inorganic inputs and to precipitation of authigenic mineral.

In the Meso-Adriatic and South Adriatic Depression low sedimentation rates and strongly reworked organic and inorganic matter produce very low benthic nutrient fluxes.

In Ionian Sea slope sediments are characterized by very low particulate inputs and by negative fluxes of DIC acting in this way as CO<sub>2</sub> traps while basin sediments show higher benthic fluxes due to increases of organic matter inputs.

## AMERIGO: A new benthic lander for dissolved flux measurements at sediment-water-interface

F. SPAGNOLI<sup>1\*</sup>, G. CICERI<sup>2</sup>, G. GIULIANI<sup>1</sup>, V. MARTINOTTI<sup>2</sup> AND P. PENNA<sup>1</sup>

<sup>1</sup>CNR-ISMAR, Largo Fiera della Pesca, 60125, Ancona, Italy

<sup>2</sup>RSE SpA, Via Rubattino 54, 20134, Italy

Amerigo is a new autonomous and automatic benthic lander for the measurements of dissolved benthic fluxes at the sediment-water interface. The lander is able to measure fluxes of nutrients such as ammonium, nitrites, nitrates, phosphates and silica, gases such as oxygen, carbon dioxide and methane, trace elements such as heavy metals, and also other dissolved pollutants resulting from human activity. AMERIGO is able to operate from transitional environments to continental shelf and abyssal plain. The Lander can include various components, at present it is equipped with 3 benthic chambers for measuring the fluxes at the water-sediment interface and is prepared to host a microprofiler and other benthic instruments (mini-penetrometer, gravimeter, etc.). The 3 benthic chambers are equipped with a water sampler, which also allows injection of tracers, a system for the refilling of the consumed oxygen (Oxystat) and sensors for pH and dissolved gas monitoring (oxygen, methane and in future CO<sub>2</sub>). Outside the benthic chambers a CTD probe for measuring the chemical-physical parameters (temperature, conductivity and pressure) and a niskin bottle for the sampling of the water column are present. The lander is equipped with all mechanisms for the dipping (ballast weights), positioning on the bed, raising (a timed release mechanism (burn-wire type) for the release of the ballast and glass spheres for the flotation) and recovery (radio transmitter, GPS position system and flasher) on board. A useful property of AMERIGO is the modularity and flexibility, that is different components, which can be assembled and programmed on the basis of needs and of the environmental conditions in which it will operate.

After the two first testing cruises early results of the AMERIGO functioning will be presented.

## Hydrogeochemical radiation burden in the ambiance of natural radioactivity in the hills of Vršac

<sup>1</sup>V. SPASIĆ-JOKIĆ, <sup>2</sup>V. GORDANIĆ, <sup>2</sup>M. VIDOVIĆ  
AND <sup>3</sup>D. JOVANOVIĆ

<sup>1</sup>Faculty of Technical Sciences, University of Novi Sad,  
svesna@uns.ac.rs

<sup>2</sup>IHTM, University of Belgrade gordanicv@gmail.com,  
mivibgd@yahoo.com

<sup>3</sup>Geological Survey, Belgrade, dragan.jovanovic@gzs.gov.rs

During regional hydrogeochemical prospection (500 km<sup>2</sup>) samples were collected from surface flows, springs, wells and borings. In water, contents of uranium, radium and radon were determined. Three anomaly zones of radionuclides in water were identified, and their values vary within the interval: 0.1-166 ppb for U, up to 7 Bq for Ra and 2.8-36 Bq. Risk for cancer incidence was calculated using Monte Carlo techniques. Anomalies of radioactive elements are located in the area which is built of granites, gneiss and crystalline schists. According to the available data it is considered that the granites have intruded in the crystalline schists during Hercynian orogeny which is of significance for uranium deposits formation. In the purpose of defining conditions of uranium migration and depositing at favorable geochemical barriers, beside contents of U, Ra and Rn in water, some other parameters (Eh, pH, Ep, content of microelements, etc) were determined. Identification of the areas of hydrogeochemical radiation burden caused by presence of radionuclides (U, Ra, Rn) in water is of special relevance for determination of geopathogenic zones of the influence of natural radioactivity. By applying conversion factors the radiation burden was calculated for each radionuclide. Research results are shown on maps and charts. That results are representing the influence of natural radionuclides in water, which are ingested in the ambient of living environment of rural settlements.

**Keywords:** hydrogeochemistry, radioactivity, cancer incidence, uranium, radium, radon.

This work has been financed by the Ministry of Science and Technological Development of the Republic of Serbia (project No. 45006).

[1] S. Pavlović *et al.* (1966) Study of Yugoslavian granitoid massifs, fund of Geoinstitute, Belgrade, Serbia.

## Mineral Physics in the Terapascal Regime: Dynamic Studies of Planetary Interiors

DYLAN K. SPAULDING

Origins Initiative, Harvard University,  
dylanspauling@fas.harvard.edu

Laser-driven shock wave techniques extend the reach of mineral physics to the terapascal regime, permitting unprecedented studies of planetary compositions. Such experiments probe extreme states of matter characteristic of late-stage giant impacts (such as that believed to have formed the moon) as well as the present-day interiors of several Earth-mass exoplanets. Here, I present a suite of recent results on the physical and transport properties of fundamental mineral phases in the Earth's mantle: SiO<sub>2</sub>, MgO and MgSiO<sub>3</sub>. Experiments on molten MgSiO<sub>3</sub> show the first evidence of a liquid-liquid phase transition with a 6% volume reduction over a wide temperature range, suggesting the potential for unexpectedly complex behavior in silicate liquids at ultra-high pressure. Results on MgO resolve controversial predictions for high-pressure melting and the B1-B2 transition. In addition, data for all three materials reveal thermal and electrical conductivities enhanced by one to two orders of magnitude in the fluid state relative to estimates for the present-day terrestrial mantle. These results underscore the potentially significant role of conductive liquid silicates and oxides in governing the early thermal-chemical evolution of the Earth and other extra-solar 'rocky' planets.

## Evidence from fluid inclusions extends the record of seawater chemistry by ~300 million years, from ~544 Ma to ~830 Ma

NATALIE SPEAR<sup>1\*</sup>, H.D. HOLLAND<sup>1</sup>,  
JAVIER GARCIA-VEIGAS<sup>2</sup>, T.K. LOWENSTEIN<sup>3</sup>  
AND ROBERT GIEGENGACK<sup>1</sup>

<sup>1</sup>Earth and Environmental Science, Univ. of Pennsylvania, Phila., PA 19014, USA (\*correspondence: nahilln@sas.upenn.edu)

<sup>2</sup>Univ. of Barcelona, Barcelona 08028, Spain

<sup>3</sup>Department of Geological Sciences, State Univ. of New York at Binghamton, Binghamton, NY 13902, USA

We analyzed primary fluid inclusions in halite from marine evaporites in the ~830-Ma Browne Formation of the Officer Basin in Western Australia by the Cryo-SEM-EDS technique. The parent seawater, calculated from the concentrations measured in those inclusions, contained ~565 mmolal Cl<sup>-</sup>, ~456 mmolal Na<sup>+</sup>, ~50 mmolal Mg<sup>2+</sup>, 9-12 mmolal Ca<sup>2+</sup>, ≥ 3 mmolal SO<sub>4</sub><sup>2-</sup>, and ~1 mmolal K<sup>+</sup>. The concentrations of the major ions, except K<sup>+</sup> and possibly SO<sub>4</sub><sup>2-</sup>, fall within the known range of Phanerozoic seawater composition. Ours is the first direct measurement of the composition of Mid-Neoproterozoic seawater, and extends direct documentation of seawater chemistry by ~300 Ma.

We sampled the Browne Formation from two cores (Empress 1A and Lancer 1), both from the western Officer Basin, a large intracratonic basin that covers an area of ~525,000 km<sup>2</sup> in Western and South Australia. In spite of the distance between the two studied wells (~264 km), the lithology and thicknesses throughout the sedimentary succession of the encountered Browne Formation are remarkably similar.

The amount of sulfate in the Mid-Neoproterozoic ocean was closely linked to the amount of oxygen in the atmosphere and deep ocean. Our estimates suggest that Mid-Neoproterozoic marine-sulfate concentrations were considerably lower (≥ 10%) than modern values. By terminal Neoproterozoic time, the composition of fluid inclusions in halite and the mineralogy of evaporite rocks indicate that seawater-sulfate levels rose significantly, to 50 to 80% of modern concentrations, a trend that parallels a similar increase in atmospheric and oceanic oxygen. By imposing a tighter constraint on the sulfate levels of Neoproterozoic seawater, we can define more accurately the circumstances and timing of the oxygenation of the Earth's atmosphere and oceans.

## Geochemical evolution of prehistoric magma sources beneath Mt. Etna

E.A. SPENCE<sup>1</sup>, H. DOWNES<sup>1\*</sup>, J. BLICHERT-TOFT<sup>2</sup>,  
J.G. BRYCE<sup>3</sup> AND E. HEGNER<sup>4</sup>

<sup>1</sup>Dept of Earth and Planetary Sciences, Birkbeck University of London, UK (\*correspondence: h.downes@ucl.ac.uk)

<sup>2</sup>Ecole Normale Supérieure de Lyon, Lyon, France.

<sup>3</sup>UNH Earth Sciences, Durham, New Hampshire, USA.

<sup>4</sup>Dept of Earth and Environmental Sciences, Ludwig-Maximilians Universität, Munich, Germany.

Prehistoric alkalic lavas of Mount Etna representing a ~70 ka time span, sampled from four vertical sections in the southern wall of the Valle del Bove (VdB), exhibit geochemical and isotopic variations distinguishing them as six separate lithostratigraphic and volcanic units within the newly defined framework of Etna [1]. Intersecting geochemical correlations between lavas highlight their stratigraphic relationships, and new isotopic data such as <sup>87</sup>Sr/<sup>86</sup>Sr (0.7033-0.7036) and <sup>206</sup>Pb/<sup>204</sup>Pb (19.76-20.02), indicate subtle changes in evolution of the magma sources beneath Etna. The alkalic centres of the VdB and modern Etna no longer tap the source(s) of ancient Iblean magmatism (2.6-1.4 Ma) [2]. Isotopic variations indicate that the oldest unit Salfizio-1 (>85 ka) tapped a mantle source similar to present-day Etna (<sup>87</sup>Sr/<sup>86</sup>Sr >0.7035), while four other units relate more closely to the source of historic Etna magmatism (<sup>87</sup>Sr/<sup>86</sup>Sr <0.7035) [3]. The sixth group, part of Piano Provenzana formation (~42-30 ka) of Ellittico, has the most chemically evolved lavas (58-62 wt% SiO<sub>2</sub>) and exhibits lower Hf and Nd isotopic ratios and less radiogenic <sup>206</sup>Pb/<sup>204</sup>Pb and <sup>87</sup>Sr/<sup>86</sup>Sr than the oldest unit, implying that the temporal trend generally observed in the evolution of Nd-Sr isotope systematics breaks down over a ~70 ka period. Mt. Etna's unique position on an accretionary wedge related to the Calabrian Arc, formed during convergence of the African and Eurasian plates and close to the extensional Malta Escarpment [4], presents a complicated tectonic evolution model for Etna magmatism. Subduction processes, slab rollback of Ionian oceanic lithosphere and upwelling asthenospheric mantle are all likely to introduce chemical and isotopic heterogeneities into the convecting mantle.

[1] Branca *et al.* (2011) *Ital. J. Geosci.* **130**, 265-291. [2] Trua *et al.* (1998) *Contrib. Min. Pet.* **131**, 307-322. [3] Viccaro and Cristofolini (2008) *Lithos* **105**, 272-288. [4] Doglioni *et al.* (2001) *Terra Nova* **13**, 25-31.

## The isotopic artifacts of enhanced crustal preservation in collisional orogenesis

CHRISTOPHER J. SPENCER<sup>1\*</sup>, PETER A. CAWOOD<sup>1</sup>,  
CHRIS HAWKESWORTH<sup>1</sup> AND NICK M.W. ROBERTS<sup>2</sup>

<sup>1</sup>Department of Earth and Environmental Sciences, University of St Andrews, North Street, St Andrews KY169AL

<sup>2</sup>NERC Isotopes Geosciences Laboratory, British Geological Survey, Keyworth, Nottingham, NG12 5GG, UK

\*cs207@st-andrews.ac.uk

The generation of felsic crust at accretionary/collisional tectonic boundaries is considered globally to be in steady-state, although the rate of crustal production can vary locally.

U-Pb, Hf, and O isotopic analyses in detrital zircon are widely used to assess the timing and isotopic composition of crustal growth. The age distribution of global detrital zircon record is comprised of “peaks” and “troughs”.

This episodic temporal distribution of zircon crystallization ages has been argued to represent periods of global collisional orogenesis that isolated continental crust formed within accretionary settings within the interior of newly formed supercontinents. This is shown by comparing U-Pb, O, and Hf isotopes in detrital zircons derived from the accretionary, collisional, and post-rift stages of the assembly of the supercontinent of Rodinia based on data from Laurentia and Baltica.

Our results show that continental crust with highly negative  $\epsilon_{\text{Hf}}$  and high  $\delta^{18}\text{O}$  values that formed during the accretionary stage is largely removed from the record preserved in collisional and post-rift stages, probably via sediment subduction, subduction erosion or tectonic delamination. These relations support the hypothesis that detrital zircon age peaks do not represent non-steady state felsic crust formation, but are an artifact of selective preservation during collisional orogenesis.

## SCLM super-Si garnet traces the Archaean

DIRK SPENGLER

Institute of Earth and Environmental Science, Potsdam University, 14476 Potsdam, Germany (spengler@geo.uni-potsdam.de)

Sub-continental lithospheric mantle (SCLM) garnet that hosts oriented pyroxene lamellae, that exsolved from former super-Si garnet, have been reported only from the oldest parts of cratons including the Kalahari, Laurentia and Siberia composite cratons [1-5]. Direct implications are: the exsolution microstructure has (1) an Archaean affinity and (2) a global distribution. This study reviews reconstructed and normal garnet chemistries to evaluate proposed garnet origins and exsolution scenarios.

Proportions of pyroxene lamellae in garnet that were quantified using standard techniques range with 0.5-9.6vol.%. Re-integrated garnets have Si+Ti in the range of 2.992-3.086 (median 3.034) cations per 12 oxygen. Maximum values correspond to 7.9 GPa (median 6.4 GPa) [6] that favour a lithospheric origin of all garnet prior to exsolution. Garnet Si isopleths have negative slopes in P-T space [6] suggesting that the above P estimates are overestimated if pre-exsolved garnet formed at high T.

Ti-Na systematics shows a bimodal distribution. The larger fraction of pre-exsolved garnet (G1, G4, G5, G12) has  $\text{TiO}_2 > 0.4 \text{ wt.}\%$  and has a positive correlation between  $\text{TiO}_2$  and  $\text{Na}_2\text{O}$  with  $\text{TiO}_2/\text{Na}_2\text{O} > 10$ . These features overlap those of lamellae-free garnet megacrysts [7], consistent with an origin from re-fertilising melts. The other, minor fraction of pre-exsolved garnet (G4, G5) has  $\text{TiO}_2 < 0.4 \text{ wt.}\%$  that correlates negatively with  $\text{Na}_2\text{O}$  at dominantly  $\text{TiO}_2/\text{Na}_2\text{O} < 2$ . Major elements suggest these pre-exsolved garnets to have a pyroxenite/websterite origin. Non-eclogitic lithospheric garnet diamond inclusions from the Siberia, Kaapvaal and Slave cratons include the negative, but not the positive correlation defined by the pre-exsolved garnet chemistry. Thus, low  $\text{TiO}_2/\text{Na}_2\text{O}$  garnet (pyroxenitic/websteritic) formed part of Archaean SCLM prior to local lithospheric diamond formation.

In summary, (1) lamellae type pyroxene exsolution in garnet occurred at SCLM depth most likely by cooling and (2) appears to be a tracer of Archaean provinces, (3) high  $\text{TiO}_2/\text{Na}_2\text{O}$  pre-exsolved garnet may have formed by infiltrating melts, (4) low  $\text{TiO}_2/\text{Na}_2\text{O}$  pre-exsolved garnet is related to the origin of websterite/pyroxenite. Additional REE systematics will be presented to provide constraints on the latter.

[1] Haggerty & Sautter (1990) *Science* **248**, 993-996. [2] Roden *et al.* (2006) *Lithos* **90**, 77-91. [3] Spengler *et al.* (2006) *Nature* **440**, 913-917. [4] Bobrov *et al.* (2012) *Doklady* **444**, 574-578. [5] Alifirova *et al.* (2012) *Int. Geol. Rev.* **54**, 1071-1092. [6] Collerson *et al.* (2010) *GCA* **74**, 5939-5957. [7] Schulze (1997) *Expl. Min. Geol.* **6**, 349-366.

## Tracking environmental changes over the past 3000 years in the Region of Ria do Mamanguá, Rio de Janeiro, Southeastern Brazil using molecular organic markers

A. M. SPERA<sup>1\*</sup>, S. TANIGUCHI<sup>1</sup>, J. LEONEL<sup>1</sup>  
AND M. C. BICEGO<sup>1</sup>

<sup>1</sup>Praça do Oceanográfico, 191, Cidade Universitária, São Paulo – SP, Brazil. 05508-120

(\*correspondence: amandaspera@usp.br)

Molecular organic markers (terrestrial *n*-alkanes and alkenones) and other geochemical tracers ( $\delta^{13}\text{C}$ ,  $\delta^{15}\text{N}$  and  $\delta^{34}\text{S}$ ) were used to assess changes in rainfall patterns and in the sea surface temperature over the past 3000 years in the Region of Ria do Mamanguá, located on the southern coast of Rio de Janeiro, Brazil. It was possible to identify periods with distinctive contribution from terrestrial organic matter in the sediments cores. The wetter periods between 2733 and 2000 cal years BP and between 1100 and 200 cal years BP presented a higher contribution of terrestrial organic matter to the area. While the dryer period between 2000 and 1100 cal years BP showed a lower input. Furthermore, it was possible to identify the presence of the Little Ice Age event, that was characterized as a period of wetter conditions and with relatively low SST in the Region of Ria do Mamanguá, corroborating with other paleoclimate records in South America. A possible reduction in the termohaline circulation during these cold events may have contributed to the increase in the latitudinal temperature gradient. A lower sea surface temperature in the North Atlantic could have contributed to a displacement in the atmospheric system of the South Hemisphere through a change in the latitudinal position of the Intertropical Convergence Zone (ITCZ). The ITCZ acts as the main source of moisture to the region where the South American Summer Monsoon is formed and consequently the South Atlantic Convergence Zone (SACZ). The SACZ is one of the main features responsible for most of the rain in the Region of Ria do Mamanguá.

## The global record of local iron geochemical data from Proterozoic through Paleozoic basins

E.A. SPERLING<sup>1</sup>, C. WOLOCK<sup>2</sup>, A.H. KNOLL<sup>1,2</sup>  
AND D.T. JOHNSTON<sup>1</sup>

<sup>1</sup>Dept. of Earth and Planetary Sciences, Harvard University, Cambridge, MA, USA

(\*correspondence: sperling@fas.harvard.edu)

<sup>2</sup>Dept. of Organismic and Evolutionary Biology, Harvard University, Cambridge, MA, USA

Iron-based redox proxies represent one of the most mature tools available to sedimentary geochemists. These techniques, which benefit from decades of refinement, are based on the fact that rocks deposited under anoxic conditions tend to be enriched in highly-reactive iron. However, there are myriad local controls on the development of anoxia, and no local section is an exemplar for the global ocean. The global signal must thus be determined using techniques like those developed to solve an analogous problem in paleobiology: the inference of global diversity patterns through time from faunas seen in local stratigraphic sections. Here we analyze a dataset of over 4000 iron speciation measurements (including over 600 de novo analyses) to better understand redox changes from the Proterozoic through the Paleozoic Era. As with paleobiological diversity curves, it is expected that a number of biases affect such a dataset, including both spatial and temporal sampling bias and stochastic error.

Preliminary database analyses yield interesting observations. We find that although anoxic water columns in the middle Proterozoic were dominantly ferruginous, there was a statistical tendency towards euxinia not seen in early Neoproterozoic or Ediacaran data. Also, we find that in the Neoproterozoic oceans, oxic depositional environments—the likely home for early animals—have exceptionally low pyrite contents, and by inference low levels of porewater sulfide. This runs contrary to notions of sulfide stress on early metazoans. Finally, the current database of iron speciation data does not support an Ediacaran or Cambrian oxygenation event. This conclusion is of course only as sharp as the ability of the Fe-proxy database to track dissolved oxygen and does not rule out the possibility of a small-magnitude change in oxygen. It does suggest, however, that if changing  $p\text{O}_2$  facilitated animal diversification it did so by a limited rise past critical ecological thresholds, such as seen in the modern Oxygen Minimum Zones benthos. Oxygen increase to modern levels thus becomes a Paleozoic problem, and one in need of better sampling if a database approach is to be employed.

## Viscosity and structure of fayalite liquid at high pressure up to 9GPa

H. SPICE<sup>1\*</sup>, C. SANLOUP<sup>1</sup>, J. DREWITT<sup>1</sup>,  
C. DE GROUCHY<sup>1</sup>, C. CRÉPISSON<sup>2</sup>, Y. KONO<sup>3</sup>, C. PARK<sup>3</sup>,  
AND C. MCCAMMON<sup>4</sup>

<sup>1</sup>Centre for Science at Extreme Conditions, University of Edinburgh, UK (holly.spice@ed.ac.uk) (\*presenting author)

<sup>2</sup>UPMC Univ Paris 06, UMR 7193, ISTEP, Paris, France

<sup>3</sup>HPCAT, Geophysical laboratory, Carnegie Institution of Washington, USA

<sup>4</sup>Bayerisches GeoInstitut, Universitaet Bayreuth, Germany

Viscosity of magma is a crucial transport property of melts that influences a variety of important igneous processes, both during the evolution of the early Earth and in the present day mantle [1]. Previous experimental work on polymerized silicate melts e.g. [2] show a decrease in viscosity with increasing pressure. Viscosities of depolymerized silicate melts are poorly documented at mantle P-T due to experimental difficulties.

Here we present the results of *in situ* experiments on the viscosity and structure of pure fayalite melt at high pressure. Fayalite consists of isolated silica tetrahedra, so is as depolymerized as possible for a silicate melt. Viscosity measurements were carried out using the falling sphere viscometry technique e.g. [3]. Viscosity was found to decrease along the fayalite liquidus up to ~9GPa.

The structure and compressibility of fayalite melt was studied up to 7.5GPa. The coordination of the Fe-O bond was found to increase gradually from ambient pressure to 7.5GPa [4]. Higher coordination numbers allow for a more densely packed structure, resulting in a longer and hence weaker Fe-O bond, causing a decrease in viscosity [5]. The results suggest that deep Fe-rich melts will have a high density, but will be very mobile due to their low viscosity. Compressibility of the melt is derived from extrapolation of the structure factor to  $q=0 \text{ \AA}^{-1}$ . This enables the determination of density as a function of P with an unprecedented P resolution. This is a promising method to extract the equation of state of non-crystalline materials at mantle P.

[1] Ghosh and Karki (2011) *Geochim. Cosmochim. Acta.* 75, 4591-4600. [2] Kushiro (1976) *JGR* 81(35), 6347-6350. [3] Liebske *et al.* (2005) *EPSL* 240, 589-604. [4] Sanloup *et al.* *Geochim. Cosmochim. Acta.* Accepted. [5] Reid *et al.* (2003) *Phys Earth. Planet. Inter.* 139, 45-54.

## Origin of curved CSDs: Heterogeneous nucleation of crystals in crystallizing magmas

VÁCLAV ŠPILLAR\* AND DAVID DOLEJŠ

Institute of Petrology and Structural Geology, Charles University, Albertov 6, 128 43 Praha 2, Czech Republic (\*correspondence: vaclav.spillar@seznam.cz)

Crystal size distributions (CSDs) are becoming a routine method to quantitatively describe textures of plutonic and volcanic rocks. Simple batch or open system crystallization models involving homogeneous nucleation and crystal growth predict linear trends in the logarithmic population density vs. crystal size space. Since numerous magmatic rocks show concave-up curves, their origin was interpreted as due to multiple crystallization stages or population mixing. Many crystal populations in magmatic rocks also have a non-random, clustered, spatial distribution whose origin remains unclear. We show that both curved CSDs and clustering of crystals can be self-consistently explained by crystallization involving heterogeneous nucleation on crystal surfaces.

We performed three-dimensional numerical simulations of melt crystallization by homogeneous and heterogeneous nucleation and crystal growth. The rates of heterogeneous and homogeneous nucleation were coupled in order to simulate texture with a characteristic ratio of heterogeneous to homogeneous nuclei ( $H$ ). Quantitative parameters describing sizes, contact, and spatial relationships of crystals were evaluated as functions of the  $H$ -ratio.

As  $H$  increases above ~2, the CSD evolves from straight to progressively curved, the number of neighbors around a crystal increases, and the clustering index,  $R$ , decreases below unity. At  $H > 10$ , the resulting texture gains porphyritic appearance, and for  $H > 200$ , the crystallization proceeds as radial growth of heterogeneous nuclei on isolated centers and a spherulitic texture develops. Numerical simulations with variable nucleation and growth rate functions indicate that these results are general and robust, thus solely depend on the  $H$ -ratio. This approach allows meaningful determination of the role of the heterogeneous nucleation in natural samples without of a detailed knowledge of the underlying kinetics of crystallization.

Our simulations are consistent with the number of heterogeneous nuclei being about an order of magnitude predominant over the number of homogeneous nuclei in ordinary magmatic rocks with curved CSDs, without involvement of mechanical mineral-melt interactions or late magmatic coarsening.



## The climate impacts of natural aerosol

DOMINICK VINCENT SPRACKLEN, CATHERINE SCOTT  
AND ALEX RAP,

School of Earth and Environment, University of Leeds, Leeds,  
UK; dominick@env.leeds.ac.uk

Natural aerosol plays a significant role in the Earth system because climate controls many natural aerosol sources and because natural aerosol alters the radiative balance of the Earth. Here we explore a wide range of interactions and feedbacks between natural aerosol, anthropogenic aerosol and climate.

Firstly, we quantify the direct and first aerosol indirect effect of different natural aerosol sources. We explain the magnitude of these different radiative effects in terms of atmospheric chemistry and aerosol microphysics. Secondly, we quantify the impact of the natural aerosol background on the anthropogenic aerosol indirect effect. We find that a higher natural aerosol background tends to reduce the first aerosol indirect effect attributed to anthropogenic aerosol. Next, we explore the impact of anthropogenic aerosol on natural aerosol – climate feedbacks. We demonstrate that anthropogenic pollution aerosol in the Northern Hemisphere has reduced the climate feedback that occurs due to changes in natural aerosol emissions. Finally, we explore the impact of natural aerosol on diffuse radiation and the impact on the terrestrial biosphere.

## Age calibration of geomagnetic polarity reversals around the Cretaceous-Paleogene boundary

COURTNEY SPRAIN<sup>1\*</sup>, PAUL J., RENNE<sup>1,2</sup>  
AND GREGORY P.R. WILSON<sup>3</sup>

<sup>1</sup>Dept. Earth and Planetary Science, Univ. California,  
Berkeley, CA 94720, USA (\*correspondence:  
spra0111@berkeley.edu)

<sup>2</sup>Berkeley Geochronology Center, 2455 Ridge Rd., Berkeley,  
CA 94709, USA

<sup>3</sup>Dept. Biology, Univ. Washington, Seattle, WA 98195, USA

Improved understanding of the timing of events attending the end-Cretaceous mass extinction is limited by difficulty in correlating marine and terrestrial records. The Geomagnetic Polarity Time Scale (GPTS), if well-calibrated, offers an important means to address this problem. Terrestrial sections in the Hell Creek region of Montana, interbedded with abundant sanidine-bearing tuffs, provide an opportunity to refine the ages of polarity reversals near the Cretaceous-Paleogene boundary (KPB), ultimately providing a test on the accuracy of orbital tuning chronologies e.g. [Ogg, 2012] for these reversals. Variable sedimentation rates often render terrestrial sequences unsuitable for such purposes, but in this case close stratigraphic proximity between reversals and tuffs allows very small fractional interpolations, ranging from 0.01 to 0.25 of the distance between bounding dated tuffs.

Preliminary new <sup>40</sup>Ar/<sup>39</sup>Ar ages for 3 tuffs were combined with existing magnetostratigraphic data from two sections [Swisher *et al.*, 1993] to evaluate the potential of these records for time-scale calibration. Magnetic data gaps as large as several meters were used as conservative proxies for the uncertainty in reversal placement. Ages and uncertainties (+/- systematic sources) based on the optimization calibration of the <sup>40</sup>Ar/<sup>39</sup>Ar system [Renne *et al.*, 2011] were determined by linear interpolation for the following three polarity reversals immediately following the KPB, and are shown compared with the GTS 2012 values [Ogg, 2012].

| <u>Chron boundary</u> | <u>Age (Ma)</u> | <u>±σ (Ma)</u> | <u>GTS 2012</u> |
|-----------------------|-----------------|----------------|-----------------|
| C28r top              | 64.755          | 0.028/0.050    | 64.667          |
| C28r base             | 64.900          | 0.044/0.061    | 64.958          |
| C29r top              | 65.605          | 0.080/0.092    | 65.688          |

The uncertainties in our ages are dominated by the coarse spacing of samples defining the Chron boundaries. Our modelling indicates that with sampling at the decimeter scale and with age precision demonstrably attainable from these tuffs [Renne *et al.*, 2013], these reversals can be dated with a resolution of ±10 ka, and an absolute accuracy of ±40 ka.

## Initial $^{176}\text{Hf}/^{177}\text{Hf}$ of the Earth and early silicate differentiation

P. SPRUNG<sup>1,2</sup>, T. KLEINE<sup>1</sup> AND E.E. SCHERER<sup>3</sup>

<sup>1</sup>Institut für Planetologie, University of Münster, 48149 Münster, Germany (sprung@uni-muenster.de)

<sup>2</sup>Institute of Geochemistry and Petrology, ETH Zürich, 8092 Zürich, Switzerland

<sup>3</sup>Institut für Mineralogie, University of Münster, 48149 Münster, Germany

Investigating silicate differentiation on Earth using the  $^{176}\text{Lu}$ - $^{176}\text{Hf}$  system requires knowledge of the  $^{176}\text{Hf}/^{177}\text{Hf}$  evolution of the bulk silicate Earth (BSE). The starting point of this evolution is commonly determined by back-calculating the present-day  $^{176}\text{Hf}/^{177}\text{Hf}$  of chondrites to the age of the solar system [1]. Relative to this  $^{176}\text{Hf}/^{177}\text{Hf}$  evolution, most Hadean zircons exhibit less radiogenic  $^{176}\text{Hf}/^{177}\text{Hf}$  and were interpreted in terms of crust extraction from a primordial mantle at 4.4–4.5 Ga [e.g., 2]. However, Bizzarro *et al.* [3] argued that the initial  $^{176}\text{Hf}/^{177}\text{Hf}$  of the angrite Sahara 99555, which is  $\sim 4$   $\epsilon$ -units below the back-calculated chondrite initial [1], provides a more appropriate initial  $^{176}\text{Hf}/^{177}\text{Hf}$  of the BSE. Relative to such a revised  $^{176}\text{Hf}/^{177}\text{Hf}$  evolution of the BSE [3], Hadean zircon populations show both enriched and depleted signatures, which was inferred to imply continuous crustal growth throughout the Hadean [3].

To better constrain the initial  $^{176}\text{Hf}/^{177}\text{Hf}$  of the BSE we have initiated a Lu-Hf study on primitive meteorites, complemented by investigations of KREEP-rich lunar rocks, which provide the signature of a strongly enriched reservoir that formed at *ca.* 4.4 Ga [4]. Our data for low-Lu/Hf phases in primitive meteorites, which should directly provide the initial  $^{176}\text{Hf}/^{177}\text{Hf}$  of the solar system, overlap with the back-calculated chondrite initial [1]. Moreover, we show that the  $^{176}\text{Hf}/^{177}\text{Hf}$  of KREEP at  $\sim 3.9$  Ga is  $\sim 5.5$   $\epsilon$ -units below the contemporaneous  $^{176}\text{Hf}/^{177}\text{Hf}$  of chondrites, yielding a two-stage model age of *ca.* 4.4 Ga, assuming a chondritic Lu-Hf isotopic evolution for the bulk Moon. This Lu-Hf model age of KREEP is fully consistent with other, independent estimates for the age of KREEP. In contrast, the two-stage model age of our KREEP-rich lunar rocks relative to the revised BSE evolution of [3] is *ca.* 4.0 Ga and thus *ca.* 400 Myr too young. Thus, our new data do not support the revised initial  $^{176}\text{Hf}/^{177}\text{Hf}$  of the BSE based on Sahara 99555 [3], but rather indicate that the back-calculated chondrite composition [1] is a reliable estimate for the initial  $^{176}\text{Hf}/^{177}\text{Hf}$  of the BSE.

[1] Bouvier *et al.* (2008) *EPSL* **273**, 48–57. [2] Kemp *et al.* (2010) *EPSL* **296**, 45–56. [3] Bizzarro *et al.* (2012) *G3* **13**, Q03002. [4] Carlson & Lugmair (1979) *EPSL* **45**, 123–132.

## The structural role of iron in pantelleritic glasses

P. STABILE<sup>1\*</sup>, M.R. CICONI<sup>1</sup>, G. GIULI<sup>1</sup>, H. BEHRENS<sup>2</sup>, J. KNIPPING<sup>2</sup> AND E. PARIS<sup>1</sup>

<sup>1</sup>School of Science and Technology, Geology Division, University of Camerino, Via Gentile III da Varano, 62032 Camerino, Italy (paola.stabile@unicam.it)

<sup>2</sup>Institute of Mineralogy, Leibniz University Hannover, Callinstr.3, D-30167, Hannover, Germany

The main objects of this work are to determine the effect of oxygen fugacity and composition on the structural role of Fe in silicate glasses representative of pantelleritic magmas. Since many studies have investigated melts using glasses as a structural analogue [1, 2, 3], we have focused on the structural environments of Fe and S in synthetic glasses to relate their behaviour to natural magma with the same composition.

Several glasses have been synthesized under controlled oxygen fugacity conditions (from air to iron-wustite buffer) and with different (Na+K)/Al ratios. In fact, alkali content is known to affect strongly the Fe oxidation state in silicate glasses [4], but it is still controversial to which extent alkali can modify Fe structural role in glasses/melts. Hydrothermal syntheses have been carried out at 1.5 kbar and temperatures between 800°C and 1000°C. Additionally, glasses were produced by melting in a Ar/H<sub>2</sub> gas mixing furnace at ambient pressure and at 1250°C.

Water incorporation in the glasses has been characterized by Karl-Fischer titration (KFT) and IR spectroscopy. Additionally, the redox state of iron in the glasses has been determined by colorimetric wet-chemical analyses. Preliminary Fe K-edge X-ray Absorption Spectroscopy data allowed to study the kinetic of Fe reduction under anhydrous conditions. Here we present preliminary results on Fe oxidation state, coordination number and geometry [5]. The results will be useful for understanding the role of Fe in the polymerization of the silicate melt and the interaction Fe-S.

[1] Calas & Petiau (1983) *Solid State Communic.* **45**, 625–629. [2] Mysen *et al.* (1985) *American Mineralogist* **70**, 317–331. [3] Giuli *et al.* (2002) *Geochimica et Cosmochimica Acta* **66**, 4347–4353. [4] Moretti & Ottonello (2003) *Journal of Non-Cryst. Solids* **323**, 111–119. [5] Giuli *et al.* (2012) *American Mineralogist* **97**, 468–475.

## First-principles calculations of the lattice thermal conductivity of the lower mantle

STEPHEN STACKHOUSE<sup>1\*</sup>, LARS STIXRUDE<sup>2</sup>  
AND BIJAYA B. KARKI<sup>3</sup>

<sup>1</sup>School of Earth and Environment, University of Leeds, Leeds LS2 9JT, United Kingdom  
s.stackhouse@leeds.ac.uk (\* presenting author)

<sup>2</sup>Department of Earth Sciences, University College London, Gower Street, London WC1E 6NT, United Kingdom  
l.stixrude@ucl.ac.uk

<sup>3</sup>School of Electrical Engineering and Computer Science, Department of Geology and Geophysics, and Center for Computation and Technology, Louisiana State University, Baton Rouge, LA 70803, United States of America  
karki@csc.lsu.edu

The rate of loss of heat from Earth's core is controlled by the thermal conductivity of the minerals that comprise the overlying mantle. The heat-flux at the core-mantle boundary has implications for the thermal evolution of both the core and mantle, the size and stability of plumes, and magnetic field generation. As insulators, conduction in lower mantle phases is expected to be dominated by phonon transport. Estimates of the thermal conductivity of MgSiO<sub>3</sub> perovskite, the most abundant phase, at core-mantle boundary conditions, vary significantly, with the phonon contribution reported to lie between 1.6 and 17 Wm<sup>-1</sup>K<sup>-1</sup>. In view of this, we have performed ab initio non-equilibrium molecular dynamics simulations to determine the lattice thermal conductivity of MgSiO<sub>3</sub> perovskite at lower mantle conditions, calculating it to be 6.5 ± 0.8 Wm<sup>-1</sup> K<sup>-1</sup>, a value consistent with geophysical constraints on the thermal state at the base of the mantle. Our results suggest that the conductivity depends strongly on pressure, helping to explain the dynamical stability of superplumes, and weakly on temperature and composition, so that lateral variations in thermal conductivity at the base of the mantle are small.

## Origin of methane to n-butane in marine sediments of the New Jersey shallow shelf

S. STADLER<sup>1</sup>, R. VAN GELDERN<sup>2</sup> AND S. SCHLÖMER<sup>1</sup>

<sup>1</sup>Federal Institute for Geosciences and Natural Resources (BGR), Stilleweg 2, 30655 Hanover, Germany,  
susanne.stadler@bgr.de, stefan.schloemer@bgr.de

<sup>2</sup>GeoZentrum Nordbayern, Schlossgarten 5, FAU Erlangen–Nürnberg, 91054 Erlangen, Germany,  
robert.van.geldern@fau.de

Concentrations and stable carbon isotope compositions of C<sub>1</sub> to C<sub>4</sub> in pore fluids were measured in three cores (M0027A, M0028A and M0029A) of IODP Expedition 313 that targeted Miocene sedimentary sequences up to 67 km off the coast of New Jersey, USA (Mountain *et al.* 2010), to understand processes related to gas geochemistry and carbon cycling in the investigated shallow shelf. Stable carbon isotope data and C<sub>1</sub>/(C<sub>2</sub>+C<sub>3</sub>) ratios suggest a biogenic origin of methane. If methane is produced by a biogenic process this could in principle also be the case for C<sub>2+</sub> gases as suggested by Hinrichs *et al.* (2006). An alternative explanation could be low-temperature kerogen cracking (Rowe & Muehlenbachs 1999). Showing first data we discuss gas formation mechanisms including the potential source of the organic material, secondary alteration processes and the role of mixing of gases of different origin (biogenic versus thermal) at the investigated site.

[1] Hinrichs, K.U., Hayes, J.M., Bach, W., Spivackl, A.J., Hmelo, L.R., Holm, N.G., Johnson, C.G. and Sylva, S.P. (2006): Biological formation of ethane and propane in the deep marine subsurface. - Proceedings of the National Academy of Sciences of the United States of America 103:14684-14689. [2] Mountain, G., Proust, J.-N., McInroy, D., Cotterill, C., and the Expedition 313 Scientists (2010): Proceedings of the Integrated Ocean Drilling Program, Volume 313: Tokyo (Integrated Ocean Drilling Program Management International, Inc.). [3] Rowe, D., Muehlenbachs, A. (1999): Low-temperature thermal generation of hydrocarbon gases in shallow shales. - Nature (London) 398:61-63.

## High-pressure stability of synthetic $\text{Al}_{63}\text{Cu}_{24}\text{Fe}_{13}$ icosahedral quasicrystal

V. STAGNO<sup>1</sup>, L. BINDI<sup>2\*</sup>, C. MURPHY<sup>1</sup>, Y. FEI<sup>1</sup>,  
AND P.J. STEINHARDT<sup>3</sup>

<sup>1</sup>Carnegie Institution of Washington, USA (vstagno@ciw.edu; cmurphy@ciw.edu; yfei@ciw.edu)

<sup>2</sup>Università di Firenze, Italy (luca.bindi@unifi.it).

<sup>3</sup>Princeton University, USA (steinh@princeton.edu).

Quasiperiodic crystals are solids characterized by quasiperiodic translational order and a discrete point group impossible for ordinary periodic crystals [1]. Among synthetic quasicrystalline solids, icosahedral- $\text{Al}_{63}\text{Cu}_{24}\text{Fe}_{13}$  is of particular interest since it is representative of icosahedrite, the first quasicrystal found in nature [2, 3]. Although an extraterrestrial origin has been recently established for icosahedrite [4], pressure and temperature conditions at which the mineral would be stable are still not clear. Previous studies showed that synthetic AlCuFe quasicrystals do not undergo any phase transitions over pressures up to 35 GPa (at room temperature) [5] and over a temperature range of 500-870 °C at ambient pressure. However, no data are available for  $\text{Al}_{63}\text{Cu}_{24}\text{Fe}_{13}$  quasicrystal at high temperatures and pressures.

We have performed *in situ* high-pressure synchrotron X-ray diffraction experiments under quasi-hydrostatic conditions (neon pressure medium) using diamond anvil cell technique up to 51.5 GPa (in both compression and decompression) to investigate the possible structural evolution of the synthetic analogue of icosahedrite. We also performed a series of quenched experiments with multi anvil to determine the thermal stability of  $\text{Al}_{63}\text{Cu}_{24}\text{Fe}_{13}$  at different isobars (between 3 and 20 GPa) and employing different capsule materials to intrinsically buffer the oxygen fugacity.

Preliminary results from *in situ* X-ray diffraction data collected at ambient temperature confirm that the high degree of translational order for the  $\text{Al}_{63}\text{Cu}_{24}\text{Fe}_{13}$  icosahedral quasicrystal is retained at much higher pressures than previously reported.

Results from this study will improve our knowledge regarding the origin of icosahedrite in nature and provide constraints on the pressure and temperature conditions for its formation.

[1] Levine, D., Steinhardt, P.J. (1984) *Phys. Rev. Lett.* **53**, 2477-2480. [2] Bindi, L. *et al.* (2009) *Science* **324**, 1306-1309. [3] Bindi, L. *et al.* (2011) *Am. Mineral.* **96**, 928-931. [4] Bindi, L. *et al.* (2012) *PNAS* **109**, 1396-1401. [5] Sadoc, A. *et al.* (1994) *Phil. Mag.* **70**, 855-866.

## Impact of anthropogenic land cover changes (ALCC) on dust particle emissions and associated impact on radiation

TANJA STANELLE<sup>1</sup>, ISABELLE BEY<sup>1</sup>, CHRISTIAN REICK<sup>2</sup>,  
THOMAS RADDATZ<sup>2</sup> AND INA TEGEN<sup>3</sup>

<sup>1</sup>Institute for Atmospheric and Climate Science & Center for Climate Systems Modeling, ETH Zurich, Switzerland, tanja.stanelle@env.ethz.ch

<sup>2</sup>Max Planck Institute for Meteorology, Hamburg, Germany

<sup>3</sup>Leibniz Institute for Tropospheric Research, Leipzig, Germany

Mineral dust particles are usually considered as 'natural' aerosols. Human activities can however affect emission of dust particles by altering land properties or through an increase in desertification associated with climate change. Changes in wind speed due to climate change also alter the amount of dust particles emitted in the atmosphere. The goal of this work is to estimate the extent to which human activities contribute to dust emissions and how this has changed since the pre-industrial time taking into account both climate change and ALCC.

For this purpose, we use the global aerosol-climate model ECHAM6-HAM2.1, in which a new method to calculate potential dust source areas was implemented. This allows us to quantify emissions from agricultural sources and to account for past and future land cover changes. The results from the simulation using the new method compare relatively well to measurements and data available in the literature, indicating that the new approaches allows a reasonable representation of today's dust load and providing confidence into the new method.

In a 'best guess' simulation, where we consider the attempts of farmers to prevent ground erosion, we find that nearly 10 % of today's dust particles are emitted globally from agricultural sources. But agricultural dust sources are not necessarily new dust sources. Often natural grass or shrub land, where emissions of dust particles can take place, were converted into agricultural land. We then account for ALCC between 1850s and 2000s in the model system and simulate emissions under different climate conditions. The contribution of ALCC on changes in dust emissions between pre-industrial times and today is estimated. Further an estimate of the changes in radiative fluxes due to dust particles emitted from agricultural sources including both the direct and indirect aerosol effect is provided.

## Geochemical and isotopic monitoring of dissolved carbon dynamic in a karst aquifer, located above the Rouse site test for CO<sub>2</sub> geological storage

Y. STANISZEWSKI<sup>1</sup>, A. GROLEAU<sup>1</sup>, D. JEZEQUEL<sup>1</sup> AND P. AGRINIER<sup>1</sup>

<sup>1</sup>IPGP-Paris 7, Institut de Physique du Globe de Paris & Univ. Paris Diderot, Sorbonne Paris Cité, UMR 7154 CNRS, 75005 Paris, France (stanis@ipgp.fr)

### A new method for monitoring CO<sub>2</sub> sequestration.

A near surface perched karst aquifer is considered as an integrative system of putative CO<sub>2</sub> leaks above the Rouse site test of CO<sub>2</sub> storage (operated by Total near Pau - France). We develop a low cost and long term geochemical monitoring of spring waters in order to describe the natural forcings that drive the dynamics of the dissolved carbon. Such procedure is mandatory in order to determine dissolved carbon thresholds above which excursions can be anomalies.

The chemical composition of the groundwater is ultra-dominated by calcium and bicarbonate ions. Dataset of 4 main springs is obtained with:

(1) high frequency measurements (15') of conductivity (C<sub>25</sub>), pH & hydrodynamics (C<sub>25</sub> and pH are used to determine the dissolved carbonate system: pH, pCO<sub>2</sub>, DIC & alkalinity).

(2) bi-monthly geochemical and isotopic samples which give another appreciation of the dissolved carbon dynamics.

We show that the C<sub>25</sub> is a very robust proxy of the alkalinity because a strong linear relation has been established between C<sub>25</sub> and carbonate composition in all meteorological conditions. At present, after three years of monitoring, we note that the dominant natural forcing of dissolved carbon is the hydrodynamic which is linked to pluviometry.

Modelisation of the geochemical impact induced by an input of CO<sub>2</sub> in the aquifer is in progress, using thermodem database [1] with the software PHREEQC [2].

Other aquifers will be tested like a typical carbonate karst: "Parc des Grands Causses".

[1] Blanc, P. *et al.* (2012), *Applied Geochemistry* 27, p2107–2116 [2] Parkhurst, D.L., Appelo, C.A.J., (1999) U.S. Geol. Surv. Water Resour. Invest. Rep. 9

## Formation mechanism of hematite-rutile pseudomorphs from Mwinilunga (Zambia)

N. STANKOVIĆ\*, N. DANEU AND A. REČNIK<sup>1</sup>

<sup>1</sup>Department for Nanostructured Materials, Jožef Stefan Institute, Jamova 39, 1000 Ljubljana, Slovenia nadezda.stankovic@ijs.si

In geologic environments we often find minerals which formed by replacement reactions from a parent mineral as a consequence of solid-liquid interactions [1]. The newly formed mineral or mineral assemblages retain some characteristics of the parent minerals like their euhedral shape, whereas the chemical composition and texture of the products may be different. The changes are readily used for the interpretation of geological history of the samples.

In our work we studied rutile-hematite intergrowths from the Mwinilunga locality in Zambia. Samples can be described as euhedral hematite crystals intergrown with oriented rutile crystals. The general relationship between rutile and hematite can be determined already by macroscopic observation of hematite crystals and larger rutile crystals on their surface as  $\langle 010 \rangle (101)_{\text{RUT}} \parallel \langle 001 \rangle (110)_{\text{HEM}}$ . Besides single rutiles, also rutile twins on (101) and (301) planes are found on the surface of the samples [2].

In order to determine the mechanism of ilmenite replacement by hematite and rutile, we analyzed the sample with different methods of electron microscopy. Detailed structural analysis of the sample interior along the  $[001]_{\text{HEM}}$  confirmed the macroscopically observed orientation relationship and all six possible orientations of rutile crystals within the single-crystal hematite matrix were found. The stable hematite-rutile interface was determined from the HRTEM images. In the perpendicular orientation, i.e. along the  $[100]_{\text{HEM}}$  zone axis, we found nano-sized relicts of parent ilmenite and we observed the diffusion paths of Ti-ions towards the rutile lamellae. The results of our analyses suggest that re-crystallization of ilmenite to hematite and rutile is structurally controlled. The transformation is possible since all three minerals (ilmenite, rutile and hematite) have a common oxygen sublattice which is controlling the re-crystallization to rutile and hematite [3].

[1] Putnis A, (2009) *RevMineralGeochem* 70, 87-124. [2] Daneu *et al.* (2007) *AmMin* 92,1789-1799. [3] Armbruster (1981) *NeuesJbMinerMonat* 7,328-334.

## Mg-aenigmatite from the Tazheran massif (East Siberia, Russia)

STARIKOVA A.E.<sup>1</sup> SKLYAROV AND E.V.<sup>2</sup> KANAKIN S.V.<sup>3</sup>

<sup>1</sup>IGM SB RAS, Novosibirsk, Russia, a\_sklr@mail.ru

<sup>2</sup>IEC SB RAS, Irkutsk, Russia, skl@crust.irk.ru

<sup>3</sup>Institute of geology SB RAS, Ulan-Ude, Russia, skan\_61@mail.ru

Aenigmatite ( $\text{NaFe}^{2+}_5\text{TiSi}_6\text{O}_{20}$ ) occurs usually in high-Na magmatic rocks in association with nepheline, aegirine or augite, arfvedsonite or riebeckite, K-feldspar, sometimes fayalite. Variations of its composition are related mostly to the presence of  $\text{Fe}^{3+}$  whereas content of MnO and MgO is low (usually < 1 wt%). The Tazheran Massif of alkaline and nepheline syenites (East Siberia, Russia) [2] is the second occurrence of high-Mg aenigmatite (up to 10 wt% MgO,  $\text{Mg}/(\text{Fe}+\text{Mg}) = 0.3-0.4$ ). The only high-Mg variety have been described before in Ne-syenite on Mount Kenia [1]. In the Tazheran massif both high-Mg and typical aenigmatites occur separately at the marginal part of the Ne-syenite veins with Mll-Wo-Cpx-Grt-Ne metasomatic rocks. Both aenigmatite varieties associate with aegirine-augite, nepheline, K-feldspar, sometimes with ilmenite, Fe-olivine and richterite (only with high-Mg aenigmatite) and have low content of CaO (less than 2 wt%) and  $\text{Al}_2\text{O}_3$  (up to 5 wt%). In Mg-aenigmatite content of MgO varies from 8.5 to 10 wt%, whereas in aenigmatite – from 1 to 2 wt%. There are no transition on composition between the minerals. In most cases aenigmatites as well as Cpx and Amp occur as symplectite with nepheline. According to composition high-Mg aenigmatite does not belong to aenigmatite-rhonite ( $\text{Ca}_2(\text{Mg},\text{Fe}^{2+},\text{Fe}^{3+})_5\text{TiO}_2(\text{Si},\text{Al})_6\text{O}_{18}$ ) series, but is transitional variety of series  $\text{Na}_2\text{Fe}^{2+}_5\text{TiO}_2[\text{Si}_6\text{O}_{18}]$  (aenigmatite) -  $\text{Na}_2\text{Mg}_5\text{TiO}_2[\text{Si}_6\text{O}_{18}]$  (unknown).

The work was supported by RFBR (№ 12-05-31253, 12-05-00229) and special grant of OPTEC LLC.

[1] Price, R.C., Johnson, R.W., Gray, C.M. and Frey, F.A. (1985) *Contrib. Mineral. Petrol.*, **89**, 394-409. [2] Sklyarov E. V., Fedorovsky V. S., Kotov A. B. *et al.* (2009) *Russ. Geol. Geophys.* **50** (12), 1405–1423.

## Fe isotopic composition of sequentially extracted reactive Fe from marine sediments

MICHAEL STAUBWASSER<sup>1\*</sup>, SUSANN HENKEL<sup>1</sup>, SABINE KASTEN<sup>2</sup> AND SIMON W. POULTON<sup>3</sup>

<sup>1</sup>Institute of Geology and Mineralogy, Uni. of Cologne, GER

\*correspondence: m.staubwasser@uni-koeln.de

<sup>2</sup>Alfred Wegener Institute, Bremerhaven, GER

<sup>3</sup>School of Earth & Env., Uni. of Leeds, Leeds LS2 9JT, UK

The partitioning of Fe in sediments and soils has traditionally been studied by applying sequential leaching methods. These are based on reductive dissolution and exploit differences in dissolution rates between different reactive Fe (oxyhydr)oxide minerals. We used lab-made ferrihydrite, goethite, hematite and magnetite spiked with  $^{58}\text{Fe}$  and leached two-mineral mixtures with both phases abundant in excess of the methods dissolution capacity. Leaching was performed with 1) hydroxylamine-HCl and 2) Na-dithionite as the reactive agent. Following Poulton & Canfield (2005) [1], the first dissolution is designed to selectively leach the most reactive Fe-phases, ferrihydrite and lepidocrocite, whereas the second dissolution is designed to leach goethite and hematite. Magnetite would then be dissolved in a third dissolution step with oxalic acid.

First results show that the hydroxylamine-HCl method for ferrihydrite dissolves only insignificant amounts of goethite and hematite. However, magnetite-Fe constitutes about 10% of the total dissolved Fe. The Na-dithionite dissolved Fe from goethite-magnetite and hematite-magnetite mixtures contain about 30% of magnetite-Fe.

We applied selective sequential leaching and Fe isotope analysis to fine-grained marine sediments from a depocenter in the North Sea, which contain abundant reactive Fe (oxyhydr)oxides and show evidence for Fe sulfide formation within the upper 10 cm. Fe isotopes of the hydroxylamine-HCl leach targeting ferrihydrite shows a downcore increase of  $\delta^{56}\text{Fe}$  typical for sediments undergoing microbial reductive Fe dissolution, whereas Fe isotopes of the Na-dithionite leach (goethite and hematite) and oxalic acid leach (magnetite) are identical and show no downcore variation in  $\delta^{56}\text{Fe}$ . This means, that only the most reactive Fe phases participate in the Fe redox cycle in this location. The similar isotopic composition of goethite + hematite and magnetite suggests a detrital source, which is not utilized possibly due to the abundant ferrihydrite and lepidocrocite present.

[1] Poulton & Canfield (2005), *Chemical Geology* 214, 209–221

## The Connection Between Life and Oceanic Volcanism: Biosphere Meets Lithosphere

HUBERT STAUDIGEL<sup>1</sup>

<sup>1</sup>Scripps Institution of Oceanography, UCSD-0225, La Jolla CA 92093-0225, USA; hstaudigel@ucsd.edu

Life and volcanoes have been intimately connected since the beginning of life on Planet Earth. Microbial trace fossils in volcanic glass are amongst the earliest well preserved physical fossils on earth and we can trace the association of microbes with volcanic features throughout the geological record. Interactions between volcanoes and life may occur in diverse settings, in the deep biosphere and hydrothermal systems, in the hydrosphere and at the earth's surface and atmosphere. The total biomass associated directly or indirectly with oceanic volcanoes may comprise a substantial fraction of the total biomass on Earth. Volcanoes are known to impact life, as volcanic aerosols disrupt air traffic, change the earth's radiation budget and cause tsunamis (e.g. Thera and Krakatoa). Consequences for civilization may be substantial, with well documented changes in climate, crop failures and major loss of life and property, including the destruction of an entire culture. Oceanic volcanoes are particularly relevant as the most common and voluminous volcano type and for their immediate interaction with the oceanic/atmospheric systems that control many key global geochemical cycles.

Feedbacks between life and volcanoes are best studied using combined geo- and biological investigations. There is a clear relationship between microbial activity and many types of mineralization. Distinct microbial communities are known to preferentially colonize particular substrates. Their activity may accelerate substrate dissolution processes and distinct microbial dissolution fabrics. There are remarkable similarities in sub-sea basalt-hosted microbial communities with the ones in terrestrial soils, in terms of diversity as well as the relevance of *eukarya*, *prokarya* and *archaea*. We are beginning to understand specific microbial consortia associated with volcanic rock and their main functions such as their capabilities to gain energy from chemolithotrophic reactions and their mechanisms for carbon fixation. We are beginning to explore many details of the genetic underpinnings of microbial function specializing in volcano/ hydrothermal interactions. However, there remains much room for illuminating the geological/ geochemical controls of extremely slow-growing microbial communities, microbial evolution in the geological record and the biological controls of global geochemical cycles, amongst many other issues.

## Inert nano-reactors or dynamic micelle interfaces? CaCO<sub>3</sub> precipitation from microemulsions

TOMASZ M. STAWSKI<sup>1</sup> AND LIANE G. BENNING<sup>1</sup>

<sup>1</sup>Cohen Geochemistry Group, School of Earth and Environment, LS29JT, University of Leeds, Leeds, United Kingdom, (t.m.stawski@leeds.ac.uk and l.g.benning@leeds.ac.uk)

Reverse microemulsions are, thermodynamically stable suspensions of water droplets in oil i.e. micelles that are stabilised by an interface surfactant. Water droplets are typically 1-50 nm in diameters and can carry dissolved salt ions and exchange their content upon collisions, which lead to mineral precipitation. These droplets are believed to act as "nano-reactors" because precipitation occurs in the water pools shielded by the surfactants from the oil phase

Here we show how we can use microemulsions to elucidate the formation of CaCO<sub>3</sub> phases and stabilise initial amorphous stages. Micelles are used to confine volume in which nucleation and growth occurs. Mixing of two distinct microemulsions containing Ca<sup>2+</sup> and CO<sub>3</sub><sup>2-</sup> ions leads to a reproducible method to make nano-sized, monodisperse particles. However, there is no correlation between the initial droplet size and the size of solid CaCO<sub>3</sub> particles, which are considerably larger than the original micelles. Therefore, the notion of a "nano-reactor" may in this case be inaccurate, because it implies the formation of an inert, impenetrable water-surfactant-oil interface that limits the growth to a single droplet.

By using time-resolved and *in situ* small and wide-angle X-ray scattering and high-resolution imaging we demonstrated that CaCO<sub>3</sub> grows through a continuous but progressive and slow disintegration of the micelles, rather than precipitation inside of individual droplets. Upon destabilisation of the original salt-ion carrying micelles, new water-mineral-surfactant interfaces are created. These constitute a nucleus and they direct further growth. The formation of this interface is crucial in stabilising amorphous CaCO<sub>3</sub> in the form of nanoparticles (30-100 nm) and this also slows down or prevents further growth and crystallization.

We believe that these findings are relevant for understanding of the CaCO<sub>3</sub> growth mechanisms occurring at water-nonpolar liquid interfaces in natural and industrial environments (e.g. preventing scale formation). Microemulsions could also be a good analogue model system for mineralization of coccolith plates formed within the cell vesicles produced in the Golgi apparatuses of coccolithophores.

## Organic Carbon inventory of the Tissint meteorite.

A. STEELE<sup>1</sup>, F. MCCUBBIN<sup>2</sup>, L.G. BENNING<sup>3</sup>,  
S. SILJESTRÖEM<sup>4</sup>, G. CODY<sup>1</sup>, Y. GOREVA<sup>5</sup>, E. HAURI<sup>6</sup>,  
J. WANG<sup>6</sup>, A. KILCOYNE<sup>7</sup>, M. GRADY<sup>8</sup>, C. SMITH<sup>11</sup>,  
C. FREISSINET<sup>12</sup>, D. GLAVIN<sup>12</sup>, A. BURTON<sup>13</sup>, M. FRIES<sup>14</sup>,  
J. BLANCO<sup>3</sup>, M. GLAMOCLJA<sup>1</sup>, K. ROGERS<sup>1</sup>,  
S. MIKHAIL<sup>6</sup> AND J. DWORKIN<sup>12</sup>

<sup>1</sup>University College London, Gower St, London.  
(stealie@mac.com.)

<sup>2</sup>Inst. of Meteoritics, Dept. of Earth and Planetary Sci, Univ.  
New Mexico, Albuquerque, New Mexico, 87131 USA

<sup>3</sup>School of Earth and Environment, University of Leeds,  
Leeds, LS2 9JT, UK.

<sup>4</sup>Department of Chemistry and Materials, SP Technical  
Research Institute of Sweden, 501 15 Borås Sweden.

<sup>5</sup>Department of Mineral Sciences, Smithsonian Institution,  
Washington, DC. 20013-7012 USA.

<sup>6</sup>Department of Terrestrial Magnetism, Carnegie Institution of  
Washington, 5241 Broad Branch Rd, Washington DC.  
20015 USA.

<sup>7</sup>Advanced Light Source, 1 Cyclotron Road, MS 7R0222,  
LBNL, Berkeley, California 94720. USA.

<sup>8</sup>Centre for Earth, Planetary, Space and Astronomical  
Research. Open University, Milton Keynes, Walton Hall,  
Milton Keynes, MK7 6AA, UK.

<sup>9</sup>Université de Toulouse, UPS-OMP, IRAP, Toulouse, France.

<sup>10</sup>CNRS, IRAP, 9 Av. colonel Roche, BP 44346, 31028,  
Toulouse Cedex 4, France.

<sup>11</sup>Department of Mineralogy, The Natural History Museum,  
Cromwell Road, London, SW7 5BD. U.K.

<sup>12</sup>NASA Goddard Space Flight Center, Greenbelt Road,  
Maryland 20771, USA.

<sup>13</sup>Catholic University of America, NASA Goddard Space  
Flight Center, 8800 Greenbelt Road, Greenbelt, Maryland,  
20771, USA.

<sup>14</sup>Planetary Science Institute, 1700 East Fort Lowell, Suite  
106, Tucson, Arizona, 85719 USA

The fall of the Tissint meteorite has provided a unique opportunity to study a minimally contaminated piece of Mars. Martian organic carbon has been detected previously in igneous basalts and the carbonates of ALH 84001. Analysis of sealed maskelynite inclusions using *in situ* techniques including Raman, NanoSIMS, ToFSIMS, STXM and TEM, coupled with whole rock analysis by stepped combustion, GCMS and evolved gas analysis has revealed an inventory of organic compounds containing -CH, -CN, -CNO, -COOH, -CO and aromatic complexes. These are spatially resolved to known inorganic catalysts, i.e. magnetite, pyrite, nickel containing pyrrhotite and clays. Furthermore there is a release of nitrogen containing organics above 600°C, at which temperature  $\delta^{15}\text{N}$  is  $\sim +40\%$ . These results show that Mars has an inventory of organic carbon and nitrogen containing molecules that are probably produced through abiological hydrothermal activity.

## PTX properties of FeCl<sub>2</sub>-bearing fluids at elevated PT conditions

MATTHEW STEELE-MACINNIS<sup>1\*</sup>, PILAR LECUMBERRI-SANCHEZ<sup>1</sup> AND ROBERT J. BODNAR<sup>1</sup>

<sup>1</sup>Department of Geosciences, Virginia Tech, Blacksburg VA  
24061, USA (\*correspondence: mjmaci@vt.edu)

Iron chloride is a significant component of saline aqueous fluids in many ore-forming environments, commonly occurring at concentrations of up to several mass percent [1]. Thus the effect of FeCl<sub>2</sub> on the phase equilibria of aqueous fluids is a significant factor in interpreting fluid evolution in iron-rich systems such as tin-tungsten deposits and some porphyry copper deposits. However, there are few available experimental data on the phase equilibria and thermometric properties of iron-bearing aqueous fluids [2].

We have used the synthetic fluid inclusion technique to investigate the pressure-temperature conditions along the locus of critical points in the system H<sub>2</sub>O-FeCl<sub>2</sub>, from 0 to 35 wt% FeCl<sub>2</sub>. Our results show that the effect of FeCl<sub>2</sub> on the phase equilibria of aqueous fluids is unlike that of other divalent cation chlorides such as CaCl<sub>2</sub> or MgCl<sub>2</sub>. Specifically, the locus of critical points for H<sub>2</sub>O-FeCl<sub>2</sub> fluids occurs at significantly lower pressure (at a given temperature) compared to the critical curve of the system H<sub>2</sub>O-NaCl. For example, at 500 °C the critical point for H<sub>2</sub>O-FeCl<sub>2</sub> fluids occurs at 480 bar, compared to about 560 bar for H<sub>2</sub>O-NaCl. The low pressure along the H<sub>2</sub>O-FeCl<sub>2</sub> locus of critical points implies that immiscibility (boiling) of FeCl<sub>2</sub>-rich fluids can occur only at relatively low pressures, or relatively shallow levels in the crust. These results allow us to reinterpret the conditions of mineralization at boiling, Fe-rich hydrothermal systems.

[1] Yardley (2005) *Econ. Geol.* **100**, 613-632. [2] Liebscher (2007) *Rev. Mineral. Geochem.* **65**, 15-47.



## IR spectroscopic and quantum chemical study of metal bicarbonate and carbonate interaction in aqueous solutions

ANDRI STEFÁNSSON<sup>1</sup>, KONO LEMKE<sup>2</sup>,  
PASCALE PÉNÉZETH<sup>2</sup> AND JACQUES SCHOTT<sup>3</sup>

<sup>1</sup> University of Iceland, Sturlugata 7, 101 Reykjavík, Iceland  
(e-mail: as@hi.is)

<sup>2</sup> University of Hong Kong, Pokfulam Road, Hong Kong

<sup>3</sup> GET, CNRS/UMR 5563-Université Paul Sabatier, 14 rue  
Edouard Belin, 31400 Toulouse, France

Carbonate speciation are among the most important in aqueous systems. Carbonic acid deprotonates to form  $\text{HCO}_3^-$  and  $\text{CO}_3^{2-}$ , which further may complex with dissolved cations in solution. In this study, potentiometric and IR spectroscopic measurements were conducted as well as molecular simulation calculations to gain insight into the aqueous speciation of  $\text{H}_2\text{O}-\text{CO}_2-\text{NaCl}\pm\text{MgCl}_2$  solutions. In  $\text{H}_2\text{O}-\text{CO}_2-\text{NaCl}$  solutions  $\text{CO}_2(\text{aq})$ ,  $\text{HCO}_3^-$  and  $\text{CO}_3^{2-}$  predominates, with addition to the  $\text{NaHCO}_3(\text{aq})$  and  $\text{NaCO}_3^-$  ion-pairs. These ion-pairs are weak at low-temperatures but become increasingly important with increasing temperature under neutral to alkaline conditions in moderately dilute to concentrated NaCl solutions. With addition of  $\text{MgCl}_2$ ,  $\text{MgHCO}_3^-$  and  $\text{MgCO}_3(\text{aq})$  ion-pairs form, these accounting for significant part of the carbonate species concentrations. The combined potentiometric and IR measurements demonstrate that these ion-pairs truly exist in solution and cannot solely be explained by non-ideal ion-ion interaction. Moreover, the coordination number of  $\text{Mg}^{2+}$  is reduced upon substitution of  $\text{HCO}_3^-$  and  $\text{CO}_3^{2-}$  to the hydration shell from six to a maximum number of five. These changes may have profound effects on further reactions of  $[\text{MgCO}_3\cdot n\text{H}_2\text{O}]^0$  and  $[\text{MgHCO}_3\cdot n\text{H}_2\text{O}]^+$  to form Mg-carbonate and bicarbonate clusters and minerals. No such coordination changes were observed associated with  $\text{Na}^+$   $\text{HCO}_3^-$  and  $\text{CO}_3^{2-}$  ion pairing. Based on the experimental results the equilibrium ionization and ion-pair formation constants were retrieved that can be used to calculate aqueous speciation in  $\text{H}_2\text{O}-\text{CO}_2-\text{NaCl}+\text{MgCl}_2$  containing solutions.

## $\delta^{30}\text{Si}$ in early Archean cherts and implications for the silica cycle

E. J. T. STEFURAK\*<sup>1</sup>, W. W. FISCHER<sup>2</sup>  
AND D. R. LOWE<sup>1</sup>

<sup>1</sup>Stanford University, Stanford, CA 94305, USA

(\*correspondence: ltrower@stanford.edu)

<sup>2</sup>California Institute of Technology, Pasadena, CA 91125,  
USA

Si isotopes in Archean cherts offer insight into mass fluxes and mechanisms associated with silica concentration, precipitation, diagenesis and metamorphism. Previous studies have used Archean chert  $\delta^{30}\text{Si}$  to estimate seawater  $\delta^{30}\text{Si}$  [1-4], assuming a simple mass balance model with silica inputs from crustal weathering balanced by outputs of hydrothermal silicification and amorphous silica precipitation from seawater. This model relies on reservoir analogies, even though silicon reservoirs often have broad  $\delta^{30}\text{Si}$  ranges resulting from low temperature dissolution and precipitation reactions. We propose that process analogies are more appropriate for the early Archean system.

To connect isotope composition to process, we used secondary ion mass spectrometry (SIMS) to compare  $\delta^{30}\text{Si}$  and  $\delta^{18}\text{O}$  in distinct silica phases present in cherts, including carbonaceous bands, pure chert bands and grains, early cavity-filling cements and later quartz-filled veins. Our results indicate that low temperature processes fractionated silicon isotopes in early Archean marine basins—behavior that probably precludes the application of chert  $\delta^{30}\text{Si}$  as a paleothermometer. Relationships between  $\delta^{18}\text{O}$  and petrographic textures are consistent with setting during early burial and diagenesis [5]. The average value we observe for petrographic textures we infer to be primary silica precipitates from seawater,  $\delta^{30}\text{Si} +0.6\text{‰}$ , is heavier than expected for bulk silicate Earth ( $\delta^{30}\text{Si} -0.4\text{‰}$ ). This constraint is consistent with an isotope mass balance wherein contemporaneous iron formation deposits have negative  $\delta^{30}\text{Si}$  composition and form a notable fraction of the mass balance of Si leaving seawater. Precipitation of authigenic clay minerals may have also comprised a large part of the required  $^{30}\text{Si}$ -depleted sink, in addition to playing a role as an important non-carbonate alkalinity sink consuming cations released by silicate weathering. We present a new model for the Archean silica cycle based on process analogies and existing data sets.

[1] Robert & Chaussidon (2006), *Nature* **443**, 969-972. [2] van den Boorn *et al.* (2007), *Geology* **35**, 939-942. [3] van den Boorn *et al.* (2010), *Geochim Cosmochim Acta* **74**, 1077-1103. [4] Abraham *et al.* (2011), *EPSL* **301**, 222-230. [5] Lowe & Knauth (2003), *GSA Bulletin* **115**, 566-580.

## Impact of Natural Sulfidation of Silver Nanoparticles on Bioavailability and Biouptake

JOHN STEGEMEIER<sup>1,2</sup>, GREGORY V. LOWRY<sup>1,2</sup>,  
AMY DALE<sup>1,2</sup>, CLEMENT LEVARD<sup>3,2</sup>,  
FABIENNE SCHWAB<sup>4,2</sup>, BENJAMIN P. COLMAN<sup>4,2</sup>,  
EMILY S. BERNHARDT<sup>4,2</sup>, ELIZABETH A. CASMAN<sup>1,2</sup> AND  
MARK R. WIESNER<sup>4,2</sup>

<sup>1</sup>Carnegie Mellon University, Pittsburgh, PA 15213

<sup>2</sup>Center for Environmental Implications of Nanotechnology

<sup>3</sup>Centre de Recherche et d'Enseignement de Géosciences de  
l'Environnement, Aix-en-Provence, France

<sup>4</sup>Duke University, Durham, NC 27708

Engineered silver nanoparticles (Ag NPs), often partially or fully sulfidized, enter the environment. There, sulfidation of Ag NPs greatly decreases the rate of oxidation of Ag<sup>0</sup> and the release of Ag<sup>+</sup>. We hypothesized that sulfidation of Ag<sup>0</sup> NPs added to an emergent freshwater wetland mesocosm would greatly decrease silver bioavailability. We dosed a 1.2x1x3m freshwater wetland mesocosm with 30nm PVP-coated Ag NPs (25 mg/L Ag) and then determined the distribution and speciation of Ag NPs after 18 months. A sediment diagenetic model was developed and used to predict the distribution and speciation of Ag in the mesocosms.

Ag<sup>0</sup> NPs in sediments sulfidized over 18 months. Ag speciation was approximately 50% Ag<sub>2</sub>S, 30% Ag-S-R (likely organic matter complexed) and 20% Ag<sup>0</sup> as determined by X-ray absorption spectroscopy. Sulfidation decreased dissolved Ag concentration in the water column to below method detection (2 µg/L). The sediment diagenetic model could predict Ag distribution and speciation well using parameter values (e.g. bioturbation) and partition coefficients (e.g. Ag-organic matter) in the range expected for freshwater sediment and demonstrated seasonal fluctuations. There was measurable uptake of Ag into several sediment dwelling organisms, suggesting that Ag<sub>2</sub>S or Ag-S-R species remained bioavailable. The uptake of Ag<sub>2</sub>S in duckweed roots was confirmed with synchrotron based micro-X-ray fluorescence (µ-XRF) and µ-XANES indicates that the silver within the root cortex was predominantly Ag<sup>0</sup>.

## Cavity ring-down spectroscopy for the high-precision analysis of the triple oxygen isotope composition of water and water vapor

E. J. STEIG<sup>1</sup>, V. GKINIS<sup>2</sup>, A.J. SCHAUER<sup>1</sup>, J. HOFFNAGLE<sup>2</sup>,  
S. TAN<sup>2</sup> JAND S.W. SCHOENEMANN<sup>1</sup>

<sup>1</sup>Earth and Space Sciences, University of Washington, Seattle, WA 98195, USA, steig@uw.edu

<sup>2</sup>Institute for Arctic and Alpine Research, University of Colorado, Boulder, CO 80309, v.gkinis@nbi.ku.dk

<sup>3</sup>Picarro Inc., 3105 Patrick Henry Drive, Santa Clara, CA 95054, jhoffnagle@picarro.com

High precision analysis of the <sup>17</sup>O/<sup>16</sup>O isotope ratio is an important new tool in water isotope analysis. The <sup>17</sup>O-excess (= ln(δ<sup>17</sup>O+1)-0.528 ln(δ<sup>18</sup>O +1)) is sensitive to kinetic fractionation processes and nearly invariant with temperature [1]. For most applications, measurements of <sup>17</sup>O-excess must have a precision of ~5 per meg. This precision is normally obtained by flourination of H<sub>2</sub>O to O<sub>2</sub> and analyzed by dual-inlet isotope ratio mass spectrometry (IRMS).

Cavity ring-down spectroscopy (CRDS), commonly used for measurements of δ<sup>18</sup>O or δD in water [2, 3], provides several advantages over IRMS, including streamlined sample handling and the ability to measure ambient water vapor in the field. Use of CRDS for <sup>17</sup>O-excess poses unique challenges not addressed by existing commercial instruments. While a H<sub>2</sub><sup>17</sup>O absorption region is present in some instruments, the absorbance is influenced by the tail of the H<sub>2</sub><sup>16</sup>O spectrum; resulting precision is inadequate for distinguishing samples from the meteoric water line.

We describe a new CRDS system for high precision <sup>17</sup>O-excess measurements. Innovations include i) use of two lasers that measure absorption in different IR regions; ii) sample introduction system for continuous introduction of water vapor over long time periods (similar to [3]); iii) novel improvements to the spectroscopy. Samples can be analyzed with ~5 per meg precision in 60 min. Calibration with respect to VSMOW is achieved using working laboratory standards previously calibrated with IRMS [4]. The results show that both the precision and the accuracy of the new CDRS are competitive with IRMS methods. An additional benefit is improved precision of δ<sup>18</sup>O and δD (0.02 ‰, 0.08 ‰).

[1] Luz and Barkan (2005), RCM, 19, 3737-3742; [2] Crosson (2008) Appl. Phys. B, 92, 403-408; [3] Gkinis *et al.* (2011) Atmos. Meas. Tech., 3, 2531-2542; [4] Schoenemann *et al.* (2013) RCM, 27, 582-590.

## Eocene hydrocarbon migration, Green River Formation, Utah

HOLLY STEIN<sup>1,2</sup>, JUDITH HANNAH<sup>1,2</sup>, GANG YANG<sup>1</sup>,  
HELGE LØSETH<sup>3</sup>, LARS WENSAAS<sup>3</sup>  
AND PETER COBBOLD<sup>4</sup>

<sup>1</sup>AIRIE Program, Colorado State University, Fort Collins, CO  
80523-1482 USA; holly.stein@colostate.edu

<sup>2</sup>CEED Centre of Excellence, University of Oslo, Norway

<sup>3</sup>Statoil ASA, Research Centre Rotvoll, Trondheim, Norway

<sup>4</sup>Géosciences, Université de Rennes, France

The renowned Eocene Green River Formation presents a spectacular field setting to study both source rock and migration of hydrocarbon. From the Uinta basin, we combine field observations with Re-Os data from pristine outcrop and drill core samples to interpret hydrocarbon migration history.

To build a meaningful Re-Os data set, we employ our sampling strategy to capture just a few mm of stratigraphic section for each analysis. Larger bulk samples risk homogenization of real variations in the initial Os ratio and any time occupied by non-depositional or erosional intervals. Re-Os data for the Mahogany Bed and the petroliferous Mahogany Zone in Hells Canyon (Utah) are combined with Re-Os data from drill core from the Parachute Creek and Douglas Creek members to provide a compelling story for hydrocarbon migration. Samples from high-TOC "Rich Zones" (local stratigraphic nomenclature; the Mahogany Zone is "Rich Zone 7") show a narrow range of Re and Os concentrations and a narrow range in <sup>187</sup>Re/<sup>188</sup>Os ratios relative to low-TOC "Lean Zones"; this combination can lead to easily misinterpreted Model 1 isochron ages with low MSWDs and large age uncertainties. Such data sets do not provide accurate depositional ages. Rather, these data sets may characterize Re-Os behavior on initiation of hydrocarbon migration. In effect, we may be looking at source rock with incipient migration of its own oil (i.e., unconventional hydrocarbon), with local homogenization of organic matter and the Re and Os it carries. Samples from designated Lean Zones have nearly an order of magnitude lower Re and Os and yield Re-Os scatterchrons of 47-49 Ma. Scatterchrons and variable <sup>187</sup>Os/<sup>188</sup>Os ratios are attributed to local migration of oil still mixed with original kerogen.

Our Re-Os data and an interpretation that accommodates the full data set bring new understanding to hydrocarbon systems in lacustrine rocks. In some cases, Re-Os results inform us not just about the shale, but about hydrocarbon generation and incomplete expulsion. Field relationships are used to support this interpretation.

*Project initiated and funded by Statoil ASA, including joint field work; additional core samples from USGS library.*

## Dust transport over the late Quaternary Red Sea - Dead Sea regions from Nd-Sr isotopes in deep- sea cores and lake sediments

M. STEIN<sup>1\*</sup>, D. PALCHAN<sup>1,2</sup>, A. ALMOGI-LABIN<sup>1</sup>,  
Y. EREL<sup>2</sup> AND SL GOLDSTEIN<sup>3</sup>

<sup>1</sup>Geological Survey of Israel, 30 Malkhe Israel St. Jerusalem,  
95501 ISRAEL (motistein@gsi.gov.il)

<sup>2</sup>Institute of Earth Science, The Hebrew University of  
Jerusalem, ISRAEL 91904

<sup>3</sup>Lamont -Doherty Earth Observatory, Columbia University,  
Palisades NY 10964, USA

The Red and Dead Seas situated along the African – Syrian Rift valley between the Sahara and Arabia deserts and the subtropical Mediterranean received during the late Quaternary dust particles that were transported from the Sahara-Arabia deserts, Ethiopian Highlands and the Nile delta. Nd and Sr isotope ratios, chemical and mineralogical compositions of fine-detritus particles, that were recovered from the deep-sea cores: KL15, KL11 and KL23 and from Dead Sea and east Mediterranean sedimentary archives were used to determine the particle sources and reconstruct the synoptic conditions responsible for their transport.

The data indicate that during glacial dust was blown to the northern Red Sea and the east Mediterranean- Dead Sea area from the Sahara deserts by winds associated with the strong-glacial Mediterranean winter cyclones. At the same time dust was blown from Sahelian sources by southern winds associated with monsoonal circulation. During the last interglacial and the African Humid Period, monsoonal rains caused erosion and flooding at the ANS margins of the Red Sea, increasing the contribution of granitic ANS material to the Red Sea floor. During the Heinrich events (e.g. H11 and 1), mixed basaltic-granitic dust was blown from all sources reflecting severe regional aridity, when both monsoonal and Mediterranean cyclone activity were weak.

## Enhanced ice nucleation activity of soil dust particles

I. STEINKE<sup>1</sup>, R. FUNK<sup>2</sup>, A. DANIELCZOK<sup>3</sup>, K. HÖHLER<sup>1</sup>,  
N. HIRANUMA<sup>1</sup>, N. HOFFMANN<sup>1</sup>, M. HUMMEL<sup>1</sup>,  
S. KIRCHEN<sup>4</sup>, A. KISELEV<sup>1</sup>, M. LEUE<sup>2</sup>, O. MÖHLER<sup>1</sup>,  
H. SAATHOFF<sup>1</sup>, M. SCHNAITER<sup>1</sup>, T. SCHWARTZ<sup>4</sup>,  
B. SIERAU<sup>5</sup>, O. STETZER<sup>5</sup>, E. TOPRAK<sup>1</sup>, A. ULRICH<sup>2</sup>,  
C. HOOSE<sup>1</sup> AND T. LEISNER<sup>1,6</sup>

<sup>1</sup>Institute for Meteorology and Climate Research Atmospheric Aerosol Research, Karlsruhe Institute of Technology, Germany

<sup>2</sup>Institute of Soil Landscape Research, Leibniz Centre for Agricultural Landscape Research, Germany

<sup>3</sup>Institute for Atmospheric and Environmental Sciences, Goethe University Frankfurt, Germany

<sup>4</sup>Institute of Functional Interfaces, Karlsruhe Institute of Technology, Germany

<sup>5</sup>Institute for Atmospheric and Climate Science, ETH Zürich, Switzerland

<sup>6</sup>Institute of Environmental Physics, Heidelberg University, Germany

Primary biological particles have been identified as very efficient ice nuclei at high sub-zero temperatures. Soil dust particles emitted from agricultural areas contain large amounts of organic material such as fungi, bacteria and plant debris. Thus, soil dust particles may act as a carrier for highly ice-active biological particles. In this work, we present ice nucleation experiments conducted in the AIDA cloud chamber where we investigated the ice nucleation efficiency of three types of soil dust from different regions of the world. Results are presented for the immersion freezing and the deposition nucleation mode of these soil dust samples: all soil dusts show higher ice nucleation efficiencies than desert dusts, especially at high temperatures. In addition, inertially separated ice crystal residuals from these AIDA experiments have been analyzed in order to elucidate the ice nucleation process in more detail. The organic content of the soil dusts is investigated with regard to morphology and composition, hydrophilicity, as well as the diversity and viability of species. These characteristics are then related to the ice nucleation efficiencies of the individual dusts.

## Oceanographic control on microbial methane oxidation in the water column offshore Svalbard

LEA I. STEINLE\*<sup>1,2</sup>, CAROLYN GRAVES<sup>3,4</sup>,  
CHRISTIAN BERNDT<sup>2</sup>, TOMAS FESEKER<sup>5</sup>,  
MORITZ F. LEHMANN<sup>1</sup>, TINA TREUDE<sup>2</sup>  
AND HELGE NIEMANN<sup>1</sup>

<sup>1</sup>University of Basel, Dept. of Env. Geosciences, CH  
(\*correspondence: lea.steinle@unibas.ch)

<sup>2</sup>Helmholtz Centre for Ocean Research (GEOMAR), DE

<sup>3</sup>National Oceanography Centre Southampton, UK

<sup>4</sup>University of Southampton, UK

<sup>5</sup>University of Bremen, DE

A large number of gas flares were recently discovered at the landward termination of the methane gas hydrate stability zone off Svalbard. The gas ebullition is most probably caused by seasonal bottom water temperature fluctuations of 1-2°C, causing periodic methane hydrate formation and dissociation. During summer time, methane concentrations were consistently elevated in bottom waters (up to 825 nM), providing abundant substrate for aerobic methanotrophs. Our investigations on the spatio-temporal variation of aerobic methane oxidation (MOx) rates revealed highest rates (up to 3.1 nM/day) at ~50 m above the sea floor. Despite constant supply of methane, MOx rates displayed a high temporal variability. Comparison of MOx rates and water temperature revealed consistent spatio-temporal patterns that suggest an oceanographic control on the magnitude of MOx: Cool Arctic bottom water contains a comparably large standing stock of methanotrophic bacteria. This water mass is episodically displaced by the warmer W-Spitsbergen current, which is depleted in methanotrophic biomass. CARD-FISH analyses confirmed that high MOx rates are associated with the presence of methanotrophic cell aggregates. Our data thus imply that MOx fluctuations offshore Svalbard are indirectly controlled by ocean circulation patterns rather than methane substrate availability.

## Absorption and fractionation of Rare Earth Elements (REE) by plants

M. STEINMANN<sup>1\*</sup>, L. BRIOSCHI<sup>1</sup>, E. LUCOT<sup>1</sup>,  
MC. PIERRET<sup>2</sup>, P. STILLE<sup>2</sup>, J. PRUNIER<sup>2,3</sup>, PM. BADOT<sup>1</sup>

<sup>1</sup> Chrono-Environnement, Univ. Franche-Comté/CNRS,  
F-25030 Besançon, France (\*correspondence :  
marc.steinmann@univ-fcomte.fr)

<sup>2</sup> LHyGeS-EOST, Univ. Strasbourg/CNRS,  
F-67084 Strasbourg, France

<sup>3</sup> GET, Univ. P. Sabatier/CNRS, F-31400 Toulouse, France

Rare Earth Elements (REE) are increasingly used by man (electronics industry, medicine, agriculture) and therefore considered as emerging pollutants. The present study documents REE mobility in non-polluted natural soil-plant systems in order to characterize their environmental availability for future anthropogenic pollution.

The study is based on a field approach in non-polluted natural sites with contrasting geological environments (limestone, granite and carbonatite) and highly variable REE contents. The data show that REE uptake by plants is not primarily controlled by the plant itself, but depends on the concentration and the speciation in the soil and the adsorbed soil water pool. REE uptake by plant roots are linked with those of Fe. Roots absorb preferentially the light REE (Fig. 1). Before translocation, REE are retained by the Casparian strip leading to much lower concentrations in the aerial parts. The transport of the REE within the xylem is associated with the general nutrient flux.

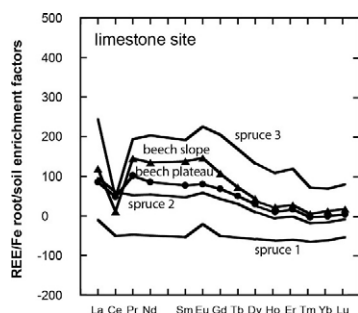


**Figure 1:** Soil-normalized REE/Fe ratios of plant roots ( $([REE/Fe]_{\text{root}}/[REE/Fe]_{\text{soil}})*100$ ) showing that roots absorb the LREE preferentially with respect to Fe. Figure from [1].

[1] Brioschi *et al.* (2012) *Plant Soil*, DOI 10.1007/s11104-012-1407-0

## Late Devonian “Kellwasser-Event” A global mass-extinction equivalent to the Precambrian-Cambrian boundary interval?

YANNIK STEINMANN<sup>1\*</sup>, ULRICH STRUCK<sup>1</sup>  
AND ANTONIA GAMPER<sup>1</sup>

<sup>1</sup>Museum für Naturkunde, Invalidenstr. 43, D-10115 Berlin,  
(\*yannik.steinmann@fu-berlin.de)

The Late Devonian Kellwasser Event characterizes a significant epoch in the evolution of the Palaeozoic ecosphere and hosts one of the five major global mass-extinction events in Earth history. During this period massive continental renovations forced seawater level changes and climate instabilities thus provoking biogeochemical perturbations of the oceans likely comparable to the Precambrian-Cambrian evolution events. Culminating in the extinction of up to 60% of the pelagic biosphere the Kellwasser period is characterized by the deposition of two black shale successions, the so-called Kellwasser horizons (e.g. Germany, France, USA). Well preserved Devonian strata crop out in sections around the Kellwassertal in the central German Harz Mountains. However, geochemical data especially sedimentary bulk nitrogen isotope values from these rock sections are rare.

We determined  $\delta^{13}\text{C}_{\text{carb}}$ ,  $\delta^{13}\text{C}_{\text{org}}$  and  $\delta^{15}\text{N}$  isotope values from an outcrop near Goslar including the basal cephalopod limestone, the lower and upper Kellwasser horizons and the overlying lower Famennian limestones. The section represents a carbonate-siliciclastic setting in a submarine rise environment permanently connected to the ocean but influenced by multiple trans- and regression events.  $\delta^{15}\text{N}$  isotope data from the Kellwasser horizons reveal two major negative excursions, one shift down to  $-1.2\text{‰}$ , the latter  $-1.7\text{‰}$ . Two positive co-occurring  $\delta^{13}\text{C}_{\text{carb}}$  and  $\delta^{13}\text{C}_{\text{org}}$  excursions represent the global Kellwasser carbon isotope signal as already reported in other upper Devonian sections worldwide.

Our data represent trustful markers for the marine palaeo-oxygenation state and nutrient availability suggesting that biogeochemical events during the Frasnian-Famennian interval can roughly be compared to the Precambrian-Cambrian boundary interval and may record phases of photic zone anoxia. Scenarios like the stepwise upper Devonian mass-extinction of biota associated with marine transgressive events and negative  $\delta^{15}\text{N}$  excursions can be paralleled to the Precambrian-Cambrian event recorded in sections e.g. of South China and Kazakhstan thus enabling new approaches of interpretation.

## Mineralogical characterization and crystallization kinetics of fibrous and acicular volcanic orthopyroxenes from Mt. Etna, Sicily, Italy

I. STELLUTI<sup>1\*</sup>, C. VITI<sup>2</sup>, A. GIANFAGNA<sup>1</sup>

<sup>1</sup> Dipartimento di Scienze della Terra, Sapienza Università di Roma, Italy (\*correspondence: igor.stelluti@uniroma1.it)

<sup>2</sup> Dipartimento di Scienze Fisiche, della Terra e dell'Ambiente, Università di Siena, Italy (cecilia.viti@unisi.it)

The present study reports mineralogical characterization of unusual acicular and fibrous orthopyroxenes occurred in the autoclastic volcanic products from Santa Maria di Licodia, belonging to "Mt. Calvario Formation", Etna Volcano. The orthopyroxene is associated to Na-feldspar, augitic clinopyroxene, apatite and Fe-Ti oxides and shows variable morphology from prismatic to fibrous, with composition enstatite to ferroan-enstatite. Prismatic and acicular morphologies highlight a composition with high Fe contents (FeO 18-20 wt%) and moderate Ca enrichments (~1 wt %), whereas the fibers present enrichment in Mg contents (FeO < 11%). Fibrous orthopyroxene has been investigated by Transmission Electron Microscopy (TEM), revealing fibers less than 1  $\mu\text{m}$  in diameter, with perfectly euhedral habit, high crystallinity and crystal order. Selected Area Electron Diffraction (SAED) patterns show sharp and intense reflections, with limited streaking effects, probably corresponding to polytypic disorder and twinning. Corresponding HRTEM images confirm the occurrence of rare packing defects and twinning, giving rise to lamellar nanostructures in both parallel and orthogonal orientations with respect to c fiber axis. A remarking feature is represented by the systematic occurrence of a very thin amorphous film that envelops the entire fiber. Focused-beam EDS microanalyses highlighted reverse zoning, with Fe-enriched cores and Mg-enriched rims.

Orthopyroxenes with fibrous morphology are rare [1, 2] and there is no evidence in literature about their presence in volcanic environment. The occurrence of the fibrous orthopyroxene in the volcanic area studied [3] allowed to undertake this detailed mineralogical investigation. The data obtained provide some preliminary constraints on crystallization kinetics pointing to conditions of high temperature crystallization and very fast cooling.

[1] Abu El-Rus et al. (2006) - *Lithos*, **89**, 29-46. [2] Bryant et al. (2007) - *Geochem. Geophys. Geosyst.*, **8**, 24 pp. [3] Gianfagna et al. (2012) *EMC2012* - **1**, 533.

## Magmatic evolution at Yellowstone: The role of isotopically juvenile magma inferred from zircon age, trace-element and Hf isotope data

MARK STELTEN<sup>1\*</sup>, KARI COOPER<sup>1</sup>, JORGE VAZQUEZ<sup>2</sup>, JOSH WIMPENNY<sup>1</sup>, QING-ZHU YIN<sup>1</sup>

<sup>1</sup>University of California – Davis, Davis, CA, USA (\*correspondance: mestelten@ucdavis.edu)

<sup>2</sup>U.S. Geological Survey, Menlo Park, CA, USA

Yellowstone caldera (USA) is a prime example of a long-lived, large-volume silicic magma system that has produced numerous eruptions of rhyolite and basalt during Quaternary time, including caldera-forming eruptions at ca. 2.1 Ma, ca. 1.3 Ma and ca. 0.640 Ma [1]. The most recent post-caldera eruptive episode at Yellowstone produced the Central Plateau Member (CPM) of the Plateau Rhyolite, which erupted between ca. 170-70 ka. Previous research (e.g., [2]) has documented that the Nd isotopic compositions of the CPM rhyolites lie between that of the local crust and Yellowstone basalts, leading to the hypothesis that both local crust and isotopically juvenile material are required to explain the genesis of the CPM rhyolites. Additionally, it is clear from oxygen isotopic studies that the low  $\delta^{18}\text{O}$  values of the CPM rhyolites (~4 to 4.5‰) require some contributions from remelted, hydrothermally altered crustal rocks [3, 4]. Here we use zircon age, trace-element and Hf isotopic compositions to explore the role of isotopically juvenile magma in the generation of the CPM rhyolites.

New Hf isotope data from CPM zircons demonstrate the presence of zircons with juvenile Hf isotope compositions (-4 to 0  $\epsilon_{\text{Hf}}$ ) relative to their host CPM glasses (-5.7 to -6.2  $\epsilon_{\text{Hf}}$ ), which requires that isotopically juvenile silicic magmas contributed mass to the CPM magma reservoir. Local crustal sources and older Yellowstone rhyolites have  $\epsilon_{\text{Hf}}$  values lower than the CPM rhyolites (<-6.5  $\epsilon_{\text{Hf}}$ ) and therefore cannot represent the sources responsible for contributing the high- $\epsilon_{\text{Hf}}$  zircons observed in the CPM rhyolites. Instead, new Hf isotope data show that the Yellowstone basalts (-0.1 to 5.5  $\epsilon_{\text{Hf}}$ ) are the only source identified to date with an appropriate isotopic composition to account for the Hf isotopic heterogeneity observed in CPM zircons. Thus, these data suggest that 1) the high  $\epsilon_{\text{Hf}}$  CPM zircons crystallized from isotopically juvenile silicic magma that is a hybrid of silicic liquids derived from Yellowstone basalts and local crust and 2) this isotopically juvenile hybrid magma is then added to the CPM reservoir periodically thorough time. In turn, these data provide direct evidence supporting the concept that both crustal-derived and mantle-derived (i.e., juvenile) components are required to generate Yellowstone rhyolites.

[1] Lanphere et al. (2002), *Geol Soc Am Bull*, **114**, 559-568. [2] Hildreth et al. (1991), *J. Pet.*, **32**, 63-138. [3] Bindeman et al. (2008), *J. Pet.*, **49**, 163-193. [4] Watts et al. (2012), *Contrib. Mineral. Petrol.*, **164**, 45-67.

## Biotite is an important host for Nb in the lower crust

STEPANOV A.S.<sup>1,2</sup>, HERMANN J.<sup>1</sup>

<sup>1</sup>RSES, Australian National University, Canberra, Australia

<sup>2</sup>CODES, University of Tasmania, Hobart, Australia  
(sasha.stepanov@utas.edu.au)

The trace element-enriched continental crust is a result of partial melting of the mantle, which displays a complementary depleted composition. Nb and Ta are elements regarded as geochemical twins showing very similar properties and they display a strong affinity to Ti minerals. Therefore it is surprising that significant fractionation of Nb and Ta are observed at global scale. The subchondritic Nb/Ta ratio of both the continental crust and the depleted mantle is known as the “missing Nb paradox”.

We present partitioning data between biotite and granitic melt for experimental and natural samples that provide evidence that Nb is compatible in biotite. Nb can thus be enriched in the residue during partial melting of crustal rocks. Additionally, biotite preferentially incorporates Nb over Ta (Stepanov and Hermann, 2013). Hence, incipient partial melting in the lower crust with biotite as residual mineral can result in restites with high Nb contents and super chondritic Nb/Ta.

Data from two key localities of crustal anatexis provide additional evidence for intracrustal Nb and Ta fractionation during partial melting of biotite-bearing rocks. Crustal, granulite facies metapelite encalves from the El Hoyazo (EH) dacite, Spain, contain melt inclusions that have significantly lower Nb and Nb/Ta than the bulk rock composition. In contrast, residual biotite is an abundant phase in the enclaves and has high Nb contents and Nb/Ta significantly higher than the bulk rock. In the classic lower crustal section in the Ivrea Verbano zone, northern Italy, metasedimentary amphibolite grade rocks have typical crustal Nb/Ta ratios, whereas granulite grade restites have higher and partial melts lower ratios. Therefore we suggest that intra-crustal differentiation might be an important process to produce Nb-rich rocks with superchondritic Nb/Ta that represent one of the missing reservoirs to balance the subchondritic Nb/Ta of the upper crust and the depleted mantle.

[1] Stepanov, A.S., Hermann, J., 2013. Fractionation of Nb and Ta by biotite and phengite: Implications for the “missing Nb paradox”. *Geology* 41, 303–306.

## The Paleoproterozoic MORB-type tholeiitic dykes as indicators of early continents breakup

A.V. STEPANOVA<sup>1\*</sup>, A.V. SAMSONOV<sup>2</sup>,  
E.B. SALNIKOVA<sup>3</sup>, YU.O. LARIONOVA<sup>2</sup>,  
A.N. LARIONOV<sup>4</sup>, V.S. STEPANOV<sup>1</sup>

<sup>1</sup>Institute of Geology, Karelian Research Centre, Russian Academy of Sciences, Petrozavodsk, Russia  
(\*correspondence: stepanov@krc.karelia.ru)

<sup>2</sup>IGEM Russian Academy of Sciences, Moscow, Russia

<sup>3</sup>IPGG, Russian Academy of Sciences, St. Petersburg, Russia

<sup>4</sup>CIR VSEGEI, St. Petersburg, Russia

The time and circumstances of the Precambrian continents fragmentation is usually highly controversial issue because of deep erosion and absence of clear evidences of breakup events. Relics of various igneous provinces occur in Precambrian Shields, but it is difficult to decide which of them is indicator of final continent breakup.

In the Karelian Craton, Eastern Fennoscandian Shield there are a lot of Paleoproterozoic (2.5 -1.97 Ga) mafic dykes that vary in composition from high-Mg to high-Fe-Ti tholeiites [1]. Among them we recognize very specific dykes of age 2.13-2.14 Ga. In spite of intracontinental tectonic setting these dykes are MORB-type tholeiites with flat REE patterns, HFSE enrichment, Nb/Nb\* = 0.7-1.6 and  $\epsilon_{\text{Nd}}$  range from +3.0 to +1.4. Geochemical modelling indicates that chemical and isotopic compositions of the dykes are best explained by derivation of their parental magmas from partial melting of depleted mantle sources in the spinel peridotite stability field, followed by fractional crystallization and low (< 6%) extent assimilation of continental crustal material. The latter suggests a rapid rise of mafic melts, accompanied by rapid crust extension, which follows from the morphology of the dykes.

Widespread MORB-type tholeiitic dykes on the Karelian Craton suggest substantial lithosphere thinning accompanied by asthenosphere rising. This allows us to consider MORB-type tholeiitic dykes as indicators of final breakup of the Achaean continent and Lapland-Kola and Svecofennian oceans opening. This statement is supported by strong compositional similarity between studied dykes and syn-breakup basalts in North Atlantic Igneous Province [2], [3] and Afar [4], [5].

[1] Vuollo & Huhma (2005) *Prec. Geol. of Finland*, 195–236.

[2] Søger & Holm (2011), *Chem. Geol.*, 297–313. [3] Waight & Baker (2012), *JP*, 1569–1596. [4] Barrat *et al.* (2003) *Lithos*, 1–13. [5] Daoud *et al.* (2010) *Lithos*, 327–336.

## Formation of Se(0) nanoparticles by *Azospirillum brasilense*

R. STEUDTNER<sup>1\*</sup>, A. MAFFERT<sup>1</sup>, M. VOGEL<sup>1</sup>,  
C. FRANZEN<sup>1</sup> AND A.C. SCHEINOST<sup>1</sup>

<sup>1</sup> Helmholtz-Zentrum Dresden-Rossendorf e.V.,  
Institute of Resource Ecology, P.O. Box 510119, D-01314  
Dresden, Germany  
(\*correspondence: r.steudtner@hzdr.de)

We investigated the reduction of  $\text{SeO}_3^{2-}$  by *Azospirillum brasilense*. The formation of fairly soluble Se(0) nanoparticles during this process is of interest for both bioremediation of Se-contaminated sites and for nanobiotechnology.

*A. brasilense* was cultured in 30 mL medium at 30 C in a shaking (100 rpm) incubator for 3 days in the presence of 1 mM Se(IV). The cellular material was then separated from the red Se precipitate by using a modified procedure of Oremland *et al.* [1]. The cleaned precipitate was resuspended in deionized water. For selective Se(IV) quantification in the culture media we used hybrid generation atomic absorption spectrometry (HG-AAS) [2]. The formed Se precipitate was characterized by scanning electron microscopy with energy-dispersive X-ray spectrometry (SEM-EDX), photon correlation spectroscopy (PCS) and zeta potential measurements.

After exposing *A. brasilense* to Se(IV), the bacterial growth continued after an extended lag-phase. After a cultivation time of 3 days, a reddish staining of the sample was observed, indicating the formation of Se(0). SEM coupled to EDX confirmed the formation of nanoparticulate, red Se(0). Only 10 % of the initial Se(IV) concentration could be recovered from the culture media by HG-AAS. The separated Se(0) suspension was stable for several hours, sufficient for the PCS and the zeta potential measurements. In contrast, Se(0) chemically formed by reduction with hydroxylamine solution produced amorphous aggregates with rapidly settled down. PCS and SEM imaging showed that the Se(0) particles had a particle size distribution between 100 and 300 nm with an averaged particle diameter of 200 nm. The isoelectric point of Se(0) particles was at  $\text{pH } 2.8 \pm 0.2$ . The preference of forming Se(0) particles with a negative charge agree very well with the literature [3].

[1] Oremland *et al.* (2004) Appl. Environ. Microb. **70**, 52-60.  
[2] Niedzielski *et al.* (2002) Pol. J. Environ. Stud. **11**, 219-224. [3] Dhanjal & Cameotra (2010) Microb. Cell Fact. **9**, 1-11.

## Stable and Radiogenic Strontium isotope behaviour in the subglacial environment

E. I. STEVENSON<sup>1\*</sup>, S. M. ACIEGO<sup>1</sup>, I. J. PARKINSON<sup>2</sup>  
K.W. BURTON<sup>3</sup>, C. ARENDT<sup>1</sup>

<sup>1</sup> Earth and Environmental Sciences, University of Michigan,  
Ann Arbor, MI 48109 USA, (\*correspondence:  
emisstev@umich.edu)

<sup>2</sup> Bristol Isotope Group, School of Earth Sciences, University  
of Bristol, Wills Memorial Building, BS8 1RJ, UK

<sup>3</sup> Department of Earth Sciences, Durham University, Science  
Labs, Durham DH1 3LE, UK

Subglacial hydrology plays a key role in determining the nutrient fluxes from glaciated terrains. Differences in the chemical and isotopic composition of the glacial outflow are controlled by variations in initial inputs, mineralogy, mineral dissolution and residence time. We present geochemical data from the glacial discharge of two geographically, geologically and climatologically distinct glaciers over two field seasons: the Athabasca Glacier, Canada (AG, Precambrian sedimentary bedrock) and the Lemon Creek Glacier, USA (LCG, Southeast Alaska metamorphic belt).

Strontium isotopes are widely utilized in studies of weathering and hydrology. Radiogenic Sr ( $^{87}\text{Sr}/^{86}\text{Sr}$ ) is a good proxy for varying hydrological inputs and weathering reactions, however Sr *stable* isotopes ( $\delta^{88/86}\text{Sr}$ ) can be fractionated by both precipitation and dissolution reactions. A combination of the two strontium systems should therefore provide improved constraints on the weathering environment.

Radiogenic Sr results indicate differences in glacial outflow composition with  $^{87}\text{Sr}/^{86}\text{Sr} \sim 0.7142$  and  $\sim 0.7106$  for AG and LCG respectively. Radiogenic Sr data from the AG show clear resolvable seasonal excursions, varying from 0.716 in May to 0.712 in July. By contrast, the meltwater from the Lemon Creek shows little variability in radiogenic strontium with time. The  $^{87}\text{Sr}/^{86}\text{Sr}$  in suspended sediments from the LCG are consistently less radiogenic than their water counterparts and show a similar trend toward more radiogenic values as the season progresses.

The  $\delta^{88/86}\text{Sr}$  data, however clearly show the difference in the underlying bedrock geology with mean  $\delta^{88/86}\text{Sr} \sim 0.19$  and  $\sim 0.33$  for AG and LCG respectively. Analysis of  $\delta^{88/86}\text{Sr}$  from suspended sediments from LCG show consistently lighter compositions than the corresponding water sample.

Variations in both  $^{87}\text{Sr}/^{86}\text{Sr}$  and  $\delta^{88/86}\text{Sr}$  in the meltwater will be analyzed using principle component analysis to reveal relationships with water mass source and elemental fluxes.



## Determining the pre-eruptive magmatic conditions and sulfur release of the AD1280 Quilotoa eruption, Ecuador

A-M. STEWART; J. CASTRO

Johannes Gutenberg Universität, 55099 Mainz, Germany  
(\*stewara@uni-mainz.de, castroj@uni-mainz.de)

Pre-eruptive conditions in the magma storage zone prior to the AD1280 eruption of Quilotoa volcano in Ecuador have been constrained using geothermobarometry; values of 240 MPa average magma pressure and  $f_{O_2}$  NNO+1.63 were calculated; a relatively oxidized, shallow magma of 800°C.

Using FTIR and EMPA on glass melt inclusions in quartz phenocrysts, total water dissolved in the melt was determined to be ~6.65 wt% ( $X_{H_2O}$  0.21), of which 5.05wt% exists as  $H_2O_m$  while 1.6wt% is OH.  $CO_2$  in the melt is variable. The average, 141ppm, corresponds to  $X_{CO_2}$   $1.8e^{-4}CO_2$ .

Using  $CO_2$ - $H_2O$  solubility models, a melt  $X_{H_2O}$  0.2 was computed – equal to the value measured in the melt, indicating water saturation at the time of trapping.

A dominance of  $H_2O$  over  $CO_2$  is revealed in the vapor phase: 0.98 and 0.02 respectively.

Melt sulfur concentrations are 47-92ppm. Petrologic methods, magma volume- $SO_2$  degassing correlations and ice core records were combined to estimate values of 969 Mt  $H_2O$  and 2.25 Mt  $SO_2$  degassed from the melt during the eruption, from which  $\leq 3.4$  Mt  $H_2SO_4$  could have been produced (assuming 100%  $SO_2$ -to- $H_2SO_4$  conversion) and a total of 35-75Mt  $SO_2$  (melt + excess S vapor phase), producing ~52-115 Mt  $H_2SO_4$ .

## Origin of dissolved solids in Marcellus shale produced water

BRIAN W. STEWART<sup>1\*</sup>, ELIZABETH C. CHAPMAN<sup>2</sup>,  
ROSEMARY C. CAPO<sup>1</sup>, JOSEPH R. GRANEY<sup>3</sup>  
AND JASON D. JOHNSON<sup>3</sup>

<sup>1</sup>Department of Geology and Planetary Science, University of Pittsburgh, Pittsburgh, PA 15217, USA (\*correspondence: bstewart@pitt.edu)

<sup>2</sup>Echelon Applied Geoscience Consulting, 1229 Twelve Oaks Ct. Murrysville, PA 15668, USA

<sup>3</sup>Department of Geological Sciences, Binghamton University, Binghamton, NY 13902, USA

Hydraulic fracturing of black shales for natural gas production results in large volumes of flowback and produced water, which rapidly (within days to weeks) achieves high levels of total dissolved solids (TDS), sometimes  $>2 \times 10^5$  ppm. This highly saline water continues to be produced, albeit at much diminished rates, over the lifetime of the well. This brine could originate from (1) interaction of injected water with salts in the formation, (2) extraction of brine trapped in pores within the shale and/or (3) formation water previously held in fractures, sandy lenses, or adjacent strata. To evaluate the origin of these dissolved solids, we carried out sequential leaching experiments on dry-drilled cuttings from the Middle Devonian Marcellus shale and adjacent units in Tioga County, New York, USA. The samples were treated with ultrapure water to dissolve soluble salts and sulfates, 1N ammonium acetate buffered to pH 8 to extract exchangeable cations, 8% acetic acid to dissolve carbonate minerals and 0.1N HCl to target other acid-soluble phases.

The water leachates had consistently higher Na/Cl and lower Ca/ $SO_4$ , Na/Ca and Sr/Ca ratios compared to produced water [1, 2]. Ba/Ca ratios were highly variable (as in the produced water) and  $>90\%$  of the Ba extracted was in the ammonium acetate fraction, suggesting it is bound in exchangeable sites within the shale.  $^{87}Sr/^{86}Sr$  ratios of water-soluble and exchangeable Sr range from 0.7093 to 0.7112, mostly within the range of  $^{87}Sr/^{86}Sr$  values measured in produced waters [1], but well above Devonian seawater and well below bulk-shale values ( $>0.731$ ). Based on the significant differences between the chemistry of the leachates and that of Marcellus produced waters, we suggest that most solutes in the latter are inherited from highly saline formation waters in fractures or adjacent strata. Long-term interaction of these waters with the shale imprinted similar Sr isotope ratios on the water-soluble and exchangeable portions.

[1] Chapman *et al.* (2012) *ES&T* **46**, 3545-3553. [2] Haluszczak *et al.* (2013) *AppGeochem* **28**, 55-61.

## Improved boron isotope pH proxy calibration for the deep sea coral *Desmophyllum dianthus* through sub-sampling of fibrous aragonite

J.A. STEWART<sup>\*1</sup>, E. ANAGNOSTOU<sup>1</sup> AND G. L. FOSTER<sup>1</sup>

<sup>1</sup>Ocean and Earth Science, National Oceanography Centre, University of Southampton, Southampton, UK, (\*Joseph.Stewart@noc.soton.ac.uk)

The isotopic composition of boron ( $\delta^{11}\text{B}$ ) in marine carbonates is well established as a proxy for past ocean pH [1,2]; however, its robust application to palaeo-environments relies on the generation of species-specific calibrations. Existing calibrations utilising the deep sea coral *Desmophyllum dianthus* highlight the potential application of  $\delta^{11}\text{B}$  measurements of this species to pH reconstructions of intermediate depth waters [3,4]. However considerable uncertainty remains regarding the estimation of seawater pH from these bulk  $\delta^{11}\text{B}$  measurements, resulting from sub-structural heterogeneities in  $\delta^{11}\text{B}$  of *D. dianthus*. To circumvent this problem, thus improving the reliability of the *D. dianthus*  $\delta^{11}\text{B}$  calibration, we present a new  $\delta^{11}\text{B}$  calibration of micro-sampled fibrous aragonite from *D. dianthus*. Modern coral specimens recovered from the Atlantic, Pacific and Southern Oceans (depth range of 274-1470 m) were micro-sampled using a MicroMill (New Wave), analysed using multi-collector ICP-MS (Neptune) and the measured  $\delta^{11}\text{B}$  was regressed against ambient pH taken from hydrographic data sets (pH range 7.4 to 8.0).  $\delta^{11}\text{B}$  values from this new fibre calibration are generally lower than bulk septal measurements [e.g. 3] and suggest a stronger and better-defined dependence on ambient seawater pH. This study confirms the utility of *D. dianthus* as an archive of palaeo-pH, provided suitable sampling strategies are applied.

[1] Sanyal *et al.* (2001) *Paleoceanography* 16, 515-519, [2] Hönisch *et al.* (2004) *EPSL* 68, 3675-3685, [3] Anagnostou *et al.* (2012) *EPSL* 349-350, 251-260, [4] McCulloch *et al.* (2012) *GCA* 87, 21-34.

## Dual sources for early Taranaki magmas: The Sr isotope story

R.B. STEWART<sup>1\*</sup>, R.C. PRICE<sup>2</sup>, I. E.M. SMITH<sup>3</sup> AND A. ZERNACK<sup>4</sup>

<sup>1</sup>Volcanic Risk Solutions, IAE, Massey University, Palmerston North 4442, New Zealand (\*correspondence: r.b.stewart@massey.ac.nz)

<sup>2</sup>Faculty of Science and Engineering, University of Waikato, Hamilton, New Zealand (rprice@waikato.ac.nz)

<sup>3</sup>School of Environment, University of Auckland, Auckland 1142, New Zealand (ie.smith@auckland.ac.nz)

<sup>4</sup>Tanenuiarangi Manawatu Inc., PO Box 1341, Palmerston North, New Zealand (a.zernack@massey.ac.nz)

Mount Taranaki, located 140 km west of the Taupo Volcanic Zone (TVZ), lies 180 km above the Wadati-Benioff Zone and is the most westerly subduction-related volcanism in New Zealand. Compositions are basaltic andesite to andesite with minor dacite and basalt. Taranaki has erupted episodically for more than 130 ka, generating debris avalanche deposits by catastrophic failure of the edifice. These deposits provide a record of the early magmatic evolution of the Taranaki volcanic system.  $\text{K}_2\text{O}$  and LILE are enriched with time, culminating in Holocene high-K andesites [1]. Pre-100 ka magmas include primitive basalts and basaltic andesites with higher silica compositions in progressively younger units and the appearance of late-stage low pressure mineral phases (high-Ti hornblende, biotite and Fe-rich orthopyroxene) confirms a gradual shift to more evolved magmas with time.

Sr isotope compositions have been constant at around 0.7046; similar to the least radiogenic compositions at Ruapehu, a long-lived active andesite volcano in the TVZ, suggesting a common mantle wedge composition for both Taranaki and the TVZ. However, the Taranaki isotope data set contains evidence for the presence prior to 100 ka of an even less radiogenic source with  $^{87}\text{Sr}/^{86}\text{Sr}$  compositions of < 0.7040, mostly in primitive basalts with < 50%  $\text{SiO}_2$ . Trace element data for these samples have only weak arc signatures. A similar dual Sr isotope source is evident in the older Pouakai volcano in Taranaki. We suggest that in the early Taranaki magma systems a component of relatively unmodified mantle was present that was eclipsed after c. 100 ka by subduction-modified material. The slab under Taranaki is near-vertical and this slab configuration might allow edge flow to contribute to the Taranaki magma source.

[1] Zernack *et al.* (2012) *J Pet* 53, 325-363.

## Rare Earth Elements origin and dynamic in contaminated river basins: Nd isotopic evidence

STILLE P.<sup>1</sup>, HISSLER C.<sup>2</sup> AND CHABAUX F.<sup>1</sup>

<sup>1</sup> LHyGeS - UMR 7517 CNRS - EOST/UdS, 1 rue Blessig  
F-67084 Strasbourg cedex (pstille@unistra.fr,  
fchabaux@unistra.fr)

<sup>2</sup> GEOSAT/EVA/CRP-GL, 41 rue du Brill L-4422 Belvaux  
(hissler@lippmann.lu)

Uncertainties in identifying the origin of pollutants in river systems and in quantifying their impact particularly exist for ecosystems in strongly contaminated river basins. The difficulty of such estimations is based on the relative significance of both anthropogenic and natural sources of trace metals in the environment. The natural geochemical background is characterized by important variations at global, regional or local scales. Moreover, elements currently considered to be undisturbed by human activities and used as tracers of continental crust derived material have become more and more involved in industrial or agricultural processes. The global production of lanthanides (REE), used in industry, medicine and agriculture, for instance, has increased exponentially from a few tons in 1950 to about 150 kt in 2012. Consequently, these contributions interfere in the estimation of natural REE sources.

The application of Nd isotope ratios has very recently been successfully used for the first time for tracing the anthropogenic contribution of atmospheric deposition in urban and industrial areas (Lahd Geagea *et al.*, 2008; Hissler *et al.*, 2008; Guéguen *et al.*, 2012). However, at our knowledge, no study focused on the fractionation of the Nd isotopic ratio due to anthropogenic activity in river systems. For this reason, this work is dedicated to the understanding of processes that control the Nd isotopic fractionation in river waters heavily contaminated by anthropogenic activities.

The upper Alzette River basin, in Luxembourg, suffers from substantial historical and current contamination principally due to the presence of the steel industry, which has been active from 1875 until now. The particulate and dissolved fractions of river waters were monitored using a multitracer approach (including REE and Nd isotopes) during two hydrological cycles (bi-weekly and flood event based sampling). This extensive sampling design allowed to understand the seasonal dynamics of the waters Nd isotopic compositions according to the REE composition of the particulate fraction of the water. Combining REE concentrations and the Nd isotopic information allowed us to quantify the annual anthropogenic fluxes of REE.

## A review of CO<sub>2</sub> and O<sub>2</sub> gas dynamics within the sub-surface Critical Zone and implications for early-atmosphere studies using paleosols

G. E. STINCHCOMB<sup>1\*</sup>, S. L. BRANTLEY<sup>1</sup>

<sup>1</sup>Department of Geosciences, Pennsylvania State University,  
University Park, PA 16802

(\*Correspondence: ges130@psu.edu, <sup>1</sup>sxb7@psu.edu)

The pCO<sub>2</sub> concentrations of early Earth's atmosphere are a key component for resolving the faint young Sun paradox and have been intensely debated for some time. Regolith models that use mass-balance geochemical arguments, based on the consumption of CO<sub>2</sub> through the neutralization of soil, saprolite and rock, prove to be one of the more reliable methods for estimating atmospheric pCO<sub>2</sub> [1, 2, 3]. Yet, many of the assumptions used to estimate the early atmosphere are difficult to test in the modern biotic Earth. This study serves as a review of modern regolith gas research and explores the potential use of deep weathering profiles for refining paleoatmosphere reconstructions. We compiled 248 soil CO<sub>2</sub> and O<sub>2</sub> assays from 29 regolith studies spanning a range of environments that includes deep (>3 m) profiles. Soil CO<sub>2</sub> values (n=174) range from 0.01 to 15.5% by vol., whereas soil O<sub>2</sub> values (n=74) range from 0.2 to 22.85% by vol. The compilation of regolith gas data shows that only 30% of the assays were collected from a depth >3 m; and few of these studies include both gas and bulk geochemical data. The data that do extend to depths >3 m show O<sub>2</sub>:CO<sub>2</sub> ratios that exponentially decline with increasing depth. This deep portion of the modern sub-surface Critical Zone has lower O<sub>2</sub>:CO<sub>2</sub> ratios and presumed lower biomass concentrations than the modern surface. These observations suggest that the highly acidic, low-oxidizing soil atmosphere *deep* in modern regolith may be a suitable analogue for Precambrian abiotic *near-surface* weathering. Contemporary deep (> 3 m) regolith studies that include both bulk geochemical and gaseous phase data are not only lacking but could provide a much-needed empirical dataset for refining Precambrian atmosphere estimates using paleosols. [1] Sheldon, 2006, *Precambrian Res* 147, 148-155. [2] Driese *et al.*, 2011, *Precambrian Res* 189, 1-17. [3] Brantley *et al.*, *in press*, *In Treatise of Geochemistry, The Atmosphere – History*.

## Environmental parameters that determine distribution coefficients of radionuclides for repositories

M. STOCKMANN<sup>1\*</sup>, V. BRENDLER<sup>1</sup>, J. FLÜGGE<sup>2</sup>, S. BRITZ<sup>2</sup>  
AND U. NOSECK<sup>2</sup>

<sup>1</sup>Helmholtz-Zentrum Dresden-Rossendorf, D-01314 Dresden, Germany (\*correspondence: m.stockmann@hzdr.de)

<sup>2</sup>GRS Braunschweig, D-38122 Braunschweig, Germany

In order to treat radionuclide sorption processes in natural systems more realistically, temporally and spatially variable distribution coefficients (smart  $K_d$ -values) are calculated as a function of important environmental parameters such as pH, ionic strength (IS), concentration of dissolved inorganic carbon [DIC], calcium [Ca] and radionuclides [RN]. This smart  $K_d$ -concept is implemented into the transport code  $r^3t$  [1].

As a test of the modified code  $r^3t$  and the sensitivity analysis of radionuclide sorption regarding the mentioned environmental parameters, a possible future climate transition (seawater transgression) at Gorleben site / Germany was modelled [2]. Seawater inundation drastically influences the distribution and values of all environmental parameters. Chemical changes cause dissolution or precipitation of calcite and these in turn affect the pH, DIC and Ca concentration. In consequence the  $K_d$ -values and therewith the transport of radionuclides is impacted.

The results of the calculations are plausible: environmental parameters follow expected trends and major dependencies. As a consequence of the low Ca and DIC concentration in seawater, calcite dissolves in the aquifer and causes an increase of the pH. The  $K_d$ -values change according to the changes in environmental parameters. The pH has the most dominant impact on the smart  $K_d$ -values for most of the considered RNs, except for Pu and Th, for which the DIC concentration has the strongest impact. Under the assessed conditions for seawater transgressions the smart  $K_d$ -values of Cs, Ni, Am and Np(V) increase, those of Se(VI) and U(VI) decrease with increasing pH. The smart  $K_d$ -value particularly of Pu and Th decreases with increasing DIC concentration.

This project is funded by the German Federal Ministry of Economics and Technology (BMW) under contract no. 02 E 11072A and 02 E 11072B.



[1] Fein (2004) Report GRS-192 [2] Noseck et al. (2012) Report GRS-297

## Detrital zircon U/Pb ages on sedimentary rocks from the South Carpathians, Romania and implications for regional tectonic provenance

A. STOICA<sup>1\*</sup>, M. N. DUCEA<sup>1,2</sup>, D. JIANU<sup>1</sup>

<sup>1</sup> Faculty of Geology and Geophysics, University of Bucharest, Bucharest, 010041, Romania

<sup>2</sup> Department of Geosciences, University of Arizona, Tucson, AZ, 85721, USA

(\*stoica.mala@gmail.com)

We present new detrital U/Pb zircon ages on six sands and sandstones collected from the South Carpathians, Romania. The Southern Carpathians have a nappe structure assembled during Middle to Late Cretaceous Alpine continental collision, consisting of several thrust nappes: the Getic-Supragetic nappe system, the underlying Severin complex and the lowermost Danubian nappe system, each composed of several amalgamated blocks of different affinities [1]. The analyzed rocks are: 3 mid-Cretaceous sandstones from Bucegi Mountains, one latest Cretaceous from Cozia Mountains, one Quaternary sandstone and one modern sand from Pianu Valley, north from Sebes Mountains. Our LA-MC-ICPMS U/Pb ages on detrital zircons confirm periods of magmatism in the Neoproterozoic and Cambro-Ordovician, as well as an episode of metamorphism in Late Devonian to Carboniferous documented by high U/Th ratio zircons.

The three early Cretaceous sedimentary rocks, collected from Bucegi Mountains, contain detrital zircons of different crystallisation ages ranging from 2.7 Ga to 340 Ma, but mostly clustering around 500 Ma. The predominant Neoproterozoic (550–850Ma) and Cambro-Ordovician (450-520 Ma) zircons indicate subaerial exposure of Leaota metamorphic unit in Aptian. Precambrian tectonics is documented by inherited zircons (cca. 900-1200 Ma, 1800-2200 Ma, 2600-2800 Ma), most likely recycled from Cumpana metasedimentary rocks due to their similarity in age distribution.

In the other samples, the most prominent population occurs between 450 and 500 Ma, followed by less abundant age group between 550 and 800 Ma. Older ages are also present but less frequent frequencies than in the early Cretaceous samples.

Age distribution patterns from all samples are consistent with derivation from basement rocks of the Getic-Supragetic thrust sheets and no contributions from Danubian units.

[1] Balintoni et al. (2009) *Gondwana Res.* **16**, 119-133.

## A coordinated in situ NanoSIMS, HR-SEM and TEM search for presolar grains in an ALHA77307 chondrule rim

A.N. STOJIC<sup>1\*</sup>, F. E. BRENKER<sup>1</sup>, J. LEITNER<sup>2</sup>  
AND P. HOPPE<sup>2</sup>

<sup>1</sup>Institute of Geosciences, Mineralogy, Goethe University,  
Altenhoferallee 1, 60438 Frankfurt/M., Germany  
(\*correspondence: stojic@em.uni-frankfurt.de)

<sup>2</sup>Max-Planck Institute for Chemistry, Hahn-Meitner Weg 1,  
55128 Mainz, Germany

Only recently, fine-grained rims around chondrules (FGRs) have been reported to contain presolar grains [e.g., 1, 2]. Competing hypotheses explaining formation history of FGRs are namely formation in the solar nebula or as a result of meteorite parent-body alteration processes [3]. FGRs and interchondrule matrix material do not differ chemically or mineralogically except for the grain size of the respective constituent minerals [4]. From the primitive CO3.0 chondrite ALHA 77307 containing a 390  $\mu\text{m}$  x 300  $\mu\text{m}$  large porphyritic chondrule surrounded by a FGR of 30  $\mu\text{m}$  - 75  $\mu\text{m}$  thickness, a transparent thin film suitable for TEM studies was prepared with a new preparation technique, ArIS [5]. Subsequently, 2,200  $\mu\text{m}^2$  of the FGR part of the thin film was analyzed with the NanoSIMS 50 ion probe in Mainz to search for O-rich presolar grains. Obtained isotope images, HR SEM images and TEM images of the same area were superimposed to unambiguously relocate the presolar grains among the surrounding solar material in the TEM. We detected 4 oxygen anomalous grains (3 silicates and one oxide), showing excesses in their <sup>17</sup>O/<sup>16</sup>O ratio relative to the solar value. These grains represent relative abundances of ~ 70ppm and ~ 33ppm for the silicates and oxides, respectively. All grains are Group I which to date constitute the bulk of identified presolar O-rich species forming around low mass RGB/AGB stars. One presolar silicate is a crystalline fayalitic olivine, 180 nm x 40 nm in size. The grain is embedded in a groundmass comprising fine-grained Fe-rich silicates, refractory silicates, sulfides and Fe-Ni metal. There is no microscopically observable evidence of equilibration and this absence more likely favours the solar nebula accretion hypothesis rather than parent body alteration, a conclusion previously obtained only by SEM and NanoSIMS studies in the case of ALHA 77307 [e.g., 6].

[1] Haenecour & Floss (2012) *LPSC*, XL III, # 1107. [2] Leitner *et al.* (2012) *MAPS*, **47**, A394. [3] Metzler *et al.* (1992) *GCA*, **56**, 2873. [4] Brearley (1993), *GCA*, **57**, 1521. [5] Stojic & Brenker (2010) *EJM*, **22**, 17-21. [6] Davidson *et al.* (2012) *AMM*, **47**, A115.

## High-precision LA-ICP-MS analysis of microanalytical reference materials for environmental research

B. STOLL<sup>1\*</sup>, K.P. JOCHUM<sup>1</sup>, U. WEIS<sup>1</sup>  
AND M.O. ANDREAE<sup>1</sup>

<sup>1</sup>Max Planck Institute for Chemistry, Mainz, Germany  
(\*correspondence: brigitte.stoll@mpic.de)

The high spatial resolution available with LA-ICP-MS microanalysis of speleothems, biogenic calcium carbonates, bones and teeth holds the promise to improve the understanding of past climate conditions and environmental change. However, there are analytical problems with this method, such as interferences, elemental fractionation and matrix-dependent mass load effects using non-matrix-matched microanalytical reference materials (MRM) [1]. We therefore have investigated new carbonate MACS-1, MACS-3 and phosphate MAPS-4, MAPS-5, STDP5, Durango apatite MRM by a sector-field ICP-MS coupled either with 213 nm or 193 nm Nd:YAG nanosecond (ns) lasers, or a 200 nm Ti-sapphire based femtosecond (fs) laser.

Our studies show that many masses are affected by interferences, such as <sup>24</sup>Mg<sup>++</sup> by <sup>48</sup>Ca<sup>++</sup> in the carbonate and <sup>47</sup>Ti<sup>+</sup> by <sup>31</sup>P<sup>16</sup>O<sup>+</sup> in the phosphate matrix. Elemental fractionation and mass-load-dependent matrix effects have been detected for the ns laser systems. They are small for refractory lithophile elements, such as Ba and Sr (< 5 – 10%). For chalcophile/siderophile trace elements with low boiling points (e.g., Pb, Zn) these effects are high (up to 20 - 40%) and different for the NIST silicate glasses, commonly used for calibration and the carbonate and phosphate MRM. Experiments with the femtosecond laser demonstrate that these matrix-related effects are negligibly small with this system [2]. This means that NIST glasses are suitable as calibration material [3] for carbonate and phosphate LA-ICP-MS microanalyses when using fs-UV lasers. They are also appropriate for the determination of lithophile element concentrations in environmental samples when using UV-ns lasers. However, when using ns lasers, matrix-matched calibration is still preferred for an accurate analysis of chalcophile/siderophile and volatile elements.

To further characterize the few available carbonate and phosphate MRM, we have analyzed them using the different laser ablation systems. Overall analytical uncertainties at the 95 % confidence level are about 5 – 10% for most elements. Our fs-UV laser results agree well with available reference values.

[1] Jochum *et al.* (2012) *Chem. Geol.* **318-319**, 31-44. [2] Weis *et al.* (2013) this conference. [3] Jochum *et al.* (2011) *GGR* **35**, 397-429.

## Combined $^{13}\text{C}$ -D and D-D clumping in $\text{CH}_4$ : Preliminary results

D.A. STOLPER<sup>1\*</sup>, S.S. SHUSTA<sup>2</sup>, D.L. VALENTINE<sup>2</sup>,  
A.L. SESSIONS<sup>1</sup>, A. FERREIRA<sup>3</sup>, E.V. SANTOS NETO<sup>3</sup> AND  
J.M. EILER<sup>1</sup>

<sup>1</sup>Caltech, Pasadena, CA, USA (\*dstolper@caltech.edu,  
eiler@gps.caltech.edu, als@gps.caltech.edu)

<sup>2</sup>University of California, Santa Barbara, CA, USA  
(sshusta@uamail.ucsb.edu, valentine@geol.ucsb.edu)

<sup>3</sup>Petrobras, Brazil (alexandrea@petrobras.com.br,  
eugenioneto@petrobras.com.br)

Methane is a key component of natural gas reservoirs, biogeochemical cycles and greenhouse gas emissions. Its cycle is often studied with stable isotopes (e.g.,  $\delta\text{D}$  and  $\delta^{13}\text{C}$ ), which help to distinguish between various environmental sources (e.g., thermogenic vs biogenic) and sinks [1]. However, as many of these processes generate methane with similar isotopic compositions, new measurements can aid in understanding various aspects of the methane cycle.

We present a new mass spectrometric technique that allows for the measurement of isotopologues of methane with more than one rare isotope ('clumped' isotopologues) at natural abundances. Specifically, we simultaneously measure  $^{13}\text{CH}_3\text{D}$  and  $^{12}\text{CH}_2\text{D}_2$  without interferences from water [2] and with external errors of 0.25-0.3‰ (in the  $\Delta_{18}$  notation [3]).

Clumped isotopologues can serve as geothermometers for equilibrated systems, quantify kinetic processes and fingerprint different sources and sinks. To better understand the information recorded by the clumped isotopes of methane, we experimentally generated a high-temperature (200-500°C) calibration of equilibrium clumping, including approaches to equilibrium from multiple starting points. Application of this calibration to thermogenic methane samples from natural gas fields generally yields high temperatures ( $\sim 190 \pm 65$  °C), which span the range of nominal natural gas formation temperatures, though with one high temperature outlier. The same calibration applied to biogenic gases gives lower temperatures ( $\sim 45$ -60°C) that are consistent with their inferred or known formation temperature.

Preliminary results indicate that the temperatures derived from combined  $^{13}\text{CH}_3\text{D}$  and  $^{12}\text{CH}_2\text{D}_2$  clumping are, in most cases, reasonable formation or storage temperatures. This suggests that methane may achieve internal isotopic equilibrium in both high and low temperature processes and retain that signature during storage. If so, then measurements of methane clumped isotopes will serve as a straightforward way to distinguish sources of methane in nature and give insight into the physics and chemistry of how methane forms.

[1] MJ Whiticar, *Chemical Geology* **161** (1999). [2] JM Eiler *et al.*, *IJMS* **335** (2012). [3] JM Eiler, *EPSL* **262** (2007).

## The petrochemistry of Jake\_M: A martian mugearite

E.M. STOLPER<sup>1\*</sup>, M.B. BAKER<sup>1</sup>, A. COUSIN<sup>2,3</sup>, M. FISK<sup>4</sup>,  
R. GELLERT<sup>5</sup>, P.L. KING<sup>6</sup>, S. MAURICE<sup>3</sup>,  
S.M. MCLENNAN<sup>7</sup>, M.E. MINITTI<sup>8</sup>, M. NEWCOMBE<sup>1</sup>,  
V. SAUTTER<sup>9</sup>, M.E. SCHMIDT<sup>10</sup>, A.H. TREIMAN<sup>11</sup>,  
R.C. WIENS<sup>2</sup> AND THE MSL SCIENCE TEAM

<sup>1</sup>Caltech, Pasadena, CA 91125, \*correspondence:  
ems@caltech.edu; <sup>2</sup>LANL, Los Alamos; <sup>3</sup>Institut de  
Recherches Astrophys. Planétol., Toulouse, France; <sup>4</sup>Oregon  
State Univ.; <sup>5</sup>Univ. Guelph; <sup>6</sup>Res. School Earth Sci., ANU;  
<sup>7</sup>SUNY, Stony Brook; <sup>8</sup>APL, Johns Hopkins Univ.; <sup>9</sup>LMCM,  
Paris, France; <sup>10</sup>Brock Univ.; <sup>11</sup>Lunar & Planet. Inst.

Jake\_M (JM), the first rock analyzed by the APXS instrument on the Curiosity rover, is an alkaline igneous rock ( $\sim 13\%$  normative nepheline). It differs significantly in composition from other known martian rocks and it is fractionated relative to typical martian igneous rocks (MgO  $\sim 3.5$  wt%; Mg#  $\sim 0.37$ ; Ni  $< 50$  ppm; normative oligoclase and orthoclase [ $\sim 13\%$ ]). JM is compositionally similar to terrestrial mugearites, a magma type typically found on ocean islands and in continental rift zones; indeed, were JM found on earth, we would be hard pressed to tell from its composition that it is a martian rock.

The discovery of this rock type on Mars likely indicates an origin by significant fractional crystallization of a primary alkaline or transitional magma generated by melting a region of the martian mantle compositionally distinct from the sources of other known martian basalts. JM's chemical composition (especially its high  $\text{Al}_2\text{O}_3$  and low FeO contents) suggest that this fractional crystallization occurred under conditions that suppressed plagioclase crystallization relative to crystallization at 1 atm. Although non-unique, MELTS calculations indicate that a reasonable match to JM's composition can be achieved at 2 kbar ( $\sim 15$  km depth on Mars) after  $\sim 50\%$  fractional crystallization of an estimated parental composition from St. Helena island containing 1.5 wt%  $\text{H}_2\text{O}$ . This result suggests a possible role for elevated pressure and/or water content in JM's petrogenesis.

The discovery of JM has implications for magmatic and eruptive processes on Mars, for the possibility of primary hydrous minerals in martian igneous rocks and for encountering even more fractionated alkaline magmas such as phonolites and trachytes. JM is also distinctly richer in potassium than other martian basalts, consistent with a metasomatized mantle source, perhaps characteristic of the mantle beneath the Gale Crater region.

## A novel approach for determining the rate of organic carbon remineralization in bioturbated marine sediments at the global scale

K. STOLPOVSKY<sup>1\*</sup>, A. W. DALE<sup>1</sup> AND K. WALLMANN<sup>1</sup>

<sup>1</sup>Helmholtz-Zentrum für Ozeanforschung Kiel (GEOMAR),  
Wischhofstr. 1-3, 24148 Kiel, Germany,

\*kstolpovsky@geomar.de

The spatial variability in benthic particulate organic carbon (POC) mineralization kinetics throughout the ocean is currently unknown. This creates considerable uncertainties when diagenetic models are used to couple benthic and pelagic biogeochemical cycles in global models. The aim of this study is to derive a predictive algorithm to calculate the depth-dependent rate of POC degradation in bioturbated surface marine sediments.

Our approach first uses measured fluxes of oxygen and nitrate across the sediment-water interface to calculate the total depth-integrated rate of POC degradation [1]. Next, a diagenetic reaction-transport model is used to simulate these fluxes to within a defined tolerance range by optimizing the parameters of a depth-dependent POC decay function. The model describes POC mineralization using oxygen, nitrite and nitrate as electron acceptors and also their transport into and out of the sediments by molecular diffusion, sediment burial and bioirrigation.

We applied this approach to published data from 151 stations around the globe to simulate the fluxes of oxygen and nitrate in the uppermost 50 cm of the sediment including the bioturbated layer. Where published data were available, the modelled and measured oxygen and nitrate concentration profiles were compared. Ongoing work attempts to search for spatial trends in the parameters of the optimized POC degradation model and relate these trends to master variables such as the rain rate of POC to the seafloor (RRPOC). Our over-arching goal is to use these results to better predict the benthic exchange fluxes between marine sediments and the overlying water column in global models. This is especially for the main ocean basins where field data is currently limited.

[1] Bohlen, L., Dale, A. W., & Wallmann, K. 2012 Simple transfer functions for calculating benthic fixed nitrogen losses and C:N:P regeneration ratios in global biogeochemical models. *Global Biogeochemical Cycles* 26, GB3029, doi:10.1029/2011GB004198.

## Soil organic matter and microbial activity in critical zones of tropical soils from Luquillo, Puerto Rico

M.M. STONE<sup>1</sup> AND A.F. PLANTE<sup>1\*</sup>

<sup>1</sup>Department of Earth & Environmental Science, University of Pennsylvania, Philadelphia, PA 19104-6316, USA

(\*correspondance: aplante@sas.upenn.edu)

The Luquillo Critical Zone Observatory (LCZO) is located in northeastern Puerto Rico in the El Yunque National Forest (18.33 °N, 65.73 °W) and seeks to understand the evolution of landscapes over time due to varying critical zone processes occurring in areas with similar climates, land use and geologic history. The critical zone is generally defined as the zone “where rock meets life” [1]. From this perspective, it is interesting to examine how microbial activity declines with depth into the critical zone as energy and substrate supplies decline and how this decline might be affected by various landscape properties.

The LCZO Soil Network consists of 216 quantitative soil pits, stratified across two parent materials (volcaniclastic and granodiorite), three forest types (Tabonuco, Palm and Colorado) and three hillslope positions (ridgetops, slopes, valleys). The current study used a subset of soils sampled to a depth of 140 cm and analyzed for organic C, total N and extractable organic P concentrations. Soil microbial biomass was determined using phospholipid fatty acid (PLFA) total lipid analysis [2] and enzyme activities were assayed according to German *et al.* [3].

All enzyme activities declined exponentially with depth, tracking exponential declines in total organic and microbial carbon. However, these trends differed when normalized by substrate or microbial C (i.e., specific activity). Soil parent material did not significantly affect microbial biomass or enzyme activity, though there were several significant depth × forest type interactions. Taken together, the results indicate that soil depth (as a surrogate for substrate availability) is the main driver of microbial activity in the critical zone of these tropical soils, rather than differences in landscape-scale variables.

[1] <http://criticalzone.org/national/research/the-critical-zone-1-national/>. [2] White *et al.* (1979) *Oecologia*. **40**, 51-62. [3] German *et al.* (2011) *Soil Biol. Biochem.* **43**, 1387-1397.

## Eliminate the organic nitrogen fraction to perform $\delta^{15}\text{N}_{\text{tot}}-\delta^{15}\text{N}_{\text{bnd}}$ analyses in bulk rocks: Application for Iguanodon-bearing Wealden facies of Bernissart (Belgium)

J.-Y. STORME<sup>1</sup>, P. IACUMIN<sup>2</sup>, G. ROCHEZ<sup>1</sup>  
AND J. YANS<sup>1\*</sup>

<sup>1</sup>University of Namur, Department of Geology, 61 rue de Bruxelles, 5000 Namur, Belgium. (\*correspondence: johan.yans@fundp.ac.be, jean-yves.storme@fundp.ac.be, gaetan.rochez@fundp.ac.be)

<sup>2</sup>Earth Sciences, Parma University, Viale G.P. Usberti 157/A, 43100 Parma, Italy (paola.iacumin@unipr.it)

$\delta^{15}\text{N}_{\text{org}}$  on bulk could be a useful proxy for reconstructing paleoclimatic and paleohydrologic conditions of the pre-Quaternary Past [1]. Total nitrogen ( $\text{N}_{\text{tot}}$ ) and inorganic nitrogen bound ( $\text{N}_{\text{bnd}}$ ) concentrations are automatically determined for each sample, to provide nitrogen isotopes on organics ( $\delta^{15}\text{N}_{\text{org}}$ ) using of a mass balance equation. The inorganic nitrogen bound is deciphered by treating decalcified subsample with KOBr–KOH solution to eliminate the organic nitrogen fraction [2,3,4]. Here we experienced this procedure on samples from a borehole cutting the lacustrine succession of the Iguanodon-bearing Wealden facies of Bernissart, middle Barremian to earliest Aptian in age [5,6,7].  $\delta^{15}\text{N}_{\text{org}}$  data show positive trend upwards whereas  $\delta^{13}\text{C}_{\text{org}}$  show negative trend, suggesting variations in paleoclimatic and paleohydrologic conditions. However samples with relatively high TOC contents, after boiling with KOH-KOBr solution by ~5 minutes, show chaotic  $\delta^{15}\text{N}_{\text{org}}$  values, maybe due to uncomplete extraction of organic nitrogen. Similar analyses are required to understand the extraction of organic nitrogen during preparations. Many tests have to be performed such as: use of HCl or other acid, analysis of the type of organic matter in the sediments, limits of TOC contents, KOH-KOBr treatment before or after HCl treatment, etc. Matching this with other proxies in other successions will improve our knowledge of  $\delta^{15}\text{N}_{\text{org}}$  variations in geological Pre-Quaternary successions.

[1] Storme *et al.* (2012). *Terra Nova* **24**, 114-122. [2] Silva & Bremner (1966). *Soil Sci. Soc. Am. Proc.* **30**, 587-594. [3] Corbeels *et al.* (2000). *Plant and Soil* **218**, 71-82. [4] Schubert & Calvert (2001). *Deep-Sea Res I* **48**, 789-810. [5] Yans *et al.* (2005). *Paleovol* **4**, 135-150. [6] Dejx *et al.* (2007). *Rev. Paleobot. Pal.* **144**, 25-38. [7] Schnyder *et al.* (2009). *Palaeogeogr. Palaeoclimatol. Palaeoecol.*, **281**, 79-91.

## Evidence for North to South Progression of Pulsed Intrusion and Metamorphism in the Lower Crust of a Gondwana Arc, Fiordland NZ

H.H. STOWELL<sup>1</sup>, C.M. HOUT<sup>1</sup>, A.J. TULLOCH<sup>2</sup>,  
K.A. ODOM-PARKER<sup>1</sup>, J. SCHWARTZ<sup>3</sup>  
AND K.A. KLEPEIS<sup>4</sup>

<sup>1</sup>Geol. Sciences, Univ. of Alabama, Tuscaloosa AL 35487  
USA (hstowell@geo.ua.edu)

<sup>2</sup>GNS Science, Dunedin, NZ

<sup>3</sup>Geol. Sciences, California State Univ., Northridge, CA, USA

<sup>4</sup>Geology, Univ. of Vermont, Burlington, VT, USA

Exhumed magmatic arcs are critical for understanding subduction processes and the growth and deformation of continents. The duration and rates of tectonic shortening and the transition from over-thickened arc crust to thinned crust and ocean floor spreading are poorly understood. This transition may be related to buoyancy changes and delamination of dense lower crust. The Cretaceous rocks of New Zealand's Median Batholith provide a natural laboratory for understanding these processes because the rocks show evidence for eclogite facies metamorphism, magmatism and granulite-facies metamorphism with local loading during metamorphism. Garnet Sm-Nd ages indicate pulses of metamorphism that closely follow magmatic pulses in the Western Fiordland Orthogneiss suite (WFO). Eclogite facies rocks (Breaksea Orthogneiss) SW of the extensional Resolution Island shear zone (RISZ) juxtaposed these ca. 1.8 Gpa rocks against one (Malaspina Pluton) of three large granulite-facies WFO plutons. Rocks on both sides of the RISZ experienced granulite facies conditions, but those on the NE were metamorphosed at a lower P of 1.2 – 1.4 Gpa. Garnet Sm-Nd ages for peritectic garnet indicate that Malaspina rocks in the hanging wall of the RISZ underwent 116-112 Ma granulite-facies metamorphism shortly after pluton emplacement. Preliminary garnet Sm-Nd ages for eclogite-facies metamorphism SW of the RISZ indicate initial high P at ca. 123 Ma, then high T granulite facies metamorphism that lasted until ca. 108 Ma, following initial extension and collapse of the magmatic arc. Granulite facies metamorphism in the Malaspina and Breaksea postdates similar metamorphism in N Fiordland (Pembroke Granulite) by 10 Ma. Compilation of igneous and metamorphic ages along the lower crust exposed in Fiordland indicates temporal pulses of high-temperature metamorphism which may have progressed from north to south over ca. 15 Ma. preceding extension and continuing during initial extensional collapse of the over-thickened arc crust.



## Insights in the methanogenic degradation of BTEX and PAH in different geological systems

N. STRAATEN<sup>1\*</sup>, N. JIMENEZ-GARCIA<sup>2</sup>, F. GRÜNDGER<sup>1</sup>,  
H. H. RICHNOW<sup>2</sup>, T. LÜDERS<sup>3</sup> AND M. KRÜGER<sup>1</sup>

<sup>1</sup>BGR, Stilleweg 2, 30655 Hannover, Germany

(\*Correspondence: Nontje.Straaten@bgr.de)

<sup>2</sup>UFZ, Permoserstraße 15, 04318 Leipzig, Germany

<sup>3</sup>GSF, Ingolstädter Landstr. 1, D-85764 Neuherberg, Germany

Biodegraded oil is found in many reservoirs worldwide. The more complex hydrocarbons belonging to the PAH and BTEX groups are harder to degrade by prokaryotes than e.g. alkanes. To understand the degradation processes of these hydrocarbons into simpler components, it is very important to get insight in the microbial communities and metabolic processes involved.

The lack of alternative electron acceptors in many habitats limits the possible anaerobic degradation pathways to methanogenesis, which has been shown to be the most important process in different hydrocarbon reservoirs. The composition of the microbial communities in enrichments from habitats with differing geochemical settings, e.g. shallow and deep subsurface terrestrial and marine systems showed a relatively similar composition, independent of the sampling site. Especially methanogenic Archaea, members of the *Syntrophaceae* and sulfate-reducing Prokaryotes contributed to the community in most enrichments. Moreover, in samples from a Chinese oilfield, the crucial process, the conversion of alcanoic, aromatic and polyaromatic hydrocarbons to methane, was proven in incubations via <sup>13</sup>C-labeling [1]. The further molecular biological analysis of this habitat confirmed the presence of methanogenic Archaea as well as of different Bacteria capable of hydrocarbon degradation. In the ongoing work <sup>13</sup>C-labeled substrates combined with SIP of proteins and DNA is used to identify the actively involved microorganisms. Preliminary analyses revealed labeled proteins belonging to methanogens, SRB and *Syntrophus* species thus confirming the 16S results. In addition the results from these enrichments are compared with data from environmental samples of gas, shale and oil reservoirs, to determine the *in situ* importance of the enriched hydrocarbon degraders.

[1] Jiménez, Morris, Cai, Gründger, Yao, Richnow, Krüger (2012) *Organic Geochemistry* 52, 44-54.

## Observed large- and meso-scale oxygen changes in the ocean

L. STRAMMA<sup>1\*</sup>, R.A. WELLER<sup>2</sup>, R. CZESCHEL<sup>1</sup>,  
S. BIGORRE<sup>2</sup>, S. SCHMIDTKO<sup>3</sup> AND A. OSCHLIES<sup>1</sup>

<sup>1</sup>GEOMAR Helmholtz Centre for Ocean Research Kiel, 24105 Kiel, Germany (\*correspondance: lstramma@geomar.de)

<sup>2</sup>Woods Hole Oceanographic Institution, Woods Hole, MA 02543, USA

<sup>3</sup>School of Environmental Sciences, University of East Anglia, Norwich, NR4 7TJ, UK

Model results predict a decline in ocean oxygen and observations confirmed declines at different locations [1]. Within the research initiative 'Climate – Biogeochemistry Interactions in the tropical Ocean' the temporal-spatial scales of oxygen changes were investigated. Large scale oxygen changes for the world ocean were derived at 300 dbar for the last 50 years and in the South Atlantic Ocean even for a 70 year period [2]. Declining upper-ocean oxygen levels in many regions, especially in the tropical oceans, are dominant, whereas areas with increasing trends are found in subtropical and in a few polar regions. A comparison to a numerical biogeochemical Earth system model reveals that the magnitude of the observed change is consistent with CO<sub>2</sub>-induced climate change, however there is a large mismatch between observed and modeled oxygen trends.

In the equatorial Pacific the zonal current bands are important in resupplying oxygen to the oxygen minimum zone in the eastern Pacific. In the Pacific strong oxygen changes are related to the Pacific Decadal Oscillation while oscillations on shorter time scales like an El Nino signal in the upper 350 m are superimposed upon this signal [3].

Meso-scale related oxygen changes are expected to be important on the poleward side of the tropical oxygen minimum zones. Recent measurements of the oxygen distribution of eddies near the Peruvian shelf as well as mooring observations at the Stratus mooring at ~20°S, 85°W show a large expanded low oxygen layer in anticyclonic eddies while in cyclonic eddies the low oxygen layer decreased.

The derived results indicate the importance of a large range of temporal-spatial scales which needs to be investigated further.

[1] Keeling *et al.* (2010) *Annu. Rev. Mar. Sci.*, **2**, 199-229.  
[2] Stramma *et al.* (2012) *Biogeosciences*, **9**, doi:10.5194/bg-9-1-2012. [3] Czeschel *et al.* (2012) *J. Geophys. Res.*, **117**, doi:10.1029/2012JC008043.

## Photochemistry of arsenite and chromate on iron oxyhydroxide

NARAYAN BHANDARI<sup>1</sup>, ELIZABETH CERKEZ<sup>1</sup>,  
RICHARD J. REEDER<sup>2</sup> AND DANIEL R. STRONGIN<sup>1,\*</sup>

<sup>1</sup>Department of Chemistry, Temple University, Philadelphia,  
PA 19122, USA (dstrongin@temple.edu)

<sup>2</sup>Department of Geosciences, Stony Brook University, Stony  
Brook, NY 11794, USA

The (photo)chemistry of arsenite [As(III)] and chromate [Cr(VI)] in the presence of ferrihydrite and goethite was investigated. A variety of techniques, including infrared spectroscopy, X-ray absorption near edge structure (XANES) and solution phase analysis were used to characterize the surface bound and aqueous phase species. The exposure of the iron oxyhydroxides to As(III) in the dark resulted in a adsorbed layer of As(III). Irradiation of the As(III)/ferrihydrite or As(III)/goethite system to simulated solar radiation resulted in the conversion of As(III) to adsorbed and aqueous phase As(V). The relative amounts of adsorbed and aqueous phase As(V) product varied whether ferrihydrite or goethite was present in solution due to differences in the rate of the heterogeneous oxidation of surface Fe(II) on the surfaces by dissolved oxygen. This particular reaction resulted in the formation of reactive oxygen species. Redox reactions of mixtures of As(III) and Cr(VI) in the presence of the two iron oxyhydroxides also were investigated. In this circumstance even in the absence of light, As(III) was oxidized to As(V) (~92% conversion) and Cr(VI) was reduced to Cr(III) if one of the small band gap semiconductor iron oxyhydroxide materials was present. As a comparison nanophase aluminum oxyhydroxide (an insulator) was exposed to As(III) and Cr(VI) under dark conditions. Under these experimental conditions far less As(III) oxidation and Cr(VI) reduction occurred (~50% conversion of As(III) to As(V)) compared to when iron oxyhydroxide was present. Furthermore, the exposure of the As(III)/Cr(VI)/ferrihydrite system to simulated solar light led to additional As(III) oxidation and Cr(VI) reduction (compared to dark conditions) while light had no effect on the As(III)/Cr(VI)/aluminum oxyhydroxide system. In general the results suggested that the semiconducting materials were able to drive the redox chemistry more efficiently due to facile surface mediated electron transfer from As(III) to Cr(VI).

## Water mass mixing in the Drake Passage during the last 40 kyrs

T. STRUVE<sup>1,\*</sup>, T. VAN DE FLIEDT<sup>1</sup>, L. F. ROBINSON<sup>2</sup>,  
A. BURKE<sup>3</sup>, K. C. CROCKET<sup>4</sup>, M. LAMBELET<sup>1</sup>  
AND M.E. AURO<sup>5</sup>.

<sup>1</sup>Imperial College London, London SW7 2AZ, UK

(\*correspondence: t.struve11@imperial.ac.uk).

<sup>2</sup>University of Bristol, Bristol BS8 1RJ, UK.

<sup>3</sup>California Institute of Technology, Pasadena, CA 91125.

<sup>4</sup>DG Research and Innovation, European Commission, Rue de  
la Loi, 1049 Brussels, Belgium.

<sup>5</sup>WHOI, Woods Hole Oceanographic Institution, MA 02543.

The modern Southern Ocean is a key area for the global ocean circulation as wind-driven mixing, upwelling and redistribution of water masses in the Antarctic Circumpolar Current (ACC) all have a significant impact on the properties and flow patterns of global water masses. It has been suggested that the Southern Ocean plays a central role in oceanographic and climatic changes observed on glacial-interglacial timescales, in particular with respect to carbon sequestration between the deep ocean and the atmosphere.

For the purpose of unravelling Southern Ocean water mass mixing over the past ~40,000 years, the aragonitic skeletons of solitary deep-sea corals collected from two cruises on the Nathaniel B. Palmer to the Drake Passage are used as archives for seawater Nd isotopes. These corals were collected from water depths between 300 and 1750 m and have previously been directly dated by U-Th and analysed for their radiocarbon content.<sup>[1]</sup>

Neodymium was extracted from the wash solution of the U-series anion-exchange chemistry using a two-stage ion chromatography (RE-spec and Ln-spec resins). Subsequent analyses of Nd were performed as NdO<sup>+</sup> on a Triton TIMS using a TaF<sub>5</sub> activator on W filaments. This method yields within run uncertainties around 10 ppm (2σ SE) and external uncertainties around 20 ppm (2σ SD) for sample loads as small as a few ng of Nd.

Preliminary Nd isotope results on *D. dianthus*, *F. curvatum* and *B. malouinensis* specimen growing during the last 40 kyrs show significant variability at intermediate water depths (εNd of ~-5 to -8) and a more stable Nd isotopic composition in the lower water column (>1000m; εNd ~-8).

We will interpret our unique data set in the context of published glacial-interglacial radiocarbon results and inferred Southern Ocean water mass variability and ventilation rates.

[1] Burke & Robinson (2012), *Science* **335**, 557-561.

## Emerging understanding of anthropogenic interferences in the ecosystem silica filter

ERIC STRUYF<sup>1\*</sup> AND DANIEL J. CONLEY<sup>2</sup>

<sup>1</sup> University of Antwerp, Department of Biology, Universiteitsplein 1C, 2610 Wilrijk, Belgium, eric.struyf@ua.ac.be

<sup>2</sup> Lund University, Dept. Geology, Sölvegatan 12, 22362 Lund, Sweden

The annual fixation of DSi into terrestrial vegetation is 60 to 200 Tmole, 10–40 times more than the yearly export of DSi from the terrestrial geobiosphere to the coastal zone and 3–6 times more than annual weathering of silicates. Ecosystems form a large filter between mobilization of DSi by silicate weathering and mobilization to rivers. A large reservoir of biogenic amorphous Si (mostly plant phytoliths) and pedogenically reworked amorphous Si (ASi) accumulates in soils. ASi is substantially more soluble than mineral Si. Still, ASi persistence and reactivity in soils, the dependence of the ASi turnover on ecological processes and ultimately the global relevance in Si budgets are poorly constrained [1]. A major challenge is presented by the difficulty to separate pedogenic and biogenic amorphous Si phases in the soil. This hampers quantification of the silicate weathering-related C-sink and accurate modelling of transport of Si to rivers and estuaries, where Si plays a crucial in phytoplankton productivity.

Human land management can cause abrupt shifts to the biogeochemical cycle in terrestrial ecosystems and their ability to sequester Si. Our results from a novel technique that allows for separation of biogenic and pedogenic ASi phases, shows that turnover rates of ASi in temperate cultivated soils are strongly reduced compared to forests and stocks of pedogenic ASi are depleted. Newly acquired analysis of Si isotopes in soil water also show this. This results in timescale dependent, 2–4 fold shifts in terrestrial Si mobilisation [2]. Human harvest of crop ASi has created a parallel anthropogenic Si cycle, which has received virtually no quantification so far [3]. Our observations show that intense domestic reindeer and cattle grazing alters physical and chemical reactivity of biogenic ASi (Si is a defense mechanism against herbivory) and can cause abrupt shifts in ecosystem ASi storage and cycling. The combination of experimental, field and modelling studies shows that land use has strongly altered mineral-soil-plant interactions.

[1] Struyf & Conley (2012), *Biogeochemistry*, 107, 9–18. [2] Struyf *et al.* (2010), *Nature Comm.*, 1, 129 [3] Vandevenne *et al.* (2012), *Front Ecol Environ*, 243–48.

## Deep-sea coral amino acids illuminate ecosystem processes on South East Australia seamounts

K.M. STRZEPEK<sup>1\*</sup>, A. REVILL<sup>2</sup>, R.E. THRESHER<sup>2</sup>, C. I. SMITH<sup>3</sup> AND S.J. FALLON<sup>1</sup>

<sup>1</sup> Research School of Earth Sciences, Australian National University, Canberra, 0200, Australia (\*correspondance: kelly.strzepek@anu.edu.au, stewart.fallon@anu.edu.au )

<sup>2</sup> CSIRO Marine and Atmosphere, Hobart, 7000, Australia (andy.revill@csiro.au, ron.thresher@csiro.au )

<sup>3</sup> Faculty of Humanities and Social Sciences, Latrobe University, Melbourne, 3086, Australia (colin.smith@latrobe.edu.au )

South-east Australian seamounts and their associated deep-sea ecosystems, are located in an oceanographically complex and climatically sensitive region. Across this region, Bamboo Corals inhabit a tremendous depth range (600–4000m) archiving surface processes by incorporating raining particulates into their banded skeletons. Bulk organic <sup>15</sup>N has previously been used to substantiate the region's shifting surface regimes in response to current climate change, but trophic enrichment was necessarily approximated, obscuring the <sup>15</sup>N-signal of the producers at the base of the foodweb [1].

In this study, we revisit the <sup>15</sup>N archive, instead using individual amino acids (AA) to reconstruct ecosystem dynamics. We are able to capture and decouple, a century of trophic interactions from the <sup>15</sup>N-signal of primary production. Furthermore, as specimens were collected between 1000–3000m, we are able to explore deep-sea particle transformations and microbial heterotrophy that connects surface and deepwater ecosystems. By exploiting previously validated <sup>15</sup>N-AA patterns [2] and considering those in the <sup>13</sup>C-AA record, we propose likely mechanisms that could support the inexplicably high biomass that has been reported within the local bathyl zone [3].

Our preliminary results indicate that clear distinctions seen between depths in the bulk record naturally reflect the isotopic signature of the most abundant AA, glycine, as well as trophic complexity. Furthermore we find evidence of differing particulate processing histories, provenance and species effects that all have important implications for the future interpretation of records from deep-sea coral organics.

[1] Sherwood *et al.* (2009) *Mar. Ecol. Prog. Ser.* **397**, 209–218. [2] McCarthy *et al.* (2007) *GCA* **71**, 4727–4744. [3] Thresher *et al.* (2011) *Nat. Sci. Reports* **1**, 119.

## Constraints on the source of mantle plumes from the first picrites erupted Ethiopian flood basalt province

F. M. STUART<sup>1\*</sup> AND N. ROGERS<sup>2</sup>

<sup>1</sup>Isotope Geosciences, SUERC, East Kilbride G75 0QF, UK  
(\*fin.stuart@glasgow.ac.uk)

<sup>2</sup>Department of Earth & Environmental Sciences, Open University, Milton Keynes MK7 6AA, UK

The earliest basalts erupted by largest mantle plumes are typically 200-300°C hotter than those derived from convecting upper mantle at mid-ocean ridges. They originate from a thermal boundary layer deep in Earth that is assumed to be the core-mantle boundary. Consequently the first plume-derived basalts provide constraints on Earth structure and differentiation history. The first picrites erupted by the Iceland plume have a high proportion of primordial He ( $^3\text{He}/^4\text{He} \sim 50 R_a$ ) yet a range in radiogenic isotope and incompatible trace element ratios that overlap the global mid-ocean ridge basalt range [1]. This is difficult to reconcile with pristine mantle dominating the plume head. The simplest interpretation is that the convecting mantle has been polluted by primordial He either at the core-mantle boundary or during ascent, thus still requires the existence of primordial volatile reservoir.

In an attempt to provide better constraints on the deep mantle source of plumes we have analysed the He-Sr-Nd-Pb isotopic composition of the earliest high-Ti picrites (HT2) from the Dilb section of the ~30 Ma Ethiopian flood basalt province. The basalts are characterized by high Fe and Ti contents for MgO = 14-15% that implies the parent magma was derived from a high temperature small melt fraction, likely the plume head. The basalts are characterized by a narrow range of  $^{87}\text{Sr}/^{86}\text{Sr}$  (0.70396–0.70412) and  $^{206}\text{Pb}/^{204}\text{Pb}$  (18.82-19.01).  $^3\text{He}/^4\text{He}$  of olivine never exceeds 21  $R_a$ . The Afar plume was sourced in a discrete mantle reservoir that is less degassed and more enriched than the convecting upper mantle. The source region is significantly more degassed than the mantle sampled by the proto-Iceland plume and more homogenous. Clearly the largest mantle plumes are not initiated in a single deep mantle domain with the same depletion/enrichment history and they do not mix with convecting mantle to the same extent.

[1] Starkey *et al.* (2009) *Earth Planet. Sci. Lett.* 277 91-100.

## Oxidative corrosion of uraninite (UO<sub>2</sub>) surfaces

JOANNE E. STUBBS<sup>1\*</sup>, PETER J. ENG<sup>1</sup>, CRAIG A. BIWER<sup>2</sup>, ANNE M. CHAKA<sup>3</sup>, GLENN A. WAYCHUNAS<sup>4</sup> AND JOHN R. BARGAR<sup>5</sup>

<sup>1</sup>Center for Advanced Radiation Sources, University of Chicago, Chicago, IL, USA, stubbs@cars.uchicago.edu (\* presenting author)

<sup>2</sup>Department of Computational Medicine and Bioinformatics, University of Michigan, Ann Arbor, MI, USA

<sup>3</sup>Physical Measurement Laboratory, National Institute of Standards and Technology, Gaithersburg, MD, USA

<sup>4</sup>Lawrence Berkeley National Laboratory, Berkeley, CA, USA

<sup>5</sup>Stanford Synchrotron Radiation Lightsource, Menlo Park, CA, USA

Uraninite (UO<sub>2</sub>) is the most abundant uranium ore mineral, the product of proposed bioremediation strategies for uranium-contaminated soils and aquifers and its synthetic analog is the primary constituent of most nuclear fuels. It incorporates interstitial oxygen up to a stoichiometry of UO<sub>2.25</sub> without disruption of the uranium lattice, but the structural details of the process are the subject of ongoing study and debate. Because the solubility and dissolution kinetics of uraninite depend heavily on the oxidation state of uranium, understanding the mechanisms of UO<sub>2</sub> surface oxidation and corrosion is essential to predicting its stability in the environment throughout the nuclear fuel cycle. To date, however, no study has addressed this process at the molecular scale at atmospheric pressure and room temperature.

We present crystal truncation rod (CTR) x-ray diffraction studies of pristine and oxidized UO<sub>2</sub> (111) and (100) surfaces. The clean (111) surface shows minimal contraction of the uppermost atomic layers and a layer of oxygen or hydroxyl group adatoms above the vacuum-terminated surface. Upon exposure to oxygen, an oxidation front proceeds into the crystal, interstitial oxygen atoms penetrate to depths of 30 Å or more, surface-normal layer distances contract (consistent with bulk uraninite oxidation) and an ordered superlattice forms, commensurate with the underlying bulk. Similar oxygen surface penetration and layer contraction are observed upon oxidation of the (100) surface. These results demonstrate that the solid state diffusion of oxygen into UO<sub>2</sub> and UO<sub>2+x</sub> surfaces is facile and that ordering kinetics are relatively rapid, even at room temperature.

*Ab initio* thermodynamics, which combines density-functional theory calculations with macroscopic thermodynamics, provides insight into the energetics, bonding and oxidation processes that occur as oxygen reacts with the surfaces and diffuses into the solid. Subsurface oxidation is predicted to contract surface-normal layers, consistent with experimental observations.

## Extraction of paleo seawater Nd isotope compositions: A case study from the Indonesian Throughflow

ROLAND STUMPF<sup>1,2\*</sup>, MARTIN FRANK<sup>2</sup>, BRIAN A. HALEY<sup>2,3</sup>, STEFFANIE KRAFT<sup>2</sup> AND WOLFGANG KUHN<sup>4</sup>

<sup>1</sup>Imperial College London, Dept. of Earth Science & Engineering, London SW7 2AZ, UK (\*presenting author)

<sup>2</sup>GEOMAR Helmholtz Centre for Ocean Research Kiel, Germany

<sup>3</sup>Oregon State University, College of Oceanic & Atmospheric Sciences (COAS), USA

<sup>4</sup>Christian-Albrechts-Universität Kiel, Institute of Geosciences, Germany

Over the past decade, radiogenic Nd isotope compositions have increasingly been used as a paleo seawater proxy for the reconstruction of past ocean currents and water mass mixing. For this purpose, the Nd isotopes have been extracted from various marine archives, such as ferromanganese crusts and nodules, Fe-Mn oxyhydroxide coatings on detrital sediment surfaces, as well as in foraminiferal shells, cold water corals and fish teeth. However, it is still under debate if all these archives reliably preserve unaltered paleo seawater Nd isotope compositions.

In this study, the Nd isotope compositions of reductively cleaned foraminiferal shells (bulk planktonic & monospecific), of Fe-Mn oxyhydroxide coatings leached from the decarbonated detrital fraction of the sediment, as well as Nd isotope compositions leached directly from the bulk sediment were extracted from carbonate-rich sediment core MD01-2378 (1783 m water depth) located in the outflow region of the Indonesian Throughflow (ITF) in the eastern Timor Sea. We focus on the comparison of the Nd isotope records from these three archives covering the time period of marine isotope stage 3 (~23 – 64 ka B.P.) in order to reconstruct variations of intensity and the relative contributions from different outflow pathways of the ITF.

A comparison of core top Nd isotope compositions extracted from planktonic foraminiferal shells shows good agreement with water column Nd isotope data [1]. Data from a core top sample at a location close to core MD01-2378 showed that there is no significant difference in Nd isotope composition between monospecific ( $\epsilon\text{Nd} = -4.3$ ) and bulk ( $\epsilon\text{Nd} = -4.4$ ) planktonic foraminiferal samples.

The Nd isotope variability observed in the downcore planktonic foraminiferal records of core MD01-2378 ranged from  $\epsilon\text{Nd} = -3.5$  to  $-5.5$  with minimum values occurring during the Last Glacial Maximum and either documents variations between different ITF outflow pathways or variable surface water contributions from Northern Australia or even from the Southern Ocean. These data are compared with bottom water Nd isotope variations newly obtained from oxyhydroxide coatings of the same sediment core.

[1] Jeandel *et al.*, (1998). *Geochim Cosmochim Acta*, 62(15), 2597-2607.

## Record of historical mercury trends in sediments from the Laguna del Plata, Córdoba, Argentina

Y.V. STUPAR<sup>1,2\*</sup>, J. SCHÄFER<sup>3</sup>, M.G. GARCIA<sup>2</sup>, S. SCHMIDT<sup>4</sup>, E. PIOVANO<sup>2</sup>, G. BLANC<sup>3</sup>, F. HUNEAU<sup>5</sup> AND P. LE COUSTOMER<sup>1</sup>

<sup>1</sup>Université de Bordeaux, EA 4592 Géorressources & Environnement, ENSEGID, 1 allée F. Daguin, F-33607 Pessac, France (\*correspondance : yohanastupar@yahoo.com.ar)

<sup>2</sup>Centro de Investigaciones en Ciencias de la Tierra (CICTERRA), CONICET/UNC, Av. Vélez Sarsfield 1611, X5016CGA, Córdoba, Argentina.

<sup>3</sup>Université de Bordeaux, EPOC, UMR 5805, F-33400 Talence, France

<sup>4</sup>CNRS, EPOC, UMR5805, F-33400 Talence, France

<sup>5</sup>Université de Corse Pascal Paoli, Laboratoire d'Hydrogéologie UMR 6134 SPE, Campus Grimaldi, BP 52, F-20250 Corte, France

Mercury concentrations and main carrier phases were determined in sediments of a 120 cm core from Laguna del Plata (LP). This lake is a part of the Laguna Mar Chiquita (LMC) system as it is connected to LMC itself during water highstands. LMC is one of the largest saline lakes in the world representing a sensitive climatic indicator due to its frequent lake level variations at millennial and interdecadal scales [1], with the most recent major variations during the early 1970s and after 2004. Total mercury ( $\text{Hg}_{\text{TP}}$ ) concentrations analyzed by Atomic Absorption spectrometry after sample calcination in an  $\text{O}_2$  stream (DMA 80) varied between ~13 and ~131  $\mu\text{g kg}^{-1}$  and reflected changes in water and sediment supply to the LP. Selective extractions performed on the sediments using ascorbate, HCl and  $\text{H}_2\text{O}_2$  revealed that in the base of the core corresponding to a low water level period, Hg is mainly associated to reactive sulfides. In contrast, in the middle and upper part of the core Hg is rather associated with sedimentary organic matter and was interpreted as reflecting Hg deposition at the watershed scale. Core dating, performed with  $^{210}\text{Pb}$  and  $^{137}\text{Cs}$ , allowed to determine that the highest Hg peak corresponds to the years 1990-1995. This was attributed to the eruption of Lascar volcano in 1993 in the Central Andes of northern Chile rather than anthropogenic pollution sources.

[1] Piovano *et al.* (2002). *Sedimentology* **49**, 1371-1384. [2] Schäfer *et al.* (2006) *Appl. Geochem.* **21**,515-527.

## Tracer applications to verify carbon mineralization in Icelandic basalts

M. STUTE<sup>1</sup>, J. HALL<sup>1</sup>, J.M. MATTER<sup>1</sup>, K. MESFIN<sup>2</sup>,  
S.R. GISLASON<sup>2</sup>, E.H. OELKERS<sup>2,3</sup>, B. SIGFUSSON<sup>4</sup>,  
E. GUNNLAUGSSON<sup>4</sup>, I. GUNNARSSON<sup>4</sup>,  
E.S. ARADOTTIR<sup>4</sup>, H. SIGURDARDOTTIR<sup>4</sup>, G. AXELSON<sup>5</sup>  
AND W.S. BROECKER<sup>1</sup>

<sup>1</sup>Lamont-Doherty Earth Observatory, 61 Route 9W, Palisades, NY 10964, USA (martins@ldeo.columbia.edu)

<sup>2</sup>Institute of Earth Sciences, University of Iceland, Sturlugata 7, 101 Reykjavík, Iceland

<sup>3</sup>GET, CNRS/URM 5563-Université Paul Sabatier, 14 av. Edouard Belin, 31400, Toulouse, France

<sup>4</sup>Reykjavík Energy, Baejarhálsi 1, 110 Reykjavík, Iceland

<sup>5</sup>Iceland GeoSurvey, Grensásvegur 9, 108 Reykjavík, Iceland

The risks associated with geologic carbon storage can be considerably reduced by subsurface carbon mineralization.

The CARBIFIX project in Iceland is a field scale pilot study where CO<sub>2</sub> and H<sub>2</sub>S emissions from the Hellisheidi geothermal power plant are dissolved in groundwater and injected into a permeable basalt formation at ~500 m depth below surface [1]. We are using non-reactive (sodium fluorescein, amidhorhodamine G, SF<sub>3</sub>CF<sub>3</sub>, and SF<sub>6</sub>) and reactive (<sup>14</sup>C and <sup>13</sup>C) tracers in an on-going injection project to characterize subsurface CO<sub>2</sub> transport and in situ CO<sub>2</sub>-water-rock reactions. In early 2012, 170 tons of pure CO<sub>2</sub> tagged with <sup>14</sup>C and SF<sub>6</sub> were dissolved in water and injected into a confined basalt aquifer. Samples were collected from injection and monitoring wells in evacuated serum bottles with butyl stoppers and analyzed by AMS and mass spectrometry for carbon isotopes, by fluorometry for Na-fluorescein and by gas chromatography for SF<sub>6</sub> and SF<sub>3</sub>CF<sub>3</sub>. The multi-tracer approach allows us to separate various injection experiments and differentiate between dilution and reaction. While the bulk of the injected CO<sub>2</sub> has not yet arrived at the monitoring wells, a fraction following a fast flowpath appeared within less than a month. δ<sup>13</sup>C shows an initial rise attributed to dissolution of aquifer carbonates and then a drop due to carbonate precipitation. The <sup>14</sup>C/SF<sub>6</sub> ratio is lower than the injection ratio providing additional evidence for carbonate precipitation. The bulk of the injected CO<sub>2</sub> is expected to arrive by the summer of 2013 and we will extend the time series accordingly. Our study demonstrates the value of tracers as a monitoring, verification and accounting tool in reactive geological carbon storage systems.

[1] Gislason *et al.* (2010), *Int. J. Greenh. Gas Con.* 4, 537–545.

## Robust Calibration Systems Based on Syringe Pumps for Water Vapor Isotopologue Measurements

ERIC STUTZ<sup>1\*</sup>, JANEK LANDSBERG<sup>2</sup>, LASZLO SARKOZY<sup>1</sup>,  
ELISABETH MOYER<sup>1</sup> AND ERIK KERSTEL<sup>2</sup>

<sup>1</sup> Department of the Geophysical Sciences, University of Chicago, Chicago, IL 60637, USA (\*correspondence: ejstutz@uchicago.edu)

<sup>2</sup> J. Fourier University of Grenoble Laboratoire Interdisciplinaire de Physique, (UMR 5588 CNRS-UJF), 38402 Grenoble, France

Advances in spectroscopic instrumentation mean that laser-based absorption spectroscopy (both direct and cavity enhanced) is increasingly used for isotopic measurements in environmental sciences. For studies involving water, this technique offers the advantages of speed and non-destructive sampling, allowing for new applications in water vapor measurements [e.g. 1] and for the support or replacement of mass spectroscopy in studies of ice cores [e.g. 2]. In both uses, instrument accuracy is tied to instrument calibration and therefore dependent on the availability of suitable calibration systems. We describe here a new calibration technique based on syringe pumps for producing air streams of known and constant water content and isotopic composition. Syringe pumps offer advantages over previous methods such as capillary flash-evaporation, water vapor "bubbling", or microdrop generation [e.g. 2,1,3], including greater control and reliability. We show the stability and time response of two calibration systems, built at the University of Chicago and the J. Fourier University of Grenoble and designed for high and low flow rates (0.1 -10 slm) and a water vapor dynamic range of 3-10,000 ppm. We discuss the optimization of parameters such as pressure, injection rate step shape, temperature and hydrophobic coatings. The designs are robust and readily modified for instrument-specific configurations, suggesting they may find wide use in the community.

[1] Sayres, D. S., *et al. Rev Sci Inst.* **80**, 2009. [2] Gkinis, V., *et al. Atm Meas Tech.* **4**, 2011. [3] Iannone, R. Q., *et al. J. Atmos. Ocean. Tech.* **26**, 2009.

## Biogeochemical controls on the product of microbial U(VI) reduction

MALGORZATA STYLO<sup>1</sup>, DANIEL S. ALESSI<sup>1</sup>, PAUL PAOYUN SHAO<sup>1</sup>, JUAN S. LEZAMA-PACHECO<sup>2</sup>, JOHN R. BARGAR<sup>2</sup> AND RIZLAN BERNIER-LATMANI<sup>1</sup>

<sup>1</sup>Environmental Microbiology Laboratory, École Polytechnique Fédérale de Lausanne, CH-1015, Lausanne, Switzerland

<sup>2</sup>Chemistry and Catalysis Division, Stanford Synchrotron Radiation Lightsource, SLAC National Accelerator Laboratory, Menlo Park, CA 94025, USA

Biologically mediated immobilization of radionuclides in the subsurface is a promising strategy for the remediation of U-contaminated sites. During this process, soluble U(VI) is reduced by indigenous microorganisms to sparingly soluble U(IV). The crystalline U(IV) phase uraninite, or UO<sub>2</sub>, is the preferable end-product of bioremediation due to its relatively high stability and low solubility in comparison to the non-crystalline biomass-associated non-uraninite U(IV) species. However, non-uraninite U(IV) species have been reported to be a predominant U(IV) product formed under field relevant conditions. Therefore the goal of this study was to delineate the biogeochemical conditions that promote the formation of non-uraninite U(IV) versus uraninite, to decipher the mechanisms of its preferential formation and to apply this knowledge to environmentally relevant cases. Batch experiments as well as biofilm reactors were set up to test the influence of biogeochemical conditions on U(IV) product formation. U(IV) products were analyzed with X-ray absorption spectroscopy (XAS), scanning transmission X-ray microscopy (STXM) and various wet chemical methods. As a result of batch experiments, we report an increasing fraction of non-uraninite U(IV) species with decreasing initial U concentration. Additionally, the presence of several common groundwater solutes (sulfate, silicate and phosphate) promote the formation of non-uraninite U(IV). Our experiments revealed that the presence of specific solutes promotes the formation of bacterial extracellular polymeric substances (EPS) and increases bacterial viability, suggesting that the formation of non-uraninite U(IV) is due to a biological response to the presence of these solutes during U(VI) reduction. Ongoing biofilm studies focus on the characterization and origin of U(IV) species formed under field relevant conditions, i.e., in the flow-through systems, under alternating redox regimes with controlled biotic and abiotic processes.

## Arsenic immobilization and transformation by zerovalent iron

CHUNMING SU

National Risk Management Research Laboratory, U.S. Environmental Protection Agency, 919 Kerr Research Drive, Ada, OK 74820

### Introduction and Experiments

Both granular [1] and nanosized zerovalent iron (NZVI) [2] are effective in removing arsenic from water. Granular ZVI also has been used as permeable reactive barrier media to intercept and remove As from contaminated groundwater at a smelting site [3] and as a filter material for removing As from Bangladesh tube well water [4]. This study focus on As removal mechanisms by NZVI. Batch tests were conducted using 25-nm NZVI to remove As(V) and As(III) under anaerobic conditions as a function of time and pH with or without phosphate and silicate. Minerals were identified.

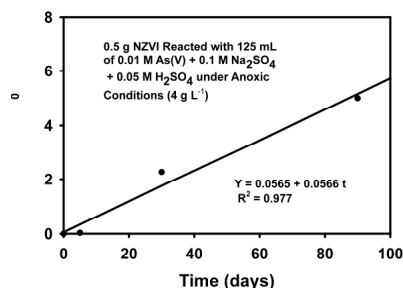


**Figure 1.** Plot of pseudo-second order removal kinetics for As(V) in the long term test.

### Results and Discussion

Both As(V) and As(III) removal increased with increasing time to approach a steady state after 4-5 days in the short-term test. There was generally more removal of As(III) than As(V). Complete or near complete removal of As(V) and As(III) was achieved at pH levels less than 10. Competition of phosphate and silicate against As(V) and As(III) was observed at alkaline pHs. New solid phases formed such as parasymplectite in the As(V) system and vivianite in the phosphate system. This study demonstrated that As(V) removal involves both solid precipitation and adsorption; whereas, As(III) removal only involves surface adsorption.

[1] Su and Puls, (2001) *Environ. Sci & Technol.* **35**, 1487-1492. [2] Kanel *et al.* (2005) *Environ. Sci & Technol.* **39**, 1291-1298. [3] Beak & Wilkin, (2009) *J. Contam. Hydrol* **106**, 15-28. [4] Leupin & Hug (2005) *Water Res.* **39**, 1729-1740.

## Evidence of underground water for the forming mechanism of high sulfur condensate reservoirs, Example from the Tazhong area

JIN SU, SHUICHANG ZHANG, GUANGYOU ZHU AND YU WANG

PetroChina Research Institute of Petroleum Exploration and Development, Beijing 100083, China,  
(susujinjin@126.com)

Condensate gas reservoirs with high content of hydrogen sulfide have been discovered on a large scale in deep marine carbonate formations in the Tarim Basin, which contain formation water with high salinity. Investigations show that, in the Tazhong area, the average negative and positive ion contents in the lower Ordovician to Cambrian formation water are higher than that in the upper Ordovician formation water. Yingshan formation with high-sulfur condensate reservoir is similar to the lower Ordovician to Cambrian formation in water properties, that is to say, the content of  $Mg^{2+}$  and  $SO_4^{2-}$  and PH value are higher than those in the upper Ordovician formation; these mineral ions and PH are crucial to thermochemical sulfate reduction. Hydrogen sulfide content in Yingshan condensate reservoir and  $Mg^{2+}$  content of formation water correlates well in the Tazhong area, which indicates a presumable TSR-origin of hydrogen sulfide according to the reaction theory of contact ion-pair. Besides, the total salinity and pH value of formation water are positively correlated with hydrogen sulfide content in the condensate reservoir, which may indicate that high salinity and pH value are important to activate and maintain TSR reaction. High sulfur condensate reservoirs are all located near the No. I faulted zone and strike-slip faults which are the major pathway for deep fluid migration in the area, showing that the formation water in condensate reservoirs may communicate with high salinity fluid in the lower Ordovician to Cambrian formation and hydrogen sulfide flowed upwards with formation water from deep zones along fractures to form condensate reservoirs with high sulfur content and high salinity. The discovery reveals the forming mechanism of high sulfur condensate reservoirs in the Tazhong area and will be helpful to predict the reservoir fluid properties.

## Tectonic setting of the Xigaze ophiolite complex in Tibet based on the characteristics of boninite

SU LI<sup>1,2</sup>, BAO PEISHENG<sup>3</sup>, SONG SHUGUANG<sup>4</sup> AND NIU YAOLING<sup>2</sup>

<sup>1</sup> Institute of Earth Science, China University of Geosciences, Beijing, 100083, China

<sup>2</sup> Department of Earth Sciences, University of Durham, Durham, DH1 3LE, UK

<sup>3</sup> Institute of Geology, Chinese Academy of Geological Sciences, Beijing, 100037, China

<sup>4</sup> Department of Earth Sciences, Beijing University, 100871, China

The Xigaze ophiolite complex contains the best preserved ophiolite blocks in the middle section of the Yarlung Zangbo ophiolite belt. It composes of several fragments and extends about 200 km long and ~ 8 km wide. The ophiolite complex consist of five lithologic units, including mantle peridotite, melanocratic to leucocratic cumulates, sheeted dyke complex, pillow lavas and diabase dykes. Most of the basic lava and sheeted dyke complex from the Dejixiang ophiolite are calc-alkaline with variable  $SiO_2$  ranging from basalt to andesite. Their LREE-depleted REE patterns show affinity of N-type MORB (or BAB). The diabase dike samples exhibit low  $TiO_2$  (<0.5%), high MgO (up to 18.24 wt%) and  $Mg^\#$  (68.3-83.7) and remarkably high mantle compatible elements Cr, Co and Ni. They exhibit low REE abundances and LREE-depleted REE patterns with  $[La/Sm]_n = 0.63-0.90$ , which are distinct from the U-shaped REE patterns of typical boninites that occur in forarc settings but similar to the boninites from the back-arc basin <sup>[1,2,3]</sup>. Ol, Sp and Opx were observed in these rocks. We conclude that (1) the Dejixiang ophiolite formed in a backarc basin setting, rather than in the mid-ocean ridge (MOR) or in a fore-arc environment and (2) the boninites are high-Ca type that formed in the late stage of back-arc basin environment during continuous extension of the spreading center that caused further melting of the depleted mantle, these melts intruded as diabase dykes into the former oceanic crust that formed the Dejixiang ophiolite during the early spreading stages of the back-arc-basin. These ophiolite blocks reflect the transition from spreading ridge to arc of the Tethys ocean.

[1] Cameron, 1985, Contrib. Mineral. Petrol. 89, 256–262.

[2] Ishikawa Nagaishi, Umino, 2002, Geology, 30, 899–902.

[3] Xia, Song, Niu, 2012, Chemical Geology, 328, 259–277.



## Subducted continental crust materials in the SW Tianshan HP-LTMB

SU WEN, LIU XIN, GAO JUN, LI JILEI AND JIANG TUO

<sup>1</sup>Institute of Geology and Geophysics, CAS, Beijing, China

The SW Tianshan HP/UHP-LT metamorphic belt (MB) in NW China occurs along a suture zone between the Yili and the Tarim blocks. It is mainly composed of blueschist, eclogite and greenschist-facies metasediments, metavolcanics, resembling typical *mélange* lithologies. Chemical compositions of mafic rocks are similar to those of typical oceanic basalts, which formed at a seamount setting in the South Tianshan ocean (Gao & Klemd, 2003). The belt has been interpreted as the typical deeper subduction of the oceanic crust in the world (Zhang *et al.*, 2007). Recent 2450-1880Ma age obtained for detrital zircons of metasediments, core of zircons of meta-basalts, implying the SW Tianshan HP/UHP-LTMB may contain subducted continental crust. Here, we therefore performed a geochemical investigation on the intimately associated eclogites and blueschists which may represent continental crust materials.

Both eclogite and blueschist have similar geochemical characteristics: an enriched LREE, flat HREE, weak negative Eu anomalies REE patterns, depleted in Ba, Sr, Nb, Ta, Ti, high Th/Yb, indicating a continental crustal source of the rocks on a Zr/Hf -Nb/Ta diagram (Pfander *et al.*, 2007). Sr-Nd isotopic data of both rocks is relatively constant with  $\epsilon_{\text{Nd}}(t) = -7.701$  to  $-4.55$ , whereas  $(^{87}\text{Sr}/^{86}\text{Sr})_i = 0.7091$  to  $0.7107$ . All  $\epsilon_{\text{Nd}}(t)$  values and Sr ratios are different with those reported for meta-N-MORBs, E-MORBs, OIBs in the Tianshan HP MB (Ai *et al.*, 2006), but within range of the continental crust. Concerning with tectonic implication for continental crust materials in the HP/UHP-LTMB, two possible mechanisms are proposed here: 1) the fragments of arc basalts derived from a Paleozoic active margin with Precambrian basement have been involved into the subduction process; 2) the continental crust of the Tarim was involved during the collision process. Although present data cannot give a clear explanation to the tectonic background, geochemical and isotopic results demonstrate some continental crust materials have been subducted in formation of HP/UHP-LTMB in the SW Tianshan orogen.

## Biochar determination in soils by applying Pyrolysis GC-MS analysis and Black Carbon (BC) concentration through dichromate and permanganate oxidation

MANUEL SUÁREZ-ABELEND<sup>1</sup>, JOERI KAAL<sup>2</sup>, HEIKE KNICKER<sup>3</sup>, MARTA CAMPS-ARBESTAIN<sup>4</sup> AND FELIPE MACÍAS<sup>1</sup>

<sup>1</sup>Department of Soil Science and Agricultural Chemistry, Biology Faculty, Santiago de Compostela University, Spain (manuel.suarez@usc.es). <sup>2</sup>Instituto de Ciencias del Patrimonio (Incipit), CSIC, Santiago de Compostela, Spain.

<sup>3</sup>Instituto de Recursos Naturales y Agrobiología de Sevilla (IRNAS-CSIC), Sevilla, Spain. <sup>4</sup>Institute of Agriculture and Environment, Massey University, Palmerston North, New Zealand.

Distinguishing pyrogenic and non-pyrogenic SOM components is a difficult task as non-selective pyrolysis products such as MAHs, PAHs and phenols can derive from multiple sources. However, black carbon (BC) may contribute significantly to the MAHs and PAHs in a given pyrolysate, especially if BC is more abundant than alternative sources. In this study, samples from a soil rich in pyrogenic material in NW Spain were subjected to  $\text{K}_2\text{Cr}_2\text{O}_7$  and  $\text{KMnO}_4$  oxidation and the residual SOM was NaOH-extracted and analyzed using analytical Py-GC-MS in order to study the susceptibility of different SOM fractions (fresh, degraded/microbial, aliphatic and specially BC) towards this oxidation agent. Besides solid-state  $^{13}\text{C}$  CP MAS-NMR was also performed to support these results. Non-oxidized samples following the same NaOH-extraction procedure were also analyzed. From Py-GC-MS, residual SOM after  $\text{K}_2\text{Cr}_2\text{O}_7$  oxidation contained BC, N-containing BC (BN) and aliphatic structures whilst carbohydrate products and lignocellulose were completely oxidized. This was corroborated by a relatively intense resonance of aromatic C and some signal of alkyl C (supporting the presence of a non-pyrogenic fraction mainly consisting of aliphatic structures) in  $^{13}\text{C}$  NMR spectra. Thus  $\text{K}_2\text{Cr}_2\text{O}_7$  effectively concentrates MAHs, PAHs and BN derived from BC. For  $\text{KMnO}_4$ , both techniques indicated that this reagent promotes the oxidation of carbohydrate products, mostly from degraded/microbial SOM but slightly oxidized lignocellulose and aromatic structures (pyrogenic and non-pyrogenic) not providing a good assessment of the BC signal.

## Contrasting patterns of bacterial weathering of granite, granulite and gabbro from tropical regions of south India

R. SUBASHRI<sup>1</sup>, J. K. DASH<sup>2</sup>, S. BALAKRISHNAN<sup>2\*</sup>,  
AND N. SAKTHIVEL<sup>1</sup>

<sup>1</sup>Department of Biotechnology, Pondicherry University,

<sup>2</sup> Department of Earth Sciences, Pondicherry University,  
Puducherry – 605014, India

(\*correspondence: balakrishnan.srinivasan@gmail.com)

Bacterial weathering of various rock forming minerals have been studied in detail. Such studies on bulk rocks are essential to better understand bacterial weathering. Results of four different bacterial activity on three different rock types are presented.

Biotite granite, garnetiferous felsic granulite and gabbro from tropical region of south India were collected and powdered to < 120 µm. The bacterial strains, RB 9, 15, 21 and 24, isolated from the rhizoplane of *Ficus* which grew on rocks were identified as *B. multivorans*, *C. malonaticus*, *E. aerogens* and *P. pleccoglossicida* respectively. They were grown for 28 days in a medium containing glucose and rock powder as the carbon and nutrient sources, respectively. Rock and abiotic controls were included. The residual pellets devoid of bacteria and other contaminants were analysed using XRD and ICP-MS.

Bacterial action on the biotite granite weathered biotites completely while microcline and albite were altered to varying degrees by different bacteria. All the major elements were depleted (30-50 %), while 25-40 % reduction of trace elements and REE were observed. P<sub>2</sub>O<sub>5</sub> and Ni reduction varied with individual strains.

Felsic granulite showed removal of almandine garnet and reduction in albite and orthoclase to a larger extent. RB15 exerted moderate reduction (10-30 %) and did not fractionate major elements. Whereas, other bacteria showed considerable depletion of MgO (> 60 %). RB24 and RB25 were found to mobilise HREE (~ 30 %) while RB15 released relatively more Eu and trace element release was bacterial dependent.

The gabbro consisting of orthopyroxene, clinopyroxene and plagioclase did not show detectable change in the mineralogy. All the strains enriched Mn while RB9 depleted it. RB25 was found to enrich more HREE compared to LREE and Eu was depleted by RB9. Each bacteria followed unique pattern in release of trace elements.

Microbial weathering of granite, felsic granulite and gabbro show distinct patterns of mineralogical and chemical changes. Each bacterial strain had unique signature in altering the major and trace element abundances of a given rock.

## LabData-GC: a database sub-system for post-processing and quality control of CFC and SF<sub>6</sub> measurements

AXEL SUCKOW<sup>1\*</sup>

<sup>1</sup>CSIRO Land and Water, Urrbrae, SA 5064, Australia

(\*correspondence: Axel.Suckow@csiro.au)

<sup>2</sup> National Centre for Groundwater Research and Training  
(NCGRT), Flinders University, Adelaide

Low-level gas-chromatography measurements, as they are needed for groundwater dating using CFCs and SF<sub>6</sub> often use commercial software for signal detection, peak detection and integration. The raw data and the parameters used during integration as well as the standards and blanks used to determine the absolute concentrations of unknown samples need to be stored for traceability of results.

A database sub-system to the LabData LIMS [1] is presented that covers:

1. storage of all raw data (signal versus time)
2. storage of parameters of peak integration
3. storage of all attribute data of the measurement (sample-ID, origin, project context etc.)

The corresponding graphical user interface and post-processing algorithms allow the calculation of absolute concentrations in water from

1. blank time series
2. sensitivity time series from standard measurements
3. linearity measurements (dependence of sensitivity from peak area)
4. graphical display of all relevant result by export to MS Excel

The database sub system is integrated in a multi-user client server architecture using MS SQL server as back-end and a graphical user interface based on MS Access. The existing modelling capabilities of age distributions using a lumped parameter approach are an add-on. The source code is public domain software and available under the GNU-GPL licence agreement.

[1] Suckow, Dumke (2001): *A database system for geochemical, isotope hydrological and geochronological laboratories*. Radiocarbon 43, No. 2, pp. 325-337.

## Abiotic methane formation not from H<sub>2</sub> but from H<sub>2</sub>O in the serpentinite-hosted Hakuba Happo hot spring

K. SUDA<sup>1\*</sup>, Y. UENO<sup>1,2</sup> AND S. MARUYAMA<sup>1,2</sup>

<sup>1</sup>Department of Earth and Planetary Sciences, Tokyo Institute of Technology, Meguro, Tokyo, 152-8551, Japan  
(\*correspondence: suda.k.ag@m.titech.ac.jp)

<sup>2</sup>Earth-Life Science Institute, Tokyo Institute of Technology, Meguro, Tokyo, 152-8551, Japan

Serpentinite-hosted hydrothermal system is considered to be important for prebiotic synthesis as well as habitat for the earliest life. Fluids derived from serpentinites are characterized by high concentrations of H<sub>2</sub> and CH<sub>4</sub> [e.g. 1]. It is generally assumed that the methane and hydrocarbons are produced abiotically from the H<sub>2</sub> and CO<sub>2</sub> via Fischer-Tropsch Type (FTT) synthesis [e.g. 1,2]. However, the production mechanism of the methane is not adequately understood yet. We report systematic isotopic study of a new serpentinite-hosted hydrothermal system: Hakuba Happo hot spring in the Shiroumadake area, Japan. The hot spring water was directly collected from 500-1000 m deep two drilling wells that show high pH over 10 and rich in H<sub>2</sub> and CH<sub>4</sub>. The δD values of H<sub>2</sub> and H<sub>2</sub>O from both wells are almost the same, whereas the δD-CH<sub>4</sub> values are different by approximately 80%. The CH<sub>4</sub>-H<sub>2</sub>-H<sub>2</sub>O hydrogen isotope systematics indicates at least two different mechanisms are required for the methane formation. The higher δD-CH<sub>4</sub> with respect to equilibrium relation is similar to other serpentinite-hosted system reported earlier and demonstrates that the source of hydrogen of CH<sub>4</sub> cannot be H<sub>2</sub> but directly derived from H<sub>2</sub>O. This implies that the CH<sub>4</sub> is not produced via the FTT synthesis, but instead, likely produced by hydration reaction of olivine. On the other hand, lower δD-CH<sub>4</sub> with respect to equilibrium relation suggests incorporation of biological methane. Based on the comparison of δD systematics between our result and other serpentinite-hosted hydrothermal system, we suggest that dominant methane formation mechanism in a general serpentinite-hosted system is not FTT reaction. Hydration of olivine may play more significant role for abiotic methane production than previously thought.

[1] Holm & Charlou (2001) *EPSL* **191**, 1-8. [2] Proskurowski *et al.* (2008) *Science* **319**(5863), 604-607.

## Organic and inorganic contaminant remediation by biogenic nanopalladium

E. SUJA<sup>1</sup>, Y. V. NANCHARAI AH<sup>1</sup>, A. J. FRANCIS<sup>2,3</sup> AND V. P. VENUGOPALAN<sup>1\*</sup>

<sup>1</sup>Biofouling and Biofilm Processes Section, Water and Steam Chemistry Division, Bhabha Atomic Research Centre, Kalpakkam 603102, Tamil Nadu, India

<sup>2</sup>Division of Advanced Nuclear Engineering, POSTECH, South Korea,

<sup>3</sup>Brookhaven National Laboratory, USA.

\* Corresponding author: E-mail: vpv@igcar.gov.in

Microbial synthesis of nanoparticles is an innovative process for precious metal recovery and preparation of nanocatalysts for transformation of environmental contaminants. Here, we report preparation of microbiologically synthesized palladium (Pd) nanoparticles (Bio-Pd) using *Clostridium* sp. BC1 [1] and microbial granules (MG) under fermentative growth conditions [Fig. 1]. Microbial granules were cultivated in bubble column sequencing batch reactors [2]. Reduction of dissolved Pd (II) to insoluble, black colored Pd (0) by BC1 or MG was instantaneous and complete. Removal of Pd (II) via sorption by BC1 or MG was negligible. Reduction of Pd (II) was mediated by the microbially generated hydrogen and the Pd (0) nanoparticles were predominantly associated with the bacterial cells or MG. The Bio-Pd catalysed the reduction of Cr (VI) to Cr (III) and the transformation of *p*-nitrophenol to *p*-aminophenol [Fig. 2]. Fermentatively produced hydrogen continued to act as the reducing agent for contaminant transformation. Our results demonstrate the potential use of MG for synthesis of Bio-Pd (0), Pd (II) recovery and efficient treatment of toxic contaminants in acidic environment. We also investigated the potential application of Bio-Pd in nitrate reduction.

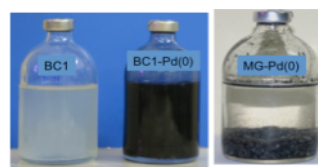


Fig 1. *Clostridium* sp. BC1 culture, Pd (0) nanoparticles associated with BC and microbial granules (MG).

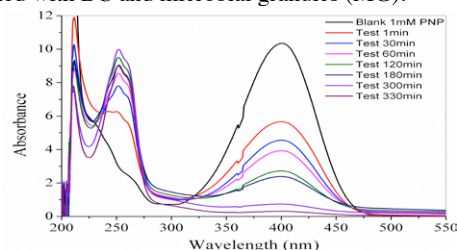


Fig 2. Bio-Pd mediated transformation of *p*-nitrophenol to *p*-aminophenol.

[1] Nancharai ah and Francis (2011) *Bioresour Technol.* 102(11)6573–8. [2] Suja *et al.* (2012) *Appl Biochem Biotechnol.* 167:1569–1577.

## Effect of K<sub>2</sub>O Addition on the Viscosity of CaO-SiO<sub>2</sub>-Al<sub>2</sub>O<sub>3</sub> Melt

S. SUKENAGA<sup>1\*</sup>, T. HIGO<sup>2</sup>, H. SHIBATA<sup>1</sup>, N. SAITO<sup>2</sup> AND K. NAKASHIMA<sup>2</sup>

<sup>1</sup>IMRAM, Tohoku University,

(\*correspondance: sukenaga@tagen.tohoku.ac.jp)

<sup>2</sup>Dept. Mater. Sci. & Eng., Kyushu University

In general, viscosity of silicate melts decreased with the addition of alkali oxides [1], which is due to the depolymerization of the silicate anions. In the case of aluminosilicate melts, the viscosity depends on not only the polymerization degree but also the average bond strength of aluminosilicate framework [2]. Roy and Navrotsky [3] reported that the average bond strength of the aluminosilicate framework could be higher when cations with lower cationic field strength (such as K, Rb, Cs) were present. Therefore, the effect of K<sub>2</sub>O on the viscosity of CaO-SiO<sub>2</sub>-Al<sub>2</sub>O<sub>3</sub> (CAS) melt was investigated to clarify relationship between the viscosity and cationic field strength using rotating cylinder method.

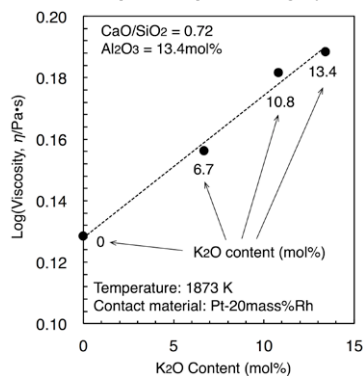


**Figure 1:** Effect of K<sub>2</sub>O addition on the viscosity of the 36.1CaO-50.5SiO<sub>2</sub>-13.4Al<sub>2</sub>O<sub>3</sub> (mol%) melt at 1873 K. CaO/SiO<sub>2</sub> ratio and Al<sub>2</sub>O<sub>3</sub> content were kept constant.

Viscosity of the CAS melt increased with the increase of K<sub>2</sub>O. On the other hand, the polymerization degree of aluminosilicate anions should be decreased. (Fig.1) This viscous behavior could be explained by an increase in the average bond strength of aluminosilicate framework with the addition of K<sub>2</sub>O.

[1] Mysen & Richet (2005) *Silicate Glasses and Melts*(Elsevier), 191. [2] Dingwell & Virgo (1988) *Geochim. Cosmochim. Acta* **52**, 395-403. [3] Roy & Navrotsky (1984), *J. Am. Ceram. Soc.* **67**, 606-610.

## Fluid flow and mineral reaction mechanisms at high pressures: Tauern window, Eastern Alps

MIROSLAV ŠULÁK<sup>1\*</sup> AND DAVID DOLEJŠ<sup>1</sup>

<sup>1</sup>Institute of Petrology and Structural Geology, Charles University, 128 43 Praha 2, Czech Republic

(\*correspondence: miroslav.sulak@natur.cuni.cz)

Aqueous fluids play major role as mass transport agents in the lithosphere but diverse approaches such as direct analysis of fluid inclusions, applications of transport theory to reaction progress, experimental mineral solubilities, time scales retrieved from isotopic tracers and microscale observations of dissolution-precipitation mechanisms still do not provide a self-consistent picture about the fluid flow mode and magnitude of intergrated fluid fluxes. We investigate synmetamorphic hydrothermal replacements, segregations and veins developed in eclogites of the Tauern Window, Eastern Alps, as a model case study to address the conditions and modes of fluid flow and efficiency of fluid-mineral reactions at very high pressures (up to c. 610 °C, 21 kbar). These hydrothermal products record a continuous sequence from volume-conserved rock-buffered replacements to fluid-buffered precipitates in open space with unidirectional growth textures recording local anisotropic stress field at peak pressures. We observe: (1) quartz-kyanite-omphacite-rutile-clinozoisite multicomponent segregations indicating nearly congruent mass transport at local scale, controlled by rheological heterogeneities, where extraction volume for immobile elements (e.g., Ti) does not exceed 2-3 centimeter in size, (2) nearly monomineralic omphacite selvages recording focused fluid flow, (3) extensional quartz veins with euhedral omphacite crystals at the wall contact and (4) large transport veins composed of kyanite and quartz, showing little or no chemical exchange with wall rock. Chemical zoning patterns of garnet and omphacite are texture-independent and indicate local interconnectivity *via* the fluid phase, from low-permeable intergranular replacements to fluid-focusing channels and transport veins. Oscillatory zoning patterns in vein omphacite and kyanite reflect pulsed flushing probably related to pressure fluctuations in crack-seal cycles. Modal variations interpreted by conventional transport theory would yield integrated fluid fluxes reaching c. 10<sup>5</sup> m<sup>3</sup> m<sup>-2</sup> but these will not be required when considering coupling of diffusional and advective mass transfer driven by pressure gradients, where precipitation is controlled by distribution and size of permeability inhomogeneities vs. extensional cavities. The observed phenomena provide a cautionary example against simple inversions of reaction progress to flux estimates.

## Using WITCH to quantify landscape and hydrologic controls on solute fluxes in the Critical Zone (Susquehanna Shale Hills Observatory, PA)

PAMELA L. SULLIVAN<sup>1,2</sup>, YVES GODDÉRIIS<sup>3</sup>,  
YUNING SHI<sup>1</sup>, JACQUES SCHOTT<sup>3</sup>,  
CHRISTOPHER J. DUFFY<sup>2</sup> AND SUSAN L. BRANTLEY<sup>1</sup>

<sup>1</sup> Earth and Environmental Systems Institute, Pennsylvania State University, University Park, PA, USA;

pls21@psu.edu, yshi@psu.edu, sxb7@psu.edu

<sup>2</sup> Department of Civil Engineering Pennsylvania State University, University Park, PA, USA; cxd11@psu.edu

<sup>3</sup> Géosciences Environnement Toulouse, CNRS-Observatoire Midi-Pyrénées, Toulouse, France; yves.godderis@get.obs-mip.fr, jacques.schott@lmtg.obs-mip.fr

To investigate the hydrologic and landscape controls on shale weathering and their influence on first-order stream solute fluxes, we coupled a numerical chemical weathering model, WITCH, with a physically-based land surface hydrologic model, Flux-PIHM (Penn State Integrated Hydrologic Model). Using this approach, we were able to simulate vertical water and chemical fluxes across two representative landscape features (planar or swale hillslopes). We extrapolate the results from the soil profiles to estimate the chemical loads to the stream over a 32 year period (1980-2012) at the Susquehanna Shale Hills Critical Zone Observatory (SSH-CZO). Observed soil water (10 cm increments) and stream water chemistry collected between 2006-2011 were used to validate the modelling results. The simulation predicted the saturation state of soil water with respect to illite, smectite and kaolinite. Saturation was driven by seasonal drying, with supersaturated conditions persistent around the rooting zone (25-70 cm) during the summer months. As expected, the modelled weathering rates of illite, chlorite and k-feldspar were elevated near the soil surface where fluids were dilute, especially at the onset of fall when solute fluxes (eg. Mg, Na and Si) reached their maximum. Results from Flux-PIHM suggest a more extensive hydrologic connection between the swale hillslopes and the stream as compared with the planar hillslopes. WITCH then documented the role of this hydrologic connection on the stream water chemistry, with swales contributing bigger solute fluxes.

## Sediment phosphorus dynamics in a marine coastal lake: Response to seasonal bottom water anoxia

FATIMAH SULU-GAMBAR<sup>1</sup>, DORINA SEITAJ<sup>2</sup>,  
FILIP MEYSMAN<sup>2</sup> AND CAROLINE P. SLOMP<sup>1</sup>

<sup>1</sup>Utrecht University, Utrecht, the Netherlands

<sup>2</sup>NIOZ, Yerseke, the Netherlands

Low-oxygen conditions are expanding in bottom waters of many coastal systems. Increased availability of the nutrient phosphorus (P) is often important in the development and sustainment of hypoxia. However, the controls on the recycling and burial of P in hypoxic and anoxic marine settings are not well understood. Here, we present results of a detailed study of the sediment biogeochemistry and P dynamics at a site in the seasonally anoxic marine Lake Grevelingen, in the Netherlands. Monthly water column and pore water profiles of oxygen and sulphide for 2012 show a short (1 month) but intense period of bottom water anoxia. Strong seasonality in the pore water profiles of dissolved Fe<sup>2+</sup> and phosphate is seen. In spring, when bottom waters were oxic, our pore water data indicate dissolution of iron sulfides and calcium carbonate due to activity of electrogenic bacteria [1]. Consequentially there is a strong release of Fe<sup>2+</sup> to the pore water without an associated release of dissolved phosphate. In this period, most released phosphate remains in the sediment. Upon the onset of anoxia, phosphate release from the sediment to the water column is enhanced, both in absolute terms, when compared to the prior oxic period and relative to dissolved inorganic carbon (DIC) and ammonium. With the return of oxic conditions, Beggiatoa establish at the sediment-water interface and the benthic flux of phosphate is again reduced. Sediment P analyses indicate most P in the sediment is present in the form of organic- and iron-bound P, even at depths where sulphide is present at high concentrations throughout the year. This suggests the presence of a reduced Fe-P phase as found recently in euxinic sediments from the Baltic Sea [2]. Further work will focus on the identification of the sedimentary Fe-bound P forms and a reconstruction of the role of the sediment as a P source and sink over past decades.

[1] Risgaard-Petersen *et al.* (2012) *Geochim Cosmochim Acta* 92: 1-13. [2] Jilbert & Slomp (2013) *Geochim Cosmochim Acta* 107: 155-169

## Noble gas and halogen recycling at subduction zones

H. SUMINO<sup>1</sup>\*, M. KOBAYASHI<sup>1</sup>, D. CHAVRIT<sup>2</sup>,  
L. JEPSON<sup>2</sup>, A. SHIMIZU<sup>3</sup>, J.-I. KIMURA<sup>4</sup>,  
R. BURGESS<sup>2</sup> AND C. J. BALLENTINE<sup>2</sup>

<sup>1</sup>GCRC, Univ. Tokyo, Tokyo 113-0033, Japan

(\*correspondence: sumino@eqchem.s.u-tokyo.ac.jp)

<sup>2</sup>SEAES, Univ. Manchester, Manchester M13 9PL, UK

<sup>3</sup>Tokyo Metropolitan Industrial Technology Research Institute,  
Tokyo 135-0064, Japan

<sup>4</sup>IFREE, Japan Agency for Marine-Earth Science and  
Technology, Yokosuka 237-0061, Japan

Recent findings of subducted halogens and noble gases with seawater and sedimentary pore-fluid signatures in exhumed mantle wedge peridotites [1], as well as seawater-derived heavy noble gases (Ar, Kr and Xe) in the convecting mantle [2], provide observations that allow us to investigate the processes that control the return of volatile and highly incompatible elements into the mantle. To verify whether and how such subduction fluids modify the composition of the mantle beneath subduction zones, we are investigating noble gas and halogen compositions of olivines and mantle-derived xenoliths in arc lavas from Western-Pacific subduction zones (Izu, Kamchatka and N. Philippines) and those of seafloor sediments and basalts from NW margin of the Pacific plate.

MORB-like <sup>3</sup>He/<sup>4</sup>He and halogen ratios of the olivines indicate insignificant contributions to the arc magmas of radiogenic <sup>4</sup>He and pore-fluid-like halogens, both of which are observed in the subduction fluids released from a slab at a depth of 100 km [1]. In contrast, mantle-derived xenoliths exhibit pore-fluid-like halogens and heavy noble gases but MORB-like He. The high I/Cl ratios of pelagic clays and radiolarian cherts can account for the enrichment of iodine in subduction fluids relative to sedimentary pore-fluids [1], whereas contributions of halogens and noble gases from altered oceanic basalts are limited.

The significantly smaller contributions of subducted noble gas and halogen in the arc magmas relative to those in the mantle wedge peridotites may result from a difference in the P-T condition of the slab in each subduction zone, or from dilution by mantle-derived halogens and He when the subduction fluid induced partial melting. The former implies a relatively small amount of the pore water subduction fluids would be released from a cold slab at a sub-arc depth resulting in further subduction of halogens, heavy noble gases and potentially water, to great depths in the mantle.

[1] Sumino *et al.* (2010) *EPSL* **294**, 163-172. [2] Holland & Ballentine (2006) *Nature* **441**, 186-191.

## Formation of Magnetite within aquifer sediments and its effects on Arsenic mobility

JING SUN<sup>1</sup>\*, STEVEN CHILLRUD<sup>2</sup>, BRIAN MAILLOUX<sup>3</sup>  
AND BENJAMIN BOSTICK<sup>4</sup>

<sup>1</sup>Columbia University, New York, U.S.A.,

jingsun@ldeo.columbia.edu

<sup>2</sup>Lamont-Doherty Earth Observatory, Palisades, U.S.A.,

chilli@ldeo.columbia.edu

<sup>3</sup>Barnard College, New York, U.S.A., bmaillou@barnard.edu

<sup>4</sup>Lamont-Doherty Earth Observatory, Palisades, U.S.A.,

bostick@ldeo.columbia.edu

One commonly attempted remediation approach for groundwater Arsenic (As) contamination involves stimulating iron (Fe) mineral transformations that affect aqueous As concentration. However, successful strategies are difficult to develop and implement, in part because many Fe minerals are only stable under a narrow window of redox conditions. Magnetite (Fe<sub>3</sub>O<sub>4</sub>) is a promising target mineral for As remediation due to its stability over a wide range of Eh-pH conditions. Recent studies have found that magnetite is capable of retaining As through surface adsorption and also trapping arsenate As(V) into its structure. However, the factors that promote magnetite formation and As incorporation and adsorption are poorly established.

Here, we did a series of columns, loaded with reduced aquifer sediments from the Dover Landfill Superfund site. We stimulated the formation of As-bearing magnetite, tested its ability of maintaining As retention and evaluated its capability of sequestering additional As. All columns were conducted at circumneutral pH, similar to site conditions but much lower than is normally considered ideal for magnetite formation. The columns were equilibrated with continuous oxygen-free artificial groundwater containing lactate and sodium arsenite As(III), during which As release was observed. Then sodium nitrate and ferrous sulfate were added to the same influent groundwater, which sequestered As on solids quickly and yielded considerable magnetite as suggested by magnetic separations of a sacrificed column. (Synchrotron X-ray absorption spectroscopy as well as sequential extraction will be used to identify and quantify solid-phase Fe and As speciation). These amended columns were able to maintain low aqueous As concentrations even when influent groundwater with high lactate concentration (and no As) were introduced to encourage reduction and also able to continue to retain As after subsequent arsenite and lactate additions.

## Porphyry deposits and oxidized magmas

WEIDONG SUN<sup>1</sup>, HUAYING LIANG<sup>1</sup>, MING-XING LING<sup>1</sup>,  
HONG ZHANG<sup>2</sup> AND XIAO-YONG YANG<sup>3</sup>

<sup>1</sup>Guangzhou Institute of Geochemistry, CAS, Guangzhou  
510640, China (weidongsun@gig.ac.cn)

<sup>2</sup>Northwest University, Xi'an 710069, China

<sup>3</sup>University of Science and Technology of China, Hefei  
230026, China

Porphyry deposits supply most of the world's Cu, Mo resources. Here we show that all the porphyry deposits are associated with oxidizing magmas. Oxidation promotes the destruction of sulfides in the magma source and thereby increases initial chalcophile element concentrations[1,2]. Sulfide remains undersaturated during the evolution of oxidized sulfur-enriched magmas where sulfate is the dominant sulfur species, leading to high chalcophile element concentrations in evolved magmas. The final porphyry mineralization is controlled by sulfate reduction, which starts with magnetite crystallization, accompanied by decreasing pH and correspondingly increasing  $fO_2$ . Hematite forms once sulfate reduction lowered the pH sufficiently and the  $fO_2$  reaches the hematite-magnetite oxygen fugacity buffer, which in turn increases the pH for a given  $fO_2$ . In addition to the oxidation of ferrous iron during the crystallization of magnetite and hematite, reducing wallrocks may also contribute to sulfate reduction and mineralization. For porphyry Cu deposits, slab melts (adakite) characterized by high Sr/Y is another controlling factor. Subduction of young ridge forms adakites with high fugacity, such that is the best geological process for porphyry Cu deposits[3,4]. Mo deposits are likely related to Mo-enriched metasediments.

[1] Sun W D *et al.* The link between reduced porphyry copper deposits and oxidized magmas. *GCA*, 2013, 103: 263-275. [2] Sun W D, *et al.* Geochemical constraints on adakites of different origins and copper mineralization. *J. Geology*, 2012, 120: 105-120. [3] Sun W D, *et al.* The genetic association of adakites and Cu-Au ore deposits. *International Geology Review*, 2011, 53: 691-703. [4] Sun W D, *et al.* Ridge subduction and porphyry copper-gold mineralization: An overview. *Science China-Earth Sciences*, 2010, 53: 475-484

## The global flux of calcium into and out of marine sediments

XIAOLE SUN<sup>1\*</sup> AND ALEXANDRA V. TURCHYN<sup>1</sup>

<sup>1</sup>Department of Earth Sciences, University of Cambridge,  
Cambridge CB2 3EQ, UK, xs243@cam.ac.uk  
(\*presenting author)

Fundamental to understanding Earth's climate is an understanding of the removal of carbon from the surface into the rock reservoir. This removal of carbon is achieved through burial of carbon-bearing minerals, both carbonate and organic carbon, in marine sediments. Much of the organic carbon buried in marine sediments is oxidized back to inorganic carbon, which may react with subsurface calcium to precipitate authigenic carbonate, or may return via diffusion to the overlying ocean. The precipitation of authigenic carbonate has recently been invoked as a critical process in the long-term carbon cycle<sup>1</sup>.

We use a compilation of 674 pore fluid profiles acquired through the various drilling programs to calculate the flux of aqueous calcium across the sediment-water interface. In coastal regions and other areas of high organic-carbon supply to marine sediments, we calculate a flux of calcium into marine sediments; this calcium consumption is linked to the production of *in situ* authigenic carbonate. Parts of the ocean are dominated by a flux of calcium out of marine sediments, where calcium is produced in the subsurface through carbonate recrystallization, ion exchange, alteration of volcanic ash, or rarely subsurface gypsum dissolution. Our compilation suggests regional heterogeneity in the subsurface calcium (and carbon) cycle, as well as a global flux of calcium between the ocean and marine sediments that is significant in the global calcium cycle.

[1] Schrag *et al.*, (2013) *Science* **339**, 540-544.

## Kerogen-generated bitumen as a source of shale gas: Experimental results and mass balance calculation

YONGGE SUN AND LIUJUE XIE

Department of Earth Science, Zhejiang University, Hangzhou 310027, P. R. China. Email: ygsun@zju.edu.cn

It is well known that most of shale gases discovered to date are thermogenetic within the late phase of hydrocarbon generation. This phenomenon was brought into questions with the fact that there is less gas potential of kerogen-cracking throughout the oil & gas window for most type I and II kerogens. Using a high pressure, semi-closed pyrolysis system, one shale from the Songliao basin, NE China with a TOC of 3.29% was selected to probe the gas generation processes throughout the oil & gas window. The results showed that there are at least two processes involved for the gas generation, which were characterized by distinctive characters of dryness ( $C_1/\sum C_{1-5}$ ) and  $\delta^{13}C_{\text{methane}}$ . The first one is associated with kerogen thermal degradation and occurs at the main phase of oil generation. The second starts at the late phase of oil generation with a decrease of dryness and  $^{13}C$  depleted methane, which is in contrast to the theoretical prediction as the increasing trend of dryness and  $\delta^{13}C_{\text{methane}}$  accompanying thermal evolution. It suggests that this process should be mainly related to the cracking of kerogen-generated products retained in shale due to the lack of aliphatic carbon in kerogen at this stage, as evidenced by FTIR and curie Py-GC-MS analyses. A rapid decreasing of polar fraction in retained bitumen could be another indicator of the process. Mass balance calculation using hydrogen content demonstrated that bitumen retained in this shale can contribute 2-3m<sup>3</sup>HC gas/t rock to shale gas during the stage of 1.3-1.7%Ro and has implications for maturity map-making and shale gas resource assessments before exploration.

## Phytoremediation for co-contaminated soils of polycyclic aromatic hydrocarbons and cadmium using willow

Y.Y. SUN<sup>1</sup>, H.X. XU<sup>1\*</sup>, J.H. LI<sup>2</sup>, J.C. WU<sup>1</sup>

<sup>1</sup>School of Earth Science and Engineering, Nanjing University, Nanjing 210093, China (sunyy@nju.edu.cn, \*correspondence: hxxu@nju.edu.cn, jcwu@nju.edu.cn)  
<sup>2</sup>Jiangsu Maritime Safety Administrations, Nanjing 210003, China (huadavid2002@163.com)

To investigate the effect of PAHs on the cadmium (Cd) phytoremediation efficiency using willow, field experiments were conducted in the lower reaches of the Yangtze River, China. Based on our previous study, a native willow (*Salix×aureo-pendula* CL 'J1011') was selected, owing to its easy propagation, fast growth, extensive root system, toleration of temporarily waterlogged environments, etc. Results showed that the growth of willow was negatively affected by PAHs (phenanthrene and pyrene) and Cd. The amendment of ethylenediaminetetraacetic acid (EDTA) and ethyl lactate could not only increase the accumulation of Cd in willow tissues, but also promote the degradation of PAHs. After 45 days, the combined treatment willow-EDTA and willow-EDTA-ethyl lactate significantly decreased the concentrations of PAHs and Cd in the soils ( $p < 0.05$ ). Willow could also accumulate phenanthrene (PHE) in tissues, while accumulation of Cd in plants was much higher than that of PHE. The effectiveness of pyrene (PYR) absorption in willow was very weak and there was no detectable PYR in willow shoots. Under the same treatment, the presence of PAHs increased the Cd accumulation in willow shoots, especially for treatment willow-EDTA, while it had no significant influence on the removal of Cd from soils ( $p > 0.05$ ). The results indicate that the native willow *Salix×aureo-pendula* CL 'J1011' together with EDTA and ethyl lactate could be used for phytoremediation of PAHs-Cd co-contaminated soils.

### Acknowledgments

This work was supported by the National Natural Science Foundation of China (41102148, 41030746) and the Specialized Research Fund for the Doctoral Program of Higher Education of China (20110091120063).



## Chemical and bacteria leaching of a low-grade and high-fluorine uranium ore in column reactors

ZHANXUE SUN\*, YAJIE LIU, JIANG LI, XUELI LI AND WEIJUN SHI

East China Institute of Technology, Nanchang, Jiangxi 330013, China (\*Correspondence: zhxsun@ecit.cn)

### The purpose of the Study and Mineralogy

The purpose of the study is to investigate the technical feasibility of using bioleaching on a low-grade and high-fluorine uranium ore from China, which is not economically exploitable with conventional technologies. The ore contains 0.19% uranium and 1.0% fluorine. Uranium is present primarily as pitchblende and secondarily as coffinite and infrequently as brannerite and uranothorite.

### Column Bioleaching Experiments

52-day column bioleaching experiment was conducted with finely ground ore (-0.8 mm) at ambient temperature to study the effect of bacteria on uranium extraction. For the sake of contrast, column chemical leaching experiment was also conducted at same time. The chemical leaching experiment used only sulfuric acid, but the bacteria leaching experiment used sulfuric acid and *A. ferrooxidans* as well.

### Results

The leaching rate of U is 91.8% for the bacteria leaching experiment and is only 78.5% for the chemical leaching experiment. The sulfuric acid consumption is 4.73% and 4.97% for bacteria leaching and for chemical leaching respectively. The microorganism used in the bioleaching test resisted high concentration of total fluorine ranging from 1.8g/L to 2.0g/L in the leachate. The experiments suggested the feasibility of bioleaching for extraction uranium from this kind of uranium ore.

This work was financially supported by International Science and Technology Cooperation Project of China (2011DFR60830).

## Flow dynamics and $^3\text{H}/^3\text{He}$ ages of deep groundwater at Gardermoen (Oslo Airport, Norway)

A. SUNDAL<sup>1\*</sup>, P. AAGARD<sup>1</sup>, B. WEJDEN<sup>2</sup> AND M.S. BRENNWALD<sup>3</sup>

<sup>1</sup>Dep. of Geosciences, University of Oslo, Norway

\*Corresponding author: anja.sundal@geo.uio.no

<sup>2</sup>Oslo Airport, Water and Soil Dep., Gardermoen, Norway

<sup>3</sup>Eawag, Dep. of Water Resources and Drinking Water, Swiss Federal Institute of Aquatic Science and Technology, Switzerland

Sandy, quaternary, deposits at Gardermoen constitute the central part of Norway's largest unconfined aquifer. The steady influx of temperate, nutrient rich groundwater is essential for ecology and geomorphology of local conservation areas. The establishment of Oslo Airport (OSL) at Gardermoen in 1998 was therefore approved by the authorities on the condition that the groundwater quality would not be deteriorated. Extensive, continuous monitoring of groundwater quality and fluxes is performed at OSL and numerous research projects have been carried out. Knowledge about the deeper parts of the aquifer, however, is limited.

The total water balance in the study area is well constrained. The sandy deposits form a ridge, with relatively permeable sediments in the North-East and decreasing permeability towards the South-West. The aquifer is solely precipitation fed (40 cm/a net recharge). The groundwater flow is directed towards the North-East (80% of flux) and South-West (20% of flux), away from a crescent shaped groundwater divide and into the effluent rivers Risa and Sogna.

In this study water samples from 20 wells (1.5 – 30m below phreatic groundwater table) have been analyzed for major ions,  $^3\text{H}$  and noble gases (He, Ne, Ar, Kr, Xe). The tritium concentrations range from 8–52 TU and the  $^3\text{H}/^3\text{He}$  water ages from 1.5–53 years. The water ages generally increase with depth and distance from the groundwater divide. The hydraulic head in some wells deviates from hydrostatic conditions due to underpressure in lower (semi-) confined units. Using water ages in multi-level wells for calibration of flow models (2D grid sections), we investigate different scenarios with respect to flow separation and vertical flow components due to geological heterogeneities. Using ionic content and water ages as tracers is complicated by indication of mixing with fossil seawater (9.5 ka BP) from basal silt deposits.

## Interactions between As(V), Fe(III) and natural organic matter

A. SUNDMAN\*, T. KARLSSON AND P. PERSSON

Department of Chemistry, Umeå University, SE-901 87

Umeå, Sweden (\*Correspondance:

anneli.sundman@chem.umu.se,

torbjorn.karlsson@chem.umu.se,

per.persson@chem.umu.se)

As is naturally occurring mainly as solid  $\text{FeAs}_x\text{S}_{2-x}$  and as adsorbed species on Fe and Al hydroxides, but it is also found associated with natural organic matter (NOM) [1]. Under oxic conditions, it has been hypothesized that, ternary complexes of As(V), Fe(III) and NOM are formed and that these play a key role in As biogeochemistry. Recently, spectroscopic evidence for the formation of these complexes in peat humic substances was published [2]. We have further investigated the fundamental properties of the interactions between As(V), Fe(III) and NOM. The experimental range covers different kinds of NOM, concentrations between 6485 and 67 243 ppm Fe, pH 3-7 and Fe(III) to As(V) ratios between 0.5 and 100. Synchrotron based Fe and As K-edge extended X-ray absorption fine structure (EXAFS) spectroscopy in combination with infrared (IR) spectroscopy have been used as molecular probes.

### Results and Discussion

The NOM suppressive effect on Fe precipitation [3] is reduced in the presence of As(V). At low pH and Fe concentration, the Fe EXAFS spectrum resembles Fe-NOM reference samples (see Figure 1). At higher Fe concentrations, i.e. 22 916 ppm Fe (or 0.085 mol Fe per mol of carboxylic functional groups), Fe(III):As(V) 1:1 quantitative Fe EXAFS results indicate a precipitated  $\text{FeAsO}_4$  phase. As EXAFS and IR data provide further support for these findings. They indicate precipitated  $\text{FeAsO}_4$  at high pH and fractions of soluble, unbound  $\text{H}_2\text{AsO}_4^-$  at low pH.

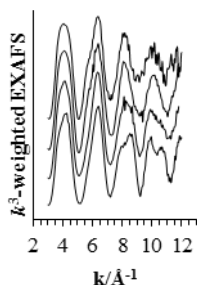


**Figure 1.** Fe EXAFS data for Suwannee River NOM samples, a) 6489 ppm Fe, pH 5.0, b) 6485 ppm Fe, Fe(III):As(V) 1:1, pH 5.0, c) 22 916 ppm Fe, Fe(III):As(V) 1:1, pH 5.3 and d) precipitated  $\text{FeAsO}_4$ .

[1] Redman *et al.* (2002) *Environ. Sci. Technol.* **36**, 2889-2896. [2] Mikutta & Kretzschmar (2011), *Environ. Sci. Technol.* **45**, 9550-9557. [3] Karlsson & Persson (2012), *Chem. Geol.* **322-323**, 19-27.

## Coupled radiogenic and stable Sr isotope variations in oceanic basalts

CHELSEA N SUTCLIFFE<sup>1\*</sup>, KEVIN W BURTON<sup>2</sup>,  
IAN J PARKINSON<sup>3</sup>, DON PORCELLI<sup>1</sup>  
AND ALEX N HALLIDAY.<sup>1</sup>

<sup>1</sup> Department of Earth Sciences, University of Oxford, Oxford, UK. (\* presenting author; chelsea.sutcliffe@st-annes.ox.ac.uk)

<sup>2</sup> Department of Earth Sciences, Durham University, Durham, UK.

<sup>3</sup> Bristol Isotope Group, School of Earth Sciences, University of Bristol.

The formation of basaltic crust at mid-ocean ridges and ocean islands provides a window into the compositional variations in Earth's upper mantle. If basalts are in equilibrium with their mantle source, then the composition of long-lived radiogenic isotopes should be identical and unaffected by partial melting or magmatic processes. Consequently, variations in the isotope composition of Sr, Nd and Pb of oceanic basalts are usually attributed to the existence of compositional heterogeneity in the mantle. In contrast, stable isotope variations can arise from mass dependent processes including partial melting, diffusional exchange or fractional crystallisation [1]. Taken together, radiogenic and stable isotopes can be used to unravel source variations from melting and magmatic processes [2].

Radiogenic Sr ( $^{87}\text{Sr}/^{86}\text{Sr}$ ) is a widely used tracer of mantle chemistry and when paired with stable Sr ( $^{88}\text{Sr}/^{86}\text{Sr}$ ) offers a unique opportunity to trace melt compositions. Moreover, using the double spike-TIMS technique, both radiogenic and stable isotopes can be measured to a high precision. However, to date there is little precise data for the stable  $^{88}\text{Sr}/^{86}\text{Sr}$  composition of mantle melts and variations cannot be detected at the precisions of existing studies [3]. This study presents high precision DS-TIMS  $^{87}\text{Sr}/^{86}\text{Sr}$  and  $^{88}\text{Sr}/^{86}\text{Sr}$  data for a geographically widespread suite of young MORBs and OIBs, including MORBs from the FAMOUS ridge section. Resolvable variations in  $\delta^{88}\text{Sr}$  of  $\sim 0.14\text{‰}$  are found for MORB and within the FAMOUS segment. In contrast, OIB possess a relatively restricted range of compositions from  $\delta^{88}\text{Sr} = +0.224 \pm 0.008$  to  $+0.280 \pm 0.008 \text{‰}$ . The extent to which coupled  $^{87}\text{Sr}/^{86}\text{Sr}$  and  $^{88}\text{Sr}/^{86}\text{Sr}$  data can be used to disentangle source heterogeneity from variations due to the effects of partial melting and magmatic processes will be discussed, as well as reasons accounting for differences in the trends seen between MORB and OIB.

[1] Teng *et al.* (2013) *Geochim. Cosmochim.* **107**, 12-26 [2] Elliott *et al.*, (2006) *Nature*, **443**, 565-568. [3] Charlier *et al.*, (2012) *EPSL*, **329**, 31-40.

## Terrestrial $\Delta^{33}\text{S}$ and the S cycle during the Archean: Evidence from paleosols

SALLY J. SUTTON<sup>1</sup>, J BARRY MAYNARD<sup>2</sup>,  
DOUGLAS RUMBLE III<sup>3</sup> AND ANDREY BEKKER<sup>4</sup>

<sup>1</sup>Department of Geosciences, Colorado State University, Fort Collins CO 80523-1482 USA, ssutton@mail.colostate.edu

<sup>2</sup>Department of Geology, University of Cincinnati, Cincinnati OH 45221-0013 USA, maynarjb@gmail.com

<sup>3</sup>Geophysical Laboratory, Carnegie Institution of Washington, 5251 Broad Branch Rd., NW, Washington, D.C., 20015-1305 USA, rumble@gl.ciw.edu

<sup>4</sup>Department of Geological Sciences, University of Manitoba, 125 Dysart Road, Winnipeg, MB R3T 2N2 Canada, bekker@cc.umanitoba.ca

Determination of multiple sulfur isotopes in Archean paleosols and diamictites shows the widespread presence of mass-independently fractionated S in the regolith developed on the pre-2.5 Ga Earth. All values of  $\Delta^{33}\text{S}$  are negative, indicating that the Archean surface environments incorporated atmospheric S as  $\text{SO}_4^{2-}$ , which carried a negative  $\Delta^{33}\text{S}$  signal. This S was subsequently converted to sulfide by sulfate reduction, most likely bacterial with terrestrial organic matter as a reductant. Pyrite with similar S isotope systematics has been reported from flood-plain deposits. Grains from these two sources were recycled into detrital pyrites now found in sandstones and conglomerates deposited before the rise of atmospheric oxygen. We suggest that atmospherically-generated S<sub>8</sub> was not similarly contained on the continents, rather was lost to the oceans, creating a continental S reservoir with dominantly negative  $\Delta^{33}\text{S}$  values and a predominantly positive S reservoir in marine sediments.

## High Energy Synchrotron X-ray Geochemical Probes

S.R. SUTTON<sup>1,2</sup>, M. NEWVILLE<sup>2</sup>, A. LANZIROTTI<sup>2</sup>,  
M.L. RIVERS<sup>1,2</sup> AND S. WIRICK<sup>2</sup>

<sup>1</sup>Department of Geophysical Sciences

<sup>2</sup>Center for Advanced Radiation Sources (CARS) University of Chicago, Chicago, IL USA [sutton@cars.uchicago.edu]

High energy synchrotron facilities produce x-radiation with high brightness making them extremely powerful tools for a wide variety of spatially-resolved geochemical research. The primary techniques, X-ray fluorescence (XRF) analysis, X-ray absorption fine structure (XAFS) spectroscopy, X-ray diffraction (XRD) and computed tomography (CT), are used to determine properties of earth, environmental and planetary materials including chemical and mineralogical compositions, crystallographic and other physical structures, oxidation states and fluid flow characteristics.

These X-ray probes are common instruments at virtually every synchrotron facility, are highly complementary in their capabilities and are typically heavily oversubscribed. Analyses at various spatial scales are required for this research necessitating the availability of a suite of instruments each optimized for analyses at different scales.

Focused X-ray beams can be produced using techniques that rely on collimation, refraction, diffraction, or reflection. The most common devices found in synchrotron X-ray probes are those based on diffraction or reflection. Flood-field modes are also utilized where high spatial resolution is achieved via the detection components. "Fly-scanning" approaches have greatly reduced mapping times.

Research using these X-ray probes has led to important insights into the geochemistry of toxic metals and metalloids in contaminated sediments and tailings, the efficiencies of contaminant remediation strategies, how bio-accumulation processes affect the distribution of trace toxic metal species and manufactured nanoparticles in soils and organisms, flow properties of porous media and valence states of multivalent elements in igneous materials, for example.

This presentation will describe currently operating instruments and recent experiments at some US synchrotron facilities, primarily at the Advanced Photon Source (APS, Argonne National Laboratory, IL USA), as well as new, advanced capabilities soon to be available at the National Synchrotron Light Source (NSLS-II, Brookhaven National Laboratory, NY USA).

## Formation of glycine from carboxylic acid and ammonia by shock conditions: Implication to chemical evolution in primitive oceans

C. SUZUKI<sup>1\*</sup>, Y. FURUKAWA<sup>1</sup>, T. KOBAYASHI<sup>2</sup>,  
T. SEKINE<sup>3</sup> AND T. KAKEGAWA<sup>1</sup>

<sup>1</sup>Graduate School of Science, Tohoku University, Japan

(\*correspondence: b2sm6018@s.tohoku.ac.jp)

<sup>2</sup>National Institute for Materials Science, Japan

<sup>3</sup>Graduate School of Science, Hiroshima University, Japan

Origins of amino acids on the early Earth have been debated by many investigators. Previous literatures indicate that intensive impacts of extraterrestrial objects had occurred during 3.8-4.0 billion years ago. These impacts seem to have delivered and produced prebiotic organic compounds including amino acids, amines and carboxylic acids as well as ammonia [1, 2]. However, the variety of biomolecules experimentally formed in the simulation of these processes was limited compared with that of the protein-constituent amino acids. In this study, we focused on the low-molecular-weight organic compounds (LOC) such as amines and carboxylic acids supplied by one impact process. LOC must have experienced further shock wave due to successive impacts in oceans. We demonstrated impact experiments on a solution of formic acid and ammonia to investigate whether amino acids form from LOC by oceanic impacts on the early Earth.

Shock-recovery experiments were performed with a single-stage propellant gun using a sample container. Starting material is a mixture of <sup>13</sup>C-formic acid and ammonia. After the impact experiments, soluble organic compounds were extracted into water. Then amines and amino acids were analyzed with liquid chromatography-mass spectrometry. Glycine, methylamine and ethylamine whose carbons are composed of <sup>13</sup>C were identified in all of the samples. The amounts of glycine were almost constant regardless of the impact velocity (0.7-0.8 km/s). The amounts of produced amines increased depending on the impact velocity. These results suggest that shock wave converts a LOC into larger-molecular-weight organic compounds including an amino acid. The successive impacts might have contributed to chemical evolution providing variety in biomolecules on the prebiotic Earth.

[1] Cronin and Pizzarello *et al.* (1988), *Meteorites and the Early Solar System*, pp. 819-857. [2] Furukawa *et al.* (2009), *Nature Geosci.*, **2**, 62-66.

## Removal Mechanisms of Silicate in the Wastewater using Aluminum Hydroxide Coprecipitation Method

SHINYA SUZUKI<sup>1\*</sup>, CHIHARU TOKORO<sup>2</sup>,  
DAISUKE HARAGUCHI<sup>3</sup>, SAYAKA IZAWA<sup>4</sup>  
AND SHUJI OWADA<sup>5</sup>

<sup>1</sup>Waseda University, Tokyo, Japan, Shinya.

(Suzuki55@gmail.com)

<sup>2</sup>Waseda University, Tokyo, Japan. (tokoro@waseda.jp)

<sup>3</sup>Waseda University, Tokyo, Japan,

(d.haraguchi@aoni.waseda.jp)

<sup>4</sup>Waseda University, Tokyo, Japan. (izasaya@uri.waseda.jp)

<sup>5</sup>Waseda University, Tokyo, Japan. (owadas@waseda.jp)

This study investigated removal mechanisms of silicate in the wastewater using aluminum hydroxide coprecipitation method. To investigate detailed silicate uptake mechanism during coprecipitation with aluminum hydroxide, adsorption process and coprecipitation process were distinguished exactly in this study [1].

In adsorption experiment, aluminum hydroxide was previously prepared at pH 9 and combined with silicate solution while pH was strictly controlled at pH 9. All sorption isotherms of silicate in adsorption experiments indicated BET like unsaturation type. Especially, dominant removal mechanisms changed from simple layer adsorption to another sorption phenomena, which was equivalent to multi-layer adsorption when Si/Al molar ratio was 2-5. XRD analysis represented the precipitation of kaolinite, which suggested that silicate uptake during adsorption experiment using aluminum hydroxide consisted of two kinds of mechanisms; one was surface complexation of silicate with aluminum hydroxide and another was precipitation of kaolinite. Results from zeta potential measurement and FT-IR analysis supported these suggestion about silicate uptake mechanism. However, in adsorption experiments, residual concentration of silicate in solution was higher than calculated value from chemical equilibrium of kaolinite precipitation. This results suggested dissolution of aluminum hydroxide to precipitate kaolinite required substantial time.

On the other hand, in coprecipitation experiments, alkaline solution consisted of aluminum and silicate ions was prepared and pH was dropped to 9. In this case, residual silicate concentration gave close agreement with calculated value from chemical equilibrium of kaolinite precipitation. This results suggested coprecipitation process was more appropriate for silicate removal than adsorption process because kaolinite could precipitate rapidly.

[1] C.Tokoro, D. Haraguchi, *Journal of MMIJ* 127(2011), pp. 26-31.

## Immobilization of selenium by biofilms of *Shewanella putrefaciens*

Y. SUZUKI<sup>1\*</sup>, H. SAIKI<sup>1</sup>, A. KITAMURA<sup>2</sup>,  
AND H. YOSHIKAWA<sup>2</sup>

<sup>1</sup>Graduate School of Bionics, Tokyo University of Technology, 1404-1 Katakura-cho, Hachioji, Tokyo 192-0982, Japan (\*correspondence: yosuzuki@stf.teu.ac.jp)

<sup>2</sup>Geological Isolation Research and Development Directorate, Japan Atomic Energy Agency, 4-33 Muramatsu, Tokai, Naka, Ibaraki 319-1194, Japan

The microbial reduction of the selenite and selenate has been widely studied using planktonic bacteria. Although bacteria are predominantly found within surface-associated cell assemblages, or biofilms in natural settings, there are little information on the interaction between biofilms and selenium. In this study, biofilms of *Shewanella putrefaciens*, which is an iron-reducing bacteria, were formed and their structure was investigated by a confocal laser scanning microscopy (CLMS). Then reduction of selenite by the biofilms was examined.

Biofilms of *S. putrefaciens* were made on circular cover glasses. Formation of biofilms was observed by CLMS. To investigate the reduction of selenite by the biofilms, a solution containing 100  $\mu\text{M}$  sodium selenite as an electron acceptor, 20 mM sodium lactate as an electron donor was added to the biofilms under an anaerobic condition. After 34 h, the selenium concentration in the solution was measured by ICP-AES. Se K-edge XANES spectra of the precipitates appeared on the biofilms were measured at the Beamline 12C, Photon Factory, KEK (Tsukuba, Japan).

The CLMS observation revealed that thickness of the biofilms was about 10-20  $\mu\text{m}$  and the cells were heterogeneously distributed in the biofilms. After 34 h incubation of the biofilms with selenite, the red precipitates were observed at the place where the biofilms were formed. The precipitates were not dissociated from the biofilms by washing with a deionized water indicating that they associated tightly with the biofilms. The selenium concentration in the solution was under detection limit. The Se K-edge XANES spectrum of the red precipitates showed that they were elemental selenium. These results suggest that the biofilms with iron-reducing bacteria in the environment can strongly immobilize the selenium on the biofilms through selenite reduction to elemental selenium.

## Prediction of Surface Organic Species at the Mineral-Water Interface vs. Spectroscopy

D.A. SVERJENSKY<sup>1</sup>

<sup>1</sup>Johns Hopkins University, Baltimore, MD 21218, USA  
(\*correspondence: cestrada@jhu.edu, sver@jhu.edu)

Surface complexation models have been widely used to model adsorption data for organic species at the mineral-water interface. However, the goal of developing truly predictive models in which the number of surface species, the nature of the surface species attachments and the variations of the proportions of the surface species as functions of environmental conditions such as pH, ionic strength and surface loading has not been reached. Recent advances in the theory and application of the extended triple-layer model (ETLM), in particular taking into account the electrical work associated with desorption of chemisorbed water molecules released during the formation of inner-sphere attachments [1] have enabled substantial progress.

For example, when the ETLM is applied to batch adsorption data referring to a wide range of environmental conditions, typically only a few reaction stoichiometries are able to fit the data. This is in marked contrast to more traditional surface complexation models that lead to highly ambiguous results. From the reaction stoichiometries, model surface species can be inferred. However, few direct *in situ* tests of such results are available. In the present study, two direct tests are described involving experimental adsorption data for the amino acids glutamate and dihydroxyphenylalanine (DOPA) on titanium dioxide. The predicted glutamate surface species and their behavior established using the ETLM [2] were tested with ATR-FTIR spectroscopy and quantum chemical calculations [3]. For DOPA the ETLM results [4] were tested with surface enhanced Raman spectroscopy (SERS) [5]. Excellent agreement is obtained between the number of surface species, the nature of their attachment to the surface and the dependence of the surface speciation on environmental conditions.

[1] Sverjensky & Fukushi (2006), *Env. Sci. & Techn.* **40**, 263-271. [2] Jonsson *et al.* (2009), *Langmuir* **25**, 12127-12135. [3] Parikh *et al.* (2011), *Langmuir* **27**, 1778-1787. [4] Bahri *et al.* (2011), *Env. Sci. & Techn.* **45**, 3959-3966. [5] Lee *et al.* (2012), *Langmuir* **28**, 17322-17330.

## Catalytic Structure of the Hammerhead Ribozyme in a Clay Mineral Environment

JACOB B. SWADLING<sup>1</sup>, JAMES L. SUTER<sup>1</sup>,  
DAVID W. WRIGHT<sup>1</sup> AND PETER V. COVENEY<sup>1</sup>.

<sup>1</sup>Department of Chemistry, University College London,  
London, WC1H 0AJ.

The hammerhead ribozyme is an RNA molecule that performs self cleavage as part of a replicative cycle [1]. We use the enhanced sampling of replica exchange molecular dynamics (REMD) performed on petascale computers to study the folding pathway and the catalytically active structure of the full-length hammerhead ribozyme in both aqueous solution and a clay mineral environment. We simulated 100 replicas of each system producing a total of 10  $\mu$ s of fully atomistic molecular dynamics simulation. Our aim was to understand the solution structure, dynamics and mechanism of the ribozyme in order to resolve hitherto open questions related to the catalytic activity of the ribozyme including the role of metal ions in mediating the reaction and to assess the effect the mineral environment has on the catalytic activity.

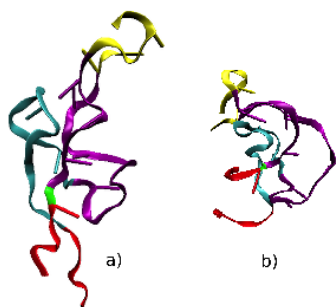


**Figure 1. The dominant principal component (PC1) projected**

The dominant mode of motion is a junction-bend Figure 1, which alters the availability of the catalytically competent conformations of the active site. We have characterized a set of highly populated structures that reveal a pathway to the native catalytically active site. We show how the montmorillonite clay environment significantly alters the structure and kinetics of the hammerhead ribozyme and discuss the implications this has on the RNA world [2].

[1] W. Scott *et al.* (1995) *Cell* **81**,991-1002. [2] E. Bondi *et al.* (2006) *Gene* **389**,10-18.

## <sup>10</sup>Be derived catchment denudation rates from the Garhwal Himalaya

ZACHARY SWANDER<sup>1</sup>, ANTHONY DOSSETO<sup>1</sup>,  
DAVID FINK<sup>3</sup>, JAN HENDRIK MAY<sup>1</sup> AND OLIVER KORUP<sup>3</sup>

<sup>1</sup>Wollongong Isotope Geochronology Lab, University of  
Wollongong, NSW, Australia (\*correspondence to  
zjs785@uow.edu.au)

<sup>2</sup>Australian Nuclear Science & Technology Organization,  
Lucas Heights, NSW, Australia

<sup>3</sup>Institute of Earth & Environmental Science, University of  
Potsdam, Potsdam, Germany.

Despite numerous Quaternary paleoclimatic reconstructions based on stable isotope records from ice core, speleothems, etc., relatively little is known about the climatic influence on terrestrial landscape processes beyond the Last Glacial Maximum (LGM). Specifically, how will changes in temperature and precipitation affect erosion rates on orbital and sub-orbital timescales? To address this question, we are measuring the concentration of *in situ* <sup>10</sup>Be, in 15 independently dated Himalayan alluvial terrace samples[1], to quantify paleo denudation rates over the past 50ka.

Within the montane landscape of the Garhwal Himalaya, the Alaknanda River endures extreme monsoon precipitation that totals greater than 2,000mm·a<sup>-1</sup> at orographic foci. The intensity of such extreme hydrologic conditions have varied spatially and through time, which should exhibit a quantifiable effect on integrated catchment erosion rates.

This research follows in the fundamental footsteps of Bierman & Steig[2] and Schaller *et al.*[3] who first utilized <sup>10</sup>Be in deciphering paleo-erosion rates from European terrace alluvium. Erosion rates are derived from the inherited TCR concentration integrated over the upstream catchment area and the, which incorporates time spent within the weathering profile, during transit and all other time before compete shielding. When measuring <sup>10</sup>Be within shielded alluvium, subsequent erosion rates may be inferred from the time of burial.

By studying how catchment wide average denudation rates have varied across the LGM transition and correlating this to regional paleoclimatic records; we will be able to quantitatively assess how erosion in the the Himalayan respond to climatic variability. Thus providing geochemically derived evidence linking climatic variability with the geomorphic evolution of Himalayan landscapes.

[1] Ray & Srivastava (2010) *QSR* **29**: 1-24. [1]Bierman & Steig (1996) *ESPL* **21**, 125-139. [2]Schaller *et al.* (2004) *Geology* **112**: 127-144.

## The quantitative contribution of oxygenic photosynthesis to Fe(II) oxidation in Precambrian oceans

ELIZABETH D. SWANNER<sup>1\*</sup>, WENFANG WU<sup>1,2</sup>,  
BETTINA VOELKER<sup>3</sup>, RONNY SCHOENBERG<sup>1</sup>  
AND ANDREAS KAPPLER<sup>1</sup>

<sup>1</sup>Department of Geoscience, University of Tuebingen, Germany, \*elizabeth.swanner@ifg.uni-tuebingen.de

<sup>2</sup>Institute of Geology and Geophysics, Chinese Academy of Sciences, Beijing, China

<sup>3</sup>Department of Chemistry and Geochemistry, Colorado School of Mines, USA

Evidence for oxidation of Fe(II) and deposition of Fe(III)-bearing minerals in anoxic or stratified Precambrian oceans has received support from decades of sedimentological and geochemical investigation of Banded Iron Formations (BIF). However, the exact mechanisms by which Fe(II) was oxidized and stabilized in anoxic sediments remain equivocal. The oxidation of Fe(II) by abiotic reaction with O<sub>2</sub> produced by oxygenic photosynthetic cyanobacteria is consistent with evidence for an iron chemocline in some Precambrian BIF basins. However, if oxygenic photosynthesis oxidized Fe in the Archean, O<sub>2</sub> release to the atmosphere must have been minimal, consistent with geochemical evidence for an anoxic atmosphere prior to 2.3 Ga.

We evaluate the hypothesis that Fe(II) oxidation and deposition was mediated by O<sub>2</sub> with laboratory experiments using *Synechococcus* PCC 7002 to represent an early marine cyanobacterium [1]. Our initial results confirm that this strain can grow in Fe(II) concentrations up to 5 mM. The kinetics of Fe(II) oxidation are consistent with an abiotic reaction between Fe(II) and O<sub>2</sub> and not via direct use of electrons from Fe(II) in photosynthesis. We also measured the isotopic fractionation factor between aqueous Fe(II) and precipitated Fe(III) during growth of *Synechococcus* PCC 7002 with Fe(II), which is similar to fractionation factors in abiotic experiments. Microscopic and spectroscopic analysis of the cell-mineral aggregates also inform the location of Fe(II) oxidation and the speciation, mineralogy and spatial relationship of iron to carbon in the resulting precipitates. Our efforts are now focused on quantifying the rates of O<sub>2</sub> production and Fe deposition in a laboratory-scale model of a ferruginous water column where Fe(II) upwells into an engineered photic zone. Our intent is that these results will provide a mechanistic and quantitative framework for evaluating the geochemical consequences of perhaps life's greatest metabolic innovation.

[1] Blank and Sánchez-Baracaldo (2010) *Geobiology*, **8**, 1-23.

## Size-dependent reactivity of magnetite nanoparticles: A bridge between lab and field investigations

A.L. SWINDLE<sup>1\*</sup>, A.S. MADDEN<sup>1</sup> AND I.M. COZZARELLI<sup>2</sup>

<sup>1</sup>University of Oklahoma, Norman, OK (\*correspondance: aswindle@ou.edu, amadden@ou.edu)

<sup>2</sup>US Geological Survey, Reston, VA (icozzare@usgs.gov)

Research on nanoparticles has exploded in recent years as we have begun to understand the extensive role these materials play in natural systems as well as their potential benefits and risks to human society. However, the very nature of nanoparticles makes them challenging to study, particularly in a field setting. As a result, many questions remain to be answered concerning how nanoparticles behave in a natural environment and how accurately laboratory results reflect reactions that occur in the field.

In this investigation magnetite nanoparticles with average diameters of 6 nm, 44 nm and 90 nm were synthesized and thoroughly characterized. The nanoparticles were emplaced in the anoxic groundwater zone of the leachate plume in the subsurface of the USGS Norman Landfill Site with custom-built TEM grid-holders. Laboratory analog experiments were also conducted using nanoparticles and synthetic groundwater modeled on the chemistry of the groundwater from the landfill site, but omitted DOC. Finally, a series of magnetite-chromate adsorption experiments was conducted with varying amounts of DOC added to investigate the impact of organics on the surface reactivity of the magnetite nanoparticles.

The field investigation revealed that a thin coating of organics developed on the particles surfaces that occluded the particles from the groundwater and inhibited dissolution. This is supported by geochemical models indicating that magnetite is not thermodynamically stable under the given chemical conditions and by the laboratory analogs which provided evidence of magnetite dissolution in the absence of organics. The chromate adsorption experiments showed that DOC concentrations as low as 1 mg/L can impact the surface reactivity of magnetite even when an excess of mineral surface area is present.

The results of this investigation revealed that under the field conditions, magnetite dissolution decreased as particle size decreased, while this trend was reversed in the laboratory experiments. Adsorption experiments indicate that this reversal is likely due to dissolved and particulate organics. Together, these experiments show that organics play a significant role in the surface reactivity of nanoscale minerals and remain integrally important to understanding the environmental fate of nanomaterials.

## U/Pb zircon age of Mistastin Lake crater, Labrador, Canada – implications for high-precision dating of small impact melt sheets and the end Eocene extinction

PAUL J. SYLVESTER<sup>1</sup>, JAMES L. CROWLEY<sup>2</sup>  
AND MARK D. SCHMITZ<sup>2</sup>

<sup>1</sup>Department of Earth Sciences, Alexander Murray Building,  
Memorial University, St John's NL A1B 3X5 Canada

<sup>2</sup>Department of Geosciences, 1910 University Drive, Boise  
State University, Boise, ID 83725 USA

Accurate and precise dating of the impact cratering record on Earth is important for determining the duration of periods of intense bombardment and their role in causing climatic perturbations and biotic extinctions. Unfortunately only four terrestrial craters are well dated by the U-Pb zircon method; all are large structures, *ca.* 100–300 km in diameter [1]. We investigated the 28-km wide, Mistastin Lake crater [2], Labrador, Canada, in order to determine whether magmatic zircon forms in small-volume impact melt sheets and may be dated precisely and accurately. A sample was collected from Discovery Hill, an 80-meter thick, wedge-shaped butte of columnar-jointed impact melt rock. An age of  $36 \pm 4$  Ma ( $2\sigma$ ) for Mistastin was reported by [3] based on  $^{40}\text{Ar}/^{39}\text{Ar}$  dating.

In addition to large elongated to equant ( $\sim 100$ – $500 \mu\text{m}$ ) zircon inherited from the country rocks, the melt rock contains tiny, elongate ( $\sim 25 \mu\text{m}$  wide  $\times$   $\sim 100$ – $175 \mu\text{m}$  long), prismatic “needle” zircon with narrow, brown-colored melt channel “spines” running through the centers of the crystals. Eleven needles were analyzed by CA-TIMS using the EARTHTIME tracer solution. With only 1–4 pg of radiogenic Pb per needle, it was critical to have low Pb blanks ( $\sim 0.4$  pg) for high-precision dating.  $^{206}\text{Pb}/^{238}\text{U}$  dates are equivalent with a weighted mean date of  $37.83 \pm 0.05$  Ma (internal error, MSWD = 1.0) that is interpreted as the crystallization age of the impact melt. The results demonstrate that magmatic zircon can crystallize in impact melt from small craters. The new radiometric age for Mistastin makes it now the most precisely and accurately dated small crater on Earth. The Mistastin U/Pb date is significantly older than  $^{40}\text{Ar}/^{39}\text{Ar}$  dates for the two largest ( $\sim 100$ km) Eocene craters, Popigai ( $35.7 \pm 0.2$  Ma,  $2\sigma$ ) and Chesapeake Bay ( $35.5 \pm 0.3$  Ma,  $2\sigma$ ) [1] and the end Eocene mass extinction event ( $\sim 34$  Ma).

[1] Jourdon *et al.* (2009) *EPSL* **286**, 1–13. [2] Marion & Sylvester (2010) *Planet Space Sci* **38**, 552–573. [3] Mak *et al.* (1976) *EPSL* **31**, 345–357.

## Modification of synthetic zeolites and characteristics of their properties

B. SZALA<sup>1\*</sup>, P. TUREK<sup>1</sup> AND T. BAJDA<sup>1</sup>

<sup>1</sup>Department of Geology, Geophysics and Environmental  
Protection, AGH University of Science and Technology,  
Krakow, Poland (\*bszala@geol.agh.edu.pl)

Synthetic zeolites are increasingly likely to be used in advanced chemical processes and industry due to their attractive properties. Ongoing research is trying to establish a way improve some of their properties, for example, the process of sorption. This process is low because it takes place only on the outer surface of the crystallites. To increase the chemical affinity of the zeolite's surface to the organic compounds, modification of zeolites' surface is necessary. The aim of the study was to perform modifications of a synthetic zeolite and evaluate its sorption properties. The material used was an X-type zeolite prepared from coal fly ash. For modification of the zeolites' surface quaternary, ammonium salts with single or double carbon chain length, such as: dodecyltrimethylammonium bromide (DDTMABr), tetradecyltrimethylammonium bromide (TDTMABr), hexadecyltrimethylammonium bromide (HDTMABr) and octadecyltrimethylammonium bromide (ODTMABr) were used. Surfactants were adsorbed onto a synthetic zeolite in amounts of 1.0 and 2.0 of the external cation exchange capacity (ECEC) in quantities of 24.4 and 48.8 mmol per 100g of zeolite respectively. Quantitative characterization of organo-zeolites and characterization of their properties has been performed. The effectiveness of the modification has been determined based on the content of carbon, hydrogen and nitrogen combined with X-ray Diffraction and IR spectroscopy. Simultaneously, the effectiveness of maximum sorption capacity on organo-zeolites in terms of organic compounds such as benzene, toluene, xylene has been established. The results obtained show an improvement of the sorption properties of the organo-zeolite modified in an amount of 2.0 ECEC in relation to the 1.0 ECEC and unmodified material. Also the carbon chain length surfactants show their importance during the modification. The results of this research can be used in environmental protection and for further studies into the properties of surfactant-modified synthetic zeolites and their potential industrial applications; for example, in petrochemistry.

We gratefully acknowledge the support of NCBiR having provided grant PBS1/A2/7/2012.



## **Petrogenesis of andesites in Mesoarchaean supracrustal belts of SW Greenland: Geodynamic implications**

KRISTOFFER SZILAS<sup>1</sup> AND J. ELIS HOFFMANN<sup>2</sup>

<sup>1</sup>Lamont-Doherty Earth Observatory, Palisades, New York,  
USA

<sup>2</sup>Institut für Geologie und Mineralogie, Universität zu Köln,  
Zùlpicher Str. 49b, 50674 Köln, Germany

We present an overview of geochemical data for the Mesoarchaean supracrustal belts from the Tasiusarsuaq terrane, SW Greenland. These ultramafic, basaltic and andesitic enclaves are located within younger tonalite-trondhjemite-granodiorite (TTG) orthogneisses and are mainly dominated by tholeiitic basalts. However, calc-alkaline andesites are also present and comprise up to ca. 50% of individual supracrustal belts. These two lithological groups can roughly be divided into tholeiitic and calc-alkaline affinity by having La/Sm ratios less than, or over 3.5, respectively. While the mafic rocks have flat trace element patterns with negative Nb- and Ta-anomalies, the andesitic rocks have strongly fractionated trace element patterns, with distinctly negative Nb-, Ta- and Ti-anomalies, as well as positive Hf- and Zr-anomalies. Thus, they are not related by fractional crystallisation and no gradational transitions between the two groups have been observed. Assimilation of pre-existing continental crust can also not explain the trace element variations of the andesites. Modelling suggests that simple binary mixing of a mafic magma and a TTG-type component in a 1:1 ratio can explain most of the variation that the andesites display. This is confirmed by Hf-isotope modelling that support the large mixing ratio and therefore that actual melting of the local felsic crust must have occurred. We suggest that the hotter conditions during the Mesoarchaean could explain the significant proportion of melting of the lower crust during addition of juvenile mafic magmas. Overall, the geochemical data are compatible with a modern-style subduction zone environment, for which recent studies have also concluded that substantial magma mixing is a significant process.